WOODY PLANTS AND FOREST ECOSYSTEMS IN A COMPLEX WORLD – ECOLOGICAL INTERACTIONS AND PHYSIOLOGICAL FUNCTIONING ABOVE AND BELOW GROUND

EDITED BY: Boris Rewald, Christian Ammer, Thorsten Grams, Henrik Hartmann, Guenter Hoch, Katharina Maria Keiblinger, Andrey V. Malyshev and Ina Christin Meier

PUBLISHED IN: Frontiers in Plant Science

frontiers Research Topics

frontiers

ISSN 1664-8714
ISBN 978-2-88963-640-2
DOI 10.3389/978-2-88963-640-2

About Frontiers

Frontiers is more than just an open-access publisher of scholarly articles: it is a pioneering approach to the world of academia, radically improving the way scholarly research is managed. The grand vision of Frontiers is a world where all people have an equal opportunity to seek, share and generate knowledge. Frontiers provides immediate and permanent online open access to all its publications, but this alone is not enough to realize our grand goals.

Frontiers Journal Series

The Frontiers Journal Series is a multi-tier and interdisciplinary set of open-access, online journals, promising a paradigm shift from the current review, selection and dissemination processes in academic publishing. All Frontiers journals are driven by researchers for researchers; therefore, they constitute a service to the scholarly community. At the same time, the Frontiers Journal Series operates on a revolutionary invention, the tiered publishing system, initially addressing specific communities of scholars, and gradually climbing up to broader public understanding, thus serving the interests of the lay society, too.

Dedication to Quality

Each Frontiers article is a landmark of the highest quality, thanks to genuinely collaborative interactions between authors and review editors, who include some of the world's best academicians. Research must be certified by peers before entering a stream of knowledge that may eventually reach the public - and shape society; therefore, Frontiers only applies the most rigorous and unbiased reviews.
Frontiers revolutionizes research publishing by freely delivering the most outstanding research, evaluated with no bias from both the academic and social point of view. By applying the most advanced information technologies, Frontiers is catapulting scholarly publishing into a new generation.

What are Frontiers Research Topics?

Frontiers Research Topics are very popular trademarks of the Frontiers Journals Series: they are collections of at least ten articles, all centered on a particular subject. With their unique mix of varied contributions from Original Research to Review Articles, Frontiers Research Topics unify the most influential researchers, the latest key findings and historical advances in a hot research area! Find out more on how to host your own Frontiers Research Topic or contribute to one as an author by contacting the Frontiers Editorial Office: researchtopics@frontiersin.org

WOODY PLANTS AND FOREST ECOSYSTEMS IN A COMPLEX WORLD – ECOLOGICAL INTERACTIONS AND PHYSIOLOGICAL FUNCTIONING ABOVE AND BELOW GROUND

Topic Editors:
Boris Rewald, University of Natural Resources and Life Sciences Vienna, Austria
Christian Ammer, University of Göttingen, Germany
Thorsten Grams, Technical University of Munich, Germany
Henrik Hartmann, Max Planck Institute for Biogeochemistry, Germany
Guenter Hoch, University of Basel, Switzerland
Katharina Maria Keiblinger, University of Natural Resources and Life Sciences Vienna, Austria
Andrey V. Malyshev, University of Greifswald, Germany
Ina Christin Meier, University of Göttingen, Germany

Citation: Rewald, B., Ammer, C., Grams, T., Hartmann, H., Hoch, G., Keiblinger, K. M., Malyshev, A. V., Meier, I. C., eds. (2020). Woody Plants and Forest Ecosystems in a Complex World – Ecological Interactions and Physiological Functioning Above and Below Ground. Lausanne: Frontiers Media SA. doi: 10.3389/978-2-88963-640-2

Table of Contents

frontiers in Plant Science

EDITORIAL
published: 28 February 2020
doi: 10.3389/fpls.2020.00173

Editorial: Woody Plants and Forest Ecosystems in a Complex World—Ecological Interactions and Physiological Functioning Above and Below Ground

Boris Rewald[1]*, *Christian Ammer*[2], *Henrik Hartmann*[3], *Andrey V. Malyshev*[4] *and Ina C. Meier*[5]

[1] Forest Ecology, Department of Forest and Soil Sciences, University of Natural Resources and Life Sciences Vienna (BOKU), Vienna, Austria, [2] Silviculture and Forest Ecology of the Temperate Zones, University of Göttingen, Göttingen, Germany, [3] Department of Biogeochemical Processes, Max Planck Institute for Biogeochemistry, Jena, Germany, [4] Experimental Plant Ecology, Institute of Botany and Landscape Ecology, University of Greifswald, Greifswald, Germany, [5] Plant Ecology, Albrecht-von-Haller Institute of Plant Sciences, University of Goettingen, Göttingen, Germany

Keywords: competition, disturbance, functional traits, forest ecosystem research, funding priorities, resource availability, stressors, trees

OPEN ACCESS

Edited and reviewed by:
Martina Pollastrini, University of Florence, Italy

***Correspondence:**
Boris Rewald
boris.rewald@boku.ac.at

Specialty section:
This article was submitted to Functional Plant Ecology, a section of the journal Frontiers in Plant Science

Received: *28 November 2019*
Accepted: *05 February 2020*
Published: *28 February 2020*

Citation:
Rewald B, Ammer C, Hartmann H, Malyshev AV and Meier IC (2020) Editorial: Woody Plants and Forest Ecosystems in a Complex World—Ecological Interactions and Physiological Functioning Above and Below Ground. Front. Plant Sci. 11:173. doi: 10.3389/fpls.2020.00173

Editorial on the Research Topic

Woody Plants and Forest Ecosystems in a Complex World—Ecological Interactions and Physiological Functioning Above and Below Ground

Forests are fundamental components of life on Earth. They are essential to global biogeochemical cycles and economies alike, shape the landscape, provide habitat for a large number of animal and plant species, are a renewable resource of wood, and provide a carbon sink that can reduce anthropogenic CO_2 pollution and mitigate climate change (FAO, 2018b). Yet despite the importance of intact forest ecosystems for future generations of humankind (Costanza et al., 1997), notoriously more research funds are directed towards agricultural systems, or wood processing at most (Lovrić et al., 2020), than towards the preservation and sustainable management of forest ecosystems under global change. This is alarming, as in times of rapidly changing environmental conditions, resource management of long-lived woody species and their ecosystems is facing new challenges (Macdicken et al., 2016; Ammer, 2019). The Intergovernmental Science-Policy Platform on Biodiversity and Ecosystem Services recently underscored that critical knowledge gaps remain for (i) ecosystem processes that underpin the contribution of nature to people and ecosystem health as well as for (ii) the consequences of changing interactions among organisms and taxa under climate change (IPBES, 2019). These knowledge gaps strongly apply to forest ecosystems. Here we call for a reconsideration of economic funding decisions that should jointly take into account forest-based bioeconomy (Kraxner et al., 2017), global biogeochemical cycles (Curtis and Gough, 2018), as well as various other regulating, ecological, cultural, and supporting services provided by forest ecosystems (Felipe-Lucia et al., 2018). This implies the explicit inclusion of (pristine and managed) forest ecosystems, incl. their soils, into the EUs' Horizons Europe research program (European Commission, 2019) and other national and supranational funding schemes worldwide.

We support our call by the large number of open questions related to forest ecology [see e.g. (Ammer et al., 2018) for Central Europe] and recent research on woody species and forest ecosystems. The 18 articles in this Research Topic (RT) not only uncover ecological interactions and physiological functioning above- and belowground, but also illustrate specific open questions and research gaps that need to be covered—allowing for better predictions of forest responses to global change and other human activity-based ecosystem modifications. The better predictions are urgently needed when it comes to adapt forest management and ensure the provision of ecosystem services under global change (Joyce et al., 2009; Keenan, 2015).

Functional traits are increasingly recognized as a useful tool to understand structure–function relationships in plants (Díaz et al., 2016; O'brien et al., 2017). In this RT, aboveground plant functional traits are shown to be useful in estimating and predicting water use efficiency, carbon stocks and competitive ability due to their inherent conservative nature. Specifically, Wang et al. report on the existence of a cross-species trade-off between the size of individual leaves and the number of leaves per yearly twig unit in a temperate forest and provide evidence for the influence of small leaf sizes on effective temperature regulation in dry environments with strong radiation. As the relationships between leaf and twig biomass as well as between leaf biomass and twig and stem dimensions are important due to their relation to plants' C metabolism and transport modes, Sun et al. focus on isometric scaling across different forest communities in the humid warm subtropics. The article by Bu et al. illustrates that plant functional traits such as specific leaf area and wood density, as affected by abiotic site conditions in a tropical montane rainforest, are key in estimating aboveground carbon stocks. Their study suggests that community-weighted means of plant functional traits are key mediators in regulating effects of abiotic site conditions on ecosystem functions. Complementary, the analysis of *Pinus sylvestris* fine-root traits by Brunner et al. reveals that a long-term increase in water availability significantly increases root biomass, length, and production, but does not alter morphological and architectural traits. Strikingly, their experiment illustrates the extended time spans necessary to reveal acclimation responses in trees—the differences in fine-root biomass between irrigated and dry plots became significant only nine years after the experiment began. This strongly suggests that more long-term experiments are needed in forest research addressing the impact of changing environments.

In dense communities, plants compete with each other for limited resources. Assessing the neighborhood of tree saplings with terrestrial laser scanners, Annighöfer et al. show that individuals of the same species perform differently under constant light conditions but differing neighborhoods. Their study confirms that the description of the neighborhood, in addition to light measurements, increases the predictive power of tree regeneration trait and performance models. However, while the amount of light is considered to be among the most important resources for saplings growing in the understory of (temperate) forest ecosystems, Bueno et al. illustrate that competition for nitrogen (N) can also modify the outcome of competitive interactions between invasive and native tree seedlings. Other articles in this RT address resource gathering and allocation patterns of woody species and their subsequent effects on growth. Assessing phosphorous (P) nutrition under continuing high N deposition and increasing drought stress, respectively, Meller et al. highlight the ability of *Fagus sylvatica* to alter resource allocation in response to soil P availability, while Dirks et al. foresee growth reductions in *Quercus calliprinos* trees due to reduced P uptake efficiency with increased drought occurrence. As plant resource uptake (capacity) is often tightly related to ectomycorrhizal fungi (EMF) in temperate and boreal forest ecosystems, identifying the biotic and abiotic factors that shape EMF communities is important for understanding terrestrial ecosystem processes and predicting the impacts of global change on plant communities. Accordingly, Defrenne et al. shed light on the ectomycorrhizal fungal diversity in *Pseudotsuga menziesii* forests across regional gradients in Canada. They find that temperature, precipitation, and the soil C:N ratio affect EMF community dissimilarities and exploration type abundances. As no evidence for a functional connection between root diameter and EMF exploration types within Douglas-fir populations was found, future studies are encouraged to simultaneously examine both fine root and fungal traits—representing the diversity of belowground resource gathering strategies.

Focusing on plant–water relations in a subtropical ecosystem, Fang et al. suggest that bamboos exchange water *via* rhizomes and that nighttime fluxes are highly important for the support of freshly sprouted culms. The study provides further insight into the benefits of physiological integration in woody monocots; water exchange may facilitate the very fast growth of bamboo shoots and the colonization of the surroundings. Gong et al. (2019) provide an example on the significance of foliar water uptake for the water balance under arid conditions—even in a deep-rooted tree species. Geißler et al. measured soil moisture dynamics at different depths with natural stable isotopes to quantify the partitioning of water between vegetation components. Consequently, potential effects of shrub encroachment on groundwater recharge rates in a climate-change affected semi-arid savanna ecosystem were determined. Finally, Martín-Sanz et al. investigated the effect of water availability on the resilience to forest fires in 19 *Pinus halepensis* provenances *via* absolute bark thickness (i.e. determining the degree of heat insulation). They show that drought-stressed trees have a higher risk to die from fires before achieving sexual maturity and building a sufficiently large aerial seed bank for post-fire regeneration. As forest fires are suggested to increase in frequency and extent, especially in the Mediterranean areas, the results highlight the unfortunate interactions between different stress and disturbance agents.

Together with forest fires, pest infestations have caused large-scale disturbances of (temperate) forests in recent years. Erfmeier et al. illustrate that younger ash trees, particularly those growing in alder-ash forests, are most susceptible to Ash dieback—thus

showing that forest community composition and age play key roles in the extent of the infection with *Hymenoscyphus fraxineus*. In a broader perspective, Rammer and Seidl argue for an increased utilization of the predictive power of machine learning techniques such as deep neural networks for a wide range of ecological problems—using bark beetle outbreaks in conifer-dominated forests as an example.

Shifting the focus towards disturbances of smaller scale, wind damage is an important factor among temperate forests (Sommerfeld et al., 2018). Dumroese et al. thus address the plasticity of *Pinus ponderosa* coarse root (systems) as a function of prevailing wind and sloping ash-cap soils, improving our functional understanding of tree anchorage. An enhanced knowledge on anchorage properties of trees will enable us to better predict the response of trees to more severe, more frequent climate change-facilitated storms, as well as to inform silvicultural practices toward improving the resilience of existing forest stands towards multiple stressors (Bolte et al., 2019). While climate change affects all seasons, the ecological effects of warming are often more pronounced in winter than summer (Kreyling et al., 2019)—i.a. leading to insufficient/pre-mature (de-)hardening with an increased risk of frost damage (Inouye, 2008). Addressing frost survival mechanism of vegetative buds in temperate trees, Neuner et al. show that the mechanism of frost resistance in temperate trees helps explain which species can withstand lower freezing temperatures and how they are distributed. The ability to withstand intracellular freezing is present in species with the best ability to withstand freezing damage at the lowest temperatures.

Green infrastructure becomes more and more important in an increasingly urbanized world (FAO, 2018a). Management of urban forests is a challenging task not only because of highly heterogeneous, often harsh growing conditions (Fitzky et al., 2019) but also because of various, often conflicting, demands and goals. In their contribution, Vitali et al. illustrate that damaging root systems of urban trees invokes long-term effects on growth and that slower growing tree species can better compensate growth reductions due to the administered damage. The paper highlights the potential of increased species functional understanding to manage (future) vegetation composition in urban environments better.

Taken together, the 18 contributions to this RT cover many aspects of timely research on woody plants and forest ecosystems. They add to the increasing evidence that one-size-fits-all tree species-to-forest type ecosystem services relationships are overly simplistic, arguing for a more nuanced empirical understanding of forest functioning under different environmental and management regimes. However, the current dominance of funding for bio-energy and bio-refinery topics over more forest ecosystem-focused studies [e.g. in the EU; (Lovrić et al., 2020)] follows the perspective of science and technology studies (Birch et al., 2010)—by which bio-economy research is focused on the innovation potential of biotechnology, and less on the sectors that manage natural resources. In contrast, we believe that an increased investment into cross-disciplinary ecological research is needed to strengthen our functional understanding of woody plants in complex ecosystems. Especially assessments of resilience and adaptive capacity of forest ecosystems under a changing climate remain important priorities of research to support evidence-based decisions by forest managers and policy makers worldwide on sustainable management practices.

AUTHOR CONTRIBUTIONS

BR, IM and AM provided the first draft of the MS. All co-authors jointly revised the manuscript and approved its publication.

ACKNOWLEDGMENTS

We thank the participants of the 48th Annual Conference of the Ecological Society of Germany, Austria and Switzerland (GfÖ) "Ecology—Meeting the Scientific Challenges of a Complex World" (Vienna, Austria, 10th–14th September 2018) for stimulating discussions, and the authors and reviewers for their support in creating this RT. Explicit thanks go to our co-editors Thorsten Grams (TUM), Günter Hoch (UNIBAS), and Katharina M. Keiblinger (BOKU) for help with the RT set-up and management.

REFERENCES

Ammer, C., Fichtner, A., Fischer, A., Gossner, M. M., Meyer, P., Seidl, R., et al. (2018). Key ecological research questions for Central European forests. *Basic Appl. Ecol.* 32, 3–25. doi: 10.1016/j.baae.2018.07.006

Ammer, C. (2019). Diversity and forest productivity in a changing climate. *New Phytol.* 221, 50–66. doi: 10.1111/nph.15263

Birch, K., Levidow, L., and Papaioannou, T. (2010). Sustainable capital? The neoliberalization of nature and knowledge in the European "knowledge-based bio-economy". *Sustainability* 2, 2898–2918. doi: 10.3390/su2092898

Bolte, A., Block, J., Eichhorn, J., Sanders, T., and Wellbrock, N. (2019). "Sustainable use and development of forests and forest soils: A resume," in *Status and dynamics of forests in Germany*. Eds. N. Wellbrock and A. Bolte (Cham, Germany: Springer), 355–374.

Costanza, R., D'arge, R., De Groot, R., Farber, S., Grasso, M., Hannon, B., et al. (1997). The value of the world's ecosystem services and natural capital. *Nature* 387, 253–260. doi: 10.1038/387253a0

Curtis, P. S., and Gough, C. M. (2018). Forest aging, disturbance and the carbon cycle. *New Phytol.* 219, 1188–1193. doi: 10.1111/nph.15227

Díaz, S., Kattge, J., Cornelissen, J. H. C., Wright, I. J., Lavorel, S., Dray, S., et al. (2016). The global spectrum of plant form and function. *Nature* 529, 167–171. doi: 10.1038/nature16489

European Commission (2019). *Orientations towards the first Strategic Plan for Horizon Europe - Revised following the co-design process (Version of 31. October 2019)*. (Brussels: European Commission).

FAO (2018a). *Forests and sustainable cities*. (Rome, Italy: Food and Agriculture Organization of the United Nations).

FAO (2018b). *State of the World's Forests 2018 - Forest pathways to ustainable developments* (Rome, Italy: Food and Agriculture Organization of the United Nations).

Felipe-Lucia, M. R., Soliveres, S., Penone, C., Manning, P., Van Der Plas, F., Boch, S., et al. (2018). Multiple forest attributes underpin the supply of multiple ecosystem services. *Nat. Commun.* 9, 1–11. doi: 10.1038/s41467-018-07082-4

Fitzky, A. C., Sandén, H., Karl, T., Fares, S., Calfapietra, C., Grote, R., et al. (2019). The Interplay Between Ozone and Urban Vegetation—BVOC Emissions,

Ozone Deposition, and Tree Ecophysiology. *Front. In Forests Global Change* 2, 1–17.

Inouye, D. W. (2008). Effects of climate change on phenology, frost damage, and floral abundance of montane wildflowers. *Ecology* 89, 353–362. doi: 10.1890/06-2128.1

IPBES (2019). *Summary for policymakers of the global assessment report on biodiversity and ecosystem services of the Intergovernmental Science-Policy Platform on Biodiversity and Ecosystem Services*. Eds. S. Díaz, J. Settele, E. S. Brondizio, H. T. Ngo, M. Guèze, J. Agard, A. Arneth, P. Balvanera, K. A. Brauman, S. H. M. Butchart, K. M. A. Chan, L. A. Garibaldi, K. Ichii, J. Liu, S. M. Subramanian, G. F. Midgley, P. Miloslavich, Z. Molnár, D. Obura, A. Pfaff, S. Polasky, A. Purvis, J. Razzaque, B. Reyers, R. R. Chowdhury, Y. J. Shin, I. J. Visseren-Hamakers, K. J. Willis and C. N. Zayas. (Bonn, Germany: IPBES secretariat).

Joyce, L. A., Blate, G. M., Mcnulty, S. G., Millar, C. I., Moser, S., Neilson, R. P., et al. (2009). Managing for multiple resources under climate change: national forests. *Environ. Manage.* 44, 1022–1032. doi: 10.1007/s00267-009-9324-6

Keenan, R. J. (2015). Climate change impacts and adaptation in forest management: a review. *Ann. For. Sci.* 72, 145–167. doi: 10.1007/s13595-014-0446-5

Kraxner, F., Fuss, S., and Verkerk, H. (2017). "Is there enough forest biomass available to meet the demands of the forest-based bioeconomy?," in *Towards a sustainable European forest-based bioeconomy – assessment and the way forward*. Ed. G. Winkel. (Joensuu, Finland: European Forest Institute), 53–66.

Kreyling, J., Grant, K., Hammerl, V., Arfin-Khan, ,.M., Malyshev, A. V., Peñuelas, J., et al. (2019). Winter warming is ecologically more relevant than summer warming in a cool-temperate grassland. *Sci. Rep.* 9, 14632. doi: 10.1038/s41598-019-51221-w

Lovrić, M., Lovrić, N., and Mavsar, R. (2020). Mapping forest-based bioeconomy research in Europe. *For. Policy Econ.* 110, 1–20. doi: 10.1016/j.forpol.2019.01.019

Macdicken, K., Jonsson, Ö., Piña, L., Maulo, S., Contessa, V., Adikari, Y., et al. (2016). *Global forest resources assessment 2015: how are the world's forests changing?* (Rome, Italy: Food and Agriculture Organization of the United Nations).

O'brien, M. J., Engelbrecht, B. M. J., Joswig, J., Pereyra, G., Schuldt, B., Jansen, S., et al. (2017). A synthesis of tree functional traits related to drought-induced mortality in forests across climatic zones. *J. Appl. Ecol.* 54, 1669–1686. doi: 10.1111/1365-2664.12874

Sommerfeld, A., Senf, C., Buma, B., D'amato, A. W., Després, T., Díaz-Hormazábal, I., et al. (2018). Patterns and drivers of recent disturbances across the temperate forest biome. *Nat. Commun.* 9, 1–9. doi: 10.1038/s41467-018-06788-9

Conflict of Interest: The authors declare that the research was conducted in the absence of any commercial or financial relationships that could be construed as a potential conflict of interest.

frontiers in Plant Science

ORIGINAL RESEARCH
published: 04 February 2019
doi: 10.3389/fpls.2019.00058

The Smaller the Leaf Is, the Faster the Leaf Water Loses in a Temperate Forest

Cunguo Wang[1,2], Junming He[1], Tian-Hong Zhao[1], Ying Cao[1], Guojiao Wang[1], Bei Sun[1], Xuefei Yan[1], Wei Guo[1] and Mai-He Li[2,3]*

[1] College of Agronomy, Shenyang Agricultural University, Shenyang, China, [2] School of Geographical Sciences, Northeast Normal University, Changchun, China, [3] Swiss Federal Institute for Forest, Snow and Landscape Research (WSL), Birmensdorf, Switzerland

Leaf size (i.e., leaf surface area and leaf dry mass) profoundly affects a variety of biological carbon, water and energy processes. Therefore, the remarkable variability in individual leaf size and its trade-off with total leaf number in a plant have particularly important implications for understanding the adaption strategy of plants to environmental changes. The various leaf sizes of plants growing in the same habitat are expected to have distinct abilities of thermal regulation influencing leaf water loss and shedding heat. Here, we sampled 16 tree species co-occurring in a temperate forest in northeastern China to quantify the variation of leaf, stomata and twigs traits, and to determine the relationships of leaf size with leaf number and leaf water loss. We examined the right-skewed distributions of leaf size, leafing intensity, stomatal size and stomatal density across species. Leafing intensity was significantly negatively correlated with leaf size, accounting for 4 and 12% of variation in leaf area and leaf mass, respectively. Species was the most important factor in explaining the variation in leaf size (conditional R^2 of 0.92 for leaf area and 0.82 for leaf mass). Leaf area and mass significantly increased with increasing diameter of twigs. Leaf water loss was strongly negatively correlated with leaf area and leaf mass during the first four hours of the measurement. Leaf area and leaf mass accounted for 38 and 30% of variation in total leaf water loss, respectively. Leaf water loss rate (k) was significantly different among tree species and markedly linearly decreased with increasing leaf area and leaf mass for simple-leaved tree species. In conclusion, the existence of a cross-species trade-off between the size of individual leaves and the number of leaves per yearly twig unit was confirmed in that temperate forest. There was strongly negative correlation between leaf water loss and leaf size across tree species, which provides evidences for leaf size in leaf temperature regulation in dry environment with strong radiation. The size-dependent leaf water relation is of central importance to recognize the functional role of leaf size in a changing climate including rapid changes in air temperature and rainfall.

Keywords: leaf area, leaf intensity, leaf mass, leaf size, leaf water loss, right-skewed distribution, trade-off

OPEN ACCESS

Edited by:
Boris Rewald, University of Natural Resources and Life Sciences, Vienna, Austria

Reviewed by:
Andreas M. Savvides, Cyprus University of Technology, Cyprus
Iván Prieto, Centro de Edafología y Biología Aplicada del Segura (CEBAS), Spain

****Correspondence:***
Wei Guo
guowei_233@163.com

Specialty section:
This article was submitted to Functional Plant Ecology, a section of the journal Frontiers in Plant Science

Received: *27 August 2018*
Accepted: *16 January 2019*
Published: *04 February 2019*

Citation:
Wang C, He J, Zhao T-H, Cao Y, Wang G, Sun B, Yan X, Guo W and Li M-H (2019) The Smaller the Leaf Is, the Faster the Leaf Water Loses in a Temperate Forest. Front. Plant Sci. 10:58. doi: 10.3389/fpls.2019.00058

INTRODUCTION

Plants are certainly modular organisms with recognized capabilities to regulate size and number of organs at the module scale (Kroon et al., 2005). Leaves are the principal photosynthetic organs of plants (Wright et al., 2004), therefore, the size of leaves (e.g., leaf surface area, leaf dry mass and leaf length) profoundly affects a variety of biological processes, for instance, plant growth, survival, reproduction, and ecosystem function (Koch et al., 2004; Tozer et al., 2015). Thus, considerable attention has been paid to the natural variations in leaf size and its ecological and evolutionary significances (Niinemets et al., 2007). For example, leaf surface area varies over six orders of magnitude across terrestrial plants (Milla and Reich, 2007; Niinemets et al., 2007), and there is a 100-fold variation in leaf dry mass within a single climatic region (Kleiman and Aarssen, 2007). Leaf length in angiosperm trees varies from a few millimeter to over one meter with more than three orders of magnitude (Jensen and Zwieniecki, 2013). Considerable variations of leaf size among species are attributed to a wide range of plant traits including morphological and physiological characteristics and leaf energy balance (Westoby and Wright, 2003; Pickup et al., 2005; Niinemets et al., 2006).

Recently, the leaf size variation has been interpreted as the trade-off between leaf size and the number of leaves produced (Kleiman and Aarssen, 2007; Yang et al., 2008; Whitman and Aarssen, 2010). Leaf size across species was linearly negatively correlated with leafing intensity, the number of leaves per unit volume/mass of the twigs on which the leaves were borne (Kleiman and Aarssen, 2007; Ogawa, 2008; Yang et al., 2008; Huang et al., 2015). Consequently, a "leafing intensity premium" hypothesis at the twig level was proposed by Kleiman and Aarssen (2007). According to Kleiman and Aarssen (2007), the fitness benefits of higher leafing intensity (namely small leaves) are primarily associated with the fitness benefits of a larger pool of axillary buds, which in turn provide greater facility for wide phenotypic plasticity in the allocation of these meristems to vegetative *versus* reproductive functions (Kleiman and Aarssen, 2007). Based on the leaf size-number trade-off theory, it was inferred that leaf biomass density per unit twig volume was constant ranging from the twig to the canopy level in fully closed forest stands (Ogawa, 2008). Hence, the leaf size-number trade-off may have particularly important implications for understanding leaf size evolution, because it is one of the fundamental adaptation strategies of plants to environmental changes (Yang et al., 2008). Trees having small *versus* large leaves can show distinct leaf deployment strategies along a leaf size-number trade-off continuum (Scott and Aarssen, 2012). For instance, smaller leaves with higher density of major vein were more tolerant to vein embolism (Scoffoni et al., 2011).

Several previous studies have found that the remarkable variability in leaf size plays a prominent role in leaf thermal regulation (Givnish and Vermeij, 1976; Ackerly et al., 2002; Jensen and Zwieniecki, 2013; Wright et al., 2017). Leaf area can regulate leaf temperature via the thickness of leaf boundary layer (Ackerly et al., 2002; Niinemets et al., 2006), where heat transfer is slower relative to the more turbulent air beyond the leaf (Givnish and Vermeij, 1976; Jensen and Zwieniecki, 2013). The thickness of leaf boundary layer increases with increasing leaf area, so that the rate of heat convection per unit leaf area is greater between leaf and air for a small leaf than for a large leaf (Leigh et al., 2017). Smaller leaves are expected to have lower leaf temperatures than large leaves at sunny habitats, and thus to avoid overheating (Niinemets and Kull, 1994). Furthermore, leaf size tends to decrease with decreasing water availability (Mcdonald et al., 2003; Basal et al., 2005; Cramer et al., 2009). Generally smaller leaves are advantageous in hot and dry environments and at high intensities of solar radiation, while large leaves with less efficient energy exchange capacity are advantageous in cooler, moister and lower irradiance environments (Niinemets et al., 2006; Meier and Leuschner, 2008; Tozer et al., 2015).

A great deal of the variability in leaf size contributes to water balance. Because plant leaf is a critical component in the plant water transport system, accounting for 30% or more of whole-plant hydraulic resistance, especially in dry environments (Sack and Holbrook, 2006). Parameters (e.g., leaf water loss and initial leaf water content) measured on excised leaves at minimum stomatal aperture have been proposed as simple but reliable indicators of drought resistance in wheat, cotton, and sorghum (Hall and Jones, 1961; Basal et al., 2005), as well as forest species in northern China (Zhang and Li, 1995). Either high irradiation or extremely negative atmospheric water potential or both will lead to severe water stress and thus stomata closure of plants (Clarke et al., 1991; Cramer et al., 2009). Therefore, water supply to a leaf may depend on rates of cuticular transpiration (Schreiber and Riederer, 1996) if water required is sufficient. Efficient cuticular transpiration is also of great importance in order to provide sufficient nutrients to leaves, because nutrients are mainly transported with water from soil to leaves via the xylem (Yates et al., 2010).

Climate models have indicated that drought episodes will become more frequently because of global warming (Salinger et al., 2005). For example, severe drought events and daily temperature extremes have been revealed to become more frequent and widespread in northeastern China (Yu et al., 2014; Yu and Li, 2015). This emphasizes the urgent need to study the morphological and physiological adaptation strategies of plants to environmental changes including future climate change. The temperate forests in northeastern China account for more than one-third of both the Chinese forest area and the stocking volume of the national forests, and play a crucial role in the national and global carbon budgets and climatic system (Wang, 2006). The 16 tree species involved in this study coexist in a naturally regenerated forest (45°25′28‴N, 127°38′55″E) nearby the Maoershan forest ecosystem research station of the Northeast Forestry University, Northeast China. However, these species significantly differed in their photosynthetic capacity and water use efficiency (water loss). For instance, *Tilia amurensis*, a simple-leaved species widely distributed at well-drained sites with relatively deep fertile soils, showed higher water use efficiency (95.1 mol H_2O m^{-2} s^{-1}), whereas *Juglans mandshurica*, a compound-leaved species occupying arid and

oligotrophic sites, had lower water use efficiency (38.6 mol H_2O m^{-2} s^{-1}; Sang et al., 2011). We, therefore, are very interested in understanding the variation and distribution of leaf, stoma, and twig traits, as well as their relationships with excised leaf water loss of all these species when they co-exist in a temperate forest with the same growth environment. Specifically, we aimed to test the hypothesis that the larger the leaf is, the faster the leaf water loses, because, compared to small leaves, large leaves have more surface area for the loss of water through transpiration.

MATERIALS AND METHODS

Study Site and Species

The present study was conducted in a temperate forest at the Maoershan forest ecosystem research station (45°25′35″N, 127°38′20″E) of the Northeast Forestry University, northeastern China. This study site has a temperate, continental monsoon climate. The mean annual temperate is 2.8°C, with the highest monthly mean temperature of 20.9°C occurring in July and the lowest monthly mean temperature of –19.6 °C occurring in January. The mean annual precipitation is 723 mm, 66% of which falls from June to August. The study site is dominated by the second-growth forest naturally regenerated after the mixed mature *Pinus koraiensis* with broad-leaved trees were harvested over 70 years ago. The soils are classified as Hap-Boric Luvisols, well drained with high organic matter (Gu et al., 2014). For each of the 16 study species in our study, three healthy, adult individual trees were randomly selected in that second-growth forest in September 2013 (**Table 1**). From each individual tree selected, we collected 3–5 current-year twigs (5–40 cm in length) from the upper sunny part of the tree canopy, giving a total of 9–15 twigs collected for each species. All twigs collected were stored in sealed plastic bags, on ice, in the dark and transported to the laboratory within 1 h for further processing.

TABLE 1 | List of sixteen tree species studied in a temperate forest in northeastern China.

No.	Species	Abbreviation	Family	Leaf type
1	*Acer ginnala*	Acgi	Aceraceae	Simple-leaved
2	*Acer mandshuricum*	Acma	Aceraceae	Compound-leaved
3	*Acer mono*	Acmo	Aceraceae	Simple-leaved
4	*Acer tegmentosum*	Acte	Aceraceae	Simple-leaved
5	*Albizia kalkora*	Alka	Leguminosae	Compound-leaved
6	*Betula costata*	Beco	Betulaceae	Simple-leaved
7	*Betula platyphylla*	Tepl	Betulaceae	Simple-leaved
8	*Fraxinus mandschurica*	Frma	Oleaceae	Compound-leaved
9	*Juglans mandshurica*	Juma	Juglandaceae	Compound-leaved
10	*Ostrya japonica*	Osja	Betulaceae	Simple-leaved
11	*Quercus mongolica*	Qumo	Fagaceae	Simple-leaved
12	*Salix pierotii*	Sapi	Salicaceae	Simple-leaved
13	*Syinga reticulata*	Syre	Oleaceae	Simple-leaved
14	*Tilia amurensis*	Tiam	Tiliaceae	Simple-leaved
15	*Ulmus japonica*	Ulja	Ulmaceae	Simple-leaved
16	*Ulmus laciniata*	Ulla	Ulmaceae	Simple-leaved

Variable Measurements

Leaf size was expressed as average individual leaf projected area and leaf dry mass (measured for the entire leaf for simple-leaved species, and for the leaflet in compound-leaved species). The two parameters on leaf size can be used to estimate various aspects of leaf functioning. For instance, leaf area characterizes leaf energy balance, leaf biomechanical efficiency and mechanical load, while leaf mass estimates leaf construction cost (Niinemets et al., 2007).

For each sample twig, the following parameters were recorded: the number of leaves borne on the twig (LN), the length (TL, mm) and diameter of the middle of twigs (TD, mm). Total projected leaf area borne on the twig (TLA, cm^2) was measured by scanning all leaves collected from a sample twig using a portable scanner (Canon LiDE 110, Japan) and the pictures were then digitized by using ImageJ software (NIH Image). Leafing intensity (LI, number cm^{-3}) was volume-based, calculated as the number of simple leaves (simple-leaved species) or leaflet (compound-leaved species) borne on a twig divided by the twig volume following Kleiman and Aarssen (2007), which could provide a metric comparable among species, representing a measure of relative investment in leaf number. Twig volume was calculated from the length and diameter of the twig by assuming the twig had the dimensions of a cylinder. The leaves were dried to constant mass at 70°C for 48 h and then weighted to acquire total leaf mass (TLM, *g*). Individual leaf area (LA, cm^2) and individual leaf mass (LM, *g*) were calculated as LA = TLA/LN and LM = TLM/LN, respectively. Specific leaf area (cm^2 g^{-1}) was then calculated as leaf area divided by leaf dry mass. The oven-dried leaf samples (70°C for 48 h) were ground to fine powder that was sieved at a 0.5 mm mesh size. Leaf total nitrogen (N), phosphorus (P) and potassium (K) concentration were determined after digesting with H_2SO_4-H_2O_2, using an elemental analyzer (N and P) and a flame photometer (K).

Three fully expanded leaves per tree were randomly selected to be used for stomatal observation based on the abaxial surface by the nail polish impression method (Franks et al., 2009). The stomatal traits were measured using a Leica DFC 450 camera (Nussloch, Germany) mounted on a Leica DM 2500 microscope at 10–20 × magnification and 20–40 × magnification, respectively. Stomatal length (SL, μm) and stomatal width (SW, μm) were measured as the guard cell length and guard cell pair width based on about forty stomata per tree species, respectively. SL and SW were then used to determine the stomatal size (SS, μm^2). Stomatal density (SD, number mm^{-2}) was calculated as the number of stomata per unit of epidermal surface based on about thirty fields of view per tree species.

From each tree, ten fully expanded leaves were randomly selected to estimate the leaf water loss using the excised leaf method (Mccaig and Romagosa, 1989), with the following details. After sampling, the leaves were stored in icebox and immediately transported to the laboratory and fresh weight of leaves was determined. After weighing, leaves were placed in a dark growth cabinet at 28–30°C with 70% relative humidity, and weighed at 1 h intervals for 6 h. They were then dried at 70°C for 48 h, and

weighed to determine the dry mass. Leaf water content (%; the percentage of fresh leaf weight), leaf water loss at every 1 h interval (%; LWL_1, LWL_2, LWL_3, LWL_4, LWL_5, LWL_6), and the total leaf water loss during 6 h (%; LWL_{1-6}) were calculated using these weights. The rates of mass loss from all reservoirs can be conveniently expressed by a parameter k, which equals the fraction of the stored quantity that is lost per unit time (Jenny et al., 1949; Olson, 1963). The water loss rate from leaves (k) was thus estimated using an exponential decay model:

$$X_t/X_o = e^{-kt}$$

where X_t is the leaf water content at a given time (t) and X_0 is the initial leaf water content.

Statistical Analyses

A Shapiro–Wilk test (*shapiro.test* function) was used to test the differences from a normal distribution for leaf size, leafing intensity, stomatal size and density. The skewness and kurtosis were also calculated to describe the distribution shape. Positive and negative values of skewness indicate a distribution is right-skewed and left-skewed, respectively. While kurtosis can measure the extent of which a distribution has a pointy peak or a rounded peak. The kurtosis value of normally distributed data should be around three (Alves-Silva et al., 2018). A linear mixed model was used to determine the variance of twig and leaf traits at both tree species and tree individual level (*lmer* function in *lme4* package). Likewise, linear mixed models were performed to determine the potential relationships of leaf size with leafing intensity, twig diameter, specific leaf area, and leaf water rate (k) after $\log_e$-transformation with tree species as the random factor. There are two values of R^2 which can be calculated according to Nakagawa and Schielzeth (2013), i.e., the marginal R^2 $\left(R^2_m\right)$, reflecting the proportion of the variance explained by fixed effects (leafing intensity), and the conditional R^2 $\left(R^2_m\right)$, reflecting the variance explained by both fixed and random effects (tree species). Satterthwaite's approximation and likelihood ratio test were used to estimate the denominator degrees of freedom and p values of the fixed effects and the random effects (*lmerTest* package). Multiple-trait relationships were analyzed by principal component analysis (PCA, *princomp* function). Non-parametric tests (*kruskal.test* function) were picked to test the effects of tree species on leaf, twig, and stoma traits, as well as leaf water loss rate (k). TukeyC test was chosen to determine differences among tree species when $p < 0.05$. Moreover, Spearman correlation (*cor* and *rcorr* function in *Hmisc* package) was used to determine correlations among all examined traits. All statistical analyses were conducted with R 3.5.1 (R Core Team, 2018).

RESULTS

The frequency distribution from Shapiro–Wilk test yielded high right-asymmetry for leaf size (leaf area and leaf mass; **Figures 1A,B**), leafing intensity (**Figure 1C**) as well as stomatal size and stomatal density (**Figures 1D,E**) when all the species sampled were pooled. The positive skewness indicated that the distributions were right-skewed (**Figure 1**). Furthermore, the distribution patterns for leaf area and leafing intensity (kurtosis > 3) were leptokurtic with a narrow peak (**Figures 1A,C**). Average individual leaf area and individual leaf mass across species varied by two and one orders of magnitude, ranging from 6.58 ± 0.71 cm^2 (*Salix pierotii*) to 166.83 ± 4.90 cm^2 (*Acer tegmentosum*), and from 0.04 ± 0.01 g (*Acer mandshuricum*) to 0.50 ± 0.01 g (*Acer tegmentosum*), respectively (**Table 2**). Leafing intensity was significantly negatively correlated with leaf size, accounting for 4% of variation in individual leaf area (marginal R^2; R^2_m 0.04, $p < 0.05$) and 12% of variation in individual leaf mass ($R^2_m = 0.12$, $p < 0.01$) (**Figure 2**). The majority of the variance was explained by the random effects (tree species), as indicated by the large difference between R^2_m and R^2_c (conditional R^2; $R^2_c = 0.92$ for leaf area, $R^2_c = 0.82$ for leaf mass, **Figure 2**). Across all species, there were marginally and significantly positive relationships between individual leaf area ($R^2_m = 0.06$, $R^2_c = 0.93$, $p = 0.09$), individual leaf mass ($R^2_m = 0.20$, $R^2_c = 0.87$, $p < 0.01$) and the corresponding twig diameter, respectively. Specific leaf area varied approximately three-fold, ranging from 123.79 ± 17.44 $cm^2\ g^{-1}$ (*Salix pierotii*) to 370.15 ± 22.31 $cm^2\ g^{-1}$ (*Ostrya japonica*; **Table 2**), and specific leaf area was positively correlated with individual leaf area ($R^2_m = 0.16$, $R^2_c = 0.80$, $p < 0.05$) but not related with individual leaf mass ($p > 0.05$). Besides, the variance of twig, leaf and stoma traits in our study was strongly dependent on species identity (**Supplementary Table S1**).

We found significant decreases in leaf water loss over time for all tree species (**Figure 3**). Significant differences in leaf water loss rate (k) were detected among tree species (**Figure 4**). LWL_1 was the highest in *Salix pierotii* (35%), which lost 90% of leaf water content during 6 h (LWL_{1-6}), resulting in the highest leaf water loss rate (k, **Figures 3**, **4**). However, LWL_1 and LWL_{1-6} of *Acer tegmentosum* were only 5.6% and 26% of leaf water content, therefore, the lowest value in leaf water loss rate (k, **Figures 3**, **4**). Leaf water loss was strongly negatively correlated with individual leaf area and individual leaf mass (with an exception for LWL_2) from 1 (LWL_1) to 4 h (LWL_4; **Table 3**). The 38 and 30% of variation in LWL_{1-6} were accounted by individual leaf area and individual leaf mass, respectively (**Table 3**). Leaf water loss rate (k) significantly linearly decreased with increasing individual leaf area and individual leaf mass for the simple-leaved tree species (**Figure 5**), but k was not related to initial leaf water content when all species pooled together (**Supplementary Table S2**). Furthermore, during the first 4 h of measurement (LWL_1 to LWL_4), leaf water loss was correlated with neither stomatal size nor stomatal density (**Supplementary Table S2**). LWL_5 and LWL_6 were markedly positively correlated with stomatal size, but leaf water loss rate (k) was significantly negatively related with stomatal size (**Supplementary Table S2**). The first axis of principal component analysis accounted for 35.6% of total variation, showing strong loadings on twig length, twig diameter, ratio of leaf nitrogen to phosphorus concentration, stomatal density and leafing intensity (**Figure 6** and **Supplementary Table S3**). The second axis, which accounted for 26.9% of the total variation, had strong loading on individual leaf area, specific leaf area, individual leaf mass and leaf water loss rate

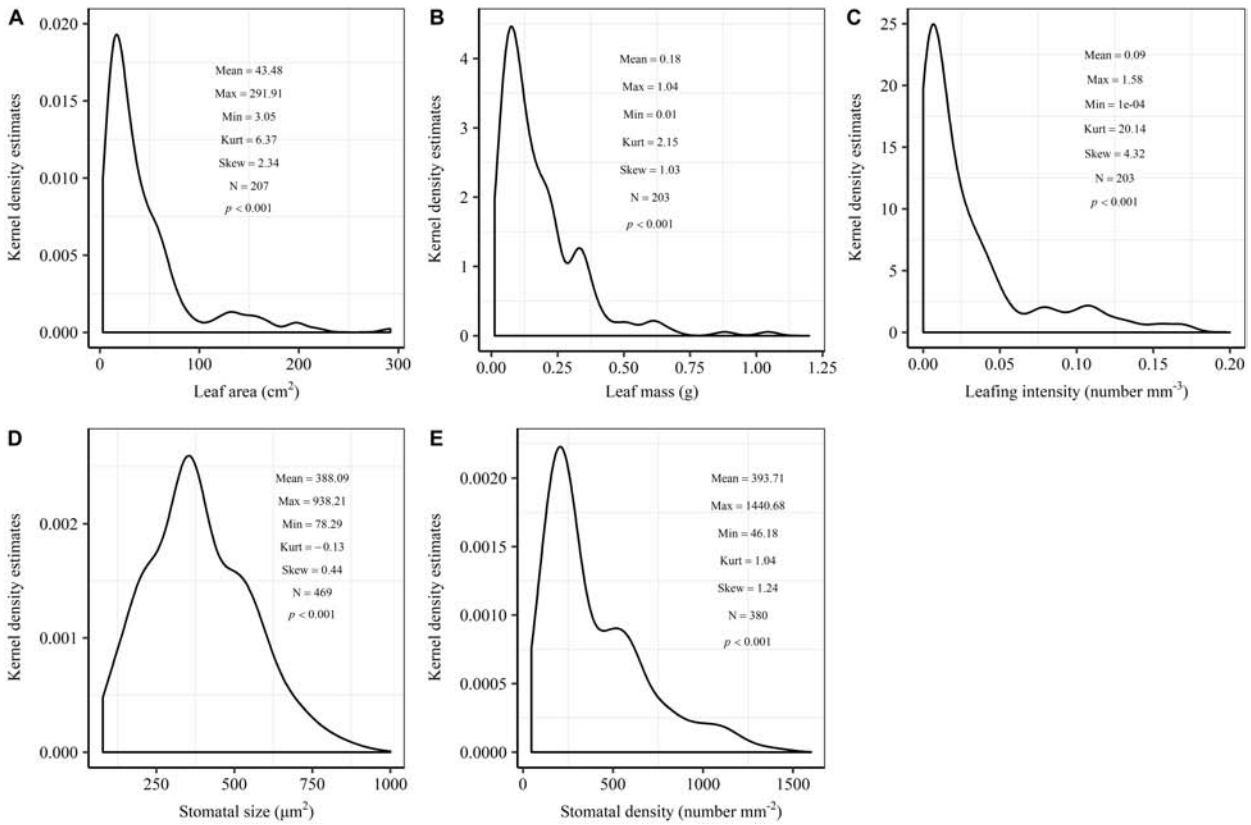

FIGURE 1 | Kernel density estimates of individual leaf area **(A)**, individual leaf mass **(B)**, leafing intensity **(C)**, stomatal size **(D)** and stomatal density **(E)**. The y-axis indicates the abundance of leaf and stomatal traits with a given value. The mean, maximum (Max), minimum (Min), kurtosis (Kurt), skewness (Skew) and sample size (N) were shown in the insets. The frequency distribution was significant different from normal distribution at $p < 0.05$.

(**Figure 6** and **Supplementary Table S3**). Leaf water loss rate (k), stomatal density, and stomatal size had high scores on the third axis (**Supplementary Table S3**).

DISCUSSION

In this study, we observed that the distributions of leaf size, leafing intensity, stomatal size and stomatal density at community-level were noticeably skewed to the right, with a long tail of larger values (**Figure 1**). Right-skewed distributions in plant assemblages have been reported recently for plant height (Moles et al., 2009), seed size (Moles et al., 2006), leaf size (Milla, 2009) and fine root diameter (Ma et al., 2018) at various scales (Ogawa, 2008; Dombroskie and Aarssen, 2010; Whitman and Aarssen, 2010). The right-skewed distributions at different taxonomical levels reported for natural vegetations indicate a pervasive signal for adaptive size metrics (Dombroskie and Aarssen, 2010). Thus, it is greatly necessary to explicitly examine the frequency distribution in the extremely similar fashion. The preponderance of small leaves (namely the right-skewed unimodal leaf size distribution) is considered to be a consequence of the left-wall effect, because the sizes of things must be greater than zero (Aarssen et al., 2006; Jensen and Zwieniecki, 2013). Most habitats for terrestrial plants have environmental conditions where adaptation is conferred through physiological optimization associated directly with relatively small leaf size (Kleiman and Aarssen, 2007). We found that the distribution for leaf area (kurtosis = 6.32) was leptokurtic with a narrow peak in our temperate forest in northeastern China (**Figure 1A**). However, platykurtic distributions of leaf area (lower kurtosis value) are observed and their degrees of platykurtosis decreased with decreased soil water in woody plant communities at Jasper Ridge, California (Cornwell and Ackerly, 2009). Skewness and kurtosis of community trait distribution are highly sensitive to climate, soil and topography (Le Bagousse-Pinguet et al., 2016). Such leptokurtosis of all examined traits in our study potentially arise from the environmental heterogeneity of habitats (Sang et al., 2011) or the existence of variations on leaf traits among the 16 tree species (**Supplementary Table S1**).

There are several well-known compromises between allocation to size and number of organs in plant bodies, or of individuals in plant populations (Yang et al., 2008; Whitman and Aarssen, 2010; Scott and Aarssen, 2012). The results in this study reinforced overall generality of a cross-species trade-off between the number of leaves attached to a unit of yearly twig and the size of individual leaves in woody species.

TABLE 2 | Descriptive statistics (mean ± 1SE, n = 3) for twig, leaf and stoma traits for the 16 tree species studied.

Species	TL	TD	LI	TLA	LA	TLM	LM	SLA
Acgi	162.88 ± 27.01^{ab}	2.58 ± 0.22^{d}	3.90 ± 0.34^{b}	154.15 ± 35.65^{b}	11.42 ± 1.53^{de}	1.21 ± 0.22^{c}	0.08 ± 0.01^{d}	141.37 ± 10.09^{f}
Acma	46.16 ± 7.98^{b}	1.90 ± 0.07^{d}	13.18 ± 2.92^{a}	176.95 ± 10.26^{b}	10.98 ± 0.38^{de}	0.63 ± 0.05^{c}	0.04 ± 0.01^{d}	289.41 ± 9.57^{abc}
Acmo	26.85 ± 8.61^{b}	1.80 ± 0.07^{d}	10.42 ± 3.13^{ab}	196.22 ± 40.90^{b}	33.17 ± 6.26^{cde}	0.55 ± 0.11^{c}	0.10 ± 0.02^{d}	362.67 ± 8.37^{a}
Acte	25.42 ± 5.00^{b}	2.91 ± 0.05^{d}	1.29 ± 0.25^{b}	333.65 ± 9.81^{b}	166.83 ± 4.90^{a}	1.01 ± 0.03^{c}	0.50 ± 0.01^{a}	337.03 ± 2.44^{ab}
Alka	278.06 ± 71.55^{a}	4.78 ± 0.65^{c}	1.87 ± 0.74^{b}	1187.90 ± 233.02^{b}	15.67 ± 2.11^{de}	5.43 ± 1.07^{c}	0.07 ± 0.01^{d}	219.68 ± 10.29^{cdef}
Beco	164.92 ± 16.57^{ab}	1.69 ± 0.09^{d}	2.13 ± 0.30^{b}	131.30 ± 16.18^{b}	16.44 ± 1.18^{cde}	0.48 ± 0.07^{c}	0.06 ± 0.01^{d}	295.32 ± 6.08^{abc}
Bepl	186.75 ± 21.32^{ab}	2.57 ± 0.24^{d}	0.78 ± 0.17^{b}	194.94 ± 27.57^{b}	27.56 ± 1.89^{cde}	1.15 ± 0.20^{c}	0.17 ± 0.02^{cd}	173.12 ± 8.19^{ef}
Frma	195.83 ± 92.19^{ab}	7.01 ± 1.01^{b}	2.06 ± 0.87^{b}	4752.40 ± 558.04^{a}	50.28 ± 7.76^{bcd}	21.24 ± 2.49^{b}	0.23 ± 0.01^{bcd}	242.86 ± 16.08^{bcde}
Juma	158.33 ± 18.33^{ab}	10.69 ± 0.19^{a}	0.66 ± 0.05^{b}	5975.82 ± 802.73^{a}	52.90 ± 9.71^{bcd}	31.08 ± 4.17^{a}	0.33 ± 0.01^{ab}	201.66 ± 3.86^{cdef}
Osja	25.49 ± 15.14^{b}	1.62 ± 0.05^{d}	14.98 ± 5.78^{a}	116.85 ± 0.45^{b}	35.31 ± 5.51^{cde}	0.32 ± 0.02^{c}	0.09 ± 0.03^{d}	370.15 ± 22.31^{a}
Qumo	118.58 ± 4.88^{ab}	2.94 ± 0.19^{cd}	0.76 ± 0.13^{b}	519.82 ± 132.90^{b}	91.67 ± 25.46^{b}	2.19 ± 0.31^{c}	0.39 ± 0.10^{ab}	233.84 ± 6.46^{bcde}
Sapi	161.12 ± 6.84^{ab}	2.09 ± 0.09^{d}	2.92 ± 0.24^{b}	114.34 ± 4.64^{b}	6.58 ± 0.71^{e}	0.91 ± 0.06^{c}	0.06 ± 0.00^{d}	123.79 ± 17.44^{f}
Syre	118.50 ± 10.48^{ab}	2.29 ± 0.06^{d}	3.28 ± 0.88^{b}	137.43 ± 15.39^{b}	20.12 ± 2.06^{cde}	0.96 ± 0.08^{c}	0.14 ± 0.01^{cd}	148.41 ± 7.47^{def}
Tiam	65.63 ± 17.07^{b}	2.14 ± 0.17^{d}	1.99 ± 0.53^{b}	188.53 ± 23.72^{b}	47.42 ± 4.37^{cde}	0.63 ± 0.11^{c}	0.16 ± 0.02^{cd}	302.35 ± 14.57^{abc}
Ulja	174.70 ± 43.87^{ab}	2.65 ± 0.38^{d}	1.31 ± 0.62^{b}	227.34 ± 53.46^{b}	22.42 ± 1.83^{cde}	1.93 ± 0.49^{c}	0.20 ± 0.03^{cd}	184.84 ± 58.30^{def}
Ulla	134.08 ± 46.13^{ab}	2.60 ± 0.23^{d}	0.92 ± 0.25^{b}	311.38 ± 42.08^{b}	59.11 ± 7.44^{bc}	1.12 ± 0.13^{c}	0.22 ± 0.05^{bcd}	286.88 ± 22.14^{abcd}

TABLE 2 | Continued

Species	*N*	*P*	*K*	*SD*	*SS*
Acgi	No data				
Acma	2.56 ± 0.12^{abcd}	0.27 ± 0.02^{b}	0.98 ± 0.04^{d}	401.14 ± 61.92^{cd}	656.46 ± 16.62^{ab}
Acmo	2.15 ± 0.23^{d}	0.26 ± 0.05^{b}	1.18 ± 0.13^{cd}	195.05 ± 43.29^{efg}	379.40 ± 19.19^{cdef}
Acte	2.41 ± 0.08^{bcd}	0.35 ± 0.01^{ab}	1.42 ± 0.09^{abcd}	207.49 ± 15.62^{efg}	438.06 ± 33.41^{cd}
Alka	3.17 ± 0.08^{a}	0.39 ± 0.02^{ab}	1.78 ± 0.10^{abc}	331.00 ± 83.19^{de}	416.34 ± 36.88^{cde}
Beco	2.66 ± 0.01^{abcd}	0.35 ± 0.01^{ab}	1.74 ± 0.05^{abc}	293.47 ± 18.70^{def}	251.38 ± 19.37^{fg}
Bepl	2.91 ± 0.08^{ab}	0.34 ± 0.04^{ab}	1.16 ± 0.07^{cd}	264.44 ± 13.80^{def}	475.89 ± 9.98^{cd}
Frma	2.93 ± 0.20^{ab}	0.37 ± 0.07^{ab}	1.34 ± 0.02^{bcd}	571.81 ± 23.32^{ab}	274.78 ± 5.44^{efg}
Juma	2.84 ± 0.07^{abc}	0.37 ± 0.02^{ab}	2.03 ± 0.13^{ab}	295.57 ± 28.96^{def}	373.43 ± 8.64^{cdefg}
Osja	2.09 ± 0.21^{d}	0.09 ± 0.00^{c}	1.62 ± 0.27^{abcd}	98.63 ± 10.75^{g}	412.85 ± 11.65^{cde}
Qumo	2.56 ± 0.02^{abcd}	0.35 ± 0.02^{ab}	1.36 ± 0.08^{abcd}	518.29 ± 23.69^{bc}	348.86 ± 14.14^{defg}
Sapi	2.56 ± 0.10^{abcd}	0.44 ± 0.02^{a}	1.80 ± 0.09^{abc}	217.39 ± 27.74^{efg}	224.56 ± 21.77^{g}
Syre	No data				
Tiam	2.75 ± 0.20^{abcd}	0.27 ± 0.02^{b}	1.66 ± 0.32^{abcd}	149.08 ± 10.63^{fg}	416.64 ± 35.95^{cde}
Ulja	2.25 ± 0.06^{cd}	0.32 ± 0.02^{ab}	1.26 ± 0.06^{cd}	697.00 ± 37.82^{a}	516.43 ± 20.20^{bc}
Ulla	2.54 ± 0.04^{abcd}	0.36 ± 0.03^{ab}	2.07 ± 0.08^{a}	219.17 ± 9.89^{efg}	688.92 ± 45.73^{a}

*TL, the length of twig (mm); TD, the diameter of twig (mm); LI, leafing intensity (100*number cm^{-3}); TLA, total leaf area per twig (cm^2); LA, individual leaf area (cm^2); TLM, total leaf mass per twig (g); LM, individual leaf mass (g); SLA, specific leaf area ($cm^2\ g^{-1}$); N, leaf nitrogen concentration (%); P, leaf phosphorus concentration (%); K, leaf potassium concentration (%); SD, stomatal density (number mm^{-2}); SS, stomatal size (μm^2). The abbreviations of tree species were shown in* ***Table 1****. Different lower case letters indicate significant differences of twig, leaf and stoma traits among tree species at $p < 0.05$.*

Leafing intensity is a whole-plant morphological trait, which can provide remarkable explanatory power in accounting for a fundamental pattern of leaf functional trait variation (Whitman and Aarssen, 2010). Therefore, a "leafing intensity premium" hypothesis has been proposed with supporting evidence of the right-skewed distribution of leaf size frequency (Kleiman and Aarssen, 2007). However, if high leafing intensity confers important general fitness advantages, why then do most species not have relatively high leafing intensity (namely the left-skewed frequency distribution)? Actually the frequency distribution of leafing intensity is also right-skewed (**Figure 1C**), which violates the assumption of leafing intensity premium that leafing intensity is left-skewed. Based on dataset covering 224 species, a similar right-skewed distribution of leafing intensity was also observed (Milla, 2009). In fact, both leaf size and leafing intensity may be direct products of natural optimizing selection (Kleiman and Aarssen, 2007; Tozer et al., 2015). Decreasing the cost of the associated twigs by deploying a given leaf mass as fewer, larger leaves, considered as the selective advantage of lower leafing intensity (Wright et al., 2017). Variation in leaf size and leaf number of plants is determined by a very precise and inevitable resource allocation trade-off relationship (Aarssen, 2012). Moreover, conditional R^2 values were quite high, whereas marginal R^2 values were quite low for the associations of leafing intensity with individual leaf area and individual leaf mass (**Figure 2** and **Supplementary Figure S1**). This indicated that the

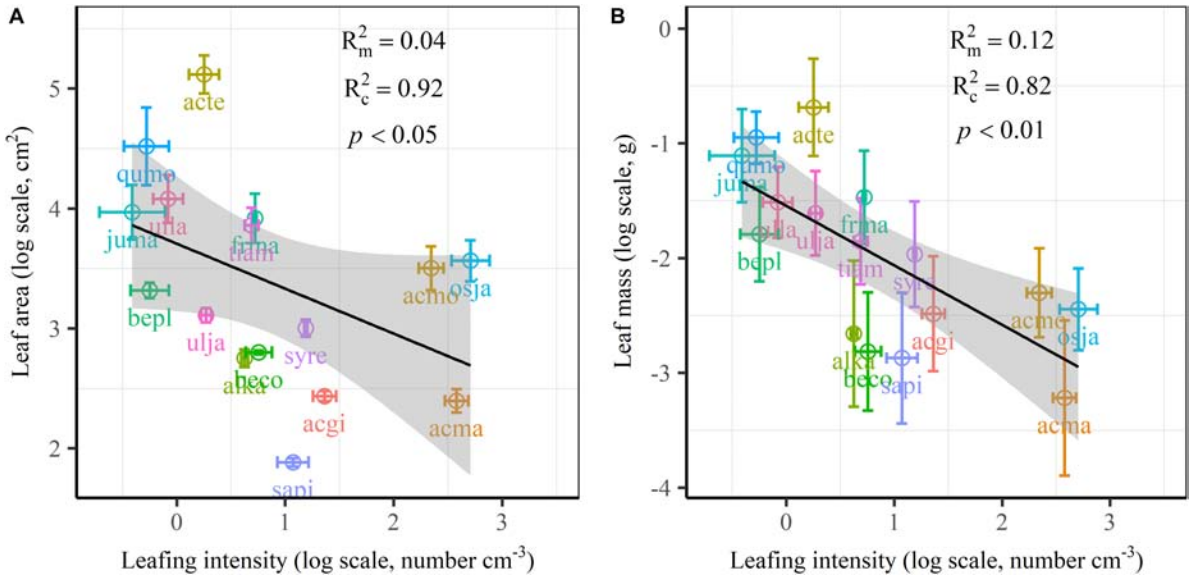

FIGURE 2 | Relationships of volume-based leafing intensity with individual leaf area **(A)** and individual leaf mass **(B)** from linear mixed models with leafing intensity as the mixed factor and tree species as the random factor. Marginal R^2 (R^2_m) reflects the proportion of the variance explained by fixed factors and conditional R^2 (R^2_c) reflects the proportion of the variance explained by both fixed and random factors. Average value per tree species and its 0.1-fold standard error were given. Gray bands show 95% confidence intervals. The abbreviations of tree species were provided in **Table 1**.

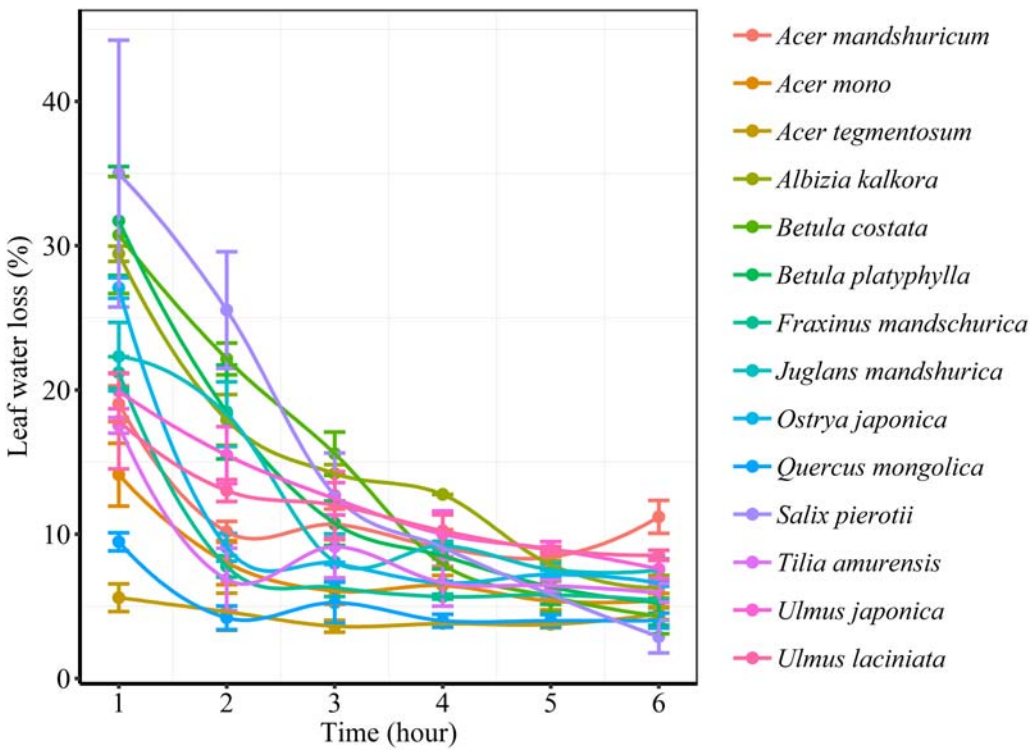

FIGURE 3 | Changes in leaf water loss (%) of different tree species over time.

leafing intensity could not solely account for the large variation in leaf size. Given the relatively small sample with only 16 species in our study, it is very necessary to enlarge the scope of plant families to claim wide generality of leaf size-number trade-off relationship, evaluating comprehensively the adaptive significance of the "leafing intensity premium" hypothesis.

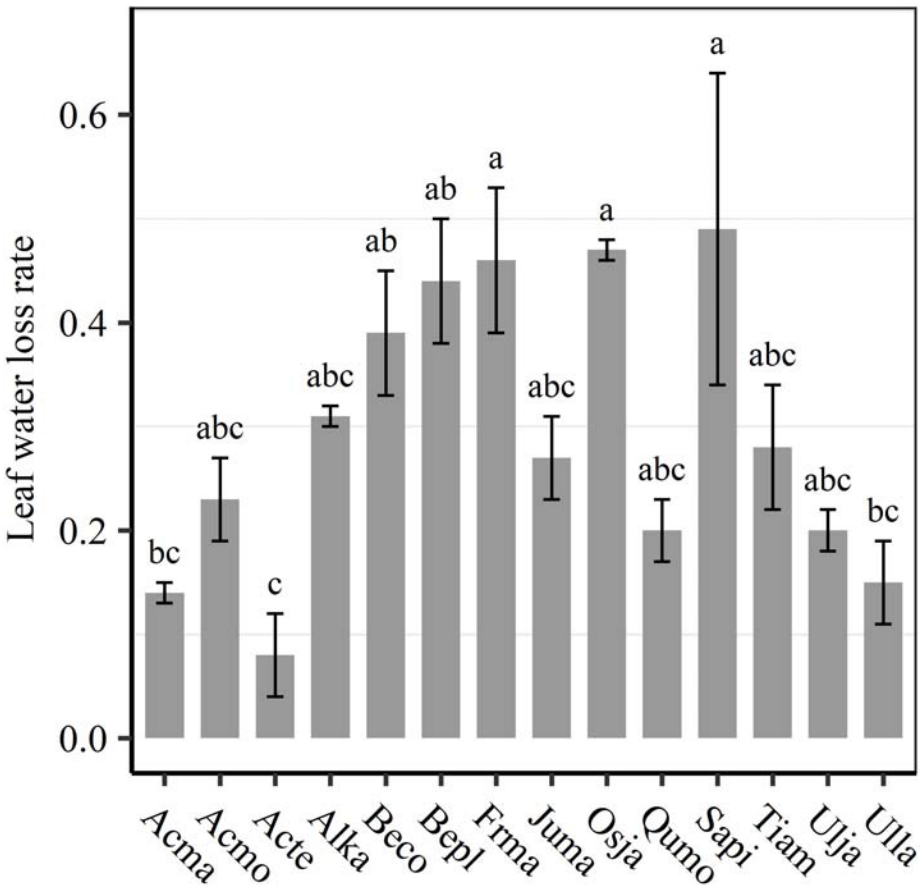

FIGURE 4 | Differences in leaf water loss rate (*k*) among tree species. Different lower case letters indicate significant differences in leaf water loss rate (*k*) among tree species at $p < 0.05$. The abbreviations of tree species were shown in **Table 1**.

TABLE 3 | Relationships between leaf size (individual leaf area, LA and individual leaf mass, LM) and leaf water loss from 1 h (LWL_1) to 6 h (LWL_6; $n = 3$), analyzed using linear mixed models with LA and LM as the mixed factor and tree species as the random factor.

	LA						LM					
	Slope	***p***	**Intercept**	***p***	$\mathbf{R_m^2}$	$\mathbf{R_c^2}$	**Slope**	***p***	**Intercept**	***p***	$\mathbf{R_m^2}$	$\mathbf{R_c^2}$
LWL_1	**–0.34**	**0.002**	**4.12**	**< 0.001**	**0.34**	**0.76**	**–0.23**	**0.034**	**2.51**	**< 0.001**	**0.13**	**0.77**
LWL_2	**–0.38**	**0.005**	**3.72**	**< 0.001**	**0.30**	**0.72**		0.102		< 0.001		
LWL_3	**–0.37**	**< 0.001**	**3.44**	**< 0.001**	**0.43**	**0.62**	**–0.32**	**< 0.001**	**1.53**	**< 0.001**	**0.28**	**0.62**
LWL_4	**–0.23**	**0.011**	**2.79**	**< 0.001**	**0.25**	**0.56**	**–0.21**	**0.026**	**1.57**	**< 0.001**	**0.17**	**0.61**
LWL_5		0.056		< 0.001				0.098		< 0.001		
LWL_6		0.71		0.002				0.679		< 0.001		
LWL_{1-6}	**–0.25**	**< 0.001**	**4.90**	**< 0.001**	**0.38**	**0.85**	**–0.17**	**0.012**	**3.72**	**< 0.001**	**0.30**	**0.56**

Marginal R^2 $\left(R_m^2\right)$ reflects the proportion of the variance explained by fixed factors, and conditional R^2 $\left(R_c^2\right)$ reflects the proportion of the variance explained by both fixed and random factors. Significant relationships were highlighted in bold.

Our results showed that the size of individual leaves across species was correlated with twig size (determined as the diameter of twigs; **Supplementary Table S2**). Thus the leaf size-number trade-off is also linked to Corner's Rules (Corner, 1949). As predicted by Corner's Rules, thin twigs bear scarcely separated nodes, with many small leaves per twig unit and vice versa for thick twigs (Corner, 1949; Pickup et al., 2005). The twig size of different tree species may influence leafing intensity and leaf size with an endogenous mechanism (Yang et al., 2008). Hence, there exists a leaf size-twig size spectrum (LSTSS), which extends from species with small leaves, small twigs and close ramification to species with large leaves, thick twigs and less frequent branching (Pickup et al., 2005; Dias et al., 2017). However, because of strong correlation among leaf size, leafing intensity and twig size

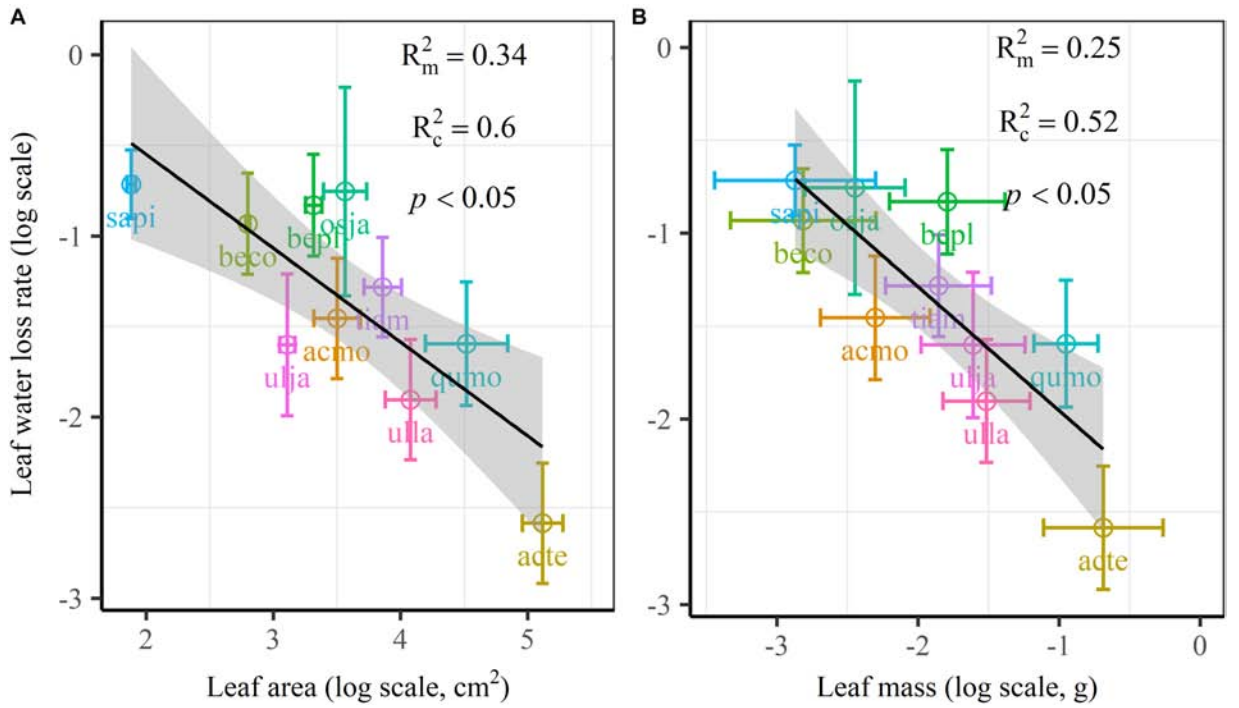

FIGURE 5 | Leaf water loss rate (*k*) in relation to individual leaf area **(A)** and individual leaf mass **(B)** of 10 simple-leaved tree species, analyzed using linear mixed models with individual leaf area or mass as the mixed factor and tree species as the random factor. Marginal R^2 (R^2_m) reflects the proportion of the variance explained by fixed factors and conditional R^2 (R^2_c) reflects the proportion of the variance explained by both fixed and random factors. Average value per tree species and its 0.1-fold standard error were given. Gray bands show 95% confidence intervals. The abbreviations of tree species were shown in **Table 1**.

across species, small leaves may be attributed to natural selection favoring either small leaves, high leafing intensity or small twigs. It is difficult to distinguish the mechanism controlling leaf size variation and/or how these mechanisms interactively influence leaf size evolution (Yang et al., 2008). But the current-year twigs have the property of permitting the leaf size-number trade-off relationship to be detected, because they include only the annual growth of the plant species with very low levels of secondary growth (Yang et al., 2008). Consequently, it is very necessary to propose synthetic approaches involving multiple scales such as leaf, twig, even whole-tree scaling, to thoroughly comprehend leaf size variation.

The most striking and potentially important pattern found in this work was the strongly negative relationship between leaf size and leaf water loss for all tree species (**Table 3**) as well as leaf water loss rate (*k*) for the simple-leaved tree species (**Figure 5** and **Supplementary Figure S2**), these results rejected our initial hypothesis that the larger the leaf is, the faster the leaf water loses. This finding furthermore highlighted a fundamental difference in leaf thermal regulation between small and large. Smaller exhibited the faster leaf water loss, which was effective in shedding heat, obtaining an adaptive advantage to high light intensity or hot environments, where smaller leaves were dominated (Leigh et al., 2017). Larger leaf species might incur higher costs in water-sourcing root biomass to supply the transpiration needed to cool leaves (Givnish and Vermeij, 1976; Yates et al., 2010). Smaller leaves intercepting more solar radiation in the upper part of the canopy have higher rates of carbon assimilation, water loss and thus are physiologically more active (Boardman, 1977). Previous studies have confirmed that the variation in leaf size can substantially modify the whole-leaf integrated photosynthetic activity, namely overall higher mass-based photosynthetic activity of smaller leaves (Poorter and Evans, 1998; Niinemets et al., 2006, 2007). Thus small leaves must ensure greater leaf hydraulic conductance to maintain greater photosynthesis (Scoffoni et al., 2011). This may be a particularly important strategy for driving nutrient mass-flow from the roots of plants that take up most of their nutrients (Cramer et al., 2009; Yates et al., 2010). However, large leaf may have fitness benefits derived from a greater boundary layer thickness for heat exchange, allowing leaves to more quickly heat up to favorable temperatures for photosynthesis, thus maximizing photosynthetic returns under cooler environments, such as cool mornings (Michaletz et al., 2016; Wright et al., 2017). Restriction of leaf water loss through the plant cuticle for large leaf species during periods of severe water stress is an important drought survival mechanism (Clarke et al., 1991). However, it may be noteworthy to mention that, due to the limited species number, we could not analyze the relationships between leaf water loss rate (*k*) and leaf size for the four compound-leaved tree species in our study. Further studies with more compound-leaved tree species are needed to better identify the leaf size-leaf water loss relationships at both leaflet and single leaf level.

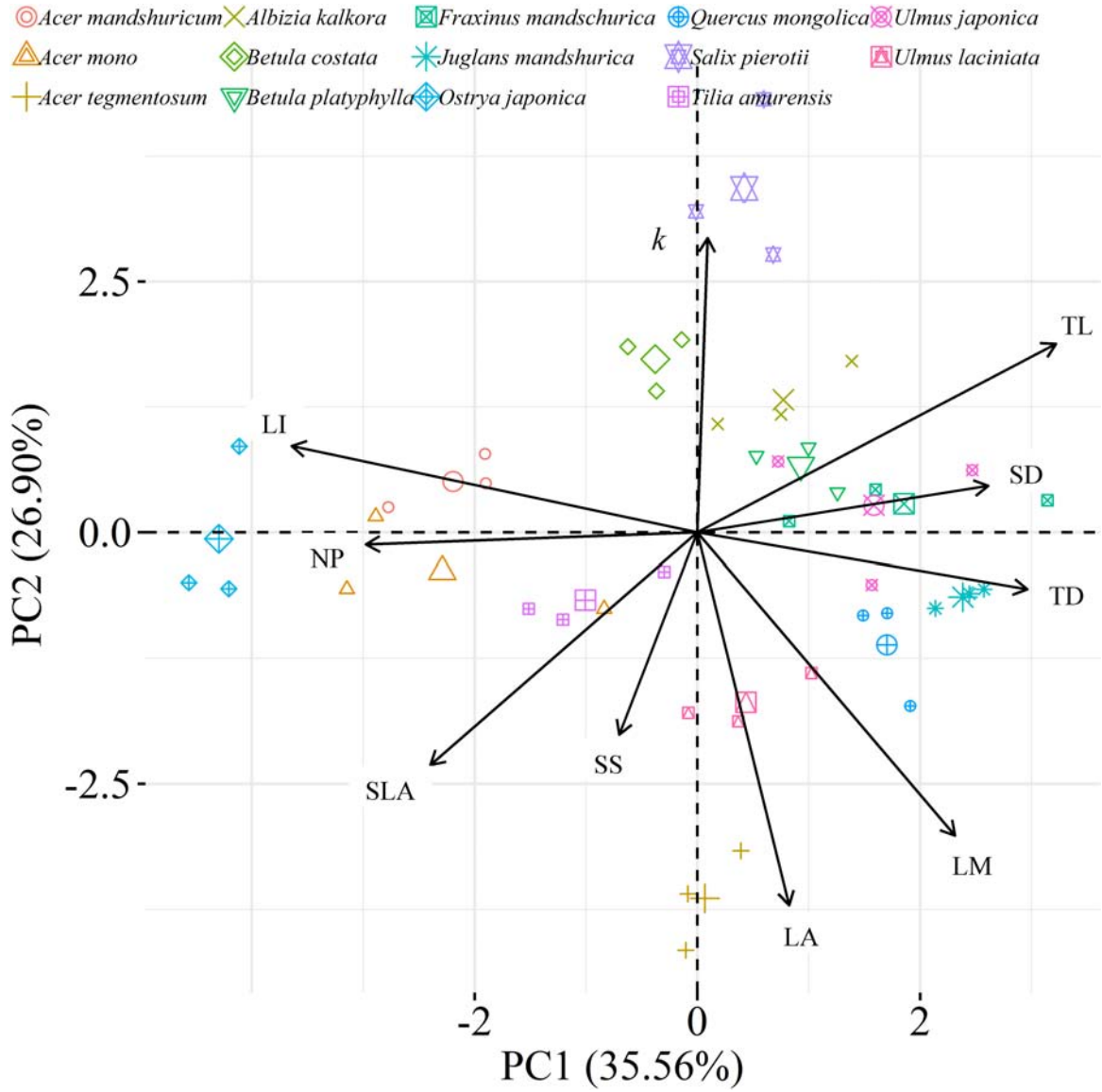

FIGURE 6 | Principal component analysis (PCA) among leaf, twig, stoma traits and leaf water loss rate as well as species distribution in the two-dimensional trait space [three points of tree species values (smaller points) and their average values (larger points)]. All data were $\log_e$-transformed before analysis. *k*, leaf water loss rate; TL, the length of twig; TD, the diameter of twig; LI, leafing intensity; SLA, specific leaf area; SS, stomatal size; SD, stomatal density; LA, individual leaf area; LM, individual leaf mass; NP, the ratio of leaf nitrogen to phosphorus concentration.

Leaf water loss occurs as stomatal and cuticular transpiration (Hall and Jones, 1961; Basal et al., 2005). The initial period of leaf water loss is assumed to be due to stomatal transpiration, and the later water loss (after stomatal closure) presumably is due to cuticular transpiration (Hall and Jones, 1961). Therefore, stomatal behavior is critical for regulating water fluxes of plants in terrestrial ecosystems (Reich and Borchert, 1988; Basal et al., 2005; Anderegg et al., 2018). In our study, the relationships between leaf water loss and stomatal size varied from non-significant relationship (LWL_1 to LWL_4) to significantly positive one (LWL_5 and LWL_6; **Supplementary Table S2**). Additionally, leaf water loss seemed to be not correlated with stomatal density. The contrasting associations indicated that stomatal characteristics in our study might be not important or sophisticated factors influencing observed leaf size-related differences in leaf water loss. This was proved by the important loadings of stomatal size and stomatal density on the third axis of principal component analysis (**Supplementary Table S3**). Moreover, residual stomatal transpiration after complete stomatal closure had been identified as the major determinant of cuticular transpiration for some species (Burghardt and Riederer, 2003). In our study, however, we failed to make critical distinctions between stomatal and cuticular transpiration. Certainly, the loss of leaf water might be related

to epicuticular wax, glaucousness or leaf rolling, which are not studied in this study (Hall and Jones, 1961; Cameron et al., 2006). In conclusion, based on our findings of increasing leaf water loss with decreasing leaf size, it was speculated that the small leaf probably exhibited the advantage in leaf temperature regulation. So we agree with the theory that leaves of small size have adaptive value for plants evolved for hot environments. This knowledge has the potential to enrich vegetation models, in which leaf temperature and water balance during photosynthesis play key roles in, potentially, contributing to well-known biogeographic trends in leaf size.

AUTHOR CONTRIBUTIONS

CW conceived the ideas. JH, YC, and GW collected the data. CW, and T-HZ performed the analysis. CW, BS, and XY wrote the first draft. WG and M-HL led the writing of the manuscript. This work has been approved for publication by all co-authors.

FUNDING

This work was financially supported by the Natural Science Foundation of China (Grant No. 31500354) and China Postdoctoral Science Foundation (Grant Nos. 2018T110232 and 2016M601343).

ACKNOWLEDGMENTS

We greatly thank M. Dawes for providing linguistic suggestions and we are grateful to Juan Sebastian Casallas and Jon Lefcheck for their modified *R* code. We also thank Zhao Chen and Hong Yin for their assistances in the field works and data analyses.

SUPPLEMENTARY MATERIAL

The Supplementary Material for this article can be found online at: https://www.frontiersin.org/articles/10.3389/fpls.2019.00058/full#supplementary-material

REFERENCES

Aarssen, L. W. (2012). Reducing size to increase number: a hypothesis for compound leaves. *Ideas Ecol. Evol.* 5, 1–5. doi: 10.4033/iee.2012.5.1.n

Aarssen, L. W., Schamp, B. S., and Pither, J. (2006). Why are there so many small plants? Implications for species coexistence. *J. Ecol.* 94, 569–580. doi: 10.1111/j.1365-2745.2006.01128.x

Ackerly, D., Knight, C., Weiss, S., Barton, K., and Starmer, K. (2002). Leaf size, specific leaf area and microhabitat distribution of chaparral woody plants: contrasting patterns in species level and community level analyses. *Oecologia* 130, 449–457. doi: 10.1007/s004420100805

Alves-Silva, E., Santos, J. C., and Cornelissen, T. G. (2018). How many leaves are enough? The influence of sample size on estimates of plant developmental instability and leaf asymmetry. *Ecol. Indicat.* 89, 912–924. doi: 10.1016/j.ecolind.2017.12.060

Anderegg, W. R. L., Wolf, A., Arango-Velez, A., Choat, B., Chmura, D. J., Jansen, S., et al. (2018). Woody plants optimise stomatal behaviour relative to hydraulic risk. *Ecol. Lett.* 21, 968–977. doi: 10.1111/ele.12962

Basal, H., Smith, C. W., Thaxton, P. S., and Hemphill, J. K. (2005). Seedling drought tolerance in upland cotton. *Crop Sci.* 45, 766–771. doi: 10.2135/cropsci2005.0766

Boardman, N. K. (1977). Comparative photosynthesis of sun and shade plants. *Annu. Rev. Plant Physiol.* 28, 355–377. doi: 10.1146/annurev.pp.28.060177.002035

Burghardt, M., and Riederer, M. (2003). Ecophysiological relevance of cuticular ranspiration of deciduous and evergreen plants in relation to stomatal closure and leaf water potential. *J. Exp. Bot.* 54, 1941–1949. doi: 10.1093/jxb/erg195

Cameron, K. D., Teece, M. A., and Smart, L. B. (2006). Increased accumulation of cuticular wax and expression of lipid transfer protein in response to periodic drying events in leaves of tree tobacco. *Plant Physiol.* 140, 176–183. doi: 10.1104/pp.105.069724

Clarke, J. M., Richards, R. A., and Condon, A. G. (1991). Effect of drought stress on residual transpiration and its relationship with water use of wheat. *Can. J. Plant Sci.* 71, 695–702. doi: 10.4141/cjps91-102

Corner, E. J. H. (1949). The durian theory or the origin of the modern tree. *Ann. Bot.* 13, 367–414. doi: 10.1093/oxfordjournals.aob.a083225

Cornwell, W. K., and Ackerly, D. D. (2009). Community assembly and shifts in plant trait distributions across an environmental gradient in coastal California. *Ecol. Monogr.* 79, 109–126. doi: 10.1890/07-1134.1

Cramer, M. D., Hawkins, H. J., and Verboom, G. A. (2009). The importance of nutritional regulation of plant water flux. *Oecologia* 161, 15–24. doi: 10.1007/s00442-009-1364-3

Dias, A. T. C., Cornelissen, J. H. C., and Berg, M. P. (2017). Litter for life: assessing the multifunctional legacy of plant traits. *J. Ecol.* 105, 1163–1168. doi: 10.1111/1365-2745.12763

Dombroskie, S. L., and Aarssen, L. W. (2010). Within-genus size distributions in angiosperms: small is better. *Perspect. Plant Ecol. Evol. Syst.* 12, 283–293. doi: 10.1016/j.ppees.2010.06.002

Franks, P. J., Drake, P. L., and Beerling, D. J. (2009). Plasticity in maximum stomatal conductance constrained by negative correlation between stomatal size and density: an analysis using *Eucalyptus globulus*. *Plant Cell Environ.* 32, 1737–1748. doi: 10.1111/j.1365-3040.2009.002031.x

Givnish, T. J., and Vermeij, G. J. (1976). Sizes and shapes of liane leaves. *Am. Nat.* 110, 743–778. doi: 10.1086/283101

Gu, J., Xu, Y., Dong, X., Wang, H., and Wang, Z. (2014). Root diameter variations explained by anatomy and phylogeny of 50 tropical and temperate tree species. *Tree Physiol.* 34, 415–425. doi: 10.1093/treephys/tpu019

Hall, D. M., and Jones, R. L. (1961). Physiological significance of surface wax on leaves. *Nature* 191, 95–96. doi: 10.1038/191095a0

Huang, Y., Lechowicz, M. J., Price, C. A., Li, L., Wang, Y., and Zhou, D. (2015). The underlying basis for the tradeoff between leaf size and leafing intensity. *Funct. Ecol.* 30, 199–205. doi: 10.1111/1365-2435.12491

Jenny, H., Gessel, S. P., and Bingham, F. T. (1949). Comparative study of decomposition of organic matter in temperate and tropical regions. *Soil Sci.* 68, 419–432. doi: 10.1097/00010694-194912000-00001

Jensen, K. H., and Zwieniecki, M. A. (2013). Physical limits to leaf size in tall trees. *Physical. Rev. Lett.* 110, 1–5. doi: 10.1103/PhysRevLett.110.018104

Kleiman, D., and Aarssen, L. W. (2007). The leaf size/number trade-off in trees. *J. Ecol.* 95, 376–382. doi: 10.1111/j.1365-2745.2006.01205.x

Koch, G. W., Sillett, S. C., Jennings, G. M., and Davis, S. D. (2004). The limits to tree height. *Nature* 428, 851–854. doi: 10.1038/nature02417

Kroon, H., Huber, H., Stuefer, J., and Van Groenendael, J. (2005). A modular concept of phenotypic plasticity in plants. *New Phytol.* 166, 73–82. doi: 10.1111/j.1469-8137.2004.01310.x

Le Bagousse-Pinguet, Y., Liancourt, P., Gross, N., De Bello, F., Fonseca, C. R. C., Kattge, J., et al. (2016). Climate, topography and soil factors interact to drive community trait distributions in global drylands. *PeerJ* 4:e1913v1. doi: 10.7287/peerj.preprints.1913v1

Leigh, A., Sevanto, S., Close, J. D., and Nicotra, A. B. (2017). The influence of leaf size and shape on leaf thermal dynamics: does theory hold up under natural conditions? *Plant Cell Environ.* 40, 237–248. doi: 10.1111/pce.12857

Ma, Z., Guo, D., Xu, X., Lu, M., Bardgett, R. D., Eissenstat, D. M., et al. (2018). Evolutionary history resolves global organization of root functional traits. *Nature* 555, 94–97. doi: 10.1038/nature25783

Mccaig, T. N., and Romagosa, I. (1989). Measurement and use of excised-leaf water status in wheat. *Crop Sci.* 29, 1140–1145. doi: 10.2135/cropsci1989.0011183X002900050008x

Mcdonald, P., Fonseca, C., Overton, J., and Westoby, M. (2003). Leaf-size divergence along rainfall and soil-nutrient gradients: is the method of size reduction common among clades? *Funct. Ecol.* 17, 50–57. doi: 10.1046/j.1365-2435.2003.00698.x

Meier, I. C., and Leuschner, C. (2008). Leaf size and leaf area index in *Fagus sylvatica* forests: competing effects of precipitation, temperature, and nitrogen availability. *Ecosystems* 11, 655–669. doi: 10.1007/s10021-008-9135-2

Michaletz, S. T., Weiser, M. D., Mcdowell, N. G., Zhou, J., Kaspari, M., Helliker, B. R., et al. (2016). The energetic and carbon economic origins of leaf thermoregulation. *Nat. Plants* 2:16129. doi: 10.1038/nplants.2016.129

Milla, R. (2009). The leafing intensity premium hypothesis tested across clades, growth forms and altitudes. *J. Ecol.* 97, 972–983. doi: 10.1111/j.1365-2745.2009.01524.x

Milla, R., and Reich, P. B. (2007). The scaling of leaf area and mass: the cost of light interception increases with leaf size. *Proc. Bio. Sci.* 274, 2109–2115. doi: 10.1098/rspb.2007.0417

Moles, A. T., Ackerly, D. D., Tweddle, J. C., Dickie, J. B., Smith, R., Leishman, M. R., et al. (2006). Global patterns in seed size. *Global Ecol. Biogeogr.* 16, 109–116. doi: 10.1111/j.1466-8238.2006.00259.x

Moles, A. T., Warton, D. I., Warman, L., Swenson, N. G., Laffan, S. W., Zanne, A. E., et al. (2009). Global patterns in plant height. *J. Ecol.* 97, 923–932. doi: 10.1111/j.1365-2745.2009.01526.x

Nakagawa, S., and Schielzeth, H. (2013). A general and simple method for obtaining R2 from generalized linear mixed-effects models. *Methods Ecol. Evol.* 4, 133–142. doi: 10.1111/j.2041-210x.2012.00261.x

Niinemets, Ü., and Kull, K. (1994). Leaf weight per area and leaf size of 85 Estonian woody species in relation to shade tolerance and light availability. *For. Ecol. Manage.* 70, 1–10. doi: 10.1016/0378-1127(94)90070-1

Niinemets, Ü., Portsmuth, A., Tena, D., Tobias, M., Matesanz, S., and Valladares, F. (2007). Do we underestimate the importance of leaf size in plant economics? Disproportional scaling of support costs within the spectrum of leaf physiognomy. *Ann. Bot.* 100, 283–303. doi: 10.1093/aob/mcm107

Niinemets, Ü., Portsmuth, A., and Tobias, M. (2006). Leaf size modifies support biomass distribution among stems, petioles and mid-ribs in temperate plants. *New Phytol.* 171, 91–104. doi: 10.1111/j.1469-8137.2006.01741.x

Ogawa, K. (2008). The leaf mass/number trade-off of Kleiman and Aarssen implies constancy of leaf biomass, its density and carbon uptake in forest stands: scaling up from shoot to stand level. *J. Ecol.* 96, 188–191. doi: 10.1111/j.1365-2745.2007.01311.x

Olson, J. S. (1963). Energy storage and the balance of producers and decomposers in ecological systems. *Ecology* 44, 322–331. doi: 10.2307/1932179

Pickup, M., Westoby, M., and Basden, A. (2005). Dry mass costs of deploying leaf area in relation to leaf size. *Funct. Ecol.* 19, 88–97. doi: 10.1111/j.0269-8463.2005.00927.x

Poorter, H., and Evans, J. R. (1998). Photosynthetic nitrogen-use efficiency of species that differ inherently in specific leaf area. *Oecologia* 116, 26–37. doi: 10.1007/s004420050560

R Core Team (2018). *R: A Language and Environment for Statistical Computing*. Vienna: R Foundation for Statistical Computing.

Reich, P. B., and Borchert, R. (1988). Changes with leaf age in stomatal function and water status of several tropical tree species. *Biotropica* 20, 60–69. doi: 10.2307/2388427

Sack, L., and Holbrook, N. M. (2006). Leaf hydraulics. *Annu. Rev. Plant Biol.* 57, 361–381. doi: 10.1146/annurev.arplant.56.032604.144141

Salinger, M. J., Sivakumar, M. V. K., and Motha, R. (2005). Reducing vulnerability of agriculture and forestry to climate variability and change: workshop summary and recommendations. *Clim. Change* 70, 341–362. doi: 10.1007/s10584-005-5954-8

Sang, Y., Wang, C., and Huo, H. (2011). Inter-specific and seasonal variations in photosynthetic capacity and water use efficiency of five temperate tree species in Northeastern China. *Scand. J. For. Res.* 26, 21–29. doi: 10.1080/02827581.2010.534499

Schreiber, L., and Riederer, M. (1996). Ecophysiology of cuticular transpiration: comparative investigation of cuticular water permeability of plant species from different habitats. *Oecologia* 107, 426–432. doi: 10.1007/bf00333931

Scoffoni, C., Rawls, M., Mckown, A., Cochard, H., and Sack, L. (2011). Decline of leaf hydraulic conductance with dehydration: relationship to leaf size and venation architecture. *Plant Physiol.* 156, 832–843. doi: 10.1104/pp.111.173856

Scott, S. L., and Aarssen, L. W. (2012). Within-species leaf size–number trade-offs in herbaceous angiosperms. *Botany* 90, 223–235. doi: 10.1139/B11-106

Tozer, W. C., Rice, B., and Westoby, M. (2015). Evolutionary divergence of leaf width and its correlates. *Am. J. Bot.* 102, 367–378. doi: 10.3732/ajb.1400379

Wang, C. (2006). Biomass allometric equations for 10 co-occurring tree species in Chinese temperate forests. *For. Ecol. Manage.* 222, 9–16. doi: 10.1016/j.foreco.2005.10.074

Westoby, M., and Wright, I. J. (2003). The leaf size-twig size spectrum and its relationship to other important spectra of variation among species. *Oecologia* 135, 621–628. doi: 10.1007/s00442-003-1231-6

Whitman, T., and Aarssen, L. W. (2010). The leaf size/number trade-off in herbaceous angiosperms. *J. Plant Ecol.* 3, 49–58. doi: 10.1093/jpe/rtp018

Wright, I. J., Dong, N., Maire, V., Prentice, I. C., Westoby, M., Díaz, S., et al. (2017). Global climatic drivers of leaf size. *Science.* 357, 917–921. doi: 10.1126/science.aal4760

Wright, I. J., Reich, P. B., Westoby, M., Ackerly, D. D., Baruch, Z., Bongers, F., et al. (2004). The worldwide leaf economics spectrum. *Nature* 428, 821–827. doi: 10.1038/nature02403

Yang, D. M., Li, G. Y., and Sun, S. C. (2008). The generality of leaf size versus number trade-off in temperate woody species. *Ann. Bot.* 102, 623–629. doi: 10.1093/aob/mcn135

Yates, M. J., Anthony Verboom, G., Rebelo, A. G., and Cramer, M. D. (2010). Ecophysiological significance of leaf size variation in proteaceae from the cape floristic region. *Funct. Ecol.* 24, 485–492. doi: 10.1111/j.1365-2435.2009.01678.x

Yu, M. X., Li, Q. F., Hayes, M. J., Svoboda, M. D., and Heim, R. R. (2014). Are droughts becoming more frequent or severe in China based on the standardized precipitation evapotranspiration index: 1951-2010? *Int. J. Climatol.* 34, 545–558. doi: 10.1002/joc.3701

Yu, Z., and Li, X. (2015). Recent trends in daily temperature extremes over northeastern China (1960–2011). *Quatern. Int.* 38, 35–48. doi: 10.1016/j.quaint.2014.09.010

Zhang, J., and Li, J. (1995). Studies on classification models and mechanisms of drought tolerance of major afforestation species in north China. *J. Hebei For. Coll.* 10, 187–193.

Conflict of Interest Statement: The authors declare that the research was conducted in the absence of any commercial or financial relationships that could be construed as a potential conflict of interest.

frontiers in Plant Science

ORIGINAL RESEARCH
published: 21 February 2019
doi: 10.3389/fpls.2019.00185

Stem Diameter (and Not Length) Limits Twig Leaf Biomass

Jun Sun[1†], Mantang Wang[1,2†], Min Lyu[3], Karl J. Niklas[4], Quanlin Zhong[3], Man Li[3] and Dongliang Cheng[1]*

[1] Fujian Provincial Key Laboratory of Plant Ecophysiology, Fujian Normal University, Fuzhou, China, [2] School of City and Civil Engineering, Zaozhuang University, Zaozhuang, China, [3] Key Laboratory of Humid Subtropical Eco-Geographical Process, Ministry of Education, Fuzhou, China, [4] Plant Biology Section, School of Integrative Plant Biology, Cornell University, Ithaca, NY, United States

The relationship between leaf and stem biomass as well as the relationship between leaf biomass and stem length and diameter are important to our understanding of a broad range of important plant scaling relationship because of their relationship to photosynthesis and thus growth. To understand how twig architecture (i.e., current year leaves, and stem diameter and length) affects stem diameter and length, and leaf number and biomass, we examined the twigs of 64 woody species collected from three forest types along an elevational gradient in the Wuyi Mountains, Jiangxi Province, China. We also compared the scaling relationships we observed with biomass allocation patterns reported at the whole tree level. Our results revealed isometric relationship between leaf and stem biomass on twigs despite differences in forest communities and despite changes in environmental factors along an elevational gradient. Across the 64 species, from twigs to individual trees, leaf biomass scaled approximately as the 2.0-power of stem diameter (but not for stem length or leaf number). These results help to identify a general rule that operates at two different levels of biological organization (twigs and whole trees). The scaling relationship between leaf biomass and stem diameter in twigs is insensitive to differences in species composition, elevation, or forest type. We speculate that this rule emerges because stem diameter serves as a proxy for the amount of resources supplied per unit cross section to developing leaves and for the flow of photosynthates from mature leaves to the rest of the plant body.

Keywords: allometry, annual growth, biomass allocation, elevation gradient, forest types, isometry, stem architecture

OPEN ACCESS

Edited by:
Boris Rewald, University of Natural Resources and Life Sciences, Vienna, Austria

Reviewed by:
Ze-Xin Fan, Xishuangbanna Tropical Botanical Garden (CAS), China
Lina Fusaro, Sapienza University of Rome, Italy
Félix P. Hartmann, INRA Physique et Physiologie Intégratives de l'Arbre Fruitier et Forestier, France

***Correspondence:**
Dongliang Cheng
chengdl02@aliyun.com

† These authors have contributed equally to this work

Specialty section:
This article was submitted to Functional Plant Ecology, a section of the journal Frontiers in Plant Science

Received: *02 November 2018*
Accepted: *05 February 2019*
Published: *21 February 2019*

Citation:
Sun J, Wang M, Lyu M, Niklas KJ, Zhong Q, Li M and Cheng D (2019) Stem Diameter (and Not Length) Limits Twig Leaf Biomass. Front. Plant Sci. 10:185. doi: 10.3389/fpls.2019.00185

INTRODUCTION

Regardless of their form, size, or longevity, the leaves on current-year shoots (i.e., twigs) provide the photosynthetic machinery that drives annual growth, whereas the stems of twigs sustain the static and dynamic mechanical forces leaves experience by gravity and wind (i.e., self-loading and wind induced drag forces, respectively) (Niklas, 1992a). The hydraulic architecture of mature twigs also provides for the efflux of photosynthates and influx of water and nutrients. Consequently, quantifying the scaling relationships between leaf and stem biomass, and the relationship between stem diameter and length is critical to our understanding of a broad spectrum of important ecological phenomena (Westoby and Wright, 2003; Niklas and Spatz, 2004; Sun et al., 2006; Olson et al., 2009; Xiang et al., 2009a).

Generally, the allocation of biomass to leaves, stems, and roots can be described using a scaling function (Enquist and Niklas, 2002), which takes the general mathematical formula $M_a = \beta M_b^{\alpha}$, where M_a and M_b are the biomass of different organs, β is the normalization constant, and α is the scaling exponent. Prior investigations using this formula have focused not only at the whole-plant level (Enquist and Niklas, 2002; Cheng and Niklas, 2007; Chave et al., 2014; Paul et al., 2016), but also at the level of individual twigs (e.g., Westoby and Wright, 2003; Sun et al., 2006; Xiang et al., 2009a; Yang et al., 2015). For example, an isometric relationship is reported for the scaling of leaf and stem growth (i.e., $G_L \propto G_S$) (Niklas and Enquist, 2002b). Therefore, it is not unreasonable to speculate that total leaf biomass might scale isometrically with respect to total stem biomass at the twig level. Indeed, some empirical results indicate that leaf biomass scales nearly isometrically with stem biomass at the level of individual twigs (Sun et al., 2006; Xiang et al., 2009a). However, other interspecific studies indicate that the smaller twigs might have a larger ratio of leaf to stem biomass (Yagi, 2000; Suzuki, 2003; Pickup et al., 2005; Wright et al., 2006). Indeed, when viewed collectively, there is considerable ambiguity about how the key functional traits of twigs (e.g., leaf and stem biomass, and stem diameter and length) actually scale with respect to one another, especially for different plant communities growing along environmental gradients, such as an elevational gradient.

In order to clarify the scaling relationships of twigs along the elevational gradient, we developed a mathematical model for the scaling of critical twig functional traits and we tested the model using data gathered from 915 twigs from 64 woody species in three different forest-types (i.e., deciduous, mixed forest, and evergreen forest) along an elevational gradient in the Wuyi Mountains. The model and the data were used to determine (1) twig biomass allocation patterns, and (2) how leaf biomass scales with respect to stem diameter and length at the twig level along a steep (2158 m) elevational gradient. Using published data, we also compared twig scaling relationships to those at the whole-tree level to provide a comprehensive view of plant biomass allocation patterns at different levels of biological organization (i.e., primary and secondary growth as well as two branching levels within tree-sized plants).

MATERIALS AND METHODS

The Model

Our model rests on the assumpt that a positive scaling relationship exists between stem diameter and total leaf biomass because (1) the transport of water and nutrients to transpiring leaves is likely to scale positively with stem cross sectional conductive area (and thus diameter) (Shinozaki et al., 1964; Niklas and Spatz, 2004) and because (2) the mechanical capacity of stems to resist bending and torsion is positively correlated with the second moment of area (and thus diameter) (Niklas and Spatz, 2010). The theoretical relationship between stem diameter and length at the twig level is less clear. However, it is reasonable to surmise that, for any stem biomass, a negative correlation exists between stem diameter and length, provided that the bulk density of stem tissues is invariant (Niklas and Spatz, 2010). Accordingly, stem diameter and length should negatively correlate with wood density. Turning to the whole plant level, prior research indicates that plant height (H) scales approximately isometrically with respect to basal stem diameter (D) across seedlings and non-woody or very small woody species (i.e., $H \propto D$), but as the 2/3 power of D across the larger trees (i.e., $H \propto D^{2/3}$) (Niklas and Spatz, 2004; see, however, Zhang et al., 2016). Although these relationships do not directly bear on the scaling of stem diameter with respect to stem length on twigs, a similar tactic can be taken by relating the scaling of basal stem diameter to plant height. Following the same logic as before, it is reasonable to suppose that twig length (L) might scale isometrically with respect to twig diameter (D) (i.e., $L \propto D$). Assuming that individual stems are more or less cylindrical in geometry, it follows that stem biomass (M_S) will be proportional to the product of the square of diameter and stem length (i.e., $M_S \propto D^2 L$). Assuming an invariant bulk tissue density, twig stem mass will scale as the cube of either diameter or length (i.e., $M_S \propto D^3 \propto L^3$). However, Xiang and Liu (2009b) report that L may be uncorrelated with stem diameter (D) due to phylogenetic reasons at twigs level. Therefore, whether leaf biomass scale as the cube of stem diameter at the twig level remains unclear.

Another variable of interest is leaf number because the total leaf biomass of twigs is the product of leaf number and the biomass of individual leaves. Assuming that stems can sustain a critical maximum leaf biomass (by virtue of hydraulic or mechanical limitations) (Westoby et al., 2002), the biomass of individual leaves must scale inversely with respect to total leaf number (Kleiman and Aarssen, 2007). For example, studies of leafing intensity (leaf number per unit stem volume) indicate that average leaf biomass increases with decreasing leaf number per stem volume (Kleiman and Aarssen, 2007; Milla, 2009; Huang et al., 2015). If this negative isometric relationship holds true across species, total leaf biomass should be independent of leaf number. However, a positive relationship between leaf number and total (and individual) leaf biomass has been reported at times (Smith et al., 2017). Therefore, it is still unclear how twig traits limit the total leaf biomass production across different forest communities along elevational gradients. Consequently, an empirical approach was adopted.

Study Site Description

The study site is located in National Natural Reserve of Wuyi Mountains (27°48.11′–28°00.35′ N, 117°39.30′–117°55.47′ E). The reserve is located in the humid warm subtropics in the southeast of China and has a mean annual precipitation of 2583 mm and a mean annual temperature of 14.2°C. The forests growing on Huanggang were selected for study because (1) this mountain is the highest peak in the reserve at 2158 m with a mean above sea level (m a.s.l) of 1200 m and thus provided considerable climatic variation along its elevational gradients, and (2) because the vertical zonation of vegetation types along these gradients ranges from evergreen forests in the lower elevations to mountainous steppe in the higher elevations. The major soil types of Huanggang are classified as

mountain yellow-red soil (400–600 m a.s.l), mountain yellow soil (600–1300 m a.s.l.), mountain dark yellow-brown soil (1300–1900 m a.s.l.) and mountain meadow soil (above 1900 m a.s.l.) (Li et al., 2017).

Twig Sampling

Three forest communities were selected along an elevational gradient: (1) an evergreen forest (EF) located at 1319 m a.s.l, (2) a mixed forest (MF) located at 1697 m a.s.l, and (3) a deciduous forest (DF) located at 1818 m a.s.l. Three 20 m × 20 m plots were randomly established in each forests. Forest stand density, stem diameter at breast height (DBH), plant height (H) and soil nutrient content were measured for woody species within each plot. Sample information shown in **Table 1**.

As noted in the Introduction, a twig is defined as a first-year shoot, consisting of a stem and attached leaves. In August, 2016, three to five individuals of each species were randomly selected, and 5 twigs were taken from the perimeter of the crown per individual plant. For species with less than three individuals in a plot, five twigs from each individual were harvested. The total number of species was 64, spanning 27 families and 45 genera among the three forest types. Specifically, 32, 20, and 23 species (including overlapping species) were collected in the evergreen, mixed, and deciduous forests, respectively. The dominant species in the EF were *Rhododendron simiarum*, *Schima superba*, *Cyclobalanopsis glauca*, *Rhododendron ovatum*, and *Symplocos sumuntia*. The dominant species in the MF *Symplocos sumuntia* and *Cyclobalanopsis multiervis*, *Tsuga chinensis*, *Taxus chinensis*, *Acer elegantulum*, and *Illicium minwanense*. The dominant species in the DF *Clethra barbinervis*, *Photinia beauverdiana*, *Acer nikoense*, and *Fraxinus chinensis*. All of the leaves on each twig were removed and each leaf was scanned to measure its area using the software Image J. Stem diameter at the top, middle, and bottom of each twig was measured and used to calculate a mean diameter. Twig length was measured using a vernier caliper, with an accuracy of 0.1 mm. Stem volume was calculated as the square of stem diameter times stem length, assuming that individual stems were more or less cylindrical in geometry. All leaves and stems attached on twigs were subsequently brought to the laboratory and oven-dried at 75°C to determine total leaf biomass (M_L), total stem biomass (M_S), and total biomass (the sum of leaf and stem biomass, M_T). Wood density (ρ) was calculated as stem biomass / stem volume.

The scaling relationships governing twig biomass allocation patterns were compared with those at the whole tree level. A total of 1123 records for total leaf, total stem, and total plant size (M_L, M_S, and M_T, respectively) and 548 records for plant height and DBH complied by Cannell (1982); Enquist and Niklas (2002), and Niklas and Enquist (2002a,b) were analyzed. The data included measurement taken on eudicot, monocot, and conifer species, and from seedlings and reproductively mature tree species.

Data Analysis

For each species, the mean values for all twig traits were calculated and used. All of the data were $\log_{10}$ transformed to fit a normal distribution before analysis. The relationships between all twig functional traits were best fit by the mathematical equation $\log(y) = \log(\beta) + \alpha\log(x)$, where β is the normalization constant and α is the scaling exponent. Model Type II regression was used to determine the numerical values of β and α using the (Standardized) Major Axis Estimation package 'smatr' version 3.4-3 in R software (R Core Team, 2012; Warton et al., 2012). The data from species showing no statistically significant differences in the numerical values of the two regression parameters were pooled to determine a common scaling exponent using the standardized major axis package in R (Warton et al., 2006, 2012). The significance level for testing slope heterogeneity was $P < 0.05$ (e.g., slope heterogeneity was rejected when $P > 0.05$). Further, in order to determine whether the correlation between different functional traits varied with evolutionary divergence, the phylogenetic signals of twig functional traits in the three forests were examined using Phylogenetically Independent Contrast Analysis (PIC), which was calculated using the "*pic*" function in the "ape" package in R 3.4.3 software (Paradis et al., 2004). The *K*-value method proposed by Blomberg et al. (2003) measures the intensity of phylogenetic signals of continuous functional traits, which was calculated using the "*phylosignal*" function in the "picante" package in R 3.4.3 software (Kembel et al., 2010). $K > 1$ indicates that functional traits exhibit a stronger phylogenetic signal; $K < 1$ indicates that the functional traits exhibit weak phylogenetic signals (Blomberg et al., 2003).

A structural equation model was used to create an empirical model for predicting how traits influence total leaf biomass at the twig level. The model run through SPSS AMOS 22.0 (SPSS. Inc., Chicago, IL, United States). Specifically, we constructed an initial model for expected causal relationships between total leaf biomass and twig trait variables based on prior theoretical knowledge (**Figure 3A**). Because the initial model did not provide a good fit to the data, the SEM was simplified and evaluated using maximum likelihood chi-squared tests (Grace et al., 2007). The CMIN/DF (the ratio of Chi-Square test value and degrees of freedom), GFI (Adjusted Goodness-of-fit Data), NFI (Normed

TABLE 1 | Ecological and morphometric traits of the three forest types examined in this study.

Forests	Altitude (m)	*n*	Density (trees/hm^2)	Height (m)	Mean DBH (cm)	Soil carbon content (mg/g)	Soil nitrogen content (mg/g)	Soil phosphorus content (mg/g)
EF	1319	32	3033 ± 200a	7.87 ± 0.07b	13.77 ± 1.46b	68.88 ± 0.59a	4.84 ± 0.04a	0.46 ± 0.01b
MF	1697	20	1133 ± 164b	10.56 ± 0.21a	21.39 ± 0.8a	78.71 ± 4.36a	5.25 ± 0.27a	0.38 ± 0.02c
DF	1818	23	2725 ± 164a	6.94 ± 0.24b	11.47 ± 0.67b	75.16 ± 5.23a	6.05 ± 0.22a	0.65 ± 0.01a

EF, evergreen forest; DF, deciduous forest; MF, mixed forest. Using one-way ANOVA, the values of morphometric functional traits and soil stoichiometry within columns not sharing a common letter are significantly different (post hoc LSD test, α = 0.05).

Fit Index) were used to determine whether the fit between the simplified model and data was adequate.

RESULTS

Biomass Allocation Patterns

The three traits (i.e., M_L, M_S, and M_T) scaled nearly isometrically with respect to one another (i.e., $\alpha \approx 1.0$) across the three different forest communities along the elevational gradient (**Table 2**). Also, there was no statistically significant difference in the numerical values of the scaling exponents and normalization constants within each of the three different forest communities. Specifically, the common slopes were 0.99 (95% CI = 0.89 – 1.11, $P = 0.13$) for M_S vs. M_T, 1.01 (95% CI = 0.995 – 1.02, $P = 0.19$) for M_L vs. M_T, and 1.03 (95% CI = 0.91 – 1.15, $P = 0.17$) for M_L vs. M_S (**Supplementary Figures 1A,B**). Across the three forest communities, the scaling exponents of M_S vs. M_T, M_L vs. M_T, and M_L vs. M_S were 1.02, 1.01, and 0.99, respectively (**Table 2**), each of which was statistically indistinguishable from 1.0 (all $P_{1.0} > 0.05$) (**Table 2**). The scaling of stem biomass vs. total twig biomass across the three different forest communities was consistent with our model, i.e., the scaling had a common slope of 1.08 (95% CI = 1.07 – 1.08, $P = 0.24$) (**Figure 1A**).

In contrast, at the whole tree level, the scaling exponents of M_S vs. M_T, M_L vs. M_T, and M_L vs. M_S significantly differed from 1.0 (i.e., α = 1.08, 0.82, and 0.76, all $P_{1.0} < 0.05$, respectively; **Figures 1A–C**).

The Scaling of Stem Architecture With Leaf Number, and Stem and Leaf Biomass

The scaling exponents of M_S vs. D were statistically indistinguishable among the three forest communities (see

TABLE 2 | Summary of regression parameters (slopes and *y*-intercepts, α and log β, respectively) for relationships between leaf and stem biomass, and stem biomass (leaf biomass) vs. stem diameter (and length) in three forests.

	Forest type	N	α (95%CI)	log β (95%CI)	r^2	*P*
M_S vs. M_T	EF	32	0.96 (0.77, 1.20)	−1.10 (− 1.75, −0.46)	0.65	< 0.001
	DF	23	1.17 (0.97, 1.43)	−0.37 (− 1.11, 0.36)	0.81	< 0.001
	MF	20	0.92 (0.80, 1.07)	−1.27 (− 1.72, −0.83)	0.91	< 0.001
	ALL	75	1.02 (0.92, 1.12)	−0.92 (− 1.24, −0.60)	0.82	< 0.001
M_L vs. M_T	EF	32	1.03 (1.01, 1.06)	0.05 (− 003, 0.13)	0.99	< 0.001
	DF	23	1.00 (0.96, 1.03)	−0.06 (− 0.18, 0.05)	0.99	< 0.001
	MF	20	1.01 (0.99, 1.02)	−0.02 (− 0.06, 0.03)	0.99	< 0.001
	ALL	75	1.01 (0.99, 1.02)	−0.03 (− 0.07, 0.02)	0.99	< 0.001
M_L vs. M_S	EF	32	1.07 (0.85, 1.36)	1.23 (0.19, 2.27)	0.59	< 0.001
	DF	23	0.85 (0.68, 1.07)	0.25 (− 0.54, 1.05)	0.75	< 0.001
	MF	20	1.09 (0.93, 1.28)	1.37 (0.63, 2.11)	0.90	< 0.001
	ALL	75	0.99 (0.89, 1.11)	0.89 (0.44, 1.34)	0.78	< 0.001
M_S vs. D	EF	32	1.87 (1.40, 2.50)	1.44 (1.26, 1.62)	0.38	< 0.001
	DF	23	2.13 (1.50, 3.03)	1.24 (0.97, 1.52)	0.38	< 0.001
	MF	20	1.77 (1.35, 2.32)	1.25 (1.07, 1.42)	0.69	< 0.001
	ALL	75	2.01 (1.70, 2.38)	1.34 (0.43, 2.26)	0.49	< 0.001
M_S vs. L	EF	32	1.22 (0.89, 1.67)	−0.18 (− 0.89, −0.52)	0.26	< 0.001
	DF	23	1.38 (0.98, 1.94)	−0.50 (− 1.34, −0.34)	0.42	< 0.001
	MF	20	1.92 (1.22, 3.02)	−1.25 (− 2.65, 0.14)	0.11	< 0.001
	ALL	75	1.44 (1.19, 1.74)	−2.24 (− 2.61, −1.88)	0.32	< 0.001
M_L vs. D	EF	32	2.03 (1.68, 2.45)	2.39 (1.35, 3.44)	0.73	< 0.001
	DF	23	1.81 (1.36, 2.42)	1.65 (0.22, 3.09)	0.61	< 0.001
	MF	20	1.93 (1.55, 2.41)	1.97 (0.79, 3.15)	0.80	< 0.001
	ALL	75	2.00 (1.75, 2.27)	2.22 (1.52, 2.92)	0.69	< 0.001
M_L vs. L	EF	32	−1.31(− 1.89, −0.91)	5.26 (4.38, 6.14)	0.001	0.94
	DF	23	1.20 (0.77, 1.78)	0.73 (− 0.16, 1.62)	0.11	0.14
	MF	20	2.10 (1.31, 3.38)	−0.55 (− 2.17, 1.06)	0.01	0.64
	ALL	75	1.43 (1.14, 1.79)	−1.34 (− 1.77, −0.90)	0.06	0.038
M_L vs. N_L	EF	32	1.45 (1.02, 2.07)	−4.11 (− 4.49, −3.72)	0.04	0.40
	DF	23	1.68 (1.08, 2.61)	−4.46 (− 5.05, −3.87)	0.04	0.27
	MF	20	−1.41 (− 2.24, −0.89)	3.61 (3.08, 4.14)	0.06	0.31
	ALL	75	−1.54 (− 1.94, −1.22)	−2.11 (− 2.39, −1.84)	0.001	0.89

M_T, twig mass; M_L, total leaf biomass; M_S, stem biomass; D, stem diameter; L, stem length; and N_L, leaf number.

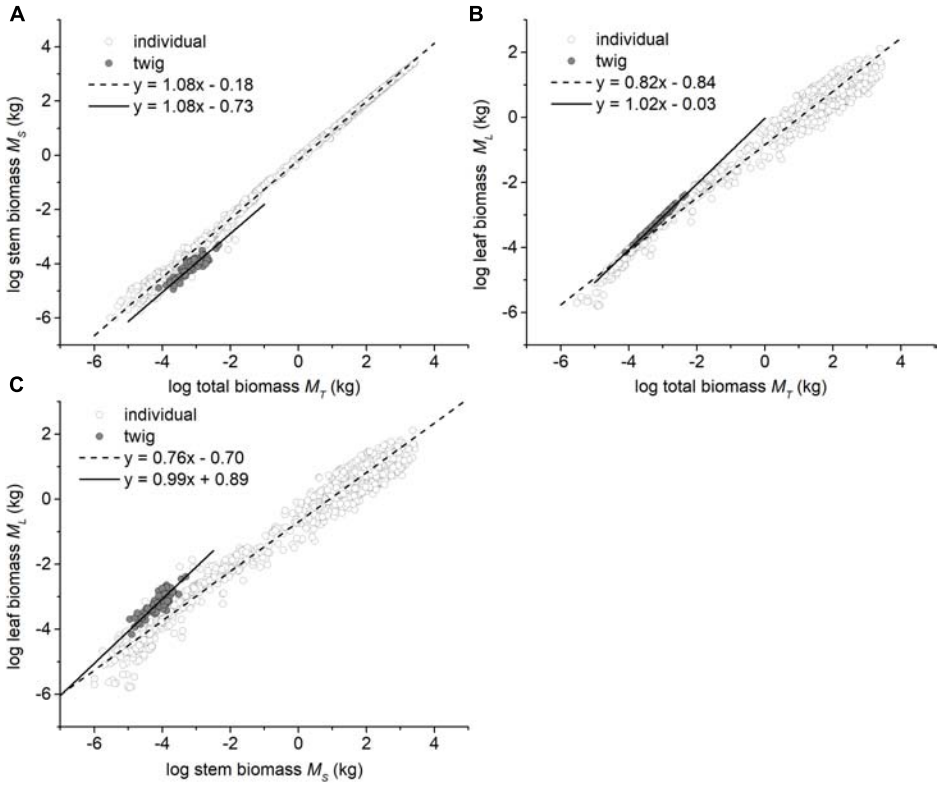

FIGURE 1 | Bivariate plots among the leaf, stem, and total biomass at the twig level and the individual plant level. **(A)** The relationship between stem and total biomass, **(B)** The relationship between leaf and total biomass, and **(C)** The relationship between leaf and stem biomass. The data of individual plants were taken from Cannell (1982), Enquist and Niklas (2002), and Niklas and Enquist (2002a,b).

Table 2 and **Supplementary Figure 1C**), with a common slope of $\alpha = 1.88$ (95% CI = 1.59 – 2.24, $P = 0.69$). However, the numerical values of normalization constants for M_S vs. D varied significantly, ranging from 0.87 for the mixed forest type to 1.09 for the evergreen forest type (**Supplementary Figure 1C**). Similarly, the scaling exponents of M_S vs. L were indistinguishable among the three forests, with a common slope of $\alpha = 1.41$ (95%CI = 1.14 – 1.73, $P = 0.26$). Additionally, the normalization constants of M_S vs. L showed no significant difference among the three forests (i.e., $\beta = -2.32$, 95%CI = −2.66 – −1.97, $P > 0.05$) (see **Table 2** and **Supplementary Figure 1D**).

Among the three forest communities, the scaling exponents of M_S vs. D were not statistically significantly different from 2.0 and had a common slope of $\alpha = 1.94$ (95%CI = 1.72 – 2.20, $P = 0.82$) (see **Table 2** and **Supplementary Figure 2**). However, the normalization constant for the data from the evergreen forest was significantly higher than that of other two forests (i.e., $\beta = 2.17$, 2.00, and 2.00 for Evergreen forest, Mixed forest, and Deciduous forest, respectively) (**Supplementary Figure 2**). Perhaps more important, the scaling exponent of M_L vs. D across the three forests (i.e., $\alpha = 1.94$) was statistically indistinguishable from that of the individual tree level (i.e., M_L vs. D, $\alpha = 1.99$), with a common slope of $\alpha = 2.00$ (95%CI = 1.93 – 2.07, $P = 0.98$) (**Figure 2A**). In contrast, M_L showed no statistically significant relationship with N_L at the twig level within each or across all of the three forests (see **Table 2** and **Supplementary Figure 3**). Although M_L was weakly correlated with L ($P = 0.038$) across the three forests, no significant correlation was observed within each of the three forests (see **Table 2**). At the level of individual plants, both stem diameter and height were significantly correlated with total leaf biomass (all $P < 0.001$, **Figures 2A,B**).

Within each and across all of the three forest communities, no significant scaling relationship was observed for leaf number (N_L) vs. stem diameter, or N_L vs. stem volume (**Table 3**). However, N_L scaled significantly with respect to L across the three forests, although little variation of N_L was explained by L (**Table 3**). Although we found the leaf number had a phylogenetic signal, it had no discernable effect on the leaf number vs. total leaf mass relationship or other stem architecture traits (see **Supplementary Table S1** and **Supplementary Figure 4**).

The final structural equation model (SEM) predicting total leaf biomass at the twig level provided an adequate fit to our data, i.e., CMIN/DF = 2.2, GFI = 0.94, and NFI = 0.96. Increasing bulk stem tissue density was negatively correlated with stem diameter, but leaf number had no effect on individual leaf biomass nor individual leaf area. Increasing stem biomass and individual leaf biomass increased with total leaf biomass at the twig level (**Figure 3B**). More importantly, although stem length did influence stem biomass (**Figure 3B**), increasing stem

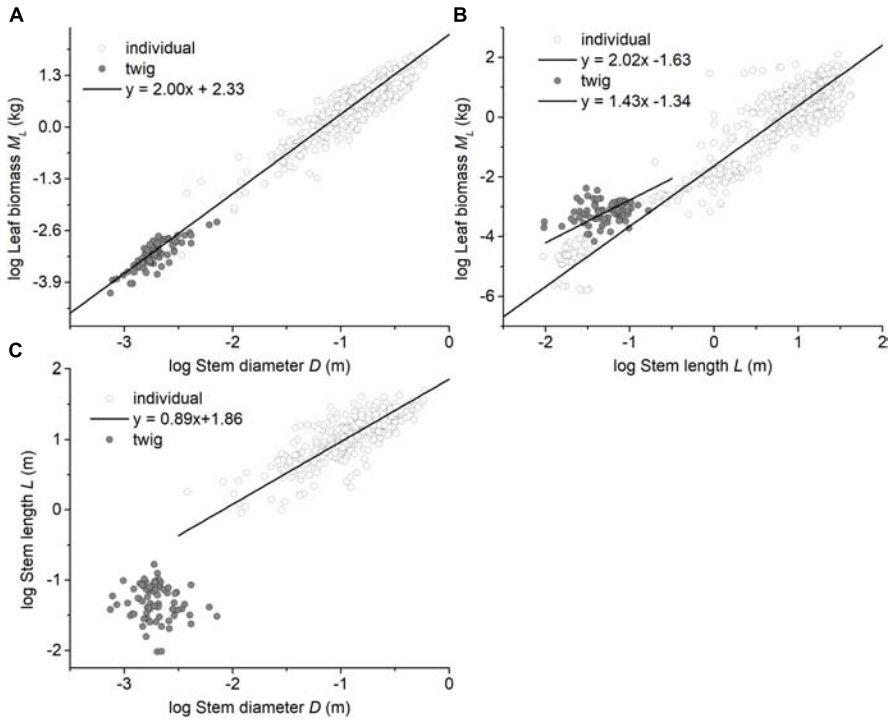

FIGURE 2 | Bivariate plots of leaf biomass with respect to stem architecture at the twig level and at the individual level. **(A)** the relationship between leaf biomass and stem diameter, **(B)** the relationship between leaf biomass and stem height (length), and **(C)** the relationship between stem diameter and stem height (length). The data for individual plants were taken from Cannell (1982), Enquist and Niklas (2002), and Niklas and Enquist (2002a,b).

TABLE 3 | Summary of regression parameters (slopes and *y*-intercepts, α and log β, respectively) for relationships between leaf number (N_L) with respect to stem diameter (*D*), length (*L*), and volume (*V*) for all twigs in three forest.

	Forest type	*n*	α (95%CI)	log β (95%CI)	r^2	*P*
N_L vs. *L*	EF	32	−0.91 (− 1.31, −0.63)	−0.41 (− 0.83, 0.01)	<0.001	0.9
	DF	23	0.70 (0.46, 1.07)	1.62 (1.22, 2.02)	0.08	0.19
	MF	20	1.49 (0.97, 2.28)	2.86 (1.89, 3.83)	0.22	0.04
	ALL	75	0.93 (0.74, 1.16)	1.91 (1.63, 2.19)	0.07	0.03
N_L vs. *D*	EF	32	1.39 (0.97, 2.01)	4.47 (3.07, 5.88)	0.005	0.69
	DF	23	1.09 (0.70, 1.68)	3.65 (2.33, 4.97)	0.02	0.51
	MF	20	−1.37 (− 2.15, −0.87)	−3.09 (− 4.85, −1.33)	0.12	0.14
	ALL	75	−1.29 (− 1.63, −1.03)	−2.81 (− 3.63, −1.99)	0.01	0.35
N_L vs. *V*	EF	32	0.64 (0.44, 0.91)	3.07 (2.18, 3.96)	<0.001	0.90
	DF	23	0.46 (0.30, 0.70)	2.46 (1.70, 3.21)	0.09	0.16
	MF	20	−0.69 (− 1.10, −0.43)	−2.12 (− 3.50, −0.73)	0.014	0.61
	ALL	75	0.57 (0.45, 0.71)	2.86 (2.35, 3.37)	0.003	0.63

EF, evergreen forest; DF, deciduous forest; and MF, mixed forest.

diameter resulted in increasing stem mass and individual leaf mass (**Figure 3B**).

DISCUSSION

Although other studies of the relationships between leaf and stem biomass at the twig level have been published (Westoby and Wright, 2003; Pickup et al., 2005; Sun et al., 2006; Xiang et al., 2009a; Li et al., 2017), this study is the first to quantify the relationship and compare it among very different forest types along the elevational gradient. It is also one the few studies comparing the leaf and stem biomass relationship at the twig level with the individual-tree level. Thus, our analyses provide a novel opportunity to draw comparisons between two different but important levels of biological organization and to understand the mechanism(s) underlying leaf biomass allocation patterns.

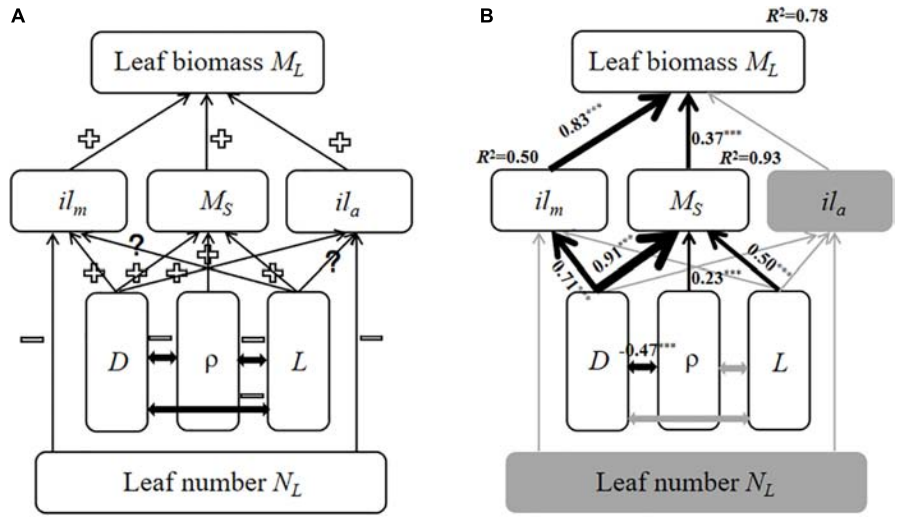

FIGURE 3 | The models of the relationship among twig trait variables based on SEM. The gray solid arrows represent statistically non-significant correlations; the black solid arrows denote significant correlations in the final model. The thickness of the solid arrows indicates the magnitude of the standardized SEM coefficients, with its level of statistical significance (***$p < 0.001$). **(A)** the initial model; **(B)** the final model. "+" indicates a positive relationship, "–" indicates a negative relationship. "?" indicates a unclear relationship. il_m, Individual leaf biomass; M_L, total leaf biomass; M_S, stem biomass; il_a, individual leaf area; D, stem diameter; ρ, wood density; and L, stem length.

Biomass Allocation at Twig and Individual Level

At the twig level, our analysis shows that there are invariant and isometric scaling relationships among M_S, M_L, and M_T (see **Table 2** and **Supplementary Figure 1**) for three different forest types. This finding is consistent with some previous studies reporting isometric scaling exponents governing the relationships among these variables at twigs level (Sun et al., 2006; Xiang et al., 2009a). Further, the seemingly invariant isometric scaling relationship observed in our study supports previous reports that the total annual growth rates of leaves and stems at the whole plant level scales isometrically (Niklas and Enquist, 2002b). In contrast, our results are in apparent contradiction with other reports that large-leaved or thick-twigged species allocate more biomass to leaves (Pickup et al., 2005; Wright et al., 2006). One possible explanation for this inconsistency is the biomechanical trade-offs among a stem's tissue bulk density, the geometric contribution to bending made by a stem's cross-sectional area (called the second moment of area), and the effect of leaf mass (and area) on stem flexure (resulting from self-loading and wind-induced drag forces). The ability of a stem to resist bending of twisting can be increased by either increasing the material properties of its tissues (which, on average, increases with density), or by increasing its second moment of area by increasing its girth. Across species comparisons show that stems composed of weaker materials (those with lower material stiffness) compensate by having greater girth (Niklas, 1992b). Indeed, our results reveal that stem bulk tissue density is negatively correlated with stem diameter (**Figure 3B**).

Perhaps more important, out data show that stem biomass scales as the 1.08 power with respect to total shoot biomass (i.e., leaf plus stem mass) at the twig level across very different forest communities (**Figure 1A**). Additionally, consistent with some previous reports (e.g., Suzuki, 2003), we see that the numerical values of the exponent of M_L vs. M_T and M_L vs. M_S (i.e., 1.01 and 0.99 for twigs) shifts to 0.82 and 0.76 at the level of individual trees (**Figures 1B,C**). This shift mirrors a shift in the numerical value of the scaling exponent for metabolic rates as the plant body increases in size (i.e., from 1.0 to 3/4; see Niklas, 2004; Reich et al., 2006, Cheng et al., 2010). When these patterns are viewed together, it is reasonable to conclude that metabolic rates likely scale isometrically as a function of current-year twig biomass and will decline as the plant body increases overall, a phenomenon that has been observed before (e.g., Westoby and Wright, 2003; Sun et al., 2006; Cheng and Niklas, 2007; Chave et al., 2014; Paul et al., 2016).

The Scaling of Leaf Biomass With Respect to Stem Architecture

The data reported here show that leaf mass (M_L) scales approximately as the 2.0-power of stem diameter (D), which is similar to the pattern reported by Enquist and Niklas (2002), i.e., total standing leaf mass (M_L) scales as the 1.99-power of basal stem diameter (D) at the individual plant level (**Table 2** and **Figure 2A**). In this context, it is useful to note that the 'Pipe model' theory argues that branches play a duel role in nutrient transport and mechanical support, such that the number of leaves per twig might be limited by the number of 'pipe' units traversing a twig (Shinozaki et al., 1964; Tyree and Ewers, 1991). In this context, Westoby and Wright (2003) argue that the cross-sectional area of twigs is expected to scale with total leaf area for both hydraulic and mechanical reasons. Because some studies report that leaf area scales, on

average, isometrically with leaf biomass (West et al., 1997, 1999; Sun et al., 2006), leaf biomass is expected to scale as the 2.0-power of stem diameter at both the individual plant level and the twig level. Moreover, for any equivalent stem diameter, our results show that twigs and individual plants have similar leaf biomass scaling relationships, despite an elevational gradient that affects ambient temperatures (**Figure 2A**). Although low temperature negatively affect metabolic rates and thus growth (Hoch and Körner, 2012; Mayor et al., 2017) and are expected to modify twig biomass allocation patterns (Xiang et al., 2009a), our results indicate a fixed "invariant" isometric relationship between leaf and stem biomass for twigs regardless of elevation (**Figure 1B**). Importantly, however, the elevational gradient did influence the numerical value of the normalization constant governing the M_S vs. D relationship (**Figure 1C**). In this context it is important to note that stem bulk tissue density (ρ) differed among the three forests examined in our study, i.e., it was highest in the evergreen forest, which also had the smallest stem diameters per stem biomass (**Supplementary Figure 1C**).

At the level of an individual plant, the data used in this study reveal a significant correlation between total standing leaf biomass and plant height, but show no clear scaling relationship at the level of individual twigs (**Table 2** and **Figure 2B**), i.e., different relationships between stem length (height) and leaf biomass exist for the twig and whole plant levels (**Figure 2C**). This finding is consistent with the observation that no single mechanical model exists across plants with and without secondary tissues or over the course of the ontogeny of woody species (Niklas and Spatz, 2004; Enquist et al., 2007; King, 2011). This phenomenology likely reflects the annual amortization of secondary tissues in progressively older stems bearing twigs that typically have little or no secondary tissues.

It is important to cast our results in the context of the hydraulic as well as the mechanical differences between twigs and the architecture of whole trees. First, the height of an individual tree height is not geometrically equivalent to the length of a stem (i.e., twig). The former is influenced by branching angles and the orientation of growth in woody stems as well as twigs, whereas the latter is a simple linear dimension reflecting growth in a single year. Second, water transport through the trunk of a tree is effected by the hydraulic efficiency of sapwood (a secondary tissue), whereas water transport in a twig is governed by the efficiency of primary xylem. Third, the diameter of a tree trunk reflects the accumulation of secondary tissues, which is lacking in twigs, which has many substantive consequences (Ryan and Yoder, 1997; West et al., 1999). Collectively, these and other factors contribute to the fact the scaling of stem diameter (D) and stem length (L) are fundamentally different at the twig and whole tree levels (**Figure 2C**).

The Scaling of Leaf Biomass With Respect to Leaf Number

Our results reveal no significant relationship between leaf number and total leaf mass on twigs (**Table 2**, $P > 0.05$). According to the leafing intensity (leaf number per unit stem volume) strategy (Kleiman and Aarssen, 2007), average leaf biomass is predicted to decrease with leaf number per stem volume such that individual leaf mass should scale negatively and isometrically with respect to leaf number for given stem volume. This negative scaling relationship might offset the relationship between total twig leaf biomass and leaf number because total twig leaf biomass is the product of leaf number and individual leaf biomass. Thus, leaf number does not invariably correlate with individual leaf mass or individual leaf area (**Figure 3B**). Furthermore, it is worth noting that our results do not support this prediction that stem length is a primary constraint on twig leaf number (Yagi, 2004) (see **Table 3**).

CONCLUSION

We have demonstrated that isometric scaling relationships hold among leaf biomass, stem biomass, and total twig biomass at the twig level within each of three different forests communities along an elevational gradient. These scaling relationships are insensitive to differences in species composition and variations in environmental conditions along an elevational gradient. Further, consistent with biomass allocation patterns reported for large trees, our analyses show that leaf biomass scales approximately as the 2.0-power of twig stem diameter across the three communities, but fail to reveal a significant relationship between leaf biomass and height/length reported for trees. These observations suggest to us that stem diameter imposes the primary constraint on the overall biomass allocation pattern in twigs because of the nature of hydrodynamic principles governing the transport of essential resources. A growth-hydraulic model rather than a growth-mechanical model appears to govern the scaling relationships among stem length, diameter, and the biomass (Niklas and Spatz, 2004; Fan et al., 2017). Indeed, recent analyses also indicate that tree diameter might be a better predictor of above-ground biomass (Chave et al., 2014; Paul et al., 2016).

AUTHOR CONTRIBUTIONS

JS and DC conceived and designed the experiments. JS, MLy, QZ, and MLi performed the experiments. JS and MW analyzed the data. JS, MW, KN, and DC wrote the manuscript. All authors contributed critically to the drafts and gave final approval for publication.

FUNDING

This work was supported by the National Natural Science Foundation of China (31722007), the National Key Research and Development Program of China (2017YFC0505400), and the Fujian Natural Science Funds for Distinguished Young Scholars (2018J07003).

ACKNOWLEDGMENTS

We thank Y. R. Guo, L. Cheng, and R. B. Yuan, for their hospitality during the implementation of our study in the National Nature Reserve of Wuyi Mountain.

SUPPLEMENTARY MATERIAL

The Supplementary Material for this article can be found online at: https://www.frontiersin.org/articles/10.3389/fpls.2019.00185/full#supplementary-material

REFERENCES

Blomberg, S. P., Garland, T., and Ives, A. (2003). Testing for phylogenetic signal in comparative data: behavioral traits are more labile. *Evolution* 57, 717–745. doi: 10.1111/j.0014-3820.2003.tb00285.x

Cannell, M. G. R. (1982). *World Forest Biomass and Primary Production Data*. London: Academic Press.

Chave, J., Rejou-Mechain, M., Burquez, A., Chidumayo, E., Colgan, M. S., Delitti, W. B., et al. (2014). Improved allometric models to estimate the aboveground biomass of tropical trees. *Glob. Chang. Biol.* 20, 3177–3190. doi: 10.1111/gcb.12629

Cheng, D. L., Li, T., Zhong, Q. L., and Wang, G. X. (2010). Scaling relationship between tree respiration rates and biomass. *Biol. Lett.* 6, 715–717. doi: 10.1098/rsbl.2010.0070

Cheng, D. L., and Niklas, K. J. (2007). Above- and below-ground biomass relationships across 1534 forested communities. *Ann. Bot.* 99, 95–102. doi: 10.1093/aob/mcl206

Enquist, B. J., Allen, A. P., Brown, J. H., Gillooly, J. F., Kerkhoff, A. J., Niklas, K. J., et al. (2007). Biological scaling: does the exception prove the rule? *Nature* 445, E9–E10.

Enquist, B. J., and Niklas, K. J. (2002). Global allocation rules for patterns of biomass partitioning in seed plants. *Science* 295, 1517–1520. doi: 10.1126/science.1066360

Fan, Z. X., Sterck, F., Zhang, S. B., Fu, P. L., and Hao, G. Y. (2017). Tradeoff between stem hydraulic efficiency and mechanical strength affects leaf-stem allometry in 28 *Ficus* tree species. *Front. Plant Sci.* 8:1619. doi: 10.3389/fpls.2017.01619

Grace, J. B., Michael, A. T., Smith, M. D., Seabloom, E., Andelman, S. J., Meche, G., et al. (2007). Does species diversity limit productivity in natural grassland communities? *Ecol. Lett.* 10, 680–689.

Hoch, G., and Körner, C. (2012). Global patterns of mobile carbon stores in trees at the high-elevation tree line. *Glob. Ecol. Biogeogr.* 21, 861–871. doi: 10.1111/j.1466-8238.2011.00731.x

Huang, Y., Lechowicz, M. J., Price, C. A., Li, L., Wang, Y., and Zhou, D. (2015). The underlying basis for the trade-off between leaf size and leafing intensity. *Funct. Ecol.* 30, 199–205. doi: 10.1111/1365-2435.12491

Kembel, S. W., Cowan, P. D., Helmus, M. R., Cornwell, W. K., Morlon, H., Ackerly, D. D., et al. (2010). Picante: R tools for integrating phylogenies and ecology. *Bioinformatics* 26, 1463–1464. doi: 10.1093/bioinformatics/btq166

King, D. A. (2011). "Size-related changes in tree proportions and their potential influence on the course of height growth," in *Size- and Age-Related Changes in Tree Structure and Function,* eds F. C. Meinzer, B. Lachenbruch, and T. E. Dawson (Dordrecht: Springer), 165–191. doi: 10.1007/978-94-007-1242-3_6

Kleiman, D., and Aarssen, L. W. (2007). The leaf size/number trade-off in trees. *J. Ecol.* 95, 376–382. doi: 10.1111/j.1365-2745.2006.01205.x

Li, M., Zheng, Y., Fan, R. R., Zhong, Q. L., and Cheng, D. L. (2017). Scaling relationships of twig biomass allocation in *Pinus hwangshanensis* along an altitudinal gradient. *PLoS One* 12:e0178344. doi: 10.1371/journal.pone.0178344

Mayor, J. R., Sanders, N. J., Classen, A. T., Bardgett, R. D., Clement, J. C., Fajardo, A., et al. (2017). Elevation alters ecosystem properties across temperate treelines globally. *Nature* 542, 91–98. doi: 10.1038/nature21027

Milla, R. (2009). The leafing intensity premium hypothesis tested across clades, growth forms and altitudes. *J. Ecol.* 97, 972–983. doi: 10.1111/j.1365-2745.2009.01524.x

Niklas, K. J. (1992a). Gravity-induced effects on material properties and size of leaves on horizontal shoots of acer saccharum (aceraceae). *Am. J. Bot.* 79, 820–827. doi: 10.1002/j.1537-2197.1992.tb13659.x

Niklas, K. J. (1992b). *Plant Biomechanics: An Engineering Approach to Plant form and Function*. Chicago, IL: University of Chicago press.

Niklas, K. J. (2004). Plant allometry: is there a grand unifying theory? *Biol. Rev.* 79, 871–889. doi: 10.1017/S1464793104006499

Niklas, K. J., and Enquist, B. J. (2002a). Canonical rules for plant organ biomass partitioning and annual allocation. *Am. J. Bot.* 89, 812–819. doi: 10.3732/ajb.89.5.812

Niklas, K. J., and Enquist, B. J. (2002b). On the vegetative biomass partitioning of seed plant leaves, stems, and roots. *Am. Nat.* 159, 482–497. doi: 10.1086/339459

Niklas, K. J., and Spatz, H. C. (2004). Growth and hydraulic (not mechanical) constraints govern the scaling of tree height and mass. *Proc. Natl. Acad. Sci. U.S.A.* 101, 15661–15663. doi: 10.1073/pnas.0405857101

Niklas, K. J., and Spatz, H. C. (2010). Worldwide correlations of mechanical properties and green wood density. *Am. J. Bot.* 97, 1587–1594. doi: 10.3732/ajb.1000150

Olson, M. E., Aguirrehernández, R., and Rosell, J. A. (2009). Universal foliage-stem scaling across environments and species in dicot trees: plasticity, biomechanics and Corner's rules. *Ecol. Lett.* 12, 210–219. doi: 10.1111/j.1461-0248.2008.01275.x

Paradis, E., Claude, J., and Strimmer, K. (2004). Ape: analyses of phylogenetics and evolution in R language. *Bioinformatics* 20, 289–290. doi: 10.1093/bioinformatics/btg412

Paul, K. I., Roxburgh, S. H., Chave, J., England, J. R., Zerihun, A., Specht, A., et al. (2016). Testing the generality of above-ground biomass allometry across plant functional types at the continent scale. *Glob. Chang. Biol.* 22, 2106–2124. doi: 10.1111/gcb.13201

Pickup, M., Westoby, M., and Basden, A. (2005). Dry mass costs of deploying leaf area in relation to leaf size. *Funct. Ecol.* 19, 88–97. doi: 10.1111/j.0269-8463.2005.00927.x

R Core Team (2012). *R: A Language and Environment for Statistical Computing*. Vienna: R Foundation for Statistical Computing.

Reich, P. B., Tjoelker, M. G., Machado, J. L., and Oleksyn, J. (2006). Universal scaling of respiratory metabolism, size and nitrogen in plants. *Nature* 439, 457–461. doi: 10.1038/nature04282

Ryan, M. G., and Yoder, B. J. (1997). Hydraulic limits to tree height and tree growth. *BioScience* 47, 235–242. doi: 10.2307/1313077

Shinozaki, K., Yoda, K., Hozumi, K., and Kira, T. (1964). A quantitative analysis of plant form: the pipe model theory. II. Further evidence of the theory and its application in forest ecology. *Jpn. J. Ecol.* 14, 133–139.

Smith, D. D., Sperry, J. S., and Adler, F. R. (2017). Convergence in leaf size versus twig leaf area scaling: do plants optimize leaf area partitioning? *Ann. Bot.* 119, 447–456. doi: 10.1093/aob/mcw231

Sun, S., Jin, D., and Shi, P. (2006). The leaf size-twig size spectrum of temperate woody species along an altitudinal gradient: an invariant allometric scaling relationship. *Ann. Bot.* 97, 97–107. doi: 10.1093/aob/mcj004

Suzuki, M. (2003). Size structure of current-year shoots in mature crowns. *Ann. Bot.* 92, 339–347. doi: 10.1093/aob/mcg144

Tyree, M. T., and Ewers, F. W. (1991). The hydraulic architecture of trees and other woody-plants. *New Phytol.* 119, 345–360. doi: 10.1111/j.1469-8137.1991.tb00035.x

Warton, D. I., Duursma, R. A., Falster, D. S., and Taskinen, S. (2012). Smatr 3-an R package for estimation and inference about allometric lines. *Methods Ecol. Evol.* 3, 257–259. doi: 10.1111/j.2041-210X.2011.00153.x

Warton, D. I., Wright, I. J., Falster, D. S., and Westoby, M. (2006). A review of bivariate line-fitting methods for allometry. *Biol. Rev.* 81, 259–291. doi: 10.1017/S1464793106007007

West, G. B., Brown, J. H., and Enquist, B. J. (1997). A general model for the origin of allometric scaling laws in biology. *Science* 276, 122–126. doi: 10.1126/science.276.5309.122

West, G. B., Brown, J. H., and Enquist, B. J. (1999). The fourth dimension of life: fractal geometry and allometric scaling of organisms. *Science* 284, 1677–1679. doi: 10.1126/science.284.5420.1677

Westoby, M., Falster, D. S., Moles, A. T., Vesk, P. A., and Wright, I. J. (2002). Plant ecological strategies: some leading dimensions of variation between species. *Ann. Rev. Ecol. Syst.* 33, 125–159. doi: 10.1146/annurev.ecolsys.33.010802.150452

Westoby, M., and Wright, I. J. (2003). The leaf size-twig size spectrum and its relationship to other important spectra of variation among species. *Oecologia* 135, 621–628. doi: 10.1007/s00442-003-1231-6

Wright, I. J., Falster, D. S., Pickup, M., and Westoby, M. (2006). Cross-species patterns in the coordination between leaf and stem traits, and their implications for plant hydraulics. *Physiol. Plant.* 127, 445–456. doi: 10.1111/j.1399-3054.2006.00699.x

Xiang, S., and Liu, Y. L. (2009b). Stem architectural effect on leaf size, leaf number, and leaf mass fraction in plant twigs of woody species. *Int. J. Plant Sci.* 170, 999–1008. doi: 10.1086/605114

Xiang, S., Wu, N., and Sun, S. C. (2009a). Within-twig biomass allocation in subtropical evergreen broad-leaved species along an altitudinal gradient: allometric scaling analysis. *Trees* 23, 637–647. doi: 10.1007/s00468-008-0308-6

Yagi, T. (2000). Morphology and biomass allocation of current-year shoots of ten tall tree species in cool temperate Japan. *J. Plant Res.* 113, 171–183. doi: 10.1007/PL00013928

Yagi, T. (2004). Within-tree variations in shoot differentiation patterns of 10 tall tree species in a Japanese cool-temperate forest. *Can. J. Bot.* 82, 228–243. doi: 10.1139/b03-124

Yang, Y., He, X., Xu, X., and Yang, D. (2015). Scaling relationships among twig components are affected by sex in the dioecious tree *Populus cathayana*. *Trees* 29, 737–746. doi: 10.1007/s00468-014-1151-6

Zhang, Z., Zhong, Q., Niklas, K. J., Liang, C., Yang, Y., and Cheng, D. (2016). A predictive nondestructive model for the covariation of tree height, diameter, and stem volume scaling relationships. *Sci. Rep.* 6:31008. doi: 10.1038/srep31008

Conflict of Interest Statement: The authors declare that the research was conducted in the absence of any commercial or financial relationships that could be construed as a potential conflict of interest.

frontiers in Plant Science

ORIGINAL RESEARCH
published: 09 January 2019
doi: 10.3389/fpls.2018.01958

Plant Functional Traits Are the Mediators in Regulating Effects of Abiotic Site Conditions on Aboveground Carbon Stock-Evidence From a 30 ha Tropical Forest Plot

Wensheng Bu[1,2,3], Jihong Huang[2,3], Han Xu[4], Runguo Zang[2,3], Yi Ding[2,3], Yide Li[4], Mingxian Lin[4], Jinsong Wang[5] and Cancan Zhang[1]*

[1] 2011 Collaborative Innovation Center of Jiangxi Typical Trees Cultivation and Utilization, Jiulianshan National Observation and Research Station of Chinese Forest Ecosystem, College of Forestry, Jiangxi Agricultural University, Nanchang, China, [2] Key Laboratory of Forest Ecology and Environment of State Forestry Administration, Institute of Forest Ecology, Environment and Protection, Chinese Academy of Forestry, Beijing, China, [3] Co-Innovation Center for Sustainable Forestry in Southern China, Nanjing Forestry University, Nanjing, China, [4] Key Laboratory of State Forestry Administration on Tropical Forestry Research, Research Institute of Tropical Forestry, Chinese Academy of Forestry, Guangzhou, China, [5] Key Laboratory of Ecosystem Network Observation and Modeling, Institute of Geographic Sciences and Natural Resources Research, Chinese Academy of Sciences, Beijing, China

OPEN ACCESS

Edited by:
Christian Ammer, Georg-August-Universität Göttingen, Germany

Reviewed by:
Mingjian Yu, Zhejiang University, China
Andreas Fichtner, Leuphana University, Germany

***Correspondence:**
Runguo Zang
zangrung@caf.ac.cn

Specialty section:
This article was submitted to Functional Plant Ecology, a section of the journal Frontiers in Plant Science

Received: *17 September 2018*
Accepted: *17 December 2018*
Published: *09 January 2019*

Citation:
Bu W, Huang J, Xu H, Zang R, Ding Y, Li Y, Lin M, Wang J and Zhang C (2019) Plant Functional Traits Are the Mediators in Regulating Effects of Abiotic Site Conditions on Aboveground Carbon Stock-Evidence From a 30 ha Tropical Forest Plot. Front. Plant Sci. 9:1958. doi: 10.3389/fpls.2018.01958

Understanding the relative contribution of abiotic and biotic factors to the formation of ecosystem functioning across scales is vital to evaluate ecosystem services. Here, we elucidate the effects of abiotic site conditions (i.e., soil and topographic properties) and plant functional traits on variations of stand aboveground carbon (AGC) stock in an old-growth tropical montane rain forest. The response-effect framework in functional ecology is adopted in examining how plant functional traits respond to environmental changes and affect ecosystem functioning. We measured specific leaf area and wood density of 270 woody plant species and estimated stand AGC stocks in a 30-ha forest plot. The relationships among environmental factors (ENVIRONMENT), community-weighted means of functional traits (TRAITS) and stand AGC stocks across nested spatial scales were disentangled by structural equation modeling. The results showed that the stands composed of 'acquisitive' species (high specific leaf area and low wood density) had low AGC, whereas stands composed of 'conservative' species (low specific leaf area and high wood density) had high AGC. TRAITS responded to ENVIRONMENT and affected AGC directly. ENVIRONMENT had an indirect effect on AGC through its direct effect on TRAITS. TRAITS were more important than ENVIRONMENT in driving variations of AGC. The effects of TRAITS on AGC increased, while the effects of ENVIRONMENT on AGC decreased with the increase of spatial scales in the tropical montane rain forest. Our study suggests that plant functional traits are the mediators in regulating effects of abiotic site conditions on ecosystem functions.

Keywords: biodiversity and ecosystem function, plant economics spectrum, response-effect framework, specific leaf area, wood density

INTRODUCTION

A variety of global changes are driving an increase in rates of species extinctions. Biodiversity loss in the 21st century has been one of the major drivers of ecosystem change (Hooper et al., 2012). Over 60% of ecosystem services are deteriorating or are already overused at global scale (Assessment, 2005), understanding the underlying mechanisms of biotic communities in regulating ecosystem processes is a pressing issue in ecology (Liu et al., 2018). Many studies have proved that ecosystem functions are affected by species composition (Liu et al., 2018), functional trait composition of the community (Liu et al., 2016); trait diversity and phylogenetic diversity (Cadotte et al., 2009) and tree size (Stephenson et al., 2014) and so on.

Functional traits are defined as morpho-physio-phenological traits that impact the fitness of individual species via their effects on growth, reproduction and survival, the three components of individual performance (Violle et al., 2007). Moreover, functional traits can indicate how a species relates and responds to its environment, which offers a powerful approach to addressing ecological questions (McGill et al., 2006). Abiotic site conditions (i.e., soil, topographic properties and light environment) can influence ecosystem processes directly by changing the ecosystem flux rate of energy and matter or indirectly by changing the physiological rate of plants, which is determined by the functional traits of plants (Boyer et al., 2009; Geert Hiddink et al., 2009; Lavorel et al., 2011; Hajek et al., 2016). As for plant functions, at least two dimensions exist, although it could be extended to include more dimensions (Westoby et al., 2002). Two of these dimensions were leaf economics spectrum (LES) and wood economics spectrum (WES). LES and WES are most commonly represented by specific leaf area (Wright et al., 2004) and wood density (Chave et al., 2009), respectively. These economics spectra can respond to environmental conditions, e.g., leaf traits are influenced by soil resource availability (Ordoñez et al., 2009) and topographical factors (Butterfield and Suding, 2013), while wood density is affected by soil fertility (Nishimua et al., 2007). Furthermore, these economics spectra also affect ecosystem functions, e.g., LES is related to biogeochemistry (Freschet et al., 2010) and above-ground net primary productivity (Mokany et al., 2008) while wood density is correlated with stem growth rate and carbon stock (Chao et al., 2008). Therefore, understanding the effects of environmental drivers on ecosystem functions through plant functional composition is central to predicting the net provisioning of multiple ecosystem services (Lavorel and Grigulis, 2012).

There is a growing consensus that community functional composition determines ecosystem functioning and related services (Garnier et al., 2004; Petchey and Gaston, 2006; Díaz et al., 2007; Lavorel, 2013). There are two hypotheses to explain how species traits within a community may influence ecosystem processes. The mass ratio hypothesis suggests that the effect of a given species on ecosystem processes is proportional to its relative contribution to the total biomass of the community (additive effect) (Grime, 1998). While the functional diversity hypothesis implies that the effects of species on ecosystem processes are not predictable from single-species traits due to antagonistic or synergistic interactions among species (Petchey et al., 2004; Mouillot et al., 2011). These non-additive effects have been considered to be mainly caused by complementary use of resources and facilitation or competition (Hooper et al., 2005; Dias et al., 2013). Several studies suggested that plant functional trait effects on ecosystem functions were mainly due to the biomass ratio mechanism (Mokany et al., 2008; Laughlin, 2011; Lavorel et al., 2011).

Global climatic change as a result of rising level of carbon dioxide in the atmosphere has greatly stimulated the interest in biological carbon sequestration in natural ecosystems, such as forests. Connecting with a series of ecosystem processes, forest carbon stock is considered as one of the paramount indicators of forest ecosystem functioning. An effective climate control by terrestrial ecosystems not only depends on the rate of carbon uptake by primary producers, but also on the rate of carbon release from the biota (Díaz et al., 2009). Carbon stocks at any given point in time reflect the net balance between these uptake, loss and retention processes. As different plant species differ in their ability to capture, store and release carbon, the functional composition of plant communities, under a given regional climatic regime, should be a major driver of carbon sequestration in terrestrial ecosystems (De Deyn et al., 2008).

Recent ecosystem research tried to incorporate functional traits into a response-effect framework, which examines the response of plants to environmental change by the "response traits" and plant effect on ecosystem functions by the "effect traits" (Grace, 2006; Suding et al., 2008). Structural equation modeling (SEM) enables scientists to use field data to test hypotheses about causal relations and pathways of ecosystem functioning (Shipley, 2002). As the response-effect framework has the potential to incorporate community level functional traits into the impacts of environmental conditions on ecosystem functioning, disentangling the complex interactions among environment, traits and ecosystem functions, it is well suited for the analysis of SEM.

Most of the studies have just focused on the relationships between environmental conditions and plant functional traits or on the relations between functional traits and ecosystem functions. A few studies have integrated environment, traits and ecosystem functions into one system to explore the interactions among these three aspects (Lavorel and Grigulis, 2012; Liu et al., 2016). For an example, a study has shown that individual-level functional traits associated with soil environment and identity of neighboring individuals strongly predict ecosystem functions (e.g., tree growth rate) in a subtropical forest (Liu et al., 2016). Therefore, knowledge about linkage between environmental factors and ecosystem functioning through functional traits in natural ecosystems is still lacking. In this paper, we assess the relative effects of environmental variations and community functional composition on aboveground carbon (AGC) stock in a 30-ha old-growth tropical montane rainforest plot on Hainan Island, China. Using the response-effect framework of Suding et al. (2008), we built a SEM to elucidate how environmental factors influence AGC stock through plant functional traits across three nested spatial scales (40 m × 40 m, 60 m × 60 m, and 80 m × 80 m) in this forest plot. We hypothesized

that: (1) Both abiotic (soil/topographic) factors and biotic factors (plant functional traits) had significant influences on the stand AGC stock at each spatial scale. (2) Plant functional traits at community level mediate the links between physical environmental variations and stand AGC stock through the response-effect framework. (3) Plant functional trait effects on stand AGC stock should increase with increasing spatial scale due to additive effects, meanwhile environmental effects on stand AGC stock should decrease with increasing spatial scale due to the homogenization of environmental variables.

MATERIALS AND METHODS

Study Site

This study was conducted in a 30-ha (500 m × 600 m) forest plot of old-growth (naturally grows over 150 years) tropical montane rainforest in Jianfengling Nature Reserve (18°23′–18°50′N, 108°36′–109°05′E) on Hainan Island in southern China. The Jianfengling Nature Reserve is located at the northern edge of the Asian tropical forest, covering ca 640 km^2, with an elevation range of ca 0–1,412 m a.s.l. The mean annual temperature is 19.7°C and annual precipitation is 2,651 mm, with a distinct wet season from May to October and a dry season from November to April of the following year. The soil type is latosol, which is broadly distributed in tropical regions of south China (Jiang et al., 2002).

Data Collection

Field investigation was conducted in the 30-ha plot of old-growth tropical montane rainforests and data collection followed the plot census protocol established by the Center for Tropical Forest Sciences Network (John et al., 2007). The entire 500 m × 600 m plot was divided into 750 quadrats of 20 m × 20 m and elevations at the four corners of each quadrat were measured by the total station (Topcon GTS332N total station, Topcon, Japan). The study area is characterized by a rugged terrain (elevations ranged from 868.3 to 975.2 m and slopes in the 20 m × 20 m quadrat ranged from 1.7° to 49.2°). All plants with diameter at breast height (DBH) ≥ 1 cm were tagged, identified, measured and mapped in the summer of 2011.

For soil sampling, 195 samples that come from the center of every 40 m × 40 m quadrat were arrayed throughout the plot in a regular grid and referred to as "base points." For every "base point," two additional sampling points were located nearby. Each additional point was located at a random compass bearing away from its associated base point. One-third (1/3) of the randomly selected additional points were located at 2 m away from their associated base points, one third (1/3) were located at 5 m away, and one third (1/3) were located at 15 m away. A soil core with 4 cm diameter and 10 cm depth was collected in each sampling point in 2012 and a total of 585 soil samples were sampled in this 30-ha plot. Soil organic matter (SOM), pH, total and available nitrogen, phosphorus, and potassium, exchangeable potassium, exchangeable sodium, exchangeable calcium, exchangeable magnesium, and exchangeable base (EB) concentrations were determined according to Forest Soil Analysis Methods (Zhang et al., 1999).

A total of 270 tree and shrub species (belonging to 145 genera and 71 families) was found in the 30-ha plot. The leaf traits were measured for all these species in at least 10 well-growth individuals per species (4,203 individuals in total) and wood density was measured for at least five individuals per species (2,015 individuals in total) in the plot or nearby the plot from July to October (growing season) in 2011, using standardized protocols for plant functional trait measurements (Cornelissen et al., 2003). For each individual, two to ten recently expanded leaves, including petioles and rachises of compound leaves were collected. Leaf surface area was measured with a leaf area meter (LI-COR 3100C Area Meter, LI-COR, Lincoln, NE, United States). Laminar dry mass was measured by drying the specimen to a constant mass at 60°C (around 72 h) and specific leaf area (SLA, $cm^2\ g^{-1}$) was calculated for each lamina as the ratio of leaf surface area to leaf mass. Wood density was determined from increment cores and trunks. The cores were taken from bark to pith of trees (DBH ≥ 5 cm) with an increment borer. Core lengths were then measured with a Mitutoyo digital micrometer and core volumes computed for cylinders of the measured length and inner diameter of the borer. For some shrub species, we had to sample trunk for individuals (DBH ≤ 5 cm) nearby the plot and removed the phloem and bark, measured fresh volume by water displacement. Each sample was quickly wrapped in a sealed plastic bag after sampling. These samples were drying in an oven at 103°C for over 72 h until they became constant weight. Wood density (WD, $g\ cm^{-3}$) was computed as the ratio of oven dry mass to fresh volume and averaged for each species.

We partitioned the 30-ha plot into three spatial scales: 40 m × 40 m (180 subplots), 60 m × 60 m (80 subplots), 80 m × 80 m (42 subplots) and measured the abundance weighted community mean trait for specific leaf area (CWM_SLA) and wood density (CWM_WD) in each scale. CWM trait values were calculated as the mean across species of their trait value weighted by the species relative abundance (Ackerly and Cornwell, 2007) using the FD package in R 2.14 (R Development Core Team, 2011) with the function dbFD (Villéger et al., 2008).

We calculated stand aboveground biomass using the following allometric regression for moist forest (Chave et al., 2014): $AGB = 0.0559\ \rho(DBH)^2H$, where ρ is the wood density for each species ($g\ cm^{-3}$), DBH is the diameter at breast height (1.30 m in cm) and H is tree height (m). We converted plant woody biomass to carbon stock multiplying it by a factor of 0.5, since carbon stock roughly represents 50% of dry woody biomass (Tomlinson et al., 2013). We focused on AGC stock because carbon stocks at any given point in time reflect the net balance between uptake, loss and retention processes (Conti and Díaz, 2013).

Statistical Analysis

To meet model assumptions, some predictors (SOM, EB, SLA, AGC) were a log-transformed. To assess how community weighted means of functional traits affect AGC, we examined the relationships between CWM_SLA/CWM_WD and AGC in

each spatial scale by linear regression. Based on the response-and-effect framework (see Figure 1a in Suding et al., 2008), to explore the causal relationship among abiotic environmental factors, functional traits, and AGC, we used SEMs to estimate the path coefficients and variation of dependent variables. We hypothesized that abiotic environmental factors affect the functional trait and AGC, respectively, and functional traits will also directly affect AGC. In other words, we expected that abiotic environment affect AGC indirectly via their effect on plant traits. To reduce the complexity of the SEM, we projected TRAITS and ENVIRONMENT in a redundancy analysis (RDA) axis at each spatial scale (40 m × 40 m, 60 m × 60 m and 80 m × 80 m) and chose the most relevant variables to reduce redundancy among these explanatory variables (see **Supplementary Figure S1**). After this procedure, the parameters retained for ENVIRONMENT were terrain convexity (TC), SOM, and EB, since TC and SOM were tightly associated with CWM_WD, as well as EB was tightly associated with CWM_SLA at each spatial scale. Thus, we assumed that functional traits (TRAITS) is a latent variable, which is related to the real measured variables (CWM_SLA and CWM_WD, the typical indicators of LES and WES); Environmental factors (ENVIRONMENT) is also a latent variable, which is related to the real measured variables (TC, SOM, and EB). The final hypothesized SEM (**Figure 1A**) will run at different spatial scales and all SEMs was fit using maximum likelihood as implemented in Amos 18.0.1 software (Amos Development Corp., Spring House, PA, United States). The quality of SEM was judged by the parameters of model (χ^2, *CMIN/df*, *CFI*, *RMSEA* and *P*-value). The direct effects were showed in the final SEMs, meanwhile the indirect effects occur if two variables are connected through paths to and from a third variable.

RESULTS

The Influence of Community-Weighted Means of Functional Traits on Stand Aboveground Carbon Stocks at Various Spatial Scales

Results of linear regressions (**Figure 2**) indicated that functional traits at community level showed significant linear relations with AGC in each spatial scale. Specific leaf area at community level (CWM_SLA) was negatively associated with AGC and the effect of CWM_SLA on AGC increased with increasing spatial scale (R^2 from 0.24 to 0.46). However, wood density at community level (CWM_WD) was positively associated with AGC and the effect of CWM_WD on AGC increased with increasing spatial scale (R^2 from 0.28 to 0.36).

The Relationships Among Environmental Factors, Functional Traits, and Carbon Stocks at Various Spatial Scales

The final SEMs showed good consistency with the field data at 40 m × 40 m (χ^2 = 14.859, *df* = 8, *n* = 180, *P* = 0.062, *CMIN/df* = 1.857, *CFI* = 0.986, *RMSEA* = 0.069), at 60 m × 60 m (χ^2 = 14.894, *df* = 8, *n* = 80, *P* = 0.061, *CMIN/df* = 1.862, *CFI* = 0.973, *RMSEA* = 0.104) and at 80 m × 80 m (χ^2 = 10.580, *df* = 8, *n* = 42, *P* = 0.227, *CMIN/df* = 1.322, *CFI* = 0.981, *RMSEA* = 0.089), respectively. Comparison with the hypothesized model, the non-significant pathway ($P > 0.05$), the direct effect of ENVIRONMENT on AGC (Environment → AGC) was removed. These final models explained 78%, 67%, and 59% variation of TRAITS for at the 40 m × 40 m, 60 m × 60 m, and 80 m × 80 m scales, respectively, and the explained variations of AGC increased from 29% through 33% to 47%, respectively (**Figures 1B–D**). The SEMs revealed direct effect of ENVIRONMENT on TRAITS as well as TRAITS on AGC, meanwhile there was no significant direct effect of ENVIRONMENT on AGC. However, ENVIRONMENT had an indirect effect on AGC through its effects on TRAITS. TRAITS in the SEM apparently mediated the direct effects of ENVIRONMENT on AGC.

Terrain convexity always had the highest effect (>0.7) among ENVIRONMENT at each scale (**Figures 1B–D**). The direct effect of SOM increased slightly (0.45 to 0.57) while that of EB increased greatly (−0.29 to −0.57) with the increase of spatial scales. TRAITS always had a large effect (>0.9) on CWM_SLA and CWM_WD. ENVIRONMENT had a strong negative effect on TRAITS and this direct effect decreased with the increase of spatial scales (−0.89 to −0.77). TRAITS also had a strong negative effect on AGC and this direct effect increased with the increase of spatial scales (−0.54 to −0.68). ENVIRONMENT only have an indirect effect on AGC through TRAITS and this indirect effect expanded gradually with the increase of spatial scales (0.45 to 0.53, in **Supplementary Table S2**). TRAITS always had a larger effect on AGC than ENVIRONMENT at each spatial scale and the difference of this effect on AGC increased gradually from 40 m × 40 m (0.45 for Environment and −0.54 for Traits) to 80 m × 80 m (0.53 for Environment and −0.68 for Traits).

Overall, TC played the most important role in affecting TRAITS and AGC among environmental variables, meanwhile SOM and EB became more and more important on driving variations of TRAITS and AGC with increasing spatial scale. ENVIRONMENT always had a strong effect on TRAITS, though this effect decreased gradually with the increase of spatial scale. TRAITS also had a large effect on AGC and its effect increased with increasing spatial scale. Therefore, TRAITS seemed to act as the mediators in regulating the effects of environmental change on AGC. Moreover, TRAITS always play a larger role in affecting AGC than environmental factors at each spatial scale.

DISCUSSION

The Response of Functional Traits to Environmental Factors

Environmental factors can be considered as filters constraining which individuals bearing specific attributes of 'response traits' are able to be sorted and persist in a community (Keddy, 1992). Different sets of response traits to environmental factors have been recognized in plants (Ackerly, 2004; Kraft et al., 2008;

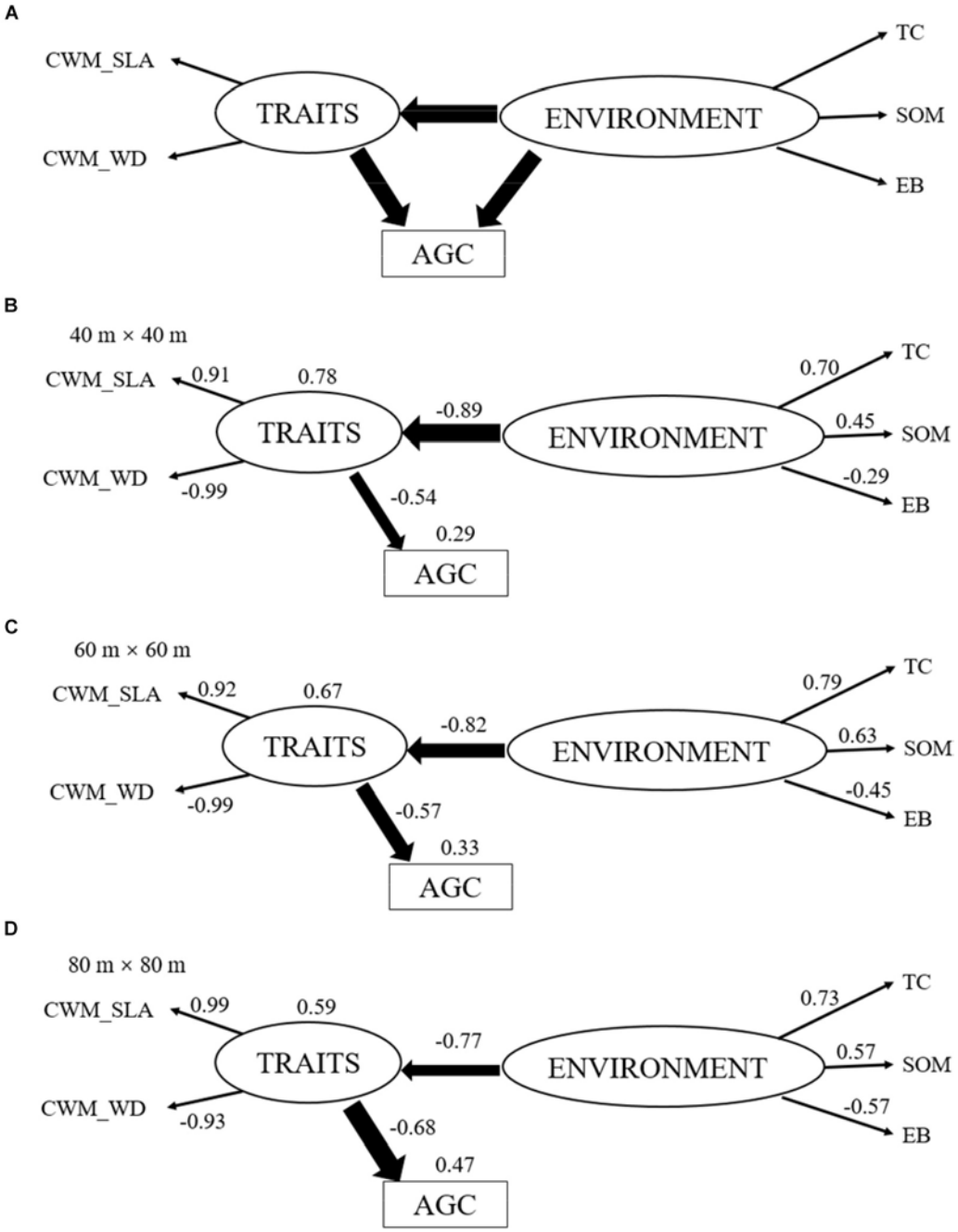

FIGURE 1 | Hypothesized structural equation model **(A)**. This model provides a multivariate perspective about how abiotic site conditions [ENVIRONMENT, including terrain convexity (TC), soil organic matter (SOM) and exchangeable base (EB)] and functional traits at community level [TRAITS, including specific leaf area and wood density at community level (CWM_SLA and CWM_WD)] interact to influence aboveground carbon stock (AGC). One-headed arrows represent the hypothesized causal relationships between variables. The final structural equation models at 40 m × 40 m scale **(B)**, 60 m × 60 m scale **(C)**, 80 m × 80 m scale **(D)**. The value nearby arrows represents for the standardized regression path coefficient ($P < 0.05$) and values at the upper right corner of variables represent for the percentage of variance explained by the model. Arrow width indicates the strength of the relationship. The paths of ENVIRONMENT to AGC at these three scales were deleted, due to the non-significant relationship ($P > 0.05$).

Poorter et al., 2009). The response of 'conservative' strategy (low specific leaf area and high wood density) to larger TC indicates that there is higher specific leaf area and low wood density in valley than in ridge. The valley habitat is often characterized by high soil water content and nutrient availability (Jobbágy and Jackson, 2003), which always lead to high specific leaf area and low wood density (Baker et al., 2004; Douma et al., 2011). The species in valley have to expand their leaf surface area to gain

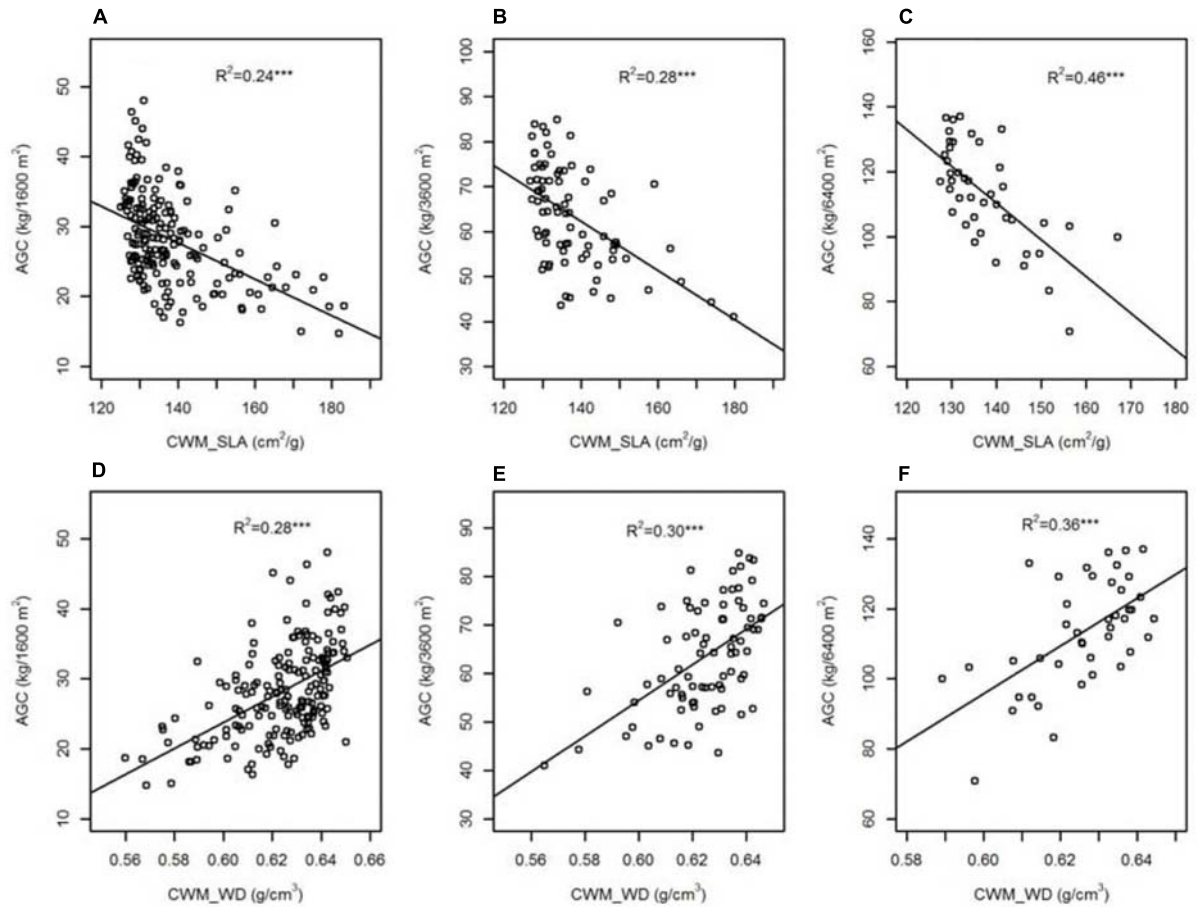

FIGURE 2 | The relationships between specific leaf area/wood density at community level (CWM_SLA/CWM_WD) and aboveground carbon stock (AGC) across nested spatial scale [**(A,D)** 40 m × 40 m, **(B,E)** 60 m × 60 m, **(C,F)** 80 m × 80 m]. ***$P < 0.001$.

a higher light availability due to a shaded condition (Andersen et al., 2012). And there is more species living in valley due to a greater light heterogeneity, especially some shrub species, which often have lower wood density than tree species (Bu, 2013). The reason that why TC plays the most important role in affecting functional traits among environmental factors may be attributed to that it is a comprehensive index of environmental heterogeneity (Kusumoto et al., 2013). In general, topographic features such as TC relate to light availability, water shifting and nutrient distribution (John et al., 2007). Unlike soil properties, topography is not a direct environmental variable but an indirect, or a proxy variable that characterizes the overall quality of a habitat (Legendre et al., 2009).

The response of 'conservative' strategy to high SOM was in line with the report of Garnier et al. (2004) in grassland. SOM is mostly derived from plant inputs that have undergone processing by microorganisms in the presence of potential reactions with soil minerals (Hobbie et al., 2007). Increases of SOM during the course of succession are well documented (Lavorel et al., 1999), even in old-growth forest with time (Zhou et al., 2006). It is probably due to a combination of an increase in the rate of litter input per unit ground area as the standing biomass of the communities increases, and a decrease in the rate of litter decomposition, as fast growing species that produce high-quality litter are progressively replaced by slow-growing species producing a litter of lower quality (Garnier et al., 2004). In our study, slow-growing species with low specific leaf area and high wood density also had a low rate of litter decomposition and then caused an increase of SOM. Therefore, 'conservative' community tends to hold high SOM.

Cation uptake and supply may explain the positive effect of EB on functional traits. Atmospheric inputs of Ca, K, and Mg are usually less than plant uptake, which is typically supplied through mineral weathering, mineralization, and leaching from plant biomass (Berthrong et al., 2009). In our study, atmospheric inputs, mineral weathering, mineralization might be similar across the 30-ha plot of old-growth forest, but leaching from plant biomass will change by different community functional traits. Fast-growing species with high specific leaf area and low wood density generally had a high rate of litter decomposition and nutrients in litter can return quickly to soil (Reich, 2014). Therefore, the change of EB in soil may correlate with the turnover of nutrients and their cycling in plant-soil feedback (Jobbágy and Jackson, 2003). Because plant litter in bark, leaves,

twigs, and reproductive structures contained the majority of the total biomass Ca and Mg (Day and Monk, 1977), community with "acquisitive" strategies tend to have higher exchangeable cations through accelerated leaching from plant biomass.

In our SEM, ENVIRONMENT was composed of TC, SOM, and EB. TRAITS composing of high specific leaf area and low wood density were corresponded to 'acquisitive' plants with fast nutrient acquisition and turnover. Thus, the negative relation between ENVIRONMENT and TRAITS implies large TC, high SOM and low EB will make community tend to 'conservative' strategy (low specific leaf area and high wood density). The tight correlation between variation in habitat preference and plant economics spectrum suggests that the topographically and edaphically associated environmental filter mediated through morphological and physiological traits of species is an important mechanism in shaping spatial patterns of tropical forest community (Kusumoto et al., 2013).

The Effects of Functional Traits on Aboveground Carbon Stock

Carbon storage in vegetation and soil underpins climate regulation through carbon sequestration. Given continuous plant growth, functional traits that optimize acquisition and efficient use of solar radiation and nutrients throughout the forest complex canopy are very important for sustained ecosystem carbon input (Reich et al., 2014). In our study, the significant negative relationship between CWM_SLA and AGC and the positive relation between CWM_WD and AGC suggested that community composing of high specific leaf area and low wood density plants ('acquisitive' strategy) will gain low AGC stock, meanwhile community composing of low specific leaf area and high wood density plants ('conservative' strategy) will gain high AGC stock in the old-growth rainforest. Because different plant species differ in their ability to capture, store and release carbon, community functional traits should be a major driver of carbon sequestration in terrestrial ecosystems (De Deyn et al., 2008). The negative relation between TRAITS (high CWM_SLA and low CWM_WD) and AGC in SEM also supports that community composing of 'acquisitive' plants will gain low AGC and that composing of 'conservative' plants will gain high AGC in old-growth rainforest. The amount of wood in the vegetation and its carbon content determined the total amount of carbon stored in biomass. Plant traits associated with a higher investment in structure per unit of biomass, such as wood density, are therefore expected to directly influence aboveground and belowground ecosystem carbon storage (Baker et al., 2004; Moles et al., 2009). Moreover, there is evidence of a trade-off between a suite of attributes promoting fast carbon acquisition and fast decomposition and another suite of attributes which promote the conservation of resources within well-protected tissues and slow decomposition (Wright et al., 2004; Luoto et al., 2007; Cornwell et al., 2008; Poorter et al., 2009). Therefore, at the ecosystem level, prevailing acquisitive trait syndromes should be conducive to higher carbon fluxes, whereas prevailing conservative trait syndromes should be conducive to higher carbon stocks (De Deyn et al., 2008; Bu, 2013; Conti and Díaz, 2013).

The role of functional traits at community level has been shown for aboveground net primary productivity (Mokany et al., 2008) and carbon-cycling (Bardgett et al., 2013). Consistently, the significant relationships between community functional traits (CWM_SLA and CWM_WD) and AGC were found in the old-growth tropical rainforest. Our result also supports the mass ratio hypothesis in agreement with the report by Garnier et al. (2004). In the mass ratio hypothesis, Grime (1998) suggested that the extent to which the trait of a species affects ecosystem properties strongly depends on the relative contribution to the total biomass of that species. Accordingly, ecosystem functions [e.g., carbon cycling (De Deyn et al., 2008)] would be determined by aggregated traits of dominant species.

The Indirect Linkage Between Environmental Factors and on Aboveground Carbon Stock Through Functional Traits

Focusing on plant functional traits rather than on species identities, allows generalizing complex community dynamics and predicting effects of ongoing environmental changes (Klumpp and Soussana, 2009). The framework proposed by Suding et al. (2008) describes an approach to scale up from individuals to communities and ecosystems in the context of environmental change. The physical environment can strongly influence variation in ecosystem functions (Boyer et al., 2009; Geert Hiddink et al., 2009; Lavorel et al., 2011), which can be due to both shifts in functional composition along environmental gradients and direct effects of the physical environment (Díaz et al., 2007; Gross et al., 2008). In our study, we expected that environmental factors would have a direct effect on AGC. Contrary to our expectations, the environmental factors had a large effect on community functional traits and only had an indirect effect on AGC through community functional traits in the old-growth forest. The tight correlation between variation in habitat preference and plant economics spectrum suggests that the topographically and edaphically associated environmental filter mediated through physiological traits of species is a vital mechanism shaping spatial patterns of tropical forest community (Kusumoto et al., 2013). These results also indicate that in forest ecosystems, plant functional traits optimize acquisition and efficient use of solar radiation and soil nutrients to sustain ecosystem carbon input and turnover by different plant strategies ("acquisitive" or "conservative" strategies). Therefore, community functional traits always had larger effects on AGC than environmental factors. Michaletz et al. (2014) studied variation in terrestrial net primary production across global climate gradients and concluded that age and biomass of plant (functional traits) explained most of the variation in production whereas temperature and precipitation (environmental factors) explained almost none, suggesting that climate indirectly (not directly) influences production.

We found that although environmental factors always had a strong effect on community functional traits, the effect decreased gradually with the increase of scale size. This could be due to the homogenizing effect of topographic variables at the larger

scales (see **Supplementary Table S1**) and other unaccounted environmental variation at the smaller scales (Punchi-Manage et al., 2013). This observation is consistent with results of other studies of tropical forests: the relationship between community functional traits and habitat heterogeneity is scale-dependent, which suggests that species functional characteristics related to resource exploitation and fitness adaptation can be spatially variable across different scales (Lavorel et al., 1999; Díaz et al., 2007; Hu et al., 2014).

We found that the effect of community functional traits on AGC increased with increasing scale size. On one hand, the sampling unit of 40 m × 40 m may be too small to well reflect the local woody species pool of a site in the species rich tropical rainforest. Thus, random effects introduce noise and impede the detection of ecological patterns, which depend on the spatial resolution (Luoto et al., 2007; Steinmann et al., 2009). On the other hand, the large effect of community functional traits on AGC supports the mass ratio hypothesis, which suggests that the effect of a given species on ecosystem processes is proportional to its relative contribution to the total biomass of the community. Therefore, community-weighted mean trait effects on AGC stock should increase with sampling scale due to additive effect and the effects of community weighted mean functional trait on ecosystem functions should be scale dependent. There are several studies, indicating that the plant community trait effects may primarily be attributed to the biomass ratio hypothesis rather than functional diversity hypothesis (Mokany et al., 2008; Laughlin, 2011; Lavorel et al., 2011).

CONCLUSION

Functional traits have a potential to describe how the functional composition of communities responds to environmental gradients and how they influence ecosystem processes and services delivery. Furthermore, the relative effects of environmental changes on ecosystem functioning in a rapidly changing world still needs to be evaluated (Hillebrand and Matthiessen, 2009). To disentangle the relative effects of these factors on the functioning of a species diverse forest ecosystem, we assessed the mechanistic linkages between environmental variations and AGC stock through functional traits across three nested spatial scales by SEM. Our results indicated that stands composed of 'acquisitive' species (high specific leaf area and low wood density) gained low AGC meanwhile stands composed of 'conservative' species (low specific leaf area and high wood density) gained high AGC. These community level functional traits effects on AGC stock increased with increasing spatial scale in accordance with the biomass ratio hypothesis. Plant functional traits at community level responded to physical environmental variations while affected stand AGC stock directly in each spatial scale. Changes in abiotic site conditions did not directly affect AGC stock significantly, but indirectly via changes in plant functional traits. Plant functional traits are more important than environmental factors in driving variations of stand AGC stock in the tropical montane rainforest. Our study suggests that plant functional traits are the mediators in regulating effects of changes in abiotic site conditions on ecosystem functioning. Although our conclusion is largely supported by the data in the old-growth tropical forest, ecosystem functions are also affected by species richness (Liu et al., 2018), trait diversity and phylogenetic diversity (Cadotte et al., 2009); tree size (Stephenson et al., 2014) and so on.

AUTHOR CONTRIBUTIONS

RZ, YL, and YD designed the study. ML, JW, and CZ collected the field samples and performed the plant traits and carbon stock measurements. WB, HX, and JH analyzed the data and performed the statistical analyses. WB and JH wrote the first version of the manuscript, which was intensively discussed and revised by all authors.

FUNDING

This study was supported by the Fundamental Research Funds for the Central Non-profit Research Institution of CAF (CAFBB2017ZB004), the National Natural Science Foundation of China (31760134) and Natural Science Foundation of Jiangxi, China (20171BAB214032).

ACKNOWLEDGMENTS

We thank Ruming Peng, Jiansheng Zhou, and Wensheng Liang from Jianfengling Natural Reserve for their help in conducting field manuscript. Furthermore, our deepest gratitude goes to the anonymous reviewers for their careful work and thoughtful suggestions that have helped improve this manuscript substantially.

SUPPLEMENTARY MATERIAL

The Supplementary Material for this article can be found online at: https://www.frontiersin.org/articles/10.3389/fpls.2018.01958/full#supplementary-material

REFERENCES

Ackerly, D. (2004). Functional strategies of chaparral shrubs in relation to seasonal water deficit and disturbance. *Ecol. Monogr.* 74, 25–44. doi: 10.1890/03-4022

Ackerly, D. D., and Cornwell, W. (2007). A trait-based approach to community assembly: partitioning of species trait values into within-and among-community components. *Ecol. Lett.* 10, 135–145. doi: 10.1111/j.1461-0248.2006.01006.x

Andersen, K. M., Endara, M. J., Turner, B. L., and Dalling, J. W. (2012). Trait-based community assembly of understory palms along a soil nutrient gradient in a lower montane tropical forest. *Oecologia* 168, 519–531. doi: 10.1007/s00442-011-2112-z

Assessment, M. E. (2005). *Ecosystems and Human Well-Being*. Washington, DC: Island Press.

Baker, T. R., Phillips, O. L., Malhi, Y., Almeida, S., Arroyo, L., et al. (2004). Variation in wood density determines spatial patterns inAmazonian forest biomass. *Glob. Chang. Biol.* 10, 545–562. doi: 10.1111/j.1365-2486.2004.00751.x

Bardgett, R. D., Manning, P., Morriën, E., and De Vries, F. T. (2013). Hierarchical responses of plant–soil interactions to climate change: consequences for the global carbon cycle. *J. Ecol.* 101, 334–343. doi: 10.1111/1365-2745.12043

Berthrong, S. T., Jobbágy, E. G., and Jackson, R. B. (2009). A global meta-analysis of soil exchangeable cations, pH, carbon, and nitrogen with afforestation. *Ecol. Appl.* 19, 2228–2241. doi: 10.1890/08-1730.1

Boyer, K. E., Kertesz, J. S., and Bruno, J. F. (2009). Biodiversity effects on productivity and stability of marine macroalgal communities: the role of environmental context. *Oikos* 118, 1062–1072. doi: 0.1111/j.1600-0706.2009.17252.x

Bu, W. (2013). *The Relationships Between Biodiversity and Ecosystem Functioning in Natural Tropical Forests of Hainan Island, China*. Ph.D. thesis, Chinese Academy of Forestry, Beijing.

Butterfield, B. J., and Suding, K. N. (2013). Single-trait functional indices outperform multi-trait indices in linking environmental gradients and ecosystem services in a complex landscape. *J. Ecol.* 101, 9–17. doi: 10.1111/1365-2745.12013

Cadotte, M. W., Cavender-Bares, J., Tilman, D., and Oakley, T. H. (2009). Using phylogenetic, functional and trait diversity to understand patterns of plant community productivity. *PLoS One* 4:e5695. doi: 10.1371/journal.pone.0005695

Chao, K. J., Phillips, O. L., Gloor, E., Monteagudo, A., Torres-Lezama, A., et al. (2008). Growth and wood density predict tree mortality in Amazon forests. *J. Ecol.* 96, 281–292. doi: 10.1111/j.1365-2745.2007.01343.x

Chave, J., Coomes, D., Jansen, S., Lewis, S. L., Swenson, N. G., et al. (2009). Towards a worldwide wood economics spectrum. *Ecol. Lett.* 12, 351–366. doi: 10.1111/j.1461-0248.2009.01285.x

Chave, J., Réjou-Méchain, M., Búrquez, A., Chidumayo, E., Colgan, M. S., et al. (2014). Improved allometric models to estimate the aboveground biomass of tropical trees. *Glob. Chang. Biol.* 20, 3177–3190. doi: 10.1111/gcb.12629

Conti, G., and Díaz, S. (2013). Plant functional diversity and carbon storage – an empirical test in semi-arid forest ecosystems. *J. Ecol.* 101, 18–28. doi: 10.1111/1365-2745.12012

Cornelissen, J., Lavorel, S., Garnier, E., Diaz, S., Buchmann, N., et al. (2003). A handbook of protocols for standardised and easy measurement of plant functional traits worldwide. *Aust. J. Bot.* 51, 335–380. doi: 10.1071/bt02124

Cornwell, W. K., Cornelissen, J. H., Amatangelo, K., Dorrepaal, E., Eviner, V. T., et al. (2008). Plant species traits are the predominant control on litter decomposition rates within biomes worldwide. *Ecol. Lett.* 11, 1065–1071. doi: 10.1111/j.1461-0248.2008.01219.x

Day, F. P. Jr., and Monk, C.D. (1977). Seasonal nutrient dynamics in the vegetation on a southern Appalachian watershed. *Am. J. Bot.* 64, 1126–1139. doi: 10.1002/j.1537-2197.1977.tb10803.x

De Deyn, G. B., Cornelissen, J. H. C., and Bardgett, R. D. (2008). Plant functional traits and soil carbon sequestration in contrasting biomes. *Ecol. Lett.* 11, 516–531. doi: 10.1111/j.1461-0248.2008.01164.x

Dias, A. T. C., Berg, M. P., De Bello, F., Van Oosten, A. R., Bílá, K., et al. (2013). An experimental framework to identify community functional components driving ecosystem processes and services delivery. *J. Ecol.* 101, 29–37. doi: 10.1111/1365-2745.12024

Díaz, S., Hector, A., and Wardle, D. A. (2009). Biodiversity in forest carbon sequestration initiatives: not just a side benefit. *Curr. Opin. Environ. Sustain.* 1, 55–60. doi: 10.1016/j.cosust.2009.08.001

Díaz, S., Lavorel, S., De Bello, F., Quétier, F., Grigulis, K., et al. (2007). Incorporating plant functional diversity effects in ecosystem service assessments. *Proc. Natl. Acad. Sci. U.S.A.* 104, 20684–20689. doi: 10.1073/pnas.0704716104

Douma, J. C., De Haan, M. W. A., Aerts, R., Witte, J.-P. M., and Van Bodegom, P. M. (2011). Succession-induced trait shifts across a wide range of NW European ecosystems are driven by light and modulated by initial abiotic conditions. *J. Ecol.* 100, 366–380. doi: 10.1111/j.1365-2745.2011.01932.x

Freschet, G. T., Cornelissen, J. H. C., Van Logtestijn, R. S. P., and Aerts, R. (2010). Substantial nutrient resorption from leaves, stems and roots in a subarctic flora: what is the link with other resource economics traits? *New Phythol.* 186, 879–889. doi: 10.1111/j.1469-8137.2010.03228.x

Garnier, E., Cortez, J., Billès, G., Navas, M.-L., Roumet, C., et al. (2004). plant functional markers capture ecosystem properties during secondary succession. *Ecology* 85, 2630–2637. doi: 10.1890/03-0799

Geert Hiddink, J., Wynter Davies, T., Perkins, M., Machairopoulou, M., and Neill, S. P. (2009). Context dependency of relationships between biodiversity and ecosystem functioning is different for multiple ecosystem functions. *Oikos* 118, 1892–1900. doi: 10.1111/j.1600-0706.2009.17556.x

Grace, J. B. (2006). *Structural Equation Modeling and Natural Systems*. London: Cambridge University Press. doi: 10.1017/CBO9780511617799

Grime, J. P. (1998). Benefits of plant diversity to ecosystems: immediate, filter and founder effects. *J. Ecol.* 86, 902–910. doi: 10.1046/j.1365-2745.1998.00306.x

Gross, N., Robson, T., Lavorel, S., Albert, C., Le Bagousse-Pinguet, Y., et al. (2008). Plant response traits mediate the effects of subalpine grasslands on soil moisture. *New Phytol.* 180, 652–662. doi: 10.1111/j.1469-8137.2008.02577.x

Hajek, P., Kurjak, D., von Wühlisch, G., Delzon, S., and Schuldt, B. (2016). Intraspecific Variation in Wood Anatomical, Hydraulic, and Foliar Traits in Ten European Beech Provenances Differing in Growth Yield. *Front. Plant Sci.* 7:791. doi: 10.3389/fpls.2016.00791

Hillebrand, H., and Matthiessen, B. (2009). Biodiversity in a complex world: consolidation and progress in functional biodiversity research. *Ecol. Lett.* 12, 1405–1419. doi: 10.1111/j.1461-0248.2009.01388.x

Hobbie, S. E., Ogdahl, M., Chorover, J., Chadwick, O. A., Oleksyn, J., et al. (2007). Tree species effects on soil organic matter dynamics: the role of soil cation composition. *Ecosystems* 10, 999–1018. doi: 10.1007/s10021-007-9073-4

Hooper, D., Chapin Iii, F., Ewel, J., Hector, A., Inchausti, P., et al. (2005). Effects of biodiversity on ecosystem functioning: a consensus of current knowledge. *Ecol. Monogr.* 75, 3–35. doi: 10.1890/04-0922

Hooper, D. U., Adair, E. C., Cardinale, B. J., Byrnes, J. E. K., Hungate, B. A., et al. (2012). A global synthesis reveals biodiversity loss as a major driver of ecosystem change. *Nature* 486, 105–108. doi: 10.1038/nature11118

Hu, G., Jin, Y., Liu, J., and Yu, M. (2014). Functional diversity versus species diversity: relationships with habitat heterogeneity at multiple scales in a subtropical evergreen broad-leaved forest. *Ecol. Res.* 29, 897–903. doi: 10.1007/s11284-014-1178-6

Jiang, Y. X., Wang, B. S., Zang, R. G., Jin, J. H., and Liao, W. B. (2002). *Tropical Forest Biodiversity and Its Forming Mechanism in Hainan Island*. Beijing: Science press.

Jobbágy, E. G., and Jackson, R. B. (2003). Patterns and mechanisms of soil acidification in the conversion of grasslands to forests. *Biogeochemistry* 64, 205–229. doi: 10.1023/a:1024985629259

John, R., Dalling, J. W., Harms, K. E., Yavitt, J. B., Stallard, R. F., et al. (2007). Soil nutrients influence spatial distributions of tropical tree species. *Proc. Natl. Acad. Sci. U.S.A.* 104, 864–869. doi: 10.1073/pnas.0604666104

Keddy, P. A. (1992). Assembly and response rules: two goals for predictive community ecology. *J. Veg. Sci.* 3, 157–164. doi: 10.2307/3235676

Klumpp, K., and Soussana, J. -F. O. (2009). Using functional traits to predict grassland ecosystem change: a mathematical test of the response-and-effect trait approach. *Glob. Chang. Biol.* 15, 2921–2934. doi: 10.1111/j.1365-2486.2009.01905.x

Kraft, N. J. B., Valencia, R., and Ackerly, D. D. (2008). Functional traits and niche-based tree community assembly in an Amazonian forest. *Science* 322, 580–582. doi: 10.1126/science.1160662

Kusumoto, B., Enoki, T., and Kubota, Y. (2013). Determinant factors influencing the spatial distributions of subtropical lianas are correlated with components of functional trait spectra. *Ecol. Res.* 28, 9–19. doi: 10.1007/s11284-012-0993-x

Laughlin, D. C. (2011). Nitrification is linked to dominant leaf traits rather than functional diversity. *J. Ecol.* 99, 1091–1099. doi: 10.1111/j.1365-2745.2011.01856.x

Lavorel, S. (2013). Plant functional effects on ecosystem services. *J. Ecol.* 101, 4–8. doi: 10.1111/1365-2745.12031

Lavorel, S., and Grigulis, K. (2012). How fundamental plant functional trait relationships scale-up to trade-offs and synergies in ecosystem services. *J. Ecol.* 100, 128–140. doi: 10.1111/j.1365-2745.2011.01914.x

Lavorel, S., Grigulis, K., Lamarque, P., Colace, M.-P., Garden, D., et al. (2011). Using plant functional traits to understand the landscape distribution of multiple ecosystem services. *J. Ecol.* 99, 135–147. doi: 10.1111/j.1365-2745.2010.01753.x

Lavorel, S., Mcintyre, S., and Grigulis, K. (1999). Plant response to disturbance in a Mediterranean grassland: how many functional groups? *J. Veg. Sci.* 10, 661–672. doi: 10.2307/3237081

Legendre, P., Mi, X., Ren, H., Ma, K., Yu, M., et al. (2009). Partitioning beta diversity in a subtropical broad-leaved forest of China. *Ecology* 90, 663–674. doi: 10.2307/27651030

Liu, X., Swenson, N. G., Lin, D., Mi, X., Umaña, M. N., et al. (2016). Linking individual-level functional traits to tree growth in a subtropical forest. *Ecology* 97:2396. doi: 10.1002/ecy.1445

Liu, X., Trogisch, S., He, J. S., Niklaus, P. A., Bruelheide, H., et al. (2018). Tree species richness increases ecosystem carbon storage in subtropical forests. *Proc. R. Soc. B.* 285:20181240. doi: 10.1098/rspb.2018.1240

Luoto, M., Virkkala, R., and Heikkinen, R. K. (2007). The role of land cover in bioclimatic models depends on spatial resolution. *Glob. Ecol. Biogeogr.* 16, 34–42. doi: 10.1111/j.1466-8238.2006.00262.x

McGill, B. J., Enquist, B. J., Weiher, E., and Westoby, M. (2006). Rebuilding community ecology from functional traits. *Trends Ecol. Evol.* 21, 178–185. doi: 10.1016/j.tree.2006.02.002

Michaletz, S. T., Cheng, D., Kerkhoff, A. J., and Enquist, B. J. (2014). Convergence of terrestrial plant production across global climate gradients. *Nature* 512, 39–43. doi: 10.1038/nature13470

Mokany, K., Ash, J., and Roxburgh, S. (2008). Functional identity is more important than diversity in influencing ecosystem processes in a temperate native grassland. *J. Ecol.* 96, 884–893. doi: 10.1111/j.1365-2745.2008.01395.x

Moles, A. T., Warton, D. I., Warman, L., Swenson, N. G., Laffan, S. W., et al. (2009). Global patterns in plant height. *J. Ecol.* 97, 923–932. doi: 10.1111/j.1365-2745.2009.01526.x

Mouillot, D., Villéger, S., Scherer-Lorenzen, M., and Mason, N. W. (2011). Functional structure of biological communities predicts ecosystem multifunctionality. *PLoS One* 6:e17476. doi: 10.1371/journal.pone.0017476

Nishimua, T., Suzuki, E., Kohyama, T., and Tsuyuzaki, S. (2007). Mortality and growth of trees in peat-swamp and heath forests in Central Kalimantan after severe drought. *Plant Ecol.* 188, 165–177. doi: 10.1007/s11258-006-9154-z

Ordoñez, J. C., Van Bodegom, P. M., Witte, J.-P. M., Wright, I. J., Reich, P. B., et al. (2009). A global study of relationships between leaf traits, climate and soil measures of nutrient fertility. *Glob. Ecol. Biogeogr.* 18, 137–149. doi: 10.1111/j.1466-8238.2008.00441.x

Petchey, O. L., and Gaston, K. J. (2006). Functional diversity: back to basics and looking forward. *Ecol. Lett.* 9, 741–758. doi: 10.1111/j.1461-0248.2006.00924.x

Petchey, O. L., Hector, A., and Gaston, K. J. (2004). How do different measures of functional diversity perform? *Ecology* 85, 847–857. doi: 10.1890/03-0226

Poorter, H., Niinemets, Ü., Poorter, L., Wright, I. J., and Villar, R. (2009). Causes and consequences of variation in leaf mass per area (LMA): a meta-analysis. *New Phytol.* 182, 565–588. doi: 10.1111/j.1469-8137.2009.02830.x

Punchi-Manage, R., Getzin, S., Wiegand, T., Kanagaraj, R., Savitri Gunatilleke, C. V., et al. (2013). Effects of topography on structuring local species assemblages in a Sri Lankan mixed dipterocarp forest. *J. Ecol.* 101, 149–160. doi: 10.1111/1365-2745.12017

R Development Core Team (2011). *R: A Language and Environment for Statistical Computing*. Available: http://www.R-project.org/

Reich, P. B. (2014). The world-wide 'fast–slow' plant economics spectrum: a traits manifesto. *J. Ecol.* 102, 275–301. doi: 10.1111/1365-2745.12211

Reich, P. B., Rich, R. L., Lu, X., Wang, Y.-P., and Oleksyn, J. (2014). Biogeographic variation in evergreen conifer needle longevity and impacts on boreal forest carbon cycle projections. *Proc. Natl. Acad. Sci. U.S.A.* 111, 13703–13708. doi: 10.1073/pnas.1216054110

Shipley, B. (2002). *Cause and Correlation in Biology: A User's Guide to Path Analysis, Structural Equations and Causal Inference*. London: Cambridge University Press.

Steinmann, K., Linder, H., and Zimmermann, N. (2009). Modelling plant species richness using functional groups. *Ecol. Model.* 220, 962–967. doi: 10.1016/j.ecolmodel.2009.01.006

Stephenson, N. L., Das, A. J., Condit, R., Russo, S. E., Baker, P. J., et al. (2014). Rate of tree carbon accumulation increases continuously with tree size. *Nature* 507, 90–93. doi: 10.1038/nature12914

Suding, K. N., Lavorel, S., Chapin, F. S., Cornelissen, J. H. C., DÍaz, S., et al. (2008). Scaling environmental change through the community-level: a trait-based response-and-effect framework for plants. *Glob. Chang. Biol.* 14, 1125–1140. doi: 10.1111/j.1365-2486.2008.01557.x

Tomlinson, K. W., Poorter, L., Sterck, F. J., Borghetti, F., Ward, D., et al. (2013). Leaf adaptations of evergreen and deciduous trees of semi-arid and humid savannas on three continents. *J. Ecol.* 101, 430–440. doi: 10.1111/1365-2745.12056

Villéger, S., Mason, N. W. H., and Mouillot, D. (2008). New multidimensional functional indices for a multifaceted framework in functional ecology. *Ecology* 89, 2290–2301. doi: 10.1890/07-1206.1

Violle, C., Navas, M.-L., Vile, D., Kazakou, E., Fortunel, C., et al. (2007). Let the concept of trait be functional! *Oikos* 116, 882–892. doi: 10.1111/j.0030-1299.2007.15559.x

Westoby, M., Falster, D. S., Moles, A. T., Vesk, P. A., and Wright, I. J. (2002). Plant ecological strategies: some leading dimensions of variation between species. *Annu. Rev. Ecol. Syst.* 33, 125–159. doi:10.1146/annurev.ecolsys.33.010802.150452

Wright, I. J., Reich, P. B., Westoby, M., Ackerly, D. D., Baruch, Z., et al. (2004). The worldwide leaf economics spectrum. *Nature* 428, 821–827. doi: 0.1038/nature02403

Zhang, W. R., Yang, G. C., and Tu, X. N. (1999). *The forestry industry standard of the People's Republic of China-Determination of forest soil*. Beijing: China Standard Press.

Zhou, G., Liu, S., Li, Z., Zhang, D., Tang, X., et al. (2006). Old-growth forests can accumulate carbon in soils. *Science* 314, 1417–1417. doi: 10.1126/science.1130168

Conflict of Interest Statement: The authors declare that the research was conducted in the absence of any commercial or financial relationships that could be construed as a potential conflict of interest.

frontiers in Plant Science

ORIGINAL RESEARCH
published: 04 June 2019
doi: 10.3389/fpls.2019.00701

Plasticity of Fine-Root Traits Under Long-Term Irrigation of a Water-Limited Scots Pine Forest

Ivano Brunner[1], Claude Herzog[1], Lucía Galiano[2,3,4] and Arthur Gessler[2]*

[1] Forest Soils and Biogeochemistry, Swiss Federal Institute for Forest, Snow and Landscape Research WSL, Birmensdorf, Switzerland, [2] Forest Dynamics, Swiss Federal Institute for Forest, Snow and Landscape Research WSL, Birmensdorf, Switzerland, [3] Centre for Research on Ecology and Forestry Applications, Barcelona, Spain, [4] Department of Animal, Plant Biology and Ecology, Universitat Autònoma de Barcelona, Barcelona, Spain

Trait-based approaches are increasingly used to investigate plant strategies for resource acquisition, growth, or competition between individual organisms or across species. However, the characterization of responses to environmental stimuli by fine-root systems of trees at the trait level is rather limited, particularly regarding the timing and degree of plasticity of the traits involved. These aspects become especially relevant under current climate-driven shifts in environmental conditions. In the present study, we examined the responses of the fine roots of Scots pines to increased soil water availability from long-term irrigation starting in the year 2003. The Scots pine forest is situated in a water-limited region in the central European Alps where increased tree mortality has been observed over the last two decades. The fine-root traits investigated include root system traits, root dynamic traits, architectural traits, and morphological traits. A first survey of fine-root traits in 2005 using ingrowth cores did not reveal any trait-based responses resulting from the irrigation treatment over a three-year period. Fine-root biomass, as periodically recorded by coring the topsoil from 2003 to 2016, showed a significant increase compared to the non-irrigated controls between three and nine years after the start of treatment. Overall, a maximum biomass increase due to the irrigation treatment was recorded in 2016 with about 80% higher biomass compared to controls. The analysis of fine-root traits revealed that irrigation significantly increased biomass, length, and production, but did not alter morphological and architectural traits, such as diameter, frequency of tips, specific root length (SRL), and root tissue density (RTD). In contrast, clear significant differences were found for all traits except for length when comparing the two root sampling methods, namely, ingrowth cores and soil coring. However, there were no interactions between the irrigation treatment and the sampling methods used and, therefore, the methods used did not affect the documented patterns, just the actual measured trait values.

Keywords: architectural traits, biomass, drought, dynamic traits, ingrowth cores, morphological traits, production, soil coring

OPEN ACCESS

Edited by:
Boris Rewald, University of Natural Resources and Life Sciences, Vienna, Austria

Reviewed by:
Louise Comas, United States Department of Agriculture, United States
Jorge E. Mayer, Ag RD&IP Consult P/L, Australia

****Correspondence:***
Ivano Brunner
ivano.brunner@wsl.ch

Specialty section:
This article was submitted to Functional Plant Ecology, a section of the journal Frontiers in Plant Science

Received: *31 January 2019*
Accepted: *13 May 2019*
Published: *04 June 2019*

Citation:
Brunner I, Herzog C, Galiano L and Gessler A (2019) Plasticity of Fine-Root Traits Under Long-Term Irrigation of a Water-Limited Scots Pine Forest. Front. Plant Sci. 10:701. doi: 10.3389/fpls.2019.00701

INTRODUCTION

Trait-based approaches are increasingly being used to investigate plant strategies for resource acquisition, growth, and competition, as well as for plant impacts on ecosystem processes (McCormack et al., 2017). However, most efforts have thus far focused on aboveground plant traits, while belowground traits and strategies still remain under-researched. To fill this gap, a Fine-Root Ecology Database (FRED[1]) was created exclusively for fine-root traits and which now includes over 70,000 observations (Iversen et al., 2017).

Ideally, the range of a trait's response to environmental stimuli or plant-intrinsic factors should be known. Regrettably, this knowledge is still limited for belowground traits (Shipley et al., 2016). Part of the problem may stem from the inconsistency and inaccuracy of belowground measurements (Freschet et al., 2015; McCormack et al., 2017).

The variability of a trait in response to environmental changes, either across environmental gradients or in experimental treatments, is called "phenotypic plasticity" (Callaway et al., 2003; Iversen et al., 2017). The capacity of organisms to alter their phenotype under changing conditions is widely recognized as an important mechanism to avoid migration or extinction (Valladares et al., 2014). The term phenotypic plasticity is currently applied in a broad sense, and is used to describe the phenotypic responses of organisms to environmental change, e.g., acclimation (equivalent to acclimatization) (Kelly et al., 2012). One aboveground example is the particular plasticity of the leaves of tropical trees, which grow differently depending on light conditions. In the light, leaves are thicker, whereas in the shade they tend to be thinner (Rozendaal et al., 2006). Weemstra et al. (2017) and Zadworny et al. (2017) have recently shown that phenotypic plasticity occurs in tree roots, where physical and chemical soil parameters are the influencing factors instead of light.

Plasticity is understood as an adaptive mechanism that allows plants to optimally respond to environmental heterogeneity (Palacio-Lopez et al., 2015). The phenotypic shift can either be the result of a genetic differentiation of populations to become locally adapted, or of the phenotypic plasticity of individuals expressing the optimal phenotype for the corresponding environment via physiological and molecular regulatory mechanism (Palacio-Lopez et al., 2015). However, the ability of an organism to express plasticity within a given trait is most likely mediated at the molecular level (Nicotra et al., 2010).

Here, we examine the response of Scots pine (*Pinus sylvestris* L.) fine-root traits to precipitation changes using a unique long-term irrigation experiment in a water-limited pine forest ecosystem in the central European Alps (Dobbertin et al., 2010; Hartmann et al., 2017). The irrigation experiment was established in the Pfyn forest in 2003 to better understand how forest ecosystems respond to water limitation (Dobbertin et al., 2010). The Pfyn forest represents the largest continuous forest of Scots pine in Switzerland, and is located in the dry Rhone Valley. Large-scale Scots pine forests in the transition zone between continental and Mediterranean climates are characteristic landscape elements in dry and warm inner Alpine valleys in the Central Alps (Rigling et al., 2013). Increasing Scots pine mortality has been recorded for several decades, with a dieback of up to 50% in particularly water-limited stands in the Swiss Rhone Valley since 1995, as well as in other valleys in the central Alps in Italy and Austria (Rebetez and Dobbertin, 2004; Vacchiano et al., 2012). High mortality of Scots pine on long-term monitoring sites in the Swiss Rhone valley, with up to 20% of the trees in a stand dying in a given year, was observed in 1999, 2004, and 2017. At the Pfynwald site, cumulated mortality between 2003 (when the irrigation treatment started) and 2016 was about 16% in the control plots and about 9% in the irrigated plots. Although average annual precipitation has remained constant in recent decades, there is evidence that climate warming has increased evaporation rates, and that water has become the main factor limiting growth and reducing stress resilience in trees (Rigling et al., 2013). It was therefore hypothesized that reducing stress from water limitation using irrigation could improve tree vitality and reduce mortality. Indeed, after 3–9 years of irrigation, trees showed increased leaf area and increased fine-root biomass (Dobbertin et al., 2010; Herzog et al., 2014). Furthermore, irrigation was found to cause significant shifts in plant community composition and increased vegetation cover (Herzog et al., 2014). In response to the doubling of precipitation over the decade-long experimental period, the monthly mean volumetric water content in the top soil increased significantly, from 28% in the controls to 34% in the irrigated plots (Hartmann et al., 2017).

In the present study, our research question was to determine whether the irrigation treatment (i.e., dry controls vs. irrigation) would affect the recorded fine-root traits. The second research question was to determine whether the method of recording roots (soil cores vs. ingrowth cores) under the irrigation treatment would influence the traits. It was the aim of the study to investigate the fine-root traits of several trait categories (McCormack et al., 2017), such as "root system," "morphology," "architecture," and "root dynamics."

MATERIALS AND METHODS

Study Site and Experimental Setup

The study site is located in the Pfynwald forest situated in the Rhone Valley in Switzerland (46°180 N, 07°370 E, 615 m.a.s.l.), in a Scots pine forest containing trees of about 100 years of age, a stand density of about 730 stems ha^{-1}, and with occasional interspersed pubescent oak (*Quercus pubescens* Willd) (Brunner et al., 2009). The mean yearly precipitation of the nearby climate station Sion is 603 mm, with a mean annual temperature 10.2°C (1980–2010; MeteoSchweiz, 2018). Over the last three decades, precipitation has dropped toward 90% of the long-term average and the temperature has risen by more than 1°C (1980–2010; MeteoSchweiz, 2018). For the long-term irrigation treatment, a 1.23-ha study area containing about 1,100 tree individuals, was subdivided into eight plots of 25 × 40 m (1,000 m^2) with 5 m buffer areas between and around each plot. The plots were aligned side by side along a channel fed by the Rhone River, from where

[1]http://roots.ornl.gov

water was taken to irrigate four randomly selected plots (hereafter referred to as "irrigated"). Four plots were left untreated as control plots (hereafter "dry"). Irrigation started for the first time in spring 2003. The irrigation system was activated on rainless nights during the vegetation period (May-October), doubling the annual rainfall amount. Volumetric soil water content was monitored hourly using time-domain reflectometry (Tektronix 1502B cable tester, Beaverton, OR) at soil depth of 10 cm at four different locations in irrigated and dry plots. The mean volumetric water content in the soil significantly increased from 28% in the dry plots to 34% in the irrigated plot (Herzog et al., 2014). In 2013, irrigation was stopped in about a third of the area of each of the irrigated plots to track the return to a 'dry' forest. More details on the study site and experimental setup are described in Brunner et al. (2009), Herzog et al. (2014), and Hartmann et al. (2017), and data on long-term growth as well as on relative leaf areas of trees from the irrigated and control plots are given by Schönbeck et al. (2018).

Soil Cores

Fine roots (<2 mm in diameter) were sampled from healthy sample trees with a soil-coring cylinder (diameter 4.5 cm) about 0.5–1 m away from the stems and down to the rocks of the subsoil to a depth of 8–12 cm. Two soil cores per tree were taken, and three trees per plot were sampled before irrigation treatment started and in April / May in 2003, 2004, 2005, 2012, 2014, and 2016 (Brunner et al., 2009; Herzog et al., 2014). The same trees were sampled throughout the duration of the experiment. Overall, twelve trees in the dry- and nine trees in the irrigation-treatment were included in the analysis. After sampling, the soil cores were packed in plastic bags, transported to the laboratory, and stored at a low temperature (in a cold room at 4°C) until they were analyzed. The soil cores were then washed in a sieve, the roots collected, and the fine roots of Scots pine sorted out by hand, dried at 60°C for 3 days, and weighed. In order to compare data over the 13-year period, the two samples per tree were averaged. Fine roots were calculated per cm^3 of soil and then balanced for 0–10 cm depth and per m^2 to obtain comparable data.

Ingrowth Cores

A first series of ingrowth cores (glass-fiber-netting cylinders 11 cm in height, 5 cm in diameter, with a 5 mm mesh size) were set in April 2003 with the ingrowth cores inserted into the holes where soil core samples had been taken previously for the fine-root biomass (Brunner et al., 2009). The ingrowth cores were refilled with sieved topsoil from outside the plots. The ingrowth cores were then harvested with a large soil corer 8.5 cm in diameter after 2 years in May 2005. After harvest, the ingrowth cores were packed undisturbed in plastic bags, transported to the laboratory, and stored at 4°C until they were analyzed several days later. The ingrowth cores were then cut out with a knife, the core length of the samples recorded, the netting removed with scissors, the soils sieved, and the fine roots rinsed with tap water. The fine roots of the Scots pine were then sorted out by hand, and stored in tap water in a refrigerator until fine-root morphology and architecture was analyzed (Brunner et al., 2009).

A second series of ingrowth cores, using identical ingrowth cores as before, was installed in April 2014 and harvested in spring 2016. The ingrowth cores were installed in the same way as the first series, at a distance of about 0.5–1 m from the stems. However, trees other than those from the first series were probed, and three ingrowth cores per tree instead of two were installed. In total, six trees were selected from the dry treatment and six trees from the irrigated treatment.

In order to compare the datasets of the two series of ingrowth cores, the data were averaged per tree. If one of the ingrowth cores per sample tree remained without roots, then only those with roots were taken into consideration.

Fine-Root Scanning and Analyses

The fine roots from the ingrowth campaign of 2005 and 2016, and from the soil-coring sampling in 2016 were scanned for morphological characteristics before drying and weighing. The scanned pictures were then analyzed using the WinRHIZO software package (version 4.1c, Regent Instruments Inc., Quebec, Canada) for morphological and architectural traits such as length, diameter, root volume, tips, and forks.

Fine-Root Traits

The measured fine-root traits were root biomass density ($g\ m^{-2}$), root length density ($m\ m^{-2}$), mean diameter (mm), tip frequency ($n\ cm^{-1}$), and fork frequency ($n\ cm^{-1}$). The calculated fine-root traits were specific root length (SRL; $m\ g^{-1}$) and root tissue density (RTD; $g\ cm^{-3}$). Biomass and length were calculated per soil area and to a soil depth of 10 cm (topsoil), tips and forks to the root length, SRL to the fine-root biomass, and RTD to the fine-root volume (Brunner et al., 2009). The fine-root turnover rate ($year^{-1}$) was calculated by dividing annual production by standing biomass (Gill and Jackson, 2000; Brunner et al., 2013) by using ingrowth core data for the annual production and soil-coring data for the standing biomass for the years 2005 and 2016. The method used to determine turnover rate, however, is only a rough estimate because of root pruning that occurs when ingrowth cores are installed (Hendricks et al., 2006). The lifespan of the fine roots (year) is equal to the inverse value of the turnover rate (Brunner et al., 2013).

Statistical Analyses

The statistical analyses performed were one- and two-way analyses of variance (ANOVA), repeated-measures ANOVA, and simple linear regression with ANOVA using StatView software (Version 5.0, SAS Institute, Cary, NC). Repeated-measures ANOVA was applied when samples were taken consecutively from the same trees at different times. The significance of the differences between treatments was tested by pairwise comparison of the sample means using Fisher's protected least significant difference at $P < 0.05$. All data were tested for normal distributions using the Kolmogorov-Smirnov Test of Normality[2].

[2]https://www.socscistatistics.com/tests/kolmogorov/Default.aspx

RESULTS

Fine-Root Biomass

The fine-root biomass of the Scot pines, as recorded with soil coring over more than a decade, changed considerably over the duration of the experiment (**Figure 1A**). Under the dry (control) condition, biomass varied from 87 to 311 g m^{-2} in the first 10 cm of the soil. In the first 2 years after the beginning of irrigation treatment, no significant change in the fine-root biomass was measured. Only when fine-roots were recorded again after a gap of 7 years in 2012, did they show a significant difference, with a biomass increase of approximately 50% in the irrigated compared to the dry plots (**Figure 1B**). This difference between treatments increased steadily over the following years (2014, 2016) resulting in the fine-root biomass of irrigated plots being more than 50% higher than in controls, with a maximum biomass of 411 g m^{-2} in 2012.

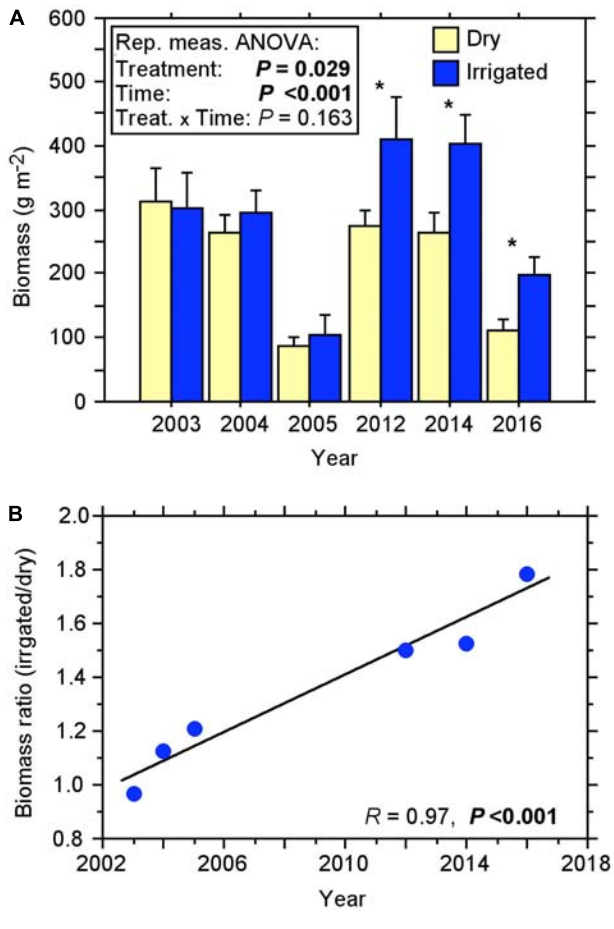

FIGURE 1 | Fine-root biomass of the topsoil (0–10 cm) under dry and irrigated conditions of the Scots pine forest for the years 2003 to 2016 recorded by soil coring. **(A)** Course of biomass (±SE). Repeated measures ANOVA, significant effects ($P < 0.05$) are shown in bold; One-way ANOVA, significant effects ($P < 0.05$) are indicated with *. **(B)** Relationship between the biomass ratio (irrigated/dry) and the sample years, a significant effect ($P < 0.05$) is shown in bold.

Repeated measures ANOVA revealed that the biomass increase in the irrigation treatment was statistically significant over the 13-year period (**Figure 1A**). Considering the ratio of biomass from the irrigated plots to dry plots, it is evident that over the years there has been a steady increase in the biomass ratio with a high coefficient of determination R^2 of 0.95 (**Figure 1B**). We found no indication for a slowdown or reversal of this increase over time.

Fine-Root Production and Turnover Rate

Comparing the 2005 fine-root production with that of 2016 reveals that values in general can be highly plastic, ranging from 33 to 66 g m^{-2} $year^{-1}$ (**Table 1**). The data also show that production in 2005 was not significantly affected by the irrigation treatment. In contrast, in 2016, fine-root production significantly increased by a factor of 2. However, the turnover rate in 2016 was only slightly influenced by the irrigation treatment (**Table 1**) because the biomass recorded through soil coring had also greatly increased due to irrigation (compare also **Figure 1A**). The lifespan of the fine-roots, as calculated from the turnover rates, was from 1.4 to 1.6 year in 2005, whereas in 2016 it was found to range from 3.0 to 3.3 year (**Table 1**).

Fine-Root Traits

Analysis of ingrowth cores sampled in 2005 showed that the fine-root traits measured were not significantly influenced by the irrigation treatment after 2 years of growth (**Table 2**). However, when the traits were again measured in 2016 from ingrowth cores, significant increases were then recorded for the biomass, length, and frequency of forks, but not for the average diameter or frequency of root tips, SRL, or RTD (**Table 2**). The strongest effects due to irrigation were recorded for root biomass, which grew 1.9-fold, and for overall root length, which increased 1.8-fold. When the 2016 soil coring samples were evaluated, only root biomass and overall root length increased significantly, 1.6 and 1.8-fold, respectively. This is slightly lower compared to the ingrowth cores (**Table 2**). Overall, fine-root architectural traits, such as the frequency of tips and forks, and morphological traits, such as average diameter, SRL and RTD, were not significantly influenced by the irrigation treatment (with one exception, namely, the frequency of forks in ingrowth cores in 2016). However, traits varied considerably across survey years and the method applied. Specifically, average diameters ranged from 0.7 to 1.1 mm, root tips from 1.1 to 3.4 cm^{-1}, fork frequency from 1.1 to 5.9 cm^{-1}, that of SRL from 7.2 to 13.3 m g^{-1}, and that of RTD from 0.17 to 0.32 g cm^{-3} (**Table 2**).

Soil Cores vs. Ingrowth Cores

When fine-root traits from both ingrowth cores collected after two-year of growth and soil cores were sampled and analyzed in 2016, significant differences between irrigated and control samples were obtained for biomass, length and forks, but not for other fine-root traits (**Table 3**). A significant effect for the sampling method (ingrowth cores vs. soil cores) was observed for almost all fine-root traits, except for root length (**Table 3**). The greatest significant differences were recorded for fine-root tips, forks, average diameter, and SRL. Interactions between the two

TABLE 1 | Biomass, production, turnover rate, and lifespan of fine roots in the years 2005 and 2016 of the Scots pine forest under dry and irrigated conditions.

Fine-root traits	Year 2005			Year 2016		
	Dry	Irrigated	*P*	Dry	Irrigated	*P*
Biomass (g m^{-2})	87.2	105.3	0.55	111.5	198.5	**0.01**
Production (g m^{-2} y^{-1})	54.9	53.2	0.89	33.8	66.1	**0.02**
Turnover (y^{-1})	0.73	0.61	–	0.30	0.33	–
Lifespan (year)	1.38	1.64	–	3.31	3.00	–

Biomass corresponds to standing biomass estimated by soil coring, production corresponds to annual production estimated by ingrowth cores, turnover corresponds to turnover rate (calculated as production divided by biomass), lifespan corresponds to root age and is the inverse of turnover. Turnover and lifespan were calculated per treatment. One-way ANOVA; significant effects ($P < 0.05$) are shown in bold.

TABLE 2 | Comparison of fine-root traits of roots from ingrowth cores from 2005 and 2016 after 2 years of growth, and of roots from the soil-coring sample from 2016 of the Scots pine forest under dry and irrigated conditions.

Fine-root traits	Ingrowth cores (2005)			Ingrowth cores (2016)			Soil cores (2016)		
	Dry	Irrigated	*P*	Dry	Irrigated	*P*	Dry	Irrigated	*P*
Biomass (g m^{-2})	109.9	106.3	0.89	67.6	132.2	**0.02**	111.9	198.5	**0.01**
Length (m m^{-2})	38.9	59.9	0.14	87.3	157.0	**0.01**	100.2	155.4	**0.049**
Diameter (mm)	1.10	1.05	0.63	0.73	0.70	0.37	0.91	0.93	0.55
Tips (n cm^{-1})	1.12	1.10	0.81	3.21	3.43	0.26	2.39	2.40	0.85
Forks (n cm^{-1})	1.04	1.17	0.60	4.72	5.91	**0.01**	3.42	3.74	0.23
SRL (m g^{-1})	8.11	7.19	0.77	12.5	13.3	0.61	9.79	8.56	0.33
RTD (g cm^{-3})	0.32	0.37	0.64	0.20	0.22	0.19	0.17	0.18	0.50

One-way ANOVA; significant effects ($P < 0.05$) are indicated in bold. SRL, specific root length; RTD, root tissue density.

TABLE 3 | Results of two-way ANOVA testing the effect of the irrigation treatments (dry vs. irrigated) and the fine-root sampling methods (ingrowth cores vs. soil cores) on fine-root traits in 2016.

Fine-root traits	Treatment			Method			Treatment × Method		
	dF	*F*	*P*	*dF*	*F*	*P*	*dF*	*F*	*P*
Biomass (g m^{-2})	1	11.9	**0.002**	1	6.36	**0.02**	1	0.25	0.62
Length (m m^{-2})	1	10.2	**0.003**	1	0.09	0.77	1	0.14	0.71
Diameter (mm)	1	0.12	0.73	1	67.5	**<0.001**	1	1.21	0.28
Tips (n cm^{-1})	1	1.82	0.19	1	110.6	**<0.001**	1	1.34	0.26
Forks (n cm^{-1})	1	12.1	**0.002**	1	63.4	**<0.001**	1	4.06	0.05
SRL (m g^{-1})	1	0.05	0.83	1	14.4	**<0.001**	1	1.06	0.31
RTD (g cm^{-3})	1	1.70	0.20	1	7.85	**0.01**	1	0.15	0.71

Significant effects ($P < 0.05$) are shown in bold. SRL, specific root length; RTD, root tissue density.

factors, irrigation treatment and fine-root sampling method were, however, not detected (**Table 3**).

DISCUSSION

Several attributes in the ecosystem of the experimentally irrigated pine forest changed due to the prolonged treatment over more than a decade. Herb and moss coverage increased significantly, as did crown cover (from 57 to 71%), tree biomass (from 6.8 to 7.9 kg m^{-2}), and litter-fall (from 0.31 to 0.46 kg m^{-2} $year^{-1}$) (Herzog et al., 2014; Hartmann et al., 2017). The increase in fine-root biomass only became apparent 9 years after the irrigation experiment began (Herzog et al., 2014). Although the exact time-point of a significant increase in fine-root biomass was not recorded, root biomass acclimation had started before year nine as indicated by the slight but not significant irrigation effects in 2004 and 2005. It also appears that the ratio of irrigated to dry treatment biomass was still increasing, rising from 1.5 in 2012 to 1.8 in 2016. This indicates that, on the one hand, a saturation of the fine-root biomass in the topsoil had not yet been reached, and, on the other hand, the density of fine-roots is strongly dependent on water availability. Thus, water rather than nutrients (e.g., nitrogen) seems to be the primarily limiting factor for fine-root abundance in this Scots pine forest. Long-term irrigation did not affect the carbon-to-nitrogen ratio, although the fine-root biomass increased by approximately 50% (Herzog et al., 2014). Thus,

higher water availability did not mobilize more nutrients from the topsoil, which, in fact, could also promote fine-root growth (e.g., Yuan and Chen, 2012). An additional indication for the water limitation is the decrease in the δ^{13}C-values in fine-roots from −26 to −27‰ (Herzog et al., 2014), and in trunk tree rings, from −22 to −24‰ (Timofeeva et al., 2017) in the irrigation treatment. These lower values are most likely a result of higher stomatal conductance, leading to higher leaf internal CO_2 concentrations and subsequent higher photosynthetic carbon isotope fractionation (Farquhar et al., 1989).

Only recently, Solly et al. (2018) unraveled the real age of fine roots by counting annual rings, and discovered a mean age (=lifespan) of fine roots of 1 to 2 year (including the fine roots of the Scots pines in the Pfyn forest). Thus, the short lifespan of the fine roots explains the strong fluctuation between 2004 and 2005 and between 2014 and 2016, when fine-root biomass was reduced by more than half. This decrease was most likely due to the heat waves and summer droughts in 2003 and 2015, respectively (Ciais et al., 2005; Dietrich et al., 2018), which negatively affected fine-root biomass build-up with a delay of one to two years, which is when reduced storage reserves came to bear.

The fine-root turnover rate, estimated by dividing annual production by standing biomass, revealed turnover values of 0.30 to 0.73 year^{-1}. These values appear to be lower than the mean values (0.76–1.40 year^{-1}) determined for Scots pine in European forests (Brunner et al., 2013), and reach lower values than those of other tree species (0.48 ± 0.52 year^{-1}; Finer et al., 2011), both estimated by the ingrowth method. Yuan and Chen (2010) analyzed fine roots worldwide, obtaining a mean turnover rate of 0.61 ± 0.17 year^{-1} for pines. While our values are still in the range covered by these studies, Finer et al. (2011) stated that the ingrowth core method usually yields lower turnover values than those obtained by the sequential coring or minirhizotron method, most likely because of a shorter exposure (<2 year). Keeping in mind the turnover values of 0.5 to 1.0 year^{-1} obtained by Solly et al. (2018), our values are in a similar range, with the exception of 2016, which was remarkably low at 0.3 year^{-1}.

Comparing the two methods, soil coring and ingrowth cores, has been done previously (e.g., Persson, 1983; Neill, 1992; Makkonen and Helmisaari, 1999), but mainly to compare dynamic fine-root traits and not to compare morphological or architectural traits. Our data shows that the experimental treatment in the Pfynwald forest had a similar effect across methods, although absolute values significantly differed between methods for most traits. Hendricks et al. (2006) concluded that ingrowth core estimates are in general comparable with soil core estimates, although ingrowth cores may underestimate root production in water-limited environments. In our study, we observed a similar trend regarding fine-root biomass, where values obtained from ingrowth cores were about one-third of those from soil cores.

Drought is known to affect both fine-root traits, such as the dynamic traits of biomass and length, and physiological and molecular traits (Gessler et al., 2005; Brunner et al., 2015; Volkmann et al., 2016; Polle et al., 2019). The production of the plant hormone abscisic acid (ABA) is strongly enhanced, influencing root growth, as well as aquaporins and proline synthesis, which help to regulate water uptake and contribute to osmotic adjustment. Hydraulic conduits and suberin are increasingly produced to better handle water transport and water loss, respectively (Fonti and Jansen, 2012; Barberon et al., 2016). Morphological and architectural traits, in contrast, do not appear to be strongly affected by water limitation. Weemstra et al. (2017) investigated fine-root trait plasticity in European beech and Norway spruce in two contrasting soils (clay vs. sand) and observed that dynamic traits, such as biomass and length, were variable, but that morphological traits such as diameter, SRL and RTD were not. It is indeed hypothesized that dynamic traits follow the resource economics spectrum (Grime, 1977; Bardgett et al., 2014; Reich, 2014), and are thus influenced by soil resource availability (i.e., water and nutrients). This study has come to the same conclusion, that while biomass and length were found to be positively affected by the irrigation treatment – and thus by soil water availability – diameter, SRL, and RTD remained unaffected.

In general, roots can show considerable trait plasticity (Callaway et al., 2003). A recent meta-analysis of the effects of precipitation changes on fine-root traits at a global scale concluded that the responses of fine-root biomass, production, decomposition, and morphology to precipitation can be either positive or negative (Zhang et al., 2019). Joslin et al. (2000) previously reviewed the dynamics of fine-root biomass in long-term stand-level irrigation experiments (2–4 year) with no conclusive results. Particularly with European beech, results were ambiguous, as decreases in precipitation resulted in more fine-root biomass in some cases (e.g., Hertel et al., 2013) and less in others (e.g., Meier and Leuschner, 2008). Hommel et al. (2016) showed that the allocation of assimilates to roots in European beech and Norway maple (*Acer platanoides*) increased under mild, but strongly decreased under more intensive drought, suggesting that drought regimes may impact fine-root biomass production. While there are indications that water sensing by the root cap might stimulate root growth along moisture gradients allowing plants to forage water (Eapen et al., 2005; Dietrich, 2018) strong drought will impair root metabolic activity (Chaves et al., 2003; Beck et al., 2007). Hagedorn et al. (2016) showed that the allocation of assimilates to the roots under drought is driven by this root metabolic activity rather than by an impairment of phloem transport. In coordination with impaired root activity and growth, supply with new carbon is ceased. Some studies with conifers have shown biomass increases (e.g., Gower et al., 1992; De Visser et al., 1994), while others have not (e.g., Bredemeier et al., 1998). Bakker et al. (2009) also conducted a long-term irrigation experiment on 13-year-old maritime pine (*Pinus pinaster*), and overall found no effects on fine-root length, SRL, or ramification after 7 years of treatment. However, in the latter study, we must assume that non-irrigated control plants did not suffer from a lack of water, because the mean annual precipitation of the study site is approximately 950 mm. This means that plants under both treatments, control and irrigation, were most likely not water-limited. In contrast, Konopka and Lukac (2013), conducting a rain-shelter experiment in a 90-year-old Norway spruce (*Picea abies*) stand, found that water shortage reduced fine-root biomass and increased necromass, which supports the

hypothesis that biomass is expected to be affected only when water is limited. Gaul et al. (2008), in a rain-shelter experiment with Norway spruce, showed that experimental drought did not result in significant changes in fine-root biomass during a six-week treatment period. We can assume here, however, that 6 weeks is too short a period to observe acclimation of tree root biomass.

Investigating the fine roots of Scots pine across a temperature and latitudinal gradient in Europe, Zadworny et al. (2017) observed that the root diameter of absorptive roots (defined by the absence of a suberized cell layer) was variable, with the diameter decreasing as the mean annual temperature (MAT) increased (0.4 mm at −2°C; 0.15 mm at 8°C). In contrast, SRL and the carbon-to-nitrogen ratio of absorptive roots were not dependent on the MAT. The average root age of transport roots (seventh to ninth root order), however, was variable with the MAT, with root age decreasing with increasing MAT (4 year at −2°C; 1.4 year at 8°C). Other studies with Scots pine, especially on precipitation gradients, are, unfortunately, lacking. Nevertheless, Zadworny et al. (2017) study provide insight into which Scots pine root traits are potentially plastic and which are not.

Zadworny et al. (2017) proposed that there are two major strategic paths that plants use. Either plants produce thin roots (with a high SRL), which grow quickly and are able to enhance water and nutrient acquisition, or they produce thick roots (with low SRL and high RTD), which grow slowly and are able to live longer, store resources, and are better protected against environmental hazards. In fact, having larger root diameters may be a more effective strategy to enhance resource acquisition when the environment is nutrient-limited (Zadworny et al., 2017). In our study, however, larger diameters and altered SRL or RTD were not obvious due to the irrigation treatment. Even though we investigated these traits with two different methods (soil coring and ingrowth cores), no significant shift in either direction was observed.

In a recent analysis of root traits, Liese et al. (2017) demonstrated that the branching pattern of roots enables a plastic response to a changing environment. Species with high branching intensity are able to rapidly and extensively proliferate into resource-rich patches. Consequently, fine-root branching, including tips and forks, and not necessarily the diameter, reflects the environment. It should be noted, however, that the goal of that study was to investigate inter-species and not intra-species variation. A better understanding could potentially be gained from the new global Fine-Root Ecology Database FRED, introduced by Iversen et al. (2017). In their review, the authors ask the question "How do root traits vary along environmental gradients?" and refer to the studies of Larson and Funk (2016) and Zadworny et al. (2016) in relation to phenotypic responses to environmental change, although the former study did not investigate trees. Overall, it appears that soil factors have a strong effect on intra-species plasticity, as Valverde-Barrantes et al. (2013) pointed out when investigating 14 angiosperm tree species. Biomass, diameter, SRL, and RTD, were found to be significantly correlated with soil fertility, fractals (=tip abundance) with soil moisture, and length with soil carbon.

The use of single-pool and diameter-based classification of fine-roots, defined here as <2 mm diameter roots, has limitations. Functional aspects of the fine roots can hardly be described with this classification system. To overcome these limitations, McCormack et al. (2015) proposed an alternative approach using an order-based classification that allows more standardized comparisons of root traits, and a functional classification that allows for the distinction between absorption and transport functions. Absorptive fine roots in their concept correspond to the most distal roots, which are mainly involved in acquisition and uptake, while transport fine roots in the branching hierarchy are higher ordered and serve mainly structural and transport functions (McCormack et al., 2015). Such a new approach would allow for more consistent and accurate comparisons of root traits as well as comparisons between functionally similar roots in the future.

CONCLUSION

Our study demonstrates that the fine-root biomass of Scots pine in the topsoil of a water-limited site increases when water is added to the soil. Other studies with broader purposes (meta-analyses and reviews) have shown, in contrast, that the reactions of fine roots can be ambiguous and divergent, with increasing soil moisture leading either to an increase in fine-root biomass, a decrease, or no reaction at all. In these cases, the experimental design or the climatic gradient under study played a crucial role, and factors such as the length of the experiment, soil type, or method used to measure the fine roots influenced the results. Even though we observed in our study an increase in the fine-root biomass in the topsoil, we did not record root acclimation at deeper soil horizons. Given that the Pfynwald is located on a former alluvial fan composed of large rocks, a change in fine-root biomass at deeper levels is likely, although its measurement is not feasible. Since we observed a positive change solely in terms of fine-root biomass and length, and not in other morphological or architectural traits, such as diameter, SRL, RTD, tips, or forks, we can assume that the majority of root traits are not plastic. As Rewald et al. (2014) and Pierret et al. (2016) correctly pointed out, it is complicated to study whole root systems, and intra-root variability occurs with respect to dynamic, morphological, and architectural traits. As observed in our study, some traits undergo a change only after several years of treatment, suggesting that more research on long-term experiments in natural forests is needed. To understand why certain fine-root traits do adjust to soil environment changes and some do not, requires "more attention to the underlying drivers of fine-root mass and morphology, and to other mechanisms that are involved in soil resource uptake" (Weemstra et al., 2017). The same authors speculate that plasticity in fine-root biomass may be even more important than morphological plasticity. Further, it must be taken into

consideration that the plasticity of certain fine-root traits might be species-specific, or dependent on the evolutionary status (gymnosperms, angiosperms, monocots, dicots) or mycorrhizal status (ectomycorrhizal, arbuscular mycorrhizal, ericoid, non-mycorrhizal) of the trees in question (Comas et al., 2014; Valverde-Barrantes et al., 2017). In conclusion, more studies are needed to investigate the main drivers and patterns of root-trait plasticity to finally link those to overall tree performance. Under future global change scenarios, it will be highly relevant to know which fine-root traits are susceptible to environmental changes, whether they be water, temperature, pH, or nutrients, and which are not.

AUTHOR CONTRIBUTIONS

IB and CH dealt with the 2005 ingrowth cores and the soil coring from 2003–2016 and analyzed the data with WinRHIZO Software. LG and AG dealt with the 2016 ingrowth cores. All authors contributed to the writing of the manuscript.

FUNDING

CH was supported by the Swiss National Science Foundation (SNF), Grant number SNF 31003A_149507. LG was supported by a postdoctoral fellowship from the Alexander von Humboldt-Foundation (AvH).

ACKNOWLEDGMENTS

The analysis was based on data from the long-term Pfynwald forest irrigation experiment, which is part of the Swiss Long-term Forest Ecosystem Research Program LWF (www.lwf.ch). We are particularly grateful to Andreas Rigling and Marcus Schaub who are responsible for the Pfynwald irrigation experiment. We are also grateful for the assistance of Peter Bleuler and Christian Hug, who provided technical support for the experiment, as well as the long-standing support received from HYDRO Exploitation SA in Sion. We also thank Curtis Gautschi for correcting the English language.

REFERENCES

Bakker, M. R., Jolicoeur, E., Trichet, P., Augusto, L., Plassard, C., Guinberteau, J., et al. (2009). Adaptation of fine roots to annual fertilization and irrigation in a 13-year-old *Pinus pinaster* stand. *Tree Physiol.* 29, 229–238. doi: 10.1093/treephys/tpn020

Barberon, M., Vermeer, J. E., De Bellis, D., Wang, P., Naseer, S., Andersen, T. G., et al. (2016). Adaptation of root function by nutrient-induced plasticity of endodermal differentiation. *Cell* 164, 447–459. doi: 10.1016/j.cell.2015.12.021

Bardgett, R. D., Mommer, L., and de Vries, F. T. (2014). Going underground: root traits as drivers of ecosystem processes. *Trends Ecol. Evol.* 29, 692–699. doi: 10.1016/j.tree.2014.10.006

Beck, E. H., Fettig, S., Knake, C., Hartig, K., and Bhattarai, T. (2007). Specific and unspecific responses of plants to cold and drought stress. *J. Biosci.* 32, 501–510.

Bredemeier, M., Blanck, K., Dohrenbusch, A., Lamersdorf, N., Meyer, A. C., Murach, D., et al. (1998). The Solling roof project - site characteristics, experiments, and results. *For. Ecol. Manag.* 101, 281–293.

Brunner, I., Bakker, M. R., Björk, R. G., Hirano, Y., Lukac, M., Aranda, X., et al. (2013). Fine-root turnover rates of European forests revisited: an analysis of data from sequential coring and ingrowth cores. *Plant Soil* 362, 357–372. doi: 10.1007/s11104-012-1313-52013

Brunner, I., Graf Pannatier, E., Frey, B., Rigling, A., Landolt, W., Zimmermann, S., et al. (2009). Morphological and physiological responses of Scots pine fine roots to water supply in a climatic dry region in Switzerland. *Tree Physiol.* 29, 541–550. doi: 10.1093/treephys/tpn046

Brunner, I., Herzog, C., Dawes, M. A., Arend, M., and Sperisen, C. (2015). How tree roots respond to drought. *Front. Plant Sci.* 6:547. doi: 10.3389/fpls.2015.00547

Callaway, R. M., Pennings, S. C., and Richards, C. L. (2003). Phenotypic plasticity and interactions among plants. *Ecology* 84, 1115–1128.

Chaves, M. M., Maroco, J. P., and Pereira, J. S. (2003). Understanding plant responses to drought - from genes to the whole plant. *Funct. Plant Biol.* 30, 239–264. doi: 10.1071/FP02076

Ciais, P., Reichstein, M., Viovy, N., Granier, A., Ogée, J., Allard, V., et al. (2005). Europe-wide reduction in primary productivity caused by the heat and drought in 2003. *Nature* 437, 529–533. doi: 10.1038/nature03972

Comas, L. H., Callahan, H. S., and Midford, P. E. (2014). Patterns in root traits of woody species hosting arbuscular and ectomycorrhizas: implications for the evolution of belowground strategies. *Ecol. Evol.* 4, 2979–2990. doi: 10.1002/ece3.1147

De Visser, P. H., Beier, B. C., Rasmussen, L., Kreutzer, K., Steinberg, N., Bredemeier, M., et al. (1994). Biological response of 5 forest ecosystems in the EXMAN project to input changes of water, nutrients and atmospheric loads. *For. Ecol. Manag.* 68, 15–29.

Dietrich, D. (2018). Hydrotropism: how roots search for water. *J. Exp. Bot.* 69, 2759–2771. doi: 10.1093/jxb/ery034

Dietrich, L., Delzon, S., Hoch, G., and Kahmen, A. (2018). No role for xylem embolism or carbohydrate shortage in temperate trees during the severe 2015 drought. *J. Ecol.* 107, 334–349. doi: 10.1111/1365-2745.13051

Dobbertin, M., Eilmann, B., Bleuler, P., Giuggiola, A., Graf Pannatier, E., Landolt, W., et al. (2010). Effect of irrigation on needle morphology, shoot and stem growth in a drought-exposed *Pinus sylvestris* forest. *Tree Physiol.* 30, 346–360. doi: 10.1093/treephys/tpp123

Eapen, D., Barroso, M. L., Ponce, G., Campos, M. E., and Cassab, G. I. (2005). Hydrotropism: root growth responses to water. *Trends Plant Sci.* 10, 44–50. doi: 10.1016/j.tplants.2004.11.004

Farquhar, G. D., Ehleringer, J. R., and Hubick, K. T. (1989). Carbon isotope discrimination and photosynthesis. *Annu. Rev. Plant Phys. Plant Mol. Biol.* 40, 503–537.

Finer, L., Ohashi, M., Noguchi, K., and Hirano, Y. (2011). Fine root production and turnover in forest ecosystems in relation to stand and environmental characteristics. *For. Ecol. Manag.* 262, 2008–2023. doi: 10.1016/j.foreco.2011.08.042

Fonti, P., and Jansen, S. (2012). Xylem plasticity in response to climate. *New Phytol.* 195, 734–736. doi: 10.1111/j.1469-8137.2012.04252.x

Freschet, G., Swart, E., and Cornelissen, J. (2015). Integrated plant phenotypic responses to contrasting above and belowground resources: key roles of specific leaf area and root mass fraction. *New Phytol.* 206, 1247–1260. doi: 10.1111/nph.13352

Gaul, D., Hertel, D., Borken, W., Matzner, E., and Leuschner, C. (2008). Effects of experimental drought on the fine root system of mature Norway spruce. *For. Ecol. Manag.* 256, 1151–1159. doi: 10.1016/j.foreco.2008.06.016

Gessler, A., Jung, K., Gasche, R., Papen, H., Heidfelder, A., Börner, E., et al. (2005). Climate and forest management influence nitrogen balance of European beech forests: microbial N transformations and inorganic N net uptake capacity of mycorrhizal roots. *Eur. J. Forest Res.* 124, 95–111. doi: 10.1007/s10342-005-0055-9

Gill, R. A., and Jackson, R. (2000). Global patterns of root turnover for terrestrial ecosystems. *New Phytol.* 147, 13–31. doi: 10.1046/j.1469-8137.2000.00681.x

Gower, S. T., Vogt, K. A., and Grier, C. C. (1992). Carbon dynamics of Rocky -Mountain Douglas-fir: influence of water and nutrient availability. *Ecol. Monogr.* 62, 43–65.

Grime, J. P. (1977). Evidence for the existence of three primary strategies in plants in relevance to ecological and evolutionary theory. *Am. Nat.* 111, 1169–1194. doi: 10.1086/283244

Hagedorn, F., Joseph, J., Peter, M., Luster, J., Pritsch, K., Geppert, U., et al. (2016). Recovery of trees from drought depends on belowground sink control. *Nat. Plants* 2:16111. doi: 10.1038/nplants.2016.111

Hartmann, M., Brunner, I., Hagedorn, F., Bardgett, R., Stierli, B., Herzog, C., et al. (2017). A decade of irrigation transforms the soil microbiome of a semi-arid pine forest. *Mol. Ecol.* 26, 1190–1206. doi: 10.1111/mec.13995

Hendricks, J. J., Hendrick, R. L., Wilson, C. A., Mitchell, R. J., Pecot, S. D., and Guo, D. (2006). Assessing the patterns and controls of fine root dynamics: an empirical test and methodological review. *J. Ecol.* 94, 40–57. doi: 10.1111/j.1365-2745.2005.01067.x

Hertel, D., Strecker, T., Müller-Haubold, H., Leuschner, C., and Guo, D. (2013). Fine root biomass and dynamics in beech forests across a precipitation gradient - is optimal resource partitioning theory applicable to water-limited mature trees? *J. Ecol.* 101, 1183–1200. doi: 10.1111/1365-2745.12124

Herzog, C., Steffen, J., Graf Pannatier, E., Hajdas, I., and Brunner, I. (2014). Nine years of irrigation cause vegetation and fine root shifts in a water-limited pine forest. *PLoS One* 9:e96321. doi: 10.1371/journal.pone.0096321

Hommel, R., Siegwolf, R., Zavadlav, S., Arend, M., Schaub, M., Galiano, L., et al. (2016). Impact of interspecific competition and drought on the allocation of new assimilates in trees. *Plant Biol.* 18, 785–796. doi: 10.1111/plb.12461

Iversen, C. M., McCormack, M. L., Powell, A. S., Blackwood, C. B., Freschet, G. T., Kattge, J., et al. (2017). A global fine-root ecology database to address belowground challenges in plant ecology. *New Phytol.* 215, 15–26. doi: 10.1111/nph.14486

Joslin, J. D., Wolfe, H. M., and Hanson, P. J. (2000). Effects of altered water regimes on forest root systems. *New Phytol.* 147, 117–129.

Kelly, S. A., Panhuis, T. M., and Stoehr, A. M. (2012). Phenotypic plasticity: molecular mechanisms and adaptive significance. *Compr. Physiol.* 2, 1417–1439. doi: 10.1002/cphy.c110008

Konopka, B., and Lukac, M. (2013). Moderate drought alters biomass and depth distribution of fine roots in Norway spruce. *For. Pathol.* 43, 115–123. doi: 10.1111/efp.12005

Larson, J. E., and Funk, J. L. (2016). Seedling root responses to soil moisture and the identification of a belowground trait spectrum across three growth forms. *New Phytol.* 210, 827–838. doi: 10.1111/nph.13829

Liese, R., Alings, K., and Meier, I. C. (2017). Root branching is a leading root trait of the plant economics spectrum in temperate trees. *Front. Plant Sci.* 8:315. doi: 10.3389/fpls.2017.00315

Makkonen, K., and Helmisaari, H.-S. (1999). Assessing fine-root biomass and production in a Scots pine stand – comparison of soil core and root ingrowth core methods. *Plant Soil* 210, 43–50.

McCormack, M. L., Dickie, I. A., Eissenstat, D. M., Fahey, T. J., Fernandez, C. W., Guo, D., et al. (2015). Redefining fine roots improves understanding of below-ground contributions to terrestrial biosphere processes. *New Phytol.* 207, 505–518. doi: 10.1111/nph.13363

McCormack, M. L., Guo, D., Iversen, C. M., Chen, W., Eissenstat, D. M., Fernandez, C. W., et al. (2017). Building a better foundation: improving root-trait measurements to understand and model plant and ecosystem processes. *New Phytol.* 215, 27–37. doi: 10.1111/nph.14459

Meier, I. C., and Leuschner, C. (2008). Genotypic variation and phenotypic plasticity in the drought response of fine roots of European beech. *Tree Physiol.* 28, 297–309. doi: 10.1111/j.1365-2486.2008.01634.x

MeteoSchweiz (2018). *Klimabulletin Jahr 2017*. Zürich. Available at: https://www.meteoschweiz.admin.ch/home/service-und-publikationen/publikationen.html?topic=/content/meteoswiss/tags/topics/klima/publication/klimabulletin-jahr (accessed May 22, 2019).

Neill, C. (1992). Comparison of soil coring and ingrowth methods for measuring belowground production. *Ecology* 73, 1918–1921.

Nicotra, A. B., Atkin, O. K., Bonser, S. P., Davidson, A. M., Finnegan, E. J., Mathesius, U., et al. (2010). Plant phenotypic plasticity in a changing climate. *Trends Plant Sci.* 15, 684–692. doi: 10.1016/j.tplants.2010.09.008

Palacio-Lopez, K., Beckage, B., Scheiner, S., and Molofsky, J. (2015). The ubiquity of phenotypic plasticity in plants: a synthesis. *Ecol. Evol.* 5, 3389–3400. doi: 10.1002/ece3.1603

Persson, H. (1983). The distribution and productivity of fine roots in boreal forests. *Plant Soil* 71, 87–101.

Pierret, A., Maeght, J.-L., Clément, C., Montoroi, J.-P., Hartmann, C., and Gonkhamdee, S. (2016). Understanding deep roots and their functions in ecosystems: an advocacy for more unconventional research. *Ann. Bot.* 118, 621–635. doi: 10.1093/aob/mcw130

Polle, A., Chen, S. L., Eckert, C., and Harfouche, A. (2019). Engineering drought resistance in forest trees. *Front. Plant Sci.* 9:1875. doi: 10.3389/fpls.2018.01875

Rebetez, M., and Dobbertin, M. (2004). Climate change may already threaten Scots pine stands in the Swiss Alps. *Theor. Appl. Climatol.* 79, 1–9. doi: 10.1007/s00704-004-0058-3

Reich, P. B. (2014). The world-wide 'fast-slow' plant economics spectrum: a traits manifesto. *J. Ecol.* 102, 275–301. doi: 10.1111/1365-2745.12211

Rewald, B., Rechenmacher, A., and Godbold, D. L. (2014). It's complicated: intraroot system variability of respiration and morphological traits in four deciduous tree species. *Plant Physiol.* 166, 736–745. doi: 10.1104/pp.114.240267

Rigling, A., Bigler, C., Eilmann, B., Feldmeyer-Christe, E., Gimmi, U., Ginzler, C., et al. (2013). Driving factors of a vegetation shift from Scots pine to pubescent oak in dry Alpine forests. *Glob. Chang. Biol.* 19, 229–240. doi: 10.1111/gcb.12038

Rozendaal, D. M., Hurtado, V. H., and Poorter, L. (2006). Plasticity in leaf traits of 38 tropical tree species in response to light; relationships with light demand and adult stature. *Funct. Ecol.* 20, 207–216. doi: 10.1111/j.1365-2435.2006.01105.x

Schönbeck, L., Gessler, A., Hoch, G., McDowell, N. G., Rigling, A., Schaub, M., et al. (2018). Homeostatic levels of nonstructural carbohydrates after 13 yr of drought and irrigation in *Pinus sylvestris*. *New Phytol.* 219, 1314–1324. doi: 10.1111/nph.15224

Shipley, B., De Bello, F., Cornelissen, J. H. C., Laliberté, E., Laughlin, D. C., and Reich, P. B. (2016). Reinforcing loose foundation stones in trait-based plant ecology. *Oecologia* 180, 923–931. doi: 10.1007/s00442-016-3549-x

Solly, E. F., Brunner, I., Helmisaari, H.-S., Herzog, C., Leppälammi-Kujansuu, J., Schöning, I., et al. (2018). Unravelling the age of fine roots of temperate and boreal forests. *Nat. Commun.* 9:3006. doi: 10.1038/s41467-018-05460-6

Timofeeva, G., Treydte, K., Bugmann, H., Rigling, A., Schaub, M., Siegwolf, R., et al. (2017). Long-term effects of drought on tree-ring growth and carbon isotope variability in Scots pine in a dry environment. *Tree Physiol.* 37, 1028–1041. doi: 10.1093/treephys/tpx041

Vacchiano, G., Garbarino, M., Mondino, E. B., and Motta, R. (2012). Evidences of drought stress as a predisposing factor to Scots pine decline in Valle d'Aosta (Italy). *Eur. J. For. Res.* 131, 989–1000. doi: 10.1007/s10342-011-0570-9

Valladares, F., Matesanz, S., Guilhaumon, F., Araujo, M. B., Balaguer, L., Benito-Garzon, M., et al. (2014). The effects of phenotypic plasticity and local adaptation on forecasts of species range shifts under climate change. *Ecol. Lett.* 17, 1351–1364. doi: 10.1111/ele.12348

Valverde-Barrantes, O. J., Freschet, G. T., Roumet, C., and Blackwood, C. B. (2017). A worldview of root traits: the influence of ancestry, growth form, climate and mycorrhizal association on the functional trait variation of fine-root tissues in seed plants. *New Phytol.* 215, 1562–1573. doi: 10.1111/nph.14571

Valverde-Barrantes, O. J., Smemo, K. A., Feinstein, L. M., Kershner, M. W., and Blackwood, C. B. (2013). The distribution of below-ground traits is explained by intrinsic species differences and intraspecific plasticity in response to root neighbours. *J. Ecol.* 101, 933–942. doi: 10.1111/1365-2745.12087

Volkmann, T. H. M., Haberer, K., Gessler, A., and Weiler, M. (2016). High-resolution isotope measurements resolve rapid ecohydrological dynamics at the soil–plant interface. *New Phytol.* 210, 839–849. doi: 10.1111/nph.13868

Weemstra, M., Sterck, F. J., Visser, E. J. W., Kuyper, T. W., Goudzwaard, L., and Mommer, L. (2017). Fine-root trait plasticity of beech (*Fagus sylvatica*) and spruce (*Picea abies*) forests on two contrasting soils. *Plant Soil* 415, 175–188. doi: 10.1007/s11104-016-3148-y

Yuan, Z. Y., and Chen, H. Y. H. (2010). Fine root biomass, production, turnover rates, and nutrient contents in boreal forest ecosystems in relation to species, climate, fertility, and stand age: literature review and meta-analyses. *Crit. Rev. Plant Sci.* 29, 204–221. doi: 10.1080/07352689.2010.483579

Yuan, Z. Y., and Chen, H. Y. H. (2012). A global analysis of fine root production as affected by soil nitrogen and phosphorus. *Proc. R. Soc. B* 279, 3796–3802. doi: 10.1098/rspb.2012.0955

Zadworny, M., McCormack, M. L., Mucha, J., Reich, P. B., and Oleksyn, J. (2016). Scots pine fine roots adjust along a 2000-km latitudinal climatic gradient. *New Phytol.* 212, 389–399. doi: 10.1111/nph.14048

Zadworny, M., McCormack, M. L., Zytkowiak, R., Karolewski, P., Mucha, J., and Oleksyn, J. (2017). Patterns of structural and defense investments in fine roots of Scots pine (*Pinus sylvestris* L.) across a strong temperature and latitudinal gradient in Europe. *Global Change Biol.* 23, 1218–1231. doi: 10.1111/gcb.13514

Zhang, X., Xing, Y., Yan, G., Han, S., and Wang, Q. (2019). Effects of precipitation change on fine root morphology and dynamics at a global scale: a meta-analysis. *Can. J. Soil Sci.* 99, 1–11. doi: 10.1139/CJSS-2018-0114

Conflict of Interest Statement: The authors declare that the research was conducted in the absence of any commercial or financial relationships that could be construed as a potential conflict of interest.

frontiers in Plant Science

ORIGINAL RESEARCH
published: 28 May 2019
doi: 10.3389/fpls.2019.00690

Advanced Aboveground Spatial Analysis as Proxy for the Competitive Environment Affecting Sapling Development

Peter Annighöfer[1], Dominik Seidel[1], Andreas Mölder[2] and Christian Ammer[1]*

[1] Silviculture and Forest Ecology of the Temperate Zones, University of Göttingen, Göttingen, Germany, [2] Department A (Forest Growth), Northwest German Forest Research Institute, Göttingen, Germany

Tree saplings are exposed to a competitive growth environment in which resources are limited and the ability to adapt determines general vitality and specific growth performance. In this study we analyzed the aboveground spatial neighborhood of oak [*Quercus petraea* (Matt.) Liebl.] and beech (*Fagus sylvatica* L.) saplings growing in Germany, by using hemispherical photography and terrestrial laser scanning as proxy for the competitive pressure saplings were exposed to. The hemispherical images were used to analyze the light availability and the three-dimensional (3D) point clouds from the laser scanning were used to assess the space and forest structure around the saplings. The aim was to increase the precision with which the biomass allocation, growth, and morphology of the saplings could be predicted by including more detailed information of their environment. The predictive strength of the models was especially increased through direct neighborhood variables (e.g., relative space filling), next to the light availability being the most important predictor variable. The biomass allocation patterns within the more light demanding oak were strongly driven by the space availability around the saplings. Diameter and height growth variables of both species reacted significantly to changes in light availability, and partly also to the neighborhood variables. The leaf morphology [as leaf-area ratio (LAR)] was also driven by light availability and decreased with increasing light availability. However, the branch morphology (as mean branch weight) could not be explained for oak and the model outcome for beech was hard to interpret. The results could show that individuals of the same species perform differently under constant light conditions but differing neighborhoods. Assessing the neighborhood of trees with highly precise measurement devices, like terrestrial laser scanners, proved to be useful. However, the primary response to a dense neighborhood seemed to be coping with a reduction of the lateral light availability aboveground, rather than responding to an increase of competition belowground. The results suggest continuing efforts to increase the precision with which plant environments can be described through innovative and efficient methods, like terrestrial laser scanning.

Keywords: biomass allocation, tree morphology, competition, light gradient, spatial analysis, growth environment, terrestrial laser scanning, hemispherical photography

OPEN ACCESS

Edited by:
Erik T. Nilsen,
Virginia Tech, United States

Reviewed by:
Thomas Ting Lei,
Ryukoku University, Japan
Enrique Andivia,
Complutense University of Madrid, Spain

****Correspondence:***
Peter Annighöfer
pannigh@gwdg.de

Specialty section:
This article was submitted to Functional Plant Ecology, a section of the journal Frontiers in Plant Science

Received: *08 February 2019*
Accepted: *08 May 2019*
Published: *28 May 2019*

Citation:
Annighöfer P, Seidel D, Mölder A and Ammer C (2019) Advanced Aboveground Spatial Analysis as Proxy for the Competitive Environment Affecting Sapling Development. Front. Plant Sci. 10:690. doi: 10.3389/fpls.2019.00690

INTRODUCTION

Every plant competes with other plants or organisms for limited resources. The survival and general plant performance is primarily determined by the amount of resources the individual plant can capture. More specifically, the resource availability influences competitive ability (Funk and Vitousek, 2007), primary and secondary growth (Pretzsch et al., 2017), biomass allocation (McConnaughay and Coleman, 1999; Shipley and Meziane, 2002), and plant morphology (Hutchings and de Kroon, 1994; Kimmins, 2004). For saplings growing in the understory of (temperate) forest ecosystems the amount of light is considered to be among the most important resources (Lambers et al., 2008). Aside of its importance, the availability of light is known to influence different species in various ways, especially when considering light demanding or shade tolerant species (Poorter, 1999; Lödige et al., 2014; Annighöfer et al., 2017), resulting in species-specific traits as reaction to varying levels of light (Petriţan et al., 2009; Schall et al., 2012). Several studies were able to measure the light availability and show its effects on the sapling performance (e.g., Beaudet and Messier, 1998; Williams et al., 1999; Drever and Lertzman, 2001; Claveau et al., 2002; Ammer, 2003; Delagrange et al., 2004; Messier and Nikinmaa, 2016; Annighöfer et al., 2017). Plants in general also compete for other resources above- and belowground, including water, nutrients and growing space (Casper and Jackson, 1997; Leuschner and Ellenberg, 2017). Effects of belowground competition on sapling performance induced by mature trees have been shown by exclusionary experimental setups, e.g., root-trenching experiments (Leuschner et al., 2001; Ammer, 2002; Petriţan et al., 2011), even though still comparably little is known about belowground competition.

In addition to directly measuring the availability of resources and relating it to plant performance, or directly measuring the resource uptake by individual plants (e.g., Ehleringer and Dawson, 1992; Silla and Escudero, 2003), a common approach to explain plant performance is to measure the competitive pressure an individual is exposed to (e.g., Wagner et al., 2009; Seidel et al., 2015). For mature trees, several indices exist to quantify the aboveground competitive pressure an individual might be exposed to at its growth site, among which the Hegyi index (Hegyi, 1974) is a widely applied measure. For saplings, however, many of the competition measures are laborious to derive in the field and rarely used (e.g., Elliot and Vose, 1995). Furthermore, many competition indices are strongly focused on the dimensions and competitive interactions of neighboring full-grown trees. In light-limited surroundings the abundance of shrubs, grasses and herbs can generally be considered to play an insignificant role for the performance of mature trees, even though some studies also show their effect on ecosystem traits (Gebhardt et al., 2014). For smaller saplings however, the abundance and density of shrubs, grass and herbs in their direct neighborhood can be expected to have a more severe impact (Löf, 2000; Coll et al., 2003; Harmer et al., 2005), but quantifying these is complicated. So far, these vegetation layers are usually described in view of their cover, e.g., through Braun-Blanquet (1932) and other visual assessments (Wagner and Radosevich, 1991), or their effect is studied by setting up desired levels of competition through planting and weeding or the use of herbicides (Morris et al., 1990, 1993; Jylhä and Hytönen, 2006). Also, depending on the growth form, some species of these vegetation layers might intercept light, but other species with similar biomass but different growth form might more strongly capture nutrients or water, making the competitive environment of saplings rather complex (Elliot and Vose, 1995).

In this study, we explored a novel approach to quantify the forest structure and neighborhood of saplings through spatial analysis of terrestrial laser scans (TLS). The quantifications derived from the TLS were combined with light measurements derived from a fisheye-lens camera. We expected that a detailed quantification of the individual neighborhood and surrounding forest structure, as addition to the light measurements, would increase the precision with which plant characteristics can be predicted (comp. Wagner et al., 2011). This expectation is based on the assumption that the general availability of resources is not only related to canopy density and thus light availability above each sapling (determined by overstorey density and recorded with the camera), but also linked to the direct neighborhood within the immediate lateral proximity of the saplings and overall indices of forest structure (recorded with TLS). Combining this information should result in a more accurate proxy of the competitive pressure the saplings are exposed to, respectively. To follow-up on this expectation we decided to harvest saplings of a shade-tolerant (*Fagus sylvatica* L.) and a more light-demanding species [*Quercus petraea* (Matt.) Liebl.] growing along light gradients in the understory of two different Central European temperate forests. Since all individuals of both species had regenerated naturally, we expected their growth, morphology, and biomass allocation to be a result of the resources at their growth site which they could capture.

We hypothesized that (1) traits and general performances (in view of growth and allocation) of saplings could be better predicted by not only using light measurements as explanatory variable, but additionally considering information of the saplings' immediate neighborhood and the surrounding forest structure. Specific hypotheses concerning biomass allocation, growth and sapling morphology were:

(2) Following the "functional equilibrium hypothesis," above- and belowground biomass is allocated in the direction of the limiting resource (Brouwer, 1963; Shipley and Meziane, 2002), e.g., increasing light availability or decreasing aboveground neighborhood density result in an increase of the belowground root-mass fraction (RMF) (Hofmann and Ammer, 2008).

(3) Diameter growth increases with increasing light availability (Beaudet and Messier, 1998) and decreasing neighborhood density, whereas height growth increases with increasing light availability (Lüpke, 2004; Lüpke and Hauskeller-Bullerjahn, 2004) but also with increasing neighborhood density.

(4) Mean branch weight increases with increasing light availability and decreases with increasing neighborhood density, especially for shade-intolerant species, like beech (Smith, 1994; Ammer, 2003).

(5) The leaf area ratio (LAR) decreases with increasing light availability and is higher under low light intensities for shade-tolerant species (Poorter and Remkes, 1990; Cornelissen et al., 1996).

MATERIALS AND METHODS

Study Area

The saplings were collected from two study locations in Germany. The oak saplings originated from the forestry district "Unterlüß" in Lower Saxony (52°50′ N, 10°16′ O). The stand under investigation is managed as high forest system. Parts of the stand have been naturally regenerated through removing overstorey trees and maintaining regularly distributed seed trees (shelterwood). Retained overstorey trees are mainly comprised of sessile oak (*Q. petraea*) admixed with scattered individuals of Scots pine (*Pinus sylvestris* L.), Norway spruce [*Picea abies* (L.) H. Karst.] and European beech (*F. sylvatica*) trees. The overstorey has an age of about 130–170 years, depending on the species. The Unterlüß study site is situated in the northwest German lowlands at an altitude of approximately 120 m a.s.l. The climate is temperate oceanic, with an average temperature of 8.4°C year^{-1}. The long-term annual precipitation lies around 760 mm year^{-1} (Gauer and Aldinger, 2005). The trees are growing on rather nutrient-poor sandy soils, moderately moist (on average sufficient water supply for plant growth) during the growing season, with top soil layers occasionally running dry or water pooling in the deeper soil horizons. The general growth site conditions are considered quite suitable for sessile oak.

The beech saplings were collected in stands of the forestry district "Leinefelde" in Thuringia (10.36° E, 51.32° N). The stand is also a high forest, dominated by beech with admixed single pedunculate oak (*Quercus robur* L.) and sycamore maple (*Acer pseudoplatanus* L.) trees. The age of the overstorey lies around 130–140 years. Following a mast year and partial target diameter harvest, beech regeneration has established. In winter 2013/2014, additionally six gap cuts (three larger, three smaller gaps, range 500–1170 m^2; Seidel et al., 2015) were added to study the natural succession in these gaps in a long term project (not part of this study). The Leinefelde site is located at 450 m a.s.l. in the central German low mountain ranges. The climate is temperate with a tendency toward subcontinentality. The average annual temperature is 8.2°C year^{-1} and the annual precipitation lies around 680 mm year^{-1} (Gauer and Aldinger, 2005). The trees are growing on a nutrient-rich clayed-silt soil with sufficient water supply, representing very good growth conditions for beech.

Sapling Collection and Further Field Measurements

Both study sites were divided into systematic grids of 25 × 25 m (Leinfelde) and 18 × 18 m (Unterlüß) with randomized starting points. This grid was chosen to assure covering a variety of light and neighborhood conditions the saplings were growing in. The grid size was derived from the size of the area under regeneration to result in about 50 sampling points. Saplings were collected along the grid points at both sites, by choosing the sapling closest to the grid point, respectively. The only selection criteria were sapling vitality (free of apparent damage) and sapling dimensions (i.e., height and diameter) to assure morphological and age wise comparability of the saplings. If saplings belonged to a regeneration group, the most vital sapling of the group was chosen. Saplings were identified, marked and harvested as whole plants (above- and belowground plant compartments) for further analysis in the laboratory. This resulted in a total of 51 beech saplings in Leinefelde and 44 oak saplings in Unterlüß (**Table 1**).

TABLE 1 | Properties and dimensions of the beech (Fs) and oak (Qp) saplings in the year of harvest.

	Fs	Qp	*p*-value
Number of observations (n)	51	44	
Mean RCD (cm)	18.18 ± 3.36	19.51 ± 6.93	0.23
Mean H (cm)	189.8 ± 25.11	161.46 ± 57.56	<0.05
Mean age (years)	11.88 ± 1.67	6.61 ± 1.85	<0.05

Presented are the number of saplings harvested (number of observations), their mean root-collar diameter (mean RCD), height (mean H), and counted stem disc age (mean age) with standard deviation (±SD). The p-value shows significant differences between Fs and Qp.

The light environment the saplings were exposed to prior to harvest, was measured at each harvesting location using an automated fisheye lens camera (Solariscope, Behling SOL300, contact: hb.messtechnik@gaia.de). This device calculates measures of light availability (e.g., indirect site factor (ISF), direct site factor, total site factor, openness, gap fraction, and leaf area index) by automatically analyzing hemispherical photographs according to seven threshold values (comp. Pryor, 2010). At each harvesting location one solariscope measurement was conducted at 2 m above ground (comp. **Table 1**).

Next to the light measurements we assessed the detailed neighborhood conditions and surrounding forest structural conditions of each sapling by taking a TLS at each saplings' growing position. To ensure capturing the immediate and relevant neighborhood of each sapling each single scan was conducted at 0.8 m above ground, close to 50% of the mean sapling height (comp. **Table 1**). Scans were captured with the Faro Focus three-dimensional (3D) 120 laser scanner (Faro Technologies Inc., Lake Mary, FL, United States). This terrestrial laser scanner emits 44 Mio laser beams per single scan, which are reflected and received by the instrument, if surrounding objects are hit (comp. Seidel et al., 2015; Ehbrecht et al., 2016). The information stored by the instrument consists of the object's coordinate in a 3D coordinate system (x, y, z). Since coordinates are dimensionless, they can be converted to voxels (3D pixels) with varying resolution (as presented in **Figure 1**). Maximum scanning distance of the instrument was 120 m. Resulting 3D point cloud representations of the different forest scenes were processed with FaroScene.

Sapling Processing and Laboratory Measurements

The harvested saplings were partitioned according to the plant organs leaves, branches, stems and roots. One random fresh-leaf sample of at least 15 leaves was collected from each sapling. These

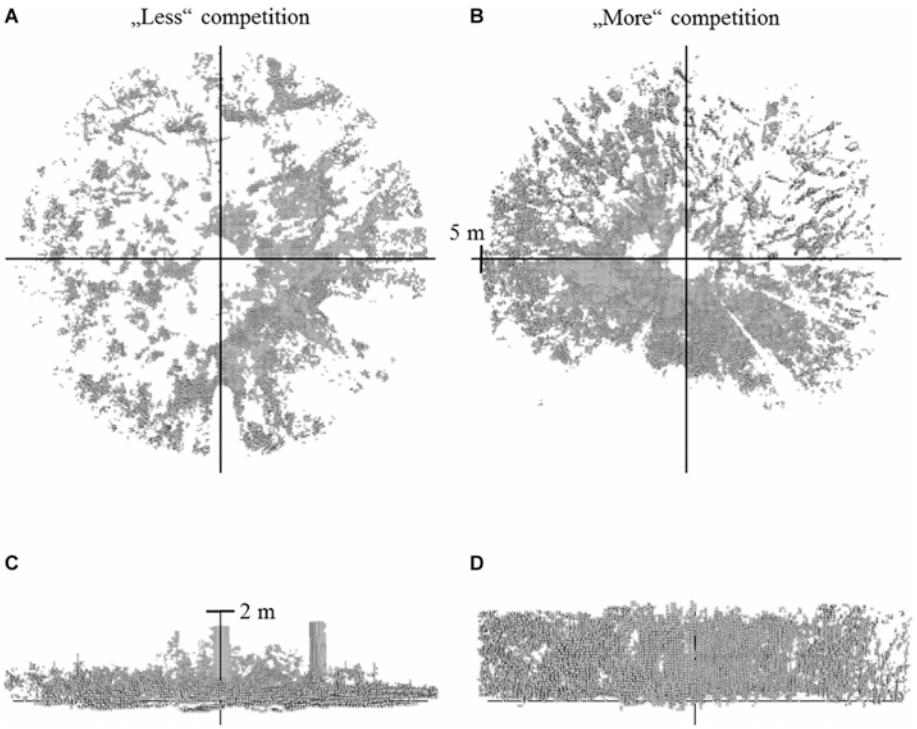

FIGURE 1 | Voxel data (gray) resulting from single scans of two different forest scenes. Left **(A,C)**: situation with less understory vegetation. Right **(B,D)**: situation with more understory vegetation in the vicinity (radius = 5 m) of the sapling (view from top: **A,B**; view from side: **C,D**). Two single stems can be made out in the left view from the side **(C)**, whereby the very dense understory vegetation on the right **(D)** does now allow identifying single objects visually.

15 leaves were scanned on a flatbed scanner (Mustek Systems Inc. A3 2400S) and their leaf area was measured with ImageJ (open source; developer: Wayne Rasband). The branches on each sapling were counted. All plant compartments were then dried in a temperature-controlled oven at 70°C to constant weight and weighed (mg). The random leaf samples were dried separately, allowing to use the ratio of leaf area and dry weight to estimate the total leaf area of each sapling. An age estimation and the annual diameter increment of all saplings was measured by extracting a stem disc from each sapling (5 cm above ground), sanding it, and counting and measuring the annual rings, respectively. Year ring widths were measured in two to four (for stem discs strongly deviating from circularity) directions on scanned images (1200 dpi) of the disks, with a precision of 1/100 mm using the software Lignovision (Rinntech version 1.37). Annual height increment was assessed along each stem by measuring the distance between two consecutive annual internodes on the stem surface. Additionally, the root-collar diameter (RCD) was measured 5 cm above ground (where the stem disc was extracted) and the total height (H) of the sapling was measured along the stem axis by measuring its length.

Data Analysis

Analyzing the Growth Environment – Light Environment

Analyzing the light environment was based on the Solariscope measurements. From the resulting seven threshold-based interpretations of the hemispherical photos from each harvesting location, the operator needs to visually choose the one showing the best distinction between sky and non-sky. Two independent operators underwent this procedure for quality assurance, especially for stand conditions which are well represented by more than one threshold value. The quantification of the light environment was based on the ISF. The ISF quantifies the proportion of indirect or diffuse radiation reaching the measurement point.

Analyzing the Growth Environment – Forest Structure

The forest structure was analyzed by calculating published indices based on the full 3D point clouds or parts of the 3D point clouds created through the TLS (single scans). These indices were the effective number of layers (Ehbrecht et al., 2016), the stand structural complexity index (Ehbrecht et al., 2017), and the so called MeanFrac, which is part of the stand structural complexity index presented in Ehbrecht et al. (2017), but used in isolation here. MeanFrac stands for the mean fractal dimension index, based on McGarigal and Marks (1995). It is defined as the arithmetic mean of perimeter to area ratios of vertical point cloud polygons, similar to what can be seen in **Figure 2B**. A detailed description of its calculation is presented in Ehbrecht et al. (2017).

Analyzing the Growth Environment – Neighborhood

The 3D point clouds derived from the single scans were further used to analyze the direct neighborhood of the saplings.

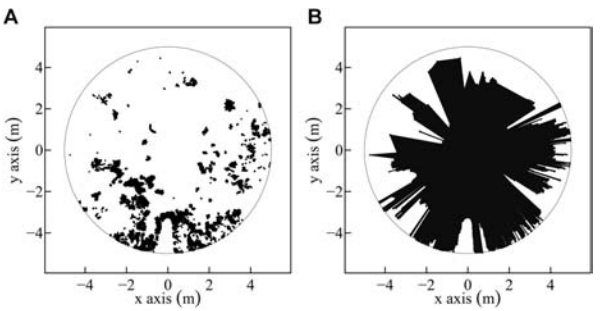

FIGURE 2 | Exemplary understory three-dimensional (3D) point cloud projection onto a two-dimensional (2D) horizontal plane. Transformation of a two-dimensional (2D) point cloud (scatterplot) **(A)** within a radius of 5 m to a polygon **(B)** by connecting all points. The polygon area is colored black **(B)**.

We assumed that the immediate neighborhood of a sapling was well represented by all elements of neighboring plants located in a cylindrical selection of the point cloud with a radius of 5 m around the target sapling. For separating the neighborhood information from the light measurements (space vs. light), the cylinder was reduced to a height of 2 m, to only include information on the neighborhood not already recorded by hemispherical photography. These point cloud cylinders were further processed and analyzed applying two different approaches:

The first approach was based on creating voxel-models from the 3D point clouds. The voxel size was 125 cm^3 (5 cm side length) and voxels served as proxy to calculate a relative space filling value around the individual saplings (**Figure 1**). An edge length of 5 cm was considered appropriate to maintain the details of the point clouds representing a forest scene, without giving too much weight to single stray points in the original point cloud. Relative filling values were calculated for the full cylinder (radius = 5 m, height = 2 m) and for gradual radius reductions in steps of 1 m by applying the following formula:

$$RF_i = \frac{V\_vox \times n\_vox_i}{\pi \times R_i^2 \times H} \times 100 \quad (1)$$

[with RF_i = relative filling of cylinder with radius i; V_vox = volume of voxel (125 cm^3); n_vox_i = number of voxels in cylinder with radius i; R_i = radius i of cylinder (with i = 500, 400,. . .100 cm); H = height of cylinder (200 cm)].

In the second approach, point clouds were not voxeled but each point coordinate was used to span a horizontal polygon, as proxy for the space available around the saplings within the predefined cylinder. Also here resulting polygon areas were calculated for the maximal radius of 5 m and for successive reductions of the radius. To create the polygons, the 3D points within the cylinder were projected onto a two-dimensional (2D) surface, whereas the points below 30 cm height were excluded to reduce the effect of forest ground hits (**Figure 2**).

Analyzing the Saplings

The effects of light availability, forest structure, and neighborhood on biomass allocation (root, stem, branch, and leaves), increment measurements (height and diameter), and sapling morphology (mean branch weight, LAR) were assessed. Mass fractions of each plant organ were calculated in relation to the total plant mass by applying Eq. 2 for each sapling.

$$MF_i = \frac{BM_i}{BM_T} \quad (2)$$

[with MF_i = mass fraction of plant organ i (g g^{-1}); BM_i = biomass of plant organ i (g); BMT = total biomass of sapling (g), with i = root, stem, branch, and leaf].

Next to absolute diameter and height increment measures (comp. above), the increment measures were also converted to relative values (Eq. 3) for each sapling:

$$Rel\_inc_i = \frac{Inc_i}{i} \quad (3)$$

[with Rel_inc_i = relative increment of i (1/100); Inc_i = increment of i (cm; 1/100 mm), with i = height, diameter (cm; 1/100 mm)].

The morphology was quantified by using the total number of branches to calculate the mean branch weight (Eq. 4) for each sapling:

$$Mean\_BW = \frac{B\_bm}{B\_n} \quad (4)$$

[with Mean_BW = mean branch weight (g n^{-1}); B_bm = branch biomass (g); B_n = number of branches].

The morphology was further quantified by calculating the LAR (Eq. 5) for each sapling:

$$LAR = \frac{LA}{BM_T} \quad (5)$$

[with LAR = leaf area ratio (cm^2 g^{-1}); LA = total leaf area (cm^2); BM_T = total biomass of sapling (g)].

Statistical Analysis

The comparisons between groups (e.g., **Table 1**, between "Beech" and "Oak") were conducted with parametric and non-parametric tests, depending on the data structure. For data that was normally distributed (Shapiro–Wilk test) and had homogenous variances (Fligner–Killeen test of homogeneity of variances) an analysis of variance model (AOV) was used. For data that was not normally distributed or data that had inhomogeneous variances, a non-parametric Kruskal–Wallis rank sum test was applied.

The relationships between response (y) and explanatory (x) variables were analyzed with multiple-regression techniques. Data was separately analyzed for both species. To reduce the total number of predictor variables and especially to reduce variance inflation through collinearity, single predictors were removed from pairs of predictors with $R^2 > 0.7$, in reference to Dormann et al. (2013). The remaining explanatory variables were (1) the ISF, as descriptor for the light environment the saplings were exposed to, (2) the relative filling of the cylinder with 5 m radius (RF_5m) and the (3) horizontal polygon area within a radius of 2 m (PA_2m), as descriptors for the direct neighborhood of the saplings; (4) MeanFrac as descriptor for the complexity

of the general forest structure of the stands where the saplings were growing.

The multiple regressions as generalized linear models (GLM) were started as full models, including interactions between the light measure (ISF) and the neighborhood variables (RF_5m and PA_2m) as representatives for competitive interactions in view of different resources. To correct for inhomogeneous standard deviations (non-normally distributed regression residuals, visual verification, Shapiro–Wilk test), logarithmic transformations were applied (McDonald, 2014), wherever necessary. The full models were then simplified through backward selection, starting with non-significant interactions and then subsequently removing single variables with highest *p*-values until all remaining variables were significant or significant in interactions, controlled through AOV tables (Crawley, 2013). Models were evaluated through residual standard error (RSE), R^2 (for models with a single predictor variable) and adjusted R^2 (as robust measure against overfitted models with more than a single predictor variable). The relative importance of significant explanatory variables in models with more than one explanatory variable was assessed using the proportional marginal decomposition method and metric proposed by Feldman (2005) and recommended by Groemping (2006). For higher order terms (interactions) variable importance was assessed through R^2 partitioning by averaging over orders according to Lindeman et al. (1980) and also as recommended by Groemping (2006).

Significant interactions were visualized in 3D plots. Selected variables comparing the response of beech and oak to one another were visualized through non-linear Generalized Additive Modeling (GAM) techniques (Hastie and Tibshirani, 1990; Wood, 2006). The GAM visualization was used for comparison because no data transformation was required. The effective degrees of freedom (EDF) were limited to a maximum of 3 (number of knots = 4). However, the amount of smoothing was chosen automatically through generalized cross-validation (Cianelli et al., 2004). The data family was set to Gaussian type with an identity-link function (Wood, 2011). The statistical significance of the GAM models was evaluated by considering the *p*-values tested by an *F*-test.

The significance level for this study was $p < 0.05$. All statistical analyzes, model fitting, and graphs were processed and produced using the free software environment R, version 3.4.0 (R Core Team, 2017).

RESULTS

The four predictor variables were able to explain 18 out of 20 response variables (unexplained: branch mass fraction, mean branch weight of oak). For these 18 response variables the model quality varied considerably, with adjusted R^2-values ranging from around 0.1 (e.g., stem mass fraction and leaf mass fraction of beech) up to maximum values around 0.5 (absolute diameter increment of oak; absolute and relative diameter increment of beech). A total of 7 out of 18 response variables was explained best by a single variable, which were light availability (ISF, $n = 4$) and relative space filling (RF_5m, $n = 3$). All other models had more than one predictor variable, with their relative importance ranging from 0.03 up to 0.52, respectively. The most abundant significant predictors in all models were the light availability (ISF, $n = 16$, including $n = 2$ significant interactions), followed by the relative space filling (RF_5m, $n = 11$, including $n = 2$ significant interactions). MeanFrac was significant in $n = 4$ models and the polygon area (PA_2m) was significant in $n = 2$ models (comp. **Table 2**).

Biomass Allocation

The RMF of oak was sensitive to neighborhood variables but not to light and forest structure (**Table 2**). An increase of relative space filling (RF_5m) reduced the RMF, whereas an increase in space (PA_2m) around the sapling increased the RMF. The RMF of the beech saplings did not respond to the neighborhood variables, but only reacted positively to light availability (ISF) and negatively to structural complexity (MeanFrac). The explanatory strength of the model for beech was much lower than for oak (comp. **Figure 3A** for RF_5m). Stem-mass fraction for oak increased with increasing RF_5m and could nearly not be explained for beech ($R^2 = 0.08$), even though RF_5m was also the significant predictor here (**Figure 3B** and **Table 2**). Leaf-mass fraction generally decreased with increasing ISF, whereas it was part of a significant interaction with RF_5m for oak. **Figure 4** shows the interaction, as opposed trends. Under low light availability (ISF) and increasing relative space filling (RF_5m), leaf-mass fraction approaches zero. Under low RF_5m and increasing ISF values leaf-mass fraction also decreases. Under high RF_5m and increasing ISF values leaf-mass fraction increases, as also for high ISF and increasing RF_5m. The branch-mass fraction could not be explained for oak, but increased with increasing RF_5m for beech.

Increment

The absolute and relative height growth (H_inc and H_inc_rel) for oak and beech saplings increased with increasing light availability (ISF) (**Figures 3C,E** and **Table 2**). But absolute height growth was partly more strongly driven by neighborhood. It decreased with increasing polygon area (PA_2m) for oak and increased with increasing relative space filling (RF_5m) for beech (same results for relative height increment of beech). Absolute height increment was higher for beech over the whole light gradient. Absolute and relative diameter increment (D_inc, D_inc_rel) for both species was most strongly driven by light availability and increased with increasing ISF (**Figures 3D,F**). For beech, also MeanFrac was significant, negatively reacting with increasing diameter growth.

Morphological Traits

The mean branch weight could not be explained by the considered predictor variables for oak. For beech, it increased with light (ISF) and relative space filling (RF_5m), whereas the explanatory strength was also not high for this model.

The LAR of both species decreased with increasing light availability, whereas this trend was explicit for beech, not so for oak (**Table 2**). The leaf-area ratio (LAR) model for oak

TABLE 2 | Generalized linear model (GLM) performance table for both species (SP), oak (Qp), and beech (Fs).

SP	Resp	Pred	Est	*p*-value	R^2	Adj. R^2	RSE	Rel. Imp.
Qp	RMF	(Int)	0.3243	0.000	0.40	0.37	0.065	
Qp	RMF	RF_5m	−0.0412	0.001				0.23
Qp	RMF	PA_2m	0.0208	0.003				0.17
Qp	SMF	(Int)	0.1860	0.006	0.31	0.29	0.092	
Qp	SMF	RF_5m	0.0664	0.000				1.00
Qp	LMF	(Int)	0.2030	0.000	0.33	0.28	0.019	
Qp	LMF	ISF	−0.0040	0.010				0.04
Qp	LMF	RF_5m	−0.0340	0.001				0.14
Qp	LMF	ISF:RF_5m	0.0010	0.005				0.15
Qp	BMF	(Int)	0.1606	0.000	0.00	0.00	0.062	n.a.
Qp	LAR	(Int)	48.2485	0.000	0.24	0.18	5.221	
Qp	LAR	ISF	−0.8750	0.042				0.03
Qp	LAR	RF_5m	−7.5537	0.005				0.11
Qp	LAR	ISF:RF_5m	0.2178	0.027				0.10
Qp	Mean_BW (log)	(Int)	0.5716	0.000	0.00	0.00	0.800	n.a.
Qp	D_inc (log)	(Int)	4.1020	0.000	0.50	0.48	0.239	
Qp	D_inc (log)	ISF	0.0241	0.000				0.43
Qp	D_inc (log)	MeanFrac	0.1298	0.015				0.07
Qp	H_inc (log)	(Int)	3.6410	0.000	0.32	0.29	0.456	
Qp	H_inc (log)	ISF	0.0162	0.019				0.11
Qp	H_inc (log)	PA_2m	−0.1545	0.002				0.21
Qp	D_inc_rel (log)	(Int)	−2.9953	0.000	0.22	0.21	0.365	
Qp	D_inc_rel (log)	ISF	0.0184	0.001				1.00
Qp	H_inc_rel (log)	(Int)	−2.7335	0.000	0.20	0.18	0.473	
Qp	H_inc_rel (log)	ISF	0.0220	0.003				1.00
Fs	RMF	(Int)	0.3852	0.000	0.21	0.18	0.038	
Fs	RMF	ISF	0.0016	0.009				0.10
Fs	RMF	MeanFrac	−0.1058	0.007				0.11
Fs	SMF	(Int)	0.5427	0.000	0.08	0.06	0.046	
Fs	SMF	RF_5m	−0.0328	0.042				1.00
Fs	LMF	(Int)	0.1215	0.000	0.13	0.11	0.011	
Fs	LMF	ISF	−0.0004	0.010				1.00
Fs	BMF	(Int)	0.0613	0.111	0.23	0.21	0.031	
Fs	BMF	RF_5m	0.0401	0.000				1.00
Fs	LAR (log)	(Int)	3.8907	0.000	0.46	0.45	0.211	
Fs	LAR (log)	ISF	−0.0203	0.000				1.00
Fs	Mean_BW (log)	(Int)	−1.1926	0.049	0.22	0.18	0.466	
Fs	Mean_BW (log)	ISF	0.0191	0.008				0.11
Fs	Mean_BW (log)	RF_5m	0.4127	0.012				0.10
Fs	D_inc	(Int)	233.4056	0.001	0.58	0.56	43.848	
Fs	D_inc	ISF	5.3324	0.000				0.52
Fs	D_inc	MeanFrac	−118.4924	0.009				0.06
Fs	H_inc	(Int)	−4.5314	0.716	0.23	0.20	9.763	
Fs	H_inc	ISF	0.4246	0.005				0.13
Fs	H_inc	RF_5m	8.6585	0.012				0.10
Fs	D_inc_rel (log)	(Int)	−2.2205	0.000	0.51	0.49	0.236	
Fs	D_inc_rel (log)	ISF	0.0249	0.000				0.46
Fs	D_inc_rel (log)	MeanFrac	−0.5124	0.033				0.05
Fs	H_inc_rel	(Int)	0.0067	0.915	0.23	0.20	0.049	
Fs	H_inc_rel	ISF	0.0024	0.002				0.16
Fs	H_inc_rel	RF_5m	0.0364	0.034				0.07

Presented are response variables (Resp) and significant predictor variables (Pred) with their estimates (Est), significance level (p-value) and relative importance (Rel. Imp.; n.a. = not applicable). Model performance is presented as R^2/adjusted R^2 (Adj. R^2) and residual standard error of the models (RSE). RMF, root-mass fraction; SMF, stem-mass fraction; LMF, leaf-mass fraction; BMF, branch-mass fraction; LAR, leaf-area ratio; Mean_BW, mean branch weight; D_inc, absolute diameter increment; H_inc, absolute height increment; D_inc_rel, relative diameter increment; H_inc_rel, relative height increment; ISF, indirect site factor; RF_5m, relative filling of the cylinder with 5 m radius; PA_2m, horizontal polygon area within a radius of 2 m; MeanFrac, mean fractal dimension index; int, model intercept.

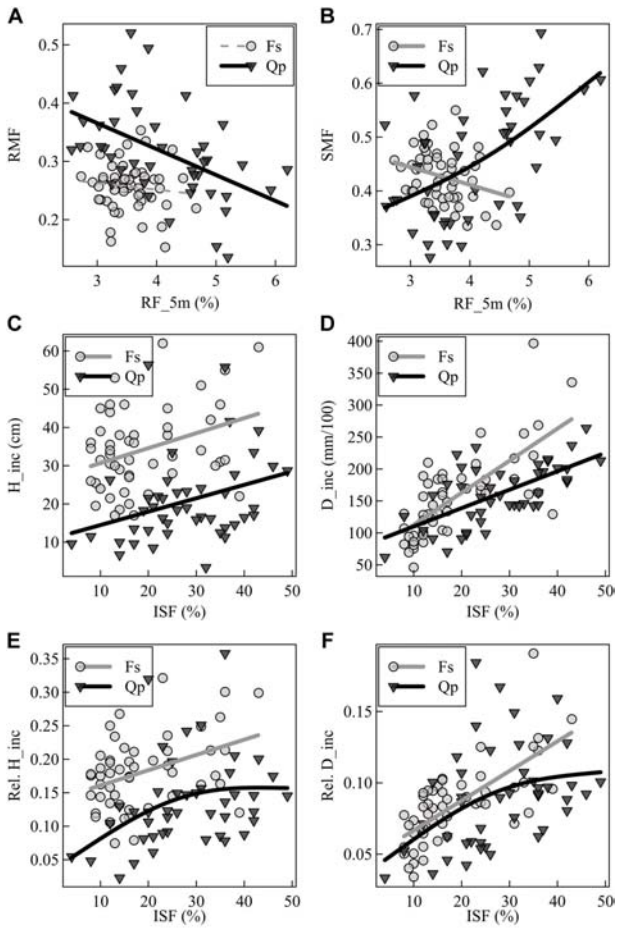

FIGURE 3 | Generalized additive model (GAM) visualization of two selected single predictors (relative space filling = RF_5m; indirect site factor = ISF) of **(A)** root-mass fraction (RMF), **(B)** stem-mass fraction (SMF), **(C)** absolute height increment (H_inc), **(D)** absolute diameter increment (D_inc), **(E)** relative height increment (Rel. H_inc), and **(F)** relative diameter increment (Rel. D_inc) for direct response comparison of beech (Fs) and oak (Qp) saplings. Solid bold lines show significant trends, dotted thin lines show non-significant trends at the level of $p < 0.05$.

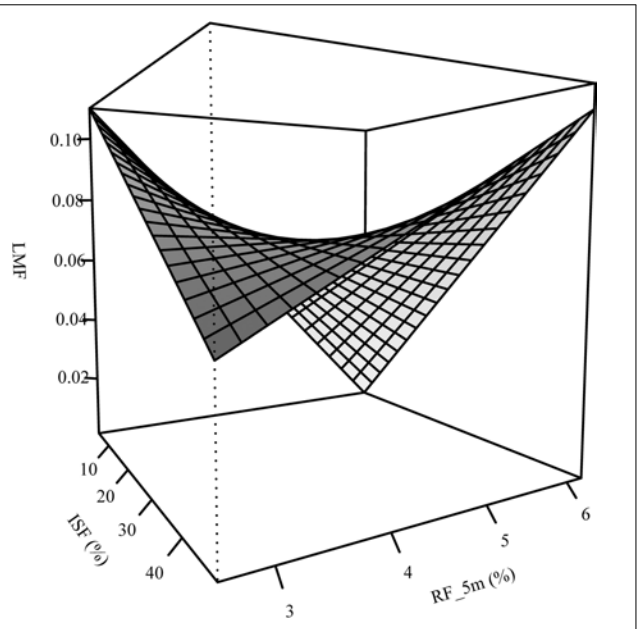

FIGURE 4 | Interaction between light (ISF) and relative filling (RF_5m) as explanatory variables of the leaf-mass fraction (LMF) – analogous to leaf area ratio (LAR) – for the oak saplings.

contained an interaction term between ISF and RF_5m again and the explanatory strength of the model was not high (Adj. $R^2 = 0.18$). The trend of the interaction was analogous to leaf-mass fraction (**Figure 4**). It suggests that oak LAR was low when light availability was high and space filling with competing vegetation was low. In contrast, LAR increased if either light availability decreased or if space filling increased.

DISCUSSION AND CONCLUSION

Our study confirmed our major hypothesis that (1) adding explanatory variables, describing the neighborhood of saplings, in addition to light measurements increase the predictive power of tree regeneration trait and performance models. The results showed that more than 50% (11/20) of the models contained more than one predictor variable. Out of all other models with a single predictor variable, light availability was not always the one with the highest explanatory power. Also the relative space filling variable (RF_5m) performed well as single predictor. This finding reflects that plants of the same species perform differently under the same level of light availability, depending on their immediate surrounding (Hofmann and Ammer, 2008). The latter may be determined by intraspecific competitors of the same cohort or by competing vegetation such as grasses or herbs. Such differences in growth environment will inevitable result in different levels of resource depletion (water and nutrients) but also affect other mechanisms that shape plant diversity (morphology), like signaling mechanisms and chemical interactions (comp. Schenk, 2006).

By separating the growth space into a zone above 2 m, in which the light availability was measured, and below 2 m, for which the neighborhood variables were derived, we aimed at getting a more precise proxy of the true competitive pressure a sapling is exposed to. By including the neighborhood we tried to give more weight to the resources other than light, i.e., water and nutrients, by assuming a correlation between above- and belowground competition. However, as in many other temperate forests, light proved to be the dominant driver for sapling performance. On the one side, light is considered to be the decisive factor of plant development (Lambers et al., 2008; Leuschner and Ellenberg, 2017). On the other side, responses to a certain level of light *in situ* always also reflect a cumulated effect of other factors (Beaudet and Messier, 1998) that vary among the microsites with differing canopy openness and light regimes (Collins et al., 1985). For example, root competition by overstorey trees for belowground resources corresponds to low light availability. Disentangling

these two drivers would require experimental approaches such as trenching (e.g., Ammer, 2002; Petriţan et al., 2011).

The general predictive strength of the models (considering all response variables together) did not differ greatly between the two species, as a possible consequence of their shade-tolerance levels (Niinemets, 2006), neither by the mean R^2-values of the models, nor by the amount of response variables that could be explained (n = 8 for oak; n = 10 for beech). When looking at the response variables separately, however, a different picture emerged, especially when considering the biomass allocation based on the growth-environment. Here, allocation toward the different plant organs (root, stem, leaves, not for branches) was better explained for oak than for beech (comp. **Figures 3A,B** and **Table 2**). So responses of oak seedlings seem to suggest that they are more sensitive to their immediate surrounding in view of allocation patterns.

In general, the findings for oak and beech confirmed our second hypothesis, namely that biomass is invested in the direction of resource limitation, so that increasing light availability or decreasing neighborhood density would result in an increase of RMF. Both species confirmed the hypothesis differently, however. ISF was not significant for oaks but the neighborhood variables were. The oaks reacted quite sensitive to occupied space around them, so reducing RMF when relative space filling (RF_5m) increased and polygon area (PA_2m) decreased. Considering this response of the oak saplings (decreasing RMF), the primary effect of a dense neighborhood seems to be a reduction of the lateral amount of light the oaks receive. This is supported by the increased stem-mass fraction with increasing relative filling (RF_5m). Our results suggest, that young oaks seem to be less sensitive to low overstorey light levels than to reductions in lateral light availability. In this respect, our investigation goes beyond other studies that have not differentiated between the two directions of light. Accordingly, they reported the more general finding that young oaks are sensitive to light availability (Jarvis, 1964; Ziegenhagen and Kausch, 1995; Lüpke and Hauskeller-Bullerjahn, 2004; Annighöfer et al., 2015; Mölder et al., 2019), However, since aboveground biomass is correlated with belowground biomass (e.g., Jackson et al., 1996; Cairns et al., 1997; Litton et al., 2003), an increase of neighborhood density should also lead to an increase in belowground competition for water and nutrients. This would mean that belowground resources might also become limiting with increasing neighborhood density. Following the "functional equilibrium hypothesis" (Brouwer, 1963; Shipley and Meziane, 2002), an increase of RMF to capture the limiting belowground resources could have also been expected (e.g., Pearson et al., 1984; Comeau and Kimmins, 1989). On the contrary, we could not find indications for this effect of neighborhood density. For a light demanding species, like oak, a kind of allocation-prioritization (hierarchical allocation) might come into play. If above- and belowground resources become limiting, biomass might primarily be allocated to the aboveground compartments. This, of course goes at the expense of root biomass and seems to be independent of a simultaneous limitation of belowground resources. Thus, the need to not lose the connection to light, which might be mortal (comp. Messier et al., 1999) and is referred to as "light-seeking strategy" (Beaudet and Messier, 1998), seems to be of higher priority than to develop the rooting system. However, this strategy may be typical for primarily light-limited settings and may be different in water-limited surroundings (Canham et al., 1996; Poorter and Nagel, 2000). McConnaughay and Coleman (1999) studied annual plants and found that biomass allocation did not strongly react to water availability but only to a light and nutrient gradient, which also allows questioning the equality of resource importance for allocation patterns. Presumably, resource importance also changes during ontogeny (Ammer et al., 2008). Interestingly, beech saplings did not react to the neighborhood variables, but to ISF. Their RMF increased and leaf-mass fraction decreased with increasing ISF, which confirmed the second hypothesis. Also a reduced complexity (MeanFrac) of the forest structure around the beech saplings increased the RMF. Apparently the complexity measure is somewhat linked to the light availability (comp. above). Opposite to the oaks, beech saplings showed decreased stem-mass fraction and increased branch-mass fraction with increasing neighborhood density, which stands quite opposite to other studies and meta-analyzes (e.g., Poorter et al., 2012). However, since the SMF model had a low predictive power the finding should be treated cautiously and may be explained by the fact that the gradient of the neighborhood variables was not as large for beech, compared to oak. Aside of a wider gradient, it is also important to mention that the growth site conditions in terms of water and nutrients were considered good for both species. So even with increasing neighborhood densities, the main driver of competition may have been light, because neither water nor nutrients apparently became as limiting.

The third hypothesis (diameter growth increases with increasing light availability) was partly confirmed for oak and beech. The positive trend between light availability and radial growth increment found here has often been reported in literature (e.g., Beaudet and Messier, 1998; Finzi and Canham, 2000; Chan et al., 2003). Expected effects of the neighborhood variables on diameter growth (diameter growth decreases with increasing neighborhood density) could not be found for both species. Neighborhood effects seem to be negligible and superimposed by the high importance of ISF for diameter growth in both cases. However, relative and absolute height growth of both species showed the expected positive relation to ISF (e.g., Collet et al., 1997; Lüpke and Hauskeller-Bullerjahn, 2004), but also to neighborhood (height growth increases with increasing neighborhood density), eventhough the explanatory strength of the models was not as high as for diameter growth. So since a dense neighborhood increased the height growth for both species (negative PA_2m for oak and positive RF_5m for beech), we can conclude for juvenile trees that a reduction of horizontal space paired with maximal vertical light availability significantly promotes height growth.

Aside of promoting juvenile height growth, a further objective of high densities of juvenile trees in forest management is to reduce their branchiness, which was expressed in the fourth hypothesis. It stated that the mean branch weight increases with light availability and space. This was surprisingly not confirmed for oak (no model could be fitted) and only partly

for beech. The mean branch weight increased with ISF but also with increasing RF_5m. Latter contradicts with practical experience and scientific publications or textbooks on silviculture (Mäkinen and Hein, 2006; Röhrig et al., 2006; Weidig et al., 2014) and cannot be explained. However, this finding should not be overrated, since the model quality was also rather low.

Finally, in line with many other studies (Popma and Bongers, 1988; Walters et al., 1993; Lusk, 2002), this study confirmed the negative relationship between LAR and ISF as stated in the fifth hypothesis. It also confirmed that the LAR values and absolute slopes were generally higher for the shade tolerant beech. This is explained by the characteristic of shade tolerant species to increase their light interception rates at low light levels, by growing shade-leaves and generally allocating more biomass to their leaves. The increased leaf-mass fraction in combination with a larger leaf area per unit leaf biomass (shade-leaves) leads to a larger leaf area per unit plant mass (LAR) (Poorter, 2001).

Overall our study could only partly disentangle the effects of overstorey tree density from lateral competition by the local neighborhood. This result may be partly due to methodological shortcomings. Maybe the relevant space defined as neighborhood (here height = 2 m, radius = 5 m) should have been kept flexible, because it presumably differs depending on sapling size. We tried to give more weight to the resources water and nutrients, by assuming a stronger correlation between the availability of these resources and the neighborhood recorded by the TLS approach than between their availability and the light environment. Apparently without actual measurements of resource availability (soil moisture, N-availability) a separation is not really possible. Also, increasing the gradient of growth site conditions, especially toward limited conditions, could result in stronger responses to the neighborhood, as opposed to conditions, in which mainly light availability is limiting. A scanner-based point could cannot efficiently discriminate point qualities yet, i.e., a return from a tree trunk with a high DBH or a small DBH, from a branch, a leaf or a blade of grass is simply a return. Current and future approaches combining the information from TLS and photogrammetry or beams widening the range of spectral wavelengths that can be retrieved aim at overcoming this limitation. A continuously improved analysis of growth environments and neighborhoods will further on increase the quality of models predicting traits and characteristics of plants. This should be further elaborated in future studies.

AUTHOR CONTRIBUTIONS

PA conceived and designed the study and wrote the manuscript with support and substantial contributions from DS, AM, and CA. PA collected the data. PA and DS performed the data analysis. CA supervised the findings of this work. All authors commented on and contributed to the final version of the manuscript and approved it.

FUNDING

We thank the German Research Foundation (DFG) for funding parts of this research through Grant SE 2383/5-1 provided to DS. The German Federal Environmental Foundation (DBU) funded AM through the QuerCon project (Grant No. DBU 32694), which is also gratefully acknowledged.

ACKNOWLEDGMENTS

Much gratitude is owed to the forestry offices Leinefelde (ThüringenForst) and Unterlüß (Niedersächsische Landesforsten) for allowing us to set up this experiment on their sites. We want to thank Ulrike Westphal and Sarah Hasstedt from Silviculture and Forest Ecology of the Temperate Zones, and two students from the University of Göttingen, for their help with performing the lab work.

REFERENCES

Ammer, C. (2002). Response of *Fagus sylvatica* seedlings to root trenching of overstorey *Picea abies*. *Scand. J. For. Res.* 17, 408–416. doi: 10.1080/028275802320435423

Ammer, C. (2003). Growth and biomass partitioning of *Fagus sylvatica* L. and *Quercus robur* L. seedlings in response to shading and small changes in the R/FR-ratio of radiation. *Ann. For. Sci.* 60, 163–171. doi: 10.1051/forest:2003009

Ammer, C., Stimm, B., and Mosandl, R. (2008). Ontogenetic variation in the relative influence of light and belowground resources on European beech seedling growth. *Tree Physiol.* 28, 721–728. doi: 10.1093/treephys/28.5.721

Annighöfer, P., Beckschäfer, P., Vor, T., and Ammer, C. (2015). Regeneration patterns of European oak species (*Quercus petraea* (Matt.) Liebl., *Quercus robur* L.) in dependence of environment and neighborhood. *PLoS One* 10:e0134935. doi: 10.1371/journal.pone.0134935

Annighöfer, P., Petritan, A. M., Petritan, I. C., and Ammer, C. (2017). Disentangling juvenile growth strategies of three shade-tolerant temperate forest tree species responding to a light gradient. *For. Ecol. Manag.* 391, 115–126. doi: 10.1016/j.foreco.2017.01.010

Beaudet, M., and Messier, C. (1998). Growth and morphological responses of yellow birch, sugar maple, and beech seedlings growing under a natural light gradient. *Can. J. For. Res.* 28, 1007–1015. doi: 10.1139/x98-077

Braun-Blanquet, J. (1932). *Plant Sociology (Transl. G. D. Fuller and H. S. Conrad)*. New York, NY: McGraw-Hill.

Brouwer, R. (1963). Some aspects of the equilibrium between overground and underground plant parts. *Meded. Inst. Biol. Scheikd. Onderzoek Landbouwgewassen* 213, 31–39.

Cairns, M. A., Brown, S., Helmer, E. H., and Baumgardner, G. A. (1997). Root biomass allocation in the world's upland forests. *Oecologia* 111, 1–11. doi: 10.1007/s004420050201

Canham, C. D., Berkowitz, A. R., Kelly, V. R., Lovett, G. M., Ollinger, S. V., and Schnurr, J. (1996). Biomass allocation and multiple resource limitation in tree seedlings. *Can. J. For. Res.* 26, 1521–1530. doi: 10.1139/x26-171

Casper, B. B., and Jackson, R. B. (1997). Plant competition underground. *Annu. Rev. Ecol. Syst.* 28, 545–570. doi: 10.1146/annurev.ecolsys.28.1.545

Chan, S. S., Radosevich, S. R., and Grotta, A. T. (2003). Effects of contrasting light and soil moisture availability on the growth and biomass allocation of douglas-fir and red alder. *Can. J. For. Res.* 33, 106–117. doi: 10.1139/x02-148

Cianelli, L., Chan, K.-S., Bailey, K. M., and Stenseth, N. C. (2004). Nonadditive effects of the environment on the survival of a large marine fish population. *Ecology* 85, 3418–3427. doi: 10.1002/ece3.2832

Claveau, Y., Messier, C., Comeau, P. G., and Coates, K. D. (2002). Growth and crown morphological responses of boreal conifer seedlings and saplings with

contrasting shade tolerance to a gradient of light and height. *Can. J. For. Res.* 32, 458–468. doi: 10.1139/x01-220

Coll, L., Balandier, P., Picon-Cochard, C., Prévosto, B., and Curt, T. (2003). Competition for water between beech seedlings and surrounding vegetation in different light and vegetation composition conditions. *Ann. For. Sci.* 60, 593–600. doi: 10.1051/forest:2003051

Collet, C., Colin, F., and Bernier, F. (1997). Height growth, shoot elongation and branch development of young *Quercus petraea* grown under different levels of resource availability. *Ann. For. Sci.* 54, 65–81. doi: 10.1051/forest:19970106

Collins, B. S., Dunne, K. P., and Pickett, S. (1985). "Response of forest herbs to canopy gaps: chapter 12," in *The Ecology of Natural Disturbance and Patch Dynamics*, eds S. Pickett and P. S. White (New York, NY: Academic Press), 217–234. doi: 10.1016/b978-0-08-050495-7.50017-x

Comeau, P. G., and Kimmins, J. P. (1989). Above- and below-ground biomass and production of lodgepole pine on sites with differing soil moisture regimes. *Can. J. For. Res.* 19, 447–454. doi: 10.1139/x89-070

Cornelissen, J. H. C., Diez, P. C., and Hunt, R. (1996). Seedling growth, allocation and leaf attributes in a wide range of woody plant species and types. *J. Ecol.* 84, 755–765. doi: 10.2307/2261337

Crawley, M. J. (2013). *The R book*, 2nd Edn. Chichester: John Wiley & Sons.

Delagrange, S., Messier, C., Lechowicz, M. J., and Dizengremel, P. (2004). Physiological, morphological and allocational plasticity in understory deciduous trees: importance of plant size and light availability. *Tree Physiol.* 24, 775–784. doi: 10.1093/treephys/24.7.775

Dormann, C. F., Elith, J., Bacher, S., Buchmann, C., Carl, G., Carré, G., et al. (2013). Collinearity: a review of methods to deal with it and a simulation study evaluating their performance. *Ecography* 36, 27–46. doi: 10.1111/j.1600-0587.2012.07348.x

Drever, C. R., and Lertzman, K. P. (2001). Light-growth responses of coastal Douglas-fir and western redcedar saplings under different regimes of soil moisture and nutrients. *Can. J. For. Res.* 31, 2124–2133. doi: 10.1139/x01-149

Ehbrecht, M., Schall, P., Ammer, C., and Seidel, D. (2017). Quantifying stand structural complexity and its relationship with forest management, tree species diversity and microclimate. *Agric. For. Meteorol.* 242, 1–9. doi: 10.1016/j.agrformet.2017.04.012

Ehbrecht, M., Schall, P., Juchheim, J., Ammer, C., and Seidel, D. (2016). Effective number of layers: a new measure for quantifying three-dimensional stand structure based on sampling with terrestrial LiDAR. *For. Ecol. Manag.* 380, 212–223. doi: 10.1016/j.foreco.2016.09.003

Ehleringer, J. R., and Dawson, T. E. (1992). Water uptake by plants: perspectives from stable isotope composition. *Plant Cell Environ.* 15, 1073–1082. doi: 10.1111/j.1365-3040.1992.tb01657.x

Elliot, K. J., and Vose, J. M. (1995). Evaluation of the competitive environment for white pine (*Pinus strobus* L.) seedlings planted on prescribed burn sites in the southern appalachians. *Forest Sci.* 41, 513–530.

Feldman, B. E. (2005). *Relative Importance and Value*. Amsterdam: Elsevier.

Finzi, A. C., and Canham, C. D. (2000). Sapling growth in response to light and nitrogen availability in a southern New England forest. *For. Ecol. Manag.* 131, 153–165. doi: 10.1016/S0378-1127(99)00206-6

Funk, J. L., and Vitousek, P. M. (2007). Resource-use efficiency and plant invasion in low-resource systems. *Nature* 446, 1079–1081. doi: 10.1038/nature05719

Gauer, J., and Aldinger, E. (2005). Waldökologische Naturräume Deutschlands: Forstliche Wuchsgebiete und Wuchsbezirke (Forest ecologically based natural geographic regions of Germany: Forest growth areas and growth districts). *Mitt. Ver. forstl. Standortskd. Forstpflanzenzücht.* 43, 1–324.

Gebhardt, T., Häberle, K.-H., Matyssek, R., Schulz, C., and Ammer, C. (2014). The more, the better? Water relations of norway spruce stands after progressive thinning. *Agric. For. Meteorol.* 197, 235–243. doi: 10.1016/j.agrformet.2014.05.013

Groemping, U. (2006). Relative importance for linear regression in R: the package relaimpo. *J. Stat. Softw.* 17, 1–27.

Harmer, R., Boswell, R., and Robertson, M. (2005). Survival and growth of tree seedlings in relation to changes in the ground flora during natural regeneration of an oak shelterwood. *Forestry* 78, 21–32. doi: 10.1093/forestry/cpi003

Hastie, T. J., and Tibshirani, R. J. (1990). *Generalized Additive Models*. Boca Raton: Chapman & Hall.

Hegyi, F. (1974). "A simulation model for managing Jack-pine stands," in *Growth Models for Tree and Stand Simulation*, ed. J. Fries (Stockholm: Department of Forest Yield Research), 74–90.

Hofmann, R., and Ammer, C. (2008). Biomass partitioning of beech seedlings under the canopy of spruce. *Aust. J. For. Sci.* 125, 51–66.

Hutchings, M. J., and de Kroon, H. (1994). Foraging in plants: the role of morphological plasticity in resource acquisition. *Adv. Ecol. Res.* 25, 159–238. doi: 10.1016/s0065-2504(08)60215-9

Jackson, R. B., Canadell, J., Ehleringer, J. R., Mooney, H. A., Sata, O. E., and Schulze, E. D. (1996). A global analysis of root distributions for terrestrial biomes. *Oecologia* 108, 389–411. doi: 10.1007/BF00333714

Jarvis, P. G. (1964). The adaptability to light intensity of seedlings of *Quercus petraea* (Matt.) Liebl. *J. Ecol.* 52, 545–571. doi: 10.2307/2257848

Jylhä, P., and Hytönen, J. (2006). Effect of vegetation control on the survival and growth of scots pine and Norway spruce planted on former agricultural land. *Can. J. For. Res.* 36, 2400–2411. doi: 10.1139/x06-053

Kimmins, J. P. (2004). *Forest Ecology: A Foundation for Sustainable Forest Management and Environmental Ethics in Forestry*. London: Pearson.

Lambers, H., Chapin, F. S., and Pons, T. L. (2008). *Plant Physiological Ecology*. New York, NY: Springer.

Leuschner, C., and Ellenberg, H. (2017). *Ecology of Central European Forests (Vegetation Ecology of Central Europe)*. Cham: Springer.

Leuschner, C., Hertel, D., Coners, H., and Büttner, V. (2001). Root competition between beech and oak: a hypothesis. *Oecologia* 126, 276–284. doi: 10.1007/s004420000507

Lindeman, R. H., Merenda, P. F., and Gold, R. Z. (1980). *Introduction to Bivariate and Multivariate Analysis*. Glenview, IL: Scott, Foresman and Company.

Litton, C. M., Ryan, M. G., Tinker, D. B., and Knight, D. H. (2003). Belowground and aboveground biomass in young postfire lodgepole pine forests of contrasting tree density. *Can. J. For. Res.* 33, 351–363. doi: 10.1139/X02-181

Lödige, C., Schall, P., and Ammer, C. (2014). How do size and resource availability control aboveground biomass allocation of tree seedlings? *Forest Res* 3:100123. doi: 10.4172/2168-9776.1000123

Löf, M. (2000). Establishment and growth in seedlings of *Fagus sylvatica* and *Quercus robur*: influence of interference from herbaceous vegetation. *Can. J. For. Res.* 30, 855–864. doi: 10.1139/x99-257

Lüpke, B. v. (2004). "Regeneration of beech-oak-mixed stands in central europe under continuous cover management," in *Proceedings of the 7th International Beech Symposium, IUFRO Research Group 1.10.00*, Tehran, 128–134.

Lüpke, B. v., and Hauskeller-Bullerjahn, K. (2004). Beitrag zur Modellierung der Jungwuchsentwicklung am Beispiel von Traubeneichen-Buchen-Mischverjüngungen (A contribution to modelling juvenile growth examplified by mixed oak-beech regeneration). *Allg. Forst- u. J.-Ztg.* 175, 61–69.

Lusk, C. H. (2002). Leaf area accumulation helps juvenile evergreen trees tolerate shade in a temperate rainforest. *Oecologia* 132, 188–196. doi: 10.1007/s00442-002-0974-9

Mäkinen, H., and Hein, S. (2006). Effect of wide spacing on increment and branch properties of young Norway spruce. *Eur. J. For. Res.* 125, 239–248. doi: 10.1007/s10342-006-0115-9

McConnaughay, K. D. M., and Coleman, J. S. (1999). Biomass allocation in plants. Ontogeny or optimality? A test along three resource gradients. *Ecology* 80, 2581–2593. doi: 10.1890/0012-9658(1999)080%5B2581:baipoo%5D2.0.co;2

McDonald, J. H. (2014). *Handbook of Biological Statistics*. Baltimore, ML: Sparky House Publishing.

McGarigal, K., and Marks, B. J. (1995). *FRAGSTATS: Spatial Pattern Analysis Program for Quantifying Landscape Structure*. Portland, OR: U.S. Department of Agriculture.

Messier, C., Doucet, R., Ruel, J.-C., Claveau, Y., Kelly, C., and Lechowicz, M. J. (1999). Functional ecology of advance regeneration in relation to light in boreal forests. *Can. J. For. Res.* 29, 812–823. doi: 10.1139/x99-070

Messier, C., and Nikinmaa, E. (2016). Effects of light availability and sapling size on the growth, biomass allocation, and crown morphology of understory sugar maple, yellow birch, and beech. *Ecoscience* 7, 345–356. doi: 10.1080/11956860.2000.11682604

Mölder, A., Meyer, P., and Nagel, R.-V. (2019). Integrative management to sustain biodiversity and ecological continuity in Central European temperate oak (*Quercus robur*, *Q. petraea*) forests: an overview. *For. Ecol. Manag.* 437, 324–339. doi: 10.1016/j.foreco.2019.01.006

Morris, D. M., MacDonald, G. B., and McClain, K. M. (1990). Evaluation of morphological attributes as response variables to perennial competition for 4-year-old black spruce and jack pine seedlings. *Can. J. For. Res.* 20, 1696–1703. doi: 10.1139/x90-226

Morris, L. A., Moss, S. A., and Garbett, W. S. (1993). Competitive interference between selected herbaceous and woody plants and *Pinus taeda* L. during two growing seasons following planting. *Forest Sci.* 39, 166–187.

Niinemets, Ü. (2006). The controversy over traits conferring shade-tolerance in trees: ontogenetic changes revisited. *J. Ecol.* 94, 464–470. doi: 10.1111/j.1365-2745.2006.01093.x

Pearson, J. A., Fahey, T. J., and Knight, D. H. (1984). Biomass and leaf area in contrasting lodgepole pine forests. *Can. J. For. Res.* 14, 259–265. doi: 10.1139/x84-050

Petriţan, A. M., Lüpke, B. v., and Petriţan, I. C. (2009). Influence of light availability on growth, leaf morphology and plant architecture of beech (*Fagus sylvatica* L.), maple *(Acer pseudoplatanus* L.) and ash (*Fraxinus excelsior* L.) saplings. *Eur. J. For. Res.* 128, 61–74. doi: 10.1007/s10342-008-0239-1

Petriţan, I. C., Lüpke, B. v., and Petriţan, A. M. (2011). Effects of root trenching of overstorey Norway spruce (*Picea abies*) on growth and biomass of underplanted beech (*Fagus sylvatica*) and Douglas fir (*Pseudotsuga menziesii*) saplings. *Eur. J. For. Res.* 130, 813–828. doi: 10.1007/s10342-010-0473-1

Poorter, H., and Nagel, O. (2000). The role of biomass allocation in the growth response of plants to different levels of light, CO_2, nutrients and water: a quantitative review. *Funct. Plant Biol.* 27:1191. doi: 10.1071/PP99173_CO

Poorter, H., Niklas, K. J., Reich, P. B., Oleksyn, J., Poot, P., and Mommer, L. (2012). Biomass allocation to leaves, stems and roots: meta-analyses of interspecific variation and environmental control. *New Phytol.* 193, 30–50. doi: 10.1111/j.1469-8137.2011.03952.x

Poorter, H., and Remkes, C. (1990). Leaf area ratio and net assimilation rate of 24 wild species differing in relative growth rate. *Oecologia* 83, 553–559. doi: 10.1007/BF00317209

Poorter, L. (1999). Growth responses of 15 rain-forest tree species to a light gradient: the elative importance of morphological and physiological traits. *Funct. Ecol.* 13, 396–410. doi: 10.1046/j.1365-2435.1999.00332.x

Poorter, L. (2001). Light-dependent changes in biomass allocation and their importance for growth of rain forest tree species. *Funct. Ecol.* 15, 113–123. doi: 10.1046/j.1365-2435.2001.00503.x

Popma, J., and Bongers, F. (1988). The effect of canopy gaps on growth and morphology of seedlings of rain forest species. *Oecologia* 75, 625–632. doi: 10.1007/BF00776429

Pretzsch, H., Forrester, D. I., and Bauhus, J. (eds) (2017). *Mixed-Species Forests: Ecology and Management*. Berlin: Springer.

Pryor, D. (2010). *Analysis of Light Environments Under Forest Canopies Using an Integrated Digital Hemispherical Image System*. Ph.D. dissertation, Staffordshire University, Staffordshire.

R Core Team (2017). *R: A Language and Environment for Statistical Computing*. Vienna: R Foundation for Statistical Computing.

Röhrig, E., Bartsch, N., and Lüpke, B. v. (2006). *Waldbau Auf Ökologischer Grundlage (Silviculture on and ecological basis)*. Stuttgart: Ulmer.

Schall, P., Lödige, C., Beck, M., and Ammer, C. (2012). Biomass allocation to roots and shoots is more sensitive to shade and drought in European beech than in Norway spruce seedlings. *For. Ecol. Manag.* 266, 246–253. doi: 10.1016/j.foreco.2011.11.017

Schenk, H. J. (2006). Root competition: beyond resource depletion. *J. Ecol.* 94, 725–739. doi: 10.1111/j.1365-2745.2006.01124.x

Seidel, D., Hoffmann, N., Ehbrecht, M., Juchheim, J., and Ammer, C. (2015). How neighborhood affects tree diameter increment new insights from terrestrial laser scanning and some methodical considerations. *For. Ecol. Manag.* 336, 119–128. doi: 10.1016/j.foreco.2014.10.020

Shipley, B., and Meziane, D. (2002). The balanced-growth hypothesis and the allometry of leaf and root biomass allocation. *Funct. Ecol.* 16, 326–331. doi: 10.1046/j.1365-2435.2002.00626.x

Silla, F., and Escudero, A. (2003). Uptake, demand and internal cycling of nitrogen in saplings of mediterranean *Quercus* species. *Oecologia* 136, 28–36. doi: 10.1007/s00442-003-1232-5

Smith, H. (1994). "Sensing the light environment: the functions of the phytochrome family," in *Photomorphogenesis in Plants*, eds R. E. Kendrick and G. H. M. Kronenberg (Dordrecht: Springer), 377–416. doi: 10.1007/978-94-011-1884-2_15

Wagner, R. G., and Radosevich, S. R. (1991). Neighborhood predictors of interspecific competition in young Douglas-fir plantations. *Can. J. For. Res.* 21, 821–828. doi: 10.1139/x91-115

Wagner, S., Fischer, H., and Huth, F. (2011). Canopy effects on vegetation caused by harvesting and regeneration treatments. *Eur. J. For. Res.* 130, 17–40. doi: 10.1007/s10342-010-0378-z

Wagner, S., Madsen, P., and Ammer, C. (2009). Evaluation of different approaches for modelling individual tree seedling height growth. *Trees* 23, 701–715. doi: 10.1007/s00468-009-0313-4

Walters, M. B., Kruger, E. L., and Reich, P. B. (1993). Growth, biomass distribution and CO_2 exchange of northern hardwood seedlings in high and low light: relationships with successional status and shade tolerance. *Oecologia* 94, 7–16. doi: 10.1007/BF00317294

Weidig, J., Wagner, S., and Huth, F. (2014). Qualitätsentwicklung von Buchenvoranbauten (*Fagus sylvatica* L.) im Thüringer Wald nach unplanmäßigem sturmbedingtem Verlust des Fichtenschirms (Quality of advanced planted European beech (*Fagus sylvatica* L.) in the Thuringian Forest after the unscheduled loss of Norway spruce shelterwood in storms). *Forstarchiv* 85, 122–133.

Williams, H., Messier, C., and Kneeshaw, D. D. (1999). Effects of light availability and sapling size on the growth and crown morphology of understory douglas-fir and lodgepole pine. *Can. J. For. Res.* 29, 222–231. doi: 10.1139/x98-189

Wood, S. N. (2006). *Generalized Additive Models: an Introduction with R*. Boca Raton: Chapman & Hall.

Wood, S. N. (2011). Fast stable restricted maximum likelihood and marginal likelihood estimation of semiparametric generalized linear models. *J. R. Stat. Soc.* 73, 3–36. doi: 10.1111/j.1467-9868.2010.00749.x

Ziegenhagen, B., and Kausch, W. (1995). Productivity of young shaded oaks (*Quercus robur* L.) as corresponding to shoot morphology and leaf anatomy. *For. Ecol. Manag.* 72, 97–108. doi: 10.1016/0378-1127(94)03482-C

Conflict of Interest Statement: CA is currently guest editor of Frontiers in Plant Science hosting the research topic "Woody Plants and Forest Ecosystems in a Complex World – Ecological Interactions and Physiological Functioning Above and Below Ground."

The remaining authors declare that the research was conducted in the absence of any commercial or financial relationships that could be construed as a potential conflict of interest.

frontiers in Plant Science

ORIGINAL RESEARCH
published: 29 March 2019
doi: 10.3389/fpls.2019.00337

Species-Specific Outcome in the Competition for Nitrogen Between Invasive and Native Tree Seedlings

Andrea Bueno[1], Karin Pritsch[2] and Judy Simon[1]*

[1] Plant Interactions Ecophysiology Group, Department of Biology, University of Konstanz, Konstanz, Germany, [2] Institute of Biochemical Plant Pathology, Helmholtz Zentrum München, Deutsches Forschungszentrum für Gesundheit und Umwelt GmbH, Neuherberg, Germany

The outcome of competition for nitrogen (N) between native and invasive tree species is a major concern when considering increasing anthropogenic N deposition. Our study investigated whether three native (i.e., *Fagus sylvatica, Quercus robur*, and *Pinus sylvestris*) and two invasive woody species (i.e., *Prunus serotina* and *Robinia pseudoacacia*) showed different responses regarding morphological and physiological parameters (i.e., biomass and growth indices, inorganic vs. organic N acquisition strategies, and N allocation to N pools) depending on the identity of the competing species, and whether these responses were mediated by soil N availability. In a greenhouse experiment, tree seedlings were planted either single or in native-invasive competition at low and high soil N availability. We measured inorganic and organic N acquisition using ^{15}N labeling, total biomass, growth indices, as well as total soluble amino acid-N and protein-N levels in the leaves and fine roots of the seedlings. Our results indicate that invasive species have a competitive advantage via high growth rates, whereas native species could avoid competition with invasives via their higher organic N acquisition suggesting a better access to organic soil N sources. Moreover, native species responded to competition with distinct species- and parameter-specific strategies that were partly mediated by soil N availability. Native tree seedlings in general showed a stronger response to invasive *P. serotina* than *R. pseudoacacia*, and their strategies to cope with competition reflect the different species' life history strategies and physiological traits. Considering the responses of native and invasive species, our results suggest that specifically *Q. robur* seedlings have a competitive advantage over those of *R. pseudoacacia* but not *P. serotina*. Furthermore, native and invasive species show stronger responses to higher soil N availability under competition compared to when growing single. In conclusion, our study provides insights into the potential for niche differentiation between native and invasive species by using different N forms available in the soil, the combined effects of increased soil N availability and competition on tree seedling N nutrition, as well as the species-specific nature of competition between native and invasive tree seedlings which could be relevant for forest management strategies.

Keywords: inorganic nitrogen, nitrogen pools, nitrogen uptake, organic nitrogen, plant competition, woody invaders

OPEN ACCESS

Edited by:
Boris Rewald, University of Natural Resources and Life Sciences Vienna, Austria

Reviewed by:
Bruce Arthur Osborne, University College Dublin, Ireland
Brian D. Strahm, Virginia Tech, United States

****Correspondence:***
Andrea Bueno
andrea.bueno@uni-konstanz.de

Specialty section:
This article was submitted to Functional Plant Ecology, a section of the journal Frontiers in Plant Science

Received: *20 August 2018*
Accepted: *04 March 2019*
Published: *29 March 2019*

Citation:
Bueno A, Pritsch K and Simon J (2019) Species-Specific Outcome in the Competition for Nitrogen Between Invasive and Native Tree Seedlings. Front. Plant Sci. 10:337. doi: 10.3389/fpls.2019.00337

INTRODUCTION

Biological plant invasions have consequences on plant interactions in native communities, thus severely affecting ecosystems in the future given that plant community composition and structure are largely determined by the outcome of plant–plant interactions such as facilitation and/or competition for limiting resources (Goldberg and Barton, 1992). Considering that nutrients, especially nitrogen (N), limit woody plant growth (Körner, 2003; Miller et al., 2007; Millard and Grelet, 2010) and that resource acquisition and internal allocation play an important role in achieving maximum growth and reproductive fitness in plants, particularly long-living woody species, competition for N between native and non-native woody species is of great relevance. Although evidence points in the direction that species in native plant communities have evolved different strategies to avoid competition for N via preference of different N sources to effectively avoid competition via niche differentiation (Näsholm et al., 2009; Hodge and Fitter, 2013; Simon et al., 2017), via N acquisition at different times during the growing season (Simon et al., 2017), and/or via the interaction with soil microorganisms to enhance N acquisition (e.g., Hodge and Fitter, 2013), these strategies might no longer be effective in competition with non-native plant species because of their higher competitive ability compared to native species (Gioria and Osborne, 2014). Considering their higher capacity to exploit limited resources, better resource use efficiency, inhibition of growth, as well as establishment of potential competitors (D´Antonio and Vitousek, 1992; Gioria and Osborne, 2014), non-native plant species have a large potential to become invasive (Keller et al., 2011) and as a result induce profound changes in forest ecosystem structure and functioning (Holmes et al., 2009; Vilà et al., 2011; Aerts et al., 2017).

The outcome of plant interactions is not only determined by biotic interactions but also shifts depending on the environmental conditions (Aschehough et al., 2016). Abiotic factors, such as light availability (Simon et al., 2014), water availability (Fotelli et al., 2001, 2002), air temperature (Fotelli et al., 2005) as well as soil N availability (e.g., Li et al., 2015) influence the competition for N between plants, thereby shifting the outcome of plant–plant competition. For example, nitrate acquisition of sycamore maple (*Acer pseudoplatanus* L.) decreased when competing with European beech (*Fagus sylvatica* L.) compared to intraspecific competition at high but not low soil N availability suggesting that the response to competition for N is mediated by soil N availability (Li et al., 2015). Furthermore, plant–plant competition and soil N availability showed combined effects on plant N nutrition by inducing changes in N pools in the fine roots such as total soluble protein-N and total amino acid-N (Li et al., 2015). Overall, the interplay between interspecific competition for N and varying environmental conditions can impact on plant N acquisition and N nutrition with consequences for plant growth and survival, which in turn may affect plant community composition and structure (Aerts et al., 2017). However, in general, non-woody species are investigated preferably in plant interaction studies, thus the understanding of the mechanisms underlying tree interactions is rather scarce (Trinder et al., 2013; Pommerening and Sánchez Meador, 2018), although resource acquisition and internal allocation are particularly important for resource-storing and -remobilizing in long-living trees.

Woody invasive species are a potential threat for forest habitats throughout Europe (Campagnaro et al., 2018), and studies indicate their highly competitive characteristics. For example, root competition with seedlings of *Prunus serotina* and *Robinia pseudoacacia* – the most important invaders in natural and semi-natural woodlands in Central Europe (Halarewicz et al., 2017; Campagnaro et al., 2018) – decreased total biomass and modified biomass allocation of seedlings of the native species *Quercus robur* and *Carpinus betulus* (i.e., by increased root biomass at the expense of aboveground production) (Kawaletz et al., 2013, 2014). Furthermore, competition intensity increased more over time for the native species when competing with the two invasive species compared to intraspecific competition or competition among natives (Kawaletz et al., 2013, 2014). On the other hand, competition with *P. serotina* stimulated the height growth of seedlings of *Q. petraea*, suggesting a potential for species-specific competitive effects (Robakowski and Bielinis, 2011).

Although these studies stress the competitive effects of invasive *P. serotina* and *R. pseudoacacia* on the growth of native species, the understanding on the interactions between native and invasive woody species with regard to N cycling in forest ecosystems depending on abiotic stressors (i.e., soil N availability) is very limited. Soil N availability is expected to rise in terrestrial ecosystems of Central Europe as a result of increased atmospheric deposition (Rennenberg et al., 2009; Waldner et al., 2014), which will also impact on the outcome of invasion processes in plant communities (Bradley et al., 2010; Littschwager et al., 2010; Luo et al., 2014). Therefore, it is key to understand the processes of interspecific competition for N between native and invasive tree species, as well as the effects of soil N availability on the outcome of this competition with regard to plant N acquisition and N nutrition to predict the future dynamics of forest ecosystems. Thus, we conducted a greenhouse experiment using different native and invasive tree species to investigate whether native and invasive tree species show species-specific responses in terms of growth, N acquisition strategies and N allocation to N pools depending on the identity of their competitor, and whether those responses are influenced by increased soil N availability. The native species (i.e., *F. sylvatica* L., *Q. robur* L., and *Pinus sylvestris* L.), represent the most abundant species in Central European forests (Ellenberg and Leuschner, 2010). The two invasive species (i.e., *P. serotina* Ehrh. and *R. pseudoacacia* L.) are among the top five invasive tree species in Central European forests (Campagnaro et al., 2018). The selected species differ in their physiology and growth strategies: *F. sylvatica* and *Q. robur* are late successional, broadleaved species differing in their drought tolerance – i.e., *Q. robur* is drought tolerant, found on fertile, loamy-clay soils, whereas *F. sylvatica* is sensitive to drought, and is mostly found on moderately fertile, calcareous soils (Cavin et al., 2013; Eaton et al., 2016; Houston et al., 2016a). *P. sylvestris*

is an evergreen conifer with needles present throughout the year functioning as N storage organs (Millard and Grelet, 2010), as opposed to the broadleaved species which lose their leaves in the autumn season. Regarding the invasive species, *P. serotina* produces cyanogenic compounds that negatively affect other plant species (Csiszár, 2009) by reducing their germination and growth rates (Robakowski et al., 2016), while *R. pseudoacacia* can fix atmospheric N_2 via symbiotic bacteria in root nodules and is potentially dominant at nutrient poor sites (Danso et al., 1995; Vítková et al., 2017). Moreover, we have chosen seedlings of uniform age to incorporate the aspect of the different demands for nitrogen between species according to their growth strategies (Reich, 2014). These differences in physiological aspects between the species may result in different response strategies to interspecific competition and also shift with increasing soil N availability. We hypothesized that: (1) Invasive species have traits that allow them to successfully grow and establish compared to native species. (2) Higher soil N availability has a positive effect on the growth and N strategies of invasive species compared to native species. (3) Native tree species respond species-specific depending on the identity of the invasive competitor species. (4) Invasive species respond differently to different native competitor species. (5) Seedling responses to competition are mediated by soil N availability.

MATERIALS AND METHODS

Plant Material and Growth Conditions

We chose three tree species native to and widely found in Central European forests: (i) European beech (*F. sylvatica* L., Fagaceae), (ii) pedunculate oak (*Q. robur* L., Fagaceae), and (iii) Scots pine (*P. sylvestris* L., Pinaceae). As invasive species we chose two tree species native to North America that were introduced to Europe in the 17^{th} century as ornamental plants and later widely planted for restoration and reforestation purposes: (i) black cherry (*P. serotina* Ehrh., Rosaceae), and (ii) black locust (*R. pseudoacacia* L., Leguminosae) (Starfinger et al., 2003; Vítková et al., 2017). From here on, species used in this study will be referred to by their genus, i.e., *Fagus, Quercus, Pinus, Prunus* and *Robinia*. For all species, 1-year-old seedlings were purchased from a commercial tree nursery (Müller Münchehof Pflanzen GmbH, Seesen/Münchehof, Germany) and planted in different competition regimes (one or two seedlings per pot, see section "Experimental Design") in a 1:1 mixture of sand and vermiculite in 3 L plastic pots (25 cm × 12 cm) at the end of November 2015. Pots overwintered outdoors and were brought into the greenhouse in early March 2016. For the next 10 days, pots were watered regularly and sufficiently with tap water. From mid-March, pots received 100 ml of a low N nutrient solution (see solution composition below) every second day as watering until the end of leaf development (early May) when the soil N availability treatments started (see section "Experimental Design"). The pots were exposed to natural light conditions and day/night regime. The average air temperature was 19.3 ± 4.0°C/16.0 ± 3.8°C (day/night, mean ± standard deviation). The average relative humidity was 54.7 ± 13.0%/63.4 ± 10.1% (day/night, mean ± standard deviation).

Experimental Design

The experiment was conducted in a fully orthogonal design with two factors, "soil N availability" (i.e., low or high) and "competitor identity" (i.e., native and invasive species in interspecific competition). Seedlings were planted in interspecific competition between native and invasive species (i.e., one seedling of a native species and one seedling of an invasive species per pot). Interspecific competition pots were established for every combination of native and invasive species. Furthermore, seedlings were planted without competition (i.e., one seedling per pot) to compare parameters between species and to determine the species general strategies and their responses to soil N availability without competition. For each species, a total of 24 pots were established as single seedlings as well as for each combination of competitor identity, summing up to a total of 264 pots. In early May, pots were assigned to either the low or high soil N availability treatment (i.e., n = 12 per combination of species, competitor identity, and soil N availability treatment). Pots were irrigated every second day with 100 ml of either low N or high N artificial nutrient solution mimicking a low (Dannenmann et al., 2009) or high soil N field site (Stoelken et al., 2010) for 6 weeks. Tests prior to the experiment showed that 100 ml of water were sufficient under the moderate air temperatures that prevailed early in the experiment. When temperatures increased in late May, additional irrigation was provided (see below). The artificial low N nutrient solution consisted of 100 μM KNO_3, 90 μM $CaCl_2{*}2H_2O$, 70 μM $MgCl_2{*}6H_2O$, 50 μM KCl, 24 μM $MnCl_2{*}4H_2O$, 20 μM NaCl, 10 μM $AlCl_3$, 7 μM $FeSO_4{*}7H_2O$, 6 μM K_2HPO_4, 1 μM NH_4Cl, 25 μM glutamine, and 25 μM arginine. The artificial high N nutrient solution consisted of 20 μM $Al_2(SO_4)_3$, 75 μM $CaCl_2{*}2H_2O$, 4 μM $FeCl_3{*}6H_2O$, 14 μM KCl, 10 μM $MnCl_2{*}4H_2O$, 40 μM $MgCl_2{*}6H_2O$, 4.5 μM Na_2HPO_4, 20 μM NaCl, 50 μM NH_4Cl, 300 μM KNO_3, 100 μM glutamine, and 100 μM arginine. Additionally, from the end of May, pots were irrigated with tap water every second day (i.e., alternating with the days when the low/high soil N solutions were applied) to avoid drought stress related to increased air temperatures and solar radiation until the ^{15}N uptake experiments and final harvest commenced in mid-June.

^{15}N Uptake Experiments

To quantify net inorganic (i.e., ammonium and nitrate) and organic (i.e., glutamine and arginine) N uptake capacity of the fine roots of the seedlings, the ^{15}N enrichment technique was used as described by Gessler et al. (1998) and modified by Simon et al. (2010) prior to the harvest of the seedlings. Seedlings were carefully removed from the pots, and their roots thoroughly washed with tap water to remove adherent substrate particles. Fine roots still attached to the seedlings were then incubated for 2 h in the artificial soil solution (n = 4–6) according to their treatment (either low or high N as described above) containing all four N sources, but with only one of them labeled as either $^{15}NH_4^+$, $^{15}NO_3^-$, $^{13}C/^{15}N$-glutamine, or $^{13}C/^{15}N$-arginine. The remaining roots were carefully wrapped in wet tissue to avoid

desiccation. After incubation, the fine roots were cut off and washed twice in 0.5 M $CaCl_2$ to remove the incubation solution from the root surface. The fresh weight was determined, followed by oven-drying at 60°C for 48 h and determination of the dry weight. Amino acids were $^{13}C/^{15}N$-labeled to determine whether they are taken up as intact molecules (Simon et al., 2011). Controls with no ^{15}N or ^{13}C label were included to account for natural abundance of ^{15}N and ^{13}C in the fine roots. Incubation took place between 10 am and 2 pm to avoid diurnal variation in net N uptake capacity (Gessler et al., 2002).

Harvest and Quantification of Plant Growth Indices

To calculate relative growth rates (RGRs), 3 to 4 pots per combination of species and competitor identity were harvested after leaf development and before commencing the soil N availability treatments to determine initial seedling biomass. Initial total seedling biomass (mean ± SD) was for *Fagus* 1.65 ± 0.53 g dw, for *Quercus* 6.43 ± 4.50 g dw, for *Pinus* 3.05 ± 1.16 g dw, for *Prunus* 10.62 ± 7.91 g dw, and for *Robinia* 4.23 ± 3.00 g dw (mean ± SD). Initial stem length was 21.7 ± 3.8 cm for *Fagus*, 33.4 ± 5.2 cm for *Quercus*, 29.2 ± 5.3 cm for *Pinus*, 63.8 ± 16.3 cm for *Prunus*, and 54.8 ± 8.4 cm for *Robinia*. Subsequent to the ^{15}N uptake experiments, all remaining seedlings were separated into leaves, stems, and roots. After determining their fresh weight, all organs were oven-dried at 60°C for 48 h, and their dry weight was determined. On the final harvest, a subset of 8 to 10 representative leaves was collected from each seedling and leaf area was measured (LI-3100C Area Meter, LI-COR, Lincoln, NE, United States) as well as fresh and dry weight determined to calculate specific leaf area (SLA). Based on Liu and van Kleunen (2017), a subset of fine roots was collected, stained, scanned, and their total length measured (WinRhizo 2012, Regent Instruments, Inc., Quebec City, QC, Canada) to calculate specific root length (SRL) before oven-drying and subsequent dry weight determination. Additionally, leaf and fine root samples were collected from each seedling for quantification of total soluble amino acid and total soluble protein levels, shock-frozen in liquid N_2 immediately after determining their fresh weight, and stored at −80°C until further analyses. Root:shoot ratio was calculated as the ratio between total root biomass and the combined biomass of stem and leaves. RGR was calculated for each seedling following the formula: $RGR = (\ln b_2 - \ln b_1) * t^{-1}$, where b_1 is total seedling biomass in grams at initial harvest, b_2 is total seedling biomass in grams at the final harvest, and t is the time period in days between the initial harvest and the final harvest (Grubb et al., 1996).

Quantification of Total N and C, ^{15}N, and ^{13}C in Fine Roots

To quantify total N and C as well as ^{15}N and ^{13}C enrichment, dried fine root samples were ground to a fine homogenous powder using a ball mill (TissueLyser, Retsch, Haan, Germany). Aliquots of 1.2 to 2.4 mg were weighed into 4 mm × 6 mm tin capsules (IVA Analysentechnik, Meerbusch, Germany) and analyzed with an isotope ratio mass spectrometer (Delta V Advantage, Thermo Electron, Dreieich, Germany) coupled to an elemental analyzer (Euro EA, Eurovector, Milan, Italy). Δ Values were calculated using a laboratory standard (acetanilide) that was part of every sequence in intervals also used in different weights to determine isotope linearity of the system. The laboratory standard was calibrated against several suitable international isotope standards (IAEA, Vienna). Final correction of isotope values was done with several international isotope standards and other suitable laboratory standards which cover the range of ^{15}N and ^{13}C results. Net N uptake capacity (nmol N g^{-1} fw h^{-1}) was calculated based on the incorporation of ^{15}N into the fine root according to Gessler et al. (1998): N uptake capacity = $((^{15}N_l\text{-}^{15}N_c)*N_{tot}*dw*10^5)/(MW*fw*t)^{-1}$, where $^{15}N_l$ and $^{15}N_c$ are the atom% of ^{15}N in labeled (N_l) and control plants (N_c, natural abundance), respectively, N_{tot} is the total N percentage, MW is the molecular weight (^{15}N g mol^{-1}), and t represents the incubation time. Net uptake capacity of the amino acids glutamine and arginine was lower based on ^{13}C incorporation than on ^{15}N incorporation indicating either (1) the degradation of amino acids in the solution or on the root surface, and/or (2) the respiration of amino acid-derived C inside the roots (Simon et al., 2011).

Quantification of Total Soluble Protein and Total Soluble Amino Acid Levels in Leaves and Fine Roots of Seedlings

Total soluble protein levels in the leaves and fine roots were extracted based on Dannenmann et al. (2009). Aliquots of ∼50 mg ground frozen organ were incubated in 1.5 ml extraction buffer (50 mM Tris-HCl pH 8.0, 1 mM EDTA, 15% (v/v) glycerol, 0.6 mM dithiothreitol, 1% Triton X-100, 2 EDTA-free protease inhibitor cocktail tablets per 100 ml buffer solution) at 4°C for 30 min and subsequently centrifuged for 10 min at 14,000 rpm and 4°C. The extraction was repeated once to increase the yield. Then, 500 μL of the combined supernatant were incubated with 1 ml 10% (v/v) trichloroacetic acid for 10 min at room temperature followed by centrifugation for 10 min at 14,000 rpm and 4°C. The protein pellet was dissolved in 1 ml 1 M KOH. To quantify total soluble protein levels according to Simon et al. (2010), 1 ml of Bradford reagent was added to 50 μL of extract. After 10 min incubating in the dark at room temperature, the absorbance at 595 nm was measured in a spectrophotometer (Ultrospec 3100pro, Amersham Biosciences). Bovine serum albumin (BSA) was used as standard.

To quantify total soluble amino acid levels in the leaves and fine roots, aliquots of ∼50 mg of frozen organ were extracted in 200 μL Hepes-buffer (5 mM EGTA, 20 mM HEPES, 10 mM NaF) and 1 ml 3.5:1.5 (v:v) methanol/chloroform, according to Winter et al. (1992). After 30 min incubation on ice, 600 μL of distilled water were added and the samples centrifuged for 5 min at 14,000 rpm and 4°C. The addition of distilled water was repeated once to increase the yield. For the quantification, according to Liu et al. (2005), 50 μL ninhydrin solution was added to a 50 μL aliquot of the combined extract and boiled for 30 min. The ninhydrin solution consisted of a 1:1 mixture of solution A (i.e., 3.84 g citric acid, 0.134 g $SnCl_2$, and 40 ml 1 M NaOH,

filled up to 100 ml with distilled water at pH 5), and solution B (i.e., 4 g ninhydrin in 100 ml ethylene-glycol-monomethyl-ether). After cooling to room temperature, 1 ml 50% isopropanol was added to the extract and incubated for 15 min. The absorption was measured at 570 nm in a spectrophotometer (Ultrospec 3100pro, Amersham Biosciences). L-Glutamine was used as standard.

Statistical Analyses

For all species, differences between treatment levels (i.e., competitor identity and low/high soil N availability) were tested (alpha level of 0.050) for total biomass, root:shoot ratio, SLA, SRL, RGR, total soluble amino acid, and total soluble protein contents in the leaves and fine roots, as well as inorganic and organic net N uptake capacity by performing Permutational ANOVAs (PERMANOVA) based on a Euclidean resemblance matrix between samples (Anderson et al., 2008). We performed two-way PERMANOVAs using "soil N availability" and "competitor identity" as orthogonal factors. The factor "soil N availability" had two levels: (i) low N and (ii) high N. The factor "competitor identity" had two levels for native species: (i) competition with *Prunus* and (ii) competition with *Robinia*; and three levels for the invasive species: (i) competition with *Fagus*, (ii) competition with *Quercus*, and (iii) competition with *Pinus*. When a significant interaction between factors was found, *post hoc* PERMANOVA pair-wise comparisons were performed. To test for differences between species in terms of SLA, SRL, RGR, total soluble amino acid and total soluble protein contents in the leaves and roots, as well as net uptake capacity of the four N sources, two-way PERMANOVAs were performed on the single seedlings data (i.e., no competition), using "species" and "soil N availability" as factors. To test for significant differences between low and high soil N availability for each species growing in absence of competition, Mann–Whitney *U*-tests were performed for all measured parameters. Furthermore, to test for preferences in net N uptake capacity, one-way PERMANOVAs were performed for each combination of species and competitor identity using "N source" as factor at both levels of soil N availability. All PERMANOVA analyses were performed using PRIMER 6.0 with the PERMANOVA+ add-on (PRIMER-E, Ltd., Plymouth, United Kingdom), while Mann–Whitney-*U* tests were performed using SigmaPlot 14.0 (Systat Software, San Jose, CA, United States).

RESULTS

Comparison Between Species and Responses to Soil N Availability Without Competition

General Differences in N Acquisition and Growth Strategies Between Tree Species

Seedlings of invasive species had a significantly higher total biomass and RGR than native seedlings, with *Prunus* having the largest total biomass among all species considered (**Table 1** and **Supplementary Table 1**). Moreover, invasive *Robinia* had significantly higher SLA and SRL than both *Prunus* and the three native species (*Fagus*, *Quercus,* and *Pinus*) (**Table 1** and **Supplementary Table 1**). Similarly, *Robinia* had in general significantly higher levels of total soluble amino acid-N and protein-N in the leaves and fine roots than all other investigated species (**Table 1** and **Supplementary Table 2**). Regarding N acquisition, inorganic N net uptake capacity did not differ significantly between species. However, seedlings of native tree species had significantly higher organic N net uptake capacity than seedlings of invasive tree species (**Table 1** and **Supplementary Table 3**).

Individual Species Responses to High Compared to Low Soil N Availability

Increased soil N availability had neither a significant effect on the total biomass nor the growth indices of the single grown species, except for a significantly lower root:shoot ratio of *Robinia* (**Table 2A** and **Supplementary Table 4**). However, inorganic and organic N net uptake capacity increased significantly for all species with high compared to low soil N availability following species-specific patterns. More specifically, an increase in net uptake capacity was shown for the native species for ammonium, nitrate, and arginine-N of *Fagus*, for ammonium and arginine-N of *Quercus*, and for all N forms of *Pinus*. Both invasive species had an increased ammonium and arginine-N net uptake capacity with higher soil N availability (**Table 2A** and **Supplementary Table 5**). Furthermore, the changes in N metabolites levels in the leaves and fine roots at high compared to low soil N availability were also species-specific: *Fagus* had higher total soluble protein-N content in the leaves, *Quercus* had lower total soluble amino acid-N content in the leaves, and *Prunus* had lower total soluble amino acid-N content in the leaves and fine roots, while for *Pinus* and *Robinia* the N metabolite content in the leaves and fine roots did not differ significantly between low and high soil N availability (**Table 2A** and **Supplementary Table 6**). No other significant differences were found between soil N availability treatments in the single grown seedlings.

Effects of Competition on Native and Invasive Tree Species

Native Tree Species – Differences in the Response to Competitor Identity Regarding Total Biomass, Growth Indices, N Acquisition, and N Pools in the Leaves and Fine Roots

Fagus seedlings grown in competition with *Prunus* had significantly lower nitrate and glutamine-N net uptake capacity as well as RGR, regardless of soil N availability than when grown with *Robinia*, while no other parameter differed significantly with different competitor species (**Figure 1**, **Table 3** and **Supplementary Tables 7**, **8A**). Unlike *Fagus*, for *Quercus* seedlings inorganic and organic N net uptake capacity did not differ between different competitor identities (**Figure 1** and **Table 3**). However, seedlings of *Quercus* had significantly lower total biomass under competition with *Prunus* compared to under competition with *Robinia*, regardless of soil N availability (**Table 3** and **Supplementary Table 7**). Moreover, total soluble

TABLE 1 | Differences in total biomass, growth indices, inorganic and organic N net uptake capacity, and N metabolite levels between single grown seedlings of *Fagus sylvatica*, *Quercus robur*, *Pinus sylvestris*, *Prunus serotina*, and *Robinia pseudoacacia*.

Biomass and growth indices					N net uptake capacity			N metabolites			
								Total soluble amino acid-N		Total soluble protein-N	
Total biomass	**Root:shoot ratio**	**RGR**	**SLA**	**SRL**	NH_4^+	NO_3^-	**Gln-N**	**Arg-N**	**Leaves**	**Fine roots**	**Leaves**	**Fine roots**
Prunus > *Robinia* > *Quercus* > *Fagus*, *Pinus*	*Pinus* > *Quercus* > *Prunus* > *Fagus* > *Robinia*	*Prunus*, *Robinia* > *Fagus*, *Quercus*, *Pinus*	*Robinia* > *Fagus* > *Quercus* > *Prunus*	*Robinia* > *Fagus*, *Quercus*, *Pinus*, *Prunus*	n.s.	n.s.	*Fagus*, *Pinus* > *Prunus*, *Robinia*	*Fagus*, *Quercus*, *Pinus* > *Prunus*, *Robinia*	*Robinia* > *Prunus* > *Fagus*, *Quercus*, *Pinus*	*Prunus*, *Robinia* > *Fagus*, *Quercus*, *Pinus*	*Robinia*, *Fagus*, *Pinus* > *Prunus*	*Robinia* > *Fagus*, *Quercus*, *Pinus*, *Prunus*

Species A > species B, seedlings of species A had significantly higher values than seedlings of species B; n.s., no significant differences between species. Total biomass (g), root:shoot ratio, ratio of belowground biomass to aboveground biomass; RGR, relative growth rate (g dw g^{-1} dw d^{-1}); SLA, specific leaf area (cm^2 g^{-1} dw); SRL, specific root length (cm g^{-1} dw); N net uptake capacity (nmol N g^{-1} fw h^{-1}); NH_4^+, ammonium; NO_3^-, nitrate; Gln-N, glutamine; Arg-N, arginine; total soluble amino acid-N (mg amino acid-N g^{-1} dw); total soluble protein-N (mg protein-N g^{-1} dw).

amino acid-N content in the fine roots of *Quercus* seedlings was also significantly lower when grown in competition with *Prunus* compared to *Robinia* only at high soil N availability (**Table 3** and **Supplementary Tables 8A,B**). For *Quercus* seedlings no differences were found between different competitor identities regarding all other parameters (**Figure 1**, **Table 3** and **Supplementary Tables 7**, **8A**). For *Pinus* seedlings the only difference between competitor identities was a significantly higher SRL for seedlings competing with *Prunus* compared to those competing with *Robinia* (**Figure 1**, **Table 3** and **Supplementary Tables 7**, **8A**).

Invasive Tree Species – Differences in the Response to Competitor Identity Regarding Total Biomass, Growth Indices, N Acquisition, and N Pools in the Leaves and Fine Roots

Seedlings of *Prunus* had a significantly lower SLA when competing with *Fagus* than when competing with *Quercus* (**Table 3** and **Supplementary Table 7**), while there were no differences between different competitor identities with respect to any of the other measured parameters (**Figure 2**, **Table 3** and **Supplementary Tables 7**, **8A**). Moreover, *Robinia* seedlings competing with *Fagus* had a significantly lower SLA (regardless of soil N availability), and higher total soluble amino acid-N content in the fine roots (only at low soil N availability) than seedlings competing with *Quercus* or *Pinus* (**Table 3** and **Supplementary Tables 7**, **8A,B**). Furthermore, seedlings of *Robinia* competing with *Quercus* had significantly lower glutamine-N net uptake capacity than those competing with either *Fagus* or *Pinus* (only at high soil N availability) (**Figure 2**). All other measured parameters did not differ significantly between different competitor identities for this species (**Figure 2**, **Table 3** and **Supplementary Tables 7**, **8A**).

Effects of High Compared to Low Soil N Availability on Native and Invasive Tree Seedlings Growing in Competition

Native Tree Species – Effects of High Compared to Low Soil N Availability on Total Biomass, Growth Indices, N Acquisition, and N Pools in the Leaves and Fine Roots

For seedlings of *Fagus* a higher soil N availability resulted in significantly higher ammonium and arginine-N net uptake capacity (**Figure 1**), as well as a significantly lower SRL (**Table 2B** and **Supplementary Table 7**) and total soluble amino acid-N content in the leaves and fine roots (**Table 2B** and **Supplementary Table 8A**), regardless of competitor identity, while the rest of the measured parameters did not change significantly. For *Quercus*, ammonium and organic N net uptake capacity increased significantly (**Figure 1**), while RGR (**Table 2B** and **Supplementary Table 7**) and total soluble protein-N content in the fine roots (**Table 2B** and **Supplementary Table 8A**) decreased significantly at high compared to low soil N availability, regardless of competitor identity. Furthermore, higher soil N availability significantly reduced the total soluble amino acid-N content in the fine

TABLE 2 | Effects of increased soil N availability on total biomass, growth indices, inorganic and organic N net uptake capacity, and N metabolite levels on **(A)** seedlings growing single and **(B)** seedlings growing in competition of *Fagus sylvatica, Quercus robur, Pinus sylvestris, Prunus serotina*, and *Robinia pseudoacacia*.

	Biomass and growth indices					N net uptake capacity				N metabolites			
										Total soluble amino acid-N		Total soluble protein-N	
	Total biomass	Root:shoot ratio	RGR	SLA	SRL	NH_4^+	NO_3^-	Gln-N	Arg-N	Leaves	Fine roots	Leaves	Fine roots
(A) Seedlings growing single													
Fagus	n.s.	n.s.	n.s.	n.s.	n.s.	↑	↑	n.s.	↑	n.s.	n.s.	n.s.	↑
Quercus	n.s.	n.s.	n.s.	n.s.	n.s.	↑	n.s.	n.s.	↑	↓	n.s.	n.s.	n.s.
Pinus	n.s.	n.s.	n.s.	n.s.	n.s.	↑	↑	↑	↑	n.s.	n.s.	n.s.	n.s.
Prunus	n.s.	n.s.	n.s.	n.s.	n.s.	↑	n.s.	n.s.	↑	n.s.	n.s.	n.s.	n.s.
Robinia	n.s.	↓	n.s.	n.s.	n.s.	↑	n.s.	n.s.	↑	n.s.	n.s.	n.s.	n.s.
(B) Seedlings growing in competition													
Fagus	n.s.	n.s.	n.s.	n.s.	↓	↑	n.s.	n.s.	↑	↓	↓	n.s.	n.s.
Quercus	n.s.	n.s.	↓	n.s.	n.s.	↑	n.s.	↑	↑	n.s.	↓(b)	n.s.	↓
Pinus	n.s.	n.s.	↓	n.s.	n.s.	↑	n.s.	n.s.	↑	↓	n.s.	n.s.	n.s.
Prunus	n.s.	n.s.	n.s.	n.s.	↓	↑	n.s.	↑	↑	↓	↓	↓	n.s.
Robinia	n.s.	n.s.	n.s.	n.s.	n.s.	↑	↑	↑(a)	↑	↓	↓(c)	n.s.	↓

↑, significant increase with increased soil N availability; ↓, significant decrease with increased soil N availability; n.s., no significant differences between high and low soil N availability. Total biomass (g), root:shoot ratio, ratio of belowground biomass to aboveground biomass; RGR, relative growth rate (g dw g^{-1} dw d^{-1}); SLA, specific leaf area (cm^2 g^{-1} dw); SRL, specific root length (cm g^{-1} dw); N net uptake capacity (nmol N g^{-1} fw h^{-1}); NH_4^+, ammonium; NO_3^-, nitrate; Gln-N, glutamine; Arg-N, arginine; total soluble amino acid-N (mg amino acid-N g^{-1} dw); total soluble protein-N (mg protein-N g^{-1} dw). (a) Only in competition with Fagus and Pinus. (b) Only in competition with Prunus. (c) Only in competition with Fagus and Quercus. No letter: effect of soil N availability regardless of competitor identity.

roots for *Quercus* seedlings when grown in competition with *Prunus* but not in seedlings grown in competition with *Robinia* (**Table 2B** and **Supplementary Tables 8A,B**). All other measured parameters remained unchanged between soil N availability treatments. For seedlings of *Pinus*, a high soil N availability significantly increased ammonium and arginine-N net uptake capacity (**Figure 1**), whereas RGR (**Table 2B** and **Supplementary Table 7**) and total soluble amino acid-N content in the leaves decreased (**Table 2B** and **Supplementary Table 8A**) compared to low soil N availability regardless of competitor identity, while the other measured parameters did not differ significantly.

Invasive Tree Species – Effects of High Compared to Low Soil N Availability on Total Biomass, Growth Indices, N Acquisition, and N Pools in the Leaves and Fine Roots

Prunus seedlings at high compared to low soil N availability significantly increased their ammonium and organic N net uptake capacity (**Figure 2**), and decreased SRL (**Table 2B** and **Supplementary Table 7**), total soluble amino acid-N contents in the leaves and fine roots, as well as total soluble protein-N content in the leaves (**Table 2B** and **Supplementary Table 8A**) regardless of the competing species. There were no effects of soil N availability on any other measured parameter. For seedlings of *Robinia*, higher soil N availability resulted in significant increases in inorganic N and arginine-N net uptake capacity (**Figure 2**), as well as significantly decreased total soluble amino acid-N content in the leaves and total soluble protein-N content in the fine roots regardless of competition (**Table 2B** and **Supplementary Table 8A**). However, glutamine-N net uptake capacity increased significantly with higher soil N availability in seedlings competing with *Fagus* and *Pinus*, but not when competing with *Quercus* (**Figure 2**). Similarly, total soluble amino acid-N content in the fine roots decreased significantly with higher soil N availability in seedlings grown in competition with *Fagus* and *Quercus*, but not when grown in competition with *Pinus* (**Table 2B** and **Supplementary Tables 8A,B**). Soil N availability did not affect other parameters measured in *Robinia*.

N Acquisition Preferences of Native and Invasive Species for Specific N Sources at Low and High Soil N Availability

Comparing inorganic and organic N acquisition among N forms for each combination of species and competitor identity as well as for the single grown seedlings, we found general preference patterns at low and high soil N availability. At low soil N availability, organic N was preferred over inorganic N across species and competitor identities (**Tables 4**, **5**), with a few exceptions that showed no preference for any N source: single seedlings of *Quercus* and *Prunus*, seedlings of *Quercus* competing with *Robinia*, and seedlings of *Prunus* and *Robinia* competing with *Fagus* (**Tables 4**, **5**). At high soil N availability, a general pattern of preference for ammonium was found followed by organic N sources over nitrate. However, no preferences were found in single seedlings of *Prunus* and *Robinia*, seedlings of *Pinus* competing with *Robinia*, seedlings of *Robinia* competing with

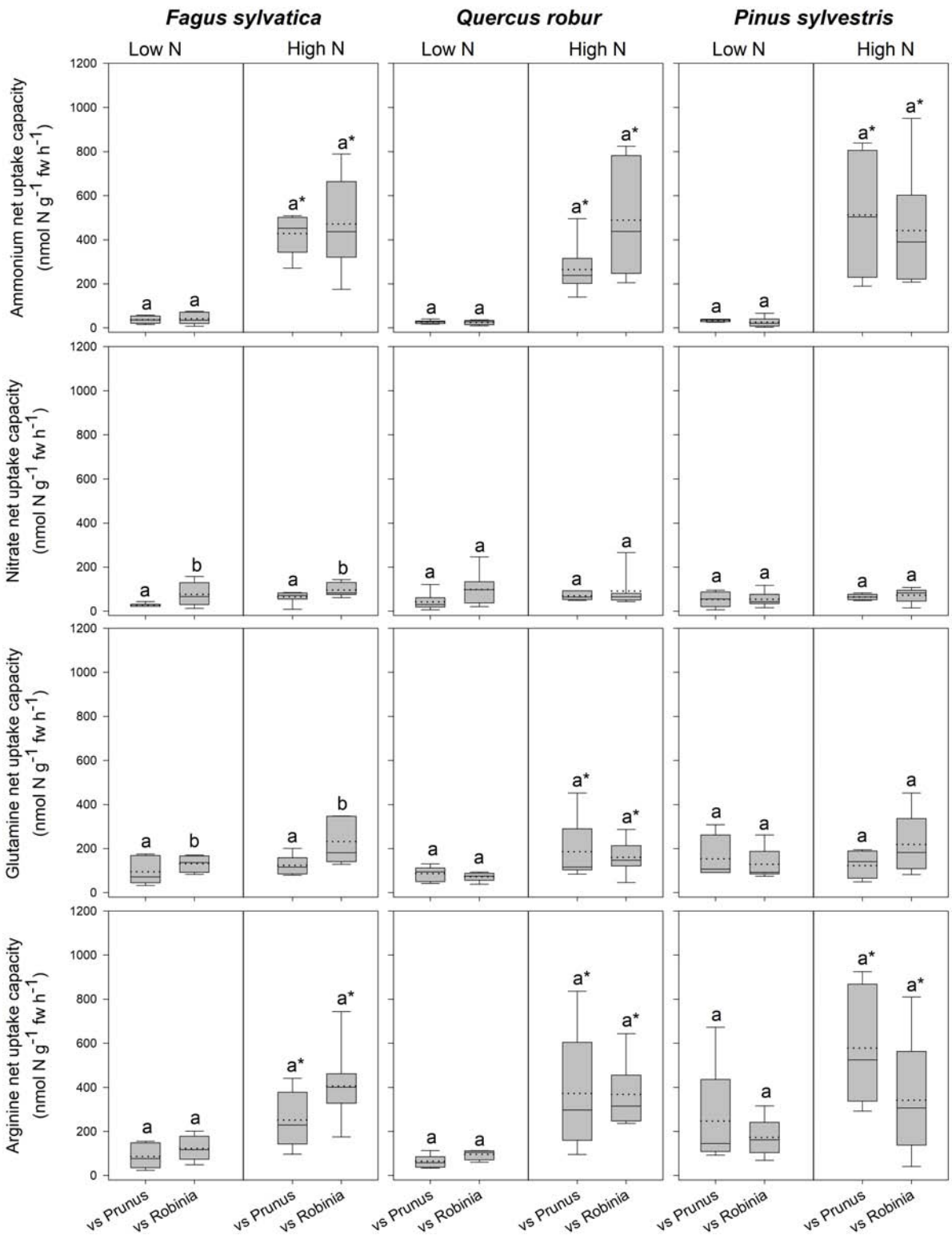

FIGURE 1 | Ammonium, nitrate, glutamine-N, and arginine-N net uptake capacity (nmol N g^{-1} fw h^{-1}) by fine roots of *Fagus sylvatica*, *Quercus robur,* and *Pinus sylvestris* seedlings at low and high soil N availability under different competition regimes. vs. Prunus = competition with *Prunus serotina*; vs. Robinia = competition with *Robinia pseudoacacia*. Box plots show mean (dotted line) and median (continuous line). Different letters indicate significant differences between competition regimes within a specific soil N availability treatment, and asterisks indicate significant differences between soil N availability treatments detected using permutational analysis of variance ($p < 0.05$).

TABLE 3 | Effects of competitor identity on total biomass, growth indices, inorganic and organic N net uptake capacity, and N metabolite levels of *Fagus sylvatica*, *Quercus robur*, *Pinus sylvestris*, *Prunus serotina*, and *Robinia pseudoacacia* seedlings.

	Biomass and growth indices					N net uptake capacity				N metabolites			
										Total soluble amino acid-N		Total soluble protein-N	
	Total biomass	Root: shoot ratio	RGR	SLA	SRL	NH_4^+	NO_3^-	Gln-N	Arg-N	Leaves	Fine roots	Leaves	Fine roots
Fagus	n.s.	n.s.	*Prunus* < *Robinia*	n.s.	n.s.	n.s.	*Prunus* < *Robinia*	*Prunus* < *Robinia*	n.s.	n.s.	n.s.	n.s.	n.s.
Quercus	*Prunus* <*Robinia*	n.s.	n.s.	n.s.	n.s.	n.s.	n.s.	n.s.	n.s.	n.s.	*Prunus* < *Robinia* (a)	n.s.	n.s.
Pinus	n.s.	n.s.	n.s.	n.s.	*Robinia* < *Prunus*	n.s.	n.s.	n.s.	n.s.	n.s.	n.s.	n.s.	n.s.
Prunus	n.s.	n.s.	n.s.	*Fagus* < *Quercus*	n.s.	n.s.	n.s.	n.s.	n.s.	n.s.	n.s.	n.s.	n.s.
Robinia	n.s.	n.s.	n.s.	*Fagus* < *Quercus*, *Pinus*	n.s.	n.s.	n.s.	*Quercus* < *Fagus*, *Pinus* (a)	n.s.	n.s.	*Quercus*, *Pinus* < *Fagus* (b)	n.s.	n.s.

Species A < species B, seedlings competing with species A had significantly lower values than seedlings competing with species B; n.s., no significant differences between competitor identities. Total biomass (g), root:shoot ratio, ratio of belowground biomass to aboveground biomass; RGR, relative growth rate (g dw g^{-1} dw d^{-1}); SLA, specific leaf area (cm^2 g^{-1} dw); SRL, specific root length (cm g^{-1} dw); N net uptake capacity (nmol N g^{-1} fw h^{-1}), NH_4^+, ammonium; NO_3^-, nitrate; Gln-N, glutamine; Arg-N, arginine; total soluble amino acid-N (mg amino acid-N g^{-1} dw); total soluble protein-N (mg protein-N g^{-1} dw). (a) Only at high soil N availability. (b) Only at low soil N availability. No letter: effect of competition regardless of soil N availability.

Quercus, and seedlings of *Prunus* and *Robinia* competing with *Pinus* (**Tables 4**, **5**).

With regard to the specific preferences of each species across different competitor identities and single grown seedlings, native *Fagus* and *Pinus* had in general similar preferences for N sources regardless of competitor identity or whether they grow single or in competition (**Table 4**). However, native *Quercus* showed no preference for any N source either when grown single or in competition with *Robinia*, but preferred organic N over ammonium when grown in competition with *Prunus* (at low soil N availability). Moreover, at high soil N availability, the preferences of *Quercus* shifted from no preference when grown single to preferring ammonium and organic N over nitrate when grown in competition with *Prunus* or *Robinia* (**Table 4**). For the invasive species, *Prunus* had no preference of N sources when grown single but generally preferred arginine-N over glutamine-N and inorganic N when competing with *Quercus* or *Pinus* at low soil N availability, while preferences for N sources did not shift across competitor identities at high soil N availability (**Table 5**). Seedlings of *Robinia* preferred organic over inorganic N sources regardless of competitor identity as well as when grown single at low soil N availability, except for seedlings competing with *Fagus* which showed no preference. However, at high soil N availability, *Robinia* seedlings preferred ammonium and organic N over nitrate when competing with *Fagus*, while seedlings competing with other native species or grown single took up all N forms without preference (**Table 5**).

DISCUSSION

Strategies of Native and Invasive Species Growing Without Competition

Invasive Species Succeed With Fast Growth, but Natives Could Counter With Preference of Organic N Acquisition

Comparing single grown invasive and native species, invasive species showed traits characteristic for fast-growing species. The invasive species had higher total biomass, RGR, and SRL, as well as total soluble amino acid-N and protein-N levels in both leaves and fine roots compared to the natives. A fast RGR is related to a rapid increase in biomass as well as high leaf nutrient concentrations, whereas slow RGR is related to a higher investment of resources in defense (Reich et al., 1997; Aerts, 1999). A higher SRL allows to forage larger soil volumes and is linked to a higher competitive ability for belowground resources (Aerts, 1999). Our results suggest a potential of the studied invasive species to outcompete the native ones via rapid growth and exploitation of above- and below-ground resources (Vilà and Weiner, 2004; Gioria and Osborne, 2014), which is in line with previous studies that found higher biomass (e.g., Lee et al., 2004; Closset-Kopp et al., 2007; Ding et al., 2012; Kawaletz et al., 2013), and monthly height increments (e.g., Ding et al., 2012) of *P. serotina* and *R. pseudoacacia* compared to plant species native to Europe and Asia. Moreover, the higher content of N metabolites in the fine roots is also linked to fast growing species

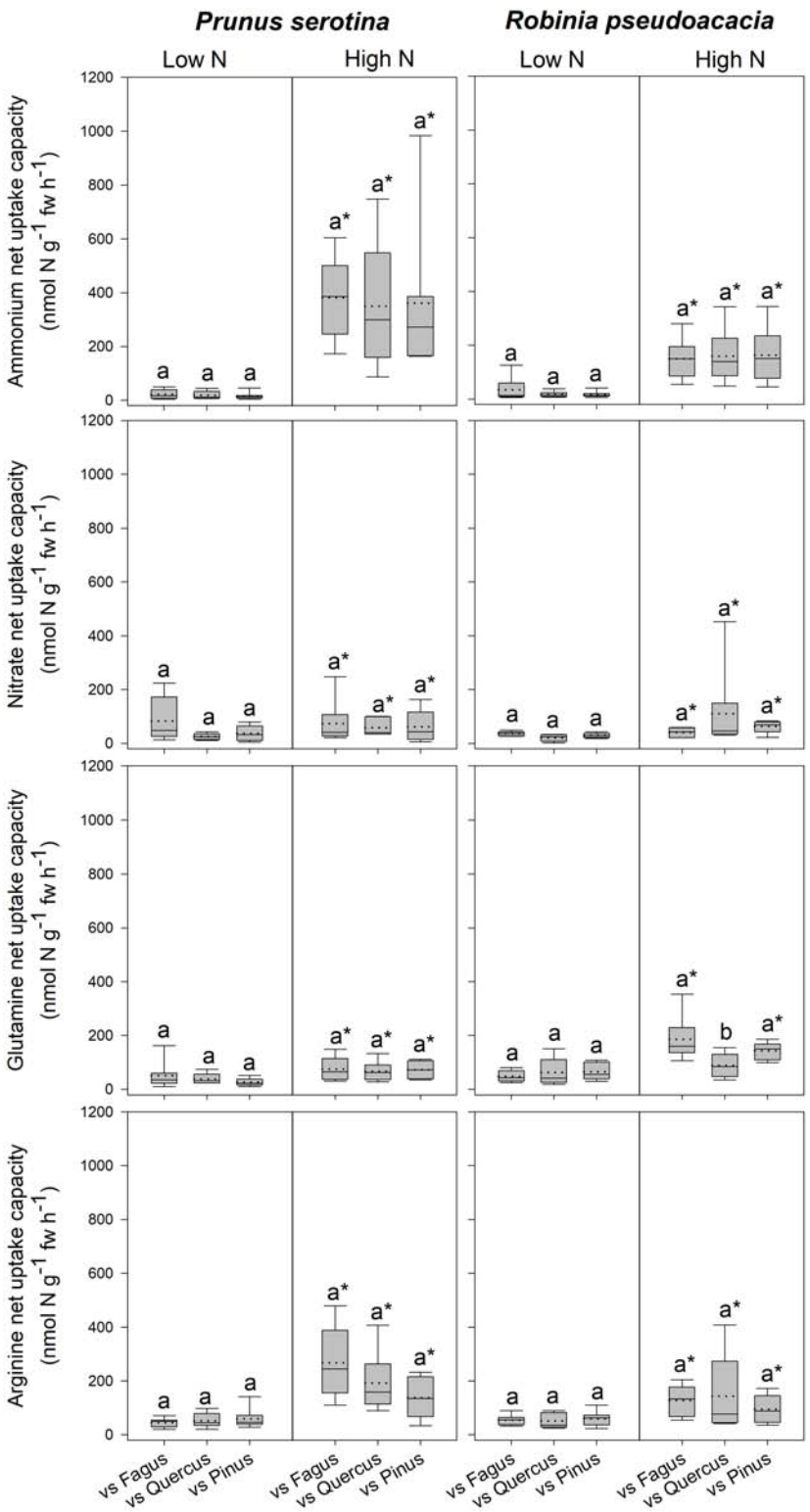

FIGURE 2 | Ammonium, nitrate, glutamine-N, and arginine-N net uptake capacity (nmol N g^{-1} fw h^{-1}) by fine roots of *Prunus serotina* and *Robinia pseudoacacia* seedlings at low and high soil N availability under different competition regimes. vs. Fagus = competition with *Fagus sylvatica*; vs. Quercus = competition with *Quercus robur*; vs. Pinus = competition with *Pinus sylvestris*. Box plots show mean (dotted line) and median (continuous line). Different letters indicate significant differences between competition regimes within a specific soil N availability treatment, and asterisks indicate significant differences between soil N availability treatments detected using permutational analysis of variance ($p < 0.05$).

TABLE 4 | Differences between ammonium (NH_4^+), nitrate (NO_3^-), glutamine-N (Gln-N), and arginine-N (Arg-N) net uptake capacity of the fine roots of *Fagus sylvatica*, *Quercus robur*, and *Pinus sylvestris* seedlings grown single and in competition at low and high soil N availability.

	Soil N availability	*Fagus*	*Quercus*	*Pinus*
Single grown seedlings	Low	Gln-N, Arg-N > NH_4^+ Gln-N > NO_3^-	n.s.	Gln-N, Arg-N > NH_4^+ Gln-N > NO_3^-
	High	NH_4^+, Arg-N > Gln-N > NO_3^-	n.s.	NH_4^+, Gln-N, Arg-N > NO_3^-
Seedlings in competition with *Prunus*	Low	Gln-N, Arg-N > NO_3^- Gln-N > NH_4^+	Gln-N, Arg-N > NH_4^+	Gln-N, Arg-N > NH_4^+, NO_3^-
	High	NH_4^+ > Arg-N > Gln-N > NO_3^-	NH_4^+, Gln-N, Arg-N > NO_3^-	NH_4^+, Arg-N > Gln-N > NO_3^-
Seedlings in competition with *Robinia*	Low	Gln-N, Arg-N > NH_4^+	n.s.	Gln-N, Arg-N > NH_4^+, NO_3^-
	High	NH_4^+ > Gln-N > NO_3^- Arg-N > NO_3^-	NH_4^+, Arg-N > NO_3^-, Gln-N	n.s.

Only significant differences are presented. n.s., no significant differences between net uptake capacity of different N forms.

TABLE 5 | Differences between ammonium (NH_4^+), nitrate (NO_3^-), glutamine-N (Gln-N), and arginine-N (Arg-N) net uptake capacity of the fine roots of *Prunus serotina* and *Robinia pseudoacacia* seedlings grown single and in competition at low and high soil N availability.

	Soil N availability	*Prunus*	*Robinia*
Single grown seedlings	Low	n.s.	Gln-N, Arg-N > NH_4^+
	High	NH_4^+, Arg-N > Gln-N > NO_3^-	n.s.
Seedlings in competition with *Fagus*	Low	n.s.	n.s.
	High	NH_4^+, Arg-N > Gln-N, NO_3^-	NH_4^+, Gln-N, Arg-N > NO_3^-
Seedlings in competition with *Quercus*	Low	Arg-N > NH_4^+, NO_3^-	Gln-N, Arg-N > NH_4^+
	High	NH_4^+, Arg-N > NO_3^-, Gln-N	n.s.
Seedlings in competition with *Pinus*	Low	Arg-N > NH_4^+, Gln-N	Gln-N, Arg-N > NH_4^+, NO_3^-
	High	n.s.	n.s.

Only significant differences are presented. n.s., no significant differences between net uptake capacity of different N forms.

compared to slow growers (e.g., *A. pseudoplatanus* compared to *F. sylvatica* in Li et al., 2015). For *Robinia*, a higher total N content in the leaves and fine roots compared to the other species is most likely associated with its N_2-fixing ability (McKey, 1994; De Marco et al., 2013; Salpagarova et al., 2014). With regard to the N acquisition strategies, inorganic N acquisition was similar between invasive and native species. However, the lower organic N acquisition for the invasive compared to the native species suggests that native species could have a competitive advantage over the invasives via better exploitation of soil organic N. Although the invasives have faster growth, their species-specific N acquisition does not suggest a competitive advantage over natives.

With Higher Soil N Availability N Acquisition Strategies of Native and Invasive Seedlings Are Similar, Whereas N Allocation to N Pools in the Leaves and Fine Roots Is Species-Specific

In our study, the responses of single growing native and invasive species to high compared to low soil N availability were similar for all species for N acquisition, biomass and growth indices, whereas the allocation of N to N pools in the fine roots and leaves depended on the species. More specifically, inorganic and organic N acquisition increased with rising soil N levels, while biomass and growth indices showed no response, except for an increased root:shoot ratio for *Robinia* indicating a greater allocation to root biomass with increasing soil N supply. The allocation of N to N pools in the leaves and fine roots was species-specific with one of three responses with higher compared to lower soil N availability: (1) an increase in total soluble protein-N levels in the leaves (i.e., for native *Fagus*), (2) a decrease in total soluble amino acid-N levels in the leaves (i.e., for native *Quercus*), and (3) no change of total soluble amino acid-N or protein-N levels in neither leaves nor fine roots (i.e., for native *Pinus* and both invasives *Prunus* and *Robinia*).

The increase in total soluble protein-N levels in the leaves of *Fagus* with higher soil N availability in combination with no change in overall biomass suggests that N is stored as Rubisco for later mobilization (Millard, 1988; Masclaux-Daubresse et al., 2010). In contrast, *Quercus* had a reduced total soluble amino acid-N levels in the leaves which suggests that soluble amino acids are used to produce other compounds not quantified here, e.g., compounds related to defense. N allocation to N pools did not differ with increased soil N availability in *Pinus*, *Prunus*, and *Robinia* which is likely related to life history traits resulting in a relative independence of external soil N supply: *Pinus* is a conifer with needles present throughout the year in which N is stored (Houston et al., 2016b), *Robinia* can fix atmospheric N_2 (Vítková et al., 2017), and *Prunus* allocates N to allelopathic compounds, such as cyanogenic glycosides (Csiszár, 2009), thereby potentially inhibiting N uptake by competitors.

Overall, for all studied species, the increased inorganic and organic N acquisition as well as the reduced levels of N metabolites in leaves and fine roots with rising soil N availability indicate plant physiological adjustments to meet the N demands with different soil N supply (BassiriRad, 2000). The lack of response with regard to biomass or growth indices suggests that the acquired N is either used for metabolism maintenance or assigned to storage (Millard and Grelet, 2010). Plant N acquisition is directly related to soil N supply, thus, higher organic and inorganic N acquisition with higher soil N availability reflects the active regulation of N uptake (Kulmatiski et al., 2017) which has already been reported for seedlings of *F. sylvatica* (e.g., Li et al., 2015) and *P. sylvestris* (e.g., Simon et al., 2013).

Native Species Respond to Competition With Invasives With Distinct Species-Specific Strategies

The native species showed distinct species- and also parameter-specific strategies in their responses to competition with different invasive species that were partly mediated by soil N availability. When competing with *Prunus* compared to *Robinia*: (1) *Fagus* had lower RGR and N acquisition without changes in biomass or N metabolite levels, (2) *Quercus* had lower biomass and total soluble amino acid-N levels without changes in N acquisition, whereas (3) *Pinus* only had higher SRL, without changes in biomass, N acquisition or N metabolite levels. More specifically, the lower RGR combined with N acquisition in *Fagus* in competition with *Prunus* compared to *Robinia* suggests that the response strength to competition with an invasive species depends on the competitor. The slower growth combined with a reduced N acquisition from the soil indicates a remobilization of internal N in compensation for the impaired N acquisition from the soil assuming a similar N demand. This strategy of a reduced growth rate (Li et al., 2015) and N acquisition (Simon et al., 2010, 2014) was found also in response to competition with fast-growing *A. pseudoplatanus*, thus indicating a general response of *F. sylvatica* to fast-growing competitors. In contrast, *Quercus* had a decreased biomass as well as total soluble amino acid-N content in the fine roots (only at high soil N availability) in competition with *Prunus* compared to *Robinia*, with no change in N acquisition suggesting a shift in the allocation of N from growth to storage and/or the synthesis of defense compounds depending on the competing species (Millard and Grelet, 2010). The lower total soluble amino acid-N levels in the fine roots when competing with *Prunus* compared to *Robinia* but only a high soil N availability indicates a mediation of the competitive response by soil N supply. Lower amino acid-N levels in the fine roots have been related to slower growth (Simon et al., 2010), whereas an increase in total soluble amino acid levels in the fine roots as a result of competition (Li et al., 2015) was found in fast-growing sycamore maple (*A. pseudoplatanus* L.). However, *Fagus* showed a different response, despite also being a slow growing species which indicates that other species-specific factors regulate the response to competition in terms of total soluble amino acid-N content in the fine roots that were not considered in our study. For seedlings of *Pinus* the sole response to competition with *Prunus* compared to *Robinia* was a higher SRL which regulates the access to N (Andersen et al., 2017). Growing longer, thinner roots allows *Pinus* seedlings to maximize resource capture without changing N acquisition capacity per root, thereby being able to tolerate competition with no effects on productivity. Unlike both deciduous species *Fagus* and *Quercus*, coniferous *Pinus* did not show different responses to different invasive competitors regarding N acquisition and N pools in leaves and fine roots, likely because conifers maintain needles in which N is stored throughout the year (Millard and Grelet, 2010) and can be utilized when needed. By drawing on these resources, *Pinus* can buffer the different competitive effects of the invasive species. Noticeably, none of our native study species responded differently depending on the competitor with regard to their total soluble protein-N levels in the leaves or fine roots. Previous studies on temperate tree seedlings including *F. sylvatica* (Simon et al., 2010, 2014; Li et al., 2015) found changes in total soluble protein-N contents in the fine roots when grown in intraspecific or interspecific competition indicating *de novo* protein synthesis as an adaptive response to competition. In the present study, we compare native species responses to different invasive species rather than intraspecific vs. interspecific competition within native species. Thus, it is possible that protein-N levels changed for the single species when grown in competition, but the response was similar with different competitors.

Overall, the response of native seedlings in competition with invasive species is species-specific and reflects different coping mechanisms related to the species life history and growth strategies. For instance, coniferous species such as *Pinus* maintain their needles throughout the year resulting in higher N storage capacities compared to deciduous species like *Fagus* and *Quercus* (Millard and Grelet, 2010). As a consequence, conifers might be less responsive to the different competitive effects of the invasive species in terms of the competition for N. All three native species responded stronger when competing with *Prunus* than *Robinia*.

Why Is *P. serotina* a Stronger Competitor Than *R. pseudoacacia* for the Studied Native Species?

In our study, the native tree seedlings competing with *Prunus* responded with decreases in N acquisition, total biomass, RGR, and total soluble amino acid-N levels in the fine roots than when competing with *Robinia* which can be explained by its relatively high root biomass, and, in turn, a better exploitation of belowground resources of *Prunus* (Casper and Jackson, 1997; Kawaletz et al., 2014) compared to all other species in our study which is linked to increased success rates of invasive plants (e.g., Grotkopp and Rejmánek, 2007; Robakowski and Bielinis, 2011; Kawaletz et al., 2013; Gioria and Osborne, 2014). Moreover, *Prunus* produces cyanogenic compounds also in the roots, a strategy that might have had an allelopathic effect on the neighboring plants (Csiszár, 2009; Robakowski et al., 2016) and contributed to the general negative influence of *Prunus* on the native species in our study. Overall, the higher competitive ability of *Prunus* in our study is in accordance with earlier work by others; however, previous studies investigated the effects of *Prunus* and *Robinia* when competing with native species mainly

considering plant growth and biomass (e.g., Closset-Kopp et al., 2011; Robakowski and Bielinis, 2011; Kawaletz et al., 2013, 2014), whereas we found not only competition effects on growth and biomass but also on N acquisition and N allocation to different N pools depending on the species.

Invasive *R. pseudoacacia* Reacts Stronger to Competition With Native Seedlings Than *P. serotina*

The invasive species used in our study responded to competition depending on the native competitor species and soil N availability: the response of *Prunus* to competition with native seedlings was an increase in SLA when grown in competition with *Quercus* compared to competition with *Fagus*, but not *Pinus*. Usually, plants with a high SLA have a lower competitive effect related to a shorter leaf lifespan resulting in a lower leaf mass fraction (Kuster et al., 2016); which is, however mostly related to limiting resource conditions (Knops and Reinhart, 2000). In contrast, having a higher SLA when belowground resources are sufficient becomes a competitive advantage as a strategy of fast resource acquisition (Liu et al., 2017). Therefore, given the higher root biomass of *Prunus* compared to our native study species (see section "Invasive Species Succeed With Fast Growth, But Natives Could Counter With Preference of Organic N Acquisition"), *Prunus* was a strong competitor for belowground resources, and enhanced its competitive ability and fast growth strategy by increasing light interception via a higher SLA (Liu et al., 2017).

In contrast, seedlings of *Robinia* responded to competition depending on the native species, with a decrease in organic N acquisition in competition with *Quercus* compared to *Pinus* and *Fagus*, as well as an increased SLA combined with a decrease in fine root total soluble amino acid-N content in competition with *Quercus* and *Pinus* compared to *Fagus*. Notably, the decrease in fine root total soluble amino acid-N content with competition was found only at low soil N availability, the decrease in organic N acquisition only at high soil N availability. This response dependency on soil N availability for *Robinia* but not *Prunus* indicates that *Robinia* shows a strong response to the combined effects of competition and soil N availability, whereas the response of *Prunus* is not mediated by soil N supply. The increase in SLA when competing with *Quercus* compared to *Fagus* was found regardless of soil N availability and suggests a potential reduced competitive ability of *Robinia* competing with *Quercus*, especially in combination with the reduced organic N acquisition and total soluble amino acid-N content in the fine roots indicating an impaired N nutrition. In general, leaves with a high SLA represent a disadvantage for plant growth under limiting nutrient conditions, because of the negative correlation with leaf lifespan, and therefore increased N losses through leaf senescence (Reich et al., 1997; Knops and Reinhart, 2000).

Overall, the investigated invasive species responded at different levels (i.e., morphological and physiological) depending on the identity of the native competitor suggesting that *Robinia* represents a lesser threat than *Prunus* at the investigated time scale. However, the impact of *Robinia* might become more important in the long run as a result of its capacity to fix atmospheric N_2 and therefore potentially alter biogeochemical processes in invaded ecosystem (Strayer et al., 2006; Medina-Villar et al., 2016). By modifying soil N availability, for example, N_2-fixing plants might influence community composition and diversity (i.e., by favoring the establishment of nitrophilous species) (Staska et al., 2014), and consequently impact on plant–plant interactions such as competition.

Higher Soil N Availability Results in Increased N Acquisition but No Change in Biomass or Growth Indices for All Species in Competition, While a Reduction in N Pool Levels Is Species- and Organ-Specific

Seedlings of native and invasive species growing in competition in our study varied their responses with high soil N supply. Although, none of them increased in biomass with high soil N supply seedlings of *Fagus* and *Prunus* had lower SRL indicating that foraging for nutrients via an investment in longer, thinner roots is only required when soil nutrients are limiting (Zhu et al., 2016). In all species, organic and inorganic N uptake increased with high compared to low soil N supply which is a key driver of N acquisition in woody species (Simon et al., 2017) as reported for *F. sylvatica* (Stoelken et al., 2010; Li et al., 2015), *P. sylvestris* (Simon et al., 2013), and *A. pseudoplatanus* (Li et al., 2015). However, reduced total soluble amino acid-N and total soluble protein-N levels with higher soil N availability were species- as well as organ-specific in our study. In general, plants have to rely less on internal N storage to maintain growth and metabolic functions when N is readily available in the soil (Millard and Grelet, 2010). For *Fagus*, our results are in contrast with a previous study that found no changes in total soluble amino acid-N contents in the fine roots with increasing soil N availability neither in intraspecific competition nor in competition with *A. pseudoplatanus* (Li et al., 2015). However, in our study, the response of native species to competition with invasive species in terms of N strategies is evaluated for the first time and suggests a specific response of native species to combined soil N availability and competition with the invasive species *Prunus* and *Robinia*.

Species responded to soil N availability mostly regardless of competitor identity, however, for some species an interaction between soil N availability and competitor was detected. For example, the reduction in total soluble amino acid-N levels in the fine roots with at high compared to low soil N availability described above was found in some species only with specific competitors (i.e., for *Quercus* when competing with *Prunus*, and for *Robinia* when competing with *Fagus* or *Quercus*). Specifically, for *Quercus* this suggests that invasive species *Prunus* induces a stronger response than invasive *Robinia*, a result that is consistent with the general responses of *Quercus* to *Prunus* described in Section "Native Species Respond to Competition With Invasives With Distinct Species-Specific Strategies." We found no effects of competition on seedling total soluble amino acid-N or total soluble protein-N levels in the leaves which contrasts with studies reporting the invasion by *Prunus* to affect foliar N levels of

native mature tree species including the ones considered here (e.g., Aerts et al., 2017). This suggests an effect of plant age on the competition response, as well as the possibility that soil N availability in our study was a strong driver of foliar N levels, thereby overriding the potential effects of competition.

Native and Invasive Species Share Common Preferences for N Sources Regardless of Soil N Availability, but There Are Species-Specific Patterns Between Competition Regimes and Competitor Identities

The common N preference patterns across species in our study depended on soil N availability and species strategies in response to competition. At low soil N availability, organic N was taken up preferentially over inorganic N by seedlings of both native and invasive suggesting that tree seedlings maintain their metabolism and growth by drawing upon a wider variety of N sources. However, at high soil N availability, ammonium-N was the preferred N form followed by organic N, while nitrate-N was the least preferred N form taken up by tree seedlings, as also found for *F. sylvatica* (Stoelken et al., 2010) and *P. sylvestris* (Simon et al., 2010). Nitrate acquisition from the soil is inhibited by high concentrations of amino acids (particularly glutamine) and ammonium (Näsholm et al., 2009; Stoelken et al., 2010). Both native and invasive species preferred specific N sources linked to other aspects considered in our study. For example, *Quercus* preferred organic N forms over ammonium only when grown in competition with invasive *Prunus*. *Pinus* did not shift N source preferences. Both invasive species also lacked a preference for certain N forms when competing with *Fagus* (at low soil N availability) or *Pinus* (at high soil N availability) which corresponds with their general stronger reaction to competition with *Quercus* (see section "Invasive *R. pseudoacacia* Reacts Stronger to Competition With Native Seedlings Than *P. serotina*"). Overall, N form preferences matched the general response strategies of native and invasive species to differing competitors that were found for growth, N acquisition and allocation of N to N pools.

CONCLUSION

In our study, we found that invasive species display traits that grant them competitive advantage, such as fast growth rates, which however did not result in a generally higher N acquisition of invasive species, because native species had a higher organic N net uptake capacity that would allow them to better utilize soil N sources, and thus potentially avoid competition with neighboring invasive species. When growing in competition, native tree seedlings showed a stronger response to competition with *Prunus* than *Robinia*, although the response variable changed between native species indicating the use of species-specific strategies of native seedlings to cope with the competition with invasive plants. These are further mediated by soil N availability in some cases. These strategies reflected the differences between native species in terms of life history and growth traits. The stronger response to *Prunus* could be related to the higher total biomass of this species and its ability to produce allelopathic compounds. Furthermore, when comparing the responses of invasive species, *Robinia* responded to different native competitors at different morphological and physiological levels, further influenced by soil N availability, while *Prunus* only showed changes in SLA, without interaction with soil N availability. This suggests that *Prunus* might have a stronger competitive advantage over native species than *Robinia* at least at the time scale of our study. Moreover, considering that native *Quercus* responded more negative to competition with *Prunus* than *Robinia*, as well as the several responses of *Robinia* to competition with *Quercus*, our results suggest that specifically *Quercus* could have a competitive advantage over invasive *Robinia*, but not over invasive *Prunus*. However, it is possible that the impact of *Robinia* becomes more important in the longer run at the plant community level, as a result of its capacity to fix atmospheric N_2 and therefore potentially alter biogeochemical processes in an invaded ecosystem. With regard to the effects of high compared to low soil N availability on competing seedlings, we found common patterns among species similar to those displayed by single grown seedlings regarding N acquisition (increased with soil N availability), but not regarding N allocation, i.e., in single seedlings N allocation was scarcely influenced by soil N availability, while in competing seedlings there was a general decrease in total soluble amino acid-N levels for most species, which suggests stronger responses to increased soil N availability when in combination with competition. Generally, our results highlight *Prunus* as a potential greater threat to seedlings of native species than *Robinia* in the time frame considered here. Overall, our results provide novel insights into the different species-specific effects of invasive species on native seedlings not only with regard to growth parameters, but also underlying physiological processes such as N acquisition and internal allocation. However, our study included only five species (three natives, two invasives) differing in their ecological background, with a focus on the competition for N rather than other resources, such as light and/or space, thus more detailed studies are still required in the future. Furthermore, the results should be validated in long term studies conducted in the field. In conclusion, the species-specific nature of competition between native and invasive tree seedlings should be considered in forest management strategies in the future.

DATA AVAILABILITY

The raw data supporting the conclusions of this manuscript will be made available by the authors, without undue reservation, to any qualified researcher.

AUTHOR CONTRIBUTIONS

AB and JS conceived the experimental design and manuscript writing. AB conducted the ^{15}N uptake experiments and evaluated the data. KP contributed stable isotope analyses and ideas to

data interpretation. All authors agreed on the final version of the manuscript.

FUNDING

Funding was provided by the Young Scholar Fund project no. 83979115 of the University of Konstanz.

ACKNOWLEDGMENTS

We are grateful to Leonhard Schink and Leia Mijatovic for their help with ^{15}N uptake experiments, harvest, and sample processing. Furthermore, we would like to thank Silvia Kuhn and Roswitha Miller for their help with sample analyses. We thank Franz Buegger for support with EA-IRMS analyses. We would also like to thank Iljas Müller, Gudrun Winter, Dietmar Funck, Marie-Luise Kocher, Anna Märkle, Dominic Stickel, Lea Held, Inna Koleber, Julia Maier, and Jasmin Thierschmidt for their assistance with parts of the harvest and sample processing. We thank the gardeners at the Botanical Garden of the University of Konstanz for their help with experimental set up.

SUPPLEMENTARY MATERIAL

The Supplementary Material for this article can be found online at: https://www.frontiersin.org/articles/10.3389/fpls.2019.00337/full#supplementary-material

REFERENCES

Aerts, R. (1999). Interspecific competition in natural plant communities: mechanisms, trade-offs and plant-soil feedbacks. *J. Exp. Bot.* 50, 29–37. doi: 10.1093/jxb/50.330.29

Aerts, R., Ewald, M., Nicolas, M., Piat, J., Skowronek, S., Lenoir, J., et al. (2017). Invasion by the alien tree *Prunus serotina* alters ecosystem functions in a temperate deciduous forest. *Front. Plant Sci.* 8:179. doi: 10.3389/fpls.2017.00179

Andersen, K. M., Mayor, J. R., and Turner, B. L. (2017). Plasticity in nitrogen uptake among plant species with contrasting nutrient acquisition strategies in a tropical forest. *Ecology* 98, 1388–1398. doi: 10.1002/ecy.1793

Anderson, M., Gorley, R., and Clarke, K. (2008). *PERMANOVA+ for PRIMER: Guide to Software and Statistical Methods*. Plymouth: PRIMER-E.

Aschehough, E. T., Brooker, R., Atwater, D. Z., Maron, J. L., and Callaway, R. M. (2016). The mechanisms and consequences of interspecific competition among plants. *Annu. Rev. Ecol. Evol. Syst.* 47, 263–281. doi: 10.1146/annurev-ecolsys-121415-032123

BassiriRad, H. (2000). Kinetics of nutrient uptake by roots: responses to global change. *New Phytol.* 147, 155–169. doi: 10.1046/j.1469-8137.2000.00682.x

Bradley, B. A., Blumenthal, D. M., Wilcove, D. S., and Ziska, L. H. (2010). Predicting plant invasions in an era of global change. *Trends Ecol. Evol.* 25, 310–318. doi: 10.1016/j.tree.2009.12.003

Campagnaro, T., Brundub, G., and Sitzia, T. (2018). Five major invasive alien tree species in European Union forest habitat types of the alpine and continental biogeographical regions. *J. Nat. Conserv.* 43, 227–238. doi: 10.1016/j.jnc.2017.07.007

Casper, B. B., and Jackson, R. B. (1997). Plant competition underground. *Annu. Rev. Ecol. Evol. Syst.* 28, 545–570. doi: 10.1146/annurev.ecolsys.28.1.545

Cavin, L., Mountford, E. P., Peterken, G. F., and Jump, A. S. (2013). Extreme drought alters competitive dominance within and between tree species in a mixed forest stand. *Funct. Ecol.* 27, 1424–1435. doi: 10.1111/1365-2435.12126

Closset-Kopp, D., Chabrerie, O., Valentin, B., Delachapelle, H., and Decocq, G. (2007). When Oskar meets Alice: does a lack of trade-off in r/K-strategies make *Prunus serotina* a successful invader of European forests? *For. Ecol. Manage.* 247, 120–130. doi: 10.1016/j.foreco.2007.04.023

Closset-Kopp, D., Saguez, R., and Decocq, G. (2011). Differential growth patterns and fitness may explain contrasted performances of the invasive *Prunus serotina* in its exotic range. *Biol. Invasions* 13, 1341–1355. doi: 10.1007/s10530-010-9893-6

Csiszár, A. (2009). Allelopathic effects of invasive woody plant species in Hungary. *Acta Silvatica Lignaria Hung.* 5, 9–17.

Dannenmann, M., Simon, J., Gasche, R., Holst, J., Naumann, P. S., Koegel-Knabner, I., et al. (2009). Tree girdling provides insight on the role of labile carbon in nitrogen partitioning between soil microorganisms and adult European beech. *Soil Biol. Biochem.* 41, 1622–1631. doi: 10.1016/j.soilbio.2009.04.024

Danso, S. K. A., Zapata, F., and Awonaike, K. O. (1995). Measurement of biological N2 fixation in field-grown *Robinia pseudoacacia L. Soil Biol. Biochem.* 27, 415–419. doi: 10.1016/0038-0717(95)98612-R

De Marco, A., Arena, C., Giordano, M., and Virzo De Santo, A. (2013). Impact of the invasive tree black locust on soil properties of Mediterranean stone pine-holm oak forests. *Plant Soil* 372, 473–486. doi: 10.1007/s11104-013-1753-6

Ding, W., Wang, R., Yuan, Y., Liang, X., and Liu, J. (2012). Effects of nitrogen deposition on growth and relationship of *Robinia pseudoacacia* and *Quercus acutissima* seedlings. *Dendrobiology* 6, 3–13.

D´Antonio, C. M., and Vitousek, P. M. (1992). Biological invasions by exotic grasses, the grass/fire cycle, and global change. *Annu. Rev. Ecol. Evol. Syst.* 23, 63–87. doi: 10.1146/annurev.es.23.110192.000431

Eaton, E., Caudullo, G., Oliveira, S., and de Rigo, D. (2016). "*Quercus robur* and *Quercus petraea* in Europe: distribution, habitat, usage and threats," in *European Atlas of Forest Tree Species*, eds J. San-Miguel-Ayanz, D. de Rigo, G. Caudullo, T. Houston Durrant, and A. Mauri (Luxembourg: Publ. Off. EU).

Ellenberg, H., and Leuschner, C. (2010). *Vegetation Mitteleuropas Mit Den Alpen*, Vol. 6. Stuttgart: Ulmer.

Fotelli, M. N., Gessler, A., Peuke, A. D., and Rennenberg, H. (2001). Drought affects the competitive interactions between *Fagus sylvatica* seedlings and an early successional species, *Rubus fruticosus*: responses of growth, water status and δ13C composition. *New Phytol.* 151, 427–435. doi: 10.1046/j.1469-8137.2001.00186.x

Fotelli, M. N., Rennenberg, H., and Gessler, A. (2002). Effects of drought on the competitive interference of an early successional species (*Rubus fruticosus*) on *Fagus sylvatica* L. seedlings: 15N uptake and partitioning, responses of amino acids and other N compounds. *Plant Biol.* 4, 311–320. doi: 10.1055/s-2002-32334

Fotelli, M. N., Rudolph, P., Rennenberg, H., and Gessler, A. (2005). Irradiance and temperature affect the competitive interference of blackberry on the physiology of European beech seedlings. *New Phytol.* 165, 453–462. doi: 10.1111/j.1469-8137.2004.01255.x

Gessler, A., Kreuzwieser, J., Dopatka, T., and Rennenberg, H. (2002). Diurnal courses of ammonium net uptake by the roots of adult beech (*Fagus sylvatica*) and spruce (*Picea abies*) trees. *Plant Soil* 240, 23–32. doi: 10.1023/A:1015831304911

Gessler, A., Schneider, S., von Sengbusch, D., Weber, P., Hanemann, U., Huber, C., et al. (1998). Field and laboratory experiments on net uptake of nitrate and ammonium by the roots of spruce (*Picea abies*) and beech (*Fagus sylvatica*) trees. *New Phytol.* 138, 275–285.

Gioria, M., and Osborne, B. A. (2014). Resource competition in plant invasions: emerging patterns and research needs. *Front. Plant Sci.* 5:501. doi: 10.3389/fpls.2014.00501

Goldberg, D. E., and Barton, A. M. (1992). Patterns and consequences of interspecific competition in natural communities: a review of field experiments with plants. *Am. Nat.* 139, 771–801. doi: 10.1086/285357

Grotkopp, E., and Rejmánek, M. (2007). High seedling relative growth rate and specific leaf area are traits of invasive species: phylogenetically independent contrasts of woody angiosperms. *Am. J. Bot.* 94, 526–532. doi: 10.3732/ajb.94.4.526

Grubb, P. J., Lee, W. G., Kollmann, J., and Wilson, J. B. (1996). Interaction of irradiance and soil nutrient supply on growth of seedlings of ten European tall-shrub species and *Fagus sylvatica*. *J. Ecol.* 84, 827–840. doi: 10.2307/2960555

Halarewicz, A., Pruchniewicz, D., and Kawałko, D. (2017). Black cherry (*Prunus serotina*) invasion in a Scots pine forest: relationships between soil properties and vegetation. *Pol. J. Ecol.* 65, 295–302. doi: 10.3161/15052249PJE2017.65.2.011

Hodge, A., and Fitter, A. H. (2013). Microbial mediation of plant competition and community structure. *Funct. Ecol.* 27, 865–875. doi: 10.1111/1365-2435.12002

Holmes, T. P., Aukema, J. E., Von Holle, B., Liebhold, A., and Sills, E. (2009). Economic impacts of invasive species in forests - past, present, and future. *Ann. N. Y. Acad. Sci.* 1162, 18–38. doi: 10.1111/j.1749-6632.2009.04446.x

Houston, T., de Rigo, D., and Caudullo, G. (2016a). "*Fagus sylvatica* and other beeches in Europe: distribution, habitat, usage and threats," in *European Atlas of Forest Tree Species*, eds J. San-Miguel-Ayanz, D. de Rigo, G. Caudullo, T. Houston, and A. Mauri (Luxembourg: Publ. Off. EU).

Houston, T., de Rigo, D., and Caudullo, G. (2016b). "*Pinus sylvestris* in Europe: distribution, habitat, usage and threats," in *European Atlas of Forest Tree Species*, eds J. San-Miguel-Ayanz, D. de Rigo, G. Caudullo, T. Houston, and A. Mauri (Luxembourg: Publ. Off. EU).

Kawaletz, H., Mölder, I., Annighöfer, P., Terwei, A., Zerbe, S., and Ammer, C. (2014). Back to the roots: how do seedlings of native tree species react to the competition by exotic species? *Ann. For. Sci.* 71, 337–347. doi: 10.1007/s13595-013-0347-z

Kawaletz, H., Mölder, I., Zerbe, S., Annighöfer, P., Terwei, A., and Ammer, C. (2013). Exotic tree seedlings are much more competitive than natives but show underyielding when growing together. *Plant Ecol.* 6, 305–315. doi: 10.1093/jpe/rts044

Keller, R. P., Geist, J., Jeschke, J. M., and Kühn, I. (2011). Invasive species in Europe: ecology, status, and policy. *Environ. Sci. Eur.* 23:23. doi: 10.1186/2190-4715-23-23

Knops, J. M. H., and Reinhart, K. (2000). Specific leaf area along a nitrogen fertilization gradient. *Am. Midl. Nat.* 144, 265–272.

Körner, C. (2003). Carbon limitation in trees. *J. Ecol.* 91, 4–17. doi: 10.1046/j.1365-2745.2003.00742.x

Kulmatiski, A., Adler, P. B., Stark, J. M., and Tredennick, A. T. (2017). Water and nitrogen uptake are better associated with resource availability than root biomass. *Ecosphere* 8:e01738. doi: 10.1002/ecs2.1738

Kuster, T. M., Wilkinson, A., Hill, P. W., Jones, D. L., and Bardgett, R. D. (2016). Warming alters competition for organic and inorganic nitrogen between co-existing grassland plant species. *Plant Soil* 406, 117–129. doi: 10.1007/s11104-016-2856-7

Lee, C. S., Cho, H. J., and Yi, H. (2004). Stand dynamics of introduced black locust (*Robinia pseudoacacia L.*) plantation under different disturbance regimes in Korea. *For. Ecol. Manage.* 189, 281–293. doi: 10.1016/j.foreco.2003.08.012

Li, X., Rennenberg, H., and Simon, J. (2015). Competition for nitrogen between *Fagus sylvatica* and *Acer pseudoplatanus* seedlings depends on soil nitrogen availability. *Front. Plant Sci.* 6:302. doi: 10.3389/fpls.2015.00302

Littschwager, J., Lauerer, M., Blagodatskaya, E., and Kuzyakov, Y. (2010). Nitrogen uptake and utilisation as a competition factor between invasive *Duchesnea indica* and native *Fragaria vesca*. *Plant Soil* 331, 105–114. doi: 10.1007/s11104-009-0236-2

Liu, M., Wang, Z., Li, S., Lu, X., Wang, X., and Han, X. (2017). Changes in specific leaf area of dominant plants in temperate grasslands along a 2500-km transect in northern China. *Sci. Rep.* 7:10780. doi: 10.1038/s41598-017-11133-z

Liu, X. P., Grams, T., Matyssek, R., and Rennenberg, H. (2005). Effects of elevated pCO2 and/or pO3 on C-, N-, and S-metabolites in the leaves of juvenile beech and spruce differ between trees grown in monoculture and mixed culture. *Plant Physiol. Biochem.* 43, 147–154. doi: 10.1016/j.plaphy.2005.01.010

Liu, Y., and van Kleunen, M. (2017). Responses of common and rare aliens and natives to nutrient availability and fluctuations. *J. Ecol.* 105, 1111–1122. doi: 10.1111/1365-2745.12733

Luo, Y., Guo, W., Yuan, Y., Liu, J., Du, N., and Wang, R. (2014). Increased nitrogen deposition alleviated the competitive effects of the introduced invasive plant *Robinia pseudoacacia* on the native tree *Quercus acutissima*. *Plant Soil* 385, 63–75. doi: 10.1007/s11104-014-2227-1

Masclaux-Daubresse, C., Daniel-Vedele, F., Dechorgnat, J., Chardon, F., Gaufichon, L., and Suzuki, A. (2010). Nitrogen uptake, assimilation and remobilization in plants: challenges for sustainable and productive agriculture. *Ann. Bot.* 105, 1141–1157. doi: 10.1093/aob/mcq028

McKey, D. (1994). "Legumes and nitrogen: the evolutionary ecology of a nitrogen-demanding lifestyle," in *Advances in Legume Systematic 5: The Nitrogen Factor*, eds J. I. Sprent and D. McKey (Kew: Royal Botanic Gardens), 211–228.

Medina-Villar, S., Rodríguez-Echeverría, S., Lorenzo, P., Alonso, A., Pérez-Corona, E., and Castro-Díez, P. (2016). Impacts of the alien trees *Ailanthus altissima* (Mill.) *Swingle and Robinia pseudoacacia L.* on soil nutrients and microbial communities. *Soil Biol. Biochem.* 96:65e73. doi: 10.1016/j.soilbio.2016.01.015

Millard, P. (1988). The accumulation and storage of nitrogen by herbaceous plants. *Plant Cell Environ.* 11, 1–8. doi: 10.1111/j.1365-3040.1988.tb01769.x

Millard, P., and Grelet, G. A. (2010). Nitrogen storage and remobilization by trees: ecophysiological relevance in a changing world. *Tree Physiol.* 30, 1083–1095. doi: 10.1093/treephys/tpq042

Miller, A. E., Bowman, W. D., and Suding, K. N. (2007). Plant uptake of inorganic and organic nitrogen: neighbor identity matters. *Ecology* 88, 1832–1840. doi: 10.1890/06-0946.1

Näsholm, T., Kielland, K., and Ganeteg, U. (2009). Uptake of organic nitrogen by plants. *New Phytol.* 182, 31–48. doi: 10.1111/j.1469-8137.2008.02751.x

Pommerening, A., and Sánchez Meador, A. J. (2018). Tamm review: tree interactions between myth and reality. *For. Ecol. Manage.* 424, 164–176. doi: 10.1016/j.foreco.2018.04.051

Reich, P. B. (2014). The world-wide 'fast–slow' plant economics spectrum: a traits manifesto. *J. Ecol.* 102, 275–301. doi: 10.1111/1365-2745.12211

Reich, P. B., Walters, M. B., and Ellsworth, D. S. (1997). From tropics to tundra: global convergence in plant functioning. *Proc. Natl. Acad. Sci. U.S.A.* 94, 13730–13734. doi: 10.1073/pnas.94.25.13730

Rennenberg, H., Dannenmann, M., Gessler, A., Kreuzwieser, J., Simon, J., and Papen, H. (2009). Nitrogen balance in forest soils: nutritional limitation of plants under climate change stresses. *Plant Biol.* 11, 4–23. doi: 10.1111/j.1438-8677.2009.00241.x

Robakowski, P., and Bielinis, E. (2011). Competition between sessile oak (*Quercus petraea*) and black cherry (*Padus serotina*): dynamics of seedlings growth. *Pol. J. Ecol.* 59, 297–306.

Robakowski, P., Bielinis, E., Stachowiak, J., Mejza, I., and Bułaj, B. (2016). Seasonal changes affect root prunasin concentration in *Prunus serotina* and override species interactions between *P. serotina and Quercus petraea*. *J. Chem. Ecol.* 42, 202–214. doi: 10.1007/s10886-016-0678-y

Salpagarova, F. S., van Logtestijn, R. S. P., Onipchenko, V. G., Akhmetzhanova, A. A., and Agafonov, V. A. (2014). Nitrogen content in fine roots and the structural and functional adaptations of alpine plants. *Biol. Bull. Rev.* 4, 243–251. doi: 10.1007/s10886-016-0678-y

Simon, J., Dannenmann, M., Gasche, R., Holst, J., Mayer, H., Papen, H., et al. (2011). Competition for nitrogen between adult European beech and its offspring is reduced by avoidance strategy. *For. Ecol. Manage.* 262, 105–114. doi: 10.1016/j.foreco.2011.01.035

Simon, J., Dannenmann, M., Pena, R., Gessler, A., and Rennenberg, H. (2017). Nitrogen nutrition of beech forests in a changing climate: importance of plant-soil-microbe water, carbon, and nitrogen interactions. *Plant Soil* 418, 89–114. doi: 10.1007/s11104-017-3293-y

Simon, J., Dong, F., Buegger, F., and Rennenberg, H. (2013). Rhizospheric NO affects N uptake and metabolism in Scots pine (*Pinus sylvestris L.*) seedlings depending on soil N availability and N source. *Plant Cell Environ.* 36, 1019–1026. doi: 10.1111/pce.12034

Simon, J., Li, X., and Rennenberg, H. (2014). Competition for nitrogen between European beech and sycamore maple shifts in favour of beech with decreasing light availability. *Tree Physiol.* 34, 49–60. doi: 10.1093/treephys/tpt112

Simon, J., Waldhecker, P., Brüggemann, N., and Rennenberg, H. (2010). Competition for nitrogen sources between European beech (*Fagus sylvatica*)

and sycamore maple (*Acer pseudoplatanus*) seedlings. *Plant Biol.* 12, 453–458. doi: 10.1111/j.1438-8677.2009.00225.x

Starfinger, U., Kowarik, I., Rode, M., and Schepker, H. (2003). From desirable ornamental plant to pest to accepted addition to the flora? - the perception of an alien tree species through the centuries. *Biol. Invasions* 5, 323–335. doi: 10.1023/B:BINV.0000005573.14800.07

Staska, B., Essl, F., and Samimi, C. (2014). Density and age of invasive *Robinia pseudoacacia* modulate its impact on floodplain forests. *Basic Appl. Ecol.* 15, 551–558. doi: 10.1016/j.baae.2014.07.010

Stoelken, G., Simon, J., Ehlting, B., and Rennenberg, H. (2010). The presence of amino acids affects inorganic N uptake in non-mycorrhizal seedlings of European beech (*Fagus sylvatica*). *Tree Physiol.* 30, 1118–1128. doi: 10.1093/treephys/tpq050

Strayer, D. L., Eviner, V. T., Jeschke, J. M., and Pace, M. L. (2006). Understanding the long-term effects of species invasions. *Trends Ecol. Evol.* 21, 645–651. doi: 10.1016/j.tree.2006.07.007

Trinder, C. J., Brooker, R. W., and Robinson, D. (2013). Plant ecology's guilty little secret: understanding the dynamics of plant competition. *Funct. Ecol.* 27, 918–929. doi: 10.1111/1365-2435.12078

Vilà, M., Espinar, J. L., Hejda, M., Hulme, P. E., Jarosik, V., Maron, J. L., et al. (2011). Ecological impacts of invasive alien plants: a meta-analysis of their effects on species, communities and ecosystems. *Ecol. Lett.* 14, 702–708. doi: 10.1111/j.1461-0248.2011.01628.x

Vilà, M., and Weiner, J. (2004). Are invasive plant species better competitors than native plant species? - evidence from pair-wise experiments. *Oikos* 105, 229–238. doi: 10.1111/j.0030-1299.2004.12682.x

Vítková, M., Müllerová, J., Sádlo, J., Pergl, J., and Pyšek, P. (2017). Black locust (*Robinia pseudoacacia*) beloved and despised: a story of an invasive tree in Central Europe. *For. Ecol. Manage.* 384, 287–302. doi: 10.1016/j.foreco.2016.10.057

Waldner, P., Marchetto, A., Thimonier, A., Schmitt, M., Rogora, M., Granke, O., et al. (2014). Detection of temporal trends in atmospheric deposition of inorganic nitrogen and sulphate to forests in Europe. *Atmos. Environ.* 95, 363–374. doi: 10.1016/j.atmosenv.2014.06.054

Winter, H., Lohaus, G., and Heldt, H. W. (1992). Phloem transport of aminoacids in relation to their cytosolic levels in barley leaves. *Plant Physiol.* 99, 996–1004. doi: 10.1104/pp.99.3.996

Zhu, Q., Iversen, C. M., Riley, W. J., Slette, I. J., and Vander Stel, H. M. (2016). Root traits explain observed tundra vegetation nitrogen uptake patterns: implications for trait-based land models. *J. Geophys. Res.* 121, 3101–3112. doi: 10.1002/2016JG003554

Conflict of Interest Statement: The authors declare that the research was conducted in the absence of any commercial or financial relationships that could be construed as a potential conflict of interest.

frontiers in Plant Science

ORIGINAL RESEARCH
published: 06 June 2019
doi: 10.3389/fpls.2019.00744

Phosphorus Allocation to Leaves of Beech Saplings Reacts to Soil Phosphorus Availability

*Sonia Meller[1,2], Emmanuel Frossard[2] and Jörg Luster[1]**

[1] Forest Soils and Biogeochemistry, Swiss Federal Institute for Forest, Snow and Landscape Research WSL, Birmensdorf, Switzerland, [2] Institute of Agricultural Sciences, ETH Zürich, Zurich, Switzerland

Decreasing phosphorus (P) concentrations in leaves of beech (*Fagus sylvatica* L.) across Europe raise the question about the implications for forest health. Considering the distribution of beech forests on soils encompassing a broad range of nutrient availability, we hypothesized that this tree species exhibits high phenotypic plasticity allowing it to alter mass, and nutrient allocation in response to local nutrient availability. To test this, we grew two groups of 12–15 year old beech saplings originating from sites with high and low soil P availability for 2 years in mineral soil from their own site and in soil from the other site. After two growing seasons, P concentrations in leaves and stem, as well as mass allocation to leaves and fine roots were affected by both soil and plant origin. By contrast, relative P allocation to leaves and fine roots, as well as P concentrations in fine roots, were determined almost entirely by the experimental soil. Independent of the P nutritional status defined as average concentration of P in the whole plant, which still clearly reflected the soil conditions at the site of plant origin, relative P allocation to leaves was a particularly good indicator of P availability in the experimental soil. Furthermore, a high plasticity of this plant trait was indicated by a large difference between plants growing in the two experimental soils. This suggests a strong ability of beech to alter resource allocation in response to specific soil conditions.

Keywords: acclimation, beech, *Fagus sylvatica*, forest health, phenotypic plasticity, phosphorus allocation, phosphorus nutritional status, soil phosphorus availability

OPEN ACCESS

Edited by:
Christian Ammer,
University of Göttingen, Germany

Reviewed by:
Friderike Beyer,
University of Freiburg, Germany
Rodica Pena,
University of Göttingen, Germany
Werner Borken,
University of Bayreuth, Germany

***Correspondence:**
Jörg Luster
joerg.luster@wsl.ch

Specialty section:
This article was submitted to Functional Plant Ecology, a section of the journal Frontiers in Plant Science

Received: *17 February 2019*
Accepted: *20 May 2019*
Published: *06 June 2019*

Citation:
Meller S, Frossard E and Luster J (2019) Phosphorus Allocation to Leaves of Beech Saplings Reacts to Soil Phosphorus Availability. Front. Plant Sci. 10:744. doi: 10.3389/fpls.2019.00744

INTRODUCTION

Forests dominated by beech (*Fagus sylvatica* L.) cover a large part of Europe (ca 14–15 Mha) from southern Norway to southern Italy and from northern Spain to northwest Turkey (Brunet et al., 2010; Durrant et al., 2016). Throughout this area, beech populations occur on a wide variety of soils realizing a broad ecological niche in terms of soil chemical properties including pH (3.2–7.3), base saturation (3–99%), and plant-available phosphorus (P) pools in the mineral topsoil (11–1287 mol P m^{-2} 10 cm^{-1}) (Leuschner et al., 2006; Batjes, 2011; Yang et al., 2013).

Analysis of data from forest monitoring plots (ICP forest level II) across Europe between 1991 and 2010 revealed a significant decline in P concentrations and an increase of N/P ratios in beech leaves on the majority of plots (Jonard et al., 2015; Talkner et al., 2015) confirming findings of earlier regional studies (Flückiger and Braun, 1998; Duquesnay et al., 2000; Jonard et al., 2009; Braun et al., 2010). These changes in leaf nutrient status have been attributed to continuing

high nitrogen (N) deposition and increasing atmospheric carbon dioxide concentrations. Both accelerated tree growth due to high N and carbon (C) input and negative effects of elevated N on fine root biomass, mycorrhization, and litter mineralization appear to have created a higher need for other nutrients which cannot be met by the supply from the soil (Kjøller et al., 2012; Peñuelas et al., 2013; Talkner et al., 2015). On 40% of the level II plots the average leaf P concentrations indicated P deficiency (Jonard et al., 2015) and average N/P ratios on 60% of the plots were higher than "good for harmonious nutrition" (Talkner et al., 2015). The currently widely accepted critical values for nutrient concentrations and ratios in leaves (Mellert and Göttlein, 2012) are based on a large number of studies comparing leaf values with deficiency symptoms, growth or reaction to fertilization. However, results from surveys and experiments on the relation between P concentrations in plant tissues and soil P availability are partially conflicting. While concentrations of P in leaves and fine roots of mature trees across different forest sites were not well related to measures of P availability in the soil (Talkner et al., 2015; Lang et al., 2017), this relation was stronger for saplings from two acid forest sites and considering different plant compartments including leaves, stem, fine and coarse roots (Yang et al., 2016; Zavišić and Polle, 2018; Zavišić et al., 2018). Furthermore, Zavišić et al. (2018) observed a strong increase of P concentrations in all compartments upon fertilization. One reason for the conflicting results could be that often only total P concentrations in soil are available which not sufficiently reflect this elements bioavailability. Another explanation could be the strong seasonal and site dependent variability of P concentrations in plant tissues (Yang et al., 2016; Netzer et al., 2017; Zavišić and Polle, 2018). This points to the importance of seasonal dynamics of nutrient uptake and plant internal nutrient allocation.

However, surprisingly little is known on how beech adapts its internal P allocation to different P availability in soil, and thus to what degree P concentrations in leaves directly reflect soil P availability or the ability of the tree to regulate its P content on the cellular and the whole-plant level (Marschner, 1996). On the cellular level, P homeostasis can be maintained by adjusting the flux of P into and out of the vacuole (Lee et al., 1990; Lee and Ratcliffe, 1992; Mimura et al., 1996). On the whole plant level, P redistribution is regulated via vascular tissues, and it follows seasonal patterns employing storage in and recycling from various organs including senescing leaves, roots, and stem (Raghothama, 1999; Lin et al., 2009, 2014; Brant and Chen, 2015; Netzer et al., 2017; Zavišić and Polle, 2018; Zavišić et al., 2018). The seasonally varying relations between soil P availability and internal P cycling have been shown for P concentrations in various plant compartments comprising leaves, fine roots, coarse roots and stem (Netzer et al., 2017; Zavišić and Polle, 2018), for P concentrations in xylem and phloem (Yang et al., 2016; Netzer et al., 2017), and for P resorption from older and senescent leaves (Hofmann et al., 2016; Netzer et al., 2017). Furthermore, growth rates of adult beech not always reflected soil P availability (Netzer et al., 2017) highlighting the potential role of high-efficiency internal cycling in trees growing on soils with low P availability. Alteration of internal nutrient cycling can be part of the adaptive response (phenotypic plasticity) of plants to external factors. For many plants, phenotypic plasticity was shown to comprise rapid trait alterations during a lifetime of an organism (Sultan, 2004; Hodge, 2009), including morphological, anatomical, physiological, reproductive, and developmental traits. Considering the long time scales of migration and natural selection, phenotypic plasticity is the most important asset of tree populations to cope with the ongoing environmental changes (Matesanz et al., 2010; Nicotra et al., 2010; Vitasse et al., 2010). The phenotypic plasticity of beech in response to drought or increased temperature has been well studied, comprising plant traits such as phenology (e.g., Kramer, 1995; Vitasse et al., 2009), biomass and root morphology (Curt et al., 2005; Weemstra et al., 2016), leaf anatomy (Stojnić et al., 2015a,b), stem anatomy (Stojnić et al., 2013; Diaconu et al., 2016), mass allocation, and growth rate (Rolo et al., 2015).

By contrast, little is known about the adaptive response of beech to changes in P availability. Our objective was therefore to identify the respective most responsive traits of this tree species. Considering the important role the plant nutritional status plays in governing nutrient acquisition (Marschner, 1996), we performed experiments with beech saplings adapted to grow in soil with either high or low soil P availability, and assessed their response to contrasting soil conditions. We hypothesized that the response of a beech sapling with a given P nutritional status, as defined by its site of origin, to higher or lower soil P availability in terms of biomass and P allocation to different plant compartments is mainly driven by the plant striving to increase a low foliar P concentration as fast as possible or to maintain a high foliar P concentration as long as possible.

MATERIALS AND METHODS

Plant and Soil Materials

Plant and soil materials were collected on the core research sites of the priority program 1685 "Ecosystem nutrition" of the German and Swiss National Science Foundations[1] in Unterlüss (LUE, Lower Saxony, Germany) with low P availability in the soil, and Bad Brückenau (BBR, northern Bavaria, Germany) with high P availability in the soil. The sites were chosen because they both sustain mature mono-specific beech stands but differ profoundly in soil P stocks and cycling. For details on the sites refer to Lang et al. (2017).

Saplings of beech (*F. sylvatica*) of similar size (approx. 45 cm in height and approx. 8 mm base diameter) were gently dug out at the sites during their dormancy period in December 2014, and stored at 4°C with their roots embedded in soil from their own site until planting.

Soil materials were collected from the Bh horizon in LUE and the Bv horizon in BBR, air-dried at 15°C, sieved to 4 mm, and homogenized. Plant residues were removed from the soils. Basic physical and chemical properties are listed in **Table 1** and were obtained as follows. Soil texture was determined using the pipette method (Gee and Bauder, 1986). Soil pH was measured in a 1:2 slurry in 0.01 M $CaCl_2$ or water after 30 Min. equilibration.

[1] http://www.ecosystem-nutrition.uni-freiburg.de/

TABLE 1 | Physical and chemical properties of homogenized material from the Bv soil horizon at Bad Brückenau (BBR) and the Bh soil horizon at Unterlüss (LUE) used in the experiment; this includes grain size fractions, pH in two different extractants, exchangeable metal cations (M_{ex}), organic C (C_{org}), total N (N_{tot}), and the following P fractions obtained by sequential extraction: resin exchangeable inorganic P (P_{resin}), sum of inorganic P (extractable P_{inorg}) and organic P (extractable P_{org}) in various extracts (for details see text); all concentrations are given per mass dry soil; shown are means ± standard deviations of two technical replicates, except for sum parameters and element ratios.

		LUE	BBR
Sand	(g kg^{-1})	811 ± 3	287 ± 14
Clay	(g kg^{-1})	43 ± 4	253 ± 14
pH in H_2O/ 0.01 M $CaCl_2$		3.99 ± 0.01/ 3.31 ± 0.01	4.76 ± 0.04/ 3.99 ± 0.01
Al_{ex}	(mmol$_c$ kg^{-1})	19.7 ± 0.2	40.6 ± 0.2
Ca_{ex}	(mmol$_c$ kg^{-1})	0.56 ± 0.01	2.13 ± 0.04
Fe_{ex}	(mmol$_c$ kg^{-1})	1.35 ± 0.02	0.04 ± 0.006
K_{ex}	(mmol$_c$ kg^{-1})	0.49 ± 0.02	0.56 ± 0.04
Mg_{ex}	(mmol$_c$ kg^{-1})	0.33 ± 0.003	0.62 ± 0.01
Mn_{ex}	(mmol$_c$ kg^{-1})	0.10 ± 0.003	0.79 ± 0.01
Zn_{ex}	(mmol$_c$ kg^{-1})	0.02 ± 0.001	0.03 ± 0.001
C_{org}	(g kg^{-1})	18.5 ± 0.04	41.9 ± 1.0
N_{tot}	(g kg^{-1})	0.75 ± 0.01	3.22 ± 0.01
P_{resin}	(mg kg^{-1})	0.44 ± 0.04	5.5 ± 1.3
Extractable P_{inorg}	(mg kg^{-1})	29	911
Extractable P_{org}	(mg kg^{-1})	89	1256
C_{org}/N_{tot}	(g g^{-1})	24.7	13.0
C_{org}/P_{org}	(g g^{-1})	208	33
N_{tot}/P_{org}	(g g^{-1})	8.4	2.6

Organic C (C_{org}) and total N (N_{tot}) contents of ground soil samples were measured using an elemental analyzer (NC 2500, CE Instruments Ltd, Hindley Green, Wigan, United Kingdom). Exchangeable cations (Al_{ex}, Ca_{ex}, Fe_{ex}, K_{ex}, Mg_{ex}, Mn_{ex}, and Zn_{ex}) were extracted with 1M NH_4Cl for 1 h at 20°C and a soil:extractant ratio of 1:10. The filtered extracts were analyzed for total elemental concentrations by inductively coupled plasma optical emission spectrometry (ICP-OES; Optima 7300 DV; Perkin Elmer, Waltham, MA, United States). Sequential P extraction was performed according to Hedley et al. (1982) as modified by Tiessen and Moir (2006). In **Table 1**, resin exchangeable inorganic P (P_{resin}), the sum of inorganic P (P_{inorg}) in various extracts (0.5 M $NaHCO_3$, 0.1 M NaOH before and after sonication, 1 M HCl, concentrated HCl) and the sum of organic P (P_{org}) in the $NaHCO_3$ and NaOH extracts are shown. The soil from BBR exhibited much higher concentrations of both inorganic and organic extractable P than the LUE soil, but most importantly also resin exchangeable inorganic P, a measure of inorganic P in soil solution, and loosely sorbed to soil particles and thus of available P (Tamburini et al., 2012), was much higher in the BBR soil.

Experimental Setup

In April 2015, rhizoboxes were set up with beech saplings planted either in the soil from their site of origin or in the contrasting soil from the other site. In a completely randomized design, each treatment was replicated seven times. The rhizoboxes had inner dimensions of 60 cm × 25 cm × 1.5 cm. They consisted of PVC walls and a removable transparent lid made of polymethyl methacrylate. The soil was filled in at a bulk density of 1.2 kg/dm^3. After 1 week of soil conditioning under irrigation as described below, the saplings were planted. The roots of the saplings were washed with tap water to remove sticking soil, and approximately 2 cm of tap root were cut to stimulate new root formation. For each tree, the front plate of one rhizobox was opened, the roots pressed into the soil, and the front plate was closed again. At this time point, saplings possessed up to 10 cm long tap roots of 0.5–1.5 cm diameter but almost no fine roots, which presumably had died off during the storage. Rhizoboxes with trees were placed in a greenhouse with temperature control (22 ± 2°C during the day/18 ± 2°C at night), natural light and shading from the direct sun. Since shading with movable blinds was the only means for active cooling, at some days in summer temperatures higher than 22°C occurred for short periods. The soil was kept dark, and to stimulate the formation of a quasi-planar root system along the transparent lid, the rhizoboxes were inclined at an angle of about 30°. Soil water potential in the rhizoboxes was kept at approximately -8 kPa by using irrigation tubes ("Rhizon irrigators," Rhizosphere research products, Wageningen, Netherlands) providing P-free artificial rain solution based on the composition of natural precipitation [2.1 μM K_2SO_4, 3.7 μM Na_2SO_4, 3.0 μM $CaCl_2$, 4.4 μM $CaSO_4$, 1.9 μM $MgCl_2$, 26.4 μM NH_4NO_3, 2.0 μM $Ca(NO_3)_2$; Holzmann et al., 2016]. During summer, additional periodic irrigation from the top was needed to compensate for high evapotranspiration. At the end of the first growing season (end of September 2015), the rhizoboxes were placed outside of the greenhouse, but protected by a roof, to induce dormancy. In November 2015, they were moved to a dark cold room at 4°C and periodically irrigated with artificial rain from the top. End of March 2016, after the last frost, the rhizoboxes were moved first to the protected area outside of the greenhouse, and in May, after appearance of the first leaves, back into the greenhouse with temperature control set to the same conditions as in the year before.

Plant Harvest and Analyses

During the first growing season in August 2015, when plants reached the phenological stage of fully developed leaves in both soils (Yang et al., 2016), five fully expanded leaves per plant were collected. Senescent leaves were collected at the end of the season after natural leaf abscission (December 2015) into nets spread around the plants. In August 2016 of the second growing season, the whole plants were harvested. At that time point, six saplings each from BBR growing in soil from BBR and LUE, 7 saplings from LUE growing in soil from BBR, and 3 saplings from LUE growing in soil from LUE had survived. The plants were divided into leaves, stem, coarse roots, and fine roots (diameter ≤ 2 mm).

The following analyses were performed on fresh tissue samples. The age of the saplings at final harvesting was determined by staining thin sections of the stem and subsequent tree-ring analysis (Gärtner and Schweingruber, 2013). According to this, the saplings from BBR were 11.7 ± 2.7 years old, and those from LUE 14.7 ± 1.6 years old. Subsamples of fully developed

leaves were used to measure the trichloroacetic acid (TCA)-soluble P fraction (also called metabolic P; Wilcox et al., 2000). Approximately 200 mg of fresh leaves were frozen in liquid N_2 in a 15 ml reagent tube and crushed to a fine powder using metal beads and vortexing. Powdered leaves were extracted for 1 h at 4°C with 4 ml of 0.3 M TCA on a shaker. Extracts were filtered at 0.45 μm using glass fiber GF/F filters (Whatman International Ltd.). Inorganic P concentrations in TCA extracts were measured colorimetrically using malachite green (Van Veldhoven and Mannaerts, 1987). Bark and wood exudates were collected with the EDTA (Ethylene diamine tetra acetate) technique (Rennenberg et al., 1996; Gessler et al., 1998; Yang et al., 2016). Briefly, approximately 2 cm of the basal stem was collected fresh and separated into bark and wood. These parts were washed with deionized water and incubated in 2 ml of a solution 10 mM in Na_2EDTA (pH 7) and 15 μM in chloramphenicol for 5 h at room temperature. Then, inorganic P in the incubation solution was measured colorimetrically as described above.

Plant parts not used for the analyses described above, were oven dried at 60°C for 48 h (leaves and fine roots) or 72 h (stems and coarse roots), weighed, and ground to fine powder using a ball mill (Retsch MM400 Mixer Mill, Retsch GmbH, Retsch-Allee 1–5, 42781 Haan, Germany) with receptacle and balls made of agate. Total carbon and nitrogen contents of the ground material were measured by combustion using an elemental analyzer (NC 2500, CE Instruments Ltd, Hindley Green, Wigan, United Kingdom). The contents of total P were determined by ICP-OES (Optima 7300 DV; Perkin Elmer, Waltham, MA, United States) of digests obtained with a solution 8.3 M in HNO_3 and 0.6M in HF using a microwave digestion unit (MW ultraCLAV, MLS, Milestone Inc., Shelton, CT, United States).

Mass and P Allocation Parameters

Biomass allocation to a specific plant compartment was calculated as mass fraction (g) of the compartment in percent of the total dry mass of the whole plant (g) (Poorter and Sack, 2012). Phosphorus allocation to a specific plant compartment was calculated as the mass fraction of P (g) in the plant compartment in percent of total plant P (g).

Resorption efficiency (RE) of nutrient elements X (X = P, N) from senescent leaves collected in December 15 was estimated by Eq. 1.

$$\mathrm{RE(X)} = \left(1 - \left(\frac{(1 - 0.21) \times Xs}{Xf}\right)\right) \times 100 \qquad (1)$$

Here Xs and Xf stand for nutrient concentrations in senescent and full season leaves, respectively. As no specific data on mass loss during senescence for beech was available, we used the average value of mass loss (21%) based on a multiple species analysis by Van Heerwaarden et al. (2003). A similar average mass loss of 21.6% was reported for "deciduous angiosperms" by Vergutz et al. (2012).

Considering the crucial role that xylem plays for P recycling in beech (Netzer et al., 2017), the P sink strengths of leaves (S_{Leaves}), and fine roots ($S_{fine\ roots}$) were calculated as total P concentration in leaves and fine roots, respectively, divided by concentrations of inorganic P in wood exudates.

Plasticity Indices

We adapted the concept of plasticity indices (Valladares et al., 2006) to quantify the change of a given plant trait during the response of a beech sapling with a given P nutritional status to changes in soil P availability. For more on rationalizing the following equations see the respective subsection of "Discussion."

In a first step, we calculated the average potential span for a given trait (ΔTr) as the arithmetic mean of pairwise differences between trait values of the m and n replicates, respectively, within the two treatments with beech saplings from BBR ($TR_{BBRinBBR}$) and LUE ($TR_{LUEinLUE}$) growing in soil from their own site using Eq. 2.

$$\Delta Tr = \frac{|\sum_{i=1..n,\, j=1..m}(Tr_{BBR\ in\ BBR}(i) - Tr_{LUE\ in\ LUE}(j))|}{m * n} \qquad (2)$$

Only traits with significant differences between the mean trait values for the two treatments were taken into account.

In a second step, we calculated average plasticity indices for the response of saplings from LUE to soil with high P availability ($PL_{LUEplant}$) and for the response of saplings from BBR to soil with low P availability ($PL_{BBRplant}$). The plasiticity indices were calculated as the arithmetic mean of pairwise differences between trait values of the m and n replicates, respectively, within two treatments with beech saplings from a given site growing in soil from their own site and in soil from the other site, divided by the trait span (Eqs. 3 and 4).

$$PL_{LUE\ plant} = \left(\frac{|\sum_{i=1..n,\, j=1..m}(Tr_{LUE\ in\ BBR}(i) - Tr_{LUE\ in\ LUE}(j))|}{m * n}\right) / \Delta Tr \qquad (3)$$

$$PL_{BBR\ plant} = \left(\frac{|\sum_{i=1..n,\, j=1..m}(Tr_{BBR\ in\ BBR}(i) - Tr_{BBR\ in\ LUE}(j))|}{m * n}\right) / \Delta Tr \qquad (4)$$

Statistical Analysis

Using analysis of variance (ANOVA), we assessed to what extent current soil (the soil in which the beech saplings were growing during the experiment) on one hand, and plant origin (forest site where the beech saplings were collected) on the other hand, influenced the measured plant traits in the first and second growing season. All ANOVA analyses were performed in R, version 3.1.2 (R Core Team, 2014; RRID:SCR_001905) with marginal type II test (Anova, package: "car") in order to account for unequal group sizes. Prior to ANOVA, data was subjected to Levene's test (leveneTest, package: "stats") for homogeneity of variance inside the groups and to the Shapiro-Wilk normality test (shapiro.test, package: "stats") for normality of residuals. Statistical significances indicated with

letters in figures and tables are the result of a one-factorial ANOVA (with treatment as explanatory variable) with a Tukey *post hoc* test (HSD.test, package: "agricolae"). Average plasticity indices for plants from BBR and LUE were compared using multiple t-tests. Each pair was analyzed individually, without assuming a consistent standard deviation, using GraphPad Prism 7.02 Software. The standard error of the mean for the plasticity indices was computed for the true sample size using Gaussian error propagation and assumption of no error in ΔTr.

RESULTS

Foliar Element Concentrations and Nutrient Resorption in the First Growing Season

During the first growing season, both total and metabolic P concentrations in leaves were slightly higher for beech saplings originating from BBR, the site with high soil P availability, than for those from LUE, the site with low soil P availability (**Table 2**). According to ANOVA, both concentrations were significantly affected only by the factor "plant origin" (**Table 3**). The first measured reaction of the saplings to the soil they were growing in during the experiment was a higher P resorption from senescent leaves for all plants growing in LUE soil than for those growing in BBR soil, irrespective of plant origin (**Figure 1**). ANOVA revealed "current soil" as sole significant factor (**Table 3**). On the other hand, N resorption from senescent leaves did not differ among the treatments and was not affected neither by plant origin nor by current soil conditions (**Figure 1** and **Table 3**).

Phosphorus Concentrations in Different Plant Compartments in the Second Growing Season

In the second growing season, total P concentrations in stem and coarse roots, and average concentrations in the whole plant still reflected the soil P availability at the site of plant origin with higher values for the saplings from BBR than for those from LUE (**Table 4**). Plant origin dominated as factor in the ANOVA (**Table 5**). By contrast, the P concentrations in fine roots were significantly affected mainly by the factor current soil (**Table 5**) and were higher for saplings growing in the BBR soil (**Table 4**). Total and metabolic P concentrations in leaves as well as inorganic P concentrations in bark and wood exudates were similarly affected by both plant origin and current soil (**Table 5**), which led to higher values for the saplings from BBR growing in mineral soil from their own site than for all other treatments (**Table 4**).

The sink strengths of leaves and roots were still clearly dominated by the factor plant origin (**Table 5**) and were higher for the saplings from LUE (**Figure 2**).

Biomass and P Allocation to Leaves and Roots in the Second Growing Season

Total plant biomass and biomass of leaves and roots were mainly and significantly affected by the factor current soil (**Table 5**), with the smallest values for saplings from LUE growing in soil from their own site (**Table 4**). By contrast, stem biomass did not differ among the treatments.

Irrespective of the treatment, the largest percentage of biomass and P was allocated to coarse roots (**Figure 3D**). Of all measured plant traits, relative allocation of P to leaves most clearly reflected the factor current soil (**Table 5**) with significantly higher values for beech saplings growing in the BBR soil, irrespective of their site of origin (**Figure 3A**). Also, P allocation to fine roots exhibited a significant influence of current soil (**Table 5**), with

TABLE 3 | Analysis of variance for different traits of beech (*Fagus sylvatica* L.) saplings as determined in the first growing season of a rhizobox experiment; traits include concentrations of P (total P, P_{tot}; metabolic P, $P_{metabolic}$) and total N (N_{tot}) in full season and senescent leaves as well resorption efficiency for P and N; saplings originated from the sites Bad Brückenau (BBR) with high soil P availability and Unterlüss (LUE) with low soil P availability (factor plant origin), and were grown in material from the Bv horizon at BBR or from the Bh horizon at LUE (factor current soil); shown are *F* values for the factors and their interactions; statistical significance is indicated as $^{***}P < 0.001$, $^{**}P < 0.01$, $^{*}P < 0.05$, ns $P > 0.05$.

		Source of variation		
		Current soil	**Plant origin**	**Current soil × plant origin**
Full season leaves	P_{tot}	1.97 ns	9.93**	0.15 ns
	$P_{metabolic}$	1.71 ns	33.0***	0.30 ns
	N_{tot}	1.15 ns	18.6**	0.05 ns
Senescent leaves	P_{tot}	24.0***	10.8**	0.67 ns
	N_{tot}	0.01 ns	4.17 ns	0.50 ns
Resorption efficiency	P_{tot}	26.4***	0.03 ns	0.29 ns
	N_{tot}	0.27 ns	0.82 ns	0.86 ns

TABLE 2 | Concentrations of P (total P, P_{tot}; metabolic P, $P_{metabolic}$) and total N (N_{tot}) in full season and senescent leaves of beech (*Fagus sylvatica* L.) saplings, measured in the first growing season of the experiment; saplings originated from the sites Bad Brückenau (BBR) with high soil P availability and Unterlüss (LUE) with low soil P availability, and were grown in material from the Bv horizon at BBR or from the Bh horizon at LUE; data represent mean concentrations per unit mass dry weight ± SE; different letters indicate significant differences between means according to the Tukey *post hoc* test.

			BBR in BBR	**BBR in LUE**	**LUE in BBR**	**LUE in LUE**
Full season	P_{tot}	(mg g^{-1})	1.23 ± 0.09 ab	1.42 ± 0.14 a	0.94 ± 0.06 b	1.04 ± 0.13 ab
	$P_{metabolic}$	(mg g^{-1})	0.35 ± 0.07 ab	0.38 ± 0.05 a	0.12 ± 0.01 c	0.17 ± 0.05 bc
	N_{tot}	(mg g^{-1})	21.5 ± 0.9 a	21.0 ± 0.9 a	23.3 ± 0.4 a	24.2 ± 1.5 a
Senescent	P_{tot}	(mg g^{-1})	1.35 ± 0.23 a	0.68 ± 0.05 b	0.83 ± 0.05 b	0.54 ± 0.13 b
	N_{tot}	(mg g^{-1})	14.2 ± 0.7 a	13.5 ± 0.7 a	15.3 ± 0.4 a	16.0 ± 1.7 a

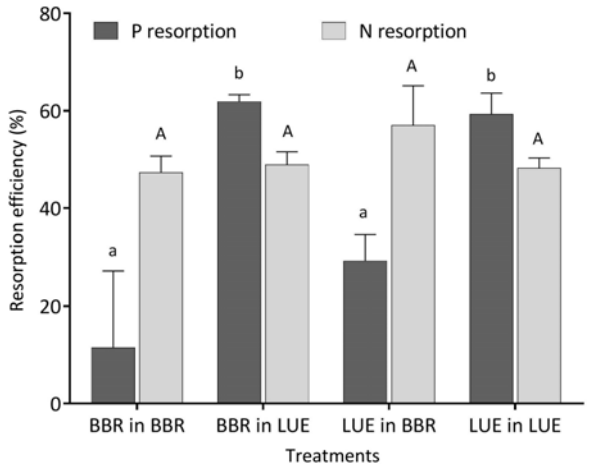

FIGURE 1 | Resorption efficiency for P (black bars) and N (gray bars) of beech (*Fagus sylvatica* L.) saplings in the first growing season of the experiment; saplings originated from the sites Bad Brückenau (BBR) with high soil P availability and Unterlüss (LUE) with low soil P availability, and were grown in material from the Bv horizon at BBR or from the Bh horizon at LUE; data represent mean values ± SE for the different treatments; different letters indicate significant differences between means according to the Tukey *post hoc* test (lowercase letters, P resorption; uppercase letters, N resorption).

values tending to be higher for saplings growing in BBR soil (**Figure 3C**). Noteworthy was the clearly highest value of all treatments for saplings from LUE growing in soil from BBR. On the other hand, allocation of biomass to the stem was still mainly determined by plant origin (**Table 5**) with a tendency to higher values for saplings from LUE (**Figure 3B**). A significant but similarly strong influence of both current soil and plant origin was detected for the allocation of biomass to leaves and fine roots (**Table 5**), with the highest and lowest values for the saplings from BBR and LUE, respectively, growing in their own soil (**Figures 3A,C**).

Plasticity Indices

Figure 4 shows the plasticity indices for beech saplings from LUE and BBR considering all plant traits for which the precondition of a significant difference between the two treatments with the saplings growing in soil from their own site was fulfilled. Total and metabolic P concentrations in full season leaves, total P concentrations in senescent leaves, and P resorption were more plastic for beech saplings from BBR responding to soil with low P availability. On the other hand, P and mass allocation to stem were more reactive for beech saplings from LUE acclimating to soil with high P availability. For all other traits, plasticity was similar for beech saplings from both origins, and thus independent on the direction of acclimation. However, values differed strongly with particularly high indices for P allocation to leaves and P concentration in fine roots and particularly low indices for P concentrations in stem and coarse roots.

DISCUSSION

Our experimental model systems employed beech saplings from forest sites strongly differing in soil P availability in terms of both measures of available P such as P_{resin} and total P stocks (Lang et al., 2017), BBR with high, and LUE with low P availability. At the end of the experiment, the saplings from the two sites still exhibited a significantly different P nutritional status in terms of average P concentration in the whole plant. Using material from mineral soil horizons from the two sites as model soils, while providing homogeneous material for the experimental replicates, possibly changed soil P availability compared to the natural situation, in particular in the case of the LUE site, where 50% of the P stock is stored in the organic surface layer (Lang et al., 2017). Nevertheless, in the second growing season total

TABLE 4 | Concentrations of P (total P, P_{tot}; metabolic P, $P_{metabolic}$; inorganic P in bark exudates, $P_{Bark\_Exudates}$; inorganic P in wood exudates, $P_{wood\_exudates}$) in and biomass of different compartments of beech (*Fagus sylvatica* L.) saplings, measured in the second growing season of a rhizobox experiment; saplings originated from the sites Bad Brückenau (BBR) with high soil P availability and Unterlüss (LUE) with low soil P availability, and were grown in material from the Bv horizon at BBR or from the Bh horizon at LUE; data represent mean concentrations per unit mass dry weight (concentrations) or g dry weight (biomass) ± SE; different letters indicate significant differences between means according to the Tukey *post hoc* test.

			BBR in BBR	BBR in LUE	LUE in BBR	LUE in LUE
Leaves (full season)	P_{tot}	(mg g^{-1})	1.53 ± 0.12 a	0.93 ± 0.09 b	0.92 ± 0.07 b	0.72 ± 0.27 b
	$P_{metabolic}$	(mg g^{-1})	0.67 ± 0.07 a	0.18 ± 0.02 b	0.19 ± 0.04 b	0.20 ± 0.11 b
	Biomass	(g)	1.62 ± 0.13 a	1.03 ± 0.16 b	1.18 ± 0.09 ab	0.37 ± 0.16 c
Stem	P_{tot}	(mg g^{-1})	0.81 ± 0.03 a	0.66 ± 0.04 b	0.36 ± 0.03 c	0.28 ± 0.07 c
	$P_{Bark\_exudates}$	(mg g^{-1})	0.134 ± 0.007 a	0.092 ± 0.006 b	0.071 ± 0.006 bc	0.052 ± 0.006 c
	$P_{Wood\_exudates}$	(mg g^{-1})	0.016 ± 0.001 a	0.009 ± 0.001 b	0.007 ± 0.0004 b	0.004 ± 0.001 c
	Biomass	(g)	4.8 ± 0.4 a	4.0 ± 0.6 a	5.8 ± 1.0 a	4.5 ± 0.4 a
Coarse roots	P_{tot}	(mg g^{-1})	0.76 ± 0.07 a	0.66 ± 0.11 a	0.31 ± 0.02 b	0.22 ± 0.05 b
	Biomass	(g)	8.8 ± 0.5 a	8.1 ± 0.4 a	8.2 ± 0.3 a	6.3 ± 0.1 b
Fine roots	P_{tot}	(mg g^{-1})	0.95 ± 0.04 a	0.66 ± 0.02 b	0.88 ± 0.07 a	0.48 ± 0.04 b
	Biomass	(g)	2.57 ± 0.35 a	1.49 ± 0.40 ab	1.86 ± 0.23 ab	0.62 ± 0.18 b
Whole plant	P_{tot}	(mg g^{-1})	0.88 ± 0.05 a	0.69 ± 0.07 b	0.43 ± 0.03 c	0.27 ± 0.05 c
	Biomass	(g)	17.7 ± 1.0 a	14.6 ± 1.5 ab	17.2 ± 1.3 a	11.7 ± 0.5 b

TABLE 5 | Analysis of variance for different traits of beech (*Fagus sylvatica* L.) saplings as determined in the second growing season of a rhizobox experiment; traits include, for different plant compartments, concentrations of P (total P, P_{tot}; metabolic P, $P_{metabolic}$; inorganic P in bark exudates, $P_{Bark\_Exudates}$; inorganic P in wood exudates, $P_{wood\_exudates}$), biomass, sink strength, and relative allocation of total P and biomass; saplings originated from the sites Bad Brückenau (BBR) with high soil P availability and Unterlüss (LUE) with low soil P availability (factor plant origin), and were grown in material from the Bv horizon at BBR or from the Bh horizon at LUE (factor current soil); shown are F values for the factors and their interactions; statistical significance is indicated as $^{***}P < 0.001$, $^{**}P < 0.01$, $^{*}P < 0.05$, ns $P > 0.05$.

		Source of variation for P concentrations, biomass, or sink strength			Source of variation for P or mass allocation		
		Current soil	Plant origin	Current soil × plant origin	Current soil	Plant origin	Current soil × plant origin
Leaves	P_{tot}	13.8**	12.6**	3.08 ns	41.8***	2.73 ns	0.24 ns
(Full season)	$P_{metabolic}$	17.6**	20.0***	8.92**			
	Biomass	29.0***	17.8**	0.80 ns	33.6***	35.3***	2.39 ns
	Sink strength	1.24 ns	10.1**	2.07 ns			
Stem	P_{tot}	10.6**	126***	1.04 ns	3.68 ns	5.78*	2.83 ns
	$P_{Bark\_exudates}$	23.8***	67.6***	2.68 ns			
	$P_{Wood\_exudates}$	43.8***	77.7***	4.38 ns			
	Biomass	3.05 ns	1.94 ns	0.02 ns	0.36 ns	19.2***	1.06 ns
Coarse roots	P_{tot}	4.01 ns	54.6***	0.49 ns	7.00*	6.63*	0.00 ns
	Biomass	10.9**	8.04*	2.79 ns	6.77*	0.57 ns	0.12 ns
Fine roots	P_{tot}	45.8***	5.38*	1.16 ns	10.1**	2.34 ns	1.95 ns
	Biomass	13.5**	6.25*	0.07 ns	12.4**	7.78*	0.12 ns
	Sink strength	2.69 ns	34.4***	0.09 ns			
Whole plant	P_{tot}	11.9**	72.4***	0.09 ns			
	Biomass	11.0**	1.36 ns	0.91 ns			

P concentrations in all plant compartments where similar to beech saplings collected at the same sites in the same year as our saplings, but were excavated together with an undisturbed soil core, and further grown this way for one season in the greenhouse (Zavišić et al., 2018).

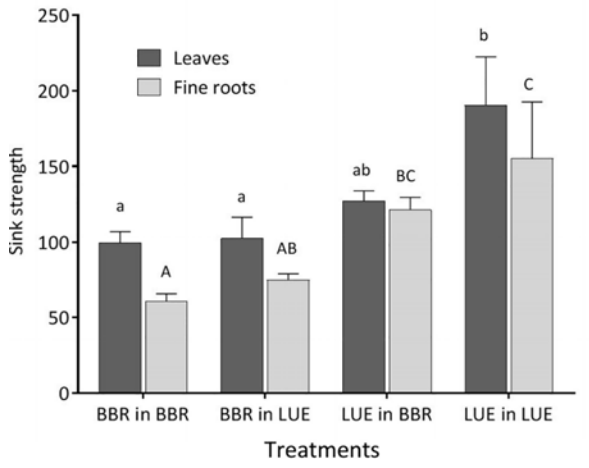

FIGURE 2 | Sink strength of leaves (black bars) and fine roots (gray bars) of beech (*Fagus sylvatica* L.) saplings in the second growing season of the experiment; saplings originated from the sites Bad Brückenau (BBR) with high soil P availability and Unterlüss (LUE) with low soil P availability, and were grown in material from the Bv horizon at BBR or from the Bh horizon at LUE; data represent mean values ± SE for the different treatments; different letters indicate significant differences between means according to the Tukey *post hoc* test (lowercase letters, leaves; uppercase letters, fine roots).

The results of our experiment thus allow to discuss the influence of P nutritional status on the plant internal allocation of P and biomass for beech saplings growing in soil with different P availability. We consider the treatments with saplings growing in the soil from their own site to represent the situation of plants adapted to a given soil situation. We furthermore assume that the results from the treatments with saplings growing in the soil from the other site provide clues on the plastic response of beech that allows it to acclimate to changes in soil nutrient conditions.

Foliar P Concentrations in Beech Depend on Both Soil P Availability and P Nutritional Status of the Plant

As pointed out in the introduction, P concentrations in tissues of trees can strongly vary with the season (Eschrich et al., 1988; Netzer et al., 2017; Zavišić and Polle, 2018) which indicates site dependent dynamics of nutrient uptake and plant internal nutrient allocation. Some studies even suggest that P utilization in beech can be decoupled from P uptake, i.e., the growth of young leaves may strongly depend on the transport of nutrients stored in the previous season in organs such as stem and coarse roots, but also from older leaves during a growing season (Schachtman et al., 1998; Güsewell, 2004; Zavišić et al., 2018). This could well explain our observations, that during the first growing season, total and metabolic P in leaves reflected the P availability of the soil at the site of plant origin rather than the soil in which the beech saplings were growing during the experiment. The results of the second growing season point to combined effects of current soil and plant origin. On one hand, the low P concentrations in leaves and roots of the beech saplings growing in the LUE soil, irrespective of their site of origin and thus their

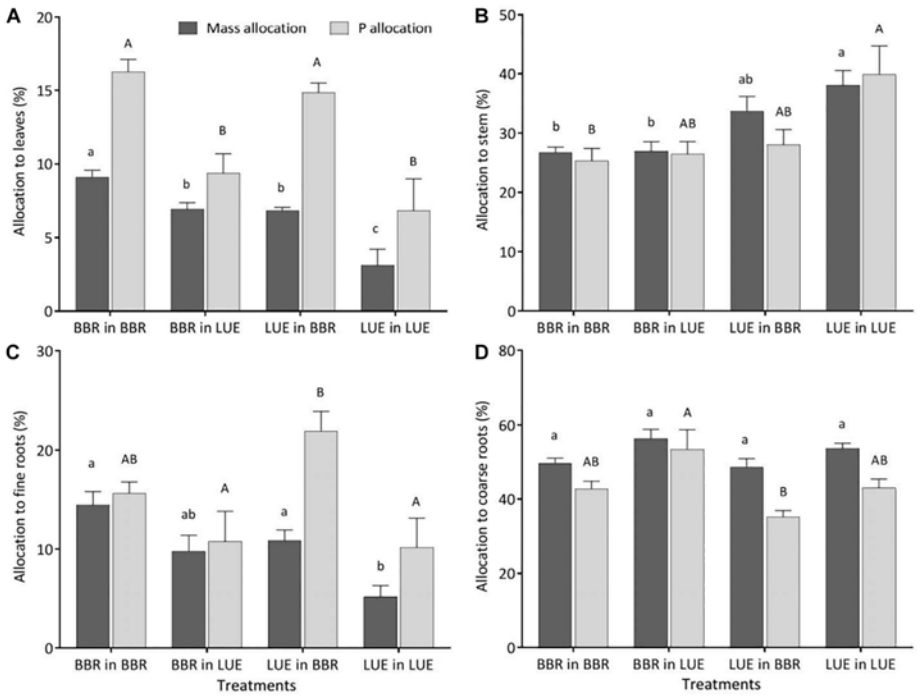

FIGURE 3 | Relative allocation of biomass (black bars) and P (gray bars) to different compartments of beech (*Fagus sylvatica* L.) saplings (**A**: leaves; **B**: stem; **C**: fine roots; **D**: coarse roots) in the second growing season of the experiment; saplings originated from the sites Bad Brückenau (BBR) with high soil P availability and Unterlüss (LUE) with low soil P availability, and were grown in material from the Bv horizon at BBR or from the Bh horizon at LUE; data represent mean values ± SE for the different treatments; different letters indicate significant differences between means according to the Tukey *post hoc* test (lowercase letters, mass allocation; uppercase letters, P allocation).

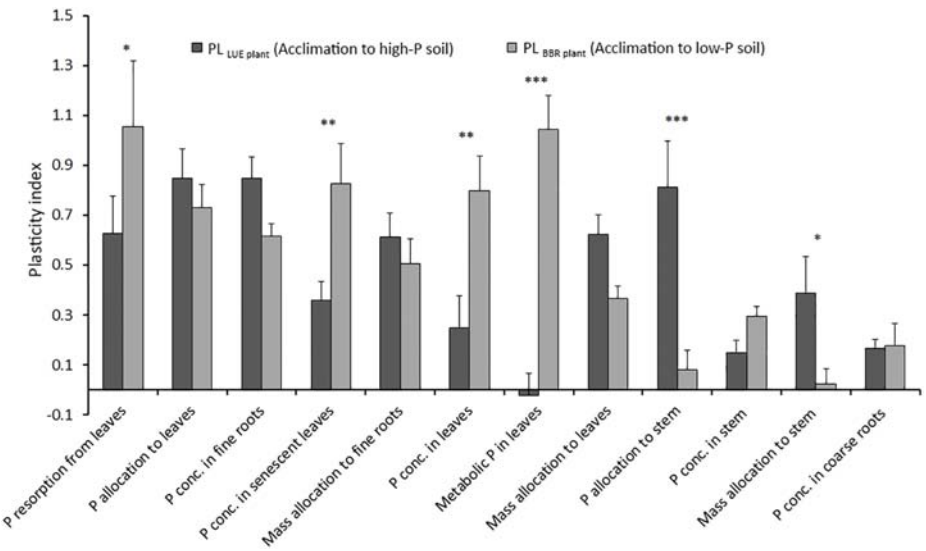

FIGURE 4 | Average plasticity indices for the response of beech (*Fagus sylvatica* L.) saplings from the site Unterlüss (LUE) with low P nutritional status to mineral soil from Bad Brückenau (BBR) with high P availability (black bars) and for saplings from the site BBR with high P nutritional status to mineral soil from LUE with low P availability (gray bars); data represent mean values ± SE of all data pairs; statistical significance is indicated as $^{***}P < 0.001$, $^{**}P < 0.01$, $^{*}P < 0.05$.

P nutritional status, were not surprising. On the other hand, the leaves of LUE saplings growing in BBR soil exhibited equally low P concentrations, despite high P uptake as indicated by relatively high P concentrations in fine roots. Taken together, and considering in addition the equally high mass allocation to leaves for LUE trees growing in BBR soil and for BBR trees

growing in LUE soil, these results point to the ability of beech to deal with different soil P availability optimally at a given P nutritional status of the plant by internal allocation of P and mass. It suggests a priority to alleviate the primary light limitation by producing as much photosynthetic organs as possible, while vacuolar P concentrations are kept low when soil P availability and/or the P nutritional status of the whole plant is low. The latter has been shown to be a successful mechanism in other plants (Lee et al., 1990; Lee and Ratcliffe, 1992; Mimura, 1995; Mimura et al., 1996). Comparing the leaf P concentrations in the second growing season with the threshold values for young beech trees published by Göttlein (2015) suggests the following. While a P concentration within the normal range (1.1–2.1 mg/g DW) indicates both a high P nutritional status of the plant and high soil P availability, a P concentration below the lower threshold of 1.1 mg/g DW may indicate that either the P nutritional status of the plant or the soil P availability or both are low. The same interpretations seem to apply to N/P ratios which, according to Mellert and Göttlein (2012) were in the normal range for BBR plants growing in BBR soil and above in all other cases.

P Resorption From Senescent Leaves Is the First Reaction to Current Soil Conditions

Phosphorus resorption from senescent leaves is a nutrient conservation mechanism, common for several plant species including beech, which reduces losses, and decreases the nutrient uptake demand for the next year (Aerts, 1996; Brant and Chen, 2015). As a consequence, there is less input of P with litter fall diminishing a recycling pool in the ecosystem (Lang et al., 2017). The higher P resorption efficiency of plants grown in the LUE soil than for those grown in the BBR soil, irrespective of their P nutritional status, are in general agreement with findings from recent chronosequence studies by Richardson et al. (2004) and Hayes et al. (2014). The sensitive reaction of this parameter to the current soil in the first growing season, when the concentrations in mature green leaves still reflected the nutrient situation at the site of plant origin, confirms the findings of Hofmann et al. (2016) who showed that fertilization of beech saplings growing in soil low in P led to a decrease in P resorption efficiency. By contrast, the similar values of N resorption efficiency, measured in our experiment for all treatments, indicate a similar degree of N availability. The observed level of about 50% falls within the average range compiled by Aerts (1996) for deciduous trees and shrubs.

P Allocation to Leaves Is a Sensitive Indicator of Soil P Availability

In this section we discuss in more detail the patterns of relative P and mass allocation to various plant compartments in the second growing season. While the link between nutrient allocation and a number of site factors such as precipitation, forest type, latitude, and plant age has been well studied (Sardans and Peñuelas, 2013), little is known about how soil P availability affects P allocation (Yang et al., 2016).

Let us first compare the saplings from LUE and BBR when growing in the soil from their site of origin. The lower allocation of mass and P to leaves and fine roots and higher allocation to the stem for the beech saplings from LUE are consistent with a conservative strategy reducing growth under nutrient limitation. Yang et al. (2016) also observed a slower growth of beech saplings from LUE than from BBR when growing in undisturbed soil cores from their own site of origin which represents a more natural situation than our experiment. A smaller root system in soil of low P availability is in line with the resource economics hypothesis (Grime, 1977; Craine, 2009) and the general characteristic that plant ecotypes from nutrient-limited environments grow slower than ecotypes from fertile soils. At the same time a tendency to a higher ratio between allocation of biomass to fine roots and leaves for the LUE saplings (mean $\pm$ SE: 2.0 $\pm$ 0.5) than for BBR saplings (mean $\pm$ SE: 1.6 $\pm$ 0.2) is in accordance with the notion that under nutrient-limited conditions plants should allocate proportionally more resources to roots (George et al., 2011). We do not know to what degree the difference in the size of the root system between these two treatments translates into volume of soil explored. In both treatments about 50% of the root tips were mycorrhized (mean $\pm$ SE: BBR in BBR, 49 $\pm$ 3%; LUE in LUE, 51 $\pm$ 10%), but extension of the hyphal system was not assessed.

When considering the two treatments with beech saplings growing in soil from the other site, the most striking result is that P allocation to leaves was the same as for the saplings adapted to the respective site, while mass allocation was intermediate in both cases. This indicates that P allocation to leaves might be a particularly good indicator of soil P availability, irrespective of P nutritional status of the plant. It further may be a key trait that the plant adjusts by balancing leaf biomass production against the transfer of nutrients from the soil or from/to internal storage organs such as stem or coarse roots.

Our results for the BBR plants growing in LUE soil indicate that the response of beech saplings with a high P nutritional status to low soil P availability is to decrease leaf P concentration, but to still produce as much leaf biomass as possible under the new low P flux into the roots. At this stage of plastic response, the substantial amount of P stored in coarse roots, and stem allows to partly compensate for the low P uptake. This compensation is also indicated by intermediate P concentrations in bark and wood exudates, maintaining the sink strength of leaves and roots at a low value similar to BBR plants growing in their own soil.

From the results for the LUE plants growing in BBR soil it appears that a beech sapling with low P nutritional status in response to high soil P availability increases leaf biomass production as much as possible under the new high P influx, while it keeps P concentrations in leaves low. Phosphorus concentrations in fine roots as high as for the saplings from BBR adapted to this soil, and the highest P allocation to fine roots of all treatments might be explained by inefficient P translocation to the aboveground plant compartments or by P recycling from stem and old leaves to support fine root growth (Marschner et al., 1996; Netzer et al., 2017). The higher sink strength of fine roots for LUE than BBR plants when growing in BBR soil argue rather in favor of inefficient translocation.

The significant difference in P allocation to leaves between beech saplings growing in BBR and LUE soil was not found for saplings growing in undisturbed soil cores from their own site (Zavišić and Polle, 2018; Zavišić et al., 2018). For a sampling time in July/August P allocation in saplings from both sites was similar to the one we measured for saplings growing in BBR soil, but also varied strongly during the growing season. This discrepancy may be explained by the presence of the organic surface layer in the undisturbed soil cores which could have increased the effective availability of soil P in the case of the LUE plants. The importance of the organic surface layer for the nutrition of young beech trees from soil low in P was clearly demonstrated by Hauenstein et al. (2018) who showed that the presence of the organic surface layer improved P nutrition and growth of beech seedlings in the LUE soil but had no effect in the BBR soil. The effect of the organic surface layer at LUE was attributed on one hand to a particularly high microbial activity promoted by a high root density, but also to a high water retention capacity minimizing loss of added or mobilized P to the mineral soil (Hauenstein et al., 2018). In particular, the high water holding capacity of the surface layer at LUE might have led to a similar effective P availability in the LUE soil as in the BBR soil during the well watered experiments with undisturbed soil cores. On the other hand, at on average drier conditions in the field one would expect a smaller effect, being consistent with the lower P nutritional status of beech saplings from LUE than from BBR.

Furthermore, we cannot exclude that stress induced by the transplantation process (accidental cutting of some roots during sampling, dying-off of fine roots during storage between sampling, and planting) may have affected P allocation even in the second growing season. In particular, "recovery" of a mycorrhized root system in the new soil could have led to a temporary elevated biomass and P allocation to the fine roots. A comparison with the more natural situation in the studies of Zavišić and Polle (2018) and Zavišić et al. (2018) revealed that biomass and P allocation were twice as high in our rhizoboxes than in the undisturbed soil columns of the mentioned studies for saplings from BBR but similar for saplings from LUE. Considering (i) the high variability among individual saplings, (ii) the differences in environmental conditions between the rhizobox and column studies, and (iii) that the larger differences occurred for the more fertile soil from BBR, this comparison does not indicate a large effect of transplantation in our rhizoboxes.

Phosphorus Allocation to Leaves and P Concentrations in Fine Roots Represent Best the Plastic Response of Beech to Changes in Soil P Availability

In this section we discuss the differences in various plant traits among the experimental treatments in terms of a plastic response of beech saplings to changes in soil P availability. For this, we assume that the trait values of saplings growing in the soil from their site of origin represent the extremes and thus define the potential trait span. We further assume, that the higher the degree to which the value of this trait changes relative to the trait span for a sapling exposed to soil from the other site, the higher is the plastic response of this trait. We did neither include P allocation to fine roots nor P and mass allocation to coarse roots, because there was no significant trait span according to the definition. We interpret the differences between the trait plasticity for BBR plants exposed to low P soil and for LUE plants exposed to high P soil as differences between the acclimation processes from high to low and from low to high soil P availability.

Considering all our plasticity indices, they indicate a rather high plasticity compared with other studies employing various plasticity quantification methods (Valladares et al., 2002; Stojnić et al., 2013, 2015a). The direction of acclimation affected the plasticity index for some traits but was unimportant for others. While the plasticity of P resorption and P concentration in leaves was higher for the beech saplings with a high P nutritional status acclimating to low P soil, P and mass allocation to the stem were more reactive for saplings with a low P nutritional status acclimating to soil with high P availability. The asymmetry in size of the reaction of the mentioned traits emphasizes the importance of taking into account the initial nutritional status of a plant when assessing plasticity. On the other hand, the strong responses of P allocation to leaves and P concentration in fine roots, which were similar for both directions of acclimation, suggest that these plant traits are most suitable to assess plasticity of beech in response to soil P availability.

CONCLUSION

A two-year cross-growth experiment with beech saplings and mineral soil from two forest sites differing strongly in soil P availability, demonstrated a high plasticity of juvenile *F. sylvatica* to differences in soil P availability. Some influence of recovery from stress implicated by the transplantation on these results, can however, not be excluded. Relative P allocation to leaves appears to be a particularly good indicator of soil P availability, irrespective of the P nutritional status of the plant.

In contrast to P allocation to leaves, foliar P concentrations were not a clear indicator of soil P availability, which may partly explain the lack of relation between leaf P concentrations and soil P availability in studies comparing forest sites on the European or regional scale (Talkner et al., 2015; Lang et al., 2017). In particular, the ambiguity with respect to the interpretation of foliar P concentrations below threshold values for normal growth implies that the observation of such low values for beech on monitoring sites (Jonard et al., 2015; Talkner et al., 2015) not necessarily indicates P deficiency and respective growth reduction, but rather a tree with still good P nutritional status but reacting to a decrease in soil P availability.

Overall, the results clearly rebut our working hypothesis, that adaptation of beech saplings to new soil conditions is driven by the plant striving to achieve or maintain high foliar P concentrations. By contrast, they point to a sensitive signaling network that allows the plant to produce as much biomass as possible under given soil conditions by regulating mass and nutrient allocation accordingly.

DATA AVAILABILITY

The datasets generated for this study are available on request to the corresponding author.

AUTHOR CONTRIBUTIONS

All authors designed the experiment and contributed significantly to the final version of the manuscript. SM and JL collected the plant and soil materials used in the study. SM set-up and carried out the experiment, performed most of the chemical analyses, analyzed the data, and wrote the first version of the manuscript.

FUNDING

This project was carried out in the framework of the Priority Program SPP 1685 "Ecosystem Nutrition" of the German and Swiss National Science Foundation (DFG and SNF, respectively). This particular project was funded by the SNF project no. 149138 and by internal funds of the Swiss Federal Research Institute WSL.

ACKNOWLEDGMENTS

The forest research stations "Bayerische Landesanstalt für Wald und Forstwirtschaft" and "Nordwestdeutsche Forstliche Versuchsanstalt" provided access to the field sites. The following groups at the Swiss Federal Research Institute WSL provided technical assistance: the technical support at Birmensdorf and the workshop at Davos helped with construction of the rhizoboxes, the experimental garden operated and maintained the greenhouse, the central analytical laboratories carried out part of the chemical analyses, and the soil physical and chemical laboratories provided various technical support. Andrea Polle (University of Göttingen) provided data from their experiments with undisturbed soil cores for comparison.

REFERENCES

Aerts, R. (1996). Nutrient resorption from senescing leaves of perennials: are there general patterns? *J. Ecol.* 84, 597–608.

Batjes, N. H. (2011). *Global Distribution of Soil Phosphorus Retention Potential*. Wageningen: ISRIC - World Soil Information, 42. .

Brant, A. N., and Chen, H. Y. H. (2015). Patterns and mechanisms of nutrient resorption in plants. *CRC Crit. Rev. Plant Sci.* 34, 471–486. doi: 10.1080/07352689.2015.1078611

Braun, S., Thomas, V. F. D., Quiring, R., and Flückiger, W. (2010). Does nitrogen deposition increase forest production? The role of phosphorus. *Environ. Pollut.* 158, 2043–2052. doi: 10.1016/j.envpol.2009.11.030

Brunet, J., Fritz, Ö, and Richnau, G. (2010). Biodiversity in european beech forests - a review with recommendations for sustainable forest management. *Ecol. Bull.* 53, 77–94.

Craine, J. (2009). *Resource Strategies of Wild Plants*. Princeton: Princeton University Press.

Curt, T., Coll, L., Prèvosto, B., Balandier, P., and Kunstler, G. (2005). Plasticity in growth, biomass allocation and root morphology in beech seedlings as induced by irradiance and herbaceous competition. *Ann. For. Sci.* 62, 51–60. doi: 10.1051/forest:2004092

Diaconu, D., Stangler, D. F., Kahle, H. P., and Spiecker, H. (2016). Vessel plasticity of European beech in response to thinning and aspect. *Tree Physiol.* 36, 1260–1271. doi: 10.1093/treephys/tpw053

Duquesnay, A., Dupouey, J. L., Clement, A., Ulrich, E., and Le Tacon, F. (2000). Spatial and temporal variability of foliar mineral concentration in beech (*Fagus sylvatica*) stands in northeastern France. *Tree Physiol.* 20, 13–22. doi: 10.1093/treephys/20.1.13

Durrant, H. T., de Rigo, D., and Caudullo, G. (2016). "Fagus sylvatica and other beeches in Europe: distribution, habitat, usage and threats," in *European Atlas of Forest Tree Species*, eds J. San-Miguel-Ayanz, D. de Rigo, G. Caudullo, H. Durrant, and T. A. Mauri (EU, Luxembourg: European Commission).

Eschrich, W., Fromm, J., and Essiamah, S. (1988). Mineral partitioning in the phloem during autumn senescence of beech leaves. *Trees* 2, 73–83.

Flückiger, W., and Braun, S. (1998). Nitrogen deposition in swiss forests and its possible relevance for leaf nutrient status, parasite attacks and soil acidification. *Environ. Pollut.* 102, 69–76. doi: 10.1016/b978-0-08-043201-4.50015-0

Gärtner, H., and Schweingruber, F. H. (2013). *Microscopic Preparation Techniques for Plant Stem Analysis*. Remagen: Dr. Norbert Kessel, 78.

Gee, G. W., and Bauder, J. W. (1986). "Particle-Size Analysis," in *Methods of Soil Analysis: Part 1 - Physical and Mineralogical Methods*, ed. A. Klute (Madison, WI: Soil Science Society of America), 383–411.

George, T. S., Fransson, A.-M., Hammond, J. P., and White, P. J. (2011). "Phosphorus nutrition: rhizosphere processes, plant response and adaptations," in *Phosphorus in Action*, *Soil Biology*, Vol. 26, eds E. K. Bünemann, A. Oberson, and E. Frossard (Berlin Heidelberg: Springer), 245–271.

Gessler, A., Schneider, S., Weber, P., Hanemann, U., and Rennenberg, H. (1998). Soluble N compounds in trees exposed to high loads of N: a comparison between the roots of Norway spruce (*Picea abies*) and beech (*Fagus sylvatica*) trees grown under field conditions. *New Phytol.* 138, 385–399. doi: 10.1046/j.1469-8137.1998.00134.x

Göttlein, A. (2015). Grenzwertbereiche für die ernährungsdiagnostische einwertung der hauptbaumarten buche, kiefer, eiche, buche. *AFJZ* 186, 110–116.

Grime, J. P. (1977). Evidence for the existence of three primary strategies in plants and its relevance to ecological and evolutionary theory. *Am. Nat.* 111, 1169–1194. doi: 10.1086/283244

Güsewell, S. (2004). N:P ratios in terrestrial plants: variation and functional significance. *New Phytol.* 164, 243–266. doi: 10.1002/ece3.2587

Hauenstein, S., Neidhardt, H., Lang, F., Krüger, J., Hofmann, D., Pütz, T., et al. (2018). Organic layers favor phosphorus storage and uptake by young beech trees (*Fagus sylvatica* L.) at nutrient poor ecosystems. *Plant Soil* 432, 289–301. doi: 10.1007/s11104-018-3804-5

Hayes, P., Turner, B. L., Lambers, H., and Laliberté, E. (2014). Foliar nutrient concentrations and resorption efficiency in plants of contrasting nutrient-acquisition strategies along a 2-million-year dune chronosequence. *J. Ecol.* 102, 396–410. doi: 10.1111/1365-2745.12196

Hedley, M. J., Nye, P. H., and White, R. E. (1982). Plant-induced changes in the rhizosphere of rape (*Brassica napus* var. Emerald) seedlings: II. Origin of the pH change. *New Phytol.* 91, 31–44. doi: 10.1111/j.1469-8137.1982.tb03290.x

Hodge, A. (2009). Root decisions. *Plant Cell Environ.* 32, 628–640. doi: 10.1111/j.1365-3040.2008.01891.x

Hofmann, K., Heuck, C., and Spohn, M. (2016). Phosphorus resorption by young beech trees and soil phosphatase activity as dependent on phosphorus availability. *Oecologia* 181, 369–379. doi: 10.1007/s00442-016-3581-x

Holzmann, S., Missong, A., Puhlmann, H., Siemens, J., Bol, R., Klumpp, E., et al. (2016). Impact of anthropogenic induced nitrogen input and liming on phosphorus leaching in forest soils. *J. Plant Nutr. Soil Sci.* 179, 443–453. doi: 10.1002/jpln.201500552

Jonard, M., André, F., Dambrine, E., Ponette, Q., and Ulrich, E. (2009). Temporal trends in the foliar nutritional status of the french,walloon and luxembourg broad-leaved plots of forest monitoring. *Ann. For. Sci.* 66, 412–421.

Jonard, M., Fürst, A., Verstraeten, A., Thimonier, A., Timmermann, V., Potočić, N., et al. (2015). Tree mineral nutrition is deteriorating in Europe. *Global Change Biol.* 21, 418–430. doi: 10.1111/gcb.12657

Kjøller, R., Nilsson, L.-O., Hansen, K., Kappel Schmidt, I., Vesterdal, L., and Gundersen, P. (2012). Dramatic changes in ectomycorrhizal community composition, root tip abundance and mycelial production along a stand-scale nitrogen deposition gradient. *New Phytol.* 194, 278–286. doi: 10.1111/j.1469-8137.2011.04041.x

Kramer, K. (1995). Phenotypic plasticity of the phenology of seven European tree species in relation to climatic warming. *Plant Cell Environ.* 18, 93–104. doi: 10.1111/j.1365-3040.1995.tb00356.x

Lang, F., Krüger, J., Amelung, W., Willbold, S., Frossard, E., Bünemann, E. K., et al. (2017). Soil phosphorus supply controls P nutrition strategies of beech forest ecosystems in central Europe. *Biogeochemistry* 136, 5–29. doi: 10.1007/s10533-017-0375-0

Lee, R. B., and Ratcliffe, R. G. (1992). Subcellular distribution of inorganic phosphate, and levels of nucleoside triphosphate, in mature maize roots at low external phosphate concentrations: measurements with 31P-NMR. *J. Exp. Bot.* 44, 587–598. doi: 10.1093/jxb/44.3.587

Lee, R. B., Ratcliffe, R. G., and Southon, T. E. (1990). 31P NMR measurements of the cytoplasmic and vacuolar Pi content of mature maize roots: relationships with phosphorus status and phosphate fluxes. *J. Exp. Bot.* 41, 1063–1078. doi: 10.1093/jxb/41.9.1063

Leuschner, C., Meier, I. C., and Hertel, D. (2006). On the niche breadth of *Fagus sylvatica*: soil nutrient status in 50 central european beech stands on a broad range of bedrock types. *Ann. For. Sci.* 63, 355–368. doi: 10.1051/forest:2006016

Lin, W.-Y., Huang, T.-K., Leong, S. J., and Chiou, T.-J. (2014). Long-distance call from phosphate: systemic regulation of phosphate starvation responses. *J. Exp. Bot.* 65, 1817–1827. doi: 10.1093/jxb/ert431

Lin, W.-Y., Lin, S.-I., and Chiou, T.-J. (2009). Molecular regulators of phosphate homeostasis in plants. *J. Exp. Bot.* 60, 1427–1438. doi: 10.1093/jxb/ern303

Marschner, H. (1996). *Mineral Nutrition of Higher Plants*, 2nd Edn. London: Academic Press, 889.

Marschner, H., Kirkby, E., and Cakmak, I. (1996). Effect of mineral nutritional status on shoot-root partitioning of photoassimilates and cycling of mineral nutrients. *J. Exp. Bot.* 47, 1255–1263. doi: 10.1093/jxb/47.Special_Issue.1255

Matesanz, S., Gianoli, E., and Valladares, F. (2010). Global change and the evolution of phenotypic plasticity in plants. *Ann. N.Y. Acad. Sci.* 1206, 35–55. doi: 10.1111/j.1749-6632.2010.05704.x

Mellert, K. H., and Göttlein, A. (2012). Comparison of new foliar nutrient thresholds derived from van den burg's literature compilation with established central european references. *Eur. J. For. Res.* 131, 1461–1472. doi: 10.1007/s10342-012-0615-8

Mimura, T. (1995). Homeostasis and transport of inorganic phosphate in plants. *Plant Cell Physiol.* 36, 1–7.

Mimura, T., Sakano, K., and Shimmen, T. (1996). Studies on distribution, retranslocation and homeostasis of inorganic phosphate in barley leaves. *Plant Cell Environ.* 19, 311–320. doi: 10.1111/j.1365-3040.1996.tb00253.x

Netzer, F., Schmid, C., Herschbach, C., and Rennenberg, H. (2017). Phosphorus-nutrition of European beech (*Fagus Sylvatica* L.) during annual growth depends on tree age and P-availability in the soil. *Environ. Exp. Bot.* 137, 194–207. doi: 10.1093/treephys/tpx126

Nicotra, A. B., Atkin, O. K., Bonser, S. P., Davidson, A. M., Finnegan, E. J., Mathesius, U., et al. (2010). Plant phenotypic plasticity in a changing climate. *Trends Plant Sci.* 15, 684–692. doi: 10.1016/j.tplants.2010.09.008

Peñuelas, J., Poulter, B., Sardans, J., Ciais, P., van der Velde, M., Bopp, L., et al. (2013). Human-induced nitrogen–phosphorus imbalances alter natural and managed ecosystems across the globe. *Nat. Commun.* 4:2934. doi: 10.1038/ncomms3934

Poorter, H., and Sack, L. (2012). Pitfalls and possibilities in the analysis of biomass allocation patterns in plants. *Front. Plant Sci.* 3:259. doi: 10.3389/fpls.2012.00259

R Core Team (2014). *R: A Language and Environment for Statistical Computing*. Vienna: R Foundation for Statistical Computing.

Raghothama, K. G. (1999). Phosphate acquisition. *Annu. Rev. Plant Biol.* 50, 665–693.

Rennenberg, H., Schneider, S., and Weber, P. (1996). Analysis of uptake and allocation of nitrogen and sulphur compounds by trees in the field. *J. Exp. Bot.* 47, 1491–1498. doi: 10.1093/jxb/47.10.1491

Richardson, S. J., Peltzer, D. A., Allen, R. B., McGlone, M. S., and Parfitt, R. L. (2004). Rapid development of phosphorus limitation in temperate rain forest along the franz josef soil chronosequence. *Oecologia* 139, 267–276. doi: 10.1007/s00442-004-1501-y

Rolo, V., Andivia, E., and Pokorny, R. (2015). Response of *Fagus Sylvatica* and *Picea abies* to the interactive effect of neighbor identity and enhanced CO2 levels. *Trees Struct. Funct.* 29, 1459–1469. doi: 10.1007/s00468-015-1225-0

Sardans, J., and Peñuelas, J. (2013). Tree growth changes with climate and forest type are associated with relative allocation of nutrients, especially phosphorus, to leaves and wood. *Glob. Ecol. Biogeogr.* 22, 494–507. doi: 10.1111/geb.12015

Schachtman, D. P., Reid, R. J., and Ayling, S. M. (1998). Phosphorus uptake by plants. From soil to cell. *Plant Physiol.* 116, 447–453. doi: 10.1104/pp.116.2.447

Stojnić, S., Orlović, S., Miljković, S., Galić, Z., Kebert, M., and von Wuehlisch, G. (2015a). Provenance plasticity of European beech leaf traits under differing environmental conditions at two Serbian common garden sites. *Eur. J. For. Res.* 134, 1109–1125. doi: 10.1007/s10342-015-0914-y

Stojnić, S., Orlović, S., Trudić, B., Živkovic, U., von Wuehlisch, G., and Milijković, D. (2015b). Phenotypic plasticity of European beech (*Fagus Sylvatica* L.) stomatal features under water deficit assessed in provenance trial. *Dendrobiology* 73, 163–173. doi: 10.12657/denbio.073.017

Stojnić, S., Sass-Klaassen, U., Orlovic, S., Matovic, B., and Eilmann, B. (2013). Plastic growth response of European beech provenances to dry site conditions. *IAWA J.* 34, 475–484. doi: 10.1163/22941932-00000038

Sultan, S. E. (2004). Promising directions in plant phenotypic plasticity. *Perspect. Plant Ecol. Syst.* 6, 227–233. doi: 10.1078/1433-8319-00082

Talkner, U., Meiwes, K. J., Potočić, N., Seletković, I., Cools, N., De Vos, B., et al. (2015). Phosphorus nutrition of beech (*Fagus Sylvatica* L.) is decreasing in Europe. *Ann. For. Sci.* 72, 919–928. doi: 10.1007/s13595-015-0459-8

Tamburini, F., Pfahler, V., Bünemann, E. K., Guelland, K., Bernasconi, S. M., and Frossard, E. (2012). Oxygen isotopes unravel the role of microorganisms in phosphate cycling in soils. *Environ. Sci. Technol.* 46, 5956–5962. doi: 10.1021/es300311h

Tiessen, H., and Moir, J. O. (2006). "Characterization of available P by sequential extraction," in *Soil Sampling and Methods of Analysis*, 2nd Edn, eds M. R. Carter and E. G. Gregorich (Boca Raton, FL: CRC Press).

Valladares, F., Chico, J. M., Aranda, I., Balaguer, L., Dizengremel, P., Manrique, E., et al. (2002). The greater seedling high-light tolerance of *Quercus robur* over *Fagus sylvatica* is linked to a greater physiological plasticity. *Trees* 16, 395–403.

Valladares, F., Sanchez-Gomez, D., and Zavala, M. A. (2006). Quantitative estimation of phenotypic plasticity: bridging the gap between the evolutionary concept and its ecological applications. *J. Ecol.* 94, 1103–1116. doi: 10.1111/j.1365-2745.2006.01176.x

Van Heerwaarden, L. M., Toet, S., and Aerts, R. (2003). Current measures of nutrient resorption efficiency lead to a substantial underestimation of real resorption efficiency: facts and solutions. *Oikos* 101, 664–669. doi: 10.1034/j.1600-0706.2003.12351.x

Van Veldhoven, P. P., and Mannaerts, G. P. (1987). Inorganic and organic phosphate measurements in the nanomolar range. *Anal. Biochem.* 161, 45–48. doi: 10.1016/0003-2697(87)90649-x

Vergutz, L., Manzoni, S., Porporato, A., Novais, R. F., and Jackson, R. B. (2012). Global resorption efficiencies and concentrations of carbon and nutrients in leaves of terrestrial plants. *Ecol. Monogr.* 82, 205–220. doi: 10.1890/11-0416.1

Vitasse, Y., Bresson, C., Kremer, A., Michalet, R., and Delzon, S. (2010). Quantifying phenological plasticity to temperature in two temperate tree species. *Funct. Ecol.* 24, 1211–1218. doi: 10.1111/j.1365-2435.2010.01748.x

Vitasse, Y., Delzon, S., Dufrêne, E., Pontailler, J.-Y., Louvet, J.-M., Kremer, A., et al. (2009). Leaf phenology sensitivity to temperature in European trees: do within-species populations exhibit similar responses? *Agric. For. Meteorol.* 149, 735–744. doi: 10.1016/j.agrformet.2008.10.019

Weemstra, M., Sterck, F. J., Visser, E. J. W., Kuyper, T. W., Goudzwaard, L., and Mommer, L. (2016). Fine-root trait plasticity of beech (*Fagus sylvatica*) and spruce (*Picea abies*) forests on two contrasting soils. *Plant Soil* 415, 175–188. doi: 10.1007/s11104-016-3148-y

Wilcox, J. R., Premachandra, G. S., Young, K. A., and Raboy, V. (2000). Isolation of high seed inorganic P, low-phytate soybean mutants. *Crop Sci.* 40, 1601–1605.

Yang, N., Zavišić, A., Pena, R., and Polle, A. (2016). Phenology, photosynthesis, and phosphorus in European beech (*Fagus Sylvatica* L.) in two forest soils with contrasting P contents. *J. Plant Nutr. Soil Sci.* 179, 151–158. doi: 10.1002/jpln.201500539

Yang, X., Post, W. M., Thornton, P. E., and Jain, A. (2013). The distribution of soil phosphorus for global biogeochemical modeling. *Biogeosciences* 10, 2525–2537. doi: 10.1016/j.chemosphere.2011.02.039

Zavišic, A., and Polle, A. (2018). Dynamics of phosphorus nutrition, allocation and growth of young beech (*Fagus sylvatica* L.) trees in P-rich and P-poor forest soil. *Tree Physiol.* 38, 37–51. doi: 10.1093/treephys/tpx146

Zavišić, A., Yang, N., Marhan, S., Kandeler, E., and Polle, A. (2018). Forest soil phosphorus resources and fertilization affect ectomycorrhizal community composition, beech P uptake efficiency, and photosynthesis. *Front. Plant Sci.* 9:463. doi: 10.3389/fpls.2018.00463

Conflict of Interest Statement: The authors declare that the research was conducted in the absence of any commercial or financial relationships that could be construed as a potential conflict of interest.

frontiers in Plant Science

ORIGINAL RESEARCH
published: 05 April 2019
doi: 10.3389/fpls.2019.00405

The Phosphorus Economy of Mediterranean Oak Saplings Under Global Change

Inga Dirks[1†], Julia Köhler[2], Shimon Rachmilevitch[1] and Ina C. Meier[2]*

[1] French Associates Institute for Agriculture and Biotechnology of Drylands, Ben Gurion University of the Negev, Beersheba, Israel, [2] Plant Ecology, Albrecht-von-Haller Institute for Plant Sciences, University of Göttingen, Göttingen, Germany

While a severe decrease in phosphorus (P) availability is already taking place in a large number of ecosystems, drought and nitrogen (N) deposition will likely further decrease the availability of P under global change. Plants have developed physiological strategies to cope with decreasing P resources, but it is unclear how these strategies respond to elevated N deposition and summer droughts. We investigated the influence of N and P availability and soil drought on P uptake ($H_3{}^{33}PO_4$ feeding experiment) and use efficiencies in young *Quercus calliprinos* Webb. trees. We hypothesized that (H1) the expected increases in soil N:P ratios will increase the efficiencies of P uptake and use of oak saplings but will decrease the efficiencies of N uptake and use, whereas (H2) drought will affect P uptake efficiency more than N uptake efficiency. In confirmation of (H1) we found that a sharp increase of the soil N:P ratio from 4 to 42 g g^{-1} significantly increased the instantaneous ^{33}P uptake efficiency ($^{33}PUptakeE$) by five-fold and long-term P uptake efficiency (PUptakeE) by six-fold, while it decreased N uptake efficiency (NUptakeE) and N use efficiency (NUE). In contradiction to (H1), P use efficiency (PUE) did not respond to the simulated extended gradient of soil N:P ratios but remained relatively constant. (H2) was only partially confirmed as soil drought reduced PUptakeE by up to a fourth at high soil N:P ratios but had no significant effect on NUptakeE. As a consequence, increasing summer droughts may decrease the response of PUptakeE to increasing P limitation, which – in the absence of adjustments of the efficiency of P use – can aggravate growth reductions in this eastern Mediterranean tree species under global change.

Keywords: drought, eastern Mediterranean, global change, nitrogen deposition, phosphorus limitation, *Quercus calliprinos*, uptake efficiency

OPEN ACCESS

Edited by:
Jian-Guo Huang,
University of Chinese Academy of Sciences (UCAS), China

Reviewed by:
Raquel Lobo-do-Vale,
Universidade de Lisboa, Portugal
Xiali Guo,
South China Botanical Garden, Chinese Academy of Sciences, China

****Correspondence:***
Ina C. Meier
imeier1@uni-goettingen.de

†Present address:
Inga Dirks,
Department of Crop Sciences, Division Agronomy/Crop Science, University of Göttingen, Göttingen, Germany

Specialty section:
This article was submitted to Functional Plant Ecology, a section of the journal Frontiers in Plant Science

Received: *29 October 2018*
Accepted: *18 March 2019*
Published: *05 April 2019*

Citation:
Dirks I, Köhler J, Rachmilevitch S and Meier IC (2019) The Phosphorus Economy of Mediterranean Oak Saplings Under Global Change. Front. Plant Sci. 10:405. doi: 10.3389/fpls.2019.00405

INTRODUCTION

Increasing N deposition and summer droughts under global change will induce nutritional imbalances and large-scale undersupply of essential plant nutrients such as P in a large number of natural forest ecosystems (Talkner et al., 2015; Sardans et al., 2016), but especially in Eastern Mediterranean forests where extreme climate conditions are already common and the effect of global change will be disproportional (Lelieveld et al., 2012). The deterioration of P availability is already indicated by decreasing P concentrations and increasing N:P ratios in leaves and fine roots, as well as by reports on growth reductions due to P limitations for various regions of Central and

Southern Europe and elsewhere (Elser et al., 2007; Peñuelas et al., 2012). This trend of increasing P deficiency of forest trees is even more pronounced in regions where P availability had already been low before (Jonard et al., 2015): Mediterranean ecosystems are commonly characterized by geological substrates poor in mineral P content and by accumulation of occluded P with longer soil development (Singer, 2007; Cramer and Hoffman, 2015) and, thus, may shift from latent to apparent P deficiency under global change.

Plants can respond to P deficiency by increasing their P uptake and use efficiencies. P uptake is generally constrained since most P occurs sorbed to or occluded in Fe and Al oxides, precipitated as secondary mineral, or integrated in humic substances but not in plant-available form (Schachtman et al., 1998; Ragothama, 1999). In addition, the low diffusion coefficient of plant-available soluble $H_2PO_4^-$ causes a distinct depletion zone in the rhizosphere. Accordingly, several adaptation or acclimation strategies for the increase of the rate and efficiency of P uptake exist. Among them the most fundamental plant response is to increase the root:shoot ratio, adjust the root architecture toward higher branching intensity, and increase root proliferation into unexplored soil regions (Lambers et al., 2006). In addition, plants can enhance the exudation of organic acids or the secretion of phosphatases and phytases, which increases the solubility of labile and organic P (Neumann and Römheld, 2007; Hofmann et al., 2016). Plant P uptake efficiency (PUptakeE) can also be increased directly by an elevated expression of high-affinity P_i-transporters and other alterations of the membrane structure (Smith et al., 2000; Kavka and Polle, 2017) and by colonization with mycorrhizal fungi (Torres Aquino and Plassard, 2004; Cairney, 2011). In contrast to PUptakeE, increases in P use efficiency (PUE) are mostly achieved by internal reallocation of plant P to photosynthetic and growth functions (Lambers et al., 2012; Veneklaas et al., 2012).

Global change executes several constraints on the relation between P availability and PUptakeE: first, atmospheric N deposition from anthropogenic sources induces nutritional imbalances and accelerates the P demand of forest trees (Jonard et al., 2015). Second, the expected increases in the duration and intensity of summer droughts will likely further impair P availability due to decreased P mineralization (Schimel et al., 2007) and reduced mobility (Schachtman et al., 1998) and diffusion rates of P in drier soil (Kreuzwieser and Gessler, 2010). Secretion of phosphatases and expression of high affinity P_i transporters are additionally expected to be interfered by drought (Sardans and Peñuelas, 2007; Lang et al., 2016) as well as the mycorrhizal symbiosis (Kleczewski et al., 2010). These negative drought effects on P uptake seem to be even more pronounced than their effects on N uptake, leading to reductions in plant P storage (Sardans and Peñuelas, 2007) and further divergence of the N:P ratios with drought (He and Dijkstra, 2014).

In the dry eastern Mediterranean climate, Palestine oak (*Quercus calliprinos* Webb) is a common evergreen broadleaf tree species which is widely distributed from northern Algeria to southern Turkey and achieves predominance in the natural Mediterranean scrub woodland of Israel (Zohary, 1966; Schiller et al., 2003). Palestine oak grows on a relatively broad spectrum of soils and is used for reforestation, erosion control, and soil conservation. Yet despite its occurrence across a wide range of mean annual precipitation (from 460 to 1000 mm a^{-1} at higher elevation and altitude; Kutiel and Naveh, 1987; Klein et al., 2013), it is more drought sensitive than other co-occurring tree species and is limited by high temperatures (Helman et al., 2017) and low nutrient availability (Tognetti et al., 2000), which could reduce its growth and vitality under a future drier and warmer climate. The predicted climate change conditions in the eastern Mediterranean include faster warming than expected for the global mean, an increasing number of very hot days in summer, and a further decline in precipitation, especially in spring and summer (Lelieveld et al., 2012; Jacob et al., 2014). Concerns are rising that climate change in combination with N deposition will have disproportional effects on the P nutrition for the forest vegetation in this region compared to other areas – especially at sites that are currently already at the drought edge of distribution of Palestine oak.

To improve our understanding of the complex responses of P and N uptake and use efficiencies to the expected global change conditions, we exposed young Palestine oak trees to an increase in soil N:P ratios and a decrease in soil moisture in a two-factorial climate chamber experiment (3 N:P ratios × 2 soil moisture levels). We examined oak uptake and use efficiencies from a ^{33}P feeding experiment, photosynthetic measurements, and elemental analyses of recent biomass. Subsequently, we analyzed the responses of P and N uptake and use efficiencies to decreasing P availability and decreasing soil moisture. We hypothesized that (H1) the increase in soil N:P ratios increases the efficiencies of P uptake and use of oak saplings but decreases the efficiencies of N uptake and use; and (H2) drought affects P uptake efficiency more than N uptake efficiency.

MATERIALS AND METHODS

Plant Material and Experimental Set-Up

Our experiment was conducted with evergreen Palestine oak (*Quercus calliprinos* Webb.) saplings that were raised from seeds collected from a mature oak forest in the Lower Galilee in northern Israel (close to Turan; N 32° 46′, E 35° 22′; plant nursery: Keren Kayemeth LeIsrael, Jerusalem, Israel). In February 2015, 48 bare-rooted 1.5-year-old oak trees of similar size were carefully transported to the botanical garden in Göttingen, Central Germany, where they were rinsed with bi-distilled water and planted in 6-L pots filled with sterilized mineral sand / very fine gravel with a particle size of ≥2 mm, a soil texture that facilitates root studies. The potted oak saplings were placed in a randomized array in a greenhouse chamber with climate control (air temperature 21/18°C day/night, day length 12 h; in representation of the growing season conditions of Palestine oak between February and October) and were cultivated for 30 weeks until the start of the physiological and biochemical measurements in September 2015. The selected saplings had an average shoot height of 67 ± 2 cm (measured from the soil surface to the top of the sapling), a crown volume of 5130 ± 570 cm^3, and a mean maximum stem diameter of 0.6 ± 0.1 cm. Oak saplings were re-randomized bi-weekly. We simulated a gradient of decreasing

P availability in response to an increase in N deposition and decrease in soil moisture as expected under global change. We established two soil moisture conditions, a well-watered (M2; 10 % soil water content, v/v; close to field capacity) and a drought treatment (M1; 6.7% soil water content, v/v; close to the permanent wilting point) based on the texture of the sandy inorganic growth medium used in the experiment. Soil water contents were biweekly adjusted for plant water consumption by homogeneous irrigation with demineralized water to bring the soil back to its target soil moisture content. We simulated low (N1; 7.3 mg kg^{-1}) and elevated N additions (N2; 15.2 mg kg^{-1}), estimated on the basis of the extremely low N content of the sand used for the experiment (N_{total} = 0.14 g kg^{-1}), typical soil N concentrations in the Mediterranean (0.8–4.9 g kg^{-1}; Carreira et al., 1994; Evrendilek et al., 2006), and the expected N deposition rates in the eastern Mediterranean (15–22 kg N ha^{-1} yr^{-1}; Roda et al., 2002; Christodoulaki et al., 2015). Our N addition schedule is, thus, a compromise between N deposition rates that are two to six times higher than the expected deposition rates (if extrapolated to a whole year: 44 and 91 kg N ha^{-1} yr^{-1}) and final soil N concentrations that were still 5–33 times lower than their average in the eastern Mediterranean (final soil N: 0.15 and 0.16 g N kg^{-1}). N was added weekly as KNO_3, $NaNO_3$, and NH_4NO_3 by watering the soil surface with a dissolved fertilizer. We did not consider leaf N uptake in our experiment. Finally, we established two P availability levels, a low (P2; 1.79 mg kg^{-1}) and an extremely low P supply treatment (P1; 0.36 mg kg^{-1}) on the basis of the estimated plant-available P content in the sandy substrate used for the experiment (*c.* 3 mg P_{resin} kg^{-1}; *cf.* Köhler et al., 2018) and typical plant-available soil P concentrations in the eastern Mediterranean (4–11 mg $P_{bicarbonate}$ kg^{-1}; Henkin et al., 1994). P was added weekly as KH_2PO_4 by watering with a dissolved fertilizer. Our fertilization regime led to three N:P treatments: the relative N:P ratio increased from N1P2 (control; N/P = 4 g g^{-1}) to N2P2 (elevated N addition; N/P = 8 g g^{-1}) and N2P1 (elevated N addition and P limitation; N/P = 42 g g^{-1}), with eight replicates per treatment. To avoid differences in salinity, we controlled for the electric conductivity of all stock solutions ($\sigma \sim 0.77$ dS m^{-1}). Micronutrients were added three times during the experiment with a diluted Hoagland solution.

Photosynthetic Carbon Assimilation

Leaf gas exchange measurements were conducted at the end of September 2015 on one canopy leaf per sapling with an infrared CO_2 analyzer (LI-6400; LI-COR Biosciences, Lincoln, NE, United States) during the midday hours, i.e., between 10.30 a.m. and 1.30 p.m. We measured area-based midday leaf photosynthesis (A_{800}; μmol CO_2 m^{-2} s^{-1}) at high photosynthetically active radiation (800 μmol PAR m^{-2} s^{-1}). During the measurements, average leaf temperature was 21°C, relative humidity 40%, vapor pressure deficit 12 hPa, and CO_2 concentrations ambient (400 μmol CO_2 mol^{-1} air). Mass-based leaf photosynthesis (in μmol CO_2 g^{-1} s^{-1}) was calculated from A_{800} and the ratio of leaf area per dry weight (specific leaf area, SLA; in cm^2 g^{-1}; for a description of the measurement see the description of the analysis of shoot biomass and morphology below). We calculated the instantaneous, late-summer photosynthetic P and N use efficiencies according to PPUE = A_{800}*SLA/P_{Leaves} and PNUE = A_{800}*SLA/N_{Leaves}, respectively (in μmol CO_2 g^{-1} P or N s^{-1}), where P_{Leaves} is the foliar P concentration and N_{Leaves} the foliar N concentration (*cf.* Li et al., 2012; Gan et al., 2016).

^{33}P Labeling Experiment

To measure ^{33}P uptake capacity at the end of the experiment, half of the experimental saplings representing all treatments were selected for a $H_3{}^{33}PO_4$ feeding experiment, which was conducted in the Laboratory for Radioisotope Research (LARI), University of Goettingen. Soils of the potted saplings were labeled with 100 mL $H_3{}^{33}PO_4$ tracer solution (total activity per sapling 1 MBq ^{33}P), which was evenly injected to the soil at ten injection points and three soil depths (2, 4, and 8 cm soil depth, respectively). After an application time of 120 min, saplings were immediately excavated and separated into fine roots (≤2 mm), coarse roots (>2 mm), the stem base (base to 10 cm stem height), the older top stem which had originated before the experiment (above 10 cm stem height), the younger top stem which developed during the experiment, the older leaves which had originated before the experiment, and the younger leaves which developed during the experiment. All compartments were immediately frozen in liquid N_2 and stored at −80°C to avoid any further progressing of ^{33}P. A subsample of mixed soil was frozen similarly and used for the determination of the specific ^{33}P activity in soil (i.e., isotope dilution of ^{33}P; determined from the amount of ^{33}P per amount of soil inorganic P_i; in Bq mg^{-1} P_i; *cf.* Zavišić and Polle, 2018). All plant samples were placed for 7 days in a freeze drier (BETA I, Christ, Osterode/Harz, Germany), weighed, and ground (Mixer Mill MM 400; Retsch, Haan, Germany). Subsequently, ground samples were digested with 65% HNO_3 at 180°C (*cf.* Heinrichs et al., 1986), filtered (filter paper grade MN 640 w; Macherey Nagel, Düren, Germany), and mixed with a scintillation cocktail (Rotiszint eco plus LSC cocktail; Roth, Karlsruhe, Germany). The ^{33}P radioisotope signature was determined with a low activity liquid scintillation analyzer (Tri-Carb 3180 TR/SL; Perkin Elmar, Waltham, MA, United States). ^{33}P uptake was determined separately for fine roots, coarse roots, and aboveground biomass. The mass-specific rate of ^{33}P uptake (^{33}PUptake) was calculated from the whole-plant amount of ^{33}P after 2 h divided by the whole-plant biomass; and division of the quotient by the specific ^{33}P activity (in g P g^{-1} DW d^{-1}; *cf.* Zavišić and Polle, 2018). The instantaneous ^{33}P uptake efficiency (^{33}PUptakeE; in Bq kBq^{-1}) was calculated according to ^{33}PUptakeE = whole-plant ^{33}P/soil ^{33}P, where *whole-plant* ^{33}*P* is the whole-plant amount of ^{33}P and *soil* ^{33}*P* is the amount of ^{33}P in soil.

Root and Shoot Biomass and Morphology

The remaining 24 plants were harvested during the following week and analyzed for biomass, morphology, and their N and P contents. Following the procedure of the ^{33}P labeled saplings, plants were divided into their compartments, namely fine roots,

coarse roots, stem bases, older top stems, younger top stems, older leaves, and younger leaves. Leaves and fine roots were dried for 24 h at 65°C until weight stability, while coarse roots and stems were dried for 72 h at 65°C until weight stability. Relative growth rates were calculated according to $RGR = (\ln DW_2 - \ln DW_1)/(t_2 - t_1)$, where DW_1 is the estimated dry weight at the beginning of the experiment in February 2015, DW_2 is the dry weight at the end of the experiment in September 2015, and $(t_2 - t_1)$ is the length of the experiment (210 days). Biomass at the beginning of the experiment was estimated from the stem diameter measured at the beginning of the experiment and the relationship between dry weight and stem diameter D established at the end of the experiment from tree harvests ($DW = 8.25 * D - 11.46$; $R^2 = 0.52$; in g). Twenty leaves per sapling were scanned to determine leaf area by using a flat-bed scanner and the computer program WinFOLIA (version 2014c; Régent Instruments Inc., Canada) and their dry mass was determined. Based on this information, SLA (in $cm^2\ g^{-1}$) was calculated. Total leaf area was extrapolated based on the subsamples.

P and N Uptake and Use Efficiencies

Dry plant compartments were ground with a vibratory disk mill (Scheibenschwingmühle TS; Siebtechnik GmbH, Mülheim, Germany) and subjected to high-pressure chemical digestion with 65% HNO_3 at 195°C. The digested samples were analyzed for P by an inductively coupled plasma optical emission spectroscopy (ICP-OES, Optima 5300 DV; Perkin Elmer, Germany). Total N in the dried plant compartments were analyzed with an elemental analyzer (vario EL III; elementar, Langenselbold, Germany). We calculated the long-term P uptake efficiency (PUptakeE; in g P g^{-1} P_{added}) by dividing the content of P in recent biomass, i.e., in fine roots and leaves that developed during the experiment, by its amount added by fertilization during the 2015 growing season. P use efficiency (PUE; in g DW g^{-1} P_{DW}) was calculated from the increment in total biomass (dry weight) for a given increase in P in biomass during a given time period (*cf.* Koide, 1991). Correspondingly, N uptake efficiency (NUptakeE) and N use efficiency (NUE) were calculated by considering N instead of P.

Data Processing and Analysis

Statistical analyses were performed with R, version 3.5.1 (R Development Core Team). Significance was determined at $p \leq 0.05$. Means and standard errors were calculated from eight replicates per treatment for P, and four replicates for N. All datasets were $\log_{10}$ transformed to resemble normality and homogeneity of residuals. The probability of fit to normal distribution was tested by a Shapiro-Wilk test. We analyzed the effects of the soil N:P ratio and soil moisture on the analyzed parameters in two-way analyses of variance (ANOVA), where both effects were treated as fixed effect. Tukey's range *post hoc* tests (Tukey's honest significant difference test) were conducted to identify significant differences between individual factor levels. We calculated linear regressions to identify relationships between variables.

RESULTS

Plant P Concentrations and N:P Ratios in Recent Biomass

Despite the extended soil N:P gradient and different soil moisture conditions, P concentrations in fine roots and young leaves remained relatively constant in different environmental conditions (**Figure 1**). Fine roots had on average a P concentration of 0.5 ± 0.02 mg P g^{-1} DW, while the average foliar P concentration in young leaves was slightly higher at 0.9 ± 0.02 mg P g^{-1} DW. The corresponding N:P ratios in fine roots responded to soil moisture conditions and were tendentiously higher in dry than in well-watered soil (increase from 13.5 g g^{-1} in moist soil to 15.3 g g^{-1} in dry soil; $p = 0.051$; **Figure 1C**), which resulted from a relative increase in fine root N concentrations in dry soil and not from a change in fine root P concentrations. In contrast to foliar P concentrations, N:P ratios in young leaves were significantly influenced by the soil N:P ratio (**Figure 1D** and **Supplementary Table 1**). The foliar N:P ratio increased from 11 ± 1 g g^{-1} at the lowest soil N:P ratio to 15–17 g g^{-1} at intermediate and high soil N:P ratios in well-watered soil,

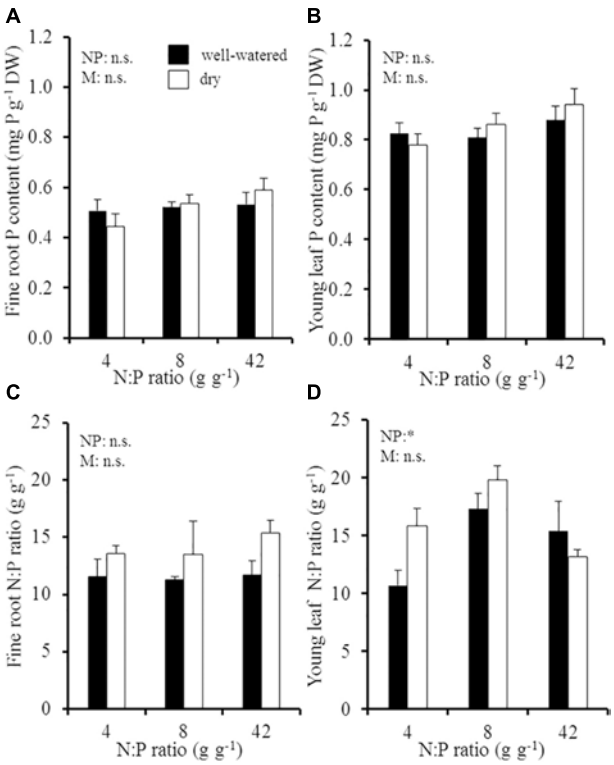

FIGURE 1 | (A) Fine root P concentration, **(B)** young leaf P concentration, **(C)** fine root N:P ratio, and **(D)** young leaf N:P ratio of young Palestine oak (*Quercus calliprinos*) trees grown at increasing soil N:P ratio and decreasing soil moisture in a climate chamber. Shown are means and standard errors for replicate saplings ($n = 48$ for P concentrations; $n = 24$ for N:P ratios). The results of two-way ANOVAs on the significance of the effect of the soil N:P ratio (NP) or soil moisture (M) are indicated by asterisks (* for $p \leq 0.05$; n.s., not significant).

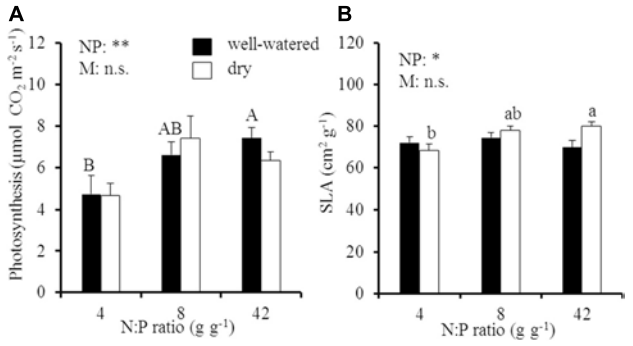

FIGURE 2 | (A) Area-based instantaneous late-summer photosynthesis (A_{800}) and **(B)** specific leaf area (SLA) of young Palestine oak (*Quercus calliprinos*) trees grown at increasing soil N:P ratio and decreasing soil moisture in a climate chamber. Shown are means and standard errors for replicate saplings (n = 24). The results of two-way ANOVAs on the significance of the effect of soil N:P ratio (NP) or soil moisture (M) are indicated by asterisks (* and ** for $p \leq 0.01$ and 0.05; n.s., not significant). Significant differences at $p \leq 0.05$ between soil N:P ratios are indicated for well-watered soil by different upper-case letters and for dry soil by different lower-case letters.

since foliar N concentrations increased at higher soil N:P ratios in well-watered soil. In dry soil, the foliar N:P ratio increased from 16 ± 1.5 g g^{-1} to 20 ± 0.5 g g^{-1} from the lowest to the intermediate soil N:P ratio; but it decreased to 13 ± 0.6 g g^{-1} at the highest soil N:P ratio ($p > 0.05$).

Plant Biomass and Photosynthetic Carbon Assimilation

Over the course of the experiment, oak biomass was not influenced by the soil N:P ratio but was significantly reduced by soil drought (on average −18%; **Supplementary Figure 1**). The reduction of plant biomass in dry soil was the most distinct at the highest soil N:P ratio, at which plant biomass was reduced by more than a third. This decrease of plant biomass occurred mostly for old leaves (because of premature litterfall), fine root biomass, and coarse root biomass, while the decrease of young leaf biomass was less pronounced.

By contrast to oak biomass, leaf morphology and photosynthesis (A_{800}) responded to a change in the soil N:P ratio but were not influenced by soil drought (SLA, $p = 0.34$ for the soil moisture effect; A_{800}, $p = 0.89$ for the soil moisture effect; **Figure 2** and **Supplementary Table 1**). Area-based carbon (C) assimilation of oak leaves increased from 4.7 to 7.4 μmol CO_2 m^{-2} s^{-1} in well-watered soil ($p < 0.05$ for the N:P effect) and from 4.7 to 6.4 μmol CO_2 m^{-2} s^{-1} in dry soil ($p > 0.05$ for the N:P effect), respectively, with an increase of the soil N:P ratio from 4 to 42 g g^{-1} (**Figure 2A**). Meanwhile, SLA significantly increased from 68 to 80 cm^2 g^{-1} with an increase of the soil N:P ratio in dry soil (**Figure 2B**), which was also accompanied by an increase of mass-based photosynthesis at high N:P ratios in dry soil (**Supplementary Figure 2**).

P and N Uptake Efficiencies in Response to Soil N:P Ratios and Drought

Elevated soil N:P ratios significantly increased instantaneous ^{33}PUptakeE and long-term PUptakeE and decreased NUptakeE (**Figure 3** and **Table 1**). More specific, instantaneous ^{33}PUptakeE increased by 4.6 and by 2.8 times under well-watered and dry conditions, respectively, when the soil N:P ratio increased by 5.3 times from 8 to 42 g g^{-1} (**Figure 3A**). The majority of the ^{33}P was retrieved from fine and coarse root biomass and only a fraction from aboveground biomass, independent of the respective treatment (**Supplementary Figure 3**). Long-term PUptakeE increased by six times under well-watered and dry conditions, respectively, when the soil N:P ratio was raised by five times, i.e., when relative P availability was reduced (**Figure 3B**). Despite the influence of the factors soil N:P ratio and soil moisture on instantaneous ^{33}PUptakeE and long-term

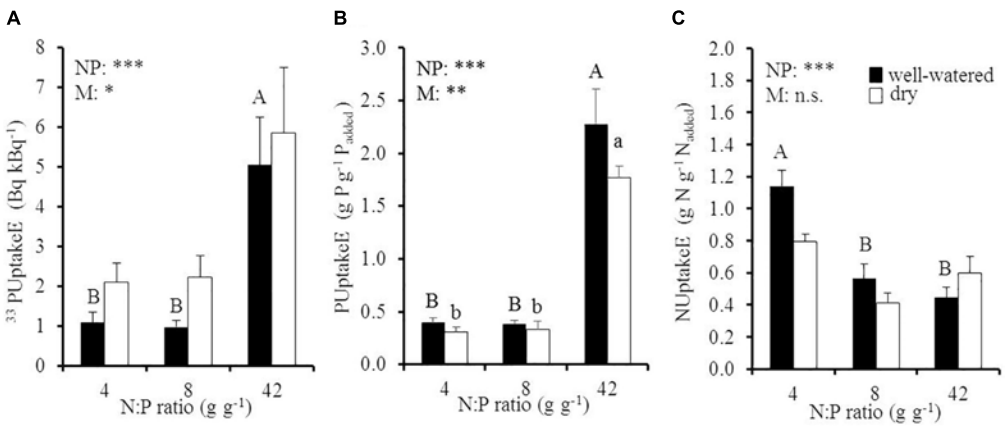

FIGURE 3 | (A) Instantaneous ^{33}P uptake efficiency (^{33}PUptakeE), **(B)** long-term P uptake efficiency (PUptakeE), and **(C)** N uptake efficiency (NUptakeE) of young Palestine oak (*Quercus calliprinos*) trees grown at increasing soil N:P ratio and decreasing soil moisture in a climate chamber. Shown are means and standard errors for replicate saplings (n = 48 for PUptakeE; n = 24 for ^{33}PUptakeE and NUptakeE). The results of two-way ANOVAs on the significance of the effect of the soil N:P ratio (NP) or soil moisture (M) are indicated by asterisks (***, **, and * for $p \leq 0.001$, 0.01, and 0.05; n.s., not significant). Significant differences at $p \leq 0.05$ between soil N:P ratios are indicated for well-watered soil by different upper-case letters and for dry soil by different lower-case letters.

TABLE 1 | Two-factorial analyses of variance (ANOVA) on the significance of the effects of the soil N:P ratio (NP), soil moisture (M), and their interaction on the variance of instantaneous ^{33}PUptake efficiency (^{33}PUptakeE), long-term P uptake efficiency (PUptakeE), P use efficiency (PUE), instantaneous late-summer photosynthetic P use efficiency (PPUE), N uptake efficiency (NUptakeE), N use efficiency (NUE), and instantaneous late-summer photosynthetic N use efficiency (PNUE) of young Palestine oak (*Quercus calliprinos*) trees.

	^{33}PUptakeE		PUptakeE		PUE		PPUE	
	F	***p***	***F***	***p***	***F***	***p***	***F***	***p***
NP	**13.3**	**<0.001**	**115.4**	**<0.001**	1.4	0.25	**5.6**	**0.01**
M	**5.0**	**0.04**	**4.7**	**0.002**	1.0	0.32	0.0	0.94
NP*M	0.1	0.87	0.3	0.97	0.31	0.74	0.5	0.58
			NUptakeE		**NUE**		**PNUE**	
			F	***p***	***F***	***p***	***F***	***p***
NP			**14.3**	**<0.001**	**4.9**	**0.03**	2.3	0.14
M			1.6	0.20	**4.9**	**0.05**	0.3	0.61
NP*M			2.7	0.11	0.2	0.79	1.5	0.27

Given are F values and the probabilities of error p. Response variables were log-transformed to resemble normality. Significant effects ($p \leq 0.05$) are indicated by bold letters (n = 24 for ^{33}PUptakeE, NUptakeE, NUE, and PNUE; n = 48 for PUptakeE, PUE, and PPUE).

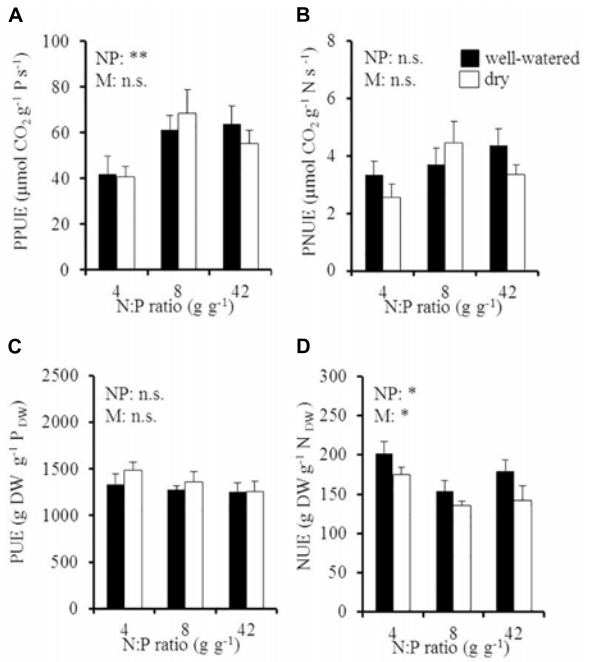

FIGURE 4 | (A) Instantaneous late-summer photosynthetic P use efficiency (PPUE), **(B)** instantaneous late-summer photosynthetic N use efficiency (PNUE), **(C)** P use efficiency (PUE), and **(D)** N use efficiency (NUE) of young Palestine oak (*Quercus calliprinos*) trees grown at increasing soil N:P ratio and decreasing soil moisture in a climate chamber. Shown are means and standard errors for replicate saplings (n = 48 for PPUE and PUE; n = 24 for PNUE and NUE). The results of two-way ANOVAs on the significance of the effect of the soil N:P ratio (NP) or soil moisture (M) are indicated by asterisks (** and * for $p \leq 0.01$ and 0.05; n.s., not significant).

PUptakeE, they had no cross-effect ($p > 0.87$; **Table 1**). We found no effect of the fine root:leaf biomass ratio on PUptakeE or NUptakeE in moist soil (PUptakeE: $p = 0.39$; NUptakeE: $p = 0.81$; not shown). Yet the absolute phosphorus uptake into recent biomass (young leaves and fine roots) related to the young leaf:fine root biomass ratio in dry soil ($R^2 = 0.58$, $p < 0.001$), where P uptake rates increased by 17 μg P d^{-1} with an increase of the young leaf:fine root biomass ratio by 1 g g^{-1} (not shown). PUptakeE of oaks increased with fine root biomass ($R = 0.56$, $p = 0.01$) and RGR ($R = 0.57$, $p < 0.001$) in well-watered soil, but decreased with increasing amount of old leaf biomass ($R = -0.50$, $p = 0.02$) in dry soil.

The reduction in NUptakeE with an increase in soil N:P ratio was far less pronounced than the concurrent increase in PUptakeE: NUptakeE was reduced by half in well-watered conditions when the soil N:P ratio increased from 4 to 8 g g^{-1}, i.e., when the relative N availability doubled, but it did not decrease much further at higher soil N:P ratio. It must be noted that both instantaneous ^{33}PUptakeE and long-term PUptakeE were drought-sensitive, while NUptakeE was not influenced by soil moisture ($p = 0.20$; **Table 1**). According to our regression analyses, the uptake efficiencies for P and N did not relate (**Supplementary Figure 4A**).

P and N Use Efficiencies in Response to Soil N:P Ratios and Drought

Elevated soil N:P ratios significantly increased instantaneous, late-summer PPUE from 41 to 65 μmol CO_2 g^{-1} P s^{-1} with an increase of the soil N:P ratio from 4 to 8 g g^{-1}, while soil moisture had no significant effect (**Figure 4A** and **Table 1**). PPUE significantly increased with foliar N concentration in young leaves (**Supplementary Figure 5A**) and with increasing instantaneous, late-summer PNUE (**Supplementary Figure 5B**) in both soil moisture treatments. PUE was on average 1328 ± 39 g DW g^{-1} P_{DW} and was neither influenced by soil N:P ratio nor by soil moisture (**Figure 4C**). PUE significantly increased with NUE in well-watered soil ($R^2 = 0.69$; **Supplementary Figure 4B**) but was independent from PUptakeE (**Supplementary Figure 4C**).

N use efficiencies responded in antagonism to the P use efficiencies to environmental conditions. Late-summer PNUE was not influenced by the soil N:P ratio or soil moisture ($p = 0.14$ for the N:P effect; $p = 0.54$ for the soil moisture effect; **Figure 4B**), whereas NUE responded to both the soil N:P ratio and the moisture content (**Figure 4D**). Accordingly, NUE significantly decreased from 201 to 153 g DW g^{-1} N_{DW} with a doubling of the soil N:P ratio in well-watered soil. Drought further reduced NUE to 142 ± 19 g DW g^{-1} N_{DW} at high soil N:P ratios (significant decrease by −18%). NUE increased with NUptakeE in dry soil ($R^2 = 0.54$, $p \leq 0.05$; **Supplementary Figure 4D**).

DISCUSSION

Elevated N deposition and summer droughts in the course of global change are assumed to deteriorate the availability of P for important forest trees, but it remains unclear to what

extent plants may adapt their uptake and use efficiencies for P and N under these conditions. Here we show that both short and long-term PUptakeE and late-summer PPUE increased with increasing soil N:P ratio, whereas PUE did not change. At the same time, both NUptakeE and NUE decreased with increasing soil N:P ratio, that is, with increasing N availability. Drought diminished the response of PUptakeE to increasing P limitation and decreased growth but had no significant effect on late-summer PPUE, PUE, and long-term NUptakeE. It seems that the efficiency of P use can be less responsive to the soil N:P and soil drought than the efficiency of P uptake in this Mediterranean oak species.

Acclimation of P Acquisition to Increasing Soil N:P Ratios

Our study demonstrates that Palestine oak can adjust its capacity for P acquisition when soil P is the limiting element to the extent that P-limitation of PUE and growth do not occur. At the same time, they down-regulate the uptake efficiency for non-limiting soil N, which is probably saving energy for the plant. In nutrient-limiting soil one of the most effective plant strategies to increase nutrient acquisition is increased resource allocation to the root system. According to optimal partitioning theory, plants allocate carbohydrates and nutrients preferentially to those organs that acquire the most growth-limiting resource, with the consequence of growth being equally limited by all resources (Bloom et al., 1985; Friedlingstein et al., 1999). Accordingly, optimal partitioning theory predicts that relative carbon allocation to fine roots and the fine root:leaf biomass ratio will increase with a limitation of soil P, but decrease with an increase in N supply. We found no effect of the fine root:leaf biomass ratio on either PUptakeE or NUptakeE, probably a consequence of the opposed influences by decreasing P supply at increasing N supply in our study. Other authors demonstrated that higher capacity for nutrient uptake and assimilation related positively to absolute root and net primary production (Norby and Iversen, 2006) and, thus, to RGR of the investigated deciduous tree species (Gan et al., 2016). Similarly, we also found a positive relationship of PUptakeE with fine root biomass and RGR in the investigated evergreen oaks. Yet this relationship is probably not the cause but rather the consequence of a more efficient P uptake, which may have been induced at the morphological (e.g., greater fine root surface area), physiological (e.g., enhanced exudation of exoenzymes involved in the decomposition of organic P), or even cellular level (e.g., increased mRNA levels of genes involved in P and N absorption and metabolism; Gan et al., 2016). While we can exclude root morphology as well as organic P decomposition as significant factors for PUptakeE of oak in our pot experiment, we can only speculate if changes at the cellular level, i.e., in the membrane structure and in the density and affinity of P_i-transporters, were the reason for increased PUptakeE of oaks under P limitation. This question of the effect of changes at the cellular level on PUptakeE of evergreen tree species deserves further study.

In contrast to our initial hypothesis, Palestine oak adjusted the efficiency of P uptake, but not the efficiency of P use under P limitation. Among different plant species, acclimation strategies to nutrient limitation differ profoundly: some species respond with changes in nutrient uptake efficiency, others with changes in nutrient use efficiency, and still others with changes in both (Nitschke et al., 2017). By contrast, PUE increased exponentially and at a higher rate than PUptakeE with increasing soil N:P ratio in temperate European beech (Köhler et al., 2018). Differences in PUE can be caused by either changes in plant P concentrations at constant biomass (Veneklaas et al., 2012; Gan et al., 2016) or changes in biomass production at constant plant P concentrations (Gan et al., 2016; Zavišić and Polle, 2018; Zavišić et al., 2018). The pronounced increase in PUE in deciduous European beech was mainly caused by a decrease in plant P concentration with increasing soil N:P, while the evergreen oak saplings of the current study had throughout a range of soil N:P ratios a comparably constant P concentration in plant tissues and constant biomass production. It seems that the young oaks have a P use economy which is independent from soil P availability. In times of low P availability, P from storage in vacuoles of coarse roots (Zavišić et al., 2018) can make plants autonomous from the amount of soil P, but this will consequently increase PUE (Gan et al., 2016). Accordingly, prominent use of P from storage in P-limited Palestine oak seems unlikely. Whereas decreased NUE under P deprivation was probably due to less efficient, waste use of N and reduced N storage in bark and wood when P (and not N) was limiting growth. NUE of the investigated Palestine oaks (135–201 g DW g^{-1} N_{DW}) was even much lower than NUE of other evergreen oak species (578–1469 g DW g^{-1} N_{DW}; Silla and Escudero, 2004). It appears that Palestine oaks can sufficiently adjust their PUptakeE to soil P availability to circumvent a shift in their PUE, while they are more opportunistic with respect to NUE.

When comparing European beech and Palestine oak it appears that PUE of the evergreen Mediterranean oak saplings (1249–1487 g DW g^{-1} P_{DW}; current study) was much less variable and in the mid-range of the PUE of the deciduous temperate beech saplings (436–2260 g DW g^{-1} P_{DW}; Köhler et al., 2018). While it has often been assumed that the dominance of evergreens in their low-nutrient habitats is due to higher nutrient use efficiencies than in deciduous species, comparisons at the whole plant level show that this is not the case (Aerts, 1995). Dominant plants on nutrient-poor and seasonally dry Mediterranean soils generally tend to have lower tissue N and P concentration in their evergreen leaves, which have longer lifespan and lower nutrient loss rates than deciduous leaves (Ribet and Drevon, 1996; Aerts and Chapin III, 2000), but they do not necessarily use foliar nutrients more efficiently for plant growth. This was also the case in the evergreen oaks, which had foliar P concentration at the lower range of the foliar P concentrations of deciduous beech from previous studies (oak: 0.8–0.9 mg P g^{-1} DW; beech: 0.5–2.8 mg P g^{-1} DW; Köhler et al., 2018; Zavišić et al., 2018). Yet, foliar P concentration also decreases with increasing plant size (Elser et al., 2010), which may also have caused lower plant P concentrations in the three times taller Palestine oak saplings of the current study than in the

much smaller European beech saplings of the previous study (Köhler et al., 2018).

Stoichiometric Homeostasis and Photosynthetic P Use Efficiency

Foliar and shoot P concentrations of Palestine oak were surprisingly constant at 0.8 mg P g^{-1} DW across the wide range of soil N:P ratios of our greenhouse study. Other field studies also showed that foliar P concentrations do not reflect soil P availability across extended P gradients (Bauer et al., 1997; Talkner et al., 2015; Lang et al., 2016), since leaves were preferred allocation sinks for P under P-poor conditions, which kept foliar P concentrations constant (Zavišić et al., 2018). This phenomenon is referred to as homeostasis, i.e., the degree to which an organism maintains its nutrient concentration around a given species-specific and size-specific value, despite variation in the availability of soil resources (Elser and Hamilton, 2007; Wang et al., 2012). Foliar P homeostasis in Palestine oak was probably maintained by acclimation of P acquisition and plant growth, with the latter having a stronger effect on foliar P homeostasis than on foliar N homeostasis. It is known that foliar P homeostasis differs from N homeostasis, since foliar P concentrations decrease more rapidly with plant size than N concentrations, resulting in a $^2/_3$ slope for the N:P scaling relationship among different plant species (Reich et al., 2010). Accordingly, foliar N:P ratios increase systematically with decreasing leaf nutrient concentrations in larger plants, which represents a disproportionate investment in N-rich proteins for high photosynthetic rates and a rising return (*sensu* Niklas et al., 2007). This allometric scaling of N and P in plants is consequence of the dependence of both acquisition and use efficiency of foliar P on the acquisition and use of N and *vice versa* (biochemically dependent co-limitation hypothesis; Ågren et al., 2012). Yet stoichiometric homeostasis is not only dependent on plant size, but also on environmental conditions, which have been suggested to exert stronger control on foliar P concentrations than on foliar N concentrations (Elser et al., 2010). In contradiction, we observed foliar P concentrations in Palestine oak saplings that remained relatively constant across different environmental conditions (and probably mainly depended on sapling size), while foliar N concentrations varied as a function of soil N availability. This led to higher foliar N:P ratios and enhanced relative P limitation when soil N availability was increased. This increase in foliar N:P ratios in Palestine oak saplings observed in our study (11–17 g g^{-1}) is comparable to other studies investigating trees in P-limited environments (8–24 g g^{-1}; Dijkstra et al., 2016).

The constant foliar P concentrations across a range of soil N:P ratios probably maintain photosynthetic rates of Palestine oak. In general, foliar P concentrations directly correlate with photosynthesis across various plant species (Wright et al., 2004a; Hidaka and Kitayama, 2009), where decreased foliar P concentrations often decrease photosynthetic rates (Pieters et al., 2001). P limitation was shown to restrict photosynthesis and leaf dark respiration in different climatic regions (Kattge et al., 2009; Domingues et al., 2010). Accordingly, Palestine oak may circumvent P limitation of photosynthesis by homeostasis of foliar P concentration even at the most extreme soil N:P ratios. Even more, late-summer photosynthesis and PPUE of oak even increased with P limitation. Woody plants can increase PPUE at constant foliar P concentration by allocating more P to the metabolites that participate in photosynthesis and less P to compounds such as nucleic acids and phospholipids, which are not involved directly in C fixation (Lambers et al., 2012). In addition, increases in SLA at high soil N:P ratios as in our study relate to higher levels of mass-based photosynthesis (**Supplementary Figure 2**; Hidaka and Kitayama, 2009), even when foliar biomass is constant. Both a change in leaf morphology and an allocation shift to photosynthetic active metabolites can be reason for increases in late-summer PPUE and increases in photosynthetic C gain of Palestine oak under enhanced P limitation. Notwithstanding this increase in late-summer PPUE, it was still comparably low in this evergreen tree species in global comparisons (Palestine oak: 55.4 $\pm$ 3.3 μmol CO_2 g^{-1} P s^{-1}; global average: 103 μmol CO_2 g^{-1} P s^{-1}; Wright et al., 2004b; Proteaceae: 305 μmol CO_2 g^{-1} P s^{-1}; Lambers et al., 2012).

Dependence of the P Economy on Soil Drought

Soil drought reduced the capacity of Palestine oaks to adjust their P acquisition to the availability of soil P. The adjustment of PUptakeE to low soil P decreased with increasing amount of old leaf biomass. In dry soil, evergreen oaks reduced their old leaf biomass at high soil N:P, probably by premature leaf drop, while sustaining a similar young leaf biomass. This decrease in leaf surface area of metabolically less active old leaves at high soil N:P ratio probably pre-empts dehydration and is primarily a drought stress syndrome characteristic for Mediterranean trees (Chaves and Oliveira, 2004). Premature leaf drop can enhance nutrient transport via sap flow, when it is improving the water status of the plant, but it also comes at a cost, since it comprises shorter P residence time in old leaves and canopy P losses, thus decreases PUE (Gleason et al., 2009). In the investigated Palestine oaks, premature leaf drop was not enough to circumvent a decrease in PUptakeE at high soil N:P ratio in dry soil. This decrease in PUptakeE was likely mainly a physical consequence of decreased mobility (Schachtman et al., 1998) and diffusion rates (Kreuzwieser and Gessler, 2010) of P in dry soil. PUptakeE was more strongly affected by drought than NUptakeE, which leads to further divergence of the foliar N:P ratios at high soil N:P ratio in dry soil (He and Dijkstra, 2014). As a consequence, growth of Mediterranean trees is increasingly P-limited in dry soil, unless PUE increases from the enhanced use of stored P from the vacuoles (Sardans and Peñuelas, 2007). The young oak trees of our study maintained their foliar P concentrations and PUE despite the P loss from premature leaf drop in dry soil constant, probably because of nutrient conservation from P resorption from senescent leaves and decreased tree biomass and growth. In global comparisons, foliar P concentrations and PUE of different plant species tend to be more strongly associated with mean annual precipitation than foliar N concentrations and NUE (Elser et al., 2010). This contrasts with our single-species study with Mediterranean oak, which is adapted to summer droughts

and low soil P availability and mainly experiences disturbance of the efficiency of N use by soil drought. This decrease in NUE when soil moisture is limiting plant growth points at a less efficient, waste use of N under these circumstances.

CONCLUSION

We investigated the effects of global change conditions on the P and N uptake and use efficiencies of evergreen Palestine oak trees, which are representatives of the Eastern Mediterranean scrub woodland. Our results demonstrate that increasing summer droughts will likely intensify nutrient imbalances for oak growth. Summer droughts decrease the acclimation of PUptakeE to increasing soil P limitation under elevated N deposition, leading to rising N:P imbalances in plants. Due to the absence of adjustment in the efficiency of P use in the investigated Palestine oaks, this effect may aggravate growth reductions from both water and P limitation under global change.

AUTHOR CONTRIBUTIONS

IM conceived and designed the research project. ID and JK performed the research. ID and JK analyzed the data. IM and ID wrote the manuscript. All authors approved the final version of the manuscript.

FUNDING

This joint research project was financially supported by the State of Lower-Saxony, Hanover, Germany. The grant was awarded by the Volkswagen Foundation [Grant #11-76251-99-34/13 (ZN 2928)] to IM and SR. We acknowledge support by the German Research Foundation and the Open Access Publication Funds of the University of Göttingen.

ACKNOWLEDGMENTS

The authors thank M. Franke-Klein, T. Klein, B. Kopka, and G. Lehmann for technical assistance in the Laboratory for Radio-Isotopes (LARI) and U. Nüsse-Hahne, C. Lau, and R. Sütterlütti for support with ICP-OES analyses. The authors also thank R. Helbig, G. Kuchenbuch, K. Rapp, B. Wetzel, and U. Yemyahu for support with fertilization and plant nurture. The authors acknowledge L. Summerfield for logistic support.

SUPPLEMENTARY MATERIAL

The Supplementary Material for this article can be found online at: https://www.frontiersin.org/articles/10.3389/fpls.2019.00405/full#supplementary-material

REFERENCES

Aerts, R. (1995). The advantages of being evergreen. *Trends Ecol. Evol.* 10, 402–407. doi: 10.1016/S0169-5347(00)89156-9

Aerts, R., and Chapin III, F. S. (2000). The mineral nutrition of wild plants revisited: a re-evaluation of processes and patterns. *Adv. Ecol. Res.* 30, 1–67. doi: 10.1016/S0065-2504(08)60016-1

Ågren, G. I., Wetterstedt, J. A. M., and Billberger, M. F. K. (2012). Nutrient limitation on terrestrial plant growth - modeling the interaction between nitrogen and phosphorus. *New Phytol.* 194, 953–960. doi: 10.1111/j.1469-8137.2012.04116.x

Bauer, G., Schulze, E.-D., and Mund, M. (1997). Nutrient contents and concentrations in relation to growth of *Picea abies* and *Fagus sylvatica* along a European transect. *Tree Physiol.* 17, 777–786. doi: 10.1093/treephys/17.12.777

Bloom, A. J., Chapin III, F. S., and Mooney, H. A. (1985). Resource limitation in plants - an economic analogy. *Annu. Rev. Ecol. Syst.* 16, 363–392. doi: 10.1146/annurev.es.16.110185.002051

Cairney, J. W. G. (2011). Ectomycorrhizal fungi: the symbiotic route to the root for phosphorus in forest soils. *Plant Soil* 344, 51–71. doi: 10.1007/s11104-011-0731-0

Carreira, J. A., Niell, F. X., and Lajtha, K. (1994). Soil nitrogen availability and nitrification in Mediterranean shrublands of varying fire history and successional stage. *Biogeochemistry* 26, 189–209. doi: 10.1007/bf00002906

Chaves, M. M., and Oliveira, M. M. (2004). Mechanisms underlying plant resilience to water deficits: prospects for water-saving agriculture. *J. Exp. Bot.* 55, 2365–2384. doi: 10.1093/jxb/erh269

Christodoulaki, S., Petihakis, G., Mihalopoulos, N., Tsiaras, K., Triantafyllou, G., and Kanakidou, M. (2015). Human-driven atmospheric deposition of N and P controls on the East Mediterranean marine ecosystem. *J. Atmos. Sci.* 73, 1611–1619. doi: 10.1175/JAS-D-15-0241.1

Cramer, M. D., and Hoffman, M. T. (2015). The consequences of precipitation seasonality for Mediterranean-ecosystem vegetation of South Africa. *PLoS One* 10:e0144512. doi: 10.1371/journal.pone.0144512

Dijkstra, F. A., Carrillo, Y., Aspinwall, M. J., Maier, C., Canarini, A., Tahaei, H., et al. (2016). Water, nitrogen and phosphorus use efficiencies of four tree species in response to variable water and nutrient supply. *Plant Soil* 406, 187–199. doi: 10.1007/s11104-016-2873-6

Domingues, T. F., Meir, P., Feldpausch, T. R., Saiz, G., Veenendaal, E. M., Schrodt, F., et al. (2010). Co-limitation of photosynthetic capacity by nitrogen and phosphorus in West Africa woodlands. *Plant Cell Environ.* 33, 959–980. doi: 10.1111/j.1365-3040.2010.02119.x

Elser, J. J., Bracken, M. E. S., Cleland, E. E., Gruner, D. S., Harpole, W. S., Hillebrand, H., et al. (2007). Global analysis of nitrogen and phosphorus limitation of primary producers in freshwater, marine and terrestrial ecosystems. *Ecol. Lett.* 10, 1135–1142. doi: 10.1111/j.1461-0248.2007.01113.x

Elser, J. J., Fagan, W. F., Kerkhoff, A. J., Swenson, N. G., and Enquist, B. J. (2010). Biological stoichiometry of plant production: metabolism, scaling and ecological response to global change. *New Phytol.* 186, 593–608. doi: 10.1111/j.1469-8137.2010.03214.x

Elser, J. J., and Hamilton, A. (2007). Stoichiometry and the new biology: the future is now. *PLoS Biol.* 5:e181. doi: 10.1371/journal.pbio.0050181

Evrendilek, F., Berberoglu, S., Taskinsu-Meydan, S., and Yilmaz, E. (2006). Quantifying carbon budgets of conifer Mediterranean forest ecosystems, Turkey. *Environ. Monit. Assess.* 119, 527–543. doi: 10.1007/s10661-005-9041-4

Friedlingstein, P., Joel, G., Field, C. B., and Fung, I. Y. (1999). Toward an allocation scheme for global terrestrial carbon models. *Glob. Change Biol.* 5, 755–770. doi: 10.1046/j.1365-2486.1999.00269.x

Gan, H. H., Jiao, Y., Jia, J. B., Wang, X. L., Li, H., Shi, W. G., et al. (2016). Phosphorus and nitrogen physiology of two contrasting poplar genotypes when exposed to phosphorus and/or nitrogen starvation. *Tree Physiol.* 36, 22–38. doi: 10.1093/treephys/tpv093

Gleason, S. M., Read, J., Ares, A., and Metcalfe, D. J. (2009). Phosphorus economics of tropical rainforest species and stands across soil contrasts in Queensland, Australia: understanding the effects of soil specialization and trait plasticity. *Funct. Ecol.* 23, 1157–1166. doi: 10.1111/j.1365-2435.2009.01575.x

He, M., and Dijkstra, F. A. (2014). Drought effect on plant nitrogen and phosphorus: a meta-analysis. *New Phytol.* 204, 924–931. doi: 10.1111/nph.12952

Heinrichs, H., Brumsack, H.-J., Loftfield, N., and König, N. (1986). Verbessertes Druckaufschlußsystem für biologische und anorganische Materialien. *J. Plant Nutr. Soil Sci.* 149, 350–353. doi: 10.1002/jpln.19861490313

Helman, D., Osem, Y., Yakir, D., and Lensky, I. M. (2017). Relationships between climate, topography, water use and productivity in two key Mediterranean forest types with different water-use strategies. *Agric. For. Meteorol.* 232, 319–330. doi: 10.1016/j.agrformet.2016.08.018

Henkin, Z., Noymeir, I., Kafkafi, U., Seligman, N., and Gutman, M. (1994). Soil phosphorus in a managed Mediterranean woodland ecosystem – herbage response and cattle grazing effects. *Agric. Ecosyst. Environ.* 47, 299–311. doi: 10.1016/0167-8809(96)01045-6

Hidaka, A., and Kitayama, K. (2009). Divergent patterns of photosynthetic phosphorus-use efficiency versus nitrogen-use efficiency of tree leaves along nutrient-availability gradients. *J. Ecol.* 97, 984–991. doi: 10.1111/j.1365-2745.2009.01540.x

Hofmann, K., Heuck, C., and Spohn, M. (2016). Phosphorus resorption by young beech trees and soil phosphatase activity as dependent on phosphorus availability. *Oecologia* 181, 369–379. doi: 10.1007/s00442-016-3581-x

Jacob, D., Petersen, J., Eggert, B., Alias, A., Christensen, O., Bouwer, L., et al. (2014). EURO-CORDEX: new high-resolution climate change projections for European impact research. *Reg. Environ. Change* 14, 563–578. doi: 10.1007/s10113-013-0499-2

Jonard, M., Furst, A., Verstraeten, A., Thimonier, A., Timmermann, V., Potocic, N., et al. (2015). Tree mineral nutrition is deteriorating in Europe. *Glob. Change Biol.* 21, 418–430. doi: 10.1111/gcb.12657

Kattge, J., Knorr, W., Raddatz, T., and Wirth, C. (2009). Quantifying photosynthetic capacity and its relationship to leaf nitrogen content for global-scale terrestrial biosphere models. *Glob. Change Biol.* 15, 976–991. doi: 10.1111/j.1365-2486.2008.01744.x

Kavka, M., and Polle, A. (2017). Dissecting nutrient-related co-expression networks in phosphate starved poplars. *PLoS One* 12:e0171958. doi: 10.1371/journal.pone.0171958

Kleczewski, N. M., Herms, D. A., and Bonello, P. (2010). Effects of soil type, fertilization and drought on carbon allocation to root growth and partitioning between secondary metabolism and ectomycorrhizae of *Betula papyrifera*. *Tree Physiol.* 30, 807–817. doi: 10.1093/treephys/tpq032

Klein, T., Shpringer, I., Fikler, B., Elbaz, G., Cohen, S., and Yakir, D. (2013). Relationships between stomatal regulation, water-use, and water-use efficiency of two coexisting key Mediterranean tree species. *For. Ecol. Manag.* 302, 34–42. doi: 10.1016/j.foreco.2013.03.044

Köhler, J., Yang, N., Pena, R., Raghavan, V., Polle, A., and Meier, I. C. (2018). Ectomycorrhizal diversity increases P uptake efficiency of European beech. *New Phytol.* 220, 1200–1210. doi: 10.1111/nph.15208

Koide, R. (1991). Nutrient supply, nutrient demand and plant response to mycorrhizal infection. *New Phytol.* 117, 365–386. doi: 10.1111/j.1469-8137.1991.tb00001.x

Kreuzwieser, J., and Gessler, A. (2010). Global climate change and tree nutrition: influence of water availability. *Tree Physiol.* 30, 1221–1234. doi: 10.1093/treephys/tpq055

Kutiel, P., and Naveh, Z. (1987). Soil properties beneath *Pinus halepensis* and *Quercus calliprinos* trees on burned and unburned mixed forest on Mt. Carmel, Israel. *For. Ecol. Manag.* 20, 11–24. doi: 10.1016/0378-1127(87)90147-2

Lambers, H., Cawthray, G. R., Giavalisco, P., Kuo, J., Laliberté, E., Pearse, S. J., et al. (2012). Proteaceae from severely phosphorus-impoverished soils extensively replace phospholipids with galactolipids and sulfolipids during leaf development to achieve a high photosynthetic phosphorus use efficiency. *New Phytol.* 196, 1096–1108. doi: 10.1111/j.1469-8137.2012.04285.x

Lambers, H., Shane, M. W., Cramer, M. D., Pearse, S. J., and Veneklaas, E. J. (2006). Root structure and functioning for efficient acquisition of phosphorus: matching morphological and physiological traits. *Ann. Bot.* 98, 693–713. doi: 10.1093/aob/mcl114

Lang, F., Bauhus, J., Frossard, E., George, E., Kaiser, K., Kaupenjohann, M., et al. (2016). Phosphorus in forest ecosystems: new insights from an ecosystem nutrition perspective. *J. Plant Nutr. Soil Sci.* 179, 129–135. doi: 10.1002/jpln.201500541

Lelieveld, J., Hadjinicolaou, P., Kostopoulou, E., Chenoweth, J., El Maayar, M., Giannakopoulos, C., et al. (2012). Climate change and impacts in the eastern Mediterranean and the Middle East. *Clim. Change* 114, 667–687. doi: 10.1007/s10584-012-0418-4

Li, H., Li, M., Luo, J., Cao, X., Qu, L., Gai, Y., et al. (2012). N-fertilization has different effects on the growth, carbon and nitrogen physiology, and wood properties of slow- and fast-growing *Populus* species. *J. Exp. Bot.* 63, 6173–6185. doi: 10.1093/jxb/ers271

Neumann, G., and Römheld, V. (2007). "The release of root exudates as affected by the plant physiological status," in *The Rhizosphere: Biochemistry and Organic Substances at the Soil-Plant Interface*, eds R. Pinton, Z. Varanini, and Z. Nannipieri (Boca Raton, FL: CRC Press), 23–72.

Niklas, K. J., Cobb, E. D., Niinemets, U., Reich, P. B., Sellin, A., Shipley, B., et al. (2007). "Diminishing returns" in the scaling of functional leaf traits across and within species groups. *Proc. Natl. Acad. Sci. U.S.A.* 104, 8891–8896. doi: 10.1073/pnas.0701135104

Nitschke, C. R., Waeber, P. O., Klaassen, J. W., Dordel, J., Innes, J. L., and Aponte, C. (2017). Nutrient uptake and use efficiency in co-occurring plants along a disturbance and nutrient availability gradient in the boreal forests of the southwest Yukon, Canada. *J. Veg. Sci.* 28, 69–81. doi: 10.1111/jvs.12468

Norby, R. J., and Iversen, C. M. (2006). Nitrogen uptake, distribution, turnover, and efficiency of use in a CO_2-enriched sweetgum forest. *Ecology* 87, 5–14. doi: 10.1890/04-1950

Peñuelas, J., Sardans, J., Rivas-Ubach, A., and Janssens, I. A. (2012). The human-induced imbalance between C, N and P in Earth's life system. *Glob. Change Biol.* 18, 3–6. doi: 10.1111/j.1365-2486.2011.02568.x

Pieters, A. J., Paul, M. J., and Lawlor, D. W. (2001). Low sink demand limits photosynthesis under Pi deficiency. *J. Exp. Bot.* 52, 1083–1091. doi: 10.1093/jexbot/52.358.1083

Ragothama, K. (1999). Phosphate acquisition. *Annu. Rev. Plant Phys.* 50, 665–693. doi: 10.1146/annurev.arplant.50.1.665

Reich, P. B., Oleksyn, J., Wright, I. J., Niklas, K. J., Hedin, L., and Elser, J. J. (2010). Evidence of a general 2/3-power law of scaling leaf nitrogen to phosphorus among major plant groups and biomes. *Proc. Biol. Sci.* 277, 877–883. doi: 10.1098/rspb.2009.1818

Ribet, J., and Drevon, J. J. (1996). The phosphorus requirement of N-2-fixing and urea-fed *Acacia mangium*. *New Phytol.* 132, 383–390. doi: 10.1111/j.1469-8137.1996.tb01858.x

Roda, F., Avila, A., and Rodrigo, A. (2002). Nitrogen deposition in Mediterranean forests. *Environ. Pollut.* 118, 205–213. doi: 10.1016/s0269-7491(01)00313-x

Sardans, J., Alonso, R., Carnicer, J., Fernandez-Martinez, M., Vivanco, M. G., and Peñuelas, J. (2016). Factors influencing the foliar elemental composition and stoichiometry in forest trees in Spain. *Perspect. Plant Ecol.* 18, 52–69. doi: 10.1016/j.ppees.2016.01.001

Sardans, J., and Peñuelas, J. (2007). Drought changes phosphorus and potassium accumulation patterns in an evergreen Mediterranean forest. *Funct. Ecol.* 21, 191–201. doi: 10.1111/j.1365-2435.2007.01247.x

Schachtman, D. P., Reid, R. J., and Ayling, S. M. (1998). Phosphorus uptake by plants: from soil to cell. *Plant Physiol.* 116, 447–453. doi: 10.1104/pp.116.2.447

Schiller, G., Unger, E. D., Moshe, Y., Cohen, S., and Cohen, Y. (2003). Estimating water use by sclerophyllous species under east Mediterranean climate. II. The transpiration of *Quercus calliprinos* Webb. in response to silvicultural treatments. *For. Ecol. Manag.* 179, 483–495. doi: 10.1016/s0378-1127(02)00536-4

Schimel, J., Balser, T. C., and Wallenstein, M. (2007). Microbial stress-response physiology and its implications for ecosystem function. *Ecology* 88, 1386–1394. doi: 10.1890/06-0219

Silla, F., and Escudero, A. (2004). Nitrogen-use efficiency: trade-offs between N productivity and mean residence time at organ, plant and population levels. *Funct. Ecol.* 18, 511–521. doi: 10.1111/j.0269-8463.2004.00872.x

Singer, A. (2007). *The Soils of Israel*. Berlin: Springer.

Smith, F. W., Rae, A. L., and Hawkesford, M. J. (2000). Molecular mechanisms of phosphate and sulphate transport in plants. *Biochim. Biophys. Acta* 1465, 236–245. doi: 10.1016/s0005-2736(00)00141-3

Talkner, U., Meiwes, K. J., Potoèiæ, N., Seletkoviæ, I., Cools, N., De Vos, B., et al. (2015). Phosphorus nutrition of beech (*Fagus sylvatica* L.) is decreasing in Europe. *Ann. For. Sci.* 72, 919–928. doi: 10.1007/s13595-015-0459-8

Tognetti, R., Cherubini, P., and Innes, J. L. (2000). Comparative stem-growth rates of Mediterranean trees under background and naturally enhanced ambient CO_2 concentrations. *New Phytol.* 146, 59–74. doi: 10.1046/j.1469-8137.2000.00620.x

Torres Aquino, M., and Plassard, C. (2004). Dynamics of ectomycorrhizal mycelial growth and P transfer to the host plant in response to low and high soil P availability. *FEMS Microbiol. Ecol.* 48, 149–156. doi: 10.1016/j.femsec.2004.01.008

Veneklaas, E. J., Lambers, H., Bragg, J., Finnegan, P. M., Lovelock, C. E., Plaxton, W. C., et al. (2012). Opportunities for improving phosphorus-use efficiency in crop plants. *New Phytol.* 195, 306–320. doi: 10.1111/j.1469-8137.2012.04190.x

Wang, H., Sterner, R. W., and Elser, J. J. (2012). On the "strict homeostasis" assumption in ecological stoichiometry. *Ecol. Model.* 243, 81–88. doi: 10.1016/j.ecolmodel.2012.06.003

Wright, I. J., Groom, P. K., Lamont, B. B., Poot, P., Prior, L. D., Reich, P. B., et al. (2004a). Leaf trait relationships in Australian plant species. *Funct. Plant Biol.* 31, 551–558. doi: 10.1071/fp03212

Wright, I. J., Reich, P. B., Westoby, M., Ackerly, D. D., Baruch, Z., Bongers, F., et al. (2004b). The worldwide leaf economics spectrum. *Nature* 428, 821–827. doi: 10.1038/nature02403

Zavišić, A., and Polle, A. (2018). Dynamics of phosphorus nutrition, allocation and growth of young beech (*Fagus sylvatica* L.) trees in P-rich and P-poor forest soil. *Tree Physiol.* 38, 37–51. doi: 10.1093/treephys/tpx146

Zavišić, A., Yang, N., Marhan, S., Kandeler, E., and Polle, A. (2018). Forest soil phosphorus resources and fertilization affect ectomycorrhizal community composition, beech P uptake efficiency, and photosynthesis. *Front. Plant Sci.* 9:463. doi: 10.3389/fpls.2018.00463

Zohary, M. (1966). Flora palaestina. *Isr. Acad. Sci. Humanit.* 1, 33–35.

Conflict of Interest Statement: The authors declare that the research was conducted in the absence of any commercial or financial relationships that could be construed as a potential conflict of interest.

frontiers in Plant Science

ORIGINAL RESEARCH
published: 22 May 2019
doi: 10.3389/fpls.2019.00643

Shifts in Ectomycorrhizal Fungal Communities and Exploration Types Relate to the Environment and Fine-Root Traits Across Interior Douglas-Fir Forests of Western Canada

Camille E. Defrenne[1], Timothy J. Philpott[2], Shannon H. A. Guichon[3], W. Jean Roach[4], Brian J. Pickles[5]* and Suzanne W. Simard[1]*

[1] Department of Forest and Conservation Sciences, Faculty of Forestry, The University of British Columbia, Vancouver, BC, Canada, [2] Ministry of Forests, Lands, Natural Resource Operations and Rural Development, Cariboo-Chilcotin Natural Resource District, Williams Lake, BC, Canada, [3] Stable Isotope Facility, Department of Forest and Conservation Sciences, University of British Columbia, Vancouver, BC, Canada, [4] Skyline Forestry Consultants Ltd., Kamloops, BC, Canada, [5] School of Biological Sciences, University of Reading, Reading, United Kingdom

OPEN ACCESS

Edited by:
Boris Rewald,
University of Natural Resources and Life Sciences, Vienna, Austria

Reviewed by:
Erik Alan Hobbie,
University of New Hampshire, United States
Sarah R. Kyker,
The Holden Arboretum, United States

***Correspondence:**
Camille E. Defrenne
camille.defrenne@ubc.ca;
camille.defrenne@gmail.com
Brian J. Pickles
b.j.pickles@reading.ac.uk

Specialty section:
This article was submitted to Functional Plant Ecology, a section of the journal Frontiers in Plant Science

Received: 18 February 2019
Accepted: 29 April 2019
Published: 22 May 2019

Citation:
Defrenne CE, Philpott TJ, Guichon SHA, Roach WJ, Pickles BJ and Simard SW (2019) Shifts in Ectomycorrhizal Fungal Communities and Exploration Types Relate to the Environment and Fine-Root Traits Across Interior Douglas-Fir Forests of Western Canada. Front. Plant Sci. 10:643. doi: 10.3389/fpls.2019.00643

Large-scale studies that examine the responses of ectomycorrhizal fungi across biogeographic gradients are necessary to assess their role in mediating current and predicted future alterations in forest ecosystem processes. We assessed the extent of environmental filtering on interior Douglas-fir (*Pseudotsuga menziesii* var. *glauca* (Beissn.) Franco) ectomycorrhizal fungal communities across regional gradients in precipitation, temperature, and soil fertility in interior Douglas-fir dominated forests of western Canada. We also examined relationships between fine-root traits and mycorrhizal fungal exploration types by combining root and fungal trait measurements with next-generation sequencing. Temperature, precipitation, and soil C:N ratio affected fungal community dissimilarity and exploration type abundance but had no effect on α-diversity. Fungi with rhizomorphs (e.g., *Piloderma* sp.) or proteolytic abilities (e.g., *Cortinarius* sp.) dominated communities in warmer and less fertile environments. Ascomycetes (e.g., *Cenococcum geophilum*) or shorter distance explorers, which potentially cost the plant less C, were favored in colder/drier climates where soils were richer in total nitrogen. Environmental filtering of ectomycorrhizal fungal communities is potentially related to co-evolutionary history between Douglas-fir populations and fungal symbionts, suggesting success of interior Douglas-fir as climate changes may be dependent on maintaining strong associations with local communities of mycorrhizal fungi. No evidence for a link between root and fungal resource foraging strategies was found at the regional scale. This lack of evidence further supports the need for a mycorrhizal symbiosis framework that is independent of root trait frameworks, to aid in understanding belowground plant uptake strategies across environments.

Keywords: biogeographic gradient, ectomycorrhizal fungi, exploration type, fine-root traits, forest ecosystems, functional ecology, mycorrhizas, *Pseudostuga menziesii* var. *glauca*

INTRODUCTION

Shifts in the taxonomic and functional structure of mycorrhizal communities across plant host distributions underpin changes in biogeochemical processes, such as modification of carbon (C) and nitrogen (N) cycles (Clemmensen et al., 2013; Koide et al., 2014; Cheeke et al., 2017; Wurzburger and Clemmensen, 2018; Jassey et al., 2018). Therefore, identifying the biotic and abiotic factors that shape mycorrhizal fungal communities is a prerequisite for understanding terrestrial ecosystem processes and predicting the impacts of global change on plant communities (Hazard and Johnson, 2018; Hoeksema et al., 2018; van der Linde et al., 2018). As climate changes, mycorrhizal fungi will likely respond to a range of environmental factors, and not necessarily the same factors as their hosts (Pickles et al., 2012), placing a premium on large-scale studies that examine communities across multiple environmental gradients (Lilleskov and Parrent, 2007; van der Linde et al., 2018).

Ectomycorrhizal fungi (EMF) play a dominant role in temperate and boreal forest ecosystems, where they control plant acquisition of soil resources (e.g., inorganic and organic forms of N and phosphorus, P; Read and Perez-Moreno, 2003; Heijden and Horton, 2009) and soil C dynamics (Simard and Austin, 2010). Biogeographic patterns in EMF diversity are now being studied (Tedersoo, 2017; Hu et al., 2019). However, there is a lack of baseline information on patterns of EMF community composition and functional trait distribution, especially at large spatial scales such as the regional (i.e., scale of a country), continental or global scales (Tedersoo, 2017; van der Linde et al., 2018; Hu et al., 2019). Yet, biogeographic data on EMF community structure are necessary to assess their role in mediating current and predicted alterations in the C cycle (Jassey et al., 2018), the hydrologic cycle (Bjorkman et al., 2018) or plant productivity (Coops et al., 2010; Richardson et al., 2018).

At the continental scale, patterns of EMF community composition of *Pinus sylvestris*, *Picea abies*, and *Fagus sylvatica* have been investigated in Europe, where host plant family and N deposition had the predominant filtering effects (Tedersoo et al., 2012; Põlme et al., 2013; Suz et al., 2014; Rosinger et al., 2018; van der Linde et al., 2018). Within Europe, at the regional scale, N deposition, rainfall and soil moisture were also found to drive shifts in the *P. sylvestris* EMF community structure (Jarvis et al., 2013), whereas other European studies highlighted the filtering effects of temperature and soil fertility on EMF communities (Sterkenburg et al., 2015; Pena et al., 2017). In Western North America, Pickles et al. (2015a) have also inferred from a common-garden greenhouse study on interior Douglas-fir (*Pseudotsuga menziesii* var. *glauca* (Beissn.) Franco; hereafter Douglas-fir) seedlings that temperature and soil fertility may drive habitat filtering in EMF communities.

Across environments, variation in EMF functional traits may relate better to ecosystem processes than variation in EMF species composition because it informs how groups of species function and the extent that there is functional redundancy in species diversity (Koide et al., 2014; Hazard and Johnson, 2018). For instance, EMF functional traits such as enzymatic activity (Courty et al., 2016), N preference (Leberecht et al., 2015; Haas et al., 2018), mycelial hydrophobicity or the differentiation of extraradical hyphae (i.e., exploration type; Agerer, 2001, 2006; Jarvis et al., 2013; Pickles et al., 2015a; Fernandez et al., 2017; Ostonen et al., 2017; Pena et al., 2017; Köhler et al., 2018; Rosinger et al., 2018) have been shown to impact ecosystem processes (Koide et al., 2014). Exploration type is a functional trait that connects the morphology and differentiation of EMF hyphae to differences in nutrient acquisition strategies. From a functional perspective, exploration type determines the ability of EMF to colonize new roots, form common mycorrhizal networks, or forage, acquire and transport resources (Agerer, 2006). Fungi with contact, short- and medium-distance smooth exploration types, for example, may preferentially use soluble, inorganic N forms (Lilleskov et al., 2002; Hobbie and Agerer, 2010). Alternatively, long-distance explorers may be more effective in capturing patchily distributed organic N (Koide et al., 2014), and are more likely to be resistant to decay due to their hydrophobicity. Hence, EMF fungi of the long-distance exploration type may drive soil C storage and C:N ratio (Suz et al., 2014), although some short-range EMF, including *Cenococcum geophilum* and *Cadophora Finlandia,* are also resistant to decay (Agerer, 2006; Fernandez et al., 2016).

Shifts in EMF exploration type may compensate for changes in fine-root structure. For example, across 13 temperate tree species, the abundance of larger absorptive fine roots, whose large diameter and associated high construction costs limits efficient resource foraging, was positively correlated with the proportion of longer distance exploration types, thus resulting in functional complementarity between fine roots and EMF with respect to soil resource capture (Chen et al., 2018a,b). This is because plants with coarser roots are less able to forage for and absorb soil resources, thus they should benefit the most from medium- or long-distance explorers that can acquire and transport resources well beyond root depletion zones (Chen et al., 2018a,b). To our knowledge, only three studies have linked root and EMF functional traits (Ostonen et al., 2011; Cheng et al., 2016; Chen et al., 2018a). Yet, studies connecting commonly measured economic fine-root traits (e.g., morphological, chemical and architectural traits) and mycorrhizal functional traits are essential for broadening root trait frameworks (McCormack et al., 2017).

Root density is also an important factor to consider when linking fine-root traits and exploration types because exploration type assemblage may be well predicted by root spacing (Peay et al., 2011) and conversely, EMF species influence root density (Pickles et al., 2010). This is especially important when working at the scale of meters or in primary succession settings (Peay et al., 2011). In this study however, we focused on economic traits commonly measured at the individual fine-root level.

To assess the extent of abiotic environmental filtering on EMF community taxonomic and functional structure, and to examine the relationship between fine root and EMF exploration type, we investigated patterns of belowground trait variation across five regions that differed in precipitation, temperature and soil fertility (pH, cation exchange capacity (CEC), total N and available P) in an area of *c.* 25, 300 km^2 (49.6 to 51.7°N) in

British Columbia, Canada. We focused on Douglas-fir in interior Douglas-fir dominated forests which are widely distributed from the Rocky Mountains of Canada and the United States to the mountains of central Mexico (Lavender and Hermann, 2014). Defrenne et al. (unpublished) have explored the variation in morphological, chemical and architectural traits among fine roots across the same biogeographic gradient and revealed that Douglas-fir trees from colder/drier climates had fine roots with higher diameter, lower root tissue density (RTD), and lower C:N, compared to trees from milder climates. In this study, we first hypothesized that temperature and soil fertility would be the main drivers of EMF diversity and community composition. Our second hypothesis was that medium-distance fringe or long-distance explorers would be more abundant in colder climates (see the third hypothesis) or in soils with high C:N ratio, because fungi with rhizomorphs that preferentially use insoluble, organic N may be more competitive for plant nutrition under these conditions. Building on the results of Defrenne et al. (unpublished), our third hypothesis was that EMF traits compensate for changes in fine-root structure, and especially root diameter, where colder/drier climates with larger diameter roots are dominated by EMF with medium-distance fringe or long-distance exploration types.

MATERIALS AND METHODS

Biogeographic Gradient

Fine roots and EMF root tips were collected from five regions in three naturally regenerated, mature, closed-canopy forest stands (30 × 30 m) per region in summer 2016 (**Figure 1**). We selected the five regions to obtain a biogeographic gradient with substantial precipitation and temperature ranges (**Table 1**). Mean annual temperature (MAT) ranged from 3.4 to 7.3°C and was lowest in Williams Lake, followed by Revelstoke, Kamloops, Salmon Arm and Nelson. The driest region was Kamloops (average mean annual precipitation- MAP, 441 mm) and the wettest was Revelstoke (average MAP 1200 mm). We picked stands that were at least 400 m apart and ecosystems that best reflected the regional climate (namely, zonal site series; Meidinger and Pojar, 1991). Average stand age ranged from 98 years (Revelstoke) to 143 years (Salmon Arm), and the proportion of Douglas-fir by basal area ranged from 49% in the mixed, even-aged forest stands of Salmon Arm to 100% in the pure, uneven-aged forest stands of Kamloops. For the basal area estimates, all the trees with a DBH > 10 cm were measured (this included only mature trees; for further details on site and stand characteristics, see **Supplementary Table 1**).

The southernmost stands (Nelson, Revelstoke and Salmon Arm) occurred predominantly on Brunisolic soils that were characterized by lower CEC, soil pH and soil N compared to the northern most stands (in Williams Lake and Kamloops) which occurred on Luvisolic soils (British Columbia Ministry of Forests and Range and British Columbia Ministry of Environment, 2010). Climatic variables for the period 1981–2010 were obtained from ClimateNA (Wang et al., 2016) and soil samples were analyzed for total soil carbon (C) and N concentrations, available phosphorus (PO_4–P; orthophosphate as phosphorus) and CEC (for further details on soil sample collection, see the next section and for details on soil sample analyses, see **Supplementary Text 1A**).

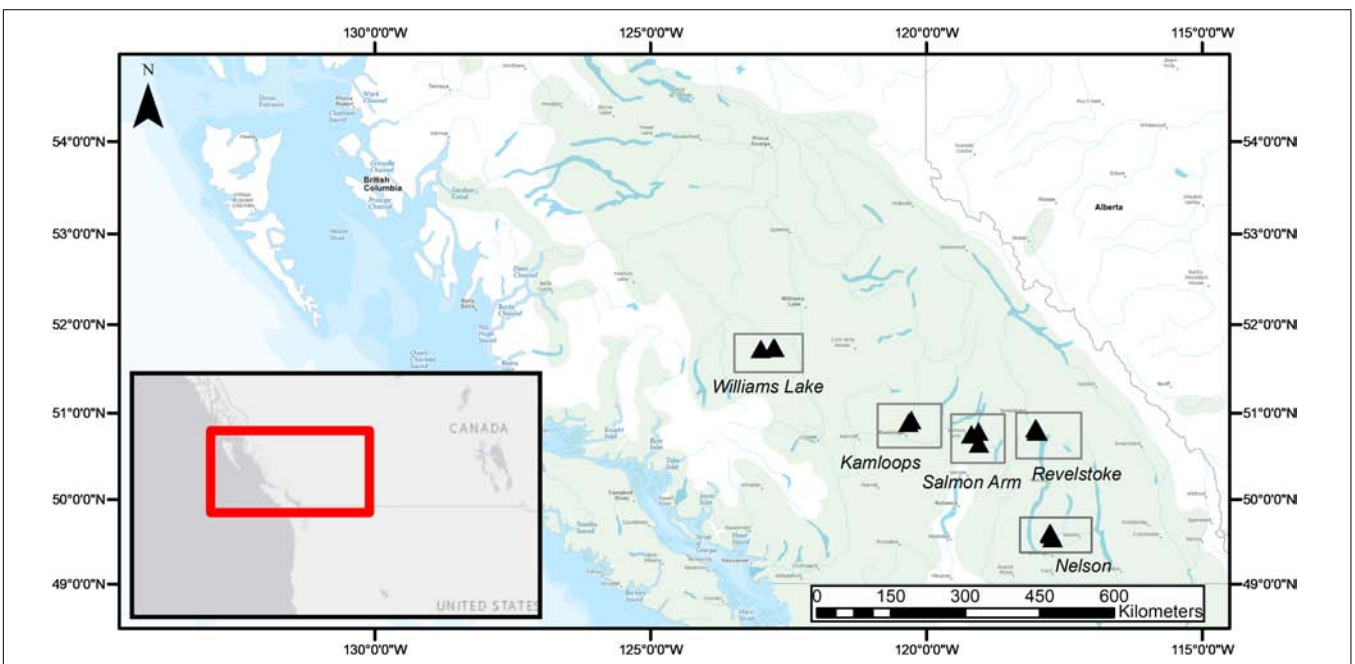

FIGURE 1 | Geographical distribution of study regions (rectangles) and forest stands (3 triangles per study region) across the current natural range of interior Douglas-fir (*Pseudotsuga menziesii* var. *glauca*; green shading) in British Columbia, Canada.

TABLE 1 | Climatic and edaphic properties of the 15 study stands selected across a biogeographic gradient in Western Canada.

		Location			Climatic properties (1981–2010)		Soil properties			
Region	**Site within region**	**Latitude (°N)**	**Longitude (°W)**	**Elevation (m)**	**MAT (°C)[a]**	**MAP (mm)[b]**	**Soil avail. P (ppm)**	**CEC (cmol(+)kg^{-1})[c]**	**Soil C:N**	**pH**
Williams Lake	WL1	51.73	123.01	1149	3.1	485	25.7 ± 8.6	11.3 ± 2.4	23.2	6.5
	WL2	51.74	122.78	1087	3.5	477	59.2 ± 24.6	15.6 ± 4.6	21.7	6.5
	WL3	51.74	122.76	1080	3.6	476	62.9 ± 9.3	21.2 ± 5.3	20.4	6.8
Revelstoke	R1	50.80	118.00	762	5.3	1216	117.5 ± 68.4	4.8 ± 1.7	24.4	5.8
	R2	50.79	117.98	706	5.6	1212	33.8 ± 9.8	4.1 ± 3.0	33.5	6.0
	R3	50.83	118.02	726	5.7	1167	232.4 ± 79.5	8.3 ± 2.0	30.1	5.6
Kamloops	K1	50.89	120.33	945	5.4	448	81.2 ± 18.3	21.5 ± 14.2	18.5	6.6
	K2	50.92	120.28	895	5.8	434	47.8 ± 17.0	21.9 ± 7.3	17.3	6.4
	K3	50.92	120.28	939	5.6	442	46.4 ± 19.3	15.5 ± 4.3	17.8	5.9
Salmon Arm	SA1	50.76	119.19	712	6.4	688	3.6 ± 1.5	34.8 ± 11	32.4	7.6
	SA2	50.65	119.05	721	6.1	701	161.8 ± 41.5	10.8 ± 6.1	28.5	6.5
	SA3	50.79	119.06	703	6.3	696	225.6 ± 95.3	12.3 ± 5.7	33.9	6.6
Nelson	N1	49.55	117.72	671	7.0	886	124.1 ± 34.1	3.8 ± 2.3	34.3	5.9
	N2	49.60	117.75	679	7.5	860	328.9 ± 77.8	5.7 ± 3.1	28.2	5.9
	N3	49.61	117.77	754	7.3	856	379.3 ± 22.1	5.9 ± 2.5	27.0	6.1

Soil properties are reported as mean ± standard error (SE, n = 5). [a]MAT, mean annual temperature; [b]MAP, mean annual precipitation; [c]CEC, effective cation exchange capacity.

Fine Root and Ectomycorrhiza Sampling and Processing

In each stand, single soil blocks (20 × 20 × 20 cm) were extracted from five Douglas-fir trees (200 cm from the trunk) in a manner that avoided clumping of sampling location (i.e., trees were at least 5 m apart). The soil blocks encompassed organic layers (L, F and H) and mineral horizons (A and B) to obtain a more complete vertical representation of the EMF community (Rosling et al., 2003). In addition, one organic (L, F, H layers) and one mineral soil sample (upper mineral horizons A and B, from the bottom of the organic layer to 10 cm depth) were collected using a trowel from each target tree (5 trees) to evaluate relationships between EMF communities and soil properties. A total of 75 sample sets were collected (5 regions, 3 stands per region, 5 trees per stand) and stored at 4°C until processing (up to 3 months).

To recover Douglas-fir fine roots and ectomycorrhizas, each soil block was soaked in water overnight before being washed over a 4 mm screen. All fine-root branches (<2 mm diameter) and fragments (>3 cm length) were collected from the sieve and sorted by tree species (based on the morphological key described in **Supplementary Table 2**). To guarantee random selection of EMF root tips, root fragments from each soil block were laid out on a numbered grid, and grid cells were selected using a random number generator. We examined and cleaned root fragments with a soft brush under the microscope until *c.* 50 live fine-root tips/soil block were collected. Excised fine-root tips were classified as individual morphotypes (based on the presence of a fungal mantle and according to Goodman et al., 1996) or uncolonized (root hairs present, or no visible mantle, usually unbranched). All tips were frozen at –80°C but only 5–10 tips per morphotype, across all soil blocks for the entire study, were used for later DNA analysis.

To assess the effect of fine-root traits on EMF taxonomic and functional diversity (exploration type), a total of 365 Douglas-fir fine-root branches was divided into individual root orders following the morphometric classification approach of Pregitzer et al. (2002). In this classification, the most distal, unbranched roots are first order and second-order roots begin at the junction of two first order roots, and so on. First-order roots were either colonized by EMF or were unbranched and the root tips uncolonized. We avoided thicker, longer pioneer first-order roots (Zadworny and Eissenstat, 2011). Each first-order group (i.e., all first-order roots of a given branch) was scanned separately and analyzed for morphological features using WinRHIZO (total length, total surface area, average diameter and total volume; 400 dpi, 165 -level gray scale, EPSON Perfection V800 Photo, STD 4800; WinRHIZO pro 2016 software, Regent Instruments Inc., Quebec City, Canada). For each first-order group, we determined specific root length, SRL (m g^{-1}), specific root area, SRA (cm^2 g^{-1}), and RTD (mg cm^{-3}). In addition, a subsample of 180 first-order roots were randomly selected and analyzed for C and N concentration (%) (see **Supplementary Text 1B**). These traits were selected for analysis due to their expected relationships with plant investment into root construction and maintenance and their benefits for soil resource foraging and acquisition.

Molecular Analyses of Ectomycorrhizas

Five to ten frozen EMF root tips for each of the 97 putative morphotypes (across all soil blocks for the entire study) were pooled and ground in liquid nitrogen before extracting fungal DNA using DNeasy® PowerSoil® kit, according to the manufacturer instructions (Qiagen®, 2017, ON, Canada). Fungal DNA extracts were sent to the Centre for Comparative Genomics and Evolutionary Bioinformatics (CGEB) at

Dalhousie University, Halifax, Canada. High-throughput sequencing (Illumina MiSeq v3 chemistry, 600 cycles; Illumina, San Diego, CA, United States) was used to identify the target EMF OTU. For the library preparation, amplicon fragments were PCR-amplified with fungal specific primers (ITS86F, GTGAATCATCGAATCTTTGAA; ITS4R, TCCTCCGCTTATTGATATGC) targeting the internal transcribed spacer region 2 (ITS2) (variable length, avg. *c.* 350 bp) of ribosomal DNA (White et al., 1990; Turenne et al., 1999; Vancov and Keen, 2009). Primers contained Illumina barcodes and overhang adaptors, allowing for a one-step PCR preparation of sequence libraries.

DNA sequencing results were analyzed using the QIIME2™ bioinformatics platform (Caporaso et al., 2010). The software package DADA2 was used to assemble bidirectional reads while filtering for quality and dereplicating sequences (Callahan et al., 2016). Prior to taxonomic assignment, representative sequences were exported from QIIME2 into fasta format and then ITS2 regions were extracted, chimeras were detected and non-ITS2 sequences were screened out using the software tool ITSx (Bengtsson-Palme et al., 2013). Extracted ITS2 sequence data were imported back into QIIME2 and the corresponding QIIME2 feature table was filtered to remove non-ITS sequence data. Demultiplexed, quality-controlled ITS2 sequence data were further screened for chimeras and then clustered into operational taxonomic units (OTUs) at 99% sequence similarity using a *de novo* clustering method with VSEARCH (Westcott and Schloss, 2015; Rognes et al., 2016).

For fungal species identification, we used the Basic Local Alignment Search Tool (BLAST) against the National Center for Biotechnology Information (NCBI) GenBank and UNITe public sequence databases (Abarenkov et al., 2010). We used two criteria to assign species or genus names to each morphotype: (i) Only EMF OTUs were considered (no consideration of root-associated fungi such as saprotrophs, root endophytes, molds or pathogens), and (ii) where pairwise identity (i.e., the amount of nucleotide that matches exactly between two different sequences) corresponding to the indicated EMF species was higher than 97%. In addition, morphotype characteristics were compared to reference photos from the Ectomycorrhizae Descriptions Database[1] and the DEEMY database[2]. Using this method, 82% of the morphotypes were identified to the species or genus level. For all but ten morphotypes, the assigned EMF species or genus corresponded to the EMF OTU with the highest number of reads; for the remaining ten morphotypes (morphotype IDs 81, 72c, 50, 55, 49, 34b, 31, 25, 3 and 2, see **Supplementary Table 3**), the EMF OTU with the highest number of reads had a low pairwise identity (<94) or was likely a contaminant. In this case, the EMF OTU with the second or third highest number of reads was chosen, but only if the morphology of the morphotype corresponded to the photos from the databases.

For each species or genus, exploration type (contact, short-distance, medium-distance smooth, medium-distance fringe and long-distance) was assigned after Agerer (2001, 2006) and compared to the published data from Ostonen et al. (2017), Pena et al. (2017), and Fernandez et al. (2017). For the genus *Sistotrema*, we referred to Ostonen et al. (2017) because it was not included in Agerer (2001, 2006). We assumed that exploration type was conserved within a genus as we did not study EMF genotypic trait variation. This assumption has been made in many other studies although plasticity of EMF mycelium can be substantial and should be taken into account more consistently (Hazard and Johnson, 2018; van der Linde et al., 2018). Hydrophobicity was assigned based on Lilleskov et al. (2011) and Fernandez et al. (2017).

Data Analyses

All statistical analyses were conducted in R version 3.5.1 (R Core Team, 2018) and results were considered statistically significant at $P < 0.05$. Fungal richness was examined across regions by estimating components of α-diversity: (i) observed species richness in each soil block and (ii) richness estimators: Chao1 (Chao, 1984), first- and second-order Jackknife (Burnham and Overton, 1979). Diversity patterns were examined by calculating the following diversity indices: Shannon–Wiener Diversity Index $\left(H' = -\sum pi \ln pi\right)$, Shannon's Evenness (E), and Simpson's Index of Diversity $\left(1 - D; D = 1 - \sum pi^2\right)$, where *pi* is the proportion of species *i* relative to the total number of species in a sample. We assessed the effect of region on EMF richness, evenness and diversity using a nested ANOVA (linear mixed effect model) with region as a fixed effect and site nested within region as a random effect using the function "*lmer*" from the *lme4* package. We did not rarefy to the lowest sampling depth (i.e., we only collected 12 root tips in a soil block from Revelstoke) because rarefaction curves indicated that our sampling effort was sufficient as it resulted in EMF species saturation (**Supplementary Figure 1**).

To investigate the effects of environment and fine-root traits on the taxonomic and functional structure of EMF communities, we first calculated the variance inflation factor (VIF) for each environmental (MAT, MAP, soil C:N, CEC, pH, soil available phosphorus) and root trait (SRL, SRA, diameter, RTD, root C:N) predictor, to avoid multicollinearity among predictive variables, using the "*vif*" function from the *usdm* package (Naimi et al., 2014). Predictors with the highest VIF were sequentially dropped until all VIF values were below three (Zuur et al., 2010). This process removed CEC and soil N from the environmental predictors and SRL from the root trait predictors. Second, unidentified morphotypes (from which DNA was not extracted and for which a sequence was not found) were removed before all analyses on the basis that reconsideration of photographic evidence suggested that they were most likely to have been dead root tips. A Hellinger transformation was applied to species and exploration type data matrices. We used a distance-based redundancy analysis (db-RDA; Legendre and Anderson, 1999) to examine β-diversity based on Bray–Curtis dissimilarities using the "*capscale*" function in *vegan*. The best model was chosen utilizing forward model selection with permutation tests (*P*-value for variable retention = 0.05). The general form of the models was:

[1] http://forestrydev.org/biodiversity/bcern

[2] www.deemy.de/

EMF Species or Exploration Type – Environmental Factors (e.g., MAT, MAP) or Root Traits (e.g., SRA, RTD)

Models were tested for significance using permutational multivariate analysis of variance (PERMANOVA, function "*adonis*" in *vegan*, 999 permutations), after assessing the multivariate homogeneity of regions dispersions (function "*betadisper*" in *vegan*; Oksanen et al., 2018; **Supplementary Figure 2**). Significant PERMANOVA effects were assessed using *post hoc* pairwise contrasts (function "*multiconstrained*" from the package *BiodiversityR*; Kindt, 2018).

The db-RDA /PERMANOVA approach was not developed to account for nested data (here, sites are nested within regions). Thus, to complement these analyses, we used a two-way approach, that only worked with two nested factors: (i) For the effect of sites within regions, we used PERMANOVA with permutations constrained within sites (strata = site in "*adonis*") and (ii) for the effect of regions, we ran a nested analysis of variance with the function "*nested.npmanova*" from the package *BiodiversityR*. These two complementary analyses were run on the models:

EMF Species or EMF Exploration Types – Regions/Sites

In addition, to account for the presence of mean-variance relationships in multivariate community analyses, we built multivariate generalized linear models using the package "*MVABUND*" (Wang et al., 2012). An offset (log of row sums) was added to the models to standardize the response variables and account for the unequal sample size. Models were run twice: with all the species and without the unresponsive species (coefficient $< |5|$). Model significance was tested with a likelihood-ratio test and univariate *P*-values were adjusted for multiple testing using a step-down resampling procedure.

RESULTS

Identification and Taxonomic Diversity

In this study, 3914 fine-root tips were extracted from 75 soil blocks and sorted into 97 putative EMF morphotypes (on average, 4.0 ± 0.2 morphotypes per soil block) of which 82 EMF morphotypes were successfully sequenced. The sequencing of the 82 morphotypes resulted in 6,322,065 sequences that were clustered into 1,901 OTUs. These OTUs comprised the following guilds: EMF, saprotrophs, root endophytes, molds or pathogens. Considering all the guilds, the average number of OTUs per morphotype was 69.0 ± 3.6 (**Supplementary Table 3**). Out of these 69 fungal OTUs per morphotype, on average, 10 OTUs were EMF (highlighted in red in **Supplementary Table 3**). After using the criteria described in the section "Molecular analyses of ectomycorrhizas," we assigned a unique EMF OTU to each of the 82 morphotypes. We then obtained 54 unique EMF OTUs because some morphotypes were assigned the same OTU (**Supplementary Table 4**). Of these 54 EMF OTU, 46 and 54% were identified to genus and species, respectively. Of the 54 EMF taxa, 91% were Basidiomycota and 9% were Ascomycota. In addition, 33% were resupinate fungi, 13% were hypogeous and 54% were mushroom-forming fungi. Tips from the 15 EMF morphotypes for which no sequences were obtained (most likely representing dead root tips) represented 10% of all the mycorrhizal root tips.

Species accumulation curves showed that almost the entirety of species richness was recovered for Kamloops. Alternatively, we recovered *c.* 80% of the estimated species richness for the remaining regions (**Supplementary Figure 1**). Richness estimators (Chao1, Jack1, Jack2) were similar to the observed species richness, which confirm that only a small number of species were not accounted for with our sampling scheme (**Supplementary Table 5A**). Revelstoke had the highest species richness per region with 25 species compared to 24 species in Salmon Arm and Williams Lake, followed by Nelson with 23 species and Kamloops with 20 species. We did not detect any differences in α-diversity among the five regions, where species richness averaged four EMF species/soil block for each region (**Supplementary Table 5B**). Similarly, species evenness and diversity estimated with Shannon and Simpson's diversity indexes were low, averaging 0.8 and 0.5, respectively, and did not vary by region.

Taxonomic Composition

Across the environmental gradients, the most abundant OTUs identified at the species level with >2% root tip abundance were *C. geophilum* (8.3%), *Lactarius rubrilacteus* (8%), *Russula mordax* (4%), *Lactarius* cf. *resimus* (2.5%), and *Cortinarius cedriolens* (2.1%), and the most abundant OTUs identified at the genus-only level were *Russula* sp. (8.4%), *Rhizopogon* sp. (5.6%), *Piloderma* cf. (3.3%), *Tomentella* sp. (3.3%), *Wilcoxina* sp. (3.4%) and *Suillus* sp. (2.5%; **Figure 2**; **Supplementary Table 4**). The five regions had five species/genera in common: *C. geophilum, Rhizopogon* sp., *Wilcoxina* sp., *Piloderma* sp. and *Russula* sp. The vast majority of fine-root tips colonized by *Russula* sp. and *Lactarius resimus* were found in the wettest region (Revelstoke; **Figure 2**), whereas the majority of root tips colonized by *C. geophilum*, *Tomentella*

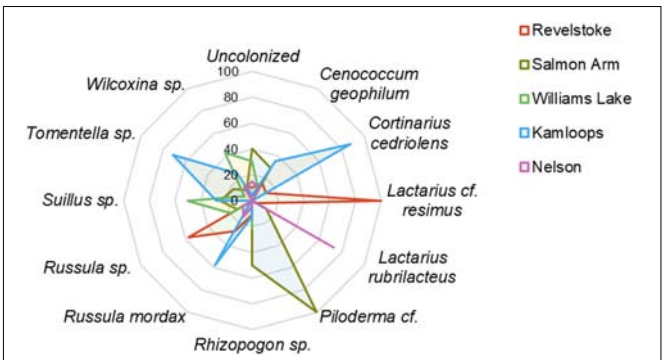

FIGURE 2 | Relative abundance (%) of ectomycorrhizal taxa on interior Douglas-fir among five regions in western Canada. Only the species/genera representing >2% of root tip abundance were included. For a given ectomycorrhizal species, numbers represent the percentage of root tips colonized by this species in each region.

sp., *Russula mordax* and *Cortinarius cedriolens* were found in the driest region (Kamloops). Almost half (43%) of the occurrence of *Wilcoxina* sp. and half of the occurrence of *Suillus* sp. were in the coldest region (Williams Lake). Alternatively, 24 and 11% of the occurrence of *Wilcoxina* sp. were in the warmest regions of Kamloops and Nelson, respectively, while the other half of *Suillus* sp. was also in warm regions (Salmon Arm and Kamloops). 75% of the occurrence of *Lactarius rubrilactus* was in the warmest region (Nelson).

Differences in climatic and edaphic conditions among the regions explained 12.2% (adjusted R^2 = 0.07) of the variation in the Douglas-fir EMF community composition (**Table 2A**). The first axis of the db-RDA was mostly explained by differences in MAT (score = –0.89) and soil C:N ratio (score = –0.55) and separated the EMF communities of the warmest region (Nelson, MAT = 7.3°C) from those in colder regions (William's Lake, MAT = 3.4°C; Kamloops, *c.* 5.6°C; Revelstoke, MAT = 5.5°C; **Figure 3A**). The second axis of the analysis was best explained by the gradients in precipitation (score = 0.53) and soil acidity (score = –0.79) and separated fungal communities in drier (Williams lake) and weakly calcareous soils (Salmon Arm) from those in wetter, strongly acidic Brunisolic soils (Revelstoke).

Genera such as *Tomentella, Cenococcum* and *Sebacina*, classified as the short-distance exploration type, were commonly associated with low MAT, soils richer in N and mid to low MAP (**Figure 3B**) and more generally, the short-distance exploration type taxa clustered in colder/drier regions. Fungal species such as *Rhizopogon* sp. and *Suillus* sp. with the long-distance type were exclusively found in drier climates while medium and medium-fringe explorers such as *Hydnum* sp., *Cortinarius* sp. and *Piloderma* sp. clustered in wet climates. Contact explorers such as *Russula* sp. and *Lactarius* sp. had a broader environmental range compared to the other exploration types but tended to be more abundant in wet climates. Uncolonized root tips occurred exclusively in regions with low MAT, low MAP and rich soils (high total N). Sites nested within regions did not have a significant effect on the EMF community composition, as revealed by the PERMANOVA with permutation restricted within sites (**Supplementary Table 6A**). However, the nested PERMANOVA confirmed the significant effect of regions (*P*-value = 0.001; **Supplementary Table 6B**)

Species-specific responses to the environmental gradients were obtained using multivariate generalized linear models (**Figure 4**; only the most responsive species, with a coefficient > |5| were included in this model, see **Supplementary Figure 3** for results with all the species). In agreement with the PERMANOVA model (except for soil pH), MAT, MAP and soil C:N ratio were all significantly related to shifts in EMF species across regions (**Table 2B**), yet EMF species were more responsive to MAP and MAT than soil C:N ratio (larger effect size; **Figure 4**). Generally, most taxa in the Russulaceae responded in a similar fashion, with species increasing in abundance with MAT and MAP (except for *Russula benwooii*). Response to climate was not similar in the Cortinariaceae and Sebacinaceae. For instance, *Cortinarius renidens* and *C. decipiens* expressed opposite responses to MAT, positive and negative, respectively, but had matching responses to MAP. Similarly, the genera *Sebacina* responded moderately but positively to MAP and negatively to MAT which was opposite to the response of the related genus *Helvellosebacina.*

TABLE 2 | Effect of climatic and edaphic conditions on interior Douglas-fir ectomycorrhizal fungal species community composition across five regions assessed by **(A)** PERMANOVA and **(B)** assessed by multivariate generalized linear model. Effect of climatic and edaphic conditions on **(C)** exploration types assessed by PERMANOVA.

(A) Ectomycorrhizal fungal community composition, PERMANOVA model

Abiotic factors	*Df*	*Pseudo F*	*Pseudo* R^2	*P*-value
MAP[a]	1	2.38	0.03	**<0.01**
MAT[b]	1	2.94	0.04	**<0.01**
soil C:N[c]	1	2.48	0.03	**<0.01**
pH	1	1.79	0.02	**0.02**
Residuals	69		0.88	
Total	73		1.00	

(B) Ectomycorrhizal fungal community composition, multivariate generalized model

Abiotic factors	*Res.Df*	*Df.diff*	*Deviance*	*P*-value
(Intercept)	61			
MAP	59	1	121.37	**0.01**
MAT	60	1	61.90	**0.01**
Soil C:N	58	1	98.22	**0.04**
pH	57	1	102.44	0.05

(C) Ectomycorrhizal fungal exploration type, PERMANOVA model

Abiotic factors	Df	Pseudo F	*Pseudo* R^2	*P*-value
MAP	1	5.4	0.07	**<0.01**
MAT	1	4.5	0.05	**<0.01**
soil C:N	1	3.94	0.05	**0.01**
Residuals	69		0.83	
Total	72		1.00	

Significant P-values (<0.05) are shown in bold. A negative binomial distribution was assumed for the multivariate model and explained deviance was tested after 999 permutations. [a]MAP, mean annual precipitation; [b]MAT, mean annual temperature; [c]soil C:N, soil carbon-to-nitrogen ratio.

Exploration Types

Considering all morphotypes, 36.4% of mycorrhizal root tips were contact-distance type, 25.5% were short-distance type, 20.0% medium-distance fringe type, 7.3%, medium-distance smooth type, and 7.3% long-distance type (**Supplementary Figure 4** and **Supplementary Table 4**). Precipitation and temperature explained 14% (adjusted R^2 = 0.14; **Table 2C**) of the variation in the dominant exploration types across the gradient. Only the first axis of the db-RDA was significant and represented the variation in MAP (score = –0.83; **Figure 5A**) and to a lesser extent MAT (score = –0.56). This axis separated long- and short-distance exploration types occurring in drier/colder regions from contact and medium-distance smooth exploration types in wetter regions (**Figure 5B**). We found no significant effect of site on exploration type abundance but found an

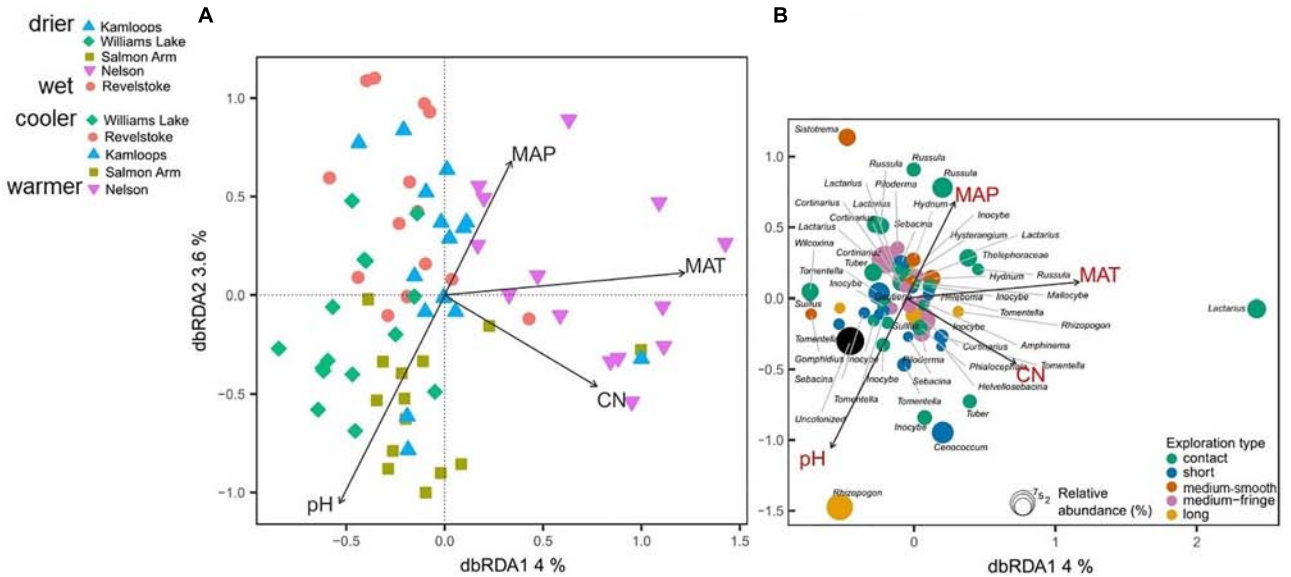

FIGURE 3 | Distance-based redundancy analysis (db-RDA) sample **(A)** and species **(B)** ordinations based on ectomycorrhizal fungal abundance on interior Douglas-fir roots across five regions in western Canada. Only the variation explained by environmental variables is visualized. The ectomycorrhizal species are color-coded by fungal exploration type and are sized according to their relative abundance. The species epithet (when known) was removed to improve readability. MAP, mean annual precipitation; MAT, mean annual temperature; CN, soil carbon-to-nitrogen ratio. To aid comparison, predictor variables were standardized (*z*-scores) prior to analysis and are therefore unitless. Contact-, short- and medium-distance smooth exploration types are hydrophylic while medium-distance fringe and long-distance exploration types are hydrophobic.

effect of region (*P*-value = 0.02; result not shown), whereas multivariate generalized linear models did not yield significant results (result not shown).

Fine-Root Traits and Fungi

Douglas-fir fine-root morphological and chemical traits explained 5% (adjusted R^2 = 0.02; **Table 3**) of shifts in EMF species community structure. Only the first axis of the db-RDA was significant and was represented by the variation in first-order root C:N ratio (score = –0.72) and RTD (score = 0.83; **Figure 6A**). This axis separated the symbionts associated with fine roots of low RTD (in Williams Lake and Nelson) from those associated with fine roots of low C:N ratio (mainly in Kamloops). Fungal taxa such as *Wilcoxina*, *Tomentella* and *Sebacina* that were classified as contact and short exploration types tended to cluster together and were related to fine roots with low RTD (**Figure 6B**). Similarly, uncolonized root tips were all associated with fine roots of low RTD. Alternatively, medium-fringe explorers such as *Cortinarius*, *Piloderma* and *Amphinema*, as well as the short distance explorer, *Cenococcum* tended to be more abundant on fine roots with high RTD. The multivariate generalized linear model did not yield significant results (result not shown).

DISCUSSION

The wide gradient in climate and soil fertility across southern British Columbia was ideal for investigating the extent of environmental filtering on EMF community taxonomic and functional structure (exploration type) across populations of Douglas-fir. Our first hypothesis was partly rejected because climate and soil fertility were not related to either EMF species richness or diversity. However, abiotic factors (MAT, MAP and soil C:N) did filter EMF community composition and the abundance of exploration types. As predicted, medium-fringe, and also contact explorers were more abundant in less fertile environments (as defined by lower pH, CEC, and available P), however, our second hypothesis was only partly confirmed because these exploration types were also associated with warmer or wetter environments. We did not find evidence for a functional connection between root diameter and EMF exploration type within Douglas-fir populations, which contradicts our third hypothesis.

Ectomycorrhizal Fungal Richness and Diversity

Contrary to our first hypothesis, we found no evidence that EMF diversity and richness varied across environmental gradients. However, most of the studies that found temperature or soil fertility to have an impact on EMF diversity used experimental treatments or covered continental gradients (Deslippe et al., 2011; Suz et al., 2014; Haas et al., 2018; Köhler et al., 2018; Rosinger et al., 2018). It is then possible that results from our regional-scale biogeographic gradient may not directly compare to these studies with regard to EMF diversity. Nonetheless, EMF richness was not affected by climatic transfer in a genecological study in temperate rainforests of coastal British Columbia (Kranabetter et al., 2015b) or by experimental warming in boreal forests of Minnesota (Fernandez et al., 2017; Mucha et al., 2018).

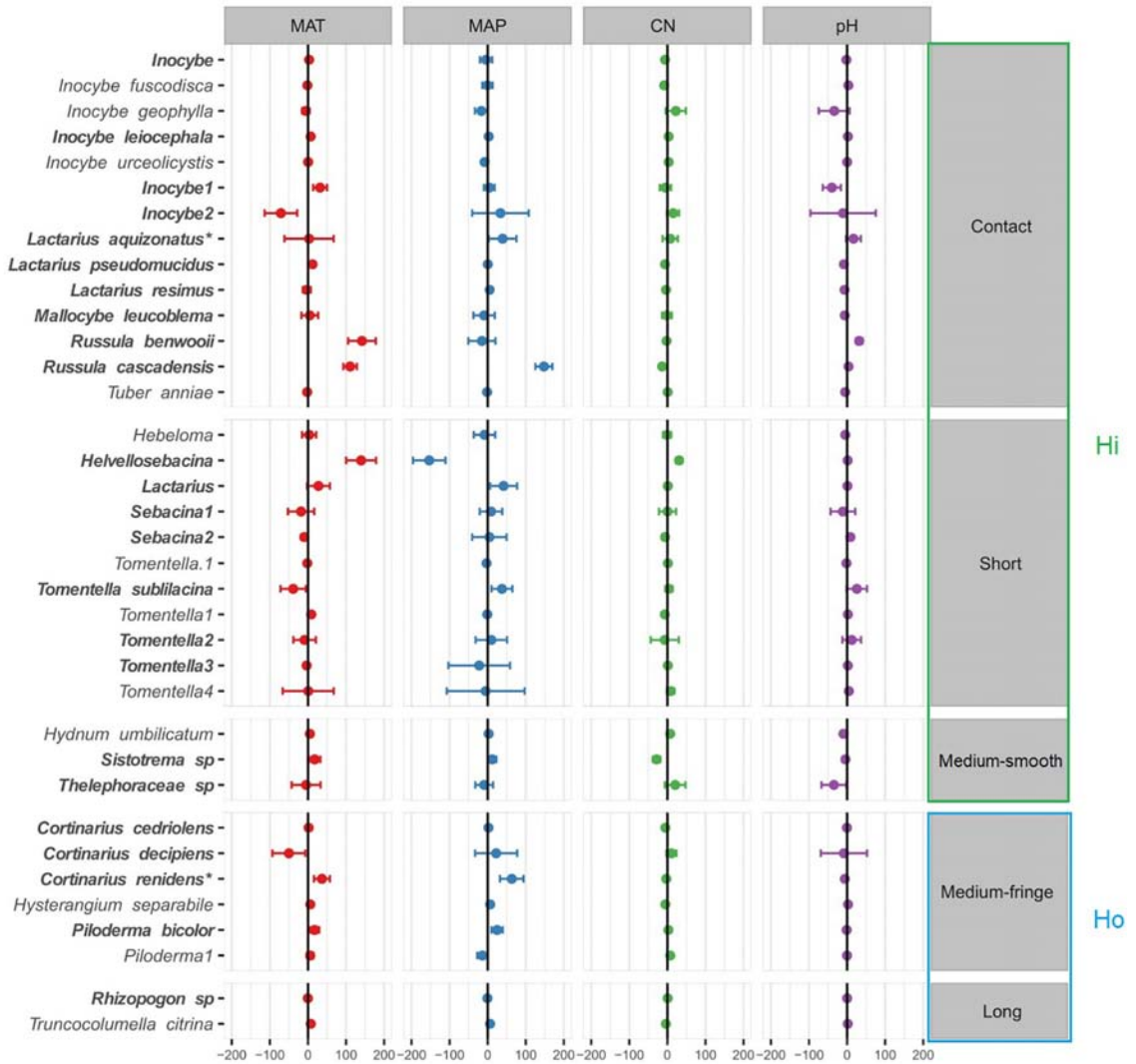

FIGURE 4 | Ectomycorrhizal fungal species-specific response to environmental factors based on multivariate generalized linear models. Only species that were responsive were added to the model (coefficient > |5|). Circles (•) represent species coefficients and lines, 95% confidence intervals. Species were grouped by exploration type indicated at the right-hand side of the plot, MAT, mean annual temperature; MAP, mean annual precipitation; CN, soil carbon-to-nitrogen ratio. To aid comparison, predictor variables were standardized (*z*-scores) prior to analysis and are therefore unitless. Hi, hydrophylic; Ho hydrophobic.

In our study, EMF communities were dominated by host-generalist taxa such as *C. geophilum, L. rubrilactus* and *Russula*, whereas taxa in *Rhizopogon* and *Suillus lakei* that are specific to the Pinaceae and Douglas-fir, respectively, represented only 8% of the total colonized root tips. This pattern could explain the lack of changes in richness and diversity because the host-generalist taxa tend to be less sensitive to environmental changes (Bahram et al., 2012; Mucha et al., 2018). Alternatively, if rare or specialist taxa were to dominate EMF communities in our study, we could have observed a change in richness and diversity (Bahram et al., 2012; Mucha et al., 2018). It is important to mention that root tips communities in our study provide a measure of the investment of the host and fungus in nutrient exchange sites and enable assessment of fungal species abundance. However, it does not necessarily represent the community of extraradical hyphae, especially in the case of long-distance colonized root tips that have higher mycelial space occupation than medium-distance smooth and short-distance colonized root tips (Weigt et al., 2012). In addition, shifts in Douglas-fir rooting depth across regions may impact EMF diversity estimates (**Supplementary Table 1**; Pickles and Pither, 2014). Our sampling scheme was consistent along the gradient, which may have hindered the detection of changes in EMF richness and diversity deeper in the soil profile.

Abiotic Drivers at the Regional Scale

In our study, temperature, precipitation and soil C:N ratio moderately but significantly explained some of the changes in EMF community assembly, despite the relatively small

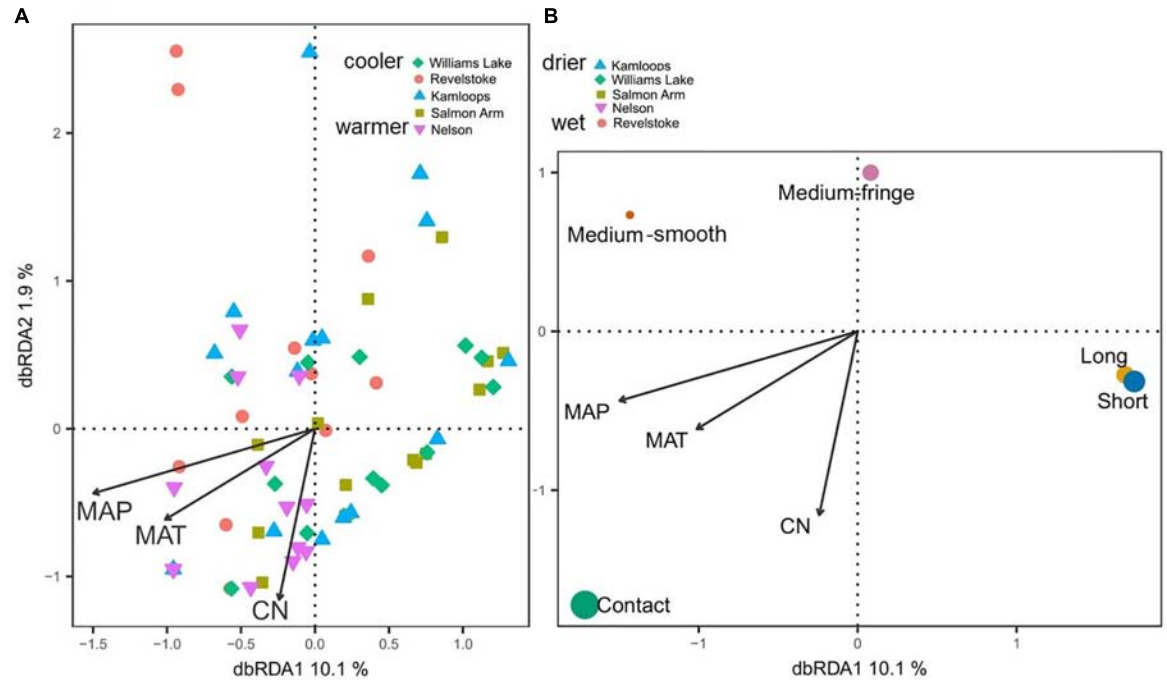

FIGURE 5 | Distance-based redundancy analysis (db-RDA) sample **(A)** and exploration type **(B)** ordinations based on ectomycorrhizal fungal exploration type on interior Douglas-fir across five regions in western Canada. The ectomycorrhizal fungal exploration types are sized according to their relative abundance. MAP, mean annual precipitation; MAT, mean annual temperature; CN, soil carbon-to-nitrogen ratio. To aid comparison, predictor variables were standardized (*z*-scores) prior to analysis and are therefore unitless. Contact-, short- and medium-distance smooth exploration types are hydrophylic while medium-distance fringe and long-distance exploration types are hydrophobic.

TABLE 3 | Effect of fine-root (first-order) morphological and chemical traits on interior Douglas-fir ectomycorrhizal fungal species community composition across five regions assessed by PERMANOVA.

Fine-root traits	*Df*	*Pseudo F*	*Pseudo* R^2	*P*-value
RTD[a]	1	1.88	0.03	**0.01**
Fine-root C:N[b]	1	1.93	0.03	**0.01**
Residuals	69		0.95	
Total	71		1.00	

Significant P-value (<0.05) effects are shown in bold. [a]*RTD, root tissue density.* [b]*Fine-root C:N, fine-root carbon-to-nitrogen ratio.*

ranges in temperature and soil fertility encompassed here. Hence, our first hypothesis was partly confirmed. We found that EMF communities varied from communities dominated by *Tomentella* and *Sebacina* in the colder, more fertile regions (higher soil pH, CEC and total N) of Douglas-fir's natural range, to communities dominated by *Hydnum* sp., *Cortinarius* sp. or Russulaceae members in the warmer, less fertile regions of the range. These results add to those of Pickles et al. (2015a), who compared variation in EMF community primarily between inside and outside the range of Douglas-fir when studying EMF communities on Douglas-fir seedlings.

Our finding that temperature, precipitation and soil C:N ratio appeared to act as filters explaining part of the regional variation in EMF assemblages was similar to that of Pena et al. (2017). However, large-scale studies in Europe have shown different responses. For example, EMF community composition varied with temperature, pH and soil nutrients but not with precipitation in some European forests (Rosinger et al., 2018; van der Linde et al., 2018), whereas elsewhere precipitation, but not temperature, influenced EMF community structure (Jarvis et al., 2013; Suz et al., 2014).

In our study, the effect of temperature and soil fertility on EMF community structure could be related to co-evolutionary history between Douglas-fir populations and fungal symbionts (Gehring et al., 2017; Pither et al., 2018; Strullu-Derrien et al., 2018) because local adaptation of Douglas-fir populations is driven by temperature and soil N availability but can also be mediated by EMF (Rehfeldt et al., 2014; Kranabetter et al., 2015b; Pickles et al., 2015b). Temperature directly influences tree growth potential and may thus impact host C supply to fungal taxa. In turn this could induce a shift in EMF community structure across our study regions as EMF taxa differ in their C cost. Alternatively, temperature may have indirectly affected EMF assemblage through its impact on soil fertility such as availability of NO_3^- and NH_4^+ (Kranabetter et al., 2015b). In addition to temperature, fitness and growth of Douglas-fir populations have been shown to relate to soil N availability (Kranabetter et al., 2015b), and close affiliation of Douglas-fir populations with local EMF symbionts may maximize tree nutritional adaptations (Kranabetter et al., 2015a; Leberecht et al., 2015). In turn this may reinforce

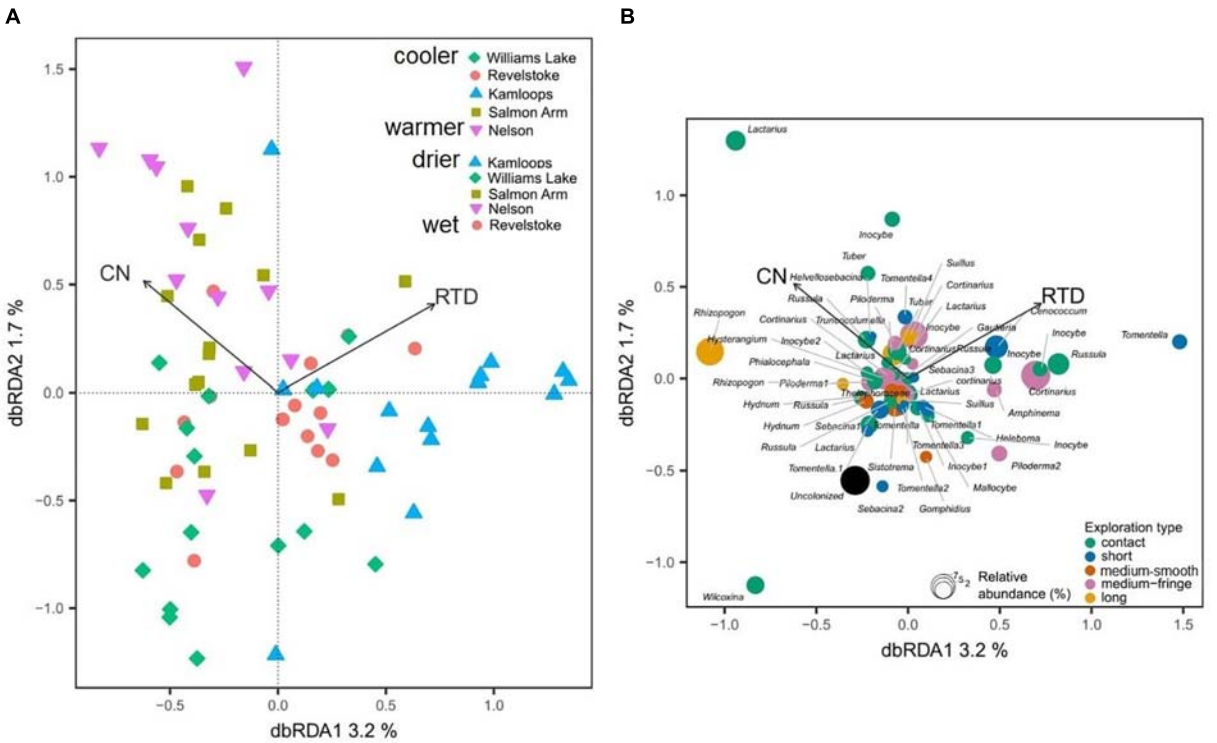

FIGURE 6 | Distance-based redundancy analysis (db-RDA) sample **(A)** and species **(B)** ordinations based on ectomycorrhizal fungal abundance on interior Douglas-fir across five regions. Only variation explained by Douglas-fir fine-root traits is visualized. The ectomycorrhizal species are color-coded by fungal exploration type and are sized according to their relative abundance. The species epithet (when known) was removed to improve readability. CN, fine-root carbon-to-nitrogen ratio; RTD, fine-root tissue density. To aid comparison, predictor variables were standardized (*z*-scores) prior to analysis and are therefore unitless. Contact-, short- and medium-distance smooth exploration types are hydrophylic while medium-distance fringe and long-distance exploration types are hydrophobic.

the filtering effect of soil C:N ratio on EMF assemblage observed in our study.

Taxonomic and Morphological Responses

We hypothesized that medium or long-distance explorers would be more abundant in colder climates or in soils with a high C:N ratio. Our results partly confirm this hypothesis as the hydrophobic, medium-fringe explorers *Cortinarius* sp., *Piloderma* sp., or *Amphinema* sp. and taxa in the Russulaceae classified as contact explorers, were more abundant in the warmer, less fertile environments of our study area, whereas the hydrophilic, short- and medium-distance smooth type, were more frequent and abundant in colder and more fertile conditions.

In our study system, this pattern of longer distance explorers associated with warmer climates can been linked to higher host photosynthetic capacity that can sustain more C demanding mycorrhizal symbionts (Jarvis et al., 2013; Fernandez et al., 2017; Köhler et al., 2018; Mucha et al., 2018; Rosinger et al., 2018). Furthermore, the positive response to temperature of the genera *Cortinarius* (except *C. decipiens*) and *Lactarius* are potentially related to the increased genetic capacity within these taxa for mobilization of N from organic matter (Bödeker et al., 2014; Kyaschenko et al., 2017). This may also hold true for the genus Russula as Jones et al. (2010) and Kyaschenko et al. (2017) highlighted the positive correlation between *Russula* taxa and enzymes mobilizing N and P from organic matter. Lilleskov et al. (2002, 2018) further classified *Cortinarius* and *Russula* as "nitrophobic" taxa. However, Looney et al. (2018) suggested that some members in the Russulaceae have lost the capacity to access C from organic matter.

The supposition that taxa associated with warmer climates tend to have competitive advantages in low N environments is supported by our data. Russulaceae and Cortinariaceae (with the exception of *C. decipiens*) were positively related to both C:N ratio and temperature. Consequently, in less fertile environments, fungi with proteolytic abilities such as *Cortinarius* or hydrophobic fungi with rhizomorphs such as *Piloderma* may be more competitive because they preferentially use insoluble, organic N. The latter fungi are likely less beneficial in richer soils (high total N concentration) where extensive exploration is not required (Ekblad et al., 2013; Koide et al., 2014; Suz et al., 2014). Similarly, Douglas-fir trees in the colder, more fertile environments of our study area may favor hydrophilic symbionts which potentially cost the plant less C, such as EMF with short emanating hyphae or "nitrophilic" EMF such as *Tomentella* (Nilsson and Wallander, 2003; Tedersoo and Smith, 2013; Haas et al., 2018).

Ascomycetes such as *Wilcoxina* sp., *Tuber* sp. and the drought-tolerant *C. geophilum*, exclusively occurred in the drier environments of our study area. This is in agreement with studies showing positive shifts in Ascomycetes abundance from mesic to xeric conditions (Allison and Treseder, 2008; Fernandez et al., 2017). It has been hypothesized that Ascomycetes have a lower C cost to their host due to their relatively thin mantles and contact or short-distance exploration types (Fernandez et al., 2017). This may be beneficial in the drier regions of southern British Columbia where water and carbon availability for growth is reduced and where lower basal area increment of Douglas-fir is accompanied by lower fine-root carbohydrate reserve concentration (Wiley et al., 2018). The long-distance explorer *Rhizopogon* also exclusively occurred in the drier climates of our study area. This likely represents host preference for drought-tolerant EMF as this taxon can transport water over long distances (e.g., Parke et al., 1983). As drier soils limit the diffusion rate of resources, this pattern of spatial niche separation could be an adaptation to stressful conditions (Pickles et al., 2015a). In addition, regions with drier soils were also phosphorus-limited, yet *C. geophilum* and *Rhizopogon,* both have a competitive advantage for plant nutrition in these conditions because the former possess acid phosphatase for P hydrolysis and mobilization, while the latter can forage for P more efficiently. This is because long-distance explorers have enhanced capacity for soil exploration and may therefore exploit soil resource such as P more completely (Kyaschenko et al., 2017; Köhler et al., 2018).

Association Between Fine-Root and Mycorrhizal Traits

We expected fine-root diameter to be correlated with abundance of exploration types along the biogeographic gradient, yet we found RTD and fine-root C:N, but not diameter, to be significantly related to EMF community structure and patterns of exploration type frequency. Fine roots with lower tissue density occurred predominantly in colder regions (Defrenne et al., unpublished) and were more frequently uncolonized or colonized by EMF with short emanating hyphae. As we do not provide evidence for a functional connection between root diameter and mycorrhizal exploration types, EMF traits might not compensate for changes in fine-root structure.

Fungi with short emanating hyphae in colder conditions may instead serve a function to protect roots from environmental stresses (e.g., frost, pathogens; Marx, 1972). This would increase root persistence without investing as much in short hyphae construction and maintenance as in hyphae for long-distance exploration. In our study area, colder environments (excluding Revelstoke) were also poorer in available phosphorus, therefore, resistance to root pathogens, potentially conferred by short-distance type EMF, could be at the expense of efficient P exploitation, for which long-distance exploration types are thought to be better adapted (Köhler et al., 2018).

Alternatively, Zadworny et al. (2017) argue that lower RTD in absorptive roots could be due to increased percentage of mycorrhizal mantle area in the root, which would then relate to enhanced capacity for resource uptake. The cost of producing new root tips with low RTD is also lower than producing roots with high RTD, this potentially leads to increased efficiency in nutrient acquisition and thus to a more precise foraging strategy. In addition to contributing to the RTD, the mycorrhizal mantle can contribute to the chemistry of first- and second-order roots (Ouimette et al., 2013). For example, a significant proportion of the fine-root N of the Kamloops region (higher root N concentration) could be from fungal origin, particularly from the mantle formed by medium-fringe taxa such as *Cortinarius cedriolens* (**Figures 2**, **6**) which colonized fine-root tips from Kamloops and had a slightly negative response to soil C:N (**Figure 3**).

In any case, selection for complementarity in foraging strategy was not a major mechanism within ectomycorrhizal tree species in a study by Chen et al. (2018a) but could be more common in arbuscular mycorrhizal tree species (Eissenstat et al., 2015; Liu et al., 2015; Zhang et al., 2019). Chen et al. (2018a) proposed bet hedging as a potential explanation because EMF traits selected for root pathogen protection may be at odds with those selected for resource foraging. Finally, the absence of a relationship between root diameter and exploration type abundance could be associated with the design of our study compared to that of Chen et al. (2018a). We used a regional scale biogeographic gradient and selected a ectomycorrhizal tree host that further expressed moderate intraspecific variation in root diameter compared to variation in RTD or root C:N, whereas Chen et al. (2018a) surveyed several ectomycorrhizal tree species with large differences in mean root diameter and investigated links between roots and ectomycorrhizal traits at the level of the nutrient patch.

CONCLUSION

We combined fine-root and EMF trait measurements with next-generation sequencing across a biogeographic gradient. Douglas-fir EMF communities were dominated by host-generalist taxa which potentially explains the low variation in EMF α-diversity across environments. We did find, however, that temperature, precipitation and soil C:N ratio affected EMF community dissimilarities and exploration type abundance. Fungi with rhizomorphs (e.g., *Piloderma* sp.) or proteolytic abilities (e.g., *Cortinarius* sp.) dominated EMF communities in warmer and less fertile environments, whereas Ascomycetes (e.g., *C. geophilum*) or shorter distance explorers, which potentially cost the plant less C, were favored in colder/drier climates and richer soils (higher total N concentration). This pattern might be associated with co-evolutionary history between Douglas-fir populations and fungal symbionts, suggesting that the success of Douglas-fir as climate changes and stress increases may be dependent on maintaining strong associations with local communities of mycorrhizal fungi. At the regional scale, we did not find evidence for a functional connection between root diameter and EMF

exploration types within Douglas-fir populations. Whether this implies no complementarity in resource foraging between fine roots and EMF is difficult to say, but this suggests that incorporating mycorrhizal symbiosis or at least EMF symbiosis into broader root trait frameworks may not be a suitable option if we are to represent the diversity of below-ground resource strategies. We thus encourage future research to simultaneously examine both root and fungal traits as separate entities.

DATA AVAILABILITY

The datasets generated for this study are available on request to the corresponding author.

AUTHOR CONTRIBUTIONS

CD, WR, BP, and SS designed the study. CED wrote the manuscript. WR and CD collected the fine-root and mycorrhizal trait data. SG and CD carried out the molecular analyses. TP and CD carried out the data analyses. TP, BP, and SS contributed to the data interpretation, and drafted and edited the manuscript. All authors contributed critically to the drafts and gave final approval for publication.

FUNDING

This research was supported by the Natural Sciences and Engineering Research Council of Canada (CREATE Grant, Strategic Partnership Grant and Discovery Grant to SS) and by the Daniel E. Stuntz Memorial Foundation (grant to CD and SG).

ACKNOWLEDGMENTS

We thank the British Columbia Ministry of Forests, Lands and Natural Resource Operations for facilitating this research. We also thank Dr. Robert D. Guy and Dr. Lori D. Daniels at the University of British Columbia, and M. Luke McCormack for providing feedback. We would like to thank our research assistants: Jaylen Bastos, Charles Cohen, Supreet Dhillon, Caitlin Low, Esmee MacDonald, Daniel Malvin, Hannah Sachs, Yifan Sun, Bailey Williams, Tong Ye, and Zuofang Zhang.

SUPPLEMENTARY MATERIAL

The Supplementary Material for this article can be found online at: https://www.frontiersin.org/articles/10.3389/fpls.2019.00643/full#supplementary-material

REFERENCES

Abarenkov, K., Henrik Nilsson, R., Larsson, K.-H., Alexander, I. J., Eberhardt, U., Erland, S., et al. (2010). The UNITE database for molecular identification of fungi–recent updates and future perspectives. *New Phytol.* 186, 281–285. doi: 10.1111/j.1469-8137.2009.03160.x

Agerer, R. (2001). Exploration types of ectomycorrhizae. *Mycorrhiza* 11, 107–114. doi: 10.1007/s005720100108

Agerer, R. (2006). Fungal relationships and structural identity of their ectomycorrhizae. *Mycol. Prog.* 5, 67–107. doi: 10.1093/treephys/tpq014

Allison, S. D., and Treseder, K. K. (2008). Warming and drying suppress microbial activity and carbon cycling in boreal forest soils. *Glob. Change Biol.* 14, 2898–2909. doi: 10.1111/j.1365-2486.2008.01716.x

Bahram, M., Põlme, S., Kõljalg, U., Zarre, S., and Tedersoo, L. (2012). Regional and local patterns of ectomycorrhizal fungal diversity and community structure along an altitudinal gradient in the Hyrcanian forests of northern Iran. *New Phytol.* 193, 465–473. doi: 10.1111/j.1469-8137.2011.03927.x

Bengtsson-Palme, J., Ryberg, M., Hartmann, M., Branco, S., Wang, Z., Godhe, A., et al. (2013). Improved software detection and extraction of ITS1 and ITS2 from ribosomal ITS sequences of fungi and other eukaryotes for analysis of environmental sequencing data. *Methods Ecol. Evol.* 4, 914–919.

Bjorkman, A. D., Myers-Smith, I. H., Elmendorf, S. C., Normand, S., Rüger, N., Beck, P. S. A., et al. (2018). Plant functional trait change across a warming tundra biome. *Nature* 562, 57–62. doi: 10.1038/s41586-018-0563-7

Bödeker, I. T. M., Clemmensen, K. E., de Boer, W., Martin, F., Olson, Å, and Lindahl, B. D. (2014). Ectomycorrhizal Cortinarius species participate in enzymatic oxidation of humus in northern forest ecosystems. *New Phytol.* 203, 245–256. doi: 10.1111/nph.12791

British Columbia Ministry of Forests and Range, and British Columbia Ministry of Environment (2010). *Field Manual for Describing Terrestrial Ecosystems*. Victoria, VIC: B.C. Ministry of Forests and Range.

Burnham, K. P., and Overton, W. S. (1979). Robust estimation of population size when capture probabilities vary among animals. *Ecology* 60, 927–936. doi: 10.2307/1936861

Callahan, B. J., McMurdie, P. J., Rosen, M. J., Han, A. W., Johnson, A. J. A., and Holmes, S. P. (2016). DADA2: High-resolution sample inference from Illumina amplicon data. *Nat. Methods* 13, 581–583. doi: 10.1038/nmeth.3869

Caporaso, J. G., Kuczynski, J., Stombaugh, J., Bittinger, K., Bushman, F. D., Costello, E. K., et al. (2010). QIIME allows analysis of high-throughput community sequencing data. *Nat. Methods* 7, 335–336.

Chao, A. (1984). Nonparametric estimation of the number of classes in a population. *Scand. J. Stat.* 11, 265–270.

Cheeke, T. E., Phillips, R. P., Brzostek, E. R., Rosling, A., Bever, J. D., and Fransson, P. (2017). Dominant mycorrhizal association of trees alters carbon and nutrient cycling by selecting for microbial groups with distinct enzyme function. *New Phytol.* 214, 432–442. doi: 10.1111/nph.14343

Chen, W., Eissenstat, D. M., and Koide, R. T. (2018a). Root diameter predicts the extramatrical hyphal exploration distance of the ectomycorrhizal fungal community. *Ecosphere* 9:e02202. doi: 10.1002/ecs2.2202

Chen, W., Koide, R. T., and Eissenstat, D. M. (2018b). Nutrient foraging by mycorrhizas: from species functional traits to ecosystem processes. *Funct. Ecol.* 32, 858–869. doi: 10.1111/nph.13451

Cheng, L., Chen, W., Adams, T. S., Wei, X., Li, L., McCormack, M. L., et al. (2016). Mycorrhizal fungi and roots are complementary in foraging within nutrient patches. *Ecology* 97, 2815–2823. doi: 10.1002/ecy.1514

Clemmensen, K. E., Bahr, A., Ovaskainen, O., Dahlberg, A., Ekblad, A., Wallander, H., et al. (2013). Roots and associated fungi drive long-term carbon sequestration in boreal forest. *Science* 339, 1615–1618. doi: 10.1126/science.1231923

Coops, N. C., Hember, R. A., and Waring, R. H. (2010). Assessing the impact of current and projected climates on douglas-fir productivity in british columbia, canada, using a process-based model (3-PG). *Can. J. For. Res.* 40, 511–524. doi: 10.1139/x09-201

Courty, P.-E., Munoz, F., Selosse, M.-A., Duchemin, M., Criquet, S., Ziarelli, F., et al. (2016). Into the functional ecology of ectomycorrhizal communities: environmental filtering of enzymatic activities. *J. Ecol.* 104, 1585–1598. doi: 10.1111/1365-2745.12633

Deslippe, J. R., Hartmann, M., Mohn, W. W., and Simard, S. W. (2011). Long-term experimental manipulation of climate alters the ectomycorrhizal community of

Betula nana in Arctic tundra. *Glob. Change Biol.* 17, 1625–1636. doi: 10.1111/j.1365-2486.2010.02318.x

Eissenstat, D. M., Kucharski, J. M., Zadworny, M., Adams, T. S., and Koide, R. T. (2015). Linking root traits to nutrient foraging in arbuscular mycorrhizal trees in a temperate forest. *New Phytol.* 208, 114–124. doi: 10.1111/nph.13451

Ekblad, A., Wallander, H., Godbold, D. L., Cruz, C., Johnson, D., Baldrian, P., et al. (2013). The production and turnover of extramatrical mycelium of ectomycorrhizal fungi in forest soils: role in carbon cycling. *Plant Soil Dordr.* 366, 1–27. doi: 10.1007/s11104-013-1630-3

Fernandez, C. W., Langley, J. A., Chapman, S., McCormack, M. L., and Koide, R. T. (2016). The decomposition of ectomycorrhizal fungal necromass. *Soil Biol. Biochem.* 93, 38–49. doi: 10.1016/j.soilbio.2015.10.017

Fernandez, C. W., Nguyen, N. H., Stefanski, A., Han, Y., Hobbie, S. E., Montgomery, R. A., et al. (2017). Ectomycorrhizal fungal response to warming is linked to poor host performance at the boreal-temperate ecotone. *Glob. Change Biol.* 23, 1598–1609. doi: 10.1111/gcb.13510

Gehring, C. A., Sthultz, C. M., Flores-Rentería, L., Whipple, A. V., and Whitham, T. G. (2017). Tree genetics defines fungal partner communities that may confer drought tolerance. *Proc. Natl. Acad. Sci. U.S.A.* 114, 11169–11174. doi: 10.1073/pnas.1704022114

Goodman, D., Durall, D., Trofymow, J., and Berch, S. (1996). *A Manual of Concise Descriptions of North American Ectomycorrhizae Including Microscopic and Molecular Characterization*. Victoria, BC: Mycologue Publications and the Canada-BC Forest Resource Development Agreement, Pacific Forestry Centre.

Haas, J. C., Street, N. R., Sjödin, A., Lee, N. M., Högberg, M. N., Näsholm, T., et al. (2018). Microbial community response to growing season and plant nutrient optimisation in a boreal Norway spruce forest. *Soil Biol. Biochem.* 125, 197–209. doi: 10.1016/j.soilbio.2018.07.005

Hazard, C., and Johnson, D. (2018). Does genotypic and species diversity of mycorrhizal plants and fungi affect ecosystem function? *New Phytol.* 220, 1122–1128. doi: 10.1111/nph.15010

Heijden, M. G. A. V. D., and Horton, T. R. (2009). Socialism in soil? The importance of mycorrhizal fungal networks for facilitation in natural ecosystems. *J. Ecol.* 97, 1139–1150. doi: 10.1111/j.1365-2745.2009.01570.x

Hobbie, E. A., and Agerer, R. (2010). Nitrogen isotopes in ectomycorrhizal sporocarps correspond to belowground exploration types. *Plant Soil* 327, 71–83. doi: 10.1007/s11104-009-0032-z

Hoeksema, J. D., Bever, J. D., Chakraborty, S., Chaudhary, V. B., Gardes, M., Gehring, C. A., et al. (2018). Evolutionary history of plant hosts and fungal symbionts predicts the strength of mycorrhizal mutualism. *Commun. Biol.* 1:116. doi: 10.1038/s42003-018-0120-9

Hu, Y., Veresoglou, S. D., Tedersoo, L., Xu, T., Ge, T., Liu, L., et al. (2019). Contrasting latitudinal diversity and co-occurrence patterns of soil fungi and plants in forest ecosystems. *Soil Biol. Biochem.* 131, 100–110. doi: 10.1016/j.soilbio.2019.01.001

Jarvis, S., Woodward, S., Alexander, I. J., and Taylor, A. F. S. (2013). Regional scale gradients of climate and nitrogen deposition drive variation in ectomycorrhizal fungal communities associated with native Scots pine. *Glob. Change Biol.* 19, 1688–1696. doi: 10.1111/gcb.12178

Jassey, V. E. J., Reczuga, M. K., Zielińska, M., Słowińska, S., Robroek, B. J. M., Mariotte, P., et al. (2018). Tipping point in plant-fungal interactions under severe drought causes abrupt rise in peatland ecosystem respiration. *Glob. Change Biol.* 24, 972–986. doi: 10.1111/gcb.13928

Jones, M. D., Twieg, B. D., Ward, V., Barker, J., Durall, D. M., and Simard, S. W. (2010). Functional complementarity of Douglas-fir ectomycorrhizas for extracellular enzyme activity after wildfire or clearcut logging. *Funct. Ecol.* 24, 1139–1151. doi: 10.1111/j.1365-2435.2010.01699.x

Kindt, R. (2018). *BiodiversityR: Package for Community Ecology and Suitability Analysis. Version 2.9-2*. Available at: https://CRAN.R-project.org/package=BiodiversityR (accessed December 15, 2018).

Köhler, J., Yang, N., Pena, R., Raghavan, V., Polle, A., and Meier, I. C. (2018). Ectomycorrhizal fungal diversity increases phosphorus uptake efficiency of European beech. *New Phytol.* 220, 1200–1210. doi: 10.1111/nph.15208

Koide, R. T., Fernandez, C., and Malcolm, G. (2014). Determining place and process: functional traits of ectomycorrhizal fungi that affect both community structure and ecosystem function. *New Phytol.* 201, 433–439. doi: 10.1111/nph.12538

Kranabetter, J. M., Hawkins, B. J., Jones, M. D., Robbins, S., Dyer, T., and Li, T. (2015a). Species turnover (β-diversity) in ectomycorrhizal fungi linked to uptake capacity. *Mol. Ecol.* 24, 5992–6005. doi: 10.1111/mec.13435

Kranabetter, J. M., Stoehr, M., and O'Neill, G. A. (2015b). Ectomycorrhizal fungal maladaptation and growth reductions associated with assisted migration of Douglas-fir. *New Phytol.* 206, 1135–1144. doi: 10.1111/nph.13287

Kyaschenko, J., Clemmensen, K. E., Hagenbo, A., Karltun, E., and Lindahl, B. D. (2017). Shift in fungal communities and associated enzyme activities along an age gradient of managed Pinus sylvestris stands. *ISME J.* 11, 863–874. doi: 10.1038/ismej.2016.184

Lavender, D. P., and Hermann, R. K. (2014). *Douglas-fir:The Genus Pseudotsuga*. Corvallis, OR: Oregon Forest Research Laboratory.

Leberecht, M., Dannenmann, M., Gschwendtner, S., Bilela, S., Meier, R., Simon, J., et al. (2015). Ectomycorrhizal communities on the roots of two beech (Fagus sylvatica) populations from contrasting climates differ in nitrogen acquisition in a common environment. *Appl. Environ. Microbiol.* 81, 5957–5967. doi: 10.1128/AEM.01481-15

Legendre, P., and Anderson, M. J. (1999). Distance-based redundancy analysis: testing multispecies responses in multifactorial ecological experiments. *Ecol. Monogr.* 69, 1–24. doi: 10.1890/0012-9615(1999)069%5B0001:dbratm%5D2.0.co;2

Lilleskov, E. A., Fahey, T. J., Horton, T. R., and Lovett, G. M. (2002). Belowground ectomycorrhizal fungal community change over a nitrogen deposition gradient in alaska. *Ecology* 83, 104–115. doi: 10.1890/0012-9658(2002)083%5B0104:befcco%5D2.0.co;2

Lilleskov, E. A., Hobbie, E. A., and Horton, T. R. (2011). Conservation of ectomycorrhizal fungi: exploring the linkages between functional and taxonomic responses to anthropogenic N deposition. *Fungal Ecol.* 4, 174–183. doi: 10.1016/j.funeco.2010.09.008

Lilleskov, E. A., Kuyper, T. W., Bidartondo, M. I., and Hobbie, E. A. (2018). Atmospheric nitrogen deposition impacts on the structure and function of forest mycorrhizal communities: a review. *Environ. Pollut.* 246, 148–162. doi: 10.1016/j.envpol.2018.11.074

Lilleskov, E. A., and Parrent, J. L. (2007). Can we develop general predictive models of mycorrhizal fungal community–environment relationships? *New Phytol.* 174, 250–256. doi: 10.1111/j.1469-8137.2007.02023.x

Liu, B., Li, H., Zhu, B., Koide, R. T., Eissenstat, D. M., and Guo, D. (2015). Complementarity in nutrient foraging strategies of absorptive fine roots and arbuscular mycorrhizal fungi across 14 coexisting subtropical tree species. *New Phytol.* 208, 125–136. doi: 10.1111/nph.13434

Looney, B. P., Meidl, P., Piatek, M. J., Miettinen, O., Martin, F. M., Matheny, P. B., et al. (2018). Russulaceae: a new genomic dataset to study ecosystem function and evolutionary diversification of ectomycorrhizal fungi with their tree associates. *New Phytol.* 218, 54–65. doi: 10.1111/nph.15001

Marx, D. H. (1972). Ectomycorrhizae as biological deterrents to pathogenic root infections. *Annu. Rev. Phytopathol.* 10, 429–454. doi: 10.1146/annurev.py.10.090172.002241

McCormack, M. L., Guo, D., Iversen, C. M., Chen, W., Eissenstat, D. M., Fernandez, C. W., et al. (2017). Building a better foundation: improving root-trait measurements to understand and model plant and ecosystem processes. *New Phytol.* 215, 27–37. doi: 10.1111/nph.14459

Meidinger, D. V., and Pojar, J. (1991). *Ecosystems of British Columbia*. Victoria, BC: Research Branch, Ministry of Forests.

Mucha, J., Peay, K. G., Smith, D. P., Reich, P. B., Stefański, A., and Hobbie, S. E. (2018). Effect of simulated climate warming on the ectomycorrhizal fungal community of boreal and temperate host species growing near their shared ecotonal range limits. *Microb. Ecol.* 75, 348–363. doi: 10.1007/s00248-017-1044-5

Naimi, B., Hamm, N. A. S., Groen, T. A., Skidmore, A. K., and Toxopeus, A. G. (2014). Where is positional uncertainty a problem for species distribution modelling? *Ecography* 37, 191–203. doi: 10.1111/j.1600-0587.2013.00205.x

Nilsson, L. O., and Wallander, H. (2003). Production of external mycelium by ectomycorrhizal fungi in a norway spruce forest was reduced in response to nitrogen fertilization. *New Phytol.* 158, 409–416. doi: 10.1046/j.1469-8137.2003.00728.x

Oksanen, J., Blanchet, F. G., Friendly, M., Kindt, R., Legendre, P., McGlinn, D., et al. (2018). *vegan: Community Ecology Package*. Available at: https://CRAN.Rproject.org/package=vegan (accessed September 1, 2018).

Ostonen, I., Helmisaari, H.-S., Borken, W., Tedersoo, L., Kukumägi, M., Bahram, M., et al. (2011). Fine root foraging strategies in norway spruce forests across a european climate gradient. *Glob. Change Biol.* 17, 3620–3632. doi: 10.1111/j.1365-2486.2011.02501.x

Ostonen, I., Truu, M., Helmisaari, H.-S., Lukac, M., Borken, W., Vanguelova, E., et al. (2017). Adaptive root foraging strategies along a boreal-temperate forest gradient. *New Phytol.* 215, 977–991. doi: 10.1111/nph.14643

Ouimette, A., Guo, D., Hobbie, E., and Gu, J. (2013). Insights into root growth, function, and mycorrhizal abundance from chemical and isotopic data across root orders. *Plant Soil* 367, 313–326. doi: 10.1007/s11104-012-1464-4

Parke, E. L., Linderman, R. G., and Black, C. H. (1983). The role of ectomycorrhizas in drought tolerance of douglas-fir seedlings. *New Phytol.* 95, 83–95. doi: 10.1111/j.1469-8137.1983.tb03471.x

Peay, K. G., Kennedy, P. G., and Bruns, T. D. (2011). Rethinking ectomycorrhizal succession: are root density and hyphal exploration types drivers of spatial and temporal zonation? *Fungal Ecol.* 4, 233–240. doi: 10.1016/j.funeco.2010.09.010

Pena, R., Lang, C., Lohaus, G., Boch, S., Schall, P., Schöning, I., et al. (2017). Phylogenetic and functional traits of ectomycorrhizal assemblages in top soil from different biogeographic regions and forest types. *Mycorrhiza* 27, 233–245. doi: 10.1007/s00572-016-0742-z

Pickles, B. J., Egger, K. N., Massicotte, H. B., and Green, D. S. (2012). Ectomycorrhizas and climate change. *Fungal Ecol.* 5, 73–84. doi: 10.1007/s004420000385

Pickles, B. J., Genney, D. R., Potts, J. M., Lennon, J. J., Anderson, I. C., and Alexander, I. J. (2010). Spatial and temporal ecology of Scots pine ectomycorrhizas. *New Phytol.* 186, 755–768. doi: 10.1111/j.1469-8137.2010.03204.x

Pickles, B. J., Gorzelak, M. A., Green, D. S., Egger, K. N., and Massicotte, H. B. (2015a). Host and habitat filtering in seedling root-associated fungal communities: taxonomic and functional diversity are altered in 'novel' soils. *Mycorrhiza* 25, 517–531. doi: 10.1007/s00572-015-0630-y

Pickles, B. J., Twieg, B. D., O'Neill, G. A., Mohn, W. W., and Simard, S. W. (2015b). Local adaptation in migrated interior Douglas-fir seedlings is mediated by ectomycorrhizas and other soil factors. *New Phytol.* 207, 858–871. doi: 10.1111/nph.13360

Pickles, B. J., and Pither, J. (2014). Still scratching the surface: how much of the 'black box' of soil ectomycorrhizal communities remains in the dark? *New Phytol.* 201, 1101–1105. doi: 10.1111/nph.12616

Pither, J., Pickles, B. J., Simard, S. W., Ordonez, A., and Williams, J. W. (2018). Below-ground biotic interactions moderated the postglacial range dynamics of trees. *New Phytol.* 220, 1148–1160. doi: 10.1111/nph.15203

Põlme, S., Bahram, M., Yamanaka, T., Nara, K., Dai, Y. C., Grebenc, T., et al. (2013). Biogeography of ectomycorrhizal fungi associated with alders (Alnus spp.) in relation to biotic and abiotic variables at the global scale. *New Phytol.* 198, 1239–1249. doi: 10.1111/nph.12170

Pregitzer, K. S., Deforest, J. L., Burton, A. J., Allen, M. F., Ruess, R. W., and Hendrick, R. L. (2002). Fine root architecture of nine north american trees. *Ecol. Monogr.* 72, 293–309. doi: 10.1890/0012-9615(2002)072%5B0293:fraonn%5D2.0.co;2

R Core Team (2018). *R: A Language and Environment For Statistical Computing*. Vienna: R Foundation for Statistical Computing. Available at: https://www.R-project.org/

Read, D. J., and Perez-Moreno, J. (2003). Mycorrhizas and nutrient cycling in ecosystems - a journey towards relevance? *New Phytol.* 157, 475–492. doi: 10.1046/j.1469-8137.2003.00704.x

Rehfeldt, G. E., Leites, L. P., Bradley St Clair, J., Jaquish, B. C., Sáenz-Romero, C., López-Upton, J., et al. (2014). Comparative genetic responses to climate in the varieties of *Pinus ponderosa* and Pseudotsuga menziesii: clines in growth potential. *For. Ecol. Manag.* 324, 138–146. doi: 10.1016/j.foreco.2014.02.041

Richardson, A. D., Hufkens, K., Milliman, T., Aubrecht, D. M., Furze, M. E., Seyednasrollah, B., et al. (2018). Ecosystem warming extends vegetation activity but heightens vulnerability to cold temperatures. *Nature* 560, 368–371. doi: 10.1038/s41586-018-0399-1

Rognes, T., Flouri, T., Nichols, B., Quince, C., and Mahé, F. (2016). VSEARCH: a versatile open source tool for metagenomics. *PeerJ* 4:e2584. doi: 10.7717/peerj.2584

Rosinger, C., Sandén, H., Matthews, B., Mayer, M., and Godbold, D. (2018). Patterns in ectomycorrhizal diversity, community composition, and exploration types in european beech, pine, and spruce forests. *Forests* 9:445. doi: 10.3390/f9080445

Rosling, A., Landeweert, R., Lindahl, B. D., Larsson, K.-H., Kuyper, T. W., Taylor, A. F. S., et al. (2003). Vertical distribution of ectomycorrhizal fungal taxa in a podzol soil profile. *New Phytol.* 159, 775–783. doi: 10.1046/j.1469-8137.2003.00829.x

Simard, S. W., and Austin, M. E. (2010). "The Role of Mycorrhizas in Forest Soil Stability with Climate Change," in *Climate Change and Variability*, ed. S. W. Simard (Rijeka: InTech Open Access).

Sterkenburg, E., Bahr, A., Brandström Durling, M., Clemmensen, K. E., and Lindahl, B. D. (2015). Changes in fungal communities along a boreal forest soil fertility gradient. *New Phytol.* 207, 1145–1158. doi: 10.1111/nph.13426

Strullu-Derrien, C., Selosse, M.-A., Kenrick, P., and Martin, F. M. (2018). The origin and evolution of mycorrhizal symbioses: from palaeomycology to phylogenomics. *New Phytol.* 220, 1012–1030. doi: 10.1111/nph.15076

Suz, L. M., Barsoum, N., Benham, S., Dietrich, H.-P., Fetzer, K. D., Fischer, R., et al. (2014). Environmental drivers of ectomycorrhizal communities in Europe's temperate oak forests. *Mol. Ecol.* 23, 5628–5644. doi: 10.1111/mec.12947

Tedersoo, L. (2017). *Biogeography of Mycorrhizal Symbiosis*. New York, NY: Springer.

Tedersoo, L., Bahram, M., Toots, M., Diédhiou, A. G., Henkel, T. W., Kjøller, R., et al. (2012). Towards global patterns in the diversity and community structure of ectomycorrhizal fungi. *Mol. Ecol.* 21, 4160–4170. doi: 10.1111/j.1365-294X.2012.05602.x

Tedersoo, L., and Smith, M. E. (2013). Lineages of ectomycorrhizal fungi revisited: foraging strategies and novel lineages revealed by sequences from belowground. *Fungal Biol. Rev.* 27, 83–99. doi: 10.1016/j.fbr.2013.09.001

Turenne, C. Y., Sanche, S. E., Hoban, D. J., Karlowsky, J. A., and Kabani, A. M. (1999). Rapid identification of fungi by using the its2 genetic region and an automated fluorescent capillary electrophoresis system. *J. Clin. Microbiol.* 37, 1846–1851.

van der Linde, S., Suz, L. M., Orme, C. D. L., Cox, F., Andreae, H., Asi, E., et al. (2018). Environment and host as large-scale controls of ectomycorrhizal fungi. *Nature* 558, 243–248. doi: 10.1038/s41586-018-0189-9

Vancov, T., and Keen, B. (2009). Amplification of soil fungal community DNA using the ITS86F and ITS4 primers. *FEMS Microbiol. Lett.* 296, 91–96. doi: 10.1111/j.1574-6968.2009.01621.x

Wang, T., Hamann, A., Spittlehouse, D., and Carroll, C. (2016). Locally downscaled and spatially customizable climate data for historical and future periods for North America. *PLoS One* 11:e0156720. doi: 10.1371/journal.pone.0156720

Wang, Y., Naumann, U., Wright, S. T., and Warton, D. I. (2012). mvabund–an R package for model-based analysis of multivariate abundance data. *Methods Ecol. Evol.* 3, 471–474. doi: 10.1111/j.2041-210x.2012.00190.x

Weigt, R. B., Raidl, S., Verma, R., and Agerer, R. (2012). Exploration type-specific standard values of extramatrical mycelium – a step towards quantifying ectomycorrhizal space occupation and biomass in natural soil. *Mycol. Prog.* 11, 287–297. doi: 10.1007/s11557-011-0750-5

Westcott, S. L., and Schloss, P. D. (2015). De novo clustering methods outperform reference-based methods for assigning 16S rRNA gene sequences to operational taxonomic units. *PeerJ* 3:e1487. doi: 10.7717/peerj.1487

White, T., Bruns, T., Lee, S., and Taylor, J. (1990). "Amplification and Direct Sequencing of Fungal Ribosomal RNA Genes for Phylogenetics," in *PCR Protocols: A Guide to Methods and Applications*, eds M. A. Innis, D. H. Gelfand, J. J. Sninsky, and T. J. White (New York, NY: Academic Press).

Wiley, E., Rogers, B. J., Griesbauer, H. P., and Landhäusser, S. M. (2018). Spruce shows greater sensitivity to recent warming than Douglas-fir in central British Columbia. *Ecosphere* 9:e02221. doi: 10.1002/ecs2.2221

Wurzburger, N., and Clemmensen, K. E. (2018). From mycorrhizal fungal traits to ecosystem properties - and back again. *J. Ecol.* 106, 463–467. doi: 10.1111/1365-2745.12922

Zadworny, M., and Eissenstat, D. M. (2011). Contrasting the morphology, anatomy and fungal colonization of new pioneer and fibrous roots. *New Phytol.* 190, 213–221. doi: 10.1111/j.1469-8137.2010.03598.x

Zadworny, M., McCormack, M. L., Żytkowiak, R., Karolewski, P., Mucha, J., and Oleksyn, J. (2017). Patterns of structural and defense investments in fine roots of Scots pine (*Pinus sylvestris* L.) across a strong temperature and latitudinal gradient in Europe. *Glob. Change Biol.* 23, 1218–1231. doi: 10.1111/gcb.13514

Zhang, J., Wang, P., Xue, K., Hao, Y., Wang, Y., and Cui, X. (2019). Trait complementarity between fine roots of Stipa purpurea and their associated arbuscular mycorrhizal fungi along a precipitation gradient in Tibetan alpine steppe. *J. Mt. Sci.* 16, 542–547. doi: 10.1007/s11629-018-5311-9

Zuur, A. F., Ieno, E. N., and Elphick, C. S. (2010). A protocol for data exploration to avoid common statistical problems. *Methods Ecol. Evol.* 1, 3–14. doi: 10.1111/j.2041-210x.2009.00001.x

Conflict of Interest Statement: The authors declare that the research was conducted in the absence of any commercial or financial relationships that could be construed as a potential conflict of interest.

frontiers in Plant Science

ORIGINAL RESEARCH
published: 12 June 2019
doi: 10.3389/fpls.2019.00786

Water Transfer Between Bamboo Culms in the Period of Sprouting

Dongming Fang[1,2], Tingting Mei[1,2], Alexander Röll[2] and Dirk Hölscher[2]*

[1] State Key Laboratory of Subtropical Silviculture, Zhejiang A&F University, Lin'an, China, [2] Tropical Silviculture and Forest Ecology, University of Göttingen, Göttingen, Germany

Bamboo culms are connected to neighboring culms via rhizomes, which enable resource exchange between culms. We assessed water transfer between established and neighboring, freshly sprouted culms by thermal dissipation probes (TDP) inserted into culms and the connecting rhizome. During the early phase of sprouting, highest sap flux densities in freshly sprouted culms were observed at night, whereas neighboring established culms had high sap flux densities during daytime. After leaf flushing on freshly sprouted culms, the nighttime peaks disappeared and culms switched to the diurnal sap flux patterns with daytime maxima as observed in established culms. TDP in rhizomes indicated water flowing from the established to the freshly sprouted culms. When the established culms of a clump were cut, freshly sprouted culms without leaves reduced sap flux densities rates by 79%. Our findings thus suggest that bamboos exchange water via rhizomes and that nighttime fluxes are highly important for the support of freshly sprouted culms. The (water) resource support may facilitate the very fast growth of the bamboo shoots, and enable the colonizing of new places.

Keywords: bamboo shoots, nighttime flux, rhizome, sap flux, water exchange

OPEN ACCESS

Edited by:
Boris Rewald, University of Natural Resources and Life Sciences, Austria

Reviewed by:
Johann Rohwer, Stellenbosch University, South Africa
Keisuke Nagai, Nagoya University, Japan

****Correspondence:***
Dongming Fang
dmfang@zafu.edu.cn

Specialty section:
This article was submitted to Functional Plant Ecology, a section of the journal Frontiers in Plant Science

Received: *31 March 2019*
Accepted: *29 May 2019*
Published: *12 June 2019*

Citation:
Fang D, Mei T, Röll A and Hölscher D (2019) Water Transfer Between Bamboo Culms in the Period of Sprouting. Front. Plant Sci. 10:786. doi: 10.3389/fpls.2019.00786

INTRODUCTION

Plants with connected roots or rhizomes have the possibility to share resources with each other directly (Baret and DesRochers, 2011). Resource exchange among connected individuals, referred to as "physiological integration" (Lau and Young, 1988; Caraco and Kelly, 1991; Kroon et al., 1996), has been intensively studied and seems to be relatively widespread in herbaceous species (Alpert and Mooney, 1986; Lau and Young, 1988; Chapman et al., 1992; Kroon et al., 1996; Stueffer et al., 1996). In tree species such as lodgepole pine (Fraser et al., 2006), aspen (Baret and DesRochers, 2011), and poplar (Adonsou et al., 2016) resource exchange via connected roots was also observed. The direction of transfer and the transferred amounts depended on the status of the connected plants; e.g., plants that suffered drought received water from watered neighbors, in which the amount of transferred water was related to the leaf water potential or leaf area of the connected plants (Kroon et al., 1996; Adonsou et al., 2016). Such resource integration was shown to be of critical importance for new ramets grown from the parental root systems of aspen (*Populus tremuloides*) (Baret and DesRochers, 2011).

As rhizomatous monocot species, bamboos are well known for their fast expansion via their underground rhizome system as well as the rapid growth of freshly sprouted culms (Liese and Köhl, 2015). After emerging from the soil, bamboo culms can attain their full heights within 1 or 2 months, with maximum growth rates up to 10–80 cm per day (Liese and Köhl, 2015;

Song et al., 2016). Some species may even grow up to 1 m per day during the fast growing phase (Ueda, 1960). This leads to the question of where developing culms, with no leaves and only few roots, get the resources to sustain such growth rates. Important mechanisms include nutrient storage in the rhizome as well as resource translocation from connected mature culms (Li et al., 1998a,b; Liese and Köhl, 2015). A study on Moso bamboo (*Phyllostachys pubescens*) revealed that the content of non-structural carbohydrates in mature culms declined substantially during the "explosive growth" period of neighboring, young bamboo shoots due to the translocation of carbohydrates from mature to young culms via the underground rhizomes (Song et al., 2016). Applying deuterium tracing on culms in a clump of *Bambusa blumeana*, Dierick et al. (2010) found higher deuterium concentration than the background values in neighboring culms close to the labeled culms. This elevated deuterium concentration was thought to imply water transfer among the culms via the rhizomes. In another study on Moso bamboo all rhizomes of several culms were cut and the culms thus disconnected from the clump's rhizome network. The culms with cut rhizomes subsequently consumed 20% less water than neighboring culms with intact rhizomes (Zhao et al., 2016).

Our study was implemented on three clumpy bamboo species during the phase of vegetative sprouting of fresh culms. The aim was to assess water transfer among established culms and sprouting culms with thermal dissipation probes (TDP) and a cutting experiment.

MATERIALS AND METHODS

Study Site and Bamboos

The study was conducted in a bamboo garden in Bogor, Indonesia (6°33′40″ S, 106°43′27″ E, 182 m asl). Rainfall in Bogor is 3978 mm per year and the mean annual temperature is 25.6°C (Van Den Besselaar et al., 2014). The months between October and May are particularly wet. During this wet period, new shoots of bamboos sprout from the soil and grow to their full height. This study was conducted in clumps of *B. vulgaris* and *Gigantochloa apus*; culm heights were 17.9 ± 0.8 m (mean ± SD) and 16.2 ± 2.7 m and culm diameters at breast height were 7.0 ± 0.4 cm and 7.9 ± 1.1 cm, respectively. In the clumps, established culms and freshly sprouted culms were connected via rhizomes of 30 to 50 cm length. Unlike the hollow culms of the bamboos, the rhizomes are solid. During the nearly 4-month experimental period from December 2012 to March 2013, fresh culms sprouted and grew to their full height. Culm growth was slowed down during the period of leaf development.

Sap Flux in Culms and the Rhizome, and Measurements of Radiation

For *B. vulgaris*, three pairs of established and attached freshly sprouted culms were selected at the culm edge (**Figures 1A,B**). The connection between established and freshly sprouted culms was verified by partially removing the topsoil and directly observing the rhizomes. Sap flux densities (J_s, g cm^{-2} h^{-1}) in bamboo culms were monitored with TDP (Granier, 1985). Each TDP consists of two probes – a heated probe and a reference one, and a thermal couple is built into each probe to detect thermal dynamic. The temperature around the heated probe is negatively correlated with J_s. The temperature differential between heated and reference probe were used for monitoring and calculating J_s (Lu et al., 2004). On each studied bamboo culm, three pairs of TDP with 1 cm sensor length were inserted into the culm walls at breast height (**Figure 1A** and **Appendix Figure S1A**). The heated probe, powered by 120 mA, was installed 10 cm above the reference probe. Voltage signals were recorded every 30 s and averaged every 10 min (CR1000 data loggers and AM16/32 multiplexer, Campbell Scientific Inc., United States). J_s of established culms was first calculated based on Granier's equation (Granier, 1985), and J_s was further corrected by multiplying it with species-specific calibration parameters (*SSCP*; 2.79 for *B. vulgaris*; 3.32 for *G. apus*; Mei et al., 2016).

$$J_s = 119 \times \left(\frac{\Delta T_{max} - \Delta T}{\Delta T}\right)^{1.231} \times 0.36 \times SSCP$$

Where ΔT is the temperature difference between the heated and reference probe and ΔT_{max} is the maximal ΔT within a given day; ΔT_{max} usually occurs during the night and is used to set zero-flux conditions (J_s = 0). The model parameters 119 and 1.231 were empirically derived by Granier (1985). These original parameters were found to substantially underestimate J_s in the bamboo species *B. vulgaris* and *G. apus* (Mei et al., 2016), which is why the mentioned *SSCP* were applied.

To measure J_s and detect directions of sap flow in the rhizome between established and freshly sprouted culms, we built self-made, modified TDP sensors with three probes instead of two. The modified TDP consisted of one central heating and two unheated reference probes. The heating probe was installed at the mid-point of the rhizome between the culms, and the two reference probes were installed at 5 cm distance from the heated probe, one on each side (**Figure 1C** and **Appendix Figure S1B**). The temperature differences between each reference probe and the heating probe were recorded, stored and used to calculate rhizome J_s in the same way as described above for the "standard" TDP sensors. The directions of sap flow in rhizome were determined by comparing the two derived voltage signals, and the reference probe with the lower signal value was assigned the downstream position of sap flow. This was based on the assumption that sap flow brought the heat energy to the downstream sensor and that this heat would increase the temperature of the downstream sensor and thus a smaller temperature difference between the heating and the downstream reference probe than that between the heating and the upstream reference probe. In this case, the signal value from the downstream sensor was smaller than that from the upstream sensor. To test this assumption, we simulated the heat field around the heating and the two reference sensors under different sap flow densities with the ANSYS model (CFX 17.0, ANSYS Inc., Pennsylvania, United States; Mei et al., 2017), and the simulated results confirmed our initial assumption (**Appendix Figures S2–S4**).

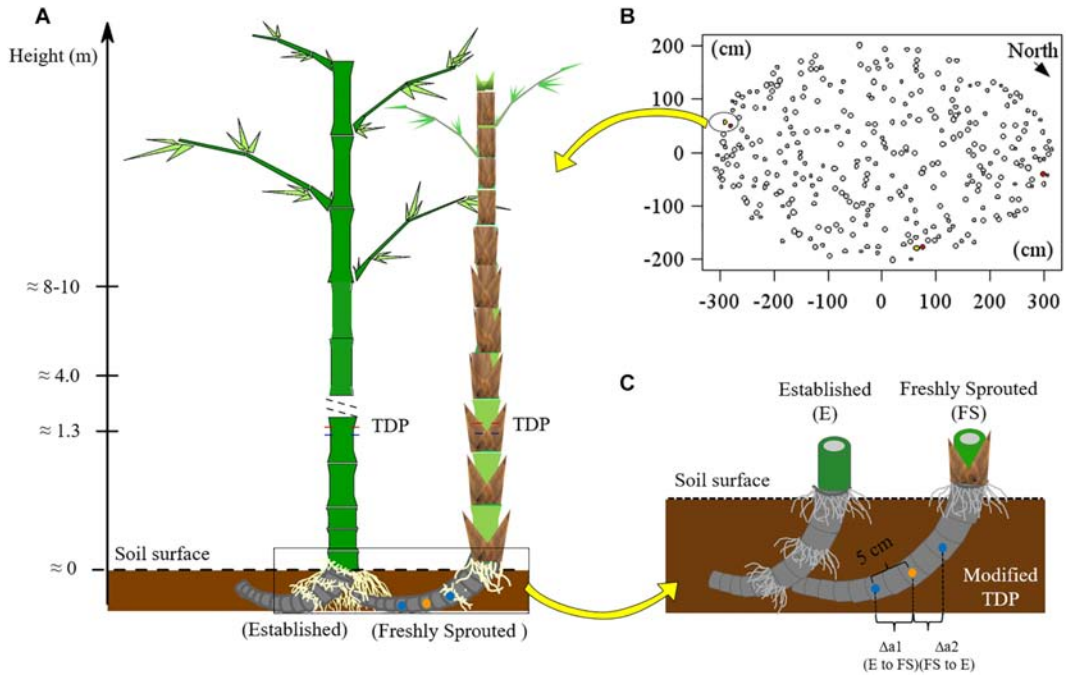

FIGURE 1 | (A) Experimental scheme for applying TDP methods; **(B)** the locations of monitored culms in a clump of *B. vulgaris* (n = 3 pairs of culms). The red, yellow and white filled circles represented the labeled established, the neighboring freshly sprouted and the other culms, respectively. **(C)** Setup of self-made modified thermal dissipation probes (TDP) with two reference probes installed at equal distance from the central heating probe on the rhizome of *B. vulgaris*. The orange point represents the heating probe, the blue points are the unheated reference probes. Photos showing the installation of TDP on bamboo culms and of modified TDP on bamboo rhizomes are provided in **Appendix Figure S1.**

Within 600 meters of the *B. vulgaris* site, we set up a micrometeorological station. A pyranometer (CS300, Campbell Scientific Inc., United States) was installed to measure radiation. The data was stored on a CR1000 data logger with the same recording intervals as described for the TDP measurements.

Cutting Experiment

Additionally to directly monitoring the water transfer via rhizome with modified TDP, a cutting experiment was implemented to explore the influence of established culms on the water status of freshly sprouted culms. Two clumps of *G. apus* in a bamboo garden were selected, one for the cutting experiment and the other as a control. Both clumps had a similar density of culms ($\sim$ 18 culms m^{-2}). All established culms in the cutting experiment clump were removed, so that only freshly sprouted culms remained. In the control clump, no culms were cut.

From 29 Dec 2012 to 10 Feb 2013, J_s of five freshly sprouted culms in the cutting experiment clump was monitored by TDP as described in section 2.2. The culms had a height of around 2 m at the beginning of the experiment and had no leaves. The monitoring stopped after about 40 days, when the culms were collapsing. Until then, the culms had reached approx. 5 – 8 m in height without any leaf development. In the control clump, we monitored J_s of five established culms but not freshly sprouted ones. To estimate the J_s of freshly sprouted culms in the *G. apus* control clump, we used an indirect assessment involving a nearby long-term monitoring *B. vulgaris* clump. There, we measured J_s of both established and freshly sprouted culms. We found a significant linear relationship (slope = 0.63, with no intercept) between J_s of established culms in the *B. vulgaris* and *G. apus* control clumps (R^2 = 0.9; $P < 0.01$; **Appendix Figure S5**). We assume that the freshly sprouted culms of the two species have the same relationship as established culms and estimated J_s of freshly sprouted culms in the control *G. apus* clump by multiplying the observed values of freshly sprouted *B. vulgaris* by 0.63 (**Appendix Figure S5**).

Statistics

To compare the patterns of J_s among the rhizome, established and freshly sprouted culms, we normalized the half-hourly J_s of each day (by fitting them to a range from 0 to 1) and plotted average hourly values of six sunny days (**Figure 2**). To further explore the relative change between established and freshly sprouted culms, we further plotted the normalized J_s values of newly sprouted culms directly versus the normalized J_s of established culms (**Figure 3**).

To explore the contribution of nighttime to whole-day sap flow, we calculated the ratio between nighttime (18:00 to 6:00 in next morning) and whole-day accumulated sap flow (24 h) of established and freshly sprouted culms and of the rhizomes connecting them (**Figure 4**).

To compare the patterns of J_s between the cutting and control freshly sprouted culms in the cutting experiment, we averaged

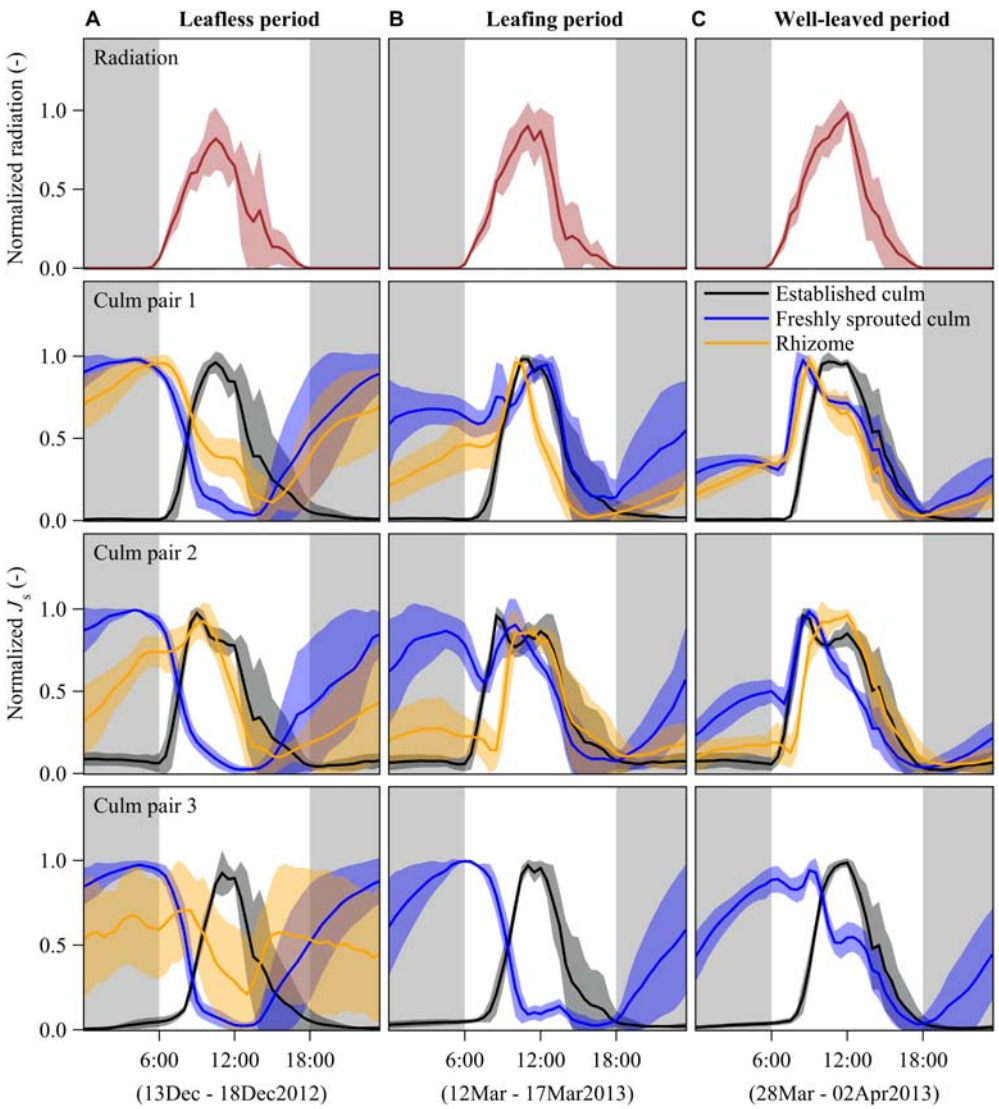

FIGURE 2 | Diurnal patterns of half-hourly radiation (first row) and sap flux densities (J_S) of *B. vulgaris* (rows 2 – 4) during leafless **(A)**, leafing **(B)**, and well-leaved period **(C)** of freshly sprouted culms. The presented lines are means of 6 days of measurements for each of the three periods; the error corridors around the lines indicate standard deviations. For each freshly sprouted culm, J_S is also displayed for the neighboring established culm and the connecting rhizome. Gray background indicates nighttime (18:00 to 6:00). Due to sensor malfunctioning, rhizome data for culm pair three is missing and thus not shown in panels **B,C**.

half-hourly J_S of 5 culms in each clump, and normalized the pooled data of both clumps by selecting one common hourly maximum (set to one) and minimum (set to zero) within three consecutive days of measurements (**Figure 5**).

All data analyses and plotting were performed with SAS 9.4 (SAS Institute Inc., Cary, NC, United States).

RESULTS

Diurnal Patterns of Sap Flux Densities in Culms and Rhizome

In established culms, sap flux density (J_S) showed a typical diurnal pattern corresponding approximately to the diurnal patterns of radiation. With rising radiation in the morning, J_S started to increase until reaching its peak values at around midday, gradually decreased in the afternoon and remained close to zero during the night (**Figure 2**).

In freshly sprouted culms, J_S switched from a day-night reversal mode through a transition mode to a similar diurnal pattern as that of established culms over the leafless, leafing, and well-leaved periods, respectively. In the leafless period, nighttime sap flux dominated. J_S increased from near zero at sunset time to its peak around sunrise. The nighttime-dominated pattern switched gradually to the normal daytime-dominated pattern after leaves developed. In the well-leaved period, 3 months after sprouting, maximum J_S was higher during the daytime than during the nighttime (**Figure 2**).

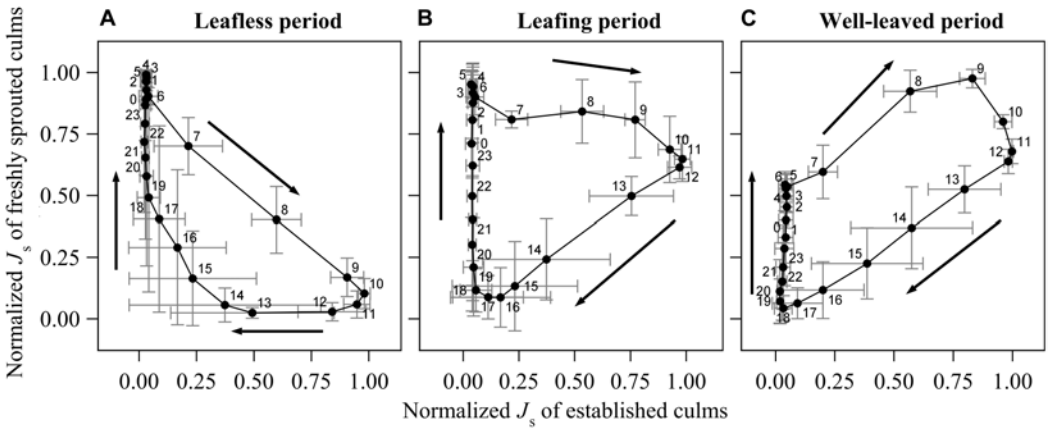

FIGURE 3 | Diurnal change of normalized sap flux density (J_S) of the freshly sprouted culms to the normalized J_S of established culms in the leafless **(A)**, leafing **(B)** and well-leaved period **(C)** of the freshly sprouted culms of *B. vulgaris*. In each sub-figure, data was averaged from six consecutive sunny days of three culm pairs. The *X*- and *Y*- error bars on each dot are standard deviations of the respective 6 days.

In rhizomes, there was substantial J_s at night during times of high J_s in freshly sprouted culms in the leafless period. During the daytime, the J_s in rhizomes differed among the three culm pairs (**Figure 2A**), which may be attributed to different culm elongation stages. Once the leaves of young culms were well established (**Figure 2B**), J_s patterns were more synchronized in rhizomes, established and young bamboo culms, usually with peaks between 9 am and midday. Based on observed temperature differences as measured with modified TDPs (**Appendix Figure S2**) and results from simulations (**Appendix Figures S3, S4**), we infer that the net sap flow in rhizomes was mainly from the established culms to the freshly sprouted culms in both the leafless and the well-leaved observation period. However, we cannot exclude the possibility of coexisting bidirectional sap flow in rhizomes.

Comparison Between Freshly Sprouted Culms and Established Culms

During the leafless period of freshly sprouted culms, they had near maximum rates of normalized hourly sap flux (J_{s_max}) from about 10 pm to 6 am, when J_s of established culms was near its minimum (<10% of J_{s_max}) (**Figure 3A**). Sap flux in leafless young culms sharply decreased as soon as sap flux in established culms increased in the morning. J_{s_max} in established culms coincided with near minimum values in freshly sprouted culms (9 am to 12 pm). J_s in freshly sprouted culms increased back to 25% of its daily maximum as soon as J_s in established culms dropped below 20% of J_{s_max} (around 4 pm).

In freshly sprouted culms in the transition period (leafing), J_{s_max} was also observed in the early morning hours, but the subsequent decline in J_s was much slower; J_s was still around 70% of J_{s_max} at noon, when J_s in established culms was at its highest (**Figure 3B**). Over the afternoon hours (12 to 6 pm), J_s in leafing young culms declined to near zero. It subsequently gradually increased until the early morning hour maximum; during this time, J_s of established culms remained below 10% of J_{s_max}.

In well-leaved freshly sprouted culms, substantial J_s as well as J_{s_max} were observed between 5 am and noon, thus coinciding with J_{s_max} in established culms. In the afternoon, J_s in the young culms gradually drops to near minimum (around 6 pm). However, in contrast to established culms (with marginal J_s between 6 pm and 6 am), J_s in well-leaved freshly sprouted culms starts to slowly and consistently rise again after sunset, reaching about 60% of J_{s_max} until sunrise (**Figure 3C**).

Contribution of Nighttime to Whole-Day Sap Flow

Over the leafless, leafing, and well-leaved periods of newly sprouted culms, nighttime accumulated J_s of neighboring established culms remained at 8 ± 1% of whole-day accumulated J_s (**Figure 4**). In contrast, the contribution of nighttime to whole-day accumulated J_s of freshly sprouted culms decreased from 69 ± 3% to 52 ± 6% to 35 ± 6% over the three periods (**Figure 4**). Nighttime accumulated J_s in rhizomes accounted for 49 ± 5%, 32 ± 4%, and 23 ± 6% of whole-day accumulated J_s over the three periods (**Figure 4**). Even though the nighttime contributions of rhizomes were thus consistently smaller than for freshly sprouted culms, they showed a similar decreasing trend over the three periods (**Figure 4**).

Influence of Cutting Established Culms on Freshly Sprouted Culms

After removing all established culms in a *G. apus* clump, daily sap flux of freshly sprouted leafless culms was estimated to be 79% lower than the corresponding values of a *G. apus* clump where established culms had not been removed (**Figure 5**); the latter was assessed indirectly by applying the ratio of 0.63 between J_s of *G. apus* and *B. vulgaris* (**Appendix Figure S5**). Taking into account uncertainties in the ratio (range: 0.55 to 0.84), the corresponding relative difference of J_s between cutting and control clump is between 76 and 84%.

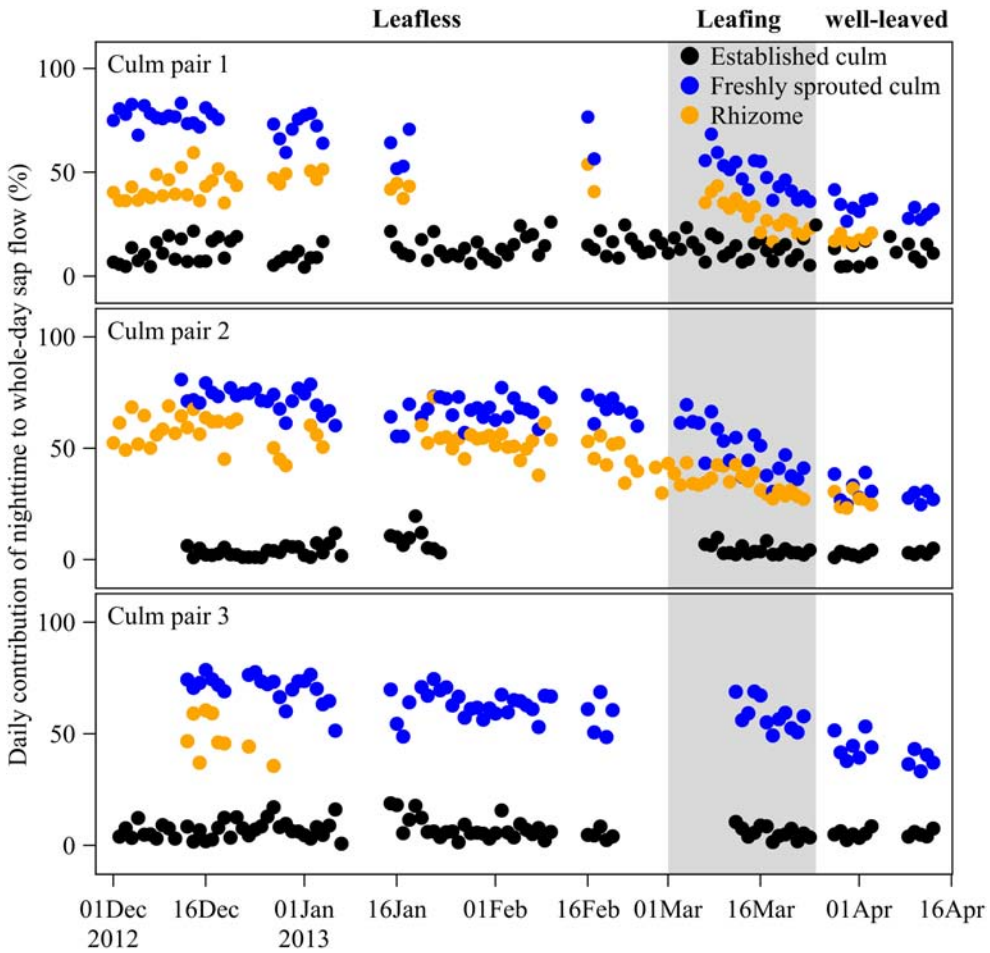

FIGURE 4 | Daily contribution (%) of nighttime to whole-day sap flow in freshly sprouted culms, established culms and the connecting rhizomes of three culm pairs of *B. vulgaris* in the first months after sprouting. The gray area indicates the leafing period of freshly sprouted culms, i.e., the transition phase from a leafless to a well-leaved state.

DISCUSSION

It is generally accepted that micrometeorological factors such as solar radiation and vapor pressure deficit are the main drivers of day-to-day fluctuations in tree water use and that limited soil water availability can constrain tree water use (O'brien et al., 2004; Kume et al., 2007). However, water use patterns may vary under special circumstances, e.g., in freshly sprouted leafless bamboo culms. In our study, we found that diurnal J_s patterns in freshly sprouted bamboo culms changed from the leafless to the well-leaved period (**Figures 2**, **3**). During the leafless period, diurnal J_s patterns in freshly sprouted bamboo culms typically differed from patterns in neighboring established culms, i.e., freshly sprouted culms had high sap flux during the night and low sap flux during the daytime. The nighttime maxima imply that the J_s pattern of freshly sprouted bamboo culms are not always controlled by the classic micrometeorological drivers, particularly during the early growing stages when culms are still without leaves and branches. The neighboring established culms most likely play an important supportive role for the freshly sprouted culms (Fraser et al., 2006; Liese and Köhl, 2015). As such, when all the established culms in a *G. apus* clump in our study were cut, J_s in neighboring, newly sprouted culms was reduced by 79% (**Figure 5**).

Tentatively applying the available adjusted J_s formula as specified for established bamboo culms (Mei et al., 2016) to the rhizomes and freshly sprouted culms in our study suggests that during the first 4 months after emerging, 48% of the daily sap flow of freshly sprouted culms was provided by established culms via the rhizomes (**Appendix Figure S6**). It may well be that freshly sprouted culms not only receive water from the nearest directly connected established culm, but from several sources interconnected via the underground rhizome network. Generally, the dependency of freshly sprouted culms on established culms may vary with their distances to established culms; as such, a previous study on water transfer between poplar ramets found that ramets benefited more from proximal root connection than from distal ones (Adonsou et al., 2016). The current elongation stage of a given newly sprouted culm may further impact its dependency on established

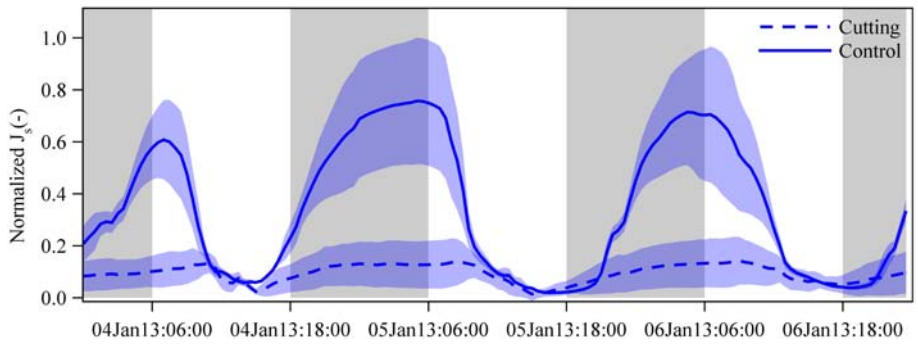

FIGURE 5 | Normalized sap flux densities (J_S) in freshly sprouted culms of *G. apus* in cutting (dashed lines) and control clumps (solid line). In the cutting experiment clump, all established culms were removed, leaving only freshly sprouted culms. Due to missing measured data, we estimated J_S of freshly sprouted *G. apus* culms in the control clump by multiplying J_S of freshly sprouted *B. vulgaris* culms in a nearby clump by a ratio of 0.63 (see section "Materials and Methods" and **Appendix Figure S5**). Averaged data from 3 and 5 culms for the control and cutting clump, respectively, normalized by setting the hourly maximum and minimum of both datasets to one and zero. Lines represent means and error corridors around the lines indicate standard deviations.

neighbors and thus the patterns and amounts of water it receives from donor culms.

Despite some previous indications of water transfer via rhizomes in bamboos (Dierick et al., 2010; Zhao et al., 2016), the mechanisms remain unclear. As such, the possible trade-offs between daytime sap flow of established culms and nighttime sap flow of freshly sprouted culms as well as the driving forces leading to the water transfer from the established donor culms to meet the water demand of the dependent freshly sprouted culms yet remain to be studied. Our results indicate that water supply from established donor culms to leafless freshly sprouted culms was reduced during the daytime, when the transpiration demand of established donor culms was high (more than 90% of whole-day transpiration; **Figures 2**, **3**). In contrast, water transfer to leafless freshly sprouted culms was high during the nighttime, when transpiration of established culms is marginal. Such sap flow patterns indicate competition for water within bamboo clumps, particularly during the phenological period of bamboo sprouting.

According to the source-sink theory, resource translocation among connected herbaceous plants depends on resource availability; the resource is transferred from resource-abundant regions (source) to resource-scarce regions (sink; Marshall, 1996). The theory could explain the opposite water use patterns observed for freshly sprouted and established bamboo culms in our study. The established bamboo culms transpired a lot of water during the daytime, probably also retrieving water stored in the culms (Yang et al., 2015; Mei et al., 2016). During the nighttime, along with the largely reduced transpiration and the refilling of the culm water storage via root pressure mechanisms (Cao et al., 2012; Yang et al., 2015), water demand in established culms is largely reduced, while demand for water in freshly sprouted culms become relatively higher than in the established culms. Such resource allocation relies largely on resource availability of the donor individuals, which can be simulated with models (Caraco and Kelly, 1991) and which has previously been observed for several tree species (Fraser et al., 2006; Baret and DesRochers, 2011; Adonsou et al., 2016) and herbaceous species (Alpert and Mooney, 1986; Lau and Young, 1988; Chapman et al., 1992; Kroon et al., 1996; Stueffer et al., 1996; Wang Z. et al., 2011; Zhang et al., 2012). The dependency of freshly sprouted culms on established culms was largely relieved after they had fully developed leaves (**Figures 2B,C**). However, some water transfer among the young culms and the interconnected established culms continued for several weeks after leaf flushing. Substantial resource translocation could potentially be reactivated at a later time, e.g., in case of resource stress of individual culms (Marshall, 1996). For example, differences in soil water availability, which have been reported even for small patches, could be balanced via interconnected rhizome networks (Hutchings and Wijesinghe, 1997; Wang Y. et al., 2011; Zhang et al., 2012).

Another finding is that for the first 4 months after emergence, freshly sprouted culms kept active nighttime sap flow regardless of whether they were with or without leaves, contributing 69, 52, and 35% of total daily sap flow over the leafless, leafing and well-leaved periods, respectively (**Figure 4**). Reduced competitive water uptake from rhizomes by the established culms during the night could be a potential reason, while another could include carbohydrate translocation from the established culms to freshly sprouted culms during the night. It has been observed that non-structural carbohydrates in established culms were largely reduced during the period of sprouting of neighboring shoots, and it was assumed that they had been transferred into the freshly sprouted culms (Song et al., 2016). Carbohydrate transport from the source (usually the leaves) to the sink (e.g., rhizome or freshly sprouted culm) is believed to be driven by hydrostatic pressure gradients in the phloem (Münch, 1930). In the carbohydrate transport process, the phloem has to withdraw water from the surrounding tissues (usually the xylem), which usually equilibrates the water potential between the phloem and the surrounding tissues (Thompson and Holbrook, 2003; Hölttä et al., 2006). However, drawing water from the xylem is more difficult when the water potential in the xylem is more negative; carbohydrate transport in the phloem thus likely occurs during the nighttime, when xylem water potential is less negative (Hölttä et al., 2009; Savage et al., 2015). Without substantial transpiration demand and with the water storage refilling via

root pressure mechanisms, the less negative water potential in established culms during the night further promotes the phloem to draw water and transport carbohydrates to freshly sprouted culms. However, the underlying mechanisms for water movement from established culms to freshly sprouted culms as well as its relationship with carbohydrate translocation remain unclear and will need to be addressed in future studies.

CONCLUSION

In the period of sprouting, young bamboo culms receive water resources from neighboring established culms via the underground rhizome network. The freshly sprouted culms show a high share of nighttime water fluxes. This resource support may facilitate the very fast growth of the bamboo shoots, and enable the colonizing of new places.

DATA AVAILABILITY

The datasets generated for this study are available on request to the corresponding author.

AUTHOR CONTRIBUTIONS

DF contributed to the experimental design, field installations, data analysis, and wrote and revised the manuscript. Particularly, DF conducted all the data analysis and figure-making, and wrote the preliminary draft of the manuscript. TM contributed to the experimental design, field installations, and revision for the manuscript. AR contributed to the field installations and revision for the manuscript. DH contributed to the experimental design and revision for the manuscript.

FUNDING

The study was funded by the German Research Foundation (DFG, code number: HO 2119 and CRC 990, A02). At the later stage of preparation to this manuscript, DF was supported by the State Key Laboratory of Subtropical Silviculture and received a scholarship from the China Scholarship Council (CSC).

ACKNOWLEDGMENTS

The authors acknowledge the support from the Departments of Facility and Property, the Ecology Laboratory and the Agriculture Faculty at the Bogor Agricultural University (IPB). Prof. Dr. Hendrayanto from the IPB Faculty of Forestry is particularly thanked by the authors for his great support during the project. The contents of the manuscript partly overlap with the doctoral thesis of the first author (DF; https://ediss.uni-goettingen.de/handle/11858/00-1735-0000-002E-E344-4).

SUPPLEMENTARY MATERIAL

The Supplementary Material for this article can be found online at: https://www.frontiersin.org/articles/10.3389/fpls.2019.00786/full#supplementary-material

REFERENCES

Adonsou, K. E., DesRochers, A., and Tremblay, F. (2016). Physiological integration of connected balsam poplar ramets. *Tree Physiol.* 36, 797–806. doi: 10.1093/treephys/tpv142

Alpert, P., and Mooney, H. A. (1986). Resource sharing among ramets in the clonal herb. *Oecologia* 70, 227–233. doi: 10.1007/BF00379244

Baret, M., and DesRochers, A. (2011). Root connections can trigger physiological responses to defoliation in nondefoliated aspen suckers. *Botany* 89, 753–761. doi: 10.1139/b11-062

Cao, K. F., Yang, S. J., Zhang, Y. J., and Brodribb, T. J. (2012). The maximum height of grasses is determined by roots. *Ecol. Lett.* 15, 666–672. doi: 10.1111/j.1461-0248.2012.01783.x

Caraco, T., and Kelly, C. K. (1991). On the adaptive value of physiological integraton in colonal plants. *Ecology* 72, 81–93. doi: 10.2307/1938904

Chapman, D. F., Robson, M. J., and Snaydon, R. W. (1992). Physiological integration in the clonal perennial herb *Trifolium repens* L. *Oecologia* 89, 338–347. doi: 10.1007/BF00317411

Dierick, D., Hölscher, D., and Schwendenmann, L. (2010). Water use characteristics of a bamboo species () in the Philippines. *Agric. For. Meteorol.* 150, 1568–1578. doi: 10.1016/j.agrformet.2010.08.006

Fraser, E. C., Lieffers, V. J., and Landhäusser, S. M. (2006). Carbohydrate transfer through root grafts to support shaded trees. *Tree Physiol.* 26, 1019–1023. doi: 10.1093/treephys/26.8.1019

Granier, A. (1985). Une nouvelle méthode pour la mesure du flux de sève brute dans le tronc des arbres. *Ann. Sci. For.* 42, 193–200. doi: 10.1051/forest:19850204

Hölttä, T., Mencuccini, M., and Nikinmaa, E. (2009). Linking phloem function to structure: analysis with a coupled xylem–phloem transport model. *J. Theor. Biol.* 259, 325–337. doi: 10.1016/j.jtbi.2009.03.039

Hölttä, T., Vesala, T., Sevanto, S., Perämäki, M., and Nikinmaa, E. (2006). Modeling xylem and phloem water flows in trees according to cohesion theory and Münch hypothesis. *Trees* 20, 67–78. doi: 10.1007/s00468-005-0014-6

Hutchings, M. J., and Wijesinghe, D. K. (1997). Patchy habitats, division of labour and growth dividends in clonal plants. *Trends Ecol. Evol.* 12, 390–394. doi: 10.1016/s0169-5347(97)87382-x

Kroon, H., Fransen, B., Rheenen, J. W., Dijk, A., and Kreulen, R. (1996). High levels of inter-ramet water translocation in two rhizomatous *Carex species*, as quantified by deuterium labelling. *Oecologia* 106, 73–84. doi: 10.1007/BF00334409

Kume, T., Takizawa, H., Yoshifuji, N., Tanaka, K., Tantasirin, C., Tanaka, N., et al. (2007). Impact of soil drought on sap flow and water status of evergreen trees in a tropical monsoon forest in northern Thailand. *For. Ecol. Manag.* 238, 220–230. doi: 10.1016/j.foreco.2006.10.019

Lau, R. R., and Young, D. R. (1988). Influence of physiological integration on survivorship and water relations in a clonal herb. *Ecology* 69, 215–219. doi: 10.2307/1943177

Li, R., Werger, M. J. A., During, H. J., and Zhong, Z. C. (1998a). Biennial variation in production of new shoots in groves of the giant bamboo in Sichuan. *China Plant Ecol.* 135, 103–112.

Li, R., Werger, M. J. A., During, H. J., and Zhong, Z. C. (1998b). Carbon and nutrient dynamics in relation to growth rhythm in the giant bamboo. *Plant Soil* 201, 113–123.

Liese, W., and Köhl, M. (2015). *Bamboo: the Plant and its Uses*. Cham: Springer.

Lu, P., Urban, L., and Zhao, P. (2004). Granier's thermal dissipation probe (TDP) method for measuring sap flow in trees: theory and practice. *Acta Bot. Sin.* 46, 631–646.

Marshall, C. (1996). Sectoriality and physiological organisation in herbaceous plants: an overview. *Vegetatio* 127, 9–16. doi: 10.1007/bf00054842

Mei, T., Fang, D., Röll, A., and Hölscher, D. (2017). The influence of bamboo culm water content on sap flux measurements with thermal dissipation probes: observations and modeling. *Trees* 32, 441–451. doi: 10.1007/s00468-017-1641-4

Mei, T., Fang, D., Röll, A., Niu, F., Hendrayanto, and Hölscher, D. (2016). Water use patterns of four tropical bamboo species assessed with sap flux measurements. *Front. Plant Sci.* 6:1202. doi: 10.3389/fpls.2015.01202

Münch, E. (1930). *Die Stoffbewegunen in der Pflanze*. Jena: Verlag von Gustav Fischer.

O'brien, J. J., Oberbauer, S. F., and Clark, D. B. (2004). Whole tree xylem sap flow responses to multiple environmental variables in a wet tropical forest. *Plant Cell Environ.* 27, 551–567. doi: 10.1111/j.1365-3040.2003.01160.x

Savage, J. A., Clearwater, M. J., Haines, D. F., Klein, T., Mencuccini, M., Sevanto, S., et al. (2015). Allocation, stress tolerance and carbon transport in plants: how does phloem physiology affect plant ecology? *Plant Cell Environ.* 39, 709–725. doi: 10.1111/pce.12602

Song, X., Peng, C., Zhou, G., Gu, H., Li, Q., and Zhang, C. (2016). Dynamic allocation and transfer of non-structural carbohydrates, a possible mechanism for the explosive growth of Moso bamboo. *Sci. Rep.* 6:25908. doi: 10.1038/srep25908

Stueffer, J. F., De Kroon, H., and During, H. J. (1996). Exploitation of environmental hetergeneity by spatial division of labor in a clonal plant. *Funct. Ecol.* 10, 328–334.

Thompson, M. V., and Holbrook, N. M. (2003). Scaling phloem transport: water potential equilibrium and osmoregulatory flow. *Plant Cell Environ.* 26, 1561–1577. doi: 10.1046/j.1365-3040.2003.01080.x

Ueda, K. (1960). Studies on the physiology of bamboo with reference to practical application. *Bull. Kyoto Univ. For.* 30, 1–169.

Van Den Besselaar, E. J. M., Klein Tank, A. M. G., Van Der Schrier, G., Abass, M. S., Baddour, O., Van Engelen, A. F. V., et al. (2014). International climate assessment & dataset: climate services across borders. *Bull. Am. Meteorol. Soc.* 96, 16–21.

Wang, Y., Dong, M., Yu, F., Jiang, H., Yu, S., Lin, X., et al. (2011). Mechanical shaking and soil water affect the growth of in the Mu Us Sandland. *J. Arid Environ.* 75, 974–977. doi: 10.1016/j.jaridenv.2011.04.019

Wang, Z., Li, Y., During, H. J., and Li, L. (2011). Do clonal plants show greater division of labour morphologically and physiologically at higher patch contrasts? *PLoS One* 6:e25401. doi: 10.1371/journal.pone.0025401

Yang, S., Zhang, Y., Goldstein, G., Sun, M., Ma, R., and Cao, K. (2015). Determinants of water circulation in a woody bamboo species: afternoon use and night-time recharge of culm water storage. *Tree Physiol.* 35, 964–974. doi: 10.1093/treephys/tpv071

Zhang, Y., Zhang, Q., and Sammul, M. (2012). Physiological integration ameliorates Negative effects of drought stress in the clonal herb. *PLoS One* 7:e44221. doi: 10.1371/journal.pone.0044221

Zhao, X., Zhao, P., Zhang, Z., Zhu, L., Niu, J., Ni, G., et al. (2016). Sap flow-based transpiration in : applicability of the TDP methodology, age effect and rhizome role. *Trees* 31, 765–779. doi: 10.1007/s00468-016-1407-4

Conflict of Interest Statement: The authors declare that the research was conducted in the absence of any commercial or financial relationships that could be construed as a potential conflict of interest.

frontiers in Plant Science

ORIGINAL RESEARCH
published: 08 May 2019
doi: 10.3389/fpls.2019.00573

High Air Humidity Causes Atmospheric Water Absorption *via* Assimilating Branches in the Deep-Rooted Tree *Haloxylon ammodendron* in an Arid Desert Region of Northwest China

Xue-Wei Gong[1,2], Guang-Hui Lü[1,2,3], Xue-Min He[1,2,3], Binoy Sarkar[4,5] and Xiao-Dong Yang[1,2]**

[1]Key Laboratory of Oasis Ecology, Xinjiang University, Urumqi, China, [2]College of Resources and Environmental Sciences, Xinjiang University, Urumqi, China, [3]Institute of Arid Ecology and Environment, Xinjiang University, Urumqi, China, [4]Department of Animal and Plant Sciences, The University of Sheffield, Sheffield, United Kingdom, [5]Future Industries Institute, University of South Australia, Mawson Lakes, SA, Australia

Atmospheric water is one of the main water resources for plants in arid ecosystems. However, whether deep-rooted, tomentum-less desert trees can absorb atmospheric water *via* aerial organs and transport the water into their bodies remains poorly understood. In the present study, a woody, deep-rooted, tomentum-less plant, *Haloxylon ammodendron* (C.A. Mey.) Bunge, was selected as the experimental object to investigate the preconditions for and consequences of foliar water uptake. Plant water status, gas exchange, and ^{18}O isotopic signatures of the plant were investigated following a typical rainfall pulse and a high-humidity exposure experiment. The results showed that a high content of atmospheric water was the prerequisite for foliar water uptake by *H. ammodendron* in the arid desert region. After atmospheric water was absorbed *via* the assimilating branches, which perform the function of leaves due to leaf degeneration, the plant transported the water to the secondary branches and trunk stems, but not to the taproot xylem or the soil, based on the ^{18}O isotopic signatures of the specimen. Foliar water uptake altered the plant water status and gas exchange-related traits, i.e., water potential, stomatal conductance, transpiration rate, and instantaneous water use efficiency. Our results suggest that atmospheric water might be a subsidiary water resource for sustaining the survival and growth of deep-rooted plants in arid desert regions. These findings contribute to the knowledge of plant water physiology and restoration of desert plants in the arid regions of the planet.

Keywords: foliar water uptake, rainfall pulse, deep-rooted woody plant, air relative humidity, ^{18}O isotopic signatures

OPEN ACCESS

Edited by:
Boris Rewald, University of Natural Resources and Life Sciences, Austria

Reviewed by:
Lars Hendrik Wegner, Karlsruhe Institute of Technology (KIT), Germany
Roman Zweifel, Swiss Federal Institute for Forest, Snow and Landscape Research (WSL), Switzerland

****Correspondence:***
Guang-Hui Lü
guanghui_xju@sina.com
Xiao-Dong Yang
xjyangxd@sina.com

Specialty section:
This article was submitted to Functional Plant Ecology, a section of the journal Frontiers in Plant Science

Received: *02 January 2019*
Accepted: *16 April 2019*
Published: *08 May 2019*

Citation:
Gong X-W, Lü G-H, He X-M, Sarkar B and Yang X-D (2019) High Air Humidity Causes Atmospheric Water Absorption via Assimilating Branches in the Deep-Rooted Tree Haloxylon ammodendron in an Arid Desert Region of Northwest China. Front. Plant Sci. 10:573. doi: 10.3389/fpls.2019.00573

INTRODUCTION

In arid ecosystems, water is the limiting factor on the ecological performance of plants (Kidron 2010; Yang et al., 2014a; Dai et al., 2015; Yang et al., 2017). In order to survive and grow in an extreme drought environment, desert plants develop special strategies to utilize all sorts of potential water resources (Yan et al., 2015). Atmospheric water is moisture that can be absorbed by the plant aerial organs, i.e., the unsaturated atmospheric water, clouds, fog, melting snow water, rainfall, and dewfall (Gotsch et al., 2014; Mayr et al., 2014; Eller et al., 2016; Pina et al., 2016; Wang et al., 2016a; Steppe et al., 2018). It is estimated that atmospheric water makes up 28–66% of the water input in the coastal prairie ecosystem of California (Corbin et al., 2005), and it can supply 74% water to plants for their growth and survival in arid desert regions (Kidron, 2000). However, owing to the differences in the absorptive pathways between atmospheric water and traditional water resources such as soil water and groundwater (Goldsmith, 2013), our understanding of how environmental conditions control plant aerial organs to absorb atmospheric water remains unclear.

The absorption of atmospheric water *via* plant aerial organs has been considered a crucial and universal phenomenon in previous studies (Schwerbrock and Leuschner, 2017). Although some recent studies have reported that the emergence of foliar water uptake might be related to the plant's root functional type and water availability (Cassana et al., 2016; Ma et al., 2017), which environmental factors actually trigger this water absorption strategy is an ongoing debate among researchers (Goldsmith, 2013; Yan et al., 2015; Cassana et al., 2016; Wang et al., 2016b). In arid desert regions, shallow-rooted herbaceous plants usually absorb atmospheric water, whereas deep-rooted woody plants rely more on groundwater or deep soil water (Pan et al., 2016; Ma et al., 2017; Yang et al., 2017; Liu et al., 2018). The water absorption preferences of desert plants might be determined by the sustainability and magnitude of different water resources. It is generally believed that atmospheric water and groundwater are the two main types of water inputs in arid desert regions (Kidron, 2000; Golkarian et al., 2018). Atmospheric water is an unstable and scarce water source, while groundwater is a more stable and abundant water source (Dawson and Pate, 1996). Due to their perennial nature, deep-rooted woody plants in arid regions must increase carbon investments in their roots to obtain a large amount of groundwater to satisfy a higher water demand (Dai et al., 2015). In contrast, because they are annual or ephemeral plants, shallow-rooted herbaceous plants only absorb a small amount of atmospheric water to guarantee their growth (Zhuang and Ratcliffe, 2012; Yang et al., 2017). Thus, the difference in predilection for water sources between deep-rooted woody trees and shallow-rooted herbaceous plants may also depend on their water demand and the distinct accessibility of various water sources in arid desert regions (Zhuang and Ratcliffe, 2012; Cassana et al., 2016; Yang et al., 2017). Desert deep-rooted woody trees generally have a considerably higher biomass than shallow-rooted herbaceous plants and therefore tend to utilize all categories of potential water resource inputs to sustain their growth and survival in water-limited environments. Additionally, simulation experiments have suggested that the emergence of uptake of atmospheric water by desert plants, to some extent, depends on the magnitude of atmospheric water (Zhuang and Ratchiffe, 2012; Yang et al., 2017). In other words, high humidity might be the precondition for the absorption of atmospheric water *via* aerial organs for the deep-rooted plants in arid ecosystems. However, whether deep-rooted desert trees can absorb atmospheric water and the assumption that the atmospheric water content is closely related to atmospheric water uptake *via* the aerial organs of deep-rooted desert plants have not yet been properly assessed in previous studies (Yan et al., 2015; Wang et al., 2016b).

The soil-plant-atmosphere continuum (SPAC) and traditional water transport theories assume that water moves from the soil through a plant and then out into atmosphere due to the difference in water potential (Ψ) (Philip, 1966). Within the SPAC, the water potential gradually decreases from soil to atmosphere. However, if atmospheric water is absorbed by plant aerial organs, water migrates from the atmosphere to trunk xylem, and even to root xylem, and finally to rhizosphere soils (Eller et al., 2013; Cassana et al., 2016). This indicates that there would be a reversal of water potential gradient from the SPAC and traditional water transport theories. Hence, there would exist two processes in plants: (1) water moves from a higher $\Psi_{atmosphere}$ to lower Ψ_{stem} through the foliar absorption of atmospheric water, while water also simultaneously rises from a higher Ψ_{soil} to lower Ψ_{stem}, thus plants obtain water from two directions; and (2) water moves from a higher $\Psi_{atmosphere}$ to a lower Ψ_{soil} only through the foliar absorption of atmospheric water (Goldsmith, 2013). In recent studies, the inverse water potential gradient in plants has been reported under artificial controlled conditions (Yan et al., 2015), but no research has found this phenomenon under field conditions. Additionally, there is no explicit conclusion on which factors control foliar water uptake in plants.

Haloxylon ammodendron (C.A. Mey.) Bunge (Chenopodiaceae) is a xerophytic woody dominant species in the arid deserts of Asia (Xu et al., 2016), which is a deep-rooted plant with many xeromorphic characteristics in its leaves and roots to adapt to drought (Huang et al., 2003; Dai et al., 2015). It has been reported that the assimilating branches of *H. ammodendron* are sensitive to changes in water inputs *via* physiological performance (Xu et al., 2007; Yang et al., 2014a). In this species, transpiration and carbon assimilation occur at the branch level due to leaf degeneration. Additionally, atmospheric water constitutes a large proportion of the available water resources in the arid desert region (Kidron, 2000). Thus, it is possible that the assimilating branches of *H. ammodendron* might absorb atmospheric water.

In this study, some plant water status and gas exchange traits of *H. ammodendron* were assessed following a natural rainfall pulse and in an artificial high-humidity exposure experiment to monitor the processes of absorption and transport of atmospheric water from the assimilating branches to the stems of *H. ammodendron*. Here, we hypothesized that (1) the high content of atmospheric water is the prerequisite

for foliar water uptake by the deep-rooted plant in arid desert regions, and (2) the absorbed water will cause changes in water status and gas exchange and will cause water potentials to reverse direction from the SPAC and traditional water transport theories.

MATERIALS AND METHODS

Study Site and Plant Species

The study site is located in the Ebinur Lake Wetland National Nature Reserve (82°36′–83°50′E, 44°30′–45°09′N) in the southwestern part of Gurbantunggut Desert, Xinjiang Uygur Autonomous Region, China. Consistent with a typical continental climate, this region is extremely dry and has scarce rainfall and frequent dust storms (He et al., 2015). Additionally, winters and summers are long, whereas springs and autumns are short in this region. The annual sunshine hours reach approximately 2,800 h. The annual precipitation is less than 100 mm, and rainfall events of ≤ 5 mm and > 10 mm account for 87.5 and 4.3% of the total rainfall, respectively (Zheng et al., 2012). The annual potential evaporation is more than 1,600 mm (Yang et al., 2017). The area is dominated by sunny days throughout the year; hence, precipitation is just an occasional event. The groundwater level is 1.50–2.30 m, and groundwater is the main water source for local plants and the desert ecosystem (Yang et al., 2014b; Ma et al., 2017).

H. ammodendron is a dominant woody species in the arid desert region, which grows naturally in a variety of habitats in the Asian and African deserts, i.e., gravel desert, clay desert, saline land, fixed and semi-fixed sandy lands (Tobe et al., 2000). Owning to its ecological roles in combating desertification and maintaining the desert forest community, *H. ammodendron* is considered a sustainer of arid desert ecosystems (Zhuang and Zhao, 2017). In the present research, 4 km^2 typical plots of *H. ammodendron* forest were first chosen as our experimental plots. Then, some young *H. ammodendron* individuals were randomly selected as our experimental subjects. Here, the selection of young *H. ammodendron* was needed due to the maneuverability of the high-humidity exposure experiment involving the plant species (see the "Experimental design" section below).

Experimental Design

To test our first hypothesis that the high content of atmospheric water is the prerequisite for foliar water uptake, a natural rainfall pulse and a high-humidity exposure experiment were conducted in this study. Precipitation in this arid desert is very scarce and is only worth 10% of evapotranspiration; hence, the atmospheric water content is low under traditional sunny conditions (e.g., the daily average air relative humidity on sunny days ranges from 25 to 50% in this region). However, a high content of atmospheric water can be reached during and following a rainfall event, which might result in direct water uptake *via* aerial organs. Similarly, a high-humidity exposure experiment could raise the atmospheric water content to a high level, which could also induce the emergence of foliar water uptake by the plant species. It is believed that the content of atmospheric water can be represented as the air relative humidity (RH); thus, our experimental objectives can be described as defining the causality between RH and foliar water uptake.

For the natural rainfall pulse experiment, three traditional sunny days (12th, 13th, and 16th July 2016) and a natural rainfall event (20th July 2016) were randomly selected as a humidity experiment to test the differences in water potentials between plant organs as well as the differences in RH between rainy and sunny days. The traditional sunny day was characterized by less than 10% cloud cover and the peaks of unimodal photosynthetic photon flux density curves greater than 1,600 mmol m^{-2} h^{-1}. The selected rainfall event occurred at 16:11–16:30 (local time, the same below) and lasted for 20 min. The total rainfall amount reached 3.56 mm. It was reported that the typical rainfall in the Gurbantunggut Desert is approximately 3–5 mm; thus, our selected rainfall was a typical rainfall pulse in this region (Zheng et al., 2012). Within the rainy and sunny days, atmospheric water conditions (RH) and soil volumetric water content (Svwc) (30 cm) were monitored using a VP-4 sensor (Decagon Devices Inc., USA) and a 5-TE probe (Decagon Devices Inc., USA), respectively. The interval of data collection on both instruments was 1 min, and the data were recorded with a data logger (EM50, Decagon Devices Inc., USA). Additionally, water potentials in the assimilating branches (Ψ_{ab}) and secondary branches (Ψ_{sb}) of *H. ammodendron* on rainy and sunny days were measured in this experiment. The occurrence of an inverse water potential gradient ($\Psi_{ab} > \Psi_{sb}$) on the rainy day was regarded as confirmation of our first hypothesis (Goldsmith, 2013). The assimilating branches refer to the tender and succulent current-year branches (phylloclades) that take over the function of gas exchange from the degenerated leaves, thus minimizing evaporative water loss (Huang et al., 2003). In the present study, the secondary branch is defined as a twig on which assimilating branches converge (the assimilating branch was regarded as the first level branch). It is easy to distinguish the assimilating branch and the secondary branch on the basis of their morphology because their colors are glossy green and greyish white, respectively (**Figure 1**).

For the high-humidity exposure experiment, a young *H. ammodendron* individual plant with a basal diameter of 4.2 cm roughly divided into two main branches was selected as our experimental subject (**Figure 1**). During the experiment, the aboveground part of the plant was divided into two types of branches: one type of branch was the treatment that was enclosed in a humidity chamber, while the other type was exposed to natural conditions and considered the control (**Figure 1**). The humidity chamber was built of polymethylmethacrylate (PMMA) and had 1.2 m × 1.2 m × 1.5 m dimensions. The joints between PMMA sheets were sealed with transparent adhesive tape. Additionally, in order to eliminate fluxes of water and heat between soil and air in the chamber, a multilayer low density polyethylene film (LDPF) was placed on the bottom of the humidity chamber (**Figure 1**). Atmospheric humidity inside the chamber was controlled by an ultrasonic humidifier placed on the LDPE,

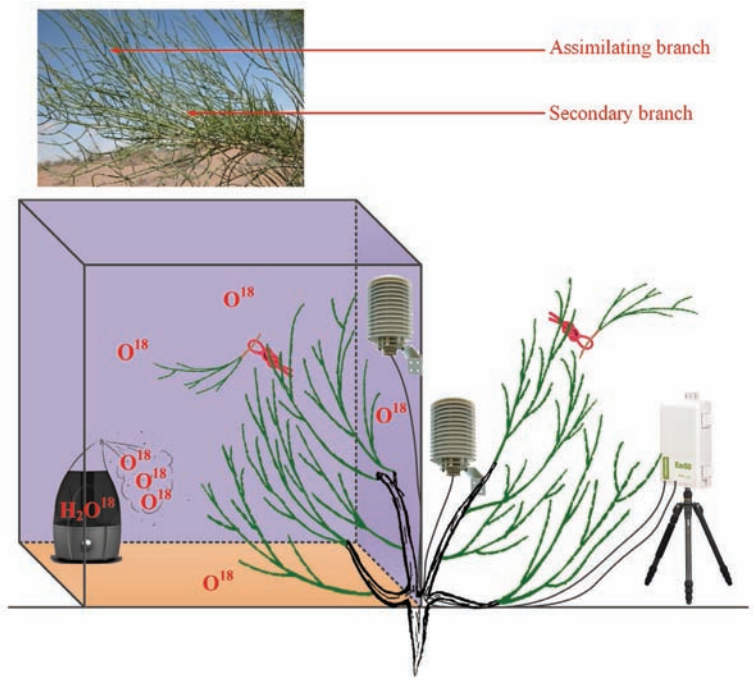

FIGURE 1 | Design of the high-humidity exposure experiment.

and RH was maintained above 90% by turning the humidifier on or off (**Figure 1**). In addition, in this experiment, a pocket weather meter (Model 5000, KestrelMeters, USA) was hung in the chamber and used to quickly obtain RH status in the chamber. At the same time, two VP-4 sensors (Decagon Devices Inc., USA) were also hung on the treatment and control branches to record the real-time changes in RH and air temperature (T) inside and outside the chamber. RH and T were measured every 1 min and recorded with a data logger (EM50, Decagon Devices Inc., USA) (**Figure 1**). In this experiment, the high-humidity exposure experiment was conducted for 8 h from 20:00 on 25th July 2016 to 04:00 on 26th July 2016. Within the experimental period, Ψ_{ab} and Ψ_{sb} of *H. ammodendron* outside and inside the chamber were also measured. In addition, since the humidifying water was ^{18}O labeled (*c.* 3008.52‰ $\delta^{18}O$) in the high-humidity exposure experiment (**Figure 1**), the emergence of the labeled ^{18}O in assimilating branches and other organs can also demonstrate our first hypothesis. Here, the ^{18}O-labeled water was composed of a mixture of groundwater (*c.* −14.39‰ $\delta^{18}O$) and water enriched in ^{18}O (98%, Shanghai Research Institute of Chemical Industry, CHN). Because of the constraints of budget and experimental operability, it was difficult to implement multiple high-humidity chambers in the field to test the atmospheric water absorption and transport within the plant body. Therefore, the high-humidity exposure experiment was conducted only once in this study (Yan et al., 2015; Wang et al., 2016b).

To test the second hypothesis that the absorbed water will cause a variability in the water transport process and cause an inversion in water potentials from the SPAC and traditional water transport theories, the difference between Ψ_{ab} and Ψ_{sb} of *H. ammodendron* was measured in both the rainfall pulse and high-humidity chamber experiments. In addition, the differences in the values of $\delta^{18}O$ among the different plant organs and soil were measured in the high-humidity exposure experiment.

In this study, the outstanding characteristics of foliar water uptake would probably be impeded by root water uptake. Thus, some inferior shoots (containing assimilating branches and secondary branches) of the treatment and control branches were cut. All the end cuts were immediately sealed with petrolatum, and the excised inferior shoots were then hung inside and outside the chamber to distinguish the effects of root and foliar water uptake (**Figure 1**). Therefore, the entire high-humidity exposure experiment was composed of four treatments: inside-attached, inside-detached, outside-attached, and outside-detached. "Attached" represents the samples connected to the main stem, and "detached" represents the samples cut from the main stem; "inside" and "outside" represent the inside and outside of the high-humidity chamber. In addition, since the foliar water uptake might cause some changes in gas exchange traits, such as stomatal conductance (g_s, mol CO_2 m^{-2} s^{-1}), transpiration rate (E, mmol H_2O m^{-2} s^{-1}), and instantaneous water use efficiency (WUEi, μmol CO_2 mmol H_2O), differences in these traits among the four treatments were also tested in this study.

Measurements

In the rainfall pulse experiment of this study, five young individual *H. ammodendron* plants with similar heights and

basal diameters (~1.5 m height and ~5 cm basal diameter) were randomly selected as subjects to test the differences in water potential between assimilating branches and secondary branches. Immediately after a natural rainfall pulse (20th July 2016) and on three representative sunny days (12th, 13th, and 16th July 2016), one shoot (containing the assimilating and the secondary branches) of each individual plant was collected (all the end cuts caused by sampling were immediately sealed with petrolatum) and sealed immediately in a plastic bag containing moist paper towels. The samples were subsequently kept in a cooler until the water potential was determined. The measurements of Ψ_{ab} and Ψ_{sb} were taken using a dew point water potential instrument (WP4C, Decagon Devices, Pullman, WA, USA). The interval of water potential measurements was 2 h, and the measurement was conducted from 20:00 to 4:00.

During the process of humidifying in the high-humidity exposure experiment, Ψ_{ab} and Ψ_{sb} were also measured at 2 h intervals from 20:00 to 04:00. For the samples in the chamber, we opened the door of the chamber every 2 h to cut the assimilating and the secondary branches to determine their differences in water potential. To decrease the effects of opening on the maintenance of high humidity in the chamber, the duration of each opening was less than 15 min. All samples from the inside and outside of the chamber with three replications were measured at each time (all the end cuts caused by sampling were immediately sealed with petrolatum). To test the effect of foliar water uptake on gas exchange traits, g_s, E, and WUEi of three assimilating branches from inside and outside of the chamber were measured at the end of the high-humidity exposure experiment (4:00) using a portable photosynthesis system (LI-6400XT, Li-COR, Inc., Lincoln, NE, USA). After that, three samples of the assimilating branches, secondary branches, and trunk xylem from inside and outside of the chamber [the samples collected from the inside of the chamber were washed with tap water and dried with paper towels to avoid potential isotopic contamination of labeled water condensed on the surface of samples (Eller et al., 2013)], as well as three samples of root xylem, rhizosphere soil, and bulk soil were carefully collected to identify the transport direction of ^{18}O water through the atmosphere, the assimilating branches, stems, roots, rhizosphere soils, and bulk soils. Meanwhile, three samples of taproot xylem, rhizosphere soil, and bulk soil of adjacent natural *H. ammodendron* plants were collected in order to test whether the ^{18}O-labeled water was transported from the atmosphere to the soil *via* plant stem. Here, the significant difference in $\delta^{18}O$ signature between humidifying and natural samples was used to illustrate the above water transport mechanisms. Following collection, all isotope samples were rapidly put in vials and sealed with parafilm. Subsequently, all samples were placed in a −20°C frozen box. The $\delta^{18}O$ measurement was conducted at the Fukang Desert Ecosystem Observation and Experiment Station, Chinese Academy of Sciences. Specifically, water was extracted from the plant tissues and soil samples using a vacuum extraction instrument (LI-2000, Lica United, Beijing, CHN), and the measurement of oxygen isotopic compositions was conducted using an isotope ratio infrared spectroscopy (IRIS) analyzer-the Liquid Water Isotope Analyzer (LWIA, DLT-100, Los Gatos Research Inc., Mountain View, CA, USA). The analytical precision of individual measurements was ± 0.25‰ for $\delta^{18}O$ (Dai et al., 2015). The isotopic abundance was expressed in delta notation (δ) in parts per thousand (‰) as $\delta = (R_{sample}/R_{standard} - 1) \times 1{,}000$, where R_{sample} and $R_{standard}$ are the molar ratios of heavy to light isotope in the sample and the international standard (Vienna Standard Ocean Water for $^{18}O/^{16}O$), respectively.

Data Analysis

In this study, the paired Student's *t*-test was used to test the differences in RH, T, Svwc, and Ψ_{ab} among different atmospheric humidity levels. In addition, the unpaired Student's *t*-test was used to indicate the differences in nocturnal Ψ_{ab} and Ψ_{sb} at each measurement time on rainy and sunny days. All statistical analyses were conducted using SPSS 17.0 (SPSS Inc., Chicago, USA). All data were tested for normality and variance constant, and $p < 0.05$ was considered to be statistically significant.

RESULTS

Atmospheric Water Uptake *via* Assimilating Branches Following a Rainfall Pulse

Our results showed that the RH values at any time during the rainfall pulse were significantly higher than those during the three typical sunny days (**Figure 2A**) ($p < 0.01$). The rainfall pulse also had a long-term effect, maintaining RH at a high level for 12 h after the rainfall (**Figure 2A**). In summary, the rainfall pulse increased the amount and availability of atmospheric water and had a great influence on the Svwc of the topsoil (**Figure 2B**). During the three typical sunny days, $\Psi_{sb} > \Psi_{ab}$ was maintained at each measurement occasion at night (**Figure 3A**). However, the inverse water potential gradient between Ψ_{sb} and Ψ_{ab} occurred during the rainy day ($\Psi_{ab} > \Psi_{sb}$) (**Figure 3B**). Specifically, after the rainfall pulse, Ψ_{sb} was lower than Ψ_{ab} from 22:00 to 04:00, whereas the other periods showed the opposite trend (**Figure 3B**). Additionally, the nocturnal mean value of Ψ_{ab} was higher on the rainy day than on the sunny days (**Figure 3C**).

Atmospheric Water Uptake *via* Assimilating Branches in the High-Humidity Exposure Experiment

Relationships between Ψ_{ab} and Ψ_{sb} differed among the four experimental treatments in the high-humidity exposure experiment (**Figure 4**). Specifically, $\Psi_{ab} > \Psi_{sb}$ occurred in inside-attached and inside-detached treatments (**Figures 4A,B**), whereas outside-attached and outside-detached treatments showed the opposite result ($\Psi_{sb} > \Psi_{ab}$) (**Figures 4C,D**). The duration of $\Psi_{ab} > \Psi_{sb}$ in the inside-attached treatment was longer than that in the inside-detached treatment (**Figures 4A,B**). All observed times showed $\Psi_{sb} > \Psi_{ab}$ in both the outside-attached and outside-detached treatments (**Figures 4C,D**). In addition, the value of $\delta^{18}O$ in the assimilating branches of

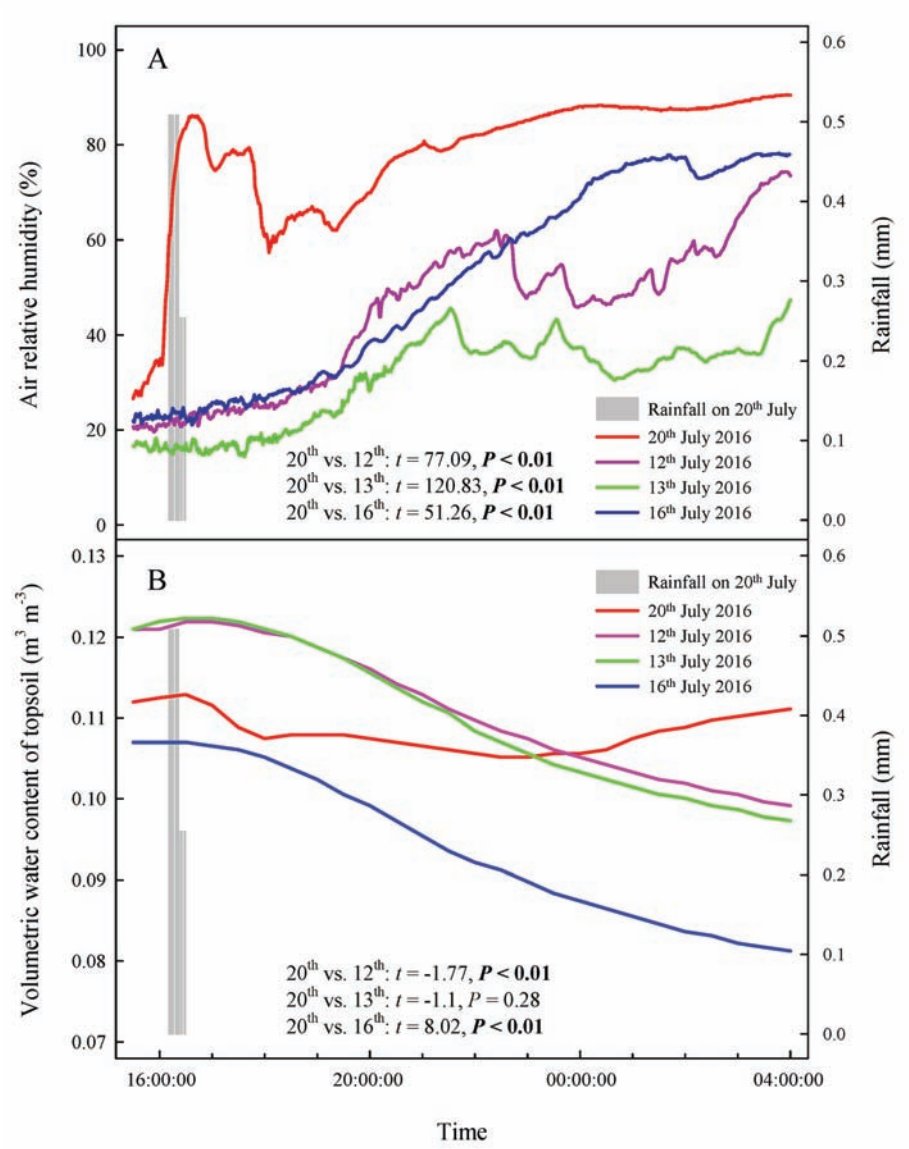

FIGURE 2 | Changes in atmospheric and soil moisture on a rainy day and three sunny days. **(A)** air relative humidity, **(B)** volumetric water content of topsoil. The bars represent a rainfall pulse at 16: 11–16: 30 on 20th July 2016. The red line represents the changes in atmospheric and soil moisture following a rainfall pulse on 20th July 2016. The purple, green and blue lines represent the changes in atmospheric and soil moisture on three representative sunny days (12th, 13th, and 16th July 2016), respectively. The *t*'s and *p*'s are the results of the paired Student's *t*-test for the variability of atmospheric and soil moisture between rainy and sunny days.

the inside-attached treatment was higher than that in the outside-attached treatment; meanwhile, the assimilating branch $\delta^{18}O$ of the inside-detached treatment was higher than that of the outside-detached treatment (**Figure 5**).

Difference in Water Transport Between the Inside and Outside of the Chamber

In the inside-attached treatment, the value of $\delta^{18}O$ was the highest in assimilating branches, intermediate in secondary branches, and the lowest in trunk xylem (**Figure 5**). In the inside-detached treatment, although the water pathway was cut-off from assimilating branches to trunk xylem, our results showed that the value of $\delta^{18}O$ was substantially higher in the assimilating branches than in the secondary branches (**Figure 5**). In contrast, the values of $\delta^{18}O$ were not different among the assimilating branches, secondary branches or trunk xylem in the outside-attached and outside-detached treatments (**Figure 5**). In addition, the values of $\delta^{18}O$ in assimilating branches, secondary branches, and trunk xylem from outside the humidity exposure chamber were lower than those from inside the chamber (**Figure 5**). The values of $\delta^{18}O$ in taproot xylem, rhizosphere soil, and bulk soil were not different between the humidifying and natural samples (**Figure 6**).

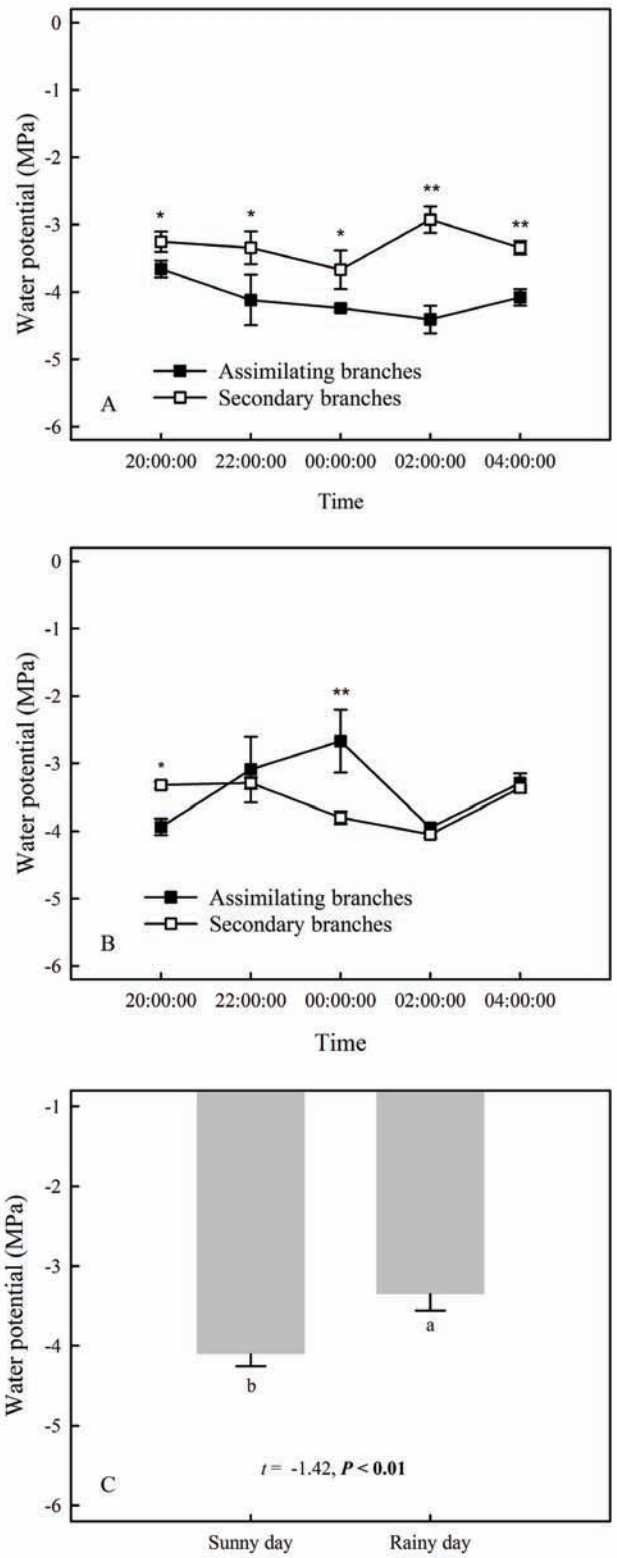

FIGURE 3 | The compared relationship of the assimilating branches to the secondary branches of *H. ammodendron* in water potential on the sunny **(A)** and rainy days **(B)**, as well as the nocturnal mean water potential of assimilating branches between sunny and rainy days **(C)**. The asterisks at each measurement time in panels **(A)** and **(B)** represent the significant differences in water potential between the assimilating branches and the secondary branches (unpaired Student's *t*-test; *, $p < 0.05$; **, $p < 0.01$). Different lowercase letters on the top of the bars in panel **(C)** represent the significant difference in nocturnal mean water potential of assimilating branches between rainy and sunny days, the *t*'s and *p*'s are the results of the paired Student's *t*-test. Values are shown as the mean ± SE.

Response of Plant Water Status and Gas Exchange to Atmospheric Water Uptake

Our results showed that the predawn Ψ, g_s, E, and WUEi in the assimilating branches were higher inside the high-humidity exposure chamber than they were outside the chamber (**Figure 7**). Physiological measurements indicated that both foliar water uptake and root water uptake had great influence on predawn Ψ, g_s, and E values (**Figures 7A–C**). Interestingly, the variability of WUEi was seemingly only influenced by foliar water uptake because the attached and detached treatments had similar WUEi values both inside and outside the chamber (**Figure 7D**). In addition, RH was significantly higher inside the high-humidity exposure chamber than outside ($p < 0.05$), whereas T did not differ between the inside and outside of the chamber (**Figure 8**). This indicated that the difference in plant water status and gas exchange inside and outside the chamber was not affected by the T but was the result of the difference in RH.

DISCUSSION

Atmospheric Water Uptake *via* Assimilating Branches

In arid desert regions, rainfall is considered the most readily obtainable atmospheric water for plants. A large proportion of rainfall is intercepted by plant foliage and is generally assumed to evaporate back into the atmosphere or fall onto the topsoil in arid desert ecosystems (Breshears et al., 2008). However, our results showed that a reverse relationship in water potential ($\Psi_{ab} > \Psi_{sb}$) appeared after a rainfall pulse (**Figure 3B**), which indicated that the assimilating branches directly absorbed rainfall water from the atmosphere (Goldsmith, 2013; Yan et al., 2015). It is believed that the availability of atmospheric water might be the decisive condition of foliar water uptake in arid desert regions (Zhuang and Ratcliffe, 2012; Yang et al., 2017). In this regard, RH might have a significant relationship with the occurrence of foliar water uptake. The results of the present study showed that the RH increased significantly after a rainfall event (**Figure 2A**) and then caused $\Psi_{ab} > \Psi_{sb}$ (**Figure 3B**). This result suggested that the high RH level was the prerequisite for foliar water uptake in this arid desert region. Similar results were also found in previous studies, e.g., the pseudostem of *Vellozia flavicans* and leaves of *Juniperus* absorbed atmospheric water after rainfall events (Oliveira et al., 2005; Breshears et al., 2008). In addition, the relationship between RH and the occurrence of foliar water uptake was also confirmed in our high-humidity exposure

experiment. Our results demonstrated an inverted water potential gradient between the assimilating branches and secondary branches ($\Psi_{ab} > \Psi_{sb}$) (**Figures 4A,B**). We also found that the labeled ^{18}O water appeared in varying amounts in the assimilating and secondary branches inside the humidity chamber, whereas the ^{18}O abundances did not differ between the two types of

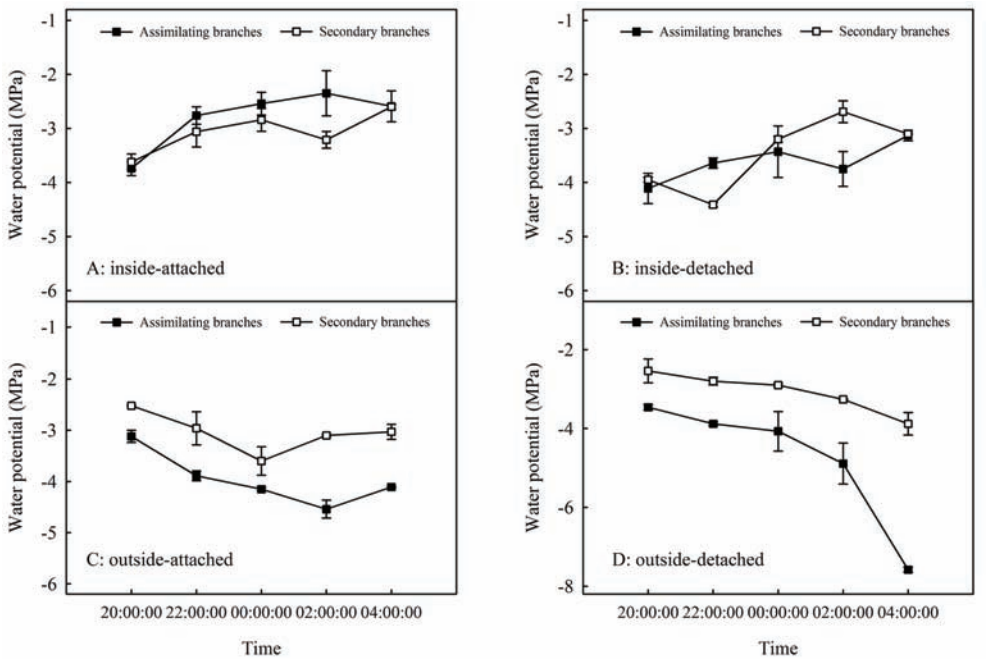

FIGURE 4 | Relationships in water potential between the assimilating branches and the secondary branches of *H. ammodendron* in inside-attached **(A)**, inside-detached **(B)**, outside-attached **(C)** and outside-detached **(D)** treatment in the high-humidity exposure experiment. "Attached" represents the samples connected to the main stem, and "detached" represents the samples cut from the main stem; "inside" and "outside" represent the inside and outside of the high-humidity chamber. Values are shown as the mean ± SE.

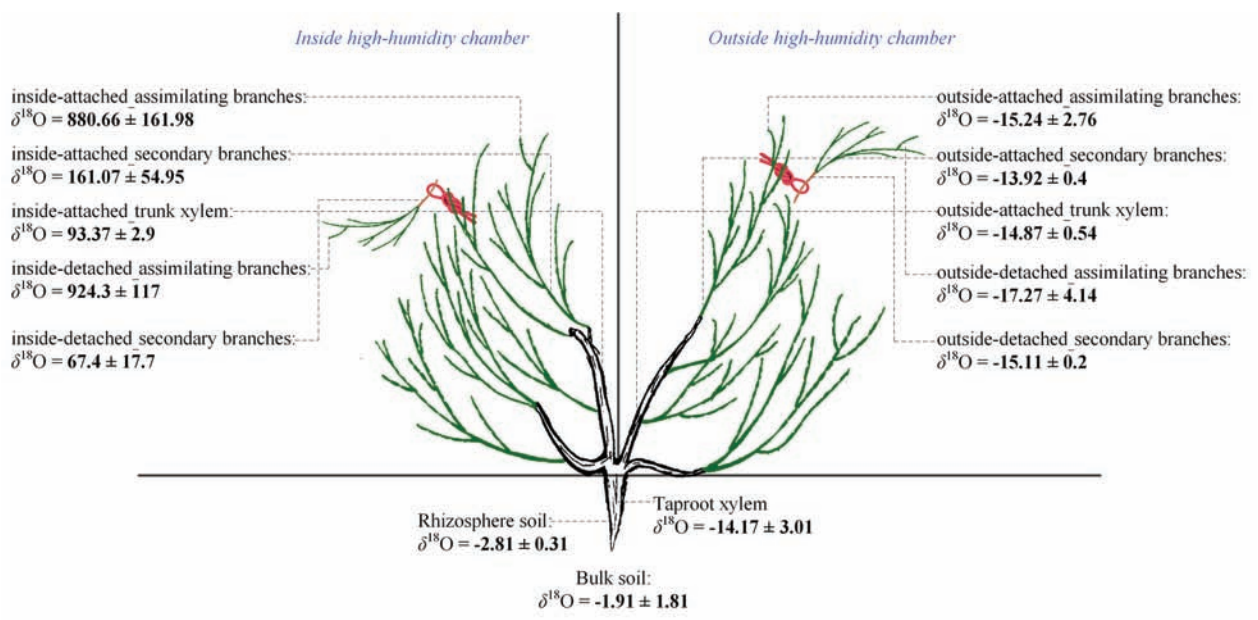

FIGURE 5 | Differences in the value of $\delta^{18}O$ across the assimilating branches, secondary branches, trunk stem, taproot xylem and soil inside and outside of the chamber, as well as in the same plant organs between the inside and outside of the chamber of the high-humidity exposure experiment. "Attached" represents the samples connected to the main stem, and "detached" represents the samples cut from the main stem; "inside" and "outside" represent the inside and outside of the high-humidity chamber. Values are shown as the mean ± SE.

branches outside the chamber (**Figure 5**). These results also indicated that the assimilating branches absorbed atmospheric water at high RH levels.

A rainfall event of approximately 6–12 mm was considered effective precipitation for *H. ammodendron* in the arid desert region because this amount of rainfall could overcome crown interception to supply soil water and could trigger a cascade of plant physiological responses (Yang et al., 2014a). However, our study showed that the assimilating branches of *H. ammodendron* absorbed atmospheric water through assimilating branches at 3.56 mm rainfall (**Figure 3B**).

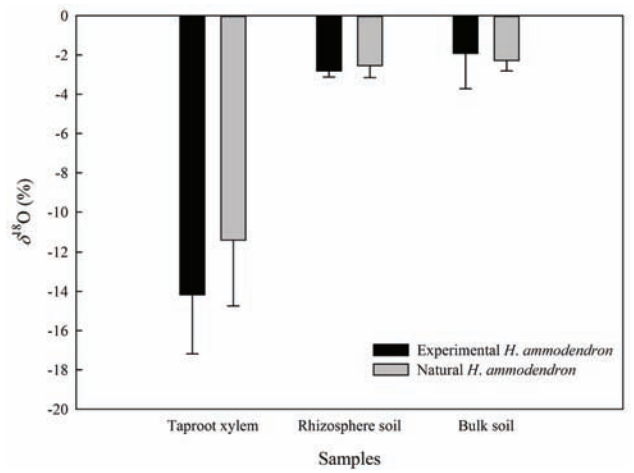

FIGURE 6 | Differences in the value of $\delta^{18}O$ of the taproot xylem, rhizosphere soil and bulk soil between the experimental and the natural *H. ammodendron* individuals. Values are shown as the mean ± SE.

This result suggested that even inappreciable precipitation, such as light rain, dew, and fog, might not directly replenish soil moisture but could play an important role in plant water physiology by rehydrating plant tissues (Dawson, 1998; Burgess and Dawson, 2004). Additionally, our study found that foliar water uptake appeared at high RH levels, which was not observed during sunny days. However, exactly what level of RH would control the switch to atmospheric water uptake still remains unclear and warrants continuous research in the future.

Previous studies indicated that the tomentum on plant aerial organ surfaces was the location of atmospheric water absorption by the plant (Vitarelli et al., 2016). It was reported that plant aerial organs without the tomentum would not absorb water from the atmosphere (Grammatikopoulos and Manetas, 1994; Zhuang and Ratcliffe, 2012). However, our results showed an opposite trend: the tomentum-less assimilating branches of *H. ammodendron* were also able to absorb water from the atmosphere under certain conditions (**Figures 4, 5**). These results suggest that there might be other specialized structures on the surfaces of assimilating branches of *H. ammodendron* that enable the plant to absorb water from the atmosphere. Previous scanning electron microscopy studies indicated that the epidermal structure of the assimilating branches of *H. ammodendron* was uneven and crinkled (Liu et al., 2016). This is conducive to the retention of atmospheric water on the surface of plants and thus might be advantageous in absorbing water from the atmosphere (Eller et al., 2013; Pan et al., 2016). In addition, a recent fluorescence labeling study indicated that the aqueous pores throughout cuticles could allow water transport from the atmosphere into the mesophyll of assimilating branches of *H. ammodendron* (Wang et al., 2016b). These aqueous pores were formed from the continuous permanent dipoles and

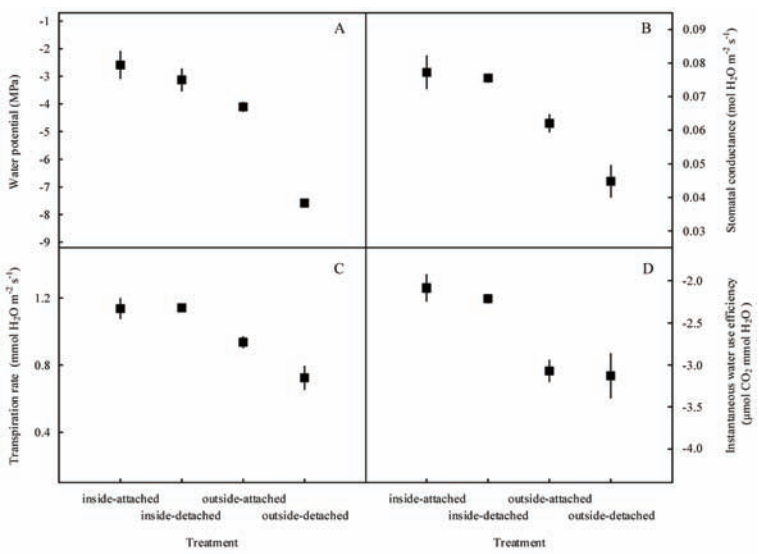

FIGURE 7 | Variations in water status and gas exchange-related traits of the assimilating branches among the four experimental treatments in the high-humidity exposure experiment. "Attached" represents the samples connected to the main stem, and "detached" represents the samples cut from the main stem; "inside" and "outside" represent the inside and outside of the high-humidity chamber. Water status and gas exchange-related traits include water potential **(A)**, stomatal conductance **(B)**, transpiration rate **(C)**, and instantaneous water use efficiency **(D)**. Values are shown as the mean ± SE.

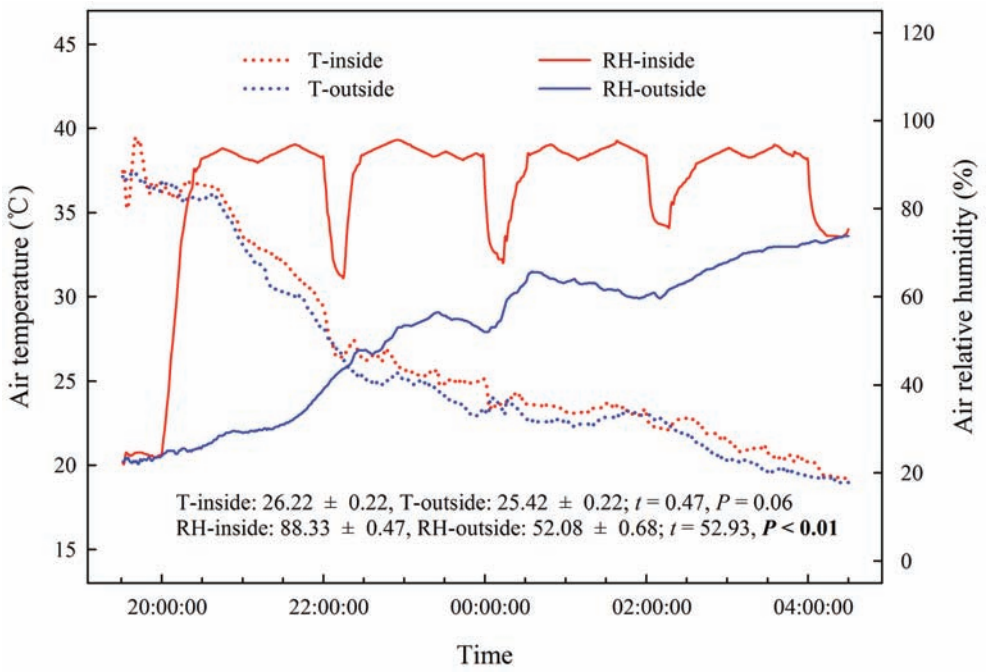

FIGURE 8 | Changes and differences in air temperature (T) and air relative humidity (RH) during the experimental time and between the inside and outside of the chamber of the high-humidity exposure experiment. Experimental time ranges from 20:00 on 25th July to 4:00 on 26th July 2016, and samples were collected at 20:00, 22:00, 0:00, 2:00 and 4:00. The *t*'s and *p*'s are the results of the paired Student's *t*-test. Values are shown as the mean ± SE.

ionizable groups across cuticles of the leaf surface under the conditions of high humidity and water deposition (Schönherr, 2006). It has been shown that direct water uptake by distal leaves from moist air might be mediated by the mucilage layers on the leaf surface and/or the epistomatal mucilage plugs set into the substomatal cavity due to the water binding capacity of acid mucopolysaccharides (Zimmermann et al., 2004, 2007; Westhoff et al., 2009). In many species, mucilage cells were also detected in the inner walls of xylem conduits, and the xylem mucilage was considered to play important roles in shifting water from the mucilage layers and epistomatal plugs to the xylem vessels *via* the apoplast-symplast pathway (Zimmermann et al., 2007; Mastroberti and de Araujo Mariath, 2008). Deng et al. (1998) proved that the assimilating branches of *H. ammodendron* contain abundant mucilage cells; thus, mucilage cells might be a potential location for atmospheric water uptake by assimilating branches and an approach transporting atmospheric water from the assimilating branches to the stem. Therefore, external microstructures, such as rough epidermis, aqueous pores, and mucilaginous substances, might be potential pathways for atmospheric water absorption in tomentum-less plants such as *H. ammodendron* (Zimmermann et al., 2007; Liu et al., 2016; Pan et al., 2016; Wang et al., 2016b).

Effect of Foliar Water Uptake on Water Transport and Physiological Performance

Root water uptake is considered the primary method by which plants absorb water in traditional plant physiology literature (Emery, 2016). Water transport from soil into the atmosphere in the SPAC framework dominated the scientific discussion on plant water movement for many years (Philip, 1966). However, whether absorbed atmospheric water can transport from leaves to the soil remains unclear (Eller et al., 2013; Goldsmith, 2013; Yan et al., 2015; Emery, 2016). The current study showed that the values of $\delta^{18}O$ differed inside and outside of the high-humidity chamber (**Figure 5**), as well as among the assimilating branches, secondary branches and stems inside the high-humidity chamber (**Figure 5**). Additionally, the values of $\delta^{18}O$ in the taproot xylem, rhizosphere soil, and bulk soil did not significantly differ between the humidifying and natural samples (**Figure 6**). These results suggested that the absorbed atmospheric water was transported from the assimilating branches to the trunk stem, but not to the taproot xylem. The above might be determined by the interrelationship between foliar water uptake, root water uptake, and water storage in trunk stems. The opposite direction of water transport during foliar water absorption and transpiration might hinder the downward movement of water uptake *via* assimilating branches at night. Our results showed that $\Psi_{sb} > \Psi_{ab}$ during sunny days in the rainfall pulse experiment (**Figure 3A**) and in outside-attached and outside-detached treatments in the high-humidity experiment (**Figures 4C,D**), which suggested that transpiration caused root absorption of soil water at night. In addition, stem water storage *via* a unique wood structure, i.e., internal secondary phloem through successive cambia, is considered an important strategy for plants surviving in a water-limited

environment (Robert et al., 2014; Barraclough et al., 2018), including *H. ammodendron* (Li et al., 2015). Thus, the small amount of labeled water in the trunk stem might result from the dilution effect of stored water in the trunk stem. On the other hand, the absorbed atmospheric water was not transported from the assimilating branches to the taproot xylem and soils, likely because the foliar water uptake was a subsidiary strategy of desert plants such as *H. ammodendron* in adapting to extreme drought; and this secondary strategy might not be sufficient alone for sustaining plant growth (Yan et al., 2015). In this study, the basal diameter of the selected *H. ammodendron* individual in the high-humidity exposure experiment was 4.2 cm. Based on the previously established relationship between basal diameter of *H. ammodendron* and its root depth under similar growth conditions (Xu et al., 2016), the calculated root depth of the selected individual plant in the current study was enough to tap groundwater, in conformity with other reports that concluded that *H. ammodendron* was a groundwater-dependent desert plant (Liu et al., 2018; Wu et al., 2019). Thus, atmospheric water might merely be a subsidiary water resource in the sustainable survival of desert woody plants. Our results are consistent with a prior study that demonstrated that the atmospheric water of foliar uptake in coastal redwood *Sequoia sempervirens* (D. Don) only accounted for a small fraction of transpirational demand (Dawson, 1998; Burgess and Dawson, 2004). However, atmospheric water is of great significance to plants since the trees possess a relatively loose stomatal control of water loss, and increases in leaf surface wettability and water status could help suppress water loss from leaves (Burgess and Dawson, 2004). Atmospheric water may occupy a decisive position in the regulation of the water balance of plants despite low availability. Additionally, it was reported that atmospheric water would transport from leaves to rhizosphere soils and neighboring plants *via* the inverse and lateral hydraulic redistribution under long-term exposure to high humidity (Caldwell et al., 1998; Eller et al., 2013; Cassana et al., 2016). In that case, foliar water uptake might play important roles in spatial water redistribution and community maintenance. However, in this study, we did not detect labeled atmospheric water in rhizosphere soils of experimental and adjacent natural trees because the high-humidity exposure experiment only lasted one night. The long-term subsidiary benefits of foliar water uptake deserve more attention in future studies in arid desert regions. In addition, quantifying the proportion of atmospheric water in a plant is also an important aspect in analyzing its influences on ecosystem maintenance (Dawson, 1998; Kidron, 2000; Corbin et al., 2005).

Atmospheric water may play a role in regulating physiological performance through foliar water uptake (McHugh et al., 2015; Tomaszkiewicz et al., 2015). As an important indicator of plant water status (Elsayed et al., 2011), the improvement in water potential of the assimilating branches suggested that atmospheric water decreased water stress in the plant. Previous studies suggested that the hygroscopic atmospheric depositions on or around the stomata transform the leaf surface around the stomata from hydrophobic to hydrophilic, which could activate the stomata in assimilating branches of *H. ammodendron* during high-humidity periods (Burkhardt, 2010; Wang et al., 2016b). During this process, water transport through assimilating branches might result in some changes in water status and gas exchange. In this study, the predawn Ψ, g_s, E, and WUEi in the assimilating branches differed between the inside and outside of the chamber (**Figure 7**). This indicated that foliar water uptake had an obvious relationship with physiological performance. In addition, traditional plant physiology theories demonstrate that plants could change their water transport-related traits to improve the capability of water absorption from soils to roots (Novák, 2012); thus, root water uptake also has an obvious relationship with water transport-related traits. In this study, foliar and root water uptake occurred simultaneously at night (**Figures 5, 7**), and our results showed that foliar water uptake, root water uptake and their interactions had significant influences on predawn Ψ, g_s and E (**Figures 7A–C**). The variability of WUEi was only determined by the foliar water uptake (**Figure 7D**) and may be due to the activation of stomata of assimilating branches inside the high-humidity chamber, which contributed to the water vaporization rate through transpiration (Ben-Asher et al., 2010; Wang et al., 2016b).

CONCLUSIONS

The current study highlights that *H. ammodendron*, a tomentum-less and deep-rooted tree, could absorb atmospheric water, and a high level of atmospheric water was the prerequisite for such foliar water acquisition strategy. Our results also found that the absorbed atmospheric water was transported from the assimilating branches to the secondary branches and the trunk stems but not to the taproot xylem or the soil. This suggested that foliar water uptake of *H. ammodendron* had the opposite mechanism as the soil-plant-atmosphere system and traditional water physiology theories. In addition, the foliar and root water uptakes affected the water potential, stomatal conductance, transpiration rate, and instantaneous water use efficiency. These results indicated that foliar water uptake could result in variation in water status and gas exchange of *H. ammodendron*. Atmospheric water might be a kind of subsidiary water resource for the sustainable survival of deep-rooted desert trees with similar characteristics as *H. ammodendron* and warrants further research on this topic in various arid regions of the world.

AUTHOR CONTRIBUTIONS

X-WG and G-HL conceived and designed the experiments. X-WG and X-MH performed the experiments. X-WG and X-DY analyzed the data. X-WG, G-HL, BS, and X-DY wrote the manuscript.

FUNDING

This study was financially supported by the National Natural Science Foundation of China (Nos. 41571034, 31500343, 31760168) and the National Basic Research Program (973 Program) of China (No. 2015CB251601).

ACKNOWLEDGMENTS

We thank Heng-Fang Wang, Zhi-Dong Liu, Yue Chen, Ya-Dong Qie, and Lei Zhang in Key Laboratory of Oasis Ecology of Xinjiang University for their indispensable help in fieldwork and laboratory analysis.

REFERENCES

Barraclough, A. D., Zweifel, R., Cusens, J., and Leuzinger, S. (2018). Daytime stem swelling and seasonal reversal in the peristaltic depletion of stored water along the stem of *Avicennia marina* (Forssk.) Vierh. *Tree Physiol.* 38, 965–978. doi: 10.1093/treephys/tpy021

Ben-Asher, J., Alpert, P., and Ben-Zvi, A. (2010). Dew is a major factor affecting vegetation water use efficiency rather than a source of water in the eastern Mediterranean area. *Water Resour. Res.* 46:W10532. doi: 10.1029/2008WR007484

Breshears, D. D., McDowell, N. G., Goddard, K. L., Dayem, K. E., Martens, S. N., Meter, C. W., et al. (2008). Foliar absorption of intercepted rainfall improves woody plant water status most during drought. *Ecology* 89, 41–47. doi: 10.1890/07-0437.1

Burgess, S. S. O., and Dawson, T. E. (2004). The contribution of fog to the water relations of *Sequoia sempervirens* (d. don): foliar uptake and prevention of dehydration. *Plant Cell Environ.* 27, 1023–1034. doi: 10.1111/j.1365-3040.2004.01207.x

Burkhardt, J. (2010). Hygroscopic particles on leaves: nutrients or desiccants? *Ecol. Monogr.* 80, 369–399. doi: 10.1890/09-1988.1

Caldwell, M. M., Dawson, T. E., and Richards, J. H. (1998). Hydraulic lift: consequences of water efflux from the roots of plants. *Oecologia* 113, 151–161. doi: 10.1007/s004420050363

Cassana, F. F., Eller, C. B., Oliveira, R. S., and Dillenburg, L. R. (2016). Effects of soil water availability on foliar water uptake of *Araucaria angustifolia*. *Plant Soil* 399, 147–157. doi: 10.1007/s11104-015-2685-0

Corbin, J. D., Thomsen, M. A., Dawson, T. E., and D'antonio, C. M. (2005). Summer water use by California coastal prairie grasses: fog, drought, and community composition. *Oecologia* 145, 511–521. doi: 10.1007/s00442-005-0152-y

Dai, Y., Zheng, X. J., Tang, L. S., and Li, Y. (2015). Stable oxygen isotopes reveal distinct water use patterns of two *Haloxylon* species in the Gurbantonggut Desert. *Plant Soil* 389, 73–87. doi: 10.1007/s11104-014-2342-z

Dawson, T. E. (1998). Fog in the California redwood forest: ecosystem inputs and use by plant. *Oecologia* 117, 476–485. doi: 10.1007/s004420050683

Dawson, T. E., and Pate, J. S. (1996). Seasonal water uptake and movement in root systems of Australian phraeatophytic plants of dimorphic root morphology: a stable isotope investigation. *Oecologia* 107, 13–20. doi: 10.1007/BF00582230

Deng, Y. B., Jiang, Y. C., and Liu, J. (1998). The xeromorphic and saline morphic structure of leaves and assimilating branches in ten Chenopodiacea species in Xinjiang. *Chin. J. Plant Ecol.* 22, 164–170 (in Chinese with English abstract). http://www.plant-ecology.com/CN/Y1998/V22/I2/164

Eller, C. B., Lima, A. L., and Oliveira, R. S. (2013). Foliar uptake of fog water and transport belowground alleviates drought effects in the cloud forest tree species, *Drimys brasiliensis* (Winteraceae). *New Phytol.* 199, 151–162. doi: 10.1111/nph.12248

Eller, C. B., Lima, A. L., and Oliveira, R. S. (2016). Cloud forest trees with higher foliar water uptake capacity and anisohydric behavior are more vulnerable to drought and climate change. *New Phytol.* 211, 489–501. doi: 10.1111/nph.13952

Elsayed, S., Mistele, B., and Schmidhalter, U. (2011). Can changes in leaf water potential be assessed spectrally? *Funct. Plant Biol.* 38, 523–533. doi: 10.1071/FP11021

Emery, N. (2016). Foliar uptake of fog in coastal California shrub species. *Oecologia* 182, 731–742. doi: 10.1007/s00442-016-3712-4

Goldsmith, G. R. (2013). Changing directions: the atmosphere–plant–soil continuum. *New Phytol.* 199, 4–6. doi: 10.1111/nph.12332

Golkarian, A., Naghibi, S. A., Kalantar, B., and Pradhan, B. (2018). Groundwater potential mapping using C5.0, random forest, and multivariate adaptive regression spline models in GIS. *Environ. Monit. Assess.* 190:149. doi: 10.1007/s10661-018-6507-8

Gotsch, S. G., Asbjornsen, H., Holwerda, F., Goldsmith, G. R., Weintraub, A. E., and Dawson, T. E. (2014). Foggy days and dry nights determine crown-level water balance in a seasonal tropical Montane cloud forest. *Plant Cell Environ.* 37, 261–272. doi: 10.1111/pce.12151

Grammatikopoulos, G., and Manetas, Y. (1994). Direct absorption of water by hairy leaves of *Phlomis fruticosa* and its contribution to drought avoidance. *Can. J. Bot.* 72, 1805–1811. doi: 10.1139/b94-222

He, X. M., Lv, G. H., Qin, L., Chang, S. L., Yang, M., Yang, J. J., et al. (2015). Effects of simulated nitrogen deposition on soil respiration in a *Populous euphratica* community in the Ebinur Lake Area, a desert ecosystem of Northwestern China. *PLoS One* 10:e0137827. doi: 10.1371/journal.pone.0137827

Huang, Z., Zhang, X., Zheng, G., and Gutterman, Y. (2003). Influence of light, temperature, salinity and storage on seed germination of *Haloxylon ammodendron*. *J. Arid Environ.* 55, 453–464. doi: 10.1016/S0140-1963(02)00294-X

Kidron, G. J. (2000). Analysis of dew precipitation in three habitats within a small arid drainage basin, Negev Highlands, Israel. *Atmos. Res.* 55, 257–270. doi: 10.1016/S0169-8095(00)00063-6

Kidron, G. J. (2010). The effect of substrate properties, size, position, sheltering and shading on dew: An experimental approach in the Negev Desert. *Atmos. Res.* 98, 378–386. doi: 10.1016/j.atmosres.2010.07.015

Li, J., Wada, H., and Matsuzaki, H. (2015). Radial growth rate through successive cambia in *Haloxylon ammodendron* (Chenopodiaceae) from the Gurbantunggut Desert, Northwestern China, determined by a series of radiocarbon dating. *Geochem. J.* 49, 39–51. doi: 10.2343/geochemj.2.0328

Liu, Y. B., Li, X. R., Li, M. M., Liu, D., and Zhang, W. L. (2016). Leaf (or assimilation branch) epidermal micromorphology of desert plant in arid and semiarid areas of China. *Chin. J. Plant Ecol.* 40, 1189–1207 (in Chinese with English abstract). doi: 10.17521/cjpe.2016.0129

Liu, R., Wang, Y. G., Li, C. J., Ma, J., and Li, Y. (2018). Partitioning water source and sinking process of a groundwater-dependent desert plant community. *Plant Soil* 430, 73–85. doi: 10.1007/s11104-018-3714-6

Ma, H. Y., Yang, X. D., Lü, G. H., He, X. M., Zhang, X. N., Wang, X. Y., et al. (2017). Water resources of dominant desert species in Ebinur Wetland Nature Resure, Xinjiang, China. *Acta Ecol. Sin.* 37, 829–840 (in Chinese with English abstract). doi: 10.5846/stxb201508311804

Mastroberti, A. A., and de Araujo Mariath, J. E. (2008). Development of mucilage cells of *Araucaria angustifolia* (Araucariaceae). *Protoplasma* 232, 233–245. doi: 10.1007/s00709-007-0274-7

Mayr, S., Schmid, P., Laur, J., Rosner, S., Charra-Vaskou, K., Dämon, B., et al. (2014). Uptake of water via branches helps timberline conifers refill embolized xylem in late winter. *Plant Physiol.* 164, 1731–1740. doi: 10.1104/pp.114.236646

McHugh, T. A., Morrissey, E. M., Reed, S. C., Hungate, B. A., and Schwartz, E. (2015). Water from air: an overlooked source of moisture in arid and semiarid regions. *Sci. Rep.* 5:13767. doi: 10.1038/srep13767

Novák, V. (2012). *Evapotranspiration in the soil-plant-atmosphere system. Chapter 6. Movement of water in the soil root zone during transpiration*. (Dordrecht: Springer).

Oliveira, R. S., Dawson, T. E., and Burgess, S. S. O. (2005). Evidence for direct water absorption by the shoot of the desiccation-tolerant plant *Vellozia flavicans* in the savannas of central Brazil. *J. Trop. Ecol.* 21, 585–588. doi: 10.1017/S0266467405002658

Pan, Z., Pitt, W. G., Zhang, Y. M., Wu, N., Tao, Y., and Truscott, T. T. (2016). The upside-down water collection system of *Syntrichia caninervis*. *Nat. Plants.* 2:16076. doi: 10.1038/nplants.2016.76

Philip, J. R. (1966). Plant water relations: some physical aspects. *Annu. Rev. Plant Physiol.* 17, 245–268. doi: 10.1146/annurev.pp.17.060166.001333

Pina, A. L. C. B., Zandavalli, R. B., Oliveira, R. S., Martins, F. R., and Soares, A. A. (2016). Dew absorption by the leaf trichomes of *Combretum leprosum* in the Brazilian semiarid region. *Funct. Plant Biol.* 43, 851–861. doi: 10.1071/FP15337

Robert, E. M. R., Jambia, A. H., Schmitz, N., De Ryck, D. J. R., De Mey, J., Kairo, J. G., et al. (2014). How to catch the patch? A dendrometer study of the radial increment through successive cambia in the mangrove *Avicennia marina*. *Ann. Bot.* 113, 741–752. doi: 10.1093/aob/mcu001

Schönherr, J. (2006). Characterization of aqueous pores in plant cuticles and permeation of ionic solutes. *J. Exp. Bot.* 57, 2471–2491. doi: 10.1093/jxb/erj217

Schwerbrock, R., and Leuschner, C. (2017). Foliar water uptake, a widespread phenomenon in temperate woodland ferns? *Plant Ecol.* 218, 555–563. doi: 10.1007/s11258-017-0711-4

Steppe, K., Vandegehuchte, M. W., Van de Wal, B. A. E., Hoste, P., Guyot, A., et al. (2018). Direct uptake of canopy rainwater causes turgor-driven growth spurts in the mangrove *Avicennia marina*. *Tree Physiol.* 38, 979–991. doi: 10.1093/treephys/tpy024

Tobe, K., Li, X., and Omasa, K. (2000). Effects of sodium chloride on seed germination and growth of two Chinese desert shrubs, *Haloxylon ammodendron* and *H. persicum* (Chenopodiaceae). *Aust. J. Bot.* 48, 455–460. doi: 10.1071/BT99013

Tomaszkiewicz, M., Abou Najm, M., Beysens, D., Alameddine, I., and Elfadel, M. (2015). Dew as a sustainable non-conventional water resource: a critical review. *Environ. Rev.* 23, 425–442. doi: 10.1139/er-2015-0035

Vitarelli, N. C., Riina, R., Cassino, M. F., and Merira, R. M. S. A. (2016). Trichome-like emergences in *Croton* of Brazilian highland rock outcrops: evidences for atmospheric water uptake. *Perspect. Plant Ecol. Evol. Syst.* 22, 23–35. doi: 10.1016/j.ppees.2016.07.002

Wang, X. H., Xiao, H. L., Cheng, Y. B., and Ren, J. (2016a). Leaf epidermal water-absorbing scales and their absorption of unsaturated atmospheric water in *Reaumuria soongorica*, a desert plant from the northwest arid region of China. *J. Arid Environ.* 128, 17–29. doi: 10.1016/j.jaridenv.2016.01.005

Wang, X. H., Xiao, H. L., Ren, J., Cheng, Y. B., and Qiu, Y. (2016b). An ultrasonic humidification fluorescent tracing method for detecting unsaturated atmospheric water absorption by the aerial parts of desert plants. *J. Arid Land* 8, 272–283. doi: 10.1007/s40333-015-0018-z

Westhoff, M., Zimmermann, D., Gessner, P., Wegner, L. H., Bentrup, F. W., and Zimmermann, U. (2009). Distribution and function of epistomatal mucilage plugs. *Protoplasma* 235, 101–105. doi: 10.1007/s00709-008-0029-0

Wu, X., Zheng, X. J., Li, Y., and Xu, G. Q. (2019). Varying responses of two *Haloxylon* species to extreme drought and groundwater depth. *Environ. Exp. Bot.* 158, 63–72. doi: 10.1016/j.envexpbot.2018.11.014

Xu, H., Li, Y., Xu, G. Q., and Zou, T. (2007). Ecophysiological response and morphological adjustment of two Central Asian desert shrubs towards variation in summer precipitation. *Plant Cell Environ.* 30, 399–409. doi: 10.1111/j.1365-3040.2006.001626.x

Xu, G. Q., Mcdowell, N. G., and Li, Y. (2016). A possible link between life and death of a xeric tree in desert. *J. Plant Physiol.* 194, 35–44. doi: 10.1016/j.jplph.2016.02.014

Yan, X., Zhou, M., Dong, X., Zou, S. B., Xiao, H. L., and Ma, X. F. (2015). Molecular mechanisms of foliar water uptake in a desert tree. *AoB Plants* 7:plv129. doi: 10.1093/aobpla/plv129

Yang, X. D., Lv, G. H., Ali, A., Ran, Q. Y., Gong, X. W., Wang, F., et al. (2017). Experimental variations in functional and demographic traits of *Lappula semiglabra* among dew amount treatments in an arid region. *Ecohydrology* 10:e1858. doi: 10.1002/eco.1858

Yang, X. D., Zhang, X. N., Lv, G. H., and Ali, A. (2014b). Linking *Populus euphratica* hydraulic redistribution to diversity assembly in the Arid Desert Zone of Xinjiang, China. *PLoS One* 9:e109071. doi: 10.1371/journal.pone.0109071

Yang, Q. Y., Zhao, W. Z., Liu, B., and Liu, H. (2014a). Physiological responses of *Haloxylon ammodendron* to rainfall pulses in temperate desert regions, Northwestern China. *Trees Struct. Funct.* 28, 709–722. doi: 10.1007/s00468-014-0983-4

Zheng, X. Q., Zheng, X. J., and Li, Y. (2012). Distribution and change of different precipitation pulse size in the southern marginal zone of the Junggar Basin, China. *Arid Zone. Res.* 29, 495–502 (in Chinese with English abstract). doi: 10.1007/s11783-011-0280-z

Zhuang, Y. L., and Ratcliffe, S. (2012). Relationship between dew presence and *Bassia dasyphylla* plant growth. *J. Arid Land* 4, 11–18. doi: 10.3724/SP.J.1227.2012.00011

Zhuang, Y. L., and Zhao, W. Z. (2017). Dew formation and its variation in *Haloxylon ammodendron* plantations at the edge of a desert oasis, northwestern China. *Agr. For. Meteorol.* 247, 541–550. doi: 10.1016/j.agrformet.2017.08.032

Zimmermann, U., Schneider, H., Wegner, L. H., and Haase, A. (2004). Water ascent in tall trees: does evolution of land plants rely on a highly metastable state? *New Phytol.* 162, 575–615. doi: 10.1111/j.1469-8137.2004.01083.x

Zimmermann, D., Westthoff, M., Zimmermann, G., Geßner, P., Gessner, A., Wegner, L. H., et al. (2007). Foliar water supply of tall trees: evidence for mucilage-facilitated moisture uptake from the atmosphere and the impact on pressure bomb measurements. *Protoplasma* 232, 11–34. doi: 10.1007/s00709-007-0279-2

Conflict of Interest Statement: The authors declare that the research was conducted in the absence of any commercial or financial relationships that could be construed as a potential conflict of interest.

frontiers in Plant Science

ORIGINAL RESEARCH
published: 13 November 2019
doi: 10.3389/fpls.2019.01411

Partitioning of Water Between Differently Sized Shrubs and Potential Groundwater Recharge in a Semiarid Savanna in Namibia

Katja Geißler[1], Jessica Heblack[1], Shoopala Uugulu[2], Heike Wanke[3] and Niels Blaum[1]*

[1] Plant Ecology and Nature Conservation, University of Potsdam, Potsdam, Germany, [2] Geology Department, University of Namibia, Windhoek, Namibia, [3] Department of Geography and Environmental Management, University of the West of England, Bristol, United Kingdom

Introduction: Many semiarid regions around the world are presently experiencing significant changes in both climatic conditions and vegetation. This includes a disturbed coexistence between grasses and bushes also known as bush encroachment, and altered precipitation patterns with larger rain events. Fewer, more intense precipitation events might promote groundwater recharge, but depending on the structure of the vegetation also encourage further woody encroachment.

Materials and Methods: In this study, we investigated how patterns and sources of water uptake of *Acacia mellifera* (blackthorn), an important encroaching woody plant in southern African savannas, are associated with the intensity of rain events and the size of individual shrubs. The study was conducted at a commercial cattle farm in the semiarid Kalahari in Namibia (MAP 250 mm/a). We used soil moisture dynamics in different depths and natural stable isotopes as markers of water sources. Xylem water of fifteen differently sized individuals during eight rain events was extracted using a Scholander pressure bomb.

Results and Discussion: Results suggest the main rooting activity zone of *A. mellifera* in 50 and 75 cm soil depth but a reasonable water uptake from 10 and 25 cm. Any apparent uptake pattern seems to be driven by water availability, not time in the season. Bushes prefer the deeper soil layers after heavier rain events, indicating some evidence for the classical Walter's two-layer hypothesis. However, rain events up to a threshold of 6 mm/day cause shallower depths of use and suggest several phases of intense competition with perennial grasses. The temporal uptake pattern does not depend on shrub size, suggesting a fast upwards water flow inside. δ^2H and $\delta^{18}O$ values in xylem water indicate that larger shrubs rely less on upper and very deep soil water than smaller shrubs. It supports the hypothesis that in environments where soil moisture is highly variable in the upper soil layers, the early investment in a deep tap-root to exploit deeper, more reliable water sources could reduce the probability of mortality during the establishment phase. Nevertheless, independent of size and time in the season, bushes do not compete with potential groundwater recharge. In a savanna encroached by *A. mellifera*, groundwater will most likely be affected indirectly.

Keywords: bush encroachment, groundwater recharge, rooting depth, Savannas, stable isotopes, shrub size, *Acacia mellifera*, rain event depth

OPEN ACCESS

Edited by:
Henrik Hartmann, Max-Planck-Institut für Biogeochemie, Germany

Reviewed by:
Iván Prieto, Spanish National Research Council, Spain
Lars Hendrik Wegner, Karlsruhe Institute of Technology, Germany

****Correspondence:***
Katja Geißler
kgeissle@uni-potsdam.de

Specialty section:
This article was submitted to Functional Plant Ecology, a section of the journal Frontiers in Plant Science

Received: *26 March 2019*
Accepted: *11 October 2019*
Published: *13 November 2019*

Citation:
Geißler K, Heblack J, Uugulu S, Wanke H and Blaum N (2019) Partitioning of Water Between Differently Sized Shrubs and Potential Groundwater Recharge in a Semiarid Savanna in Namibia. Front. Plant Sci. 10:1411. doi: 10.3389/fpls.2019.01411

INTRODUCTION

Groundwater recharge, the flux of water across the water table, is arguably the most difficult component of the hydrologic cycle to measure. In arid and semiarid regions, the problem is exacerbated by extremely small recharge fluxes that are highly variable in space and time (Phillips, 1994; Stephens, 1994; Izbicki et al., 2000). Fluctuations of precipitation and often unknown effects of vegetation are additional aggravating factors (Acharya et al., 2017; Evaristo and McDonell, 2017).

In semiarid systems, mainly large but rare rain events with deep percolation result in groundwater recharge (Le Maitre et al., 1999; Scanlon et al., 2006; Moore et al., 2012). Heavy precipitation may infiltrate where it hits the ground and moves vertically to the water table, yielding diffuse recharge but at very long time scales. Vegetation affects aquifers on very short time scales by either directly extracting groundwater from saturated strata or via uptake and interception of rainwater, thereby reducing the proportion of rainfall that is eventually recharged (Le Maitre et al., 1999). The deep-rooted soil-plant system of drylands is known to be highly rain-use efficient (Schenk and Jackson, 2002; Seyfried et al., 2005).

In many semiarid regions around the world, both, climatic conditions and vegetation are currently subject to significant changes including altered precipitation patterns with more heavy rain events and changes from open vegetation into bush and thicket (Weltzin et al., 2003; Reynolds et al., 2007; IPCC, 2014). Although such shifts in precipitation regimes may have a direct positive effect on ecosystem services such as groundwater recharge, corresponding effects on plants and vegetation dynamics might be equally substantial. A number of recent studies have shown that there are differing responses of plants to rain events of different intensity (e.g. Schwinning and Sala, 2004). Dryland systems are known to be driven by highly episodic events, which is in particular true for recruitment of bush encroaching plants (Joubert et al., 2008; Joubert et al., 2013). There is limited empirical information on what effect rain intensity may have on dryland systems with already changed vegetation pattern comprising mostly adult shrubs. Lohmann et al. (2012) demonstrated in their modelling study that more intense rain events increased the individual growth of both perennial grasses and encroaching shrubs.

In savannas of southern Africa, the area-wide bush encroachment at the cost of perennial grasses is considered a rangeland problem since many decades (Scholes and Walker, 1993; Eldridge et al., 2011; Grelliera et al., 2013; Russell and Ward, 2014). In Namibia, about 50% of the savanna is purportedly affected (De Klerk, 2004). This bush encroachment causes not only a significant reduction of the economic profitability and decrease in livelihoods but also leads to changes in vegetation structure and vegetation dynamics with major implications on different functions of the ecosystem (Reynolds et al., 2007; Eldridge et al., 2011; Soliveres and Eldridge, 2014). Ecological functions include biodiversity at many levels and the stable coexistence between bushes and perennial grasses (e.g., Blaum et al., 2009; Chown, 2010; Archer et al., 2017; Hering et al., 2019; Geissler et al., 2019). Water related ecohydrological functions that are affected by changes in vegetation include the modification of local climate, changed redistribution of water, and reductions of rainfall infiltration (Sharma, 1998; Bhark and Small, 2003; Maestre and Cortina, 2004; Wilcox and Thurow, 2006; Eldridge et al., 2011; Simonin et al., 2013). Some of these consequences have been experimentally verified at a few example sites in drylands (Shachak et al., 1998; Ludwig et al., 2005). However, only few studies focus on the possible relation to potential groundwater recharge and on the interrelation of these consequences to the specific age and/or size structure of the respective bush encroacher populations. For example, larger shrubs are likely to root independently of rainwater availability. They root deeper and may even reach saturated strata, directly utilizing groundwater, deep subsurface water pools or water from the soil that moves towards the groundwater. Recent research has demonstrated that large trees in arid savannas are indeed reliant on deep water (Shadwell and February, 2017). For shrubs, deeper rooting individuals might also allow a more stable coexistence with perennial grasses. In savannas, especially in dry savannas, densely rooting grasses obtain their water from the upper soil layer whereas woody plants escape from the competition and root mainly in deeper layers using less of the upper soil water (Walter, 1954; Scholes and Archer, 1997; Sankaran et al., 2005; Ward et al., 2013). At the same time, larger shrubs have more total transpirational surface, and consequently a higher demand for water (Meinzer et al., 2005) and might therefore take up rainwater more effectively than perennial grasses and smaller shrubs, even in upper soil layers. Consequently, competition for water increases, and precipitation is less likely to move to deeper soil parts, which is in turn negatively linked to the process of groundwater recharge. In many dryland systems woody plants tend to use water opportunistically to avoid or minimize seasonal water stress. They are able to switch from using available (sub-)surface water during the rainy season to water from greater depths as the main water source in the dry season (Dawson and Pate, 1996; Xu et al., 2011). Although being essential for anticipating the effects of climate change and bush encroachment for savanna ecosystem services, the flexibility of the encroaching woody vegetation to switch between different soil layers for predominant water uptake within a season and in particular in response to different rain event properties remains poorly understood.

The objectives of this study are to quantify relationships between rain event depth, shrub size, and sources of water use of *Acacia mellifera*, one of the most important bush encroacher species in Namibia. We aim to capture indication of feedbacks of bush encroachment to water related ecosystem services such as potential groundwater recharge or the further coexistence of perennial grasses with encroaching shrubs. The pattern of rainwater use is of specific interest, as rain accounts for an important amount of the water input in these semi-arid systems. Understanding the role of bush encroacher species at various ecological levels is a prerequisite for anticipating the effects of climate and global change on ecosystems and communities therein.

In particular, we address the following questions:

1. What is the proportional contribution of soil water at different depths and soil water intended for groundwater recharge in the water use of adult shrubs of *Acacia mellifera* during the course of the growing season?

2. What is the effect of rain event depth on water source partitioning of these shrubs?
3. Do adult shrubs of different size differ in their spatial and temporal water use?

MATERIAL AND METHODS

Study Area and Time

The study presents data of three growing seasons over a period of three years, from November 2015 to October 2018. The study area is situated in the Kalahari savanna rangeland, 180 km south-east of Windhoek, Namibia at farm Ebenhaezer (23°14'S, 18°23'E). Average annual precipitation is 250 mm/a (CV = 0.41) (Ministry of Agriculture, Water and Rural Development, Namibia, 1999). Most rainfall occurs from November to April during the hot summer months. Mean annual temperature is 19.5 °C with summer peaks of up to 45 °C. Soils are classified as red sand partially underlain by calcrete (Mendelsohn et al., 2002). The savanna is described as a Central Kalahari Camelthorn Savanna. Vegetation is characterized by open shrubland with trees and shrubs sparsely scattered in a grassy landscape (trees: *Acacia erioloba, A. haematoxylon*; shrubs: *Acacia mellifera, Acacia hebeclada, Grewia flava*; grasses: *Stipagrostis spp., Eragrostis spp., Aristida spp, Pogonathria fleckii* and *Schmidtia kalahariensis*) (Mendelsohn et al., 2002). The study area has been used for livestock farming since 1907 with heavy bush encroached areas around waterholes. Currently the rangeland is used for sheep, horse and cattle farming.

Study Species and Selection of Study Plants

The blackthorn acacia *Acacia mellifera* is one of the main bush encroachment species in the southern African savanna region (De Klerk, 2004) and is therefore of major concern to a sustainable rangeland and ecosystem management. Thirty-seven individuals of *A. mellifera* were randomly selected and measured by their canopy diameter, plant height and stem width at an inter-dune area in November 2016, several days before the first rain of the season 2016/2017. A subsample of 15 individuals was eventually chosen for the main study, ensuring the broadest range of canopy diameter and shrub height. It comprised individuals with a diameter between 35 and 952 cm and a height between 21 and 451 cm. Distance between each selected individual was >30 m to avoid effects of neighbor trees. To facilitate resampling, GPS coordinates were taken and all individuals marked with tape.

Sampling Design of Rain Water, Ground Water, Plant and Soil Water

The natural abundance of hydrogen (δ^2H) and oxygen ($\delta^{18}O$) stable isotopes in plant xylem water as an integrated signal of its sources was utilized to answer the research question, because root water uptake is generally considered a non-fractionating process (Dawson and Ehleringer, 1991). We compared the isotopic composition of plant xylem water with the composition in potential water sources such as water of five different subsurface layers and soil water of potential groundwater recharge.

Eight rain events of more than 0.5 mm were sampled during the first half of the growing season 2016/2017 from December to February (**Figure 1**). These were taken from a rain gauge (covered with a funnel shaped lid to minimize evaporation) immediately after rain ceased or in the early morning when rain fell overnight. Samples representing soil water of potential groundwater recharge were collected from a nearby well (approximately 500 m) on May 26, July 17, and September 11, 2016. As the isotopic composition of deep groundwater is less affected by precipitation (Busch et al., 1992), these samples are considered representative for the entire time period. Each sample (rain or well water) was transferred into 50 ml glass bottles, the lid tightly closed, sealed with parafilm, and stored frozen at -4°C until isotope analysis. Sampling of soil and xylem water was done following every precipitation event to characterize seasonal uptake patterns, with one exception. The very first sampling of xylem water occurred at the end of the dry season before the first rain and leaf flushing, on the 28th and 29th November 2016. Leaf flushing occurred on the 3rd of December 2016. To characterize the temporal response of plant water-use patterns to rainfall pulses, sampling took place 1, 4, and 7 days after every rainfall event.

For each individual shrub, an approximately 10 cm long outer suberized/lignified branch was collected at the base of the live crown between 4:30 and 5:30 h in the morning. All leaves

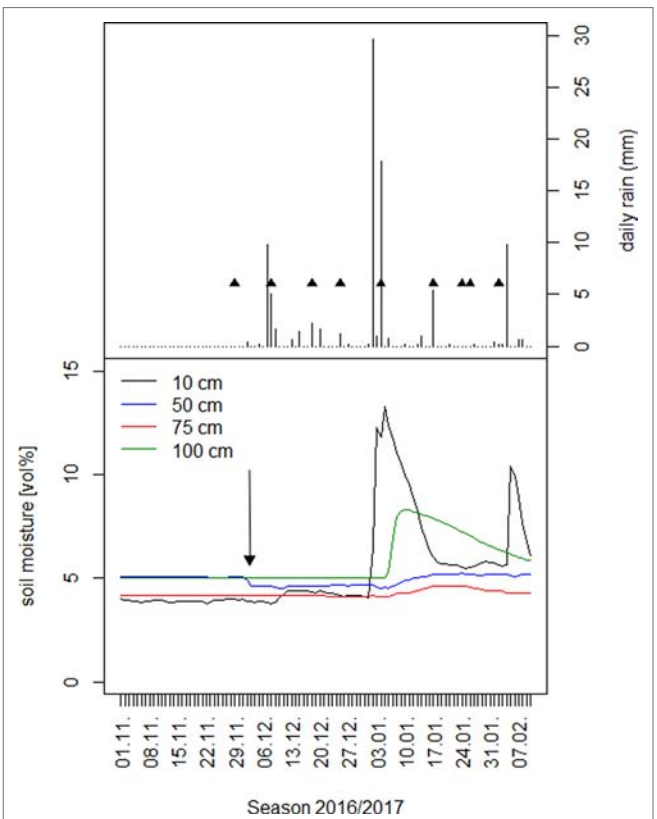

FIGURE 1 | Upper panel: Date and depth of single rain events in the first half of the season 2016/2017 together with the date of the first day of xylem and water sources sampling per rain event. Lower panel: Volumetric soil moisture under *A. mellifera* shrubs in four different soil depths. The arrow is pointing to the time of first leaf flushing on 3.12.2016.

and the first centimetre from the cut side of the branch was quickly removed from the bark and green tissue below to avoid contamination with phloem sap and isotopic enrichment of water during later extraction (Stahl et al., 2013). It was immediately infolded with Teflon tape to seal it against any water loss. All prepared samples were individually packed in aluminium foil, each locked into a zipper bag and stored in a cool bag or fridge to prevent any transpiration after sunrise. We used a Scholander pressure chamber (Soil Moisture Corp., USA) for the subsequent extraction of the xylem-water. Just before extraction, the respective sample branch was recut to receive a fresh and straight cut and immediately clamped into the pressure chamber with the prepared side of the branch facing outside. A long, cut pipette tip was tightly put over the cut end to prevent any evaporation during extraction and to also prevent loss upcoming xylem-water. The pressure inside the chamber was increased continually until a steady flow of xylem-water out of the branch was achieved. This water, approximately 0.5 to 1 ml, was immediately collected in a 2-ml tube using a small pipette. The tube was tightly closed with a screw-cap and parafilm, labelled and stored frozen until isotope analysis in the laboratory. We favoured this method over the cryogenic vacuum extraction because of lower organic contamination and in addition, we found no difference in isotopic composition between scholander pressure bomb and vacuum extraction (**Supplementary Figure S1**).

At each sampling day, early in the morning to minimize isotopic enrichment of water through evaporation, we used a soil auger (3 cm diameter) to dig a 1.2 m-deep hole at bare soil near the study plants to obtain soil samples in the depths of 10, 25, 50, 75, and 100 cm. These samples were immediately covered with a plastic sheet, placed into 8-ml glass vials, stored in a fridge and used to determine soil water content and isotopic ratios within the 0–100 cm layer. For the latter, water was extracted from the soil using a cryogenic vacuum distillation line (Ehleringer et al., 2000) at university in Munich. Extractions followed the guidelines of West et al. (2006) and were run for at least 90 minutes due to the very dry sandy soil samples. To concomitantly obtain the soil water content dynamics within the 0-100 cm layer, the three microsites 'shrub', 'bare soil', and 'grass tussock' were observed at four different soil depths of 10, 50, 75, and 100 cm using ML3 ThetaProbe Soil Moisture Sensors (Delta-T Devices). Soil moisture was measured during the whole study period.

Isotopic Analyses

For all isotopic analyses, we used an isotope ratio laser spectrometer (LGR DT-100 Liquid Water Stable Isotops Analyzer, Los Gatos Research Inc., California, USA) at the Isotope Laboratory of the Geology Department at University of Namibia. We used the Spectral Contamination Identifier (SCI) post-processing software to identify and quantify spectral contamination of organic compounds, and to correct the isotope values of contaminated water samples. About 0.5 µl of water was injected and the $\delta^{18}O$ and $\delta^{2}H$ ratios determined with a precision of ±0.8 for $\delta^{2}H$ and ±0.2‰ for $\delta^{18}O$. ^{18}O and ^{2}H values are reported in delta notation which expresses the isotopic composition relative to a standard (Vienna Standard Mean Ocean Water, V_{SMOW}) on a per mil (‰) basis:

$$\delta^{18}0 \text{ or } \delta^{2}H\left[\frac{0}{00}\right]=\left(\frac{R_{sample}}{R_{standard}}-1\right)\times 1000$$

where R_{sample} and $R_{standard}$ are the stable isotopic ratios ($^{18}O/^{16}O$ or $^{2}H/^{1}H$) of the sample and of standard water (Standard Mean Ocean Water, V_{SMOW}), respectively.

Data Analyses

All statistical analyses were performed using R 3.2.3 (R Core Team, 2016) and the R-packages "nlme" (Pinheiro et al., 2017), "lme4" (Bates et al., 2015) "piecewiseSEM" (Lefcheck, 2015) and "simmr" (Parnell, 2016), the latter using "ggplot2" (Wickham, 2016) and the software JAGS version 4.3.0 (Plummer, 2017).

Linear-mixed effects models (lmer, R-package 'lme4') were used to test for fixed effects of shrub size (expressed as canopy diameter) in interaction with rain amount, day after the rain event and time within the growing season (expressed as rain event nr.) on square root transformed $\delta^{2}H$ and $\log_e$ transformed $\delta^{18}O$ of the xylem water with day after rain nested in rain event and individual shrub ID as grouping variables in the random intercept part of the model. We assessed collinearity between fixed effects prior to the model fit using variance inflation factor (VIF) values. All predictor variables are scaled between 0 and 1 accounting for different units and to facilitate comparing coefficients for different predictors within the model (Gelman and Hill, 2007). To obtain minimal adequate models for each response variable transformed $\delta^{2}H$ and transformed $\delta^{18}O$ of the xylem water, we simplified the maximal model by removing all nonsignificant terms ($P > 0.05$) by stepwise-backward selection based on likelihood ratio tests (Crawley, 2007). Main effects included in significant interactions were retained in the minimal adequate models. For model simplification, we fitted all models by maximum likelihood (ML), but, to reliably quantify random effects, we additionally fitted the minimal adequate models with restricted maximum likelihood (REML; Bolker et al., 2009).

True probability distributions for the relative contribution of potential water sources to plant xylem water *via* Bayesian inferences (R-package "simmr"; Parnell, 2016) were determined. This framework uses linear stable isotope mixing models based on a mass balance equation of $\delta^{2}H$ and $\delta^{18}O$. It uses Markov Chain Monte Carlo (MCMC) model fitting to estimate parameters from observed data and user-specified prior distributions. The approach allows to incorporate uncertainty (variability in isotopic signatures) in both the sources and the water-mixture (xylem water) and the residuals. Moreover, it allows accounting for more than three sources in a two isotope system where usually no unique solution exists. This Bayesian framework can however not account for cases where the isotopic fractions in xylem water exceed the isotopic limits of sources. The model will then estimate negative fractional contributions of one or more sources. Implicit assumption is that the isotopic compositions of the water mixture lie inside a convex polygon bounded by all sources within a biplot. The simmr MCMC was run for 10,000 iterations with a burn rate of 1,000 and source increments of 1% for the iterative process. Source inputs included well water and

soil water of 10, 25, 50, 75, and 100 cm (Mean ± SD). Water-mixture inputs included samples from all sampling days per rain event not distinguishing between 1,4, and 7 days after the rain event because "day after rain" was non-significant in the linear mixed effect model described above. Simmr assumes that the mixture is constructed exclusively from those sources included as model inputs and that the isotopic compositions of sources differ from each other. Because root water uptake is considered a non-fractionating process (Dawson and Ehleringer, 1991), water source discrimination factors used in the mixing models were set 0 for both δ^2H and $\delta^{18}O$. Since water naturally meets the assumption of equal elemental concentrations (O and H) among the sources, the concentration dependencies was set as equal. To effectively use stable isotope data in mixing models, sources should be isotopically distinct. A two-way ANOVA was conducted for sources including rain-water at all rain events to explain the variance of mean stable isotope signatures. This was done for both isotopes separately. Variance partitioning was followed by pairwise comparisons of overall source means using Tukey's HSD test. The relationship between rain amount for a typical rain event between 0 and 6 mm and the main soil depth of water uptake was analysed by linear regression.

RESULTS

Single rain events of <6 mm were generally not reflected in any change of soil moisture under shrubs in any soil depth (**Figure 1**, **Supplementary Figure S2**). Larger rain events of around 10 mm did hardly increase soil moisture and if so, only slightly in 10 cm soil depth (**Supplementary Figure S2**). Only if occurring within short intervals of time, these moderate rain events between 6 and 10 mm became clearly reflected in an increase in soil moisture in the upper 10 cm soil depth, but again not deeper. The first of the two heavy rain events (of >10 mm) in January and March 2017 (**Figure 1**) increased soil moisture only in 10 and 100 cm depth. The second one led to a distinct increase of soil moisture in all four soil depths, but with 10 and 100 cm exhibiting the strongest and 50 and 75 cm the weakest increase. Both rain events indicate the main rooting zone of *A. mellifera* in 50 and 75 cm soil depth.

The overall mean $\delta^{18}O$ value in soil water of all depths was higher than in rain and groundwater (**Table S1**), showing evaporative enrichment in the soil. For δ^2H, only the mean value in the upper 10 cm of the soil profile was higher than in rain and groundwater and there was no difference between deeper soil, rain and groundwater. However, the isotopic composition of soil water at different depths changed abruptly from one sampling event to another (significant soil depth x rain event interaction: $\delta^{18}O$, $F_{47,76} = 2.2$, $p = 0.0009$; δ^2H, $F_{46,75} = 1.8$, $P = 0.009$), reflecting a very dynamic process of soil evaporation and rainfall percolation during the study period. It also confirms our approach identifying plant source water during each rain event using separate stable isotope mixing models (**Figure 2**). All stable isotopes of soil water plot on or slightly below the GMWL (**Figure 3**) indicating soil water originates from precipitation. An evaporation trend line is observed, with the equation: $\delta^2H = 3.10^* \delta^{18}O - 36.55$, $r^2 = 0.434$.

In the dry season 2016, before the first rain commenced it was only soil moisture in 50 cm soil depth, which apparently decreased at that time (Nov/Dec), when leaves started to flush (**Figure 1**).We were, however, unable to assess the water sources through an isotopic mixing model, because neither isotopic signature (xylem δ^2H; $\delta^{18}O$) preserved an important assumption implicit in the mixing model method that the isotopic signature must be within a convex polygon, bounded by all sources within a biplot (**Figure 4**). In the other two dry seasons 2015 and 2017 in this study period, there was little if any decrease in soil moisture in 50 cm soil depth (**Supplementary Figure S2**: Nov/Dec, open 50 cm vs. bush). In 2017, the rainy season already started mid-October.

During the very first rain event of the dry season 2016 in November 2016, which was a heavy rain event, the surface soil water in 10 cm depth accounted for 75% of the twig xylem water (**Figure 2**). During the only heavy rain event, which was also part of the isotopic sampling scheme but occurred much later in the season in January 2017, soil water at 75 cm depth constitutes the main water source with 75% (**Figure 2**). In general, the use of soil water intended for groundwater recharge was subordinated. Altogether, no clear temporal pattern in using different water sources during the course of the rainy season could be established.

The relationship between rain amount for a typical rain event between 0 and 6 mm and the main soil depth of water uptake by *A. mellifera* is significant ($F_{1,4} = 14.0$, $P = 0.02$), i.e., increasing rain amount up to a threshold of 6 mm/day increased rooting activity towards the upper soil layers (**Figure 5**). Heavy rain events (>12 mm/day) seemed to change main rooting activity back to lower soil layers. However, the isotopic dataset comprised only two such heavy rain events, making it difficult to draw conclusions about the real mechanisms.

Shrub size, expressed as canopy diameter, and time in the season, considered as rain event, both have a significant effect on stable isotope signatures in xylem (**Table 1**). Shrub size has a slightly increasing effect on both δ^2H and $\delta^{18}O$ ratios (**Figure 6**, **Table 1**). Only the smallest shrub size showed elevated values. Time in the season has a slightly decreasing effect on both isotopic values. Neither the parameter "day after the rain event" nor "depth of the rain event", nor any of the interactions with shrub size had a significant effect on either isotopic ratio in xylem water.

DISCUSSION

Proportional Contribution of Different Water Sources During the Course of the Growing Season

According to the linear stable isotope mixing model outputs soil water was in general the main source of water taken up by *A. mellifera*. Soil water of potential groundwater recharge was a subordinate source of water during the first three months of the growing season. This is consistent with a study by Kulmatiski and Beard (2013) in the Lowveld savannas of southern Krüger National Park in South Africa, where the dominating shrubs and trees seem also not to rely on soil water of potential groundwater recharge to any great extent. But it is contrary to results that

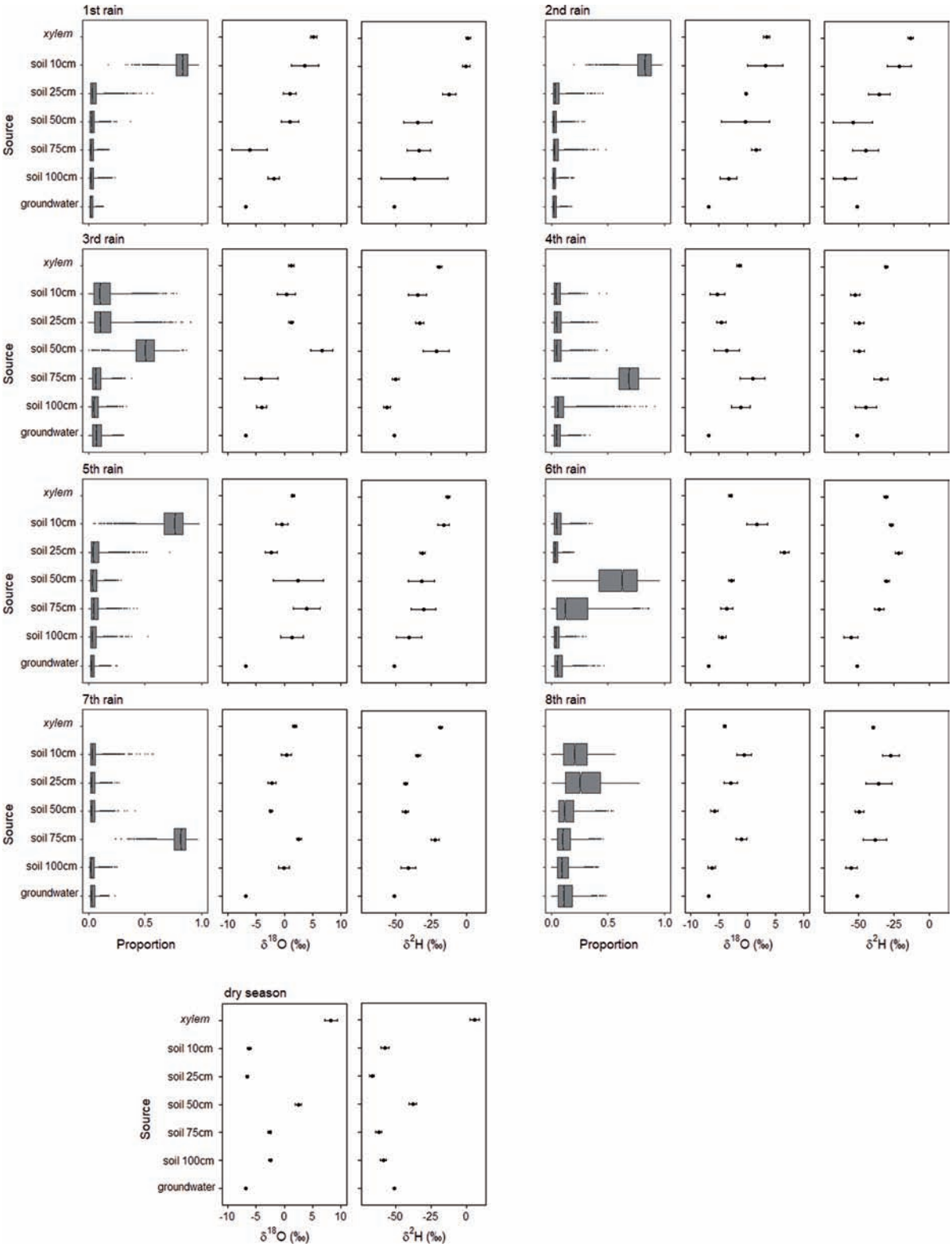

FIGURE 2 | Results of simmr Bayesian mixing models showing proportional estimates (mean, 25% and 75% percentiles) of water source composition together with oxygen and hydrogen stable isotope values for *A. mellifera* before the rainy season when leaves started to flush and during 8 consecutive rain events between November and February 2016/2017 (see **Figure 1**). groundwater = soil water intended for groundwater recharge.

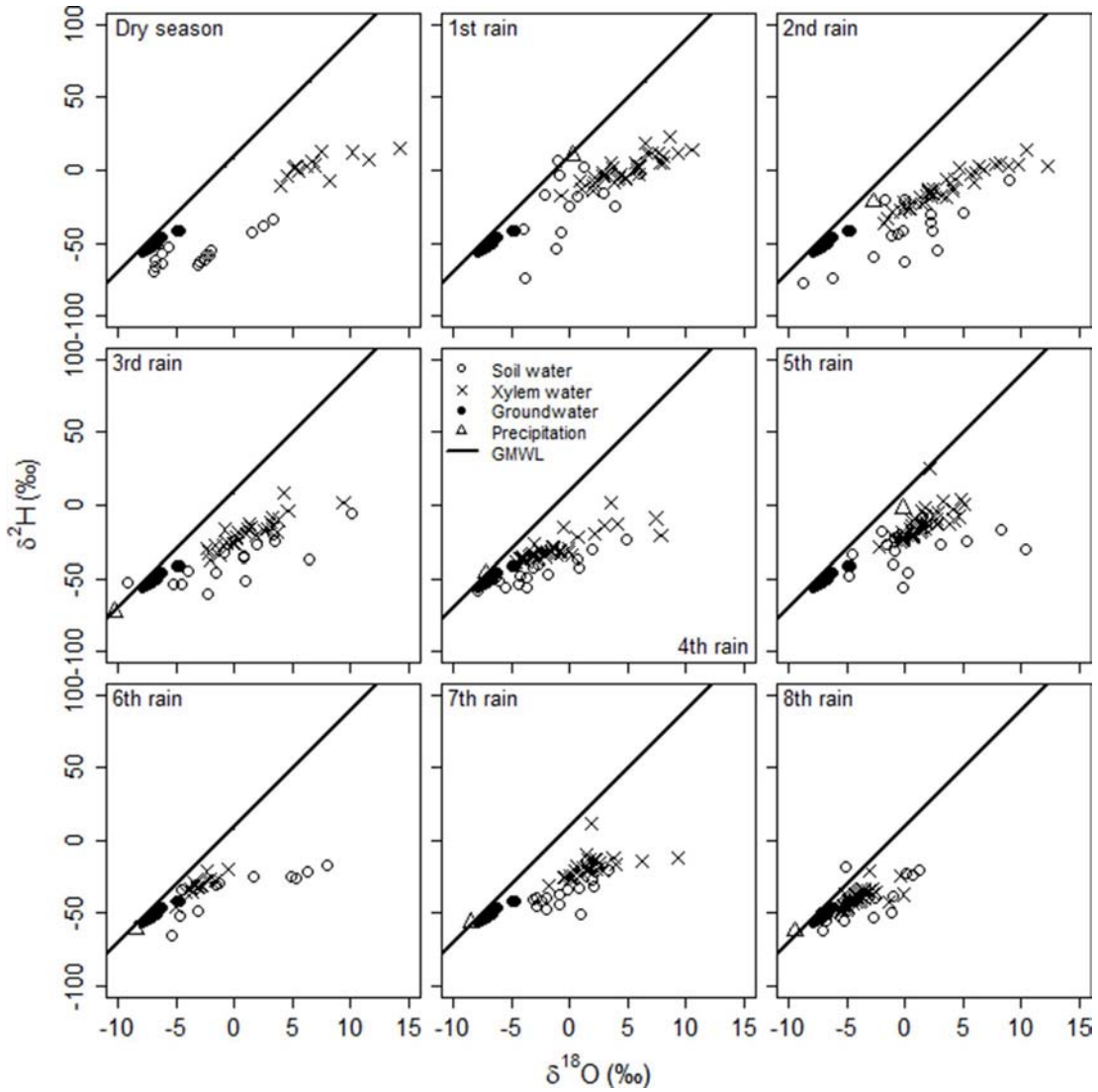

FIGURE 3 | Relationships between δ^2H and $\delta^{18}O$ in the rainwater, soil water, groundwater and twig xylem water of the *A. mellifera* shrubs from November to February 2016/2017 together with the global meteoric water line (GMWL: $\delta^2H = 8.17\ \delta^{18}O + 10.35$, Rozanski et al., 1993).

have been found in other species in semiarid regions, where members of the *Combretum*, *Terminalia, Prosopis*, and *Acacia* genera utilize groundwater (which is most likely only soil water of potential groundwater recharge) beside soil water to support the highest transpiration demand in summer (Evaristo and McDonnell, 2017; Beyer et al., 2018). Our results instead fit with the excavation study of O'Donnell et al., (2015) in the Kalahari, where the root system of *A. mellifera* did not appear to be large enough to reach the water table or saturated zones. It means that in a woody plant encroached savanna by *A. mellifera*, groundwater will most likely be affected indirectly through the impact of these plants on the process of groundwater recharge. Soil water that reaches groundwater (or deep percolation) occurs only if precipitation water passes through the soil before the vegetation can transpire it (Wilcox, 2002; Huxman et al., 2005). Consequently, the flow is directly dependent on the overall cover of the vegetation and the extent of bare soil evaporation relative to plant transpiration. C3 woody plants such as *A. mellifera* with a relatively low ability to save water (water use efficiency) should be able to transpire large amounts of water per day and therefore be very effective in preventing any groundwater flow or deep percolation (Larcher, 2003). In southern Australia, where winter precipitation exceeds evaporation, removal of Eucalyptus scrub has led instantly to rising groundwater tables (Walker et al., 1993). Unfortunately, the depth to groundwater table has not been monitored in our study. However, boreholes for groundwater use are drilled into great depths. In southern Africa, where precipitation mostly occurs in summer, complete removal of the bush encroacher *Colophermum mopane* revealed marked increases in soil moisture in the lower 45-90 cm soil zone, which could lead to deep percolation depending on rain events (Smit and Rethman, 2000). However, authors found that incidental

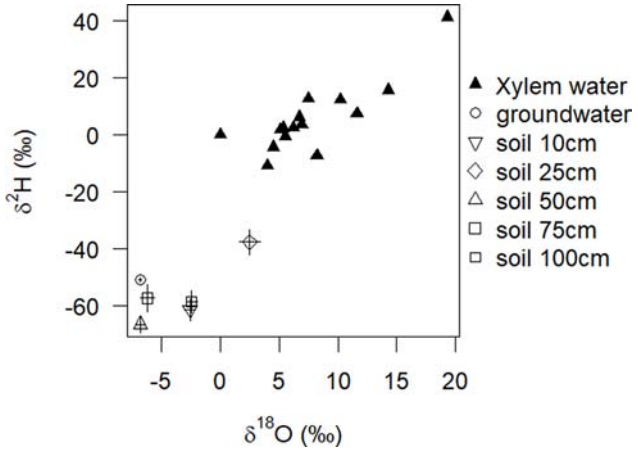

FIGURE 4 | Model input for stable isotope mixing model: oxygen and hydrogen stable isotope data from different water sources at the end of the dry season used as a potential input for simmr. Solid triangles represent the stable isotope signatures of xylem water of 15 individual *A. mellifera* shrubs (n = 1). Other symbols represent, respectively, the mean and SE of isotope signatures of water sources (n = 3).

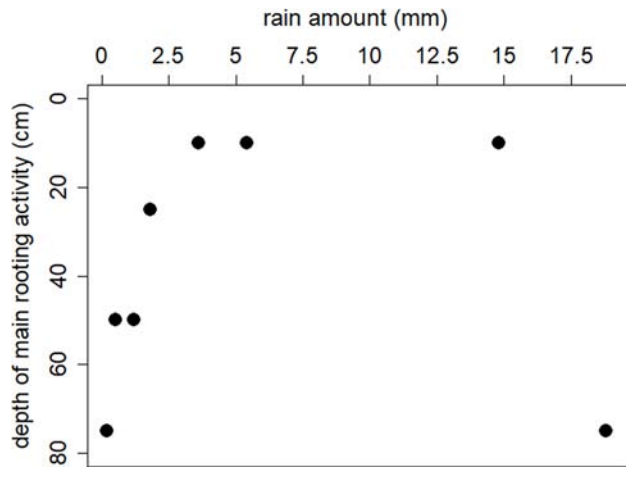

FIGURE 5 | The relationship between rain amount and the main soil depth of water uptake of by adult individuals of *A. mellifera* revealed from isotopic mixing modelling.

water losses (predominantly interception by tree canopies) were responsible for a lowering of effective rainfall and are therefore important determinants of the soil water content rather than deep soil water uptake and associated transpiration. In fact, evapotranspiration water losses from the soil even increased in plots one year after complete removal of shrubs.

Our isotopic and soil moisture data suggest that soil moisture serves as the main source of water in this sandy semiarid savanna site and accounts for over 80 % of the water needs of adult shrubs of *A. mellifera*. The global correlation between changes of soil moisture in different depths and the simple occurrence of rain events suggests a rooting activity of *A. mellifera* from 10 to 75 cm soil depth with the main activity zone in 50 and 75 cm. Isotopic analysis of xylem water during a heavy rain event suggests the main rooting activity is at 75 cm depth. The main activity zone in 50 and 75 cm fits with a recent field study along a bush cover gradient near our study site (Geissler et al., 2019). In that study, it has been found that ecophysiological traits of both shrub adults and saplings were not correlated to site specific mean soil moisture values at depths of 10 and 50 cm, while traits of annual and perennial grasses were. The proposed lower limit of active roots in 75 cm depth is in fact in the range of previously described real rooting depths for *A. mellifera* in the Kalahari (O'Donnell et al., 2015) where the authors excavated 90% of root biomass between 0 and 60 cm soil depth. However, O'Donnell et al. (2015) described the root system of *A. mellifera* as being exceptionally shallow with roots that followed an exponential distribution with depth. It suggests that in our study even the frequent missing response of soil moisture in upper soil layers to precipitation (we often observed no changes in 10 cm soil depth, although it has rained) is maybe due to woody plant water uptake from shallow soil depths and not a reflection of immediate soil evaporation or canopy interception (or both). To reduce uncertainty in reasons for soil moisture changes, we included soil moisture information of open microsites (**Supplementary Figure S1**). Results confirmed reduced movement of water into the soil due to the presence of *A. mellifera* individuals. Moreover, the isotopic composition of twig xylem water provides convincing evidence of reasonable root water uptake of the shrubs from the upper and intermediate soil layers in 10, 25, and 50 cm soil depth. Investment into shallow rooting can indeed be a successful strategy for horizontal water uptake after a low precipitation event. Nevertheless, since the main activity zone of *A. mellifera* is in 50 and 75 cm and not in the upper soil layer, and assuming O'Donnell et al. (2015) exponential root distribution with depth is prevalent, our results do not agree with the assumption that root mass distribution can serve as a proxy for rooting activity. Several authors have previously challenged this view (e.g., Eissenstat, 1992; Kulmatiski and Beard, 2013). The general inference of water uptake from measures of root biomass and changes in soil moisture might be limited because large parts of larger roots can be largely inactive. In fact, water uptake of roots preferentially goes through newly grown and relatively short-lived fine roots (Eissenstat, 1992; McCully, 1999). This is costly and the ability for a plant to survive harsh environmental conditions likely induces a cost in terms of growth capacity (Chapin, 1980), the so-called growth–stress survival trade-off. The observed increase in the 100 cm soil moisture after heavy rain events without an increase in the 50 and 75 cm soil layers might indicate a vertical subsurface flow of water, which occurs if uptake capacity of roots of *A. mellifera* has been reached. Additionally, it is likely that root channels exist. Nevertheless, the rooting activity of *A. mellifera* seems to be relatively flexible and adaptive, probably depending on the interaction between competitive situation, nutrients and rain amount, but certainly not time. Our results indicate a stationary uptake (from 50 cm soil depth) only in the beginning of the growing season, before any precipitation. However, uncertainty in the isotopic method (see **Figure 4**) prevents confidence in our conclusion. The

TABLE 1 | Effects of canopy size, rain event nr, rain depth, day after rain and all 2way-interactions with canopy size on both δ^2H and $\delta^{18}O$ values in the xylem.

Effect	β	$\chi^2_{df=1}$	P	R^2_{marg}	R^2_{cond}
δ^2H					
canopy size	**0.17**	**5.20**	**0.02**	0.05	0.73
rain event	**-0.15**	**7.30**	**0.007**	0.74	0.38
rain depth (mm)	-0.05	0.022	0.88		
day after rain	-0.15	3.65	0.06	–	–
canopy size x rain depth	–	0.013	0.91		
canopy size x day after rain	–	1.12	0.27	–	–
canopy size x rain event	–	1.47	0.23	–	–
$\delta^{18}O$					
canopy size	**0.15**	**6. 98**	**0.008**	0.05	0.76
rain event	**-0.12**	**6.08**	**0.014**	0.37	0.77
rain depth (mm)	-0.25	0.73	0.39		
rain depth^{quadratic}	-1.77	1.69	0.19		
day after rain	-0.02	0.90	0.34	–	–
canopy size x rain depth	–	0.93	0.33		
canopy size x day after rain	–	0.063	0.80	–	–
canopy size x rain event	–	0.063	0.80	–	–

Shown are parameter estimates, and the approximate χ2 distribution of the test statistic, R^2_{marg} (fixed effects alone) and R^2_{cond} (fixed + random effects). Shrub ID and day after rain nested in rain event nr. are considered as random intercept. All response and predictor variables are scaled between 0 and 1. Significant effects are shown in bold.

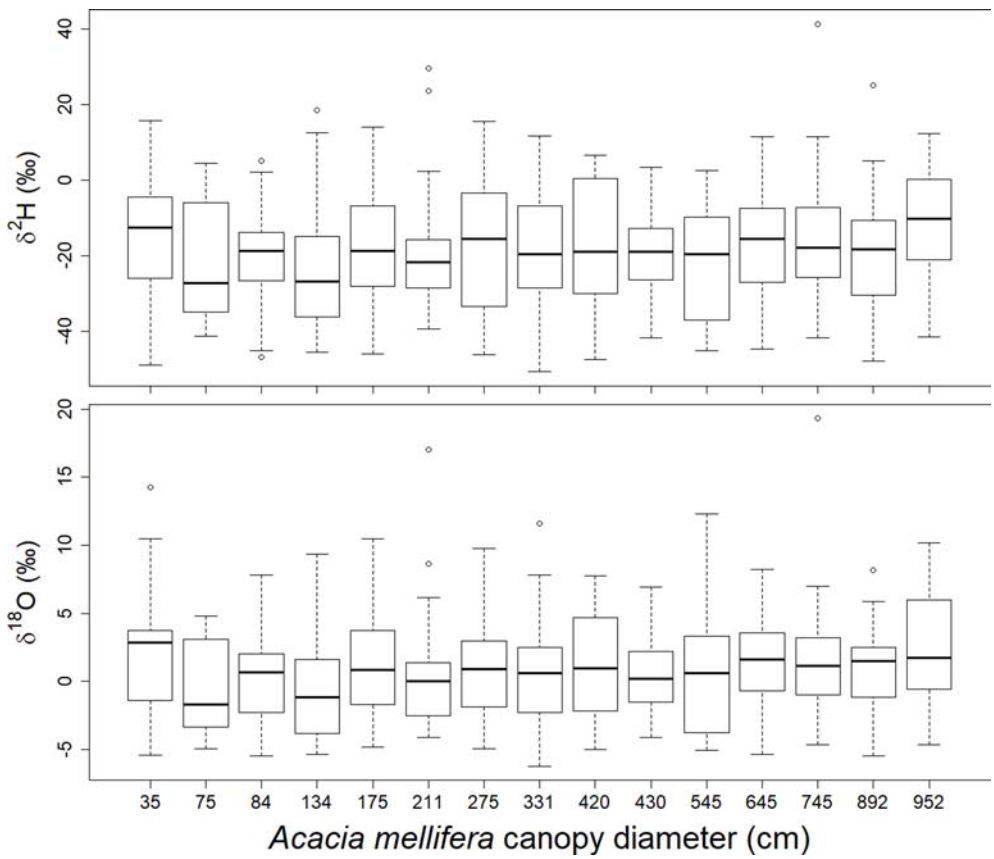

FIGURE 6 | Relationship between canopy diameter of *A. mellifera* shrubs and δ^2H and $\delta^{18}O$ in the twig xylem water over the season 2016/2017. Each box contains results of 8 rain events and within each event 3 sampling days, respectively (n = 24).

strong deviation of isotopic composition of plant water from sources at that time point towards an isotopic fractionation either along the stem due to increasing stem photosynthesis (Dawson and Ehleringer, 1993), general limited sap flow (Martin-Gómez et al., 2016) or during root uptake that does involve transport via aquaporins or simply mycorrhization (Poca et al., 2019). Many Acacia species are known for their ability to develop micorrhizal symbiosis. Further research

would be needed to obtain direct temporal quantifications of stem photosynthesis of this shrub species, root water uptake, the role of mycorrhization and related xylem water fractionation. With progressing growing season, our results on water sources of *A. mellifera* do not relate to any temporal water use pattern. In many dryland systems, woody plants tend to use water opportunistically, at switch seasonally from using water from greater depths as the main water source in the dry season to (sub-) surface water during the rainy season (Dawson and Pate, 1996; Xu et al., 2011). Gu et al. (2015) conclude that ultimately, such pattern seem to be driven by soil water availability rather than phenology, a strategy that is certainly meaningful under dryland conditions of unpredictable and erratic precipitation.

Effect of Rain Event Depth on Water Source Partitioning of *A. mellifera*

The response to soil water availability and to rain event depth occurs on very small scale and suggested a threshold of 6 mm/day rain amount. An increasing amount up to that threshold increased rooting activity further towards upper soil layers, eventually reaching the very first centimeters of soil. It strongly suggests a regulation of rooting activity depth based on fine root growth. The regulation may be controlled by both soil moisture and soil temperature and many species show optimal soil temperatures for fine root growth (Eissenstat et al., 2013). There is a delayed activation of growth in very shallow soil layers, which get very hot compared to deeper layers and stay hot for a longer time with less rain. The changes in rooting activity depth also emphasizes that woody plant growth starts with rain amounts of less than 5 mm/day, an amount, so far, many researchers regarded to be unimportant for plant growth in savannas (Lohmann et al., 2012; Tietjen, 2016). In any case, the isotopically based results on rooting activity following small rain events justifies very shallow rooting depths for *A. mellifera*. This shrub species seems to be well adapted to utilize such small rainfall events, which occur frequently in semiarid savannas of Southern Africa (De Klerk, 2004). The results also justify that small to intermediate sized rain events must lead to increasing belowground interference competition with perennial grasses. In many semiarid systems, the main water uptake zone of perennial grasses is in these upper shallower soil layers (Schenk and Jackson, 2002; Kulmatiski and Beard, 2013; Geissler et al., 2019). The potential large overlap of rooting zones between *A. mellifera* shrubs and grasses suggests limited evidence for the two-layer hypothesis (Walter, 1954; Ward et al., 2013) that savanna woody vegetation escapes competition with grasses and primarily roots in deeper soil layers. It makes a strong argument for a more comprehensive investigation of ecohydrological traits of bush encroacher species in particular compared to non- encroacher species, including functional plasticity in root architecture and distribution. A high amount of root biomass in shallow soil can already be seen as a strategy of anticipatory competition for space with perennial grasses. In fact, this strategy and related traits may constitute the widespread success of bush encroacher species in degraded savanna rangelands. Moreover, it might form the base for a negative feedback in previously bush encroached areas towards perennial grass establishment with important effects on the reversibility of a degraded ecosystem state. The grass cover at our study site was already very low. While the rooting activity depths of adult *A. mellifera* shrubs due to small rain events suggest interference competition with shallow rooting perennial grasses, the response to larger rain events (>6 mm/day) still indicates evidence for the two-layer hypothesis (Walter, 1954). It may illustrate the base of tree/shrub-grass coexistence in the thorn bush savannas of that area and the large-scale potential for savanna restoration if shallow-rooting perennial grass cover is rehabilitated.

Shrub Size and Water Use

A positive relation between shrub size and both δ^2H and $\delta^{18}O$ values in the xylem was observed during the first half of the rainy season, suggesting that larger *A. mellifera* shrubs rely less on upper and very deep soil water during times of seasonal rain events than smaller shrubs. This result is based on the soil depth isotopic pattern in **Figure 2** and **Table S1** and seems anomalous but is consistent with previous studies in other dryland ecosystems (Meinzer et al., 1999; Hasselquist et al., 2010; Bargués Tobella et al., 2017). It supports the hypothesis that in environments where soil moisture is highly variable in the upper soil layers, the early investment in a deep tap-root to exploit deeper, more reliable water sources could reduce the probability of mortality during the establishment phase (Ehleringer and Dawson, 1992). Additional horizontal root growth later in the ontogenesis may reflect an increasing nutrient demand associated with the maintenance of increasing canopy leaf area. The soil nutrient content is usually greatest in the upper soil layers. Furthermore, the ability of soil to support rhizobium bacteria and arbuscular mycorrhizal fungi populations, which are needed by nitrogen fixing leguminous shrubs such as *A. mellifera* is known to decrease with increased soil depth (Shukla et al., 2013). In this view, an increased competitive ability of *A. mellifera* towards shallow rooting perennial grasses may only be a secondary benefit.

Shrub Size and Patterns of Water Uptake During the Course of a Rain Event

Although there is most likely a shrub size effect on the depth of the main rooting activity, the temporal uptake pattern within a single rain event does not depend on shrub size. Such results suggest that the upwards water flow inside the *A. mellifera* shrubs is relatively fast. Fravolini et al. (2005) observed xylem flux rates of 1 - 5 m d^{-1} in an American encroacher bush. In our study, this would result in a recovery rate of rainwater between 1 - 4.5 days for the highest *A. mellifera* individual (451 cm) and only 1.5 – 8 h for the smallest individual (35 cm).

DATA AVAILABILITY STATEMENT

The datasets generated for this study are available on request to the corresponding author.

AUTHOR CONTRIBUTIONS

KG, HW, and NB planned and designed the research. JH, KG, NB, and SU involved in field data collection. KG and JH analyzed

the data. KG wrote the manuscript. All authors contributed to elaborating and editing the manuscript.

FUNDING

This work was supported by the German Federal Ministry of Education and Research (BMBF) project OPTIMASS (01LL1302A).

ACKNOWLEDGMENTS

We thank the Ministry of Environment and Tourism (Namibia) for granting research permission [Permit Number: 2112/2016 and 2227/2016] and Pieter Hugo, the owner of farm Ebenhaezer, for his manifold support. We are grateful to Werner Herppich for his helpful discussions considering the methodology of xylem water collections. We are grateful to the staff of the Technische Universität München (Department of Ecology & Ecosystem Sciences, Center of Life and Food Science Weihenstephan) for their technical assistance in extracting soil water, and particularly Thorsten Grams for his valuable comments.

SUPPLEMENTARY MATERIAL

The Supplementary Material for this article can be found online at: https://www.frontiersin.org/articles/10.3389/fpls.2019.01411/full#supplementary-material

SUPPLEMENTARY FIGURE S1 | Comparison of six plant stem water samples (*Acacia mellifera*) extracted via Scholander pressure bomb and via vacuum extraction. Left plot represents potentially contamination from Chemcorrect™ spectral analysis software indicating the relative degree of interference from contaminants in the sample. Right plot represents $\delta^{18}O$ value obtained via CRDS.

SUPPLEMENTARY FIGURE S2 | Upper panel: Date and depth of single rain events in the seasons 2015/2016, 2016/2017 and 2017/2018. Lower panel: Volumetric soil moisture under *A. mellifera* shrubs (bush) and open soil (open) in 2 different soil depths (10 cm dashed line, 50 cm solid line). The arrows are pointing to the time of first leaf flushing on 15.11.2015, 3.12.2016 and 17.11.2017.

REFERENCES

Acharya, B. S., Halihan, T., Zou, C. B., and Will, R. E. (2017). Vegetation Controls on the spatio-temporal heterogeneity of deep moisture in the unsaturated zone: a hydrogeophysical evaluation. *Nat. Sci. Rep.* 7, 1499. doi: 10.1038/s41598-017-01662

Archer, S. R., Andersen, E. M., Predick, K. I., Schwinning, S., Steidl, R. J., and Woods, S. R. (2017). "Rangeland systems," in *Processes, management and challenges* (Cham: Springer International Publishing), 25–84. doi: 10.1007/978-3-319-46709-2_2

Bargués Tobella, A., Hasselquist, N. J., Bazié, H. R., Nyberg, G., Laudon, H., Bayala, J., et al. (2017). Strategies trees use to overcome seasonal water limitation in an agroforestry system in semiarid West Africa. *Ecophydrology* 10, 3e1808. doi: 10.1002/eco.1808

Bates, D., Maechler, M., Bolker, B., and Walker, S. (2015). Fitting linear mixed-effects models using lme4. *J. Stat. Software* 67 (1), 1–48. doi: 10.18637/jss.v067.i01

Beyer, M., Hamutoko, J. T., Wanke, H., Gaj, M., and Koeniger, P. (2018). Examination of deep root water uptake using anomalies of soil water stable isotopes, depth-controlled isotopic labeling and mixing models. *J. Hydrol.* 566, 122–136. doi: 10.1016/j.jhydrol.2018.08.060

Bhark, E., and Small, E. (2003). Association between plant canopies and the spatial patterns of infiltration in shrubland and grassland of the Chihuahuan desert, New Mexico. *Ecosystems* 6, 185–196. doi: 10.1007/s10021-002-0210-9

Blaum, N., Seymour, C., Rossmanith, E., Schwager, M., and Jeltsch, F. (2009). Changes in arthropod diversity along a land use driven gradient of shrub cover in savanna rangelands: Identification of suitable indicators. *Biodiversity Conserv.* 18, 1187–1199. doi: 10.1007/s10531-008-9498-x

Bolker, B. M., Brooks, M. E., Clark, C. J., Geange, S. W., Poulsen, J. R., Stevens, M. H. M., et al. (2009). Generalized linear mixed models: a practical guide for ecology and evolution. *Trends Ecol. Evol.* 24, 127–135. doi: 10.1016/j.tree.2008.10.008

Busch, D., Ingraham, N., and Smith, S. (1992). Water-uptake in woody riparian phreatophytes of the Southwestern United-States - A stable isotope study. *Ecol. Appl.* 2, 450–459. doi: 10.2307/1941880

Chapin, F. S. (1980). The mineral nutrition of wild plants. *Annu. Rev. Ecol. Systematics* 11, 233–260. doi: 10.1146/annurev.es.11.110180.001313

Chown, S. (2010). Temporal biodiversity change in transformed landscapes: asouthern African perspective. Philosophical transactions of the royal society of London. Series B. *Biol. Sci.* 365, 3729–3742. doi: 10.1098/rstb.2010.0274

Crawley, M. J. (2007). *The R Book*. Chichester, UK: John Wiley & Sons Ltd.

Dawson, T. E., and Ehleringer, J. R. (1991). Streamside trees that do not use stream water. *Nature* 350, 335–337. doi: 10.1038/350335a0

Dawson, T. E., and Ehleringer, J. R. (1993). Isotopic enrichment of water in the "woody" tissues of plants: Implications for plant water source, water uptake, and other studies which use the stable isotopic composition of cellulose. *Geochimica Cosmochimica Acta* 57, 3487–3492. doi: 10.1016/0016-7037(93)90554-A

Dawson, T. E., and Pate, J. S. (1996). Seasonal water uptake and movement in root systems of Australian phraeatophytic plants of dimorphic root morphology: a stable isotope investigation. *Oecologia* 107, 13–20. doi: 10.1007/BF00582230

De Klerk, J. N. (2004). *Bush Encroachment in Namibia -Report on Phase 1 of the Bush Encroachment Research, Monitoring and Management Project*. Windhoek, Namibia: Ministry of Environment and Tourism.

Ehleringer, J. R., and Dawson, T. E. (1992). Water uptake by plants: perspectives from stable isotope composition. *Plant Cell Environ.* 15, 1073–1082. doi: 10.1111/j.1365-3040.1992.tb01657.x

Ehleringer, J. R., Roden, J., and Dawson, T. E. (2000). "Assessing ecosystem level water relations through stable isotope ratio analyses," in *Methods in ecosystem science*. Eds. Sala, O. E., Jackson, R. B., Mooney, H. A., and Howarth, R. W. (New York: Springer), 181–198. doi: 10.1007/978-1-4612-1224-9_13

Eissenstat, D. (1992). Costs and benefits of constructing roots of small diameter. *J. Plant Nutr.* 15, 763–782. doi: 10.1080/01904169209364361

Eissenstat, D. M., McCormack, M. L., and Du, Q., (2013). "Global change and root lifespan," in *Plant Roots: the Hidden Half*, , vol. 27- . Eds. Eshel, A., and Beeckman, T. (Boca Raton, USA: Taylor and Francis Group/CRC Press), 1–27-13. doi: 10.1201/b14550-32

Eldridge, D. J., Bowker, M. A., Maestre, F. T., Roger, E., Reynolds, J. F., and Whitford, W. G. (2011). Impacts of shrub encroachment on ecosystem structure and functioning: towards a global synthesis. *Ecol. Lett.* 14, 709–722. doi: 10.1111/j.1461-0248.2011.01630.x

Evaristo, J., and McDonnell, J. J. (2017). Prevalence and magnitude of groundwater use by vegetation: A global stable isotope meta-analysis. *Sci. Rep.* 7, 44110. doi: 10.1038/srep44110

Fravolini, A., Hultine, K. R., Brugnoli, E., Gazal, R., English, N. B., and Williams, D. G. (2005). Precipitation pulse use by an invasive woody legume: the role of soil texture and pulse size. *Oecologia* 144, 618–627. doi: 10.1007/s00442-005-0078-4

Geissler, K., Hahn, C., Joubert, D., and Blaum, N. (2019). Functional responses of the herbaceous plant community explain ecohydrological feedbacks of savanna shrub encroachment. *Perspect. Plant Ecol. Evol. Systematics* 39, 125458. doi: 10.1016/j.ppees.2019.125458

Gelman, A., and Hill, J. (2007). *Data analysis using regression and multilevel/hierarchical models*. Cambridge, UK: Cambridge University Press. doi: 10.1017/CBO9780511790942

Grelliera, S., Ward, D., Janeauc, J. L., Podwojewskic, P., Lorentz, S., Abbadiee, L., et al. (2013). Positive versus negative environmental impacts of tree encroachment in South Africa. *Acta Oecologica* 53, 1–10. doi: 10.1016/j.actao.2013.08.002

Gu, D., Zhang, Z., Mallik, A., Zhou, A., Mo, L., He, C., et al. (2015). Seasonal water use strategy of Cyclobalanopsis glauca in a karst area of southern China. *Environ. Earth Sci.* 74, 1007–1014. doi: 10.1007/s12665-014-3817-1

Hasselquist, N. J., Allen, M. F., and Santiago, L. S. (2010). Water relations of evergreen and drought deciduous trees along a seasonally dry tropical forest chronosequence. *Oecologia* 164, 881–890. doi: 10.1007/s00442-010-1725-y

Hering, R., Hauptfleisch, M., Geißler, K., and Blaum, N. (2019). Land use impacts in savannas: insights from beetle species niches along a grazing intensity gradient. *Land Degradation Dev.* 30, 14–24. doi: 10.1002/ldr.3197

Huxman, T. E., Wilcox, B. P., Breshears, D. D., Scott, R. L., Snyder, K. A., Small, E. E., et al. (2005). Ecohydrological implications of woody plant encroachment. *Ecology* 86, 308–319. doi: 10.1890/03-0583

IPCC. 2014. Climate Change 2014: Impacts, adaptation, and vulnerability. part a: global and 610 sectoral aspects. contribution of working group II to the fifth assessment report of the 611 intergovernmental panel on climate change [Field, C.B., V.R. Barros, D.J. Dokken, K.J. 612 Mach, M.D. Mastrandrea, T.E. Bilir, M. Chatterjee, K.L. Ebi, Y.O. Estrada, R.C. Genova, 613 B. Girma, E.S. Kissel, A.N. Levy, S. MacCracken, P.R. Mastrandrea, and L.L. White 614 (eds.)]. Cambridge, United Kingdom and New York, NY, USA: Cambridge University 615 Press.

Izbicki, J. A., Radyk, J., and Michel, R. L. (2000). Water movement through a thick unsaturated zone underlying an intermittent stream in the western Mojave Desert, southern CA, USA. *J. Hydrol.*, 238, 194–217. doi: 10.1016/S0022-1694(00)00331-0

Joubert, D. F., Rothauge, A., and Smit, G. N. (2008). A conceptual model of vegetation dynamics in the semiarid Highland savanna of Namibia, with particular reference to bush thickening by Acacia mellifera. *J. Arid. Environ.* 72, 2201–2210. doi: 10.1016/j.jaridenv.2008.07.004

Joubert, D. F., Smit, G. N., and Hoffman, M. T. (2013). The influence of rainfall, competition and predation on seed production, germination and establishment of an encroaching Acacia in an arid Namibian savanna. *J. Arid. Environ.* 91, 7–13. doi: 10.1016/j.jaridenv.2012.11.001

Kulmatiski, A., and Beard, K. H. (2013). Root niche partitioning among grasses, saplings, and trees measured using tracer technique. *Oecologia* 171, 25–37. doi: 10.1007/s00442-012-2390-0

Larcher, W. (2003). "Gas exchange in plants," in *Physiological Plant Ecology*, vol. pp. (Berlin, Germany: Springer Verlag), 81–101. doi: 10.1007/978-3-662-05214-3

Le Maitre, D. C., Scott, D. F., and Colvin, C. (1999). A review of information on interactions between vegetation and groundwater. *Water SA* 25 (2), 137–152.

Lefcheck, J. S. (2015). Piecewise SEM: Piecewise structural equation modelling in R for ecology, evolution, and systematics. *Methods Ecol. Evol.* 7, 573–579. doi: 10.1111/2041-210X.12512

Lohmann, D., Tietjen, B., Blaum, N., Joubert, D. F., and Jeltsch, F. (2012). Shifting thresholds and changing degradation patterns: climate change effects on the simulated long-term response of a semi-arid savanna to grazing. *J. Appl. Ecol.* 49, 814–823. doi: 10.1111/j.1365-2664.2012.02157.x

Ludwig, J. A., Wilcox, B. P., Breshears, D. D., Tongway, D. J., and Imeson, A. C. (2005). Vegetation patches and runoff-erosion as interacting ecohydrological processes in semiarid landscapes. *Ecology* 86, 288–297. doi: 10.1890/03-0569

Maestre, F. T., and Cortina, J. (2004). Insights into ecosystem composition and function in a sequence of degraded semiarid steppes. *Restor. Ecol.* 12, 494–502. doi: 10.1111/j.1061-2971.2004.03106.x

Martin-Gómez, P., Serrano, L., and Ferrio, J. P. (2016). Short-term dynamics of evaporative enrichment of xylem water in woody stems: implications for ecohydrology. *Tree Physiol.* 37, 511–522. doi: 10.1093/treephys/tpw115

McCully, M. E. (1999). Roots in soil: unearthing the complexities of roots and their rhizospheres. *Annu. Rev. Plant Physiol. Plant Mol. Biol.* 50, 695–718. doi: 10.1146/annurev.arplant.50.1.695

Meinzer, F. C., Andrade, J. L., Goldstein, G., Holbrook, N. M., Cavelier, J., and Wright, S. J. (1999). Partitioning of soil water among canopy trees in a seasonally dry tropical forest. *Oecologia* 121, 293–301. doi: 10.1007/s004420050931

Meinzer, F. C., Bond, B. J., Warren, J. M., and Woodruff, D. R. (2005). Does water transport scale universally with tree size. *Func. Ecol.* 19, 558–565. doi: 10.1111/j.1365-2435.2005.01017.x

Mendelsohn, J., Jarvis, A., Roberts, C., and Robertson, T., (2002). *Atlas of Namibia, 1st edn*. Cape Town: David Philip Publishers.

Moore, G. W., Barre, D. A., and Owens, M. K. (2012). Does shrub removal increase groundwater recharge in Southwestern Texas Semiarid Rangelands? *Rangeland Ecol. Manage.* 65 (1), 1–10. doi: 10.2111/REM-D-11-00055.1

O'Donnell, F. C., Caylor, K. K., Bhattachan, A., Dintwe, K., D'Odorico, P., and Okin, G. S. (2015). A quantitative description of the interspecies diversity of belowground structure in savanna woody plants. *Ecosphere* 6, 154. doi: 10.1890/ES14-00310.1

Parnell, A. (2016). simmr: a stable isotope mixing model. R package version 0.3. https://CRAN.R-project.org/package=simmr.

Phillips, F. M. (1994). Environmental tracers for water movement in desert soils of the American southwest, Soil Sci. *Soc Am. J.* 58, 15– 24. doi: 10.2136/sssaj1994.03615995005800010003x

Pinheiro, J., Bates, D., DebRoy, S., and Sarkar, D.Core Team R. (2017). _nlme: linear and nonlinear mixed effects models_. R package version 3.1-131,<URL: https://CRAN.R-project.org/package=nlme>.

Plummer, M. (2017). JAGS (Version 4.3.0) [software] doi: 10.1016/S0958-2118(17)30107-6

Poca, M., Coomans, O., Urcelay, C., Zeballos, S. R., Bode, S., and Boeckx, P. (2019). Isotope fractionation during root water uptake by Acacia caven is enhanced by arbuscular mycorrhizas. *Plant Soil* 441, 485–497. doi: 10.1007/s11104-019-04139-1

R Core Team. (2016). *A language and environment for statistical computing*. Vienna, Austria: R Foundation for Statistical Computing. URL https://www.R-project.org/.

Reynolds, J. F., Stafford Smith, D. M., Lambin, E. F., Turner, B. L., Mortimore, M., Batterbury, S. P. J., et al. (2007). Global desertification: build ing a science for dryland development. *Science* 316, 847–851. doi: 10.1126/science.1131634

Rozanski, K., Araguds-Araguds, L., and Gonfantini, R. (1993). "Isotopic patterns in modern global precipitation," in *Climate Change in Continental Isotopic records-Geophysical Monograph*, vol. 8pp . Eds. Swart, P. K., Lohman, K. C., McKenzie, J., and Savin, S. (Washington DC: American Geophysical Union), 1–36. doi: 10.1029/GM078p0001

Russell, J., and Ward, D. (2014). Vegetation change in northern KwaZulu- Natal since the Anglo-Zulu War of 1879: local or global drivers? *Afr. J. Range Forage Sci.* 31, 89–105. doi: 10.2989/10220119.2013.827740

Sankaran, M., Hanan, N. P., Scholes, R. J., Ratnam, J., Augustine, D. J., Cade, B. S., et al. (2005). Determinants of woody cover in African savannas. *Nature* 438, 846–849. doi: 10.1038/nature04070

Scanlon, B. R., Keese, K. E., Flint, A. L., Flint, L. E., Gaye, C. B., Edmunds, W. M., et al. (2006). Global synthesis of groundwater recharge in semiarid and arid regions. *Hydrolog. Processes* 20, 3335–3370. doi: 10.1002/hyp.6335

Schenk, H. J., and Jackson, R. B. (2002). The global biogeography of roots. *Ecol. Mon.* 72, 311–328. doi: 10.1890/0012-9615(2002)072[0311:TGBOR]2.0.CO;2

Scholes, R. J., and Archer, S. R. (1997). Tree-grass interactions in savannas. *Annu. Rev. Ecol. Syst.* 28, 517–544. doi: 10.1146/annurev.ecolsys.28.1.517

Scholes, R. J., and Walker, B. H., (1993). *An African Savanna: Synthesis of the Nylsvley Study;*. New York, NY, USA: Cambridge University Press.

Schwinning, S., and Sala, O. E. (2004). Hierarchy of responses to resource pulses in arid and semi-arid ecosystems. *Oecologia* 141, 211–220. doi: 10.1007/s00442-004-1520-8

Seyfried, M. S., Schwinning, S., Walvoord, M. A., Pockman, W. T., Newman, B. D., Jackson, R. B., et al. (2005). Ecohydrological control of deep drainage in arid and semiarid regions. *Ecology* 86, 277–287. doi: 10.1890/03-0568

Shachak, M., Sachs, M., and Moshe, I. (1998). Ecosystem management of desertified shrublands in Israel. *Ecosystems* 1, 475–483. doi: 10.1007/s100219900043

Shadwell, E., and February, E. (2017). Effects of groundwater abstraction on two keystone tree species in an arid savanna national park. *PeerJ* 5, e2923. doi: 10.7717/peerj.2923

Sharma, K. D. (1998). The hydrological indicators of desertification. *J. Arid. Environ.* 39, 121–132. doi: 10.1006/jare.1998.0403

Shukla, A., Vyas, D., and Jha, A. (2013). Soil depth: an overriding factor for distribution of arbuscular mycorrhizal fungi. *J. Soil Sci. Plant Nutr.* 13, 23–33. doi: 10.4067/S0718-95162013005000003

Simonin, K. A., Link, P., Rempe, D., Miller, S., Oshun, J., Bode, C., et al. (2013). Vegetation induced changes in the stable isotope composition of near surface humidity. *Ecohydrology*. 7, 936–949. doi: 10.1002/eco.1420

Smit, G. N., and Rethman, N. F. G. (2000). The influence of tree thinning on the soil water in a semi-arid savanna of southern Africa. *J. Arid. Environ.* 44, 41–59. doi: 10.1006/jare.1999.0576

Soliveres, S., and Eldridge, D. J. (2014). Do changes in grazing pressure and the degree of shrub encroachment alter the effects of individual shrubs on

understorey plant communities and soil function? *Funct. Ecol.* 28 (2), 530–537. doi: 10.1111/1365-2435.12196

Stahl, C., Hérault, B., Rossi, V., Burban, B., Bréchet, C., and Bonal, D. (2013). Depth of soil water uptake by tropical rainforest trees during dry periods: does tree dimension matter? *Oecologia* 173, 1191–1201. doi: 10.1007/s00442-013-2724-6

Stephens, D. B. (1994). A perspective on diffuse natural recharge mechanisms in areas of low precipitation. *Soil Sci. Soc Am. J.* 58, 40– 48. doi: 10.2136/sssaj1994.03615995005800010006x

Tietjen, B. (2016). Same rainfall amount different vegetation-how environmental conditions and their interactions influence savanna dynamics. *Ecol. Model* 326, 13–22. doi: 10.1016/j.ecolmodel.2015.06.013

Walker, J., Bullen, E., and Williams, B. G. (1993). Ecohydrological changes in the Murray-Darling Basin. I. The number of trees cleared over two centuries. *J. Appl. Ecol.* 30, 265–273. doi: 10.2307/2404628

Walter, H. (1954). Die Verbuschung, eine Erscheinung der subtropischen Savannengebiete und ihre ökologischen Ursachen. *Vegetatio* 5, 6–10. doi: 10.1007/BF00299544

Ward, D., Wiegand, K., and Getzin, S. (2013). Walter's two-layer hypothesis revisited: back to the roots! *Oecologia* 172, 617–630. doi: 10.1007/s00442-012-2538-y

Weltzin, J. K., Loik, M. E., Schwinning, S., Williams, D. G., Fay, P. A., Haddad, B. M., et al. (2003). Assessing the response of terrestrial ecosystems to potential changes in precipitation. *BioScience* 53, 941–952. doi: 10.1641/0006-3568(2003)053[0941:ATROTE]2.0.CO;2

West, A. G., Patrickson, S. J., and Ehleringer, J. R. (2006). Water extraction times for plant and soil materials used in stable isotope analysis. *Rapid Commun. Mass Spectrom.* 20, 1317–1321. doi: 10.1002/rcm.2456

Wickham, H. (2016). ggplot2: elegant graphics for data analysis. Springer-Verlag New York. ISBN 978-3-319-24277-4, http://ggplot2.org.

Wilcox, B. P. (2002). Shrub control and streamflow on rangelands: a process-based viewpoint. *J. Range Manage.* 55, 318–326. doi: 10.2307/4003467

Wilcox, B. P., and Thurow, T. L. (2006). Emerging issues in rangeland ecohydrology: vegetation change and the water cycle. *Rangeland Ecol. Manage.* 59, 220–224. doi: 10.2111/05-090R1.1

Xu, Q., Harbin, L., Chen, J. Q., Cheng, X. L., Liu, S. R., and An, S. Q. (2011). Water use patterns of three species in subalpine forest, Southwest China: the deuterium isotope approach. *Ecohydrology* 4, 236–244. doi: 10.1002/eco.179

Conflict of Interest: The authors declare that the research was conducted in the absence of any commercial or financial relationships that could be construed as a potential conflict of interest.

frontiers in Plant Science

ORIGINAL RESEARCH
published: 21 May 2019
doi: 10.3389/fpls.2019.00607

How Does Water Availability Affect the Allocation to Bark in a Mediterranean Conifer?

Ruth C. Martín-Sanz[1,2], Roberto San-Martín[1,2], Hendrik Poorter[3,4], Antonio Vázquez[5] and José Climent[1,5]*

[1] Sustainable Forest Management Research Institute (UVa-INIA), Palencia, Spain, [2] Escuela Técnica Superior de Ingenierías Agrarias, Universidad de Valladolid, Palencia, Spain, [3] Plant Sciences (IBG-2), Forschungszentrum Jülich GmbH, Jülich, Germany, [4] Department of Biological Sciences, Macquarie University, North Ryde, NSW, Australia, [5] Department of Forest Ecology and Genetics, Forest Research Centre (INIA-CIFOR), Madrid, Spain

Bark thickness is a key structural feature in woody plants in the protection against fire. We used 19 provenances of *Pinus halepensis*, an obligate-seeder species, in a replicated common garden at two environments contrasting in water availability to assess the interacting effects of site environment and population in the relative allocation to bark, expecting lower allocation at the drier site. Secondly, given the average fire frequency, we analyzed whether trees reached the critical absolute thickness soon enough for population persistence via aerial seed bank. Our analyses indicated that trees at the moister site allocated a rather fixed quantity of resources independent of tree size, and almost all populations reached critical absolute bark thickness to eventually survive fire. In contrast, at the drier site allocation to bark reduced with tree size, and most populations did not reach the critical bark thickness. Populations from areas with higher fire frequency had thicker basal bark, while those from areas with severe droughts and short vegetative periods, had thinner bark. In conclusion, drought-stressed trees have a higher risk to die from fires before achieving reproduction and building a sufficient aerial seed bank.

Keywords: allocation, allometry, bark thickness, fire adaptation, fire ecology, genotype-environment interaction, phenotypic plasticity, Pinaceae

OPEN ACCESS

Edited by:
Ina Christin Meier, University of Göttingen, Germany

Reviewed by:
Martin De Luis, University of Zaragoza, Spain
Sebastian Pfautsch, Western Sydney University, Australia

****Correspondence:***
Ruth C. Martín-Sanz
ruth.martin.sanz@gmail.com

Specialty section:
This article was submitted to Functional Plant Ecology, a section of the journal Frontiers in Plant Science

Received: *19 January 2019*
Accepted: *25 April 2019*
Published: *21 May 2019*

Citation:
Martín-Sanz RC, San-Martín R, Poorter H, Vázquez A and Climent J (2019) How Does Water Availability Affect the Allocation to Bark in a Mediterranean Conifer? Front. Plant Sci. 10:607. doi: 10.3389/fpls.2019.00607

INTRODUCTION

Bark is a key structural feature in woody plants, and the correlation between bark thickness and fire regime has recently attracted increasing interest by plant scientists (Pausas, 2015, 2017; Rosell, 2016). Bark includes all tissues outside the vascular cambium and is formed by two main components with contrasting functions: the living inner bark, which is related to transport and storage of photosynthates, and the dead outer bark which protects the tree from fires, pathogens and herbivores, reduces water loss or provides structural support (for details see, Evert and Eichhorn, 2006; Graves et al., 2014; Romero, 2014; Schafer et al., 2015; Rosell, 2016). However, despite its functional relevance, the role of bark in plant ecological strategies and the causes of its variation remain poorly understood.

Bark thickness is the most studied bark property so far, due to its correlation with cambial insulation and protection, especially against fires (van Mantgem and Schwartz, 2003; Bauer et al., 2010;

Hoffmann et al., 2012; Lawes et al., 2013; Pausas, 2015). The degree of heat insulation by bark increases with the square of its thickness (Hare, 1965; Vines, 1968; Peterson and Ryan, 1986). Therefore, bark thickness strongly decreases the thermal diffusivity –the most important bark protective property (Vines, 1968).

How costly bark is compared to other plant parts (especially, wood) is still poorly known. While bark and wood densities can be very similar in some species (like in conifer trees, Miles and Smith, 2009), the two tissues have different physical properties and chemical composition. Putatively high costs imply that the relative resource allocation to bark must be subjected to strong evolutionary trade-offs between the fitness benefits of a thicker bark and its costs at different ontogenetic stages (Schwilk and Ackerly, 2001).

Several studies have addressed the evolutionary consequences of bark thickness in tropical ecosystems, comparing from a few to many species in natural populations and focusing on species whose strategy against fire is adult survival (Richardson et al., 1990; Lawes et al., 2011a, 2013; Dantas and Pausas, 2013; Poorter et al., 2014; Rosell et al., 2014; Rosell, 2016). So far, few studies have addressed the intraspecific variation in bark thickness (Climent et al., 2004; Tapias et al., 2004; Stephens and Libby, 2006; Briand et al., 2014), and even fewer have used common garden experiments where genetic and environmental effects can be properly separated (Matziris, 2000; Tapias et al., 2004; Stephens and Libby, 2006; Kohnle et al., 2012). As far as we know, bark variation has only been related to different fire regimes, mainly surface fires (Keeley and Zedler, 1998; Jackson et al., 1999; Schwilk et al., 2013; Graves et al., 2014; Pausas, 2015), whereas the environmental factors determining bark thickness and allometry have barely been investigated (but see Jager et al., 2015; Richardson et al., 2015). Determining the possible phenotypic plasticity of bark thickness separately from genetic differences within species is fundamental to improve our understanding of the trade-offs related to bark that can limit adaptive evolution under a changing climate.

Resource allocation in plants changes along ontogenetic trajectories; therefore, distinguishing between environmental effects from purely developmental differences is critical when studying plasticity in allocation (Poorter and Nagel, 2000; Wright and McConnaughay, 2002; Weiner, 2004). While accounting for ontogenetic changes in such long-lived plants like trees is elusive, the concepts and theory of allometry are probably the best available tools. There are different methods to study plant allometric patterns (Poorter and Sack, 2012), but most are based on logarithmically-transformed power law allometric equations (Niklas, 1994; Ter-Mikaelian and Korzukhin, 1997). This procedure has been followed in some studies of bark allometry and allocation to bark, normally using the residuals of the log-log bark thickness-tree diameter regression (see Paine et al., 2010; Rosell, 2016). Alternative approaches have also been applied, such as the relative bark thickness (2 × absolute bark thickness divided by tree diameter; Midgley and Lawes, 2016; see Pausas, 2015, **Supplementary Information** for details on different methods).

Despite the relevance of differential allocation to bark during a plant's development, the survival of a plant facing a given fire depends on its *absolute* bark thickness rather than on the *relative* one (Midgley et al., 2010; Lawes et al., 2011b). The critical absolute bark thickness above which a tree can survive different types of fire is a highly useful parameter (VanderWeide and Hartnett, 2011; Wesolowski et al., 2014; Dehane et al., 2015; Pausas, 2015; Madrigal et al., 2019). As mentioned, above, thermal diffusivity of bark is strongly determined by its thickness (see Hare, 1965; Vines, 1968), but is independent of bark structure, density or moisture content (Martin, 1963; Uhl and Kauffman, 1990; Pinard and Huffman, 1997). In forest trees, bark thickness is generally studied at breast height (see, Harmon, 1984; Stephens and Libby, 2006; Rosell et al., 2015 for exceptions). However, bark thickness at the trunk base is ecologically relevant since trees can die by the girdling of their basal stem part in surface fires, even of low intensities (Jones et al., 2004).

We focused our research on *Pinus halepensis* Mill., a well-studied model species in Mediterranean fire-prone ecosystems (Ne'eman et al., 2004). This species is an obligate-seeder, which lacks resprouting ability. Its vital strategy is based on early building of an aerial seed bank, rather than on adult tree survival (Tapias et al., 2001; Ne'eman et al., 2004; Pausas and Keeley, 2014). However, this species is mentioned in the literature both as thin- and as moderately thick-barked (Fernandes et al., 2008; Chambel et al., 2013; Grivet et al., 2013) and some works report variable survival to low or moderate intensity fires (Ducrey et al., 1996; Trabaud and Valina, 1998; Rigolot, 2004; Fernandes et al., 2008) which coincides with our own field observations. Absolute bark thickness was observed to be moderately heritable in this species (Matziris, 2000), which implies the existence of genetic variability, but differentiation among populations and phenotypic plasticity in this trait is still unknown. Moreover, considering the contrasting natural fire regimes between eastern and western Europe (natural fires are frequent in western Europe, while virtually all fires in eastern Europe are anthropogenic, Ne'eman et al., 2004), we expected intraspecific variation for bark thickness in *P. halepensis*.

The life expectancy of *P. halepensis* trees is usually between 20 and 50 years (Agee, 1998; Vázquez de la Cueva and Moreno, 1998; Arianoutsou, 2001; Tessler, 2012), but it can be as low as 6 years under short fire return intervals (Tessler, 2012). Moreover, *P. halepensis* needs between 15 and 20 years to achieve a sufficient aerial bank of mature seeds (Moreira et al., 2011) to ensure population persistence in case of fire. Therefore, the age of the trees sampled in the present work –18 years– is key given the life-history of the species. The fact that, at this age, this species might be capable of surviving fires of low or moderate intensity thanks to a thick enough bark at the base or at breast height is of paramount importance to avoid immaturity risk. We took advantage of an adult *P. halepensis* provenance trial replicated in two sites with high contrast of water availability due to a combination of climate and soil characteristics. We used 19 range-wide, natural populations of the studied species, which allowed us to disentangle genetic and environmental effects. We wanted to know whether environmental limitations could hamper reaching a thick enough bark to survive fires

until accumulating a sufficient aerial seed bank that ensures population persistence. Thus, our first objective is to check the existence of different allocation to bark among populations under two contrasting test environments, conducive to different absolute bark thickness for each population and site both at the tree base and at breast-height. Our second objective is to determine whether provenance bark traits are related to the climate conditions and/or to fire history at provenances' origin, indicative of local adaptation.

MATERIALS AND METHODS

Research Sites

A common garden experiment was set up in 1997 using a strictly replicated experimental design at different sites in eastern and central Spain. The trial includes 52 *P. halepensis* populations from continental Spain, Balearic Islands (Spain), France, Italy, Greece and Tunisia, thus covering most of the species' range (see Climent et al., 2008 for details). We chose a subset of 19 populations (**Figure 1** and **Supplementary Table S1**) representing the main geographic and environmental gradients of origin, and with a good balance among them. Previous studies showed major significant differences among *P. halepensis* populations, with eastern populations displaying faster growth and lower investment in early reproduction (including low serotiny) and populations toward the southwest with the opposite trends (Climent et al., 2008; Santos-del-Blanco et al., 2013). One-year-seedlings were finally planted in a row-column design in four randomized complete blocks with four plants per population and block (16 trees per population). Height, diameter and cone number were periodically measured, enabling absolute and relative growth assessments and reproductive allocation estimations.

We selected two sites with contrasting environments allowing to separate population differentiation from phenotypic plasticity of bark thickness. Both sites differ in a range of environmental variables (**Table 1**), with drier site showing a 20% lower precipitation, a 100% higher drought intensity index (K) and more frequent and intense wind. Both sites contrast in soil structure, depth and water retention, which leads to a strong divergence in water availability. By contrast, soil nutrient availability between sites is very similar (Gil et al., 1996). Therefore, we refer to these differences as "drier" and "moister." Both potential forest productivity (Sánchez-Palomares and Sánchez-Serrano, 2000) and survival were higher at the moister site (1.8-fold in productivity and 9% more survival compared to the drier site; Martín-Sanz et al., 2016; **Figure 2** and **Table 2**). Moreover, site also affected significantly reproduction, degree of serotiny (long-lasting closed cones in the crown) and tree form.

Sampling and Variable Description

Sampling was carried out in both experimental sites when trees were 18 years old (271 and 241 trees were sampled at the "moister" and "drier" sites, respectively). Stem diameter and bark thickness were measured basally (10 cm above the ground; hereafter referred as D10 and BT10, respectively) and at breast height (hereafter D130 and BT130, respectively) using a tree caliper and a standard bark gauge (**Supplementary Figure S1**). Since we were obliged to preserve the common garden experiment we abstained from more precise, but invasive or destructive bark measuring methods like extraction of bark portions (Jackson et al., 1999; Paine et al., 2010; Graves et al., 2014) or cutting stem discs to remove the bark (Rosell et al., 2014, 2015; Rosell, 2016). Therefore, by bark thickness (basal: BT10 or at breast height: BT130) we refer to total (inner and outer) bark. We performed a preliminary sampling of a few trees at each test

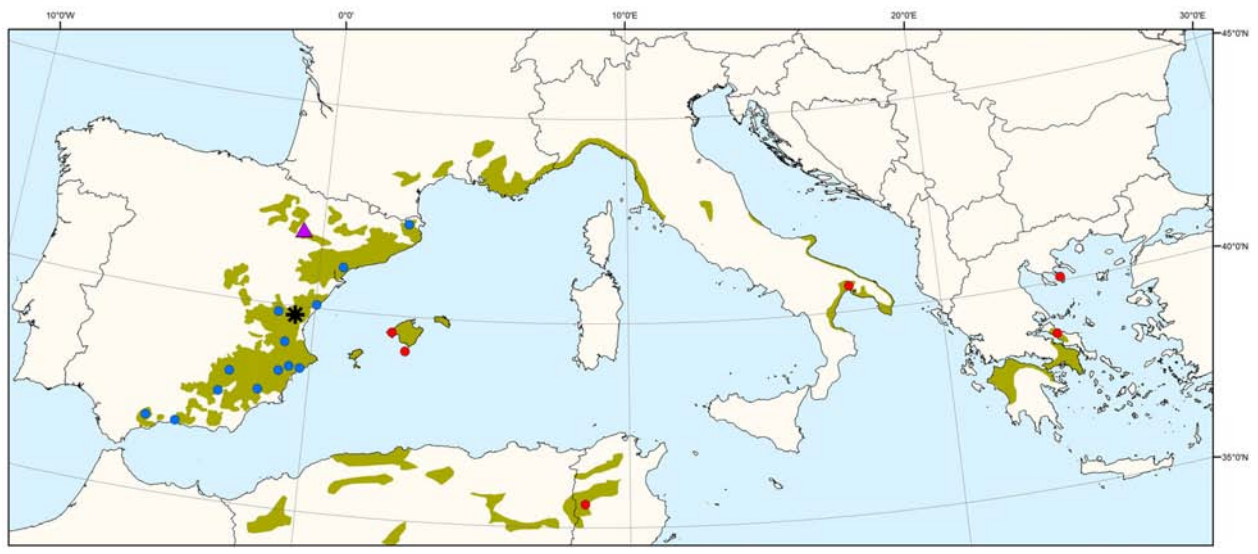

FIGURE 1 | Distribution map of *Pinus halepensis* source populations (blue circles: 13 Iberian populations; red circles: 6 non-Iberian populations) and common garden experiments (purple triangle: drier site; black asterisk: moister site). The green area indicates the species' natural distribution range.

TABLE 1 | Main climatic characteristics of the two test sites of the *Pinus halepensis* common garden experiment (n = 512 trees).

Site	Latitude	Longitude	Altitude (m)	P (mm)	T (°C)	MTWM (°C)	MTCM (°C)	A (months)	K	WS (m/s)	WSS (m/s)	Soil type	PFP (m3/ha/year)	DLI (mol/m²*day)	Sp_DLI (mol/m²*day)	A_DLI (mol/m²*day)
Drier	41° 52′ 22″ N	0° 38′ 54″ W	423	402	14.1	24.1	5.5	3.14	0.45	5.60	4.90	Gypsic Xerosol	2.25–3.00	31.10	36.0	23.7
Moister	39° 49′ 29″ N	01 34′ 22″ W	605	509	14.4	22.9	7.8	2.51	0.22	4.93	3.94	Calcic Cambisol	4.50–5.25	31.15	35.2	25.2

P, annual rainfall; T, mean annual temperature; MTWM, mean temperature of the warmest month; MTCM, mean temperature of the coldest month; A, drought duration parameter; K, drought intensity parameter, calculated as the ratio between the dry area (when 2T > P) and the wet area of the climograph (when 2T < P); all previous variables from Gonzalo-Jiménez (2010); WS, mean annual wind speed at 80 m above surface; WSS, mean summer wind speed at 80 m above surface (from Aymamí et al., 2011); Soil type classification according to FAO guidelines (FAO, 2015); PFP, Potential Forest Productivity, calculated following the Paterson Climate Index and obtained from the Potential Forest Productivity Map of Spain (Sánchez-Palomares and Sánchez-Serrano, 2000); DLI, Daily Light Integral; Sp_DLI and A_DLI, Daily Light Integral for the vegetative period (spring and autumn, respectively). DLI data from New et al. (1999).

site measuring bark thickness at three points surrounding the bole. We found that measuring bark thickness at a single point was accurate enough given the uniformity of *P. halepensis* bark at this age. Thus, for each height, we measured bark at a single point of the bole, always in the south orientation.

While simple and straightforward, we think that the linear relationship between bark thickness and diameter does not represent accurately enough the real resource allocation to bark. Our point is that allometry of bark allocation should be rather assessed through variables that are as-close-as-possible to the biomass of bark and sapwood (the functional part of the trunk). Therefore, focusing purely on the allometry of bark allocation, we looked at the allometric relationship between bark and sapwood volumes, basing the analysis on the relationship of percentage of bark volume and total volume from tree base to breast height (Martín-Sanz, 2018). Our sampled trees did not contain any heartwood (see **Appendix A** and **Supplementary Figure A.1**), so total volume is bark and sapwood (functional xylem) volumes.

Firstly, we calculated the total volume for the cone trunk from the tree base to breast height with the equation for a circular truncated cone (in dm^3):

$$V_T = \pi/3 * h * (Rb^2 + Rb * Rbh + Rbh^2) \quad (1)$$

where h is the height difference between the base (10 cm above ground) and breast height (130 cm), Rb is the basal radius and Rbh is the radius at breast height.

Sapwood volume (dm^3) was computed with the following equation:

$$V_S = \pi/3 * h * (SRb^2 + SRb * SRbh + SRbh^2) \quad (2)$$

where h is the height difference between the base (10 cm above ground) and breast height (130 cm), SRb is the sapwood basal radius and SRbh is the sapwood radius at breast height.

Finally, bark volume (dm^3) and percentage of bark volume were estimated by Equations (3) and (4), respectively:

$$V_B = V_T - V_S \quad (3)$$

$$\%V_B = V_B/V_T * 100 \quad (4)$$

Statistical Analysis

General linear mixed models (LMM) were fit with PROC MIXED procedure in SAS software (SAS Institute Inc., 2015). The incorporation of variables into the models was checked using the Akaike's Information Criterion (AIC), selecting those models with lower AIC value. This criterion favors model fit and simplicity, based on the principle of parsimony (fewer parameters in the model). Residuals of each model were examined for normality using diagnostic plots and Kolmogorov-Smirnov normality tests.

Allometric, Plastic, and Genetic Effects on Bark Allocation

We compared means of percentage of cone trunk from tree base to breast height taken up by bark volume (Equation 4) by site and populations using a LMM with environmental effect represented

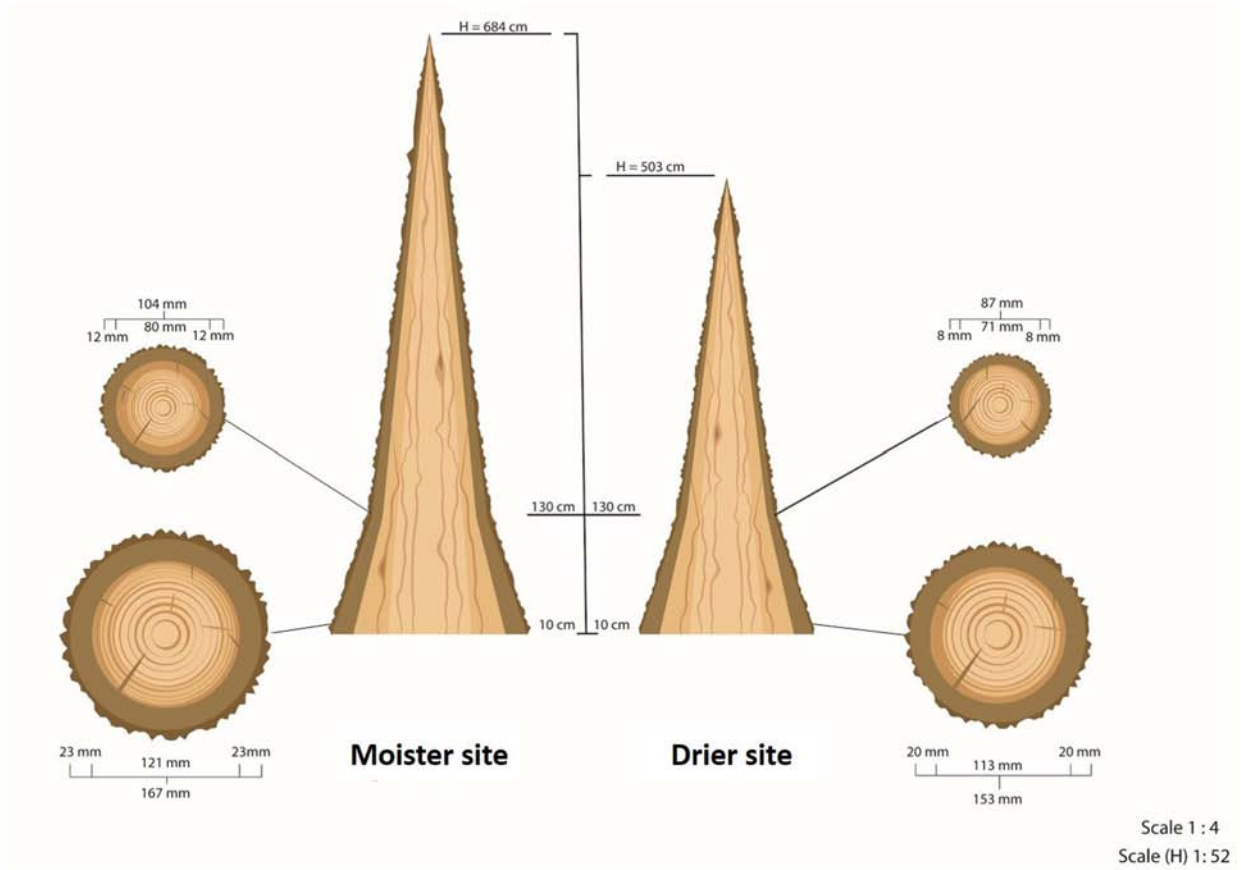

FIGURE 2 | Scheme of the average tree at each of the test sites. H is the total height of the tree. Diameters and bark thicknesses of the circular cross-sections were measured at 10 and at 130 cm from the ground. This scheme does not represent the real taper of wood and bark along the trunk above 130 cm due to the lack of measurements at higher heights. This taper is neither constant nor homogeneous.

by trial sites and genetic effect by populations. In addition, we did the same model adding total volume of the cone trunk as a covariate in order to look for tendencies in percentage of bark volume. In both models, block within site was used as random factor.

Additionally, we wanted to compare our approach with the most commonly applied allometric method, thus we also used model II regression, i.e., standardized major axis (SMA) to examine the allometry of bark volume vs. the total volume of the cone trunk from the tree base to breast height (Henry and Aarssen, 1999; Niklas, 2006; Warton et al., 2006).

The classical allometric model is $V_B = aV_T^b$ and is usually fit as $\log V_B = \log_{10} a + b \log_{10} V_T$ (Huxley, 1932; Niklas, 1994; Ter-Mikaelian and Korzukhin, 1997). Parameter *a* is the elevation or allometric coefficient and parameter *b* is the regression slope or allometric exponent. An exponent significantly different from 1 indicates an allometric relationship between the variables studied (increasing or decreasing with size, non-constant). The allometric exponents of each population at each site were compared with the isometric coefficient ($b = 1$) and to one another by multiple *post hoc* comparisons. These analyses were carried out with the smatr package (Warton et al., 2012) implemented in R software v3.3.2. (R Core Team, 2016). As the SMA analysis indicated that slopes differed among populations and sites, a general SMA test of elevation (allometric parameter) differences was not necessary.

TABLE 2 | Mean values and standard errors (SE) of different growth variables at both test sites.

	Moister (*n* = 271)	*SE*	Drier (*n* = 241)	*SE*
H (cm)	684.0	7.9	503.7	5.0
D10 (mm)	167.1	2.3	153.3	1.7
D130 (mm)	103.9	2.0	87.2	1.3
BT10 (mm)	23.5	0.3	20.7	0.2
BT130 (mm)	12.4	0.3	8.0	0.2

H, total tree height; D10, diameter at tree base (at 10 cm); D130, diameter at breast height (at 130 cm); BT10, bark thickness at tree base; BT130, bark thickness at breast height. All variables were significantly different between sites: $P < 0.0001$.

Plastic and Genetic Effects on Bark Thickness at Breast and Basal Height

We analyzed the effects of population (genetic effect), experimental site (environment) and their interaction on

absolute bark thickness at breast height and at tree base with LMM, including block within site as random factor. We compared the population per site variation of absolute bark thickness with critical thickness values –the thickness above which the risk of cambium damage decreases considerably, therefore indicating a threshold for tree survival– both at breast height and at tree base. While our bark thickness data did not differentiate between inner and outer bark neither we compared further heat insulating properties as moisture content or density, we assumed that bark anatomy should not differ significantly among provenances of a single species, as found in other species (see Wesolowski et al., 2014). Due to the lack of experimental data of critical bark thickness for *P. halepensis*, we used data published for the genetically closest available tree species: a high thickness of 20 mm, postulated to allow survival to moderate fires (for *Pinus pinea*; Madrigal et al., 2019) and a low thickness of 10 mm that would allow survival only to low-intensity fires (van Mantgem and Schwartz, 2003; VanderWeide and Hartnett, 2011).

Relationship of Bark Thickness With Seed Source Environment

Looking for ecotypic trends in bark thickness, we tested for correlations among the mean values for bark thickness of our raw data (at breast and basal heights) and continuous environmental variables, as well as with fire frequency records from the 13 Iberian populations. The nineteen original bioclimatic variables for populations' origin were obtained from Worldclim v.1.4 (Hijmans et al., 2005). We considered nine of these variables: annual precipitation, summer precipitation (June, July, and August), spring precipitation (March, April, and May), autumn precipitation (September, October, and November), precipitation of the driest month, annual mean temperature, mean temperature of the warmest month, mean temperature of the coldest month, and a continentality index (difference between mean temperature of the warmest month and mean temperature of the coldest month). Three spatial variables were also recorded for each population: longitude, latitude and altitude. We carried out a principal components analysis (PCA) with *varimax* rotation to reduce the number of environmental variables and allow a more synthetic interpretation. We decided the number of principal components to retain running a parallel analysis with 1000 iterations (Hayton et al., 2004) and selecting those principal components with eigenvalues for observed data larger than those from simulations. The analysis was performed with psych package (Revelle, 2017) on the R software v3.3.2. (R Core Team, 2016). Selected variables with loadings above 0.80 were used in Spearman correlation analysis with bark thickness. Natural fire frequency data (lightning fires, of relevance in the east part of Spain; Vázquez de la Cueva and Moreno, 1998) were defined as the number of fires in 90,000 ha of surface covered by *P. halepensis* forests each year during the period 1974–2010. A 10 × 10 km grid-unit was used to derive this fire frequency data for the 13 Iberian populations of *P. halepensis*. Unfortunately, we lacked data sources of, similarly, reliable and thorough fire information for the non-Iberian populations. Spearman correlations were done with Hmisc package (Harrell et al., 2018), implemented in R software v3.3.2. (R Core Team, 2016).

RESULTS

Allometric, Plastic, and Genetic Effects on Bark Allocation

Trees at the drier site showed a lower percentage of bark volume (43%) compared to the moister site (47%; **Table 3**), an apparently modest difference but statistically highly significant [$F_{(1,\ 6)} = 23.87$, $P = 0.003$]. Differences among populations were also significant [$F_{(18,\ 468)} = 1.87$, $P = 0.016$], with average percentages of bark volume ranging from 42 to 47% (**Supplementary Table S2**). Site by population interaction was not significant [$F_{(18,\ 468)} = 0.88$, $P = 0.608$; **Supplementary Table S3**], indicating a similar population ranking for percentage of bark between sites. Total volume as a covariate for percentage of bark was highly significant [total volume: $F_{(1,\ 430)} = 112.98$, $P < 0.001$], as well as volume × site interaction [$F_{(1,\ 430)} = 7.61$, $P = 0.006$]. The rest of factors and interactions were not significant (**Supplementary Table S4**). The allometric effect of total volume on percentage of bark volume was negative (**Figure 3**). While at lower total volumes, this allometric effect was similar between sites, at higher total volumes differences between sites were magnified.

Regarding the allometric (SMA) analysis, half of the populations showed constant investment in bark with tree size, i.e., isometric allometric exponents ($b = 1$), at the drier site and

TABLE 3 | Minimum, mean and maximum percentage of bark volume (%V_B) with confidence intervals (CI) for each test site ($n = 512$ trees).

Site	min. %V_B [CI]	Mean %V_B [CI]	max. %V_B [CI]
Moister	43.7 [39.0–48.4]	46.6 [45.3–47.9]	48.5 [45.6–51.5]
Drier	39.4 [35.5–43.4]	42.3 [41.6–44.2]	47.1 [43.7–50.4]

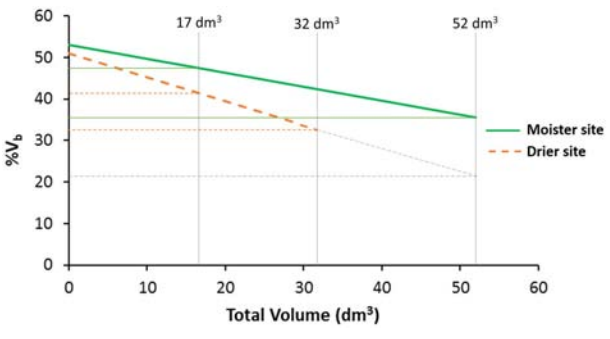

FIGURE 3 | Percentage of bark volume vs. total volume per site. Vertical lines indicate the global mean total volume for both sites (17 dm^3), and the maximum total volume reach at each test site (32 dm^3 at the drier site and 52 dm^3 at the moister site). Gray dot-dash lines represent the percentage of bark volume in the drier site if the trees would reach the same maximum total volume as in the moister site. At higher total volume, the difference between sites increases ($n = 512$ trees).

TABLE 4 | Minimum, mean and maximum absolute bark thickness at basal (BT10) and breast heights (BT130) with confidence intervals (CI) for each test site (n = 512 trees).

Site	BT10 (mm)	CI (mm)	BT130 (mm)	CI (mm)
Moister	23.5	22.8–24.2	12.5	11.8–13.1
Drier	20.6	20.1–21.2	8.1	7.6–8.5

the other half, decreasing investment with tree size ($b < 1$). At the moister site, most populations had isometric allometric exponent ($b = 1$), except three populations showing decreasing investment in bark ($b < 1$; **Supplementary Table S5**). In general, populations at the moister site showed slopes closer to 1 (mean $b = 0.92$) than the same populations at the drier site (mean $b = 0.86$; differences between slopes were significant: LRT = 5.56, $df = 1$, $P = 0.018$).

Plastic and Genetic Effects on Bark Thickness at Breast and Basal Height

Absolute bark thickness was significantly lower ($P < 0.001$) at the site with lower water availability both at breast and basal heights (**Table 4** and **Supplementary Table S6**). We performed this analysis for all 19 populations taken together and specifically for the 13 Iberian populations (for which we have fire record data). Results for the Iberian populations followed the same pattern as those for all populations, so we only show the results for all populations.

At the tree base, all populations showed bark thicker than the low critical threshold (10 mm) at both experimental sites (**Figures 4A–D**). By contrast, while all populations reached the high threshold thickness of 20 mm at the moister site (21.3–26.3 mm, **Supplementary Table S7**), not all of them did at the drier site (17.3–24.3 mm, **Supplementary Table S7** and **Figure 4**). As for the bark thickness at breast height, only three populations exceed the 10 mm thickness threshold at the drier site. At the site with higher water availability, most of the populations showed a bark thickness higher than 10 mm, but below 20 mm- only two populations did not reach the low critical value of 10 mm-. At breast height, the range of differences among populations within sites was more than twofold. Moreover, the ranking of populations for bark thickness at breast height remained rather stable: populations with higher growth rates (from Greece and Italy) had higher BT130, while the populations with lower growth rates (Tunisia and southern Spain) showed lower BT130 at both test sites. However, at the tree base the populations ranking varied considerably between the drier and moister sites, without clear patterns. Only one of the faster-growing populations (P211) had high BT10 at both test sites and one population from southern Spain remained below the average at both sites (population P172, **Supplementary Table S7**).

Bark thickness at breast height was closely linked to sapwood diameter among populations, whereas at the tree base bark thickness was little correlated to sapwood diameter, especially at the drier site (**Figures 4A–D**). To help understanding the differences in plasticity of bark thickness between sites, we depicted the sapwood-bark trends between sites for three extreme provenances: one that did not reach the minimum critical bark thickness even at the moister site (P152), another one in which the plasticity conducted to a different critical bark thickness between sites (P185), and finally a third population that achieved the critical bark thickness even at the drier site (P211, **Figures 4E,F**).

Relationship of Bark Thickness With Seed Source Environment

Parallel analysis associated with PCA for environmental variables at the populations' origins revealed two principal components (variance explained: PC1 = 45%, PC2 = 36%; Martín-Sanz, 2018). Considering loadings above 0.80, the first principal component was positively related to spring and summer rainfalls, as well as to the precipitation of the driest month. PC2 was negatively related to the continentally index and positively to autumn rainfall (see **Supplementary Table S8**). Pooling together data of both sites, BT10 was correlated (at 90% confidence, $P = 0.10$) with summer rainfall and precipitation of the driest month (Spearman rho = 0.46, $P = 0.049$, rho = 0.42, $P = 0.072$, respectively). BT10 just at the drier site was correlated with summer and spring rainfall, and precipitation of the driest month (rho = 0.50, $P = 0.031$, rho = 0.42, $P = 0.074$, and rho = 0.53, $P = 0.020$, respectively, **Figure 5**). At the moister site we did not find any association between bark thickness and environmental variables (**Supplementary Table S9**). Natural fire frequency at the original populations' habitat was positively correlated with bark thickness at the tree base, but only at the drier site (Spearman rho = 0.62, $P = 0.024$).

DISCUSSION

Allometric, Plastic, and Genetic Effects on Bark Allocation

This study highlights the existence of phenotypic plasticity for bark traits in a conifer, responding to different resource availability among environments. Using a replicated common garden experiment at two highly contrasting sites we could differentiate environmental, allometric and genetic effects (Merilä and Hendry, 2014).

Following our expectations, at the drier site our sampled *P. halepensis* trees allocated fewer resources to the bark, even considering the large difference in size among sites (see **Figure 3** where the percentage of bark volume is compared between tree equal sizes -equal total volumes-). Noteworthy, the decreasing relationship between the percentage of bark volume and the total volume was more pronounced at the drier site, confirmed also by the allometric analyses.

Instead of using the usual ratio with stem diameter (see for example, Paine et al., 2010; Pausas, 2015; Midgley and Lawes, 2016) we followed a new methodological approach intending to be closer to the real allometry between the bark and the rest of the tree. We considered this better defined by comparing the percentage of bark volume vs. the total volume of the trunk, considering also that all stem was sapwood in our sampled *P. halepensis* trees (**Supplementary Figure A.1**). As expected, due

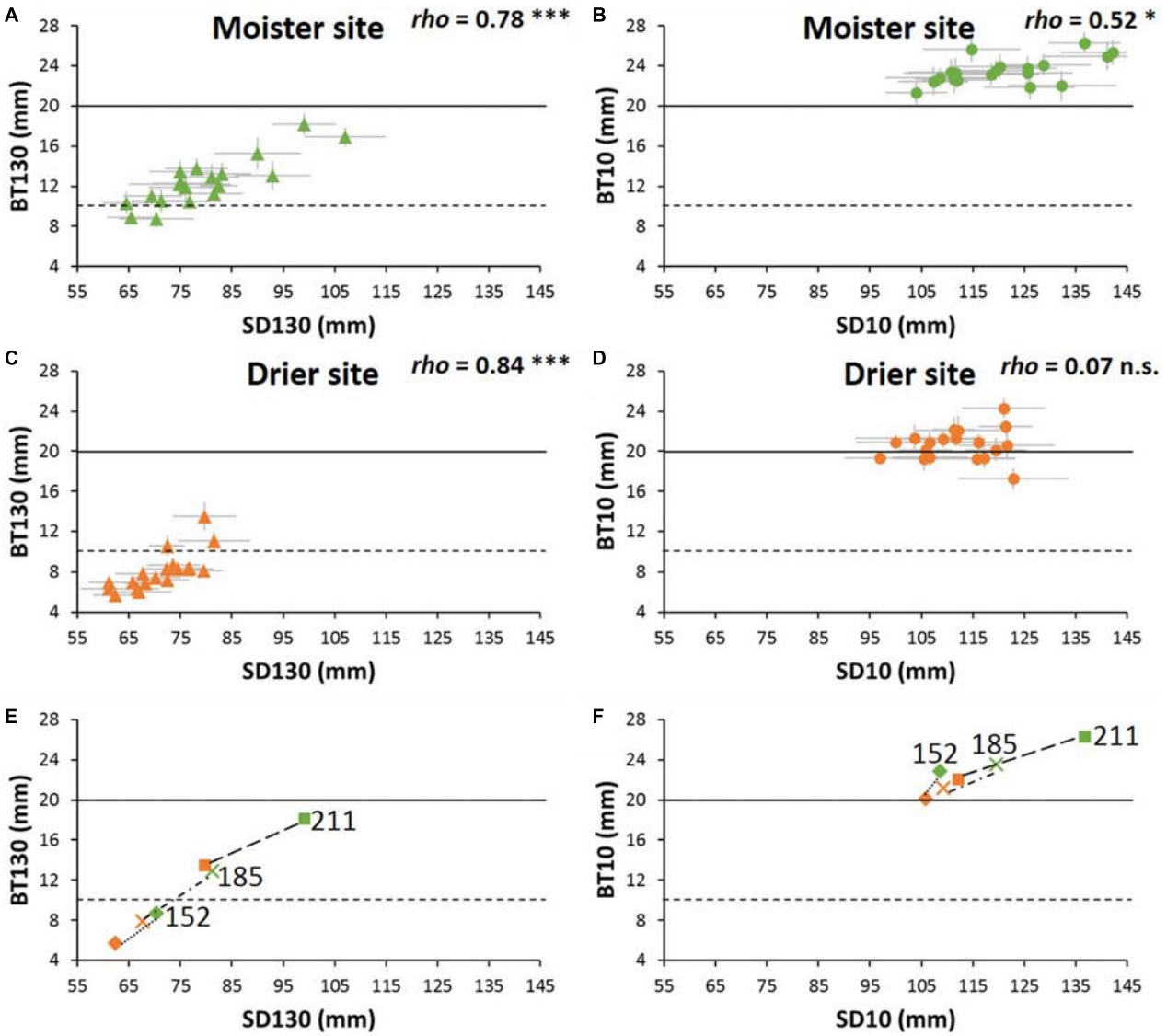

FIGURE 4 | (A–D) Bark thickness vs. sapwood diameter of *P. halepensis* populations at each experimental site. BT130 and BT10 are bark thickness at breast height and at the tree base, respectively, SD130 and SD10 are sapwood diameter at breast height and at the tree base, respectively. Horizontal black lines represent the assumed values of critical bark thickness for cambium survival (solid line: 10 mm; dashed-line: 20 mm). Significance for Spearman correlations between bark thickness and sapwood diameter at: ***$P < 0.001$, **$P < 0.01$, *$P < 0.05$, n.s. = no significant. **(E,F)** Variation between sites of the relationship between critical bark thickness and sapwood diameter of three representative *P. halepensis* populations. Numbers are the population code as in **Supplementary Table S1**. Green symbols indicate moister site and orange symbols drier site (n = 512 trees).

to the well-documented relationship between bark thickness and stem diameter (Adams and Jackson, 1995; Pinard and Huffman, 1997; Lawes et al., 2013; Poorter et al., 2014), bark volume was closely related to total volume. This allometric effect, which has an adaptive significance, implies that the evolutionary forces that act on plant size will produce changes in bark thickness (Rosell, 2016; Rosell et al., 2017). Due to this relationship, when the goal is to compare differential allocation to the bark among species or populations, plant size must be taken into account (Hempson et al., 2014; Poorter et al., 2014; Rosell and Olson, 2014). However, while differential relative allocation to bark is essential under a functional-evolutionary perspective, survival to fire clearly depends on absolute bark thickness (Midgley et al., 2010; Lawes et al., 2011b). Confirming our main hypothesis, the lower allocation to bark in the growth-limiting environment led to lower absolute bark thickness bark, such that at 18 years of age (close to an average-low fire return interval for *P. halepensis*) trees did not achieve the critical thickness of 20 mm. Moreover, our results confirmed a strong population genetic effect on absolute bark thickness, with eastern Europe populations showing thicker bark, and populations from North Africa and Southern Spain displaying thinner bark. Difference of bark thickness at breast

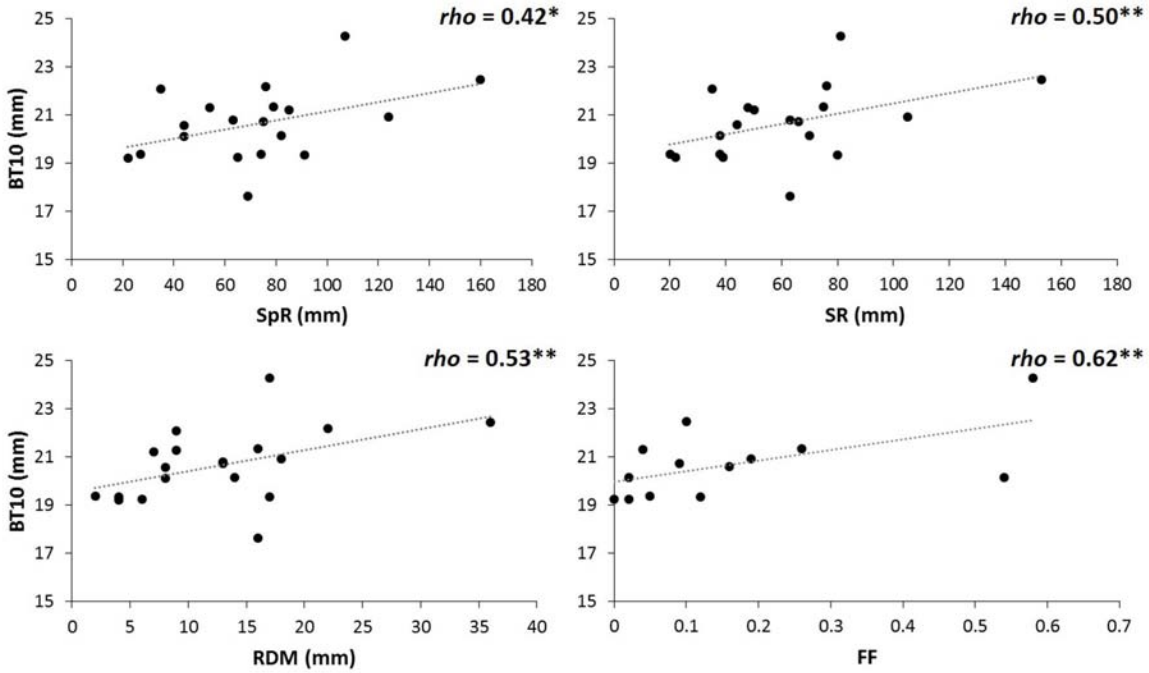

FIGURE 5 | Spearman correlations between basal bark thickness at the drier site (BT10) and spring rainfall (SpR), summer rainfall (SR), rainfall of the driest month (RDM), and fire frequency (FF). Significance for Spearman correlations at: ***$P < 0.001$, **$P < 0.01$, *$P < 0.05$, n.s. = no significant (n = 19 populations for correlations with environmental variables; n = 13 Iberian populations for correlations with fire frequency).

height among extreme populations was more than twofold (7.2 mm -population 152– and 15.8 mm –population 211–). This difference among populations is comparable to that found for trees of similar height in *P. pinaster* (Tapias et al., 2004), one of the pine species with best known strong ecotypic variation (see for example Alía et al., 1995). Moreover, plasticity of bark absolute thickness was rather homogeneous among provenances, hence the site-related scarcity of resources led to lower bark thickness affecting all populations alike.

While it has been shown that inner living bark is involved in the storage and translocation of water and photosynthates (Srivastava, 1964; Scholz et al., 2007; Romero, 2014), thermal protection depends on the outer dead bark thickness (Romero and Bolker, 2008; Pásztory and Ronyecz, 2013), rather than on the total bark thickness (Graves et al., 2014). Moreover, it seems that the decreasing rate in outer bark thickness with tree height is greater in fire-resistant species than in fire-sensitive ones, in contrast to inner bark thickness which diminishes with tree height or total bark thickness which is maintained along the bole (Graves et al., 2014). Therefore, differentiating between inner and outer bark thicknesses in future studies will help us to better understand the ecology and functional role of bark.

Environmental Correlations and Life-History Implications

The environmental correlations found in this work suggest the existence of ecotypic patterns in this species that deserve further investigation to understand their evolutionary meaning. We found a highly expected significant correlation between higher frequency of natural forest fires and thicker basal bark. Among the environmental characteristics at the provenances' seed source, the most significant correlation occurred between higher rainfall and thicker bark. These results combined may appear counter-intuitive, but it is necessary to bear in mind that in Mediterranean ecosystems higher rainfall leads to high fuel accumulation that may increase fire hazard during yearly summer droughts. Actually, permanently dry forests are usually less likely to burn due to lower fuel loads, even when trees may be physically more flammable (Fuhlendorf and Smeins, 1997; Kitzberber et al., 1997; Fernandes, 2013). A more accurate estimation of the fire regime including not only fire frequency data but also intensity, spread patterns or seasonality, and amount and type of fuel, would indeed allow us to better understand the role of fire on the variation of bark thickness in *P. halepensis*.

As an obligate seeder, the vital strategy of *P. halepensis* is the maintenance of an aerial seed bank in serotinous cones, enough for the persistence of the population in case of fire (Tapias et al., 2001; Ne'eman et al., 2004). Therefore, it is essential that trees can survive low or moderately intense fires until accumulating this "sufficient" aerial seed bank. This is usually achieved when *P. halepensis* trees are between 15 and 20 years old (Moreira et al., 2011), but both intraspecific variation and plasticity can largely modify that reference age (Martín-Sanz et al., 2016). Lacking specific data on the critical minimum bark thickness for this species, we chose

two extreme values based on the literature (see van Mantgem and Schwartz, 2003; Wesolowski et al., 2014; Pausas, 2015; Madrigal et al., 2019). We found that our trees generally reached the critical bark thickness at the base, but not at breast height. This is consistent with a greater thermal insulation at the stem base and a steep bark tapering along the bole found in several Mediterranean pine species (De Ronde, 1982; Pageaud, 1991; Jackson et al., 1999). This can be regarded as an adaptive solution to reduce immaturity risk (Lamont et al., 1991; Keeley et al., 1999), i.e., ensuring individual survival until reaching a sufficient aerial seed bank enabling recruitment after lethal fires. Importantly, our studied trees did not reach the critical breast height bark thickness of 20 mm and, at the base of the tree, this value was only achieved at the moister site. Therefore, as predicted, the plasticity associated to different resource availability (mostly water availability during the vegetative period, since light, nutrients and CO_2 are not limiting in our study sites) clearly affects the probability of *P. halepensis* to survive fires; the lesser resources, the lower expected survival facing fires. Interestingly, depending on the species and habitats, variable and even opposite relationships have been found between bark thickness and productivity or soil fertility (Climent et al., 2004; Schubert, 2014; Jager et al., 2015; Richardson et al., 2015). However, as far as we know, our study is the first to assess the strict environmental effect separated from the genotype-environment interaction; thus, the comparison with earlier works is not straightforward.

The maximum life expectancy of *P. halepensis* due to fire return interval is usually estimated between 20 and 50 years, while the average is about 25 years (Agee, 1998; Vázquez de la Cueva and Moreno, 1998; Arianoutsou, 2001; Tessler, 2012). However, fire interval could be as short as 6 years in some areas of its natural distribution (Tessler, 2012). When fire interval is shorter than 15 years, *P. halepensis* recruitment would be limited, and its populations may totally disappear (Roitemberg and Ne'eman, 2000; Eugenio et al., 2006; Herman, 2009; Tessler et al., 2014). Therefore, the age of our sampled trees -18 years- is highly meaningful considering the species' life-history.

Preceding studies in *P. halepensis* have shown relevant ecotypic trends for growth, reproduction and water use efficiency such that provenances from dry continental environments showed early and intense reproduction and serotiny, as well as conservative water use in detriment of vegetative growth (Ferrio et al., 2003; Voltas et al., 2008, 2015; Santos-del-Blanco et al., 2013). Therefore, adaptive geographic variation of this species seems to be derived from differential resource allocation among key life-history processes (growth, reproduction, fire tolerance, constitutive and induced defenses, and water stress tolerance; Sampedro et al., 2014; Climent et al., 2015).

CONCLUSION

In addition to the expected allometric effect on bark thickness, so that bigger trees had thicker bark, we found phenotypic plasticity for different bark traits in *Pinus halepensis*. Our results confirmed that growth-limiting environments hampered bark thickness such that trees did not achieve the critical bark thickness necessary to survive fires at 18 years of age, a time close to an average-low fire return interval for this species, while the relative allocation to reproduction is maximized under growth-limiting conditions (Santos-del-Blanco et al., 2013; Martín-Sanz et al., 2016). This happened not only because of lower growth, but also due to a higher negative allometry of bark thickness relative to stem size at the site with lower water availability. This could be detrimental for the resilience of this species' populations under the more intense droughts and more frequent and severe forest fires driven by ongoing climate change. Moreover, despite *P. halepensis* is considered typically an obligate seeder, our study revealed that some populations can achieve a sufficient bark thickness to survive surface and moderately-intense fires. This suggests a more variable adaptive strategy to cope with fire than has been considered so far for this species (see Ducrey et al., 1996; Rigolot, 2004; Fernandes et al., 2008); the correlations found between bark traits, fire regime and local climate among populations support the ecotypic nature of this intraspecific variation. To our knowledge, this is the first study providing experimental evidence of plasticity for this key adaptive trait in interaction with population differentiation. We still lack direct experimental data on the critical bark thickness for *P. halepensis* survival, and on the possible differences in bark morphology, its internal structure and the rate of bark thickness tapering along the entire bole; aspects that can be critical for tree survival. Moreover, the possible trade-offs with other key processes (namely reproduction or defense) deserve further investigation under a Climate Change scenario.

AUTHOR CONTRIBUTIONS

RM-S and JC conceived and designed the study. RM-S carried out fieldwork. AV collected and prepared fire data. RM-S and RS-M designed and performed the statistical analysis. RM-S wrote the original draft. JC and HP revised the manuscript. All authors have read and approved the final manuscript.

FUNDING

This work was supported by Spanish Ministry of Economy and Competitiveness through projects FENOPIN (AGL2012-40151-C03-02) and FUTURPIN (AGL2015-68274-C3-01), and through a doctoral fellowship awarded to RM-S (FPI BES-2013-064210).

ACKNOWLEDGMENTS

We thank all persons and institutions linked to the establishment of the field sites, subsequent measurements and maintenance of

the network, as well as E. Ballesteros, F. del Caño, R. Pulido, and S. San Segundo for their help with field work. We also thank J. Madrigal for his valuable comments about forest fire behavior and R. Abejón for his help in drawing up **Figure 2**. We also thank guest associate editor IM and two reviewers for valuable comments that improved a previous version. Data from the two experimental sites of the common garden experiment used in this research are part of the Spanish Network of Genetic Trials (GENFORED). Some content of this manuscript first appeared in the main author's Ph.D. thesis which can be accessed online in http://uvadoc.uva.es/handle/10324/33128.

SUPPLEMENTARY MATERIAL

The Supplementary Material for this article can be found online at: https://www.frontiersin.org/articles/10.3389/fpls.2019.00607/full#supplementary-material

REFERENCES

Adams, D. C., and Jackson, J. F. (1995). Estimating the allometry of tree bark. *Am. Midl. Nat.* 134, 99–106. doi: 10.2307/2426487

Agee, J. K. (1998). "Fire and pine ecosystems," in *Ecology and Biogeography of Pinus*, ed. D. M. Richardson (Cambridge: Cambridge University Press), 193–218.

Alía, R., Gil, L., and Pardos, J. A. (1995). Performance of 43 *Pinus pinaster* provenances on 5 locations in central Spain. *Silvae Genet.* 44, 75–81.

Arianoutsou, M. (2001). Landscape changes in Mediterranean ecosystems of Greece: implications for fire and biodiversity issues. *J. Mediterr. Ecol.* 2, 165–178.

Aymamí, J., García, A., Lacave, O., Lledó, L., Mayo, M., and Parés, S. (2011). *Análisis del Recurso. Atlas Eólico de España. Estudio Técnico PER 2011–2020*. Madrid: Instituto para la Diversificación y Ahorro de la Energía (IDAE).

Bauer, G., Speck, T., Blömer, J., Bertling, J., and Speck, O. (2010). Insulation capability of the bark of trees with different fire adaptation. *J. Mater. Sci.* 45, 5950–5959. doi: 10.1007/s10853-010-4680-4

Briand, C. H., Schwilk, D. W., Gauthier, S., and Bergeron, Y. (2014). Does fire regime influence life history traits of jack pine in the southern boreal forest of Québec, Canada? *Plant Ecol.* 216, 157–164. doi: 10.1007/s11258-014-0424-x

Chambel, M. R., Climent, J., Pichot, C., and Ducci, F. (2013). "Mediterranean pines (*Pinus halepensis* Mill. and brutia Ten.)," in *Forest Tree Breeding in Europe*, ed. L. E. Pâques (Berlin: Springer), 229–265. doi: 10.1007/978-94-007-6146-9_5

Climent, J. M., Prada, M. A., Calama, R., Chambel, M. R., de Ron, D. S., and Alía, R. (2008). To grow or to seed: ecotypic variation in reproductive allocation and cone production by young female Aleppo pine (*Pinus halepensis*, Pinaceae). *Am. J. Bot.* 95, 833–842. doi: 10.3732/ajb.2007354

Climent, J. M., Tapias, R., Pardos, J. A., and Gil, L. (2004). Fire adaptations in the canary Islands pine (*Pinus canariensis*). *Plant Ecol.* 171, 185–196. doi: 10.1023/B:VEGE.0000029374.64778.68

Climent, J. M., Voltas, J., Zas, R., Martín-Sanz, R. C., Ferrio, P., Notivol, E., et al. (2015). *Environment-Dependent Patterns of Phenotypic Integration in Aleppo pine (52267). Abstract Retrieved from Congress of the European Society for Evolutionary Biology (ESEB), Lausanne (2015)*. Lausanne: Université de Lausanne, 634.

Dantas, V. D. L., and Pausas, J. G. (2013). The lanky and the corky: fire-escape strategies in savanna woody species. *J. Ecol.* 101, 1265–1272. doi: 10.1111/1365-2745.12118

De Ronde, C. (1982). The resistance of *Pinus* species to fire damage. *S. Afr. For. J.* 122, 1–27. doi: 10.1080/00382167.1982.9628828

Dehane, B., Madrigal, J., Hernando, C., Bouhraoua, R., and Guijarro, M. (2015). New bench-scale protocols for characterizing bark flammability and fire resistance in trees: application to Algerian cork. *J. Fire Sci.* 33, 202–217. doi: 10.1177/0734904114568858

Ducrey, M., Duhoux, F., Huc, R., and Rigolot, E. (1996). The ecophysiological and growth responses of Aleppo pine (*Pinus halepensis*) to controlled heating applied to the base of the trunk. *Can. J. For. Res.* 26, 1366–1374. doi: 10.1139/x26-152

Eugenio, M., Verkaik, I., Lloret, F., and Espelta, J. M. (2006). Recruitment and growth decline in *Pinus halepensis* populations after recurrent wildfires in Catalonia (NE Iberian Peninsula). *For. Ecol. Manage.* 231, 47–54. doi: 10.1016/J.FORECO.2006.05.007

Evert, R. F., and Eichhorn, S. E. (2006). *Esau's Plant Anatomy: Meristems, Cells, and Tissues of the Plant Body: Their Structure, Function, and Development*, 3er Edn. Hoboken, NJ: John Wiley & Sons.

FAO (2015). *Global Forest Resources Assessment 2015*. Rome: FAO.

Fernandes, P. M. (2013). Fire-smart management of forest landscapes in the Mediterranean basin under global change. *Landsc. Urban Plan.* 110, 175–182. doi: 10.1016/J.LANDURBPLAN.2012.10.014

Fernandes, P. M., Vega, J. A., Jiménez, E., and Rigolot, E. (2008). Fire resistance of European pines. *For. Ecol. Manage.* 256, 246–255. doi: 10.1016/j.foreco.2008.04.032

Ferrio, J. P., Florit, A., Vega, A., Serrano, L., and Voltas, J. (2003). Δ13C and tree-ring width reflect different drought responses in *Quercus ilex* and *Pinus halepensis*. *Oecologia* 137, 512–518. doi: 10.1007/s00442-003-1372-7

Fuhlendorf, S. D., and Smeins, F. E. (1997). Long-term vegetation dynamics mediated by herbivores, weather and fire in a *Juniperus-Quercus* savanna. *J. Veg. Sci.* 8, 819–828. doi: 10.2307/3237026

Gil, L., Díaz, P., Jiménez, P., Roldán, M., Alía, R., Agúndez, M. D., et al. (1996). *Las Regiones de Procedencia de Pinus halepensis Mill. en España*. Madrid: Ministerio de Medio Ambiente.

Gonzalo-Jiménez, J. (2010). *Diagnosis Fitoclimática de la España Peninsular: Hacia un Modelo de Clasificación Funcional de la Vegetación y de los Ecosistemas Peninsulares Españoles*. Madrid: Organismo Autónomo de Parques Nacionales.

Graves, S. J., Rifai, S. W., and Putz, F. E. (2014). Outer bark thickness decreases more with height on stems of fire-resistant than fire-sensitive Floridian oaks (*Quercus* spp, Fagaceae). *Am. J. Bot.* 101, 2183–2188. doi: 10.3732/ajb.1400412

Grivet, D., Climent, J., Zabal-Aguirre, M., Neale, D. B., Vendramin, G. G., and González-Martínez, S. C. (2013). Adaptive evolution of Mediterranean pines. *Mol. Phylogenet. Evol.* 68, 555–566. doi: 10.1016/j.ympev.2013.03.032

Hare, R. C. (1965). Contribution of bark to fire resistance of southern trees. *J. For.* 63, 248–251.

Harmon, M. E. (1984). Survival of trees after low-intensity surface fires in great smoky mountains national park. *Ecology* 65, 796–802. doi: 10.2307/1938052

Harrell, F. E. Jr., with contributions from Charles Dupont and many others (2018). *Hmisc: Harrell Miscellaneous. R Package*. Available at: https://cran.r-project.org/package=Hmisc (accessed May, 2018).

Hayton, J. C., Allen, D. G., and Scarpello, V. (2004). Factor retention decisions in exploratory factor analysis: a tutorial on parallel analysis. *Organ. Res. Methods* 7, 191–205. doi: 10.1177/1094428104263675

Hempson, G. P., Midgley, J. J., Lawes, M. J., Vickers, K. J., and Kruger, L. M. (2014). Comparing bark thickness: testing methods with bark-stem data from two South African fire-prone biomes. *J. Veg. Sci.* 25, 1247–1256. doi: 10.1111/jvs.12171

Henry, H., and Aarssen, L. (1999). The interpretations of stem diameter-height allometry in trees: biomechanical constraints, neighbour effects, or biased regression? *Ecol. Lett.* 2, 89–97. doi: 10.1046/j.1461-0248.1999.22054.x

Herman, J. (2009). Fire recurrence effects on aboveground plant and soil carbon in Mediterranean shrublands with Aleppo pine (*Pinus halepensis*). *Geophys. Res. Abstract* 11, EGU2009–EGU10702.

Hijmans, R. J., Cameron, S. E., Parra, J. L., Jones, P. G., and Jarvis, A. (2005). Very high resolution interpolated climate surfaces for global land areas. *Int. J. Climatol.* 25, 1965–1978. doi: 10.1002/joc.1276

Hoffmann, W. A., Geiger, E. L., Gotsch, S. G., Rossatto, D. R., Silva, L. C. R., Lau, O. L., et al. (2012). Ecological thresholds at the savanna-forest boundary: how plant traits, resources and fire govern the distribution of tropical biomes. *Ecol. Lett.* 15, 759–768. doi: 10.1111/j.1461-0248.2012.01789.x

Huxley, J. S. (1932). *Problems of Relative Growth*, 2nd Edn. New York, NY: Dover.
Jackson, J. F., Adams, D. C., and Jackson, U. B. (1999). Allometry of constitutive defense: a model and a comparative test with tree bark and fire regime. *Am. Nat.* 153, 614–632. doi: 10.1086/303201
Jager, M. M., Richardson, S. J., Bellingham, P. J., Clearwater, M. J., and Laughlin, D. C. (2015). Soil fertility induces coordinated responses of multiple independent functional traits. *J. Ecol.* 103, 374–385. doi: 10.1111/1365-2745.12366
Jones, J. L., Webb, B. W., Jimenez, D., Reardon, J., and Butler, B. (2004). Development of an advanced one-dimensional stem heating model for application in surface fires. *Can. J. For. Res.* 34, 20–30. doi: 10.1139/X03-187
Keeley, J., and Zedler, P. (1998). "Life history evolution in pines," in *Ecology and Biogeography of Pinus*, ed. D. M. Richardson (Cambridge: Cambridge University Press), 219–242.
Keeley, J. E., Ne'eman, G., and Fotheringham, C. J. (1999). Immaturity risk in a fire dependent pine. *J. Mediterr. Ecol.* 1, 41–48.
Kitzberber, T., Veblen, O., and Villalba, R. (1997). Climatic in uences on re regimes along a rain forest-to-xeric woodland gradient, North, Patagon, Argentina. *J. Biogeogr.* 24, 35–47.
Kohnle, U., Hein, S., Sorensen, F. C., and Weiskittel, A. R. (2012). Effects of seed source origin on bark thickness of Douglas-fir (*Pseudotsuga menziesii*) growing in southwestern Germany. *Can. J. For. Res.* 42, 382–399. doi: 10.1139/x11-191
Lamont, B. B., Maitre, D. C., Cowling, R. M., and Enright, N. J. (1991). Canopy seed storage in woody plants. *Bot. Rev.* 57, 277–317. doi: 10.1007/BF02858770
Lawes, M. J., Adie, H., Russell-Smith, J., Murphy, B., and Midgley, J. J. (2011a). How do small savanna trees avoid stem mortality by fire? The roles of stem diameter, height and bark thickness. *Ecosphere* 2:art42. doi: 10.1890/ES10-00204.1
Lawes, M. J., Richards, A., Dathe, J., and Midgley, J. J. (2011b). Bark thickness determines fire resistance of selected tree species from fire-prone tropical savanna in north Australia. *Plant Ecol.* 212, 2057–2069. doi: 10.1007/s11258-011-99547
Lawes, M. J., Midgley, J. J., and Clarke, P. J. (2013). Costs and benefits of relative bark thickness in relation to fire damage: a savanna/forest contrast. *J. Ecol.* 101, 517–524. doi: 10.1111/1365-2745.12035
Madrigal, J., Souto-García, J., Calama, R., Guijarro, M., Picos, J., and Hernando, C. (2019). Resistance of *Pinus pinea* L. bark to fire. *Int. J. Wildland Fire* doi: 10.1071/WF18118
Martin, R. (1963). Thermal properties of bark. *For. Prod. J.* 13, 419–426.
Martín-Sanz, R. C. (2018). *Evolutionary Ecology of fire-Adaptive Traits in a Mediterranean Pine species*. Ph.D. thesis, Universidad de Valladolid, Valladolid.
Martín-Sanz, R. C., Santos-del-Blanco, L., Notivol, E., Chambel, M. R., and Climent, J. M. (2016). Disentangling plasticity of serotiny, a key adaptive trait in a Mediterranean conifer. *Am. J. Bot.* 103, 1–10. doi: 10.3732/ajb.1600199
Matziris, D. I. (2000). Genetic variation and realized genetic gain from aleppo pine tree improvement. *Silvae Genet.* 49, 5–10.
Merilä, J., and Hendry, A. P. (2014). Climate change, adaptation, and phenotypic plasticity: the problem and the evidence. *Evol. Appl.* 7, 1–14. doi: 10.1111/eva.12137
Midgley, J. J., and Lawes, M. J. (2016). Relative bark thickness: towards standardised measurement and analysis. *Plant Ecol.* 217, 677–681. doi: 10.1007/s11258-016-0587-8
Midgley, J. J., Lawes, M. J., and Chamaillé-Jammes, S. (2010). Savanna woody plant dynamics: the role of fire and herbivory, separately and synergistically. *Aust. J. Bot.* 58, 1–11. doi: 10.1071/BT09034
Miles, P. D., and Smith, W. B. (2009). *Specific Gravity and Other Properties of Wood and Bark for 156 Tree Species Found in North America*. Washington, DC: United States Department of Agriculture, 42.
Moreira, F., Viedma, O., Arianoutsou, M., Curt, T., Koutsias, N., Rigolot, E., et al. (2011). Landscape – Wildfire interactions in southern Europe: implications for landscape management. *J. Environ. Manage.* 92, 2389–2402. doi: 10.1016/j.jenvman.2011.06.028
Ne'eman, G., Goubitz, S., and Nathan, R. (2004). Reproductive traits of *Pinus halepensis* in the light of fire – A critical review. *Plant Ecol.* 171, 69–79. doi: 10.1023/B:VEGE.0000029380.04821.99
New, M., Hulme, M., and Jones, P. (1999). Representing twentieth-century space – Time climate variability. Part I. Development of a 1961-90 mean monthly terrestrial climatology. *J. Clim.* 12, 829–856.
Niklas, K. J. (1994). *Plant Allometry. The Scaling of form and Process*. Chicago, IL: Chicago University Press.
Niklas, K. J. (2006). Plant allometry, leaf nitrogen and phosphorus stoichiometry, and interspecific trends in annual growth rates. *Ann. Bot.* 97, 155–163.
Pageaud, D. (1991). *Reconstitution Naturelle de Peuplements Resineux Après Incendie (Pinus pinea* L. & *Pinus halepensis Mill.*). PhD Thesis, ENITEF Ecole Nationale des Ingénieurs des Travaux des Eaux et Forêts, Avignon.
Paine, C. E. T., Stahl, C., Courtois, E. A., Patiño, S., Sarmiento, C., and Baraloto, C. (2010). Functional explanations for variation in bark thickness in tropical rain forest trees. *Funct. Ecol.* 24, 1202–1210. doi: 10.1111/j.1365-2435.2010.01736.x
Pásztory, Z., and Ronyecz, I. (2013). The thermal insulation capacity of tree bark. *Acta Silv. Lignaria Hungarica* 9, 111–117. doi: 10.2478/aslh-2013-0009
Pausas, J. G. (2015). Bark thickness and fire regime. *Funct. Ecol.* 29, 315–327. doi: 10.1111/1365-2435.12372
Pausas, J. G. (2017). Letters Bark thickness and fire regime: another twist. *New Phytol.* 213, 13–15.
Pausas, J. G., and Keeley, J. E. (2014). Evolutionary ecology of resprouting and seeding in fire-prone ecosystems. *New Phytol.* 204, 55–65. doi: 10.1111/nph.12921
Peterson, D. L., and Ryan, K. C. (1986). Modeling postfire conifer mortality for long-range planning. *Environ. Manage.* 10, 797–808. doi: 10.1007/BF01867732
Pinard, M. A., and Huffman, J. (1997). Fire resistance and bark properties of trees in a seasonally dry forest in eastern Bolivia. *J. Trop. Ecol.* 13:727. doi: 10.1017/S0266467400010890
Poorter, H., and Nagel, O. (2000). The role of biomass allocation in the growth response of plants to different levels of light, CO2, nutrients and water: a quantitative review. *Aust. J. Plant Physiol.* 27, 595–607. doi: 10.1071/PP99173
Poorter, H., and Sack, L. (2012). Pitfalls and possibilities in the analysis of biomass allocation patterns in plants. *Front. Plant Sci.* 3:259. doi: 10.3389/fpls.2012.00259
Poorter, L., McNeil, A., Hurtado, V.-H., Prins, H. H. T., and Putz, F. E. (2014). Bark traits and life-history strategies of tropical dry- and moist forest trees. *Funct. Ecol.* 28, 232–242. doi: 10.1111/1365-2435.12158
R Core Team (2016). *R: A Language and Environment for Statistical Computing*. Vienna: R Found. Stat. Comput. Available at: https://www.r-project.org/ (accessed May, 2018).
Revelle, W. (2017). *Psych: Procedures for Personality and Psychological Research*. Available at: https://cran.r-project.org/package=psych (accessed May, 2018).
Richardson, D. M., Richardson, D. M., Cowling, R. M., Cowling, R. M., Le Maitre, D. C., and Le Maitre, D. C. (1990). Assessing the risk of invasive species in *Pinus* and *Banksia* in South African mountain fynbos. *J. Veg. Sci.* 1, 629–642. doi: 10.2307/3235569
Richardson, S. J., Laughlin, D. C., Lawes, M. J., Holdaway, R. J., Wilmshurst, J. M., Wright, M., et al. (2015). Functional and environmental determinants of bark thickness in fire-free temperate rain forest communities. *Am. J. Bot.* 102, 1590–1598. doi: 10.3732/ajb.1500157
Rigolot, E. (2004). Predicting postfire mortality of *Pinus halepensis* Mill. and *Pinus pinea* L. *Plant Ecol.* 171, 139–151. doi: 10.1023/B:VEGE.0000029382.59284.71
Roitemberg, D., and Ne'eman, G. (2000). The canopy stored seed bank in *Pinus* halepensis the key for post-fire recovery. *Ecol. Environ.* 6, 43–52.
Romero, C. (2014). "Bark: structure and functional ecology," in *Bark: Use, Management and Commerce in Africa*, eds A. B. Cunningham, B. M. Campell, and M. K. Luckert (Bronx, NY: The New York Botanical Garden Press).
Romero, C., and Bolker, B. M. (2008). Effects of stem anatomical and structural traits on responses to stem damage: an experimental study in the Bolivian Amazon. *Can. J. For. Res.* 38, 611–618. doi: 10.1139/X07-205
Rosell, J. A. (2016). Bark thickness across the angiosperms: more than just fire. *New Phytol.* 211, 90–102. doi: 10.1111/nph.13889
Rosell, J. A., Castorena, M., Laws, C. A., and Westoby, M. (2015). Bark ecology of twigs vs. main stems: functional traits across eighty-five species of angiosperms. *Oecologia* 178, 1033–1043. doi: 10.1007/s00442-015-3307-5
Rosell, J. A., Gleason, S., Méndez-Alonzo, R., Chang, Y., and Westoby, M. (2014). Bark functional ecology: evidence for tradeoffs, functional coordination, and environment producing bark diversity. *New Phytol.* 201, 486–497. doi: 10.1111/nph.12541

Rosell, J. A., and Olson, M. E. (2014). The evolution of bark mechanics and storage across habitats in a clade of tropical trees. *Am. J. Bot.* 101, 764–777. doi: 10.3732/ajb.1400109

Rosell, J. A., Olson, M. E., Anfodillo, T., and Martínez-Méndez, N. (2017). Exploring the bark thickness-stem diameter relationship: clues from lianas, successive cambia, monocots and gymnosperms. *New Phytol.* 215, 569–581. doi: 10.1111/nph.14628

Sampedro, L., Voltas, J., Martín-Sanz, R. C., López-Goldar, X., Zas, R., and Climent, J. (2014). "Trade-offs among life history and ecophysiological traits underlying population differentiation in Aleppo pine (*Pinus halepensis* Mill.)," in *Proceedings of the 5th International Conference on Mediterranean Pines (medPINE5), Solsona 2014*, eds L. Coll, J. Climent, L. Ximenis, A. Bravo-Oviedo, and S. Mutke (Cerdanyola del Vallès: CREAF), 139.

Sánchez-Palomares, O., and Sánchez-Serrano, F. (2000). *Mapa de la Productividad Potencial Forestal de España. Cartografía digital*. Madrid: Dirección General de Conservación de la Naturaleza, Ministerio de Medio Ambiente, Serie Cartográfica, 317.

Santos-del-Blanco, L., Bonser, S. P., Valladares, F., Chambel, M. R., and Climent, J. M. (2013). Plasticity in reproduction and growth among 52 range-wide populations of a Mediterranean conifer: adaptive responses to environmental stress. *J. Evol. Biol.* 26, 1912–1924. doi: 10.1111/jeb.12187

SAS Institute Inc. (2015). *SAS/STAT® 14.1 User's Guide*. Cary, NC: SAS Institute Inc.

Schafer, J. L., Breslow, B. P., Hohmann, M. G., and Hoffmann, W. A. (2015). Relative bark thickness is correlated with tree species distributions along a fire frequency gradient. *Fire Ecol.* 11, 74–87. doi: 10.4996/fireecology.1101074

Scholz, F. G., Bucci, S. J., Goldstein, G., Meinzer, F. C., Franco, A. C., and Miralles-Wilhelm, F. (2007). Biophysical properties and functional significance of stem water storage tissues in Neotropical savanna trees. *Plant Cell Environ.* 30, 236–248. doi: 10.1111/j.1365-3040.2006.01623.x

Schubert, A. T. (2014). *Does Fire or Productivity Drive Relative Bark Thickness From Desert to Savanna in Northern Australia?* BSc thesis, School of Environment, Faculty of Engineering, Health, Science and the Environment, Charles Darwin University, Darwin.

Schwilk, D. W., and Ackerly, D. D. (2001). Flammability and serotiny as strategies: correlated evolution in pines. *Oikos* 94, 326–336. doi: 10.1034/j.1600-0706.2001.940213.x

Schwilk, D. W., Gaetani, M. S., and Poulos, H. M. (2013). Oak bark allometry and fire survival strategies in the chihuahuan desert sky islands, Texas, USA. *PLoS One* 8:e79285. doi: 10.1371/journal.pone.0079285

Srivastava, L. M. (1964). Anatomy, chemistry and physiology of bark. *Int. Rev. For. Res.* 1, 203–277. doi: 10.1016/B978-1-4831-9975-7.50010-7

Stephens, S. L., and Libby, W. J. (2006). Anthropogenic fire and bark thickness in coastal and island pine populations from Alta and Baja California. *J. Biogeogr.* 33, 648–652. doi: 10.1111/j.1365-2699.2005.01387.x

Tapias, R., Climent, J. M., Pardos, J. A., and Gil, L. (2004). Life histories of Mediterranean pines. *Plant Ecol.* 171, 53–68. doi: 10.1023/B:VEGE.0000029383.72609.f0

Tapias, R., Gil, L., Fuentes-Utrilla, P., and Pardos, J. A. (2001). Canopy seed banks in Mediterranean pines of south- eastern Spain: a comparison between *Pinus halepensis* Mill., *P. pinaster* Ait., *P. nigra* Arn. and *P. pinea* L. *J. Ecol.* 89, 629–638. doi: 10.1046/j.1365-2745.2001.00575.x

Ter-Mikaelian, M. T., and Korzukhin, M. D. (1997). Biomass equations for sixty-five North American tree species. *For. Ecol. Manage.* 97, 1–24. doi: 10.1016/S0378-1127(97)00019-4

Tessler, N. (2012). Documentation and analysis of wildfire regimes on Mount Carmel and the Jerusalem hills. *Horizons Geogr.* 7, 184–193.

Tessler, N., Wittenberg, L., Provizor, E., and Greenbaum, N. (2014). The influence of short-interval recurrent forest fires on the abundance of Aleppo pine (*Pinus halepensis* Mill.) on Mount Carmel, Israel. *For. Ecol. Manage.* 324, 109–116. doi: 10.1016/j.foreco.2014.02.014

Trabaud, L., and Valina, J. (1998). "Importance of tree size in *Pinus* halepensis fire survival," in *Fire Management and Landscape Ecology*, ed. L. Trabaud (Farfield: International Association of Wildland Fire), 189–196.

Uhl, C., and Kauffman, J. B. (1990). Deforestation, fire susceptibility, and potential tree responses to fire in the eastern Amazon. *Ecology* 71, 437–449. doi: 10.2307/1940299

van Mantgem, P., and Schwartz, M. (2003). Bark heat resistance of small trees in California mixed conifer forests: testing some model assumptions. *For. Ecol. Manage.* 178, 341–352. doi: 10.1016/S0378-1127(02)00554-6

VanderWeide, B. L., and Hartnett, D. C. (2011). Fire resistance of tree species explains historical gallery forest community composition. *For. Ecol. Manage.* 261, 1530–1538. doi: 10.1016/j.foreco.2011.01.044

Vázquez de la Cueva, A., and Moreno, J. (1998). Patterns of lightning-, and people-caused fires in peninsular Spain. *Int. J. Wildl. Fire* 8, 103–115. doi: 10.1071/WF9980103

Vines, R. G. (1968). Heat transfer through bark, and the resistance of trees to fire. *Aust. J. Bot.* 16, 499–514. doi: 10.1071/BT9680499

Voltas, J., Chambel, M. R., Prada, M. A., and Ferrio, J. P. (2008). Climate-related variability in carbon and oxygen stable isotopes among populations of Aleppo pine grown in common-garden tests. *Trees* 22, 759–769. doi: 10.1007/s00468-008-0236-5

Voltas, J., Lucabaugh, D., Chambel, M. R., and Ferrio, J. P. (2015). Intraspecific variation in the use of water sources by the circum-Mediterranean conifer *Pinus halepensis*. *New Phytol.* 208, 1031–1041. doi: 10.1111/nph.13569

Warton, D. I., Duursma, R. A., Falster, D. S., and Taskinen, S. (2012). smatr 3 – An R package for estimation and inference about allometric lines Methods. *Ecol. Evol.* 3, 257–259.

Warton, D. I., Wright, I. J., Falster, D. S., and Westoby, M. (2006). Bivariate line-fitting methods for allometry. *Biol. Rev. Camb. Philos. Soc.* 81, 259–291. doi: 10.1017/S1464793106007007

Weiner, J. (2004). Allocation, plasticity and allometry in plants. *Perspect. Plant Ecol. Evol. Syst.* 6, 207–215. doi: 10.1078/1433-8319-00083

Wesolowski, A., Adams, M. A., and Pfautsch, S. (2014). Insulation capacity of three bark types of temperate *Eucalyptus* species. *For. Ecol. Mange.* 313, 224–232.

Wright, S. D., and McConnaughay, K. D. M. (2002). Interpreting phenotypic plasticity: the importance of ontogeny. *Plant Species Biol.* 17, 119–131. doi: 10.1046/j.1442-1984.2002.00082.x

Conflict of Interest Statement: The authors declare that the research was conducted in the absence of any commercial or financial relationships that could be construed as a potential conflict of interest.

frontiers in Plant Science

ORIGINAL RESEARCH
published: 24 May 2019
doi: 10.3389/fpls.2019.00658

Ash Dieback and Its Impact in Near-Natural Forest Remnants – A Plant Community-Based Inventory

Alexandra Erfmeier[1,2], Kerstin L. Haldan[1], Lili-M. Beckmann[3], Magdalene Behrens[3], Jonas Rotert[1] and Joachim Schrautzer[3]*

[1] Institute for Ecosystem Research, Geobotany, Kiel University, Kiel, Germany, [2] German Centre for Integrative Biodiversity Research (iDiv) Halle-Jena-Leipzig, Leipzig, Germany, [3] Applied Ecology, Institute for Ecosystem Research, Kiel University, Kiel, Germany

Temperate European forests are currently largely under attack by the infection with *Hymenoscyphus fraxineus*, a fungal pathogen introduced from Asia since at least the early 1990s and causing a major dieback of common ash (*Fraxinus excelsior*) throughout Europe. At present, ash dieback evokes major problems for forestry, in particular in sensitive forest remnants in Northern Germany, where the disease causes serious concerns for ecosystem conservation. This makes ash dieback a focal area of ecological research. In the present study, we quantified the extent of ash dieback in adult and in young ash trees in Northern Schleswig-Holstein, Germany, in relation to community composition and associated biotic and abiotic factors. Data collection was carried out in 37 plots in communities of ash-rich forests and included floristic inventory, rating of adult and young ash individuals and recording of light and soil conditions. Data were analyzed using non-metric multidimensional scaling and general linear mixed effects models. Forest type was the strongest significant predictor for variation in crown defoliation of adult ash trees. Damage was highest in communities of wet alder-ash forests and lowest in ash-rich beech forests. A further significant predictor of adult crown defoliation was individual height of the ash tree with larger trees being less affected than smaller ones. For juveniles, total species richness displayed a significant positive relationship with the proportional abundance of fungal infection, while the mean damage proportion per individual significantly increased with increasing relative light intensity in the understorey. The study clearly shows a strong relationship between forest type and ecosystem vulnerability to ash dieback. In particular, communities belonging to the species-rich wet alder-ash forests were most severely affected by ash disease, thereby deserving special attention among the vulnerable fragmented forest remnants in Schleswig-Holstein. Co-varying factors, however, seem to differ between juvenile and adult trees, hinting at the relative importance of tree performance for the adult trees and abiotic conditions for the juveniles. Accounting for such differences along a larger ecological gradient of ash forest communities will be necessary to more comprehensively understand effects of ash dieback on the ecosystem and needs to be addressed in future research.

Keywords: *Hymenoscyphus fraxineus*, fungal pathogen, *Fraxinus excelsior*, ash rejuvenation, forest community type, ash-rich forests, species richness, ecosystem vulnerability

OPEN ACCESS

Edited by:
Christian Ammer,
University of Göttingen, Germany

Reviewed by:
Gitta Jutta Langer,
Northwest German Forest Research Institute, Germany
Friderike Beyer,
University of Freiburg, Germany

****Correspondence:***
Alexandra Erfmeier
aerfmeier@ecology.uni-kiel.de

Specialty section:
This article was submitted to Functional Plant Ecology, a section of the journal Frontiers in Plant Science

Received: *17 February 2019*
Accepted: *01 May 2019*
Published: *24 May 2019*

Citation:
Erfmeier A, Haldan KL, Beckmann L-M, Behrens M, Rotert J and Schrautzer J (2019) Ash Dieback and Its Impact in Near-Natural Forest Remnants – A Plant Community-Based Inventory. Front. Plant Sci. 10:658. doi: 10.3389/fpls.2019.00658

INTRODUCTION

Due to the globalization of human activities such as world-wide trade of goods, species are translocated across the globe (Mack et al., 2000) and introduced into areas they would otherwise not be able to colonize (Richardson et al., 2000). Some of these species become invasive with the detrimental potential to alter whole ecosystems (Mack et al., 2000; Richardson et al., 2000; Bradley et al., 2010). In the case of fungal pathogens, large-scale infectious diseases can develop even more complex multitrophic interactions and, thus, may affect ecosystem functioning. Such emerging infectious diseases (Jönsson and Thor, 2012) are currently of great concern. At present, the ash dieback is a fungal infection disease, largely affecting common ash (*Fraxinus excelsior* L.) throughout its native range in temperate Europe and causing a severe dieback of this species (Kowalski et al., 2010; Kowalski et al., 2015; Dietrich, 2016). It is expected that a high proportion of ashes will die off and threaten the survival of *F. excelsior* in its natural habitats in the near future (Pautasso et al., 2013). The loss of ashes will evoke major economic and ecological consequences: Common ash produces high-quality timber (Pautasso et al., 2013; Rutjes, 2017) and in European forest ecosystems, the species fulfills ecological functions (Pautasso et al., 2013; Fussi and Konnert, 2014) as it is an important pioneer and gap-filling species (Mitchell et al., 2014; Rutjes, 2017) producing leaf litter that is easily decomposable and enabling rapid nutrient cycling in the forest (Wardle, 1961; Jacob et al., 2010). Ash foliage permits high amounts of light to penetrate the overstorey, creating a favorable light climate for understorey vegetation, thereby influencing diversity of herb and shrub layer community composition (Emborg, 1998; Härdtle et al., 2003).

The ash dieback is caused by infection with *Hymenoscyphus fraxineus* (T. Kowalski) Baral, Queloz, Hosoya (Baral et al., 2014; Kowalski et al., 2015; Lenz and Straßer, 2016), an ascomycete native to East Asia and introduced to Poland in the 1990s (Östbrant et al., 2017). Since then, it has spread all over Europe (Chavez et al., 2015), reaching Northern Germany presumably in 2002, and now being present in a large part of the distribution area of *F. excelsior* (Kowalski et al., 2010, 2015; Dietrich, 2016). The ash dieback threatens not only *F. excelsior* as its host but also much of the biodiversity associated with it. Although it is well known that such extensive diseases diminishing species occurrence can have a strong impact on the ecosystem (Loo, 2009; Jönsson and Thor, 2012), their feedback on the ecosystem has not been studied thoroughly in the past (Loo, 2009).

General knowledge, to date, suggests several factors to be involved in explaining the vulnerability to the disease. On the one hand, the extent of infection damage has been reported to vary with environmental conditions and properties of the infested trees. While generally tree individuals can be affected independent of age and size, and infections may occur in many habitat types, some studies report a variation in the severity of the disease (Kowalski and Holdenrieder, 2008; Pautasso et al., 2013; Lenz and Straßer, 2016). For example, there is evidence that ashes at wet sites may suffer from more severe damage from ash dieback than at moist and base-rich sites (Kenigsvalde et al., 2010; Schumacher, 2011; Lenz and Straßer, 2016). Yet, on the other hand, biotic covariation, as induced either by the performance of the tree species themselves, community characteristics associated with diversity and/or forest management may affect responses of *F. excelsior* individuals to the infection. For example, Bakys et al. (2013) reported a relation to ash stand density, and they found effects of ash dieback to be stronger in dense, unthinned plots compared to managed, thinned plots. In addition, age and size of a tree can be expected to have an influence on the course of an infection. A study in Latvia, e.g., revealed a difference of the extent of ash dieback between age groups, with young stands showing higher rates of decline than older ones (Kenigsvalde et al., 2010). Generally, smaller and less vital trees are presumed to be more susceptible to the disease while old trees die off slower (Skovsgaard et al., 2010; Thomas, 2016).

To date, there is a mosaic of information available on the mechanisms of fungal infection, development of the disease (Thomas, 2016) and also data on mortality rates are reported either in an European-wide census and meta-analysis (Coker et al., 2019) or in forest stand-based observations for single regions, e.g., in Latvia, Sweden or Norway (Kenigsvalde et al., 2010; Bengtsson et al., 2013; Timmermann et al., 2017). However, a thorough analysis of ash dieback extent in the context of a more comprehensive assessment of ecosystem variation in ash-rich forests is ultimately missing.

In Northern Germany, forests, by the majority, occur as postglacially imprinted remnants superimposed by management efforts for centuries, and the proportion of forest cover is largely underrepresented in comparison to other regions in temperate Europe (Häme et al., 2001). Therefore, ecological research in order to capture the extent and the context-dependency of forest susceptibility is highly demanded also for reasons of conservation. Northern Germany, and in particular the federal state of Schleswig-Holstein therein is exceptionally well-suited for such an approach since the region offers site conditions representing almost the whole abiotic gradient of common ash in Central Europe. Moreover, and due to the early occurrence of infestation, the progression of the disease can be studied more profoundly in this region than in more southern parts of Europe.

In the present study, we quantified the extent of ash dieback in adult and in young ash trees at 37 sites located in the northern part of Schleswig-Holstein in order to contribute to filling the research gaps and to test the following hypotheses: (1) Infection damage of adult ash trees differs between different forest types and landscape types, and we expect an increasing infection from dry to wet forest community types, (2) damage patterns of juvenile ashes vary accordingly along the gradient of forest type communities, and (3) a significant proportion of variation in damage patterns can be assigned to covariation with biotic and abiotic variables.

MATERIALS AND METHODS

Study System

Common ash (*F. excelsior* L.) is a deciduous tree species native to Europe and widespread throughout its range. Depending on the site conditions, adult trees can reach a size in height from

10 to 40 m (Jäger and Rothmaler, 2017) with a diameter at breast height of 1.6–1.8 m (Thomas, 2016). Ashes usually grow in mixed stands in deciduous forests covering a considerable range of soil conditions, ranging from (dry-) mesic to wet stands (Wardle, 1961), including mineral to organic soils with subacidic to alkaline ground reactions (Thomas, 2016). Leaves are characterized by having a high nutrient and a low lignin content indicating a high nutrient availability of sites. Thus, ash leaf litter is easily decomposable and nutrients are rapidly being retransferred into forest nutrient cycling (Wardle, 1961; Jacob et al., 2010; Langenbruch et al., 2012). In closed forest stands, *F. excelsior* has a narrow crown that fosters light demanding species in the understorey (Härdtle et al., 2003). While ash seedlings and juveniles are shade-tolerant, they become more light-demanding when reaching 0.5 m in height (Marigo et al., 2000).

Hymenoscyphus fraxineus is an ascomycete native to East Asia (Zhao et al., 2012; Zheng and Zhuang, 2014; Cleary et al., 2016; Thomas, 2016), where it colonizes congeneric *F. mandshurica* Rupr. and *F. chinensis* Roxb. as host species, mostly not causing any harm to the trees (Zhao et al., 2012; Gross and Han, 2015; Gross and Holdenrieder, 2015; Cleary et al., 2016). For Schleswig-Holstein, *H. fraxineus* was first referenced in 2002 and laboratory-confirmed in 2005 (Langer, 2017). The ascomycete forms fruiting bodies on ash leaf litter, releasing ascospores in the summer months (Lenz and Straßer, 2016). The infection process starts with windborne spores infecting ash leaves. The fungus enters a leaf via the rhachis, hyphae grow into the pith of the twigs and branches and later proceed into the lignified areas of the tree.

The first visible symptom of the disease is the brown discoloration of infected leaves (Kowalski and Holdenrieder, 2008; Lenz and Straßer, 2016; Thomas, 2016). In the course of the disease, bark necroses occur (Schumacher et al., 2007; Kowalski and Holdenrieder, 2008; Lenz and Straßer, 2016) as the cambium and external tissues die off (Thomas, 2016). Necroses girdling the trunk interrupt the water flow and finally kill the tree (Kowalski et al., 2010; Lenz and Straßer, 2016; Thomas, 2016). Young ashes are reported to die off faster than old trees (Schumacher, 2011). While juvenile ashes usually die off in the course of months, older trees often show a chronic course of the disease (Kowalski et al., 2010) where trees develop crown dieback and bastard branches leading to a bushy growth (Schumacher et al., 2007; Kowalski and Holdenrieder, 2008; Kowalski et al., 2010).

Study Area

Research was carried out in the northern part of Schleswig-Holstein, Germany (**Figure 1**). In the study area, the mean annual temperature is 8.9°C (1998–2010) and the mean annual precipitation is 823 mm (1981–2010) (DWD, 2017). The landscape in Schleswig-Holstein is largely shaped by its glacial and postglacial formation history: From the East to the West, forests in Schleswig-Holstein occur in the landscape regions of recent moraines ("*Östliches Hügelland*") and ancient moraines ("*Hohe Geest*"), which differ in landscape, soil type, and forest vegetation characteristics (Gripp, 1964). Recent moraines originated in the last (Weichselian) glaciation and are characterized by a hilly landscape form. Postglacial soil development gave rise to luvic Arenosols/orthic Luvisols that can turn into gleyic Luvisols at high levels of soil moisture with a potential natural vegetation of beech (*Fagus sylvatica* L.) forests. The wet extreme of the soil water gradient is represented by Gleysols with alder-ash-riparian forests (*Alnus-Fraxinus* forests) under the influence of ground water (Härdtle et al., 2003).

The ancient moraines were formed during the penultimate (Saale) glaciation. On ancient moraines, Podzols predominate with beech-oak forests (*Fagus-Quercus* forests) (LLUR, 2012). The recent forest landscape in Schleswig-Holstein is largely fragmented and represents a mosaic of ancient forest remnants and reforested, managed stands, usually distributed in small patches. Amounting to 173,412 hectares, forest covers only 11 % of the total area, making Schleswig-Holstein the federal state with least forest area in Germany (Bundesministerium für Ernährung und Landwirtschaft [BMEL], 2016).

Plot Sampling Design

In the present study, sampling addressed forest stands that represent almost the whole moisture gradient of ash on mineral soils from dry to wet conditions, not including alluvial forests and drained sites with organic soils. The following three forest vegetation types were selected to be implemented in the study:

(1) Alder-ash forests (AAF) as part of the alliance Alno-Ulmion, i.e., wet forests with black alder [*Alnus glutinosa* (L.) GÄRTN.] and common ash (*F. excelsior*) growing on gleysols,
(2) Hornbeam-ash forests (HAF) as part of the alliance Alno-Ulmion, i.e., moderately wet forests with black alder and a mixture of several other deciduous trees including the European hornbeam (*Carpinus betulus* L.) growing on stagnosols,
(3) Beech-ash forest (BAF) as part of the alliance Fagion sylvaticae, i.e., moist base-rich forests with European beech (*Fagus sylvatica* L.) and common ash growing on luvisols.

Beech forests with ash admixtures (BAF) represent the driest conditions on soils with a large supply of nutrients and bases, however, with enough moisture as they are poorly drained (Ellenberg and Leuschner, 2010). Species richness in beech-ash forests is usually lower than in the other two forest types addressed in this study. Alder-ash forests (AAF) represent the wettest forest type considered in this study and are characterized by year-round soil wetness and usually good nutrient supply. Upper soil layers are rich in humus, and alder and ash are typically the dominant tree species. Alder-ash forests belong to the most species-rich vegetation types in the Northern German lowlands. Hornbeam-ash forests having a higher soil moisture than beech forests but drier soils than the alder-ash forests represent a transitional forest type – intermediate in site conditions and species richness – characterized by a high base saturation and a narrow C/N-ratio. Here, *F. excelsior* is usually the dominating tree species under natural competitive conditions (Ellenberg and Leuschner, 2010).

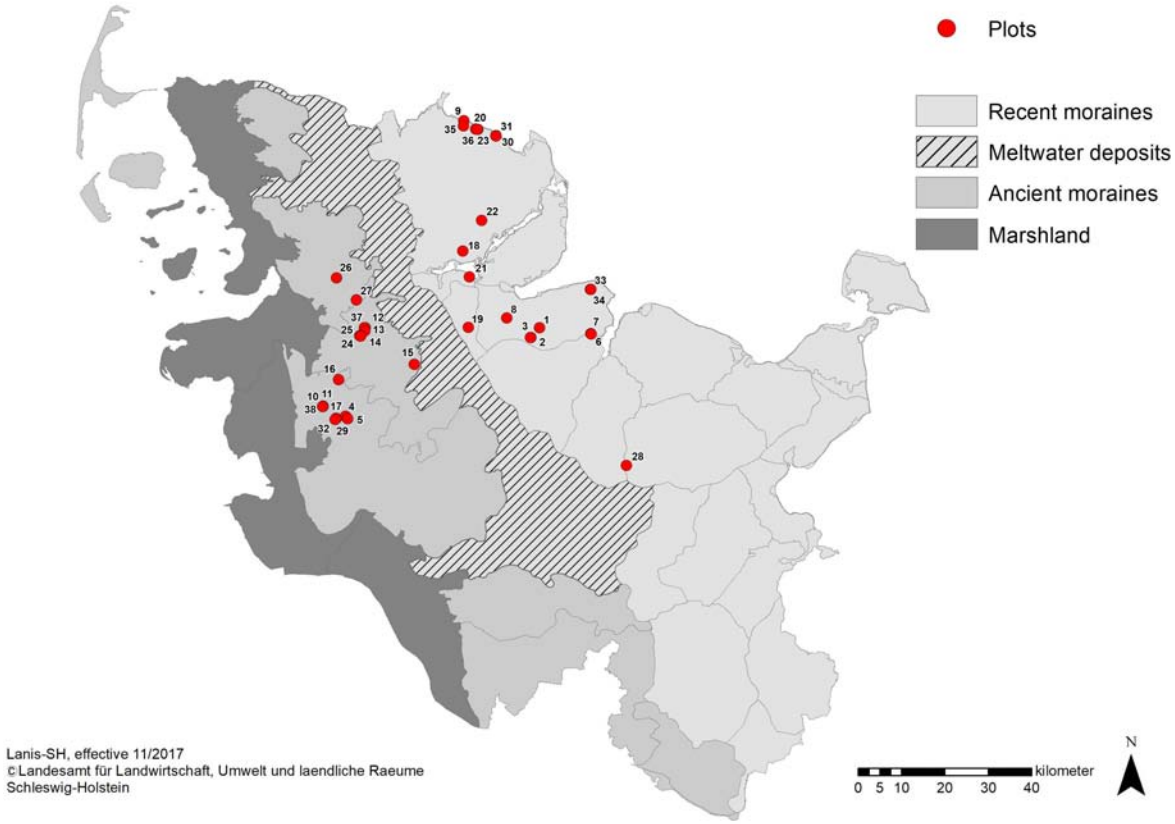

FIGURE 1 | Main landscape regions of Schleswig-Holstein with locations of forest plots. The two investigated landscape types are the ancient moraines in the west (gray) and recent moraines in the east (light gray). Location of forest plots is depicted by red dots.

We applied a stratified and balanced sampling design across the three forest types in order to represent all typical forest community types appropriately in the present study. Between May and August 2017, 37 study plots were established in 23 ash-rich forest areas in Schleswig-Holstein. The plots were randomly selected evenly filling the three forest types each in the two landscape types: the final selection included 18 and 19 plots of the landscape types ancient moraines and recent moraines, respectively (**Figure 1**), and representing at least six plots each in the three forest types ash-alder forests (AAF), hornbeam-ash forests (HAF) and beech forests (BAF, with six plots in ancient moraine landscape and seven plots in recent moraine landscape, respectively).

Data Collection

Each plot had a size of 10 × 10 m and was oriented toward the north. Within each plot, composition and cover of all vascular plant species and mosses were recorded according to the LONDO scale (Londo, 1976). Nomenclature of vascular plants and mosses followed Jäger and Rothmaler (2017) and Frahm and Frey (1992), respectively.

Species inventory was assessed separately by forest strata: Cover of the upper tree layer (i.e., trees higher than 10 m, TL1), lower tree layer (i.e., trees of 4–10 m height, TL2), shrub layer (i.e., woody species of 1–4 m height, SL), herb layer (i.e., herbaceous species up to 1 m height, HL), mosses (excluding lignicole mosses, M).

Proportion of ashes in the upper tree layer was calculated in relation to total tree layer cover.

Rating of *Fraxinus excelsior* Individuals

Effects of ash dieback were quantified on the plot level and on the individual level. Abundance of adult ash trees per plot was counted, adult ashes being defined as ash trees with a diameter at breast height (DBH) of at least 15 cm and a height of at least 4 m. On the individual level, each of five adult ashes per plot were systematically selected for additional rating: the individual closest to each one of the four corner points and the one to the center of the plot were selected, respectively. For each selected individual, basal stem diameter, DBH and total height were recorded. Damage due to the ash dieback was recorded as percentage of crown defoliation and in six damage classes following Lenz et al. (2012). In addition, we quantified wood necroses on ash trunks in three classes. As this variable was highly significantly correlated with leaf damage (Spearman' rho stat: $r = 0.902$, $p < 0.001$, data not shown), necrosis was not further considered in the analyses.

To assess the amount of ash rejuvenation in a plot, all juvenile ashes up to 4 m in height were counted, excluding seedlings with cotyledons only. Damage induced by *H. fraxineus* was assessed for each juvenile ash individual as presence/absence record of infection and quantified as relative damage by individual in percent, later calculating proportion of damaged juveniles by plot.

Environmental Site Conditions

Photosynthetically active radiation (PAR) was measured as photon flux density (PFD, $mmol/m^2s^{-1}$, wavelength 400–700 nm) with the SunScan Canopy Analysis System (Delta T Devices Ltd., Cambridge, United Kingdom). Light measurements were carried out during full foliation of the forest. Plots were subdivided into nine equal subplots and two measurements were carried out above the herb layer at a standardized measuring height of 1.3 m in each of the subplots. Relative light intensity (RLI) was calculated per plot as a mean across all subplots.

Soil samples for determination of pH, CN, and cation exchange capacity (CEC) were taken from a central location in each plot, at a depth of 10 cm. Soil samples were sieved and air dried. PH was measured potentiometrically in a 1:2.5 soil: H_2O and 0.01 molar $CaCl_2$ solution using the pH-meter Lab 860 Sen Tix HW (Schott Instruments). Total carbon and nitrogen were determined on dried (24 h at 105°C) and ground soil samples using the C/N-Analyzer EURO EA 3000 (HEKAtech GmbH, Wegberg, Germany). Since all soil samples are non-calcareous, the measured total C content equals organic carbon (C_{org}).

Extraction of exchangeable cations was performed on 2.5 g of air dried soil with 0.1 molar $BaCl_2$. The concentrations of the exchangeable cations Na^+, K^+, Ca^{2+}, Mg^{2+}, Al^{3+}, Fe^{3+}, and Mn^{2+} were measured using atomic absorption spectrophotometry (AAS), and CEC and base saturation (BS) were calculated.

Statistical Analysis

Floristic composition of all species was analyzed with non-metric multidimensional scaling (NMDS) using Bray-Curtis dissimilarity. Environmental variables were ex post-fitted to the ordination graph. Significance of correlation with NMDS axes was tested with a permutation test (n = 999). NMDS was performed using the vegan package (Oksanen et al., 2018).

The relationship between ash dieback and environmental variables was explored further using linear mixed-effect models (LMM). Before running the models, data were checked for outliers, zero inflation and autocorrelation among predictor variables. In case of significant correlation (significance threshold $r_{Spearman}$ = 0.7) only one of the variables was included in the model. Residual plots of each selected model were examined to ensure random distribution of model residuals.

A first model was run on the plot level incorporating all environmental information that was only available as one sample per plot. In a full model, we tested for effects of landscape type and forest type, and their interaction as fixed factors explaining mean crown defoliation of adult ash trees. In addition, mean diameter at breast height and mean height of adult ashes, the abundance of adult ashes and their proportion in the upper tree layer (TL1), the abundance of juveniles, and total species richness were included as biotic covariates just as soil pH and soil CN as abiotic covariates. Forest area ID was considered a random factor. Prior to analysis, each numerical predictor variable was centered around its mean. Final models were selected by comparing all possible predictor combinations based on Akaike Information Criterion with correction for small sample sizes (AICc; Sugiura, 1978). Models were fitted to the data via maximum likelihood (ML), the final model was fitted using restricted maximum likelihood (REML). Significant differences between factor levels were tested with *post hoc* pairwise *t*-tests.

A second model was run on the individual level testing for effects of environmental variables on loss of leaves of the individual adult ash trees. Again, landscape type, forest type, and their interaction were considered fixed effects. We included height and DBH of individual ash trees as covariates in the model and considered forest area ID and plot ID nested in forest area ID random effects. The model was fitted to the data via REML. Significant differences between factor levels were tested with *post hoc* pairwise Wilcoxon rank sum tests.

In the third approach, fungal infection damage of juvenile ashes was examined on the plot level. We considered fungal infection as mean response on the individual presence/absence level (i.e., damage was assessed as abundance of occurrence at the individual level) and, in addition, as a mean response of the estimated extent of damage on the individual level (i.e., as the mean of percental damage across all juveniles per plot). Mean percental damage of juveniles was log transformed prior to analysis. In the full model, we tested for effects of landscape type and forest type and their interaction as fixed factors. The plot level environmental variables mean crown defoliation of adult ashes, DBH of adult ashes, mean height of adult ashes, abundance of juvenile ashes, abundance of adult ashes, proportion of ashes in upper tree layer, soil C/N, soil pH, mean understorey RLI, and total species richness were included as covariates. Forest area ID was considered a random effect. Before running the model, each numerical predictor variable was centered around its mean. A set of linear mixed effects models with all possible combinations and subsets of fixed effects was created for the two response variables, each. Models were fitted to the data via maximum likelihood (ML) and ranked according to the second-order Akaike Information Criterion (AIC). The models with lowest AIC value were selected and fitted using REML, respectively.

All statistical analysis were performed in R, version 3.4.0 (R Core Team, 2017). All models were fitted using the lme4 package (Bates et al., 2015). Model selection was performed using the MuMin-package (Bartoń, 2018).

RESULTS

Species Composition and Environmental Variables (NMDS)

The NMDS analysis indicates differences in floristic composition among the three forest types alder-ash forest, hornbeam-ash forest and beech-ash forest (**Figure 2** and **Table 1**). The plots are scattered along NMDS axis 1 and 2 according to their

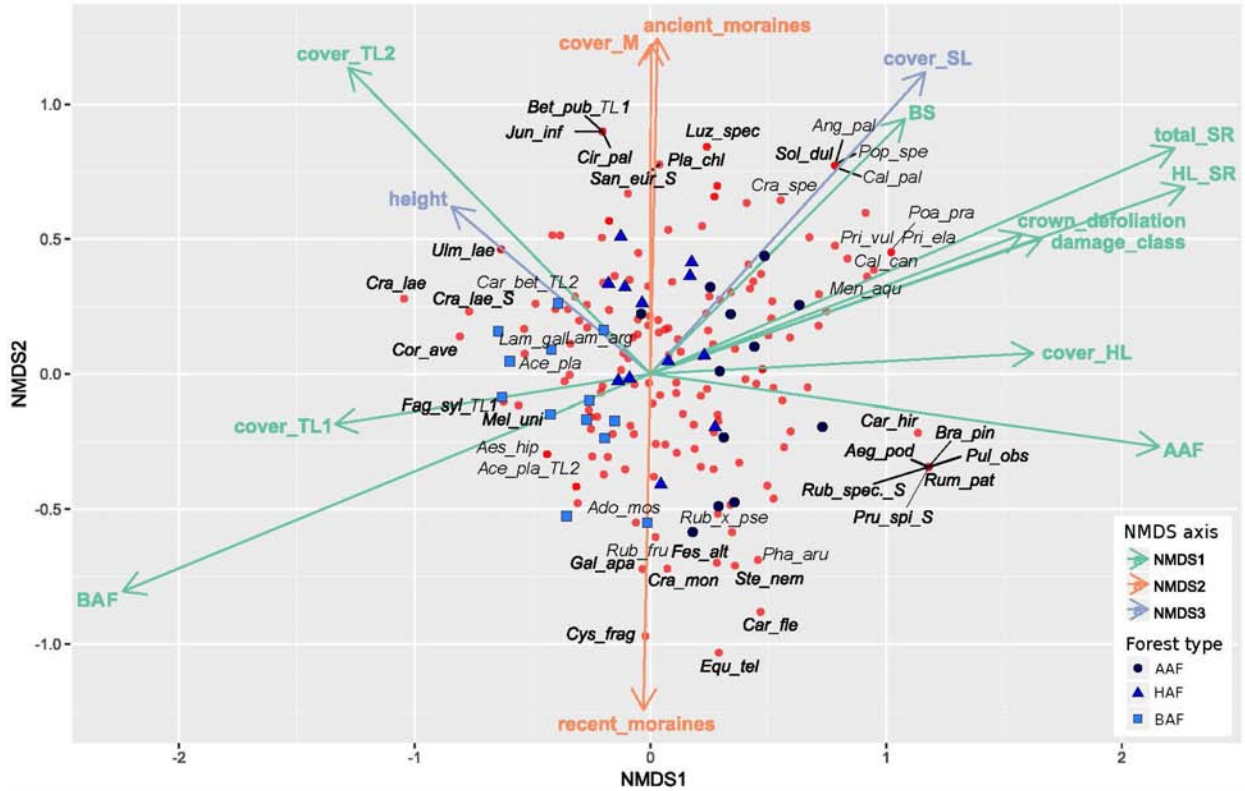

FIGURE 2 | Non-metric multidimensional scaling of cover of all herb layer species in the plots (n = 37), with blue symbols indicating the different forest types: alder-ash forest (AAF, circles), hornbeam-ash forest (HAF, triangles) and beech-ash forest (BAF; squares). Species are represented by red circles. Environmental variables that correlate significantly ($p \leq 0.05$) with one of the axes of the NMDS are shown and colored accordingly (green for correlation with NMDS axis 1, red for correlation with NMDS axis 2, blue for correlation with NMDS axis 3). For a clearer display, only 22% of species are labeled. For abbreviations of predictor variables see **Table 1**. Species names are abbreviated as follows: Ace_pla: *Acer pseudoplatanus* L., Ado_mos: *Adoxa moschatellina* L., Aeg_pod: *Aegopodium podagraria* L., Aes_hip: *Aesculus hippocastanum* L., Ang_pal: *Angelica palustris* (Besser) Hoffm., Bet_pub: *Betula pubescens* Ehrh., Bra_pin: *Brachypodium pinnatum* (L.) P. Beauv., Cal_can: *Calamagrostis canescens* (F. H. Wigg.) Roth, Cal_pal: *Caltha palustris* L., Car_bet: *Carpinus betulus* L., Car_fle: *Cardamine flexuosa* With., Car_hir: *Carex hirta* L., Cir_pal: *Cirsium_palustre* (L.) Scop., Cor_ave: *Corylus avellana* L., Cra_lae: *Crataegus laevigata* (Poir.) DC., Cra_mon: *Crataegus monogyna* Jacq., Cra_spe: *Crataegus spec*., Cys_fra: *Cystopteris fragilis* (L.) Bernh. s. str., Equ_tel: *Equisetum telmateia* Ehrh., Fag_syl: *Fagus sylvatica* L., Fes_alt: *Festuca altissima* All., Gal_apa: *Galium aparine* L., Jun_inf: *Juncus inflexus* L., Lam_arg: *Lamium argentatum* (Smejkal) G. H. Loos (=*Galeobdolon argentatum* Smejkal), Lam_gal: *Lamium galeobdolon* (L.) L. subsp. *galeobdolon* (=*Galeobdolon luteum* Huds.), Luz_spec: *Luzula spec*., Mel_uni: *Melica uniflora* Retz., Men_aqu: *Mentha aquatica* L., Pha_aru: *Phalaris arundinacea* L., Pla_chl: *Platanthera chlorantha* Custer ex Rchb., Poa_pra: *Poa pratensis* L., Pop_spe: *Populus spec.*, Pri_ela: *Primula elatior* (L.) Hill, Pri_vul: *Primula vulgaris* Huds., Pru_spi: *Prunus spinosa* L., Pul_obs: *Pulmonaria obscura* Dumort., Rub_fru: *Rubus fruticosus* agg., Rub_spec.: *Rubus spec*., Rub_×_pse: *Rubus* × *pseudidaeus* (Weihe) Lej., Rum_pat: *Rumex patientia* L., San_eur: *Sanicula europaea* L., Sol_dul: *Solanum dulcamara* L., Ste_nem: *Stellaria nemorum* L. s. str., Ulm_lae: *Ulmus laevis* Pall.

forest type with plots of the beech-ash forest (BAF, squares) displaying significant negative correlation with NMDS axis 1, thereby clustering on the left-hand side of the ordination space, whereas plots of the alder-ash forest (AAF, circles) display a positive correlation with NMDS axis 1 and are located toward the right of the axis (**Figure 2** and **Table 1**). Plots of the hornbeam-ash forest (HAF, triangles) are located in between the two other groups (**Figure 2**).

Post hoc correlation of NMDS scores with biotic and abiotic covariates indicate significant correlations (**Table 1**): NMDS axis 1 was significantly positively correlated with total species richness, herb layer species richness, herb layer cover, mean crown defoliation of adult ashes, and mean damage class of adult ashes. Cover of the upper and lower tree layer was significantly negatively correlated with NMDS axis 1.

Cover of mosses and plots of the landscape type ancient moraines displayed a significant positive correlation with NMDS axis 2, while plots of the landscape type recent moraines were negatively correlated with this axis. In addition, NMDS axis 3 was most strongly positively correlated with height of adult ashes. Abiotic soil variables pH, CN and CEC, by the majority, did not display significant correlations with neither of the first three NMDS axes. Base saturation was the only variable that significantly correlated with NMDS axis 1.

Crown Defoliation of Adult Ash Trees

The first model tested for effects of several biotic and abiotic factors on mean crown defoliation of adult ashes on the plot level. After model selection, the optimal model was run with forest type, landscape type and total species richness, as predictors. Forest

TABLE 1 | Correlation coefficients of environmental variables and of variables describing species diversity and community structure with the first three axes of the NMDS.

	NMDS1	NMDS2	NMDS3	r^2	*P*	SigCode
Alder-ash forest (AAF)	**0.989**	**−0.123**	**−0.085**	**0.529**	**0.001**	***
Hornbeam-ash forest (HAF)	0.138	0.987	−0.083	0.107	0.3	
Beech-ash forest (BAF)	**−0.935**	**−0.336**	**0.112**	**0.637**	**0.001**	***
Ancient moraines	**0.017**	**0.724**	**−0.689**	**0.328**	**0.002**	**
Recent moraines	**−0.017**	**−0.724**	**0.689**	**0.328**	**0.002**	**
Crown defoliation	**0.885**	**0.291**	**−0.363**	**0.353**	**0.002**	**
Damage class	**0.907**	**0.275**	**−0.318**	**0.373**	**0.002**	**
Fungal damage to juveniles	0.808	−0.187	−0.559	0.104	0.321	
Basal diameter	−0.159	−0.196	0.968	0.098	0.315	
Diameter at breast height (DBH)	0.004	−0.192	0.981	0.126	0.197	
Height	**−0.583**	**0.429**	**0.69**	**0.233**	**0.046**	*
Abundance of adult ashes	−0.805	0.569	−0.17	0.199	0.051	.
Total abundance ashes	−0.88	0.322	−0.349	0.136	0.134	
Density of adult ashes	−0.663	0.605	−0.441	0.064	0.494	
Proportion of ashes in tree layer 1 (TL1)	−0.721	0.515	0.464	0.15	0.126	
Abundance of juvenile ashes	−0.881	0.321	−0.348	0.135	0.143	
Cover tree layer 1 (TL1)	**−0.849**	**−0.117**	**0.516**	**0.276**	**0.016**	*
Cover tree layer 2 (TL2)	**−0.748**	**0.662**	**0.048**	**0.327**	**0.009**	**
Cover herb layer (HL)	**0.962**	**0.045**	**−0.268**	**0.316**	**0.004**	**
Cover shrub layer (SL)	**0.578**	**0.555**	**0.598**	**0.452**	**0.001**	***
Cover mosses (M)	**0.001**	**0.73**	**0.684**	**0.312**	**0.001**	***
Total species richness (SR)	**0.935**	**0.352**	**0.052**	**0.629**	**0.001**	***
Herb layer species richness (HL SR)	**0.955**	**0.291**	**0.059**	**0.627**	**0.001**	***
pH	0.663	0.41	0.626	0.166	0.092	.
C/N	−0.848	−0.495	−0.192	0.137	0.141	
Cation exchange capacity (CEC)	0.308	0.214	0.927	0.16	0.095	.
Base saturation (BS)	**0.752**	**0.658**	**0.045**	**0.229**	**0.023**	*
Understorey relative light (RLI)	0.975	0.186	0.125	0.185	0.087	.

*Variables in bold show significant correlations. SigCode, significance code (0 "***" 0.001 "**" 0.01 "*" 0.05 "." 0.1 " " 1). Letters in brackets give abbreviations used in **Figure 2**.*

type was the only variable to display a significant effect on mean crown defoliation (**Table 2**). Crown defoliation was highest in the alder-ash forest, significantly lower in hornbeam-ash forest and significantly lowest in beech-ash forest (**Figure 3**). Total species richness slightly failed to be significant and landscape type did not have any significant effect on mean crown defoliation (**Table 2**).

The second model tested for effects of biotic and abiotic factors on crown defoliation of adult ash trees at the individual level. Again, forest type displayed a highly significant effect on crown defoliation (**Figure 4A** and **Table 3**), Crown defoliation of individual adult ashes was highest in the alder-ash forest, significantly lower in hornbeam-ash forest and significantly lowest in beech-ash forest (**Figure 4A**). In addition, crown defoliation significantly co-varied with the height of the individual ash tree: The model predicted larger trees to exhibit significantly less crown defoliation compared to smaller trees (**Figure 4B**), while diameter at breast height did not show such a significant effect on crown defoliation (**Table 3**).

There was neither an effect of landscape type nor of landscape type × forest type interaction on crown defoliation (**Table 3**).

TABLE 2 | Results of the Analysis of Variance on the optimal linear mixed effects model explaining loss of leaves of adult ash trees on the plot level.

	MS	NumDF	DenDF	*F*	*P*	SigCode
Forest type	**4441.6**	2	27.2	**23.183**	**<0.001**	***
Landscape type	558.1	1	16.75	2.9131	0.106	
Species richness	776	1	24.5	4.0504	0.055	

*Variables in bold show significant correlations. SigCode, significance code (0 "***" 0.001 "**" 0.01 "*" 0.05 "." 0.1 " " 1).*

Damage to Rejuvenation of Ash

The third approach examined the relationship of biotic and abiotic factors with infection damage of juvenile ashes per plot. For mean abundance of fungal infection, total species richness was the only significant predictor for infection damage after model selection (**Table 4**). Infection damage was positively correlated with total species richness, juvenile ashes in plots with a higher species richness were predicted to exhibit higher fungal damage (**Figure 5A**). For mean percental damage of juveniles, model selection suggested only RLI as a significant predictor (**Table 4**). Log infection of juveniles increased significantly with increasing light availability in the understorey (**Figure 5B**).

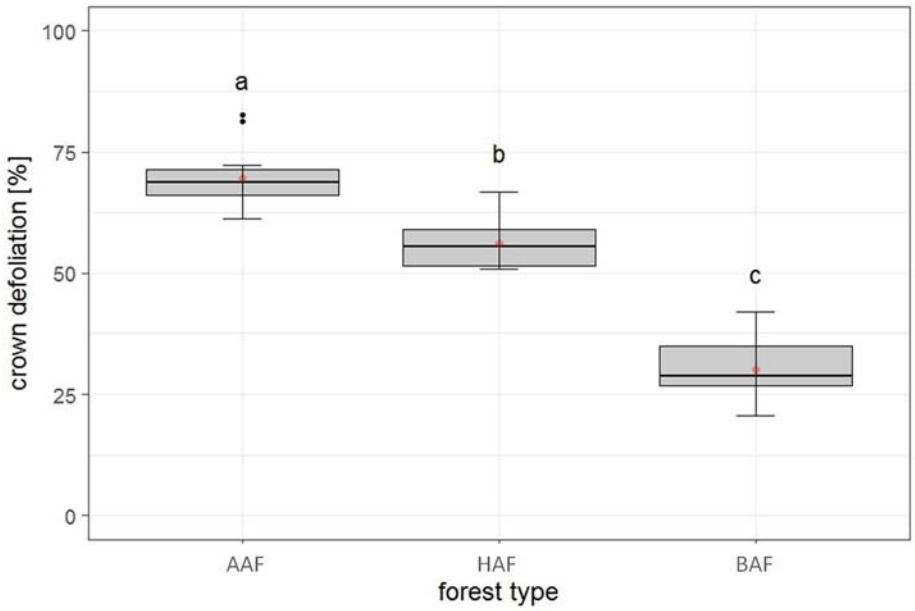

FIGURE 3 | Plot level: Estimates of crown defoliation of adult ashes by forest type AAF, alder-ash forest; HAF, hornbeam-ash forest; BAF, beech-ash forest. Box plots give medians, quartiles, minimum, and maximum per forest type (n = 12 for AAF and HAF, n = 13 for BAF). Different letters indicate significant differences according to *post hoc* test. For statistical details see **Table 2**.

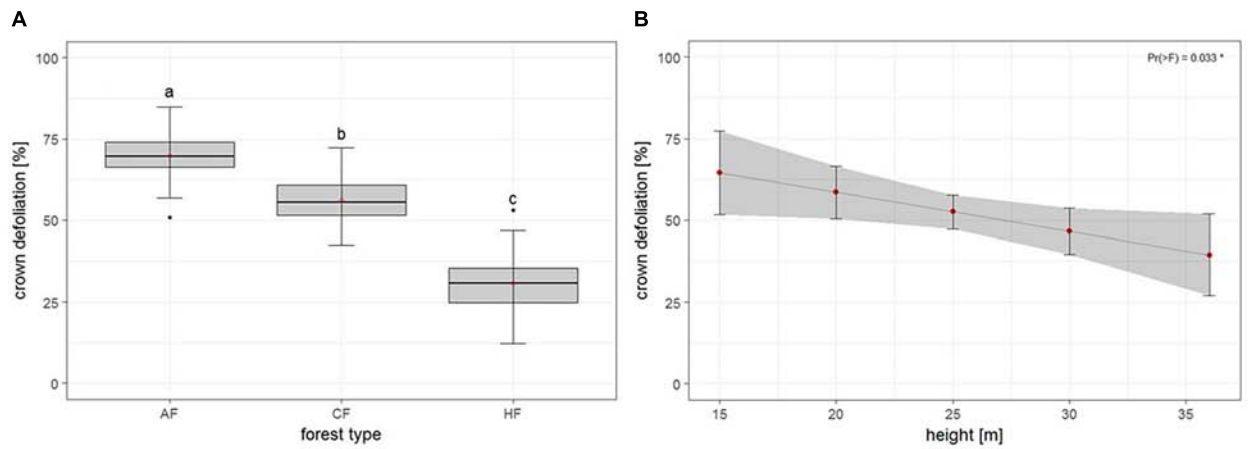

FIGURE 4 | Individual level: Estimates of crown defoliation of adult ashes **(A)** by forest type and **(B)** in relation to tree height. AAF, alder-ash forest; HAF, hornbeam-ash forest; BAF, beech-ash forest. Box plots give medians, quartiles, minimum, and maximum per forest type (n = 12 for AAF and HAF, n = 13 for BAF). Different letters indicate significant differences according to *post hoc* test. For statistical details see **Table 3**.

DISCUSSION

Infection Damage to Ash Individuals

Based on data at the plot level as well as at the individual tree level, forest type was the strongest predictor for crown defoliation thereby confirming the first hypothesis. The models predict damage to be highest in the wet alder-ash forest (AAF), lower in the hornbeam-ash forest (HAF), and least in the beech-ash forest (BAF). This finding was supported by the NMDS as the variables for damage class and crown defoliation are strongly positively correlated with axis 1 and the forest types separate along this axis.

Such floristic gradients as encountered, in principal, may be due to several environmental factors. However, in the present study, strong evidence points toward soil moisture being the major influential factor. The investigated forest types line up perfectly along a soil moisture gradient (Härdtle, 1995). Although soil moisture was not measured directly in the field, the floristic gradient along the first NMDS axis can be interpreted as a gradient of increasing soil moisture: From beech-ash forests (BAF)

TABLE 3 | Results of the Analysis of Variance on the optimal linear mixed effects model explaining loss of leaves of adult ash trees on the individual tree level.

	MS	NumDF	DenDF	*F*	*P*	SigCode
Forest type	**8951.1**	**2**	**30.219**	**15.386**	**<0.001**	***
Landscape type	998.1	1	28.538	1.716	0.201	
Landscape type × forest type	206.6	2	29.836	0.355	0.704	
Height	**2683.8**	**1**	**157.46**	**4.613**	**0.033**	*
Diameter at breast height	143.1	1	148.74	0.246	0.621	

*Variables in bold show significant correlations. SigCode, significance code (0 "***" 0.001 "**" 0.01 "*" 0.05 "." 0.1 " " 1).*

TABLE 4 | Results of the Analysis of Variance on the optimal linear mixed effects model explaining damage to young ashes (a) based on mean abundance of fungal infection of juveniles and (b) based on mean percental damage of juveniles.

Variable	MS	NumDF	DenDF	*F*	*P*	SigCode
(a) *Abundance of fungal infection*						
Species richness	**847.56**	**1**	**34.58**	**6.017**	**0.019**	*
(b) *Percental damage of juveniles*						
RLI	**3.144**	**1**	**35**	**10.698**	**0.002**	**

*Variables in bold show significant correlations. SigCode, significance code (0 "***" 0.001 "**" 0.01 "*" 0.05 "." 0.1 " " 1).*

with characteristic species as *Fagus sylvatica* L., *Melica uniflora* Retz. and *Lamium galeobdolon* (L.) L. on the left side and with wetness indicators as *Mentha aquatica* L. and *Solanum dulcamara* L. more on the right side associated with alder-ash forests (AAF). Several authors stated that, on all sites, ashes may be subject to infection (Kowalski and Holdenrieder, 2008; NW-FVA, 2011; Lenz and Straßer, 2016). In other studies, in contrast, a more severe damage was observed on wet sites, which corresponds well with our present findings (Kenigsvalde et al., 2010; Schumacher, 2011; Vacek et al., 2015; Lenz and Straßer, 2016; Timmermann et al., 2017). There are several scenarios that might apply. Most prominently, this current finding applies because the fungus *H. fraxineus* thrives better in wet microclimatic conditions (Berger et al., 2010) as such conditions promote its spore production (Kirisitis and Cech, 2009; Timmermann et al., 2011, 2017; Thomas, 2016). In addition, one might argue that increasing levels of soil moisture also reflect situations where *F. excelsior* reaches the limits of its fundamental niche, which affects performance of the tree species and thus increases susceptibility to infection. However, in the present study, we included three forest types only; in future studies, it would thus be important to broaden the range of forest community types tested to increase the degree to which these results can be generalized.

While the extent of the infection damage to adult ash trees obviously differed between the three investigated forest types, such a significant trend could not be confirmed for juvenile ashes. The second hypothesis, therefore, has to be rejected. Forest type did not appear to be a significant predictor for infection damage to juvenile ashes. A possible explanation for this result could be that the general higher infection pressure close to the litter layer, compared to higher strata within stands (cf. Chandelier et al., 2014), alleviates the effect of site conditions. As an alternative, one might assume that abiotic covariables might exert a stronger effect on juveniles than on adult trees in explaining infection damage.

Infection Damage and Abiotic Covariates

Several abiotic covariates as chemical soil parameters and understorey light conditions were suspected to potentially influence the extent of ash dieback. Firstly, we expected infection damage of adult ash trees and juvenile ashes to vary between the two landscape types ancient and recent moraines. However, the model predicted no significant differences for the landscape types neither for infection of the adult trees nor for fungal damage of the juveniles. Although there are principal differences between

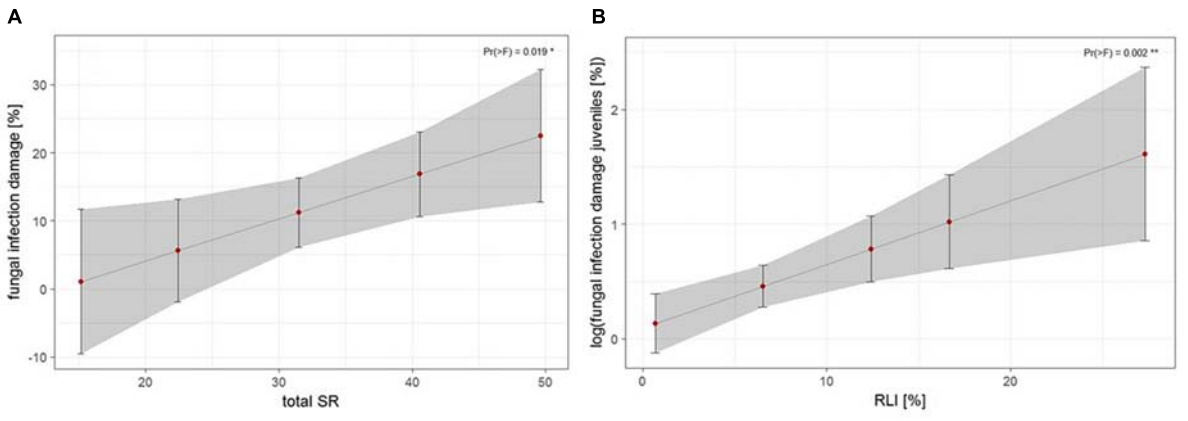

FIGURE 5 | Estimates of fungal infection damage of juvenile ashes on the plot level, **(A)** based on *mean abundance of fungal infection* of juveniles in relation to total species richness (SR) and **(B)** log fungal infection based on *mean percental damage* of juveniles in relation to relative light intensity (RLI). For statistical details see **Table 4**.

the predominant soil types of both landscapes, the subtypes can be ecologically relatively similar at the small scale (Härdtle, 1995). Basically, none of the chemical soil parameters quantified in this study displayed a significant effect for explaining the extent of the disease, thereby indicating that chemical soil parameters may not play a key role in influencing the extent of the disease. This is in line with several studies stating that ashes may become infected on all sites (Kowalski and Holdenrieder, 2008; NW-FVA, 2011; Lenz and Straßer, 2016). On the other hand, there is some evidence that ashes on soils in contact with groundwater (gleysols) may be more severely affected than on drier sites with stagnosols or luvisols (Berger et al., 2010; Kenigsvalde et al., 2010; Schumacher, 2011). Furthermore, these studies report high infection of *F. excelsior* at sites with organic soils. However, alder-ash forests at sites with organic soils were not considered in the present study because these ecosystems do not belong to the natural habitat of common ash and, furthermore, due to low species richness and the lack of endangered species they have not yet played an important role for nature protection (Schrautzer et al., 2007). However, for a more comprehensive ecological understanding of the role of site conditions for the development of the disease, the scope of habitat types should be broadened in future approaches.

In contrast, for juvenile ash individuals, we found a significant relationship between mean percental damage of juvenile individuals and understorey RLI in the final model. Although seedlings of *F. excelsior* can persist in shady conditions, they thrive better when more light is available (Wardle, 1959; Marigo et al., 2000). Apparently, this may coincide with a higher susceptibility at the individual level of juveniles. Admittedly, at this point, we are at the limits of interpretation: the extent as to which this finding is due to a causal relationship or a covarying outcome of forest community composition in the tree layer, needs to be addressed with experimental means in future approaches.

Infection Damage and Biotic Covariates

Measures of size and vitality of ashes were studied on the individual tree level as biotic covariates, and species richness and abundance of ash on the plot level. Analyzing individual adult ash trees, height of the tree was found to be a strong significant predictor of crown defoliation, with larger trees showing less crown defoliation than smaller ones. Height of a tree can be seen as a measure for its age and vitality (Dobbertin, 2005). Our study suggests that older and more vigorous ash trees currently show less symptoms of the disease. Bengtsson et al. (2013) and Timmermann et al. (2017) found a similar relationship between the extent of infection damage and age or vitality of the ash tree in Sweden and in Norway, respectively. An explanation for this phenomenon could simply be that the larger the tree is in size, the longer it takes for the fungus to spread through the tree (Berger et al., 2010). Disease symptoms may appear later in large trees (Thomas, 2016) as the fungus takes more time spreading through a large than through a small tree and additionally more fungal damage is needed to harm a large tree individual. Further studies, accordingly, suggest that ash trees of all ages or sizes are lethally infected by the disease (Pautasso et al., 2013). Nevertheless, to date, the extent of damage is not the same for all ash trees (Lenz and Straßer, 2016) and has been found to differ between age groups (Kenigsvalde et al., 2010; Timmermann et al., 2017). In addition, more attention has to be paid not only to crown symptoms, but also to collar rots associated with the ash dieback (Enderle et al., 2017). However, it has to be considered that, in our study, the forest type with highest rate of infection, the wet alder-ash forest, exhibits also the smallest adult tree individuals. So, while in our data, there is a covariation between forest type and tree size, this might indicate a true interaction effect of both, site condition and growth potential of trees, on pattern of damage. Yet, this cannot be appropriately resolved with the observational data at hand.

Species richness is a non-significant predictor for crown defoliation of adult ashes on the plot level. However, in the NMDS, damage to adult ashes and species richness are significantly positively correlated with NMDS axis 1, and therefore indicate some covariation. Regarding the abundance of fungal damage occurrence on juvenile ashes, species richness is the only significant predictor: The model predicts juvenile ashes to show more fungal damage in more species-rich sites. Previous studies have found that a disease transmitted by pathogens has less severe effects in species-rich compared to species-poor ecological communities (Keesing et al., 2006; Haas et al., 2011). This has been found to apply both to generalist (Haas et al., 2011) and specialist fungal pathogens (Mitchell et al., 2002). Authors commonly mention the "dilution effect" (Keesing et al., 2006) as cause for the observed effect. At a higher level of species diversity, host density is reduced and this reduced host density is the underlying cause for reduced transmission and severity of the disease (Keesing et al., 2006). For the present data, however, it is more probable that species richness co-varies with infection damage on young ashes.

CONCLUSION

In conclusion, the present data suggest a syndrome of factors, among those forest types (in particular those with a high species richness) associated with wet soil conditions, relatively low performance of tree individuals, building a relatively open canopy with thus high light availability in the understorey, to offer a suitable setting for the disease to develop. To identify whether all these factors only act in concert or more exclusively via some of its separate components, needs to be studied within a broader framework, ideally complemented by experimental planting trials, in the future.

DATA AVAILABILITY

The datasets generated for this study are available on request to the corresponding author.

AUTHOR CONTRIBUTIONS

AE and JS conceived the ideas and designed the methodology. KH, L-MB, JR, and MB collected the data. KH and AE analyzed

the data. AE, KH, and JS led the writing of the manuscript. All authors contributed critically to the drafts and gave final approval for the publication.

FUNDING

The study was conducted with institutional funds.

ACKNOWLEDGMENTS

We thank W. Härdtle for providing geographical data and U. Köhn and T. Buck for expert knowledge on suitable forest plot locations in Schleswig-Holstein. We are very grateful to I. Meyer for conducting the chemical soil analysis and her assistance with lab work, T. Martens for providing the distribution map, and M. Germany for support with statistical analysis.

REFERENCES

Bakys, R., Vasaitis, R., and Skovsgaard, J. P. (2013). Patterns and severity of crown dieback in young even-aged stands of European Ash (*Fraxinus excelsior* L.) in relation to stand density, bud flushing phenotype, and season. *Plant Protect. Sci.* 49, 120–126.

Baral, H.-O., Queloz, V., and Hosoya, T. (2014). *Hymenoscyphus fraxineus*, the correct scientific name for the fungus causing ash dieback in Europe. *IMA Fungus* 5, 79–80. doi: 10.5598/imafungus.2014.05.01.09

Bartoń, K. (2018). *MuMIn: Multi-Model Inference package*. Available at: https://cran.r-project.org/web/packages/MuMIn/MuMIn.pdf (accessed February 14, 2019).

Bates, D., Mächler, M., Bolker, B., and Walker, S. (2015). Fitting linear mixed-effects models using lme4. *J. Stat. Soft.* 67, 1–48. doi: 10.18637/jss.v067.i01

Bengtsson, V., Stenström, A., and Finsberg, C. (2013). The impact of ash dieback on veteran and pollarded trees in Sweden. *Q. J. Forest.* 107, 27–33.

Berger, R., Heydeck, P., Baumgart, A., and Roloff, A. (2010). Neue ergebnisse zum eschentriebsterben. *AFZ-Der Wald* 65, 18–21. doi: 10.1111/ddg.13217_g

Bradley, B. A., Blumenthal, D. M., Wilcove, D. S., and Ziska, L. H. (2010). Predicting plant invasions in an era of global change. *Trends Ecol. Evol.* 25, 310–318. doi: 10.1016/j.tree.2009.12.003

Bundesministerium für Ernährung und Landwirtschaft [BMEL] (2016). *Ergebnisse der Bundeswaldinventur 2012*. Frankfurt am Main: Druck- und Verlagshaus Zarbock GmbH & Co. KG.

Chandelier, A., Helson, M., Dvorak, M., and Gischer, F. (2014). Detection and quantification of airborne inoculum of *Hymenoscyphus pseudoalbidus* using real-time PCR assays. *Plant Pathol.* 63, 1296–1305. doi: 10.1111/ppa.12218

Chavez, V., Parnell, S., and Bosch, F. (2015). Designing strategies for epidemic control in a tree nursery: the case of ash dieback in the UK. *Forests* 6, 4135–4145. doi: 10.3390/f6114135

Cleary, M., Nguyen, D., Marčiulynienė, D., Berlin, A., Vasaitis, R., and Stenlid, J. (2016). Friend or foe? Biological and ecological traits of the European ash dieback pathogen *Hymenoscyphus fraxineus* in its native environment. *Sci. Rep.* 6:21895. doi: 10.1038/srep21895

Coker, T. L. R., Rozsypálek, J., Edwards, A., Harwood, T. P., Butfoy, L., and Buggs, R. J. A. (2019). Estimating mortality rates of European ash (*Fraxinus excelsior*) under the ash dieback (*Hymenoscyphus fraxineus*) epidemic. *Plants People Planet* 1, 48–58. doi: 10.1002/ppp3.11

Dietrich, M. (2016). *The Impact of Ash Dieback on Ash Regeneration in the Forest Reserve Dalby Söderskog*. Master's Thesis. Alnarp: Swedish University of Agricultural Sciences.

Dobbertin, M. (2005). Tree growth as indicator of tree vitality and of tree reaction to environmental stress: a review. *Eur. J. Forest Res.* 124, 319–333.

DWD. (2017). *Klimareport Schleswig-Holstein*. Offenbach am Main: Deutscher Wetterdienst.

Ellenberg, H., and Leuschner, C. (2010). *Vegetation Mitteleuropas mit den Alpen*, 6th Edn. Stuttgart: Verlag Eugen Ulmer Stuttgart.

Emborg, J. (1998). Understorey light conditions and regeneration with respect to the structural dynamics of a near-natural temperate deciduous forest in Denmark. *Forest Ecol. Manag.* 106, 83–95.

Enderle, R., Fussi, B., Lenz, H. D., Langer, G., Nagel, R., and Metzler, B. (2017). "Ash dieback in Germany: research on disease development, resistance and management options," in *Dieback of European ash (Fraxinus spp.) - Consequences and Guidelines for Sustainable Management*, eds R. Vasaitis and R. Enderle (Uppsala: Swedish University of Agricultural Sciences), 89–105.

Frahm, J.-P., and Frey, W. (1992). *Moosflora. Mit 108 Abbildungen von J. Döring*. Stuttgart: Verlag Eugen Ulmer.

Fussi, B., and Konnert, M. (2014). Genetic analysis of European common ash (*Fraxinus excelsior* L.) populations affected by ash dieback. *Silvae Genet.* 63, 198–212. doi: 10.1515/sg-2014-0026

Gripp, K. (1964). *Die Erdgeschichte Schleswig-Holsteins*. Kiel: Wachholtz Verlag.

Gross, A., and Han, J. G. (2015). *Hymenoscyphus fraxineus* and two new *Hymenoscyphus species* identified in Korea. *Mycol. Prog.* 14, 1–13. doi: 10.1007/s11557-015-1035-1

Gross, A., and Holdenrieder, O. (2015). Pathogenicity of *Hymenoscyphus fraxineus* and *Hymenoscyphus albidus* towards *Fraxinus mandshurica* var. japonica. *Forest Path.* 45, 172–174.

Haas, S. E., Hooten, M. B., Rizzo, D. M., and Meentemeyer, R. K. (2011). Forest species diversity reduces disease risk in a generalist plant pathogen invasion. *Ecol. Lett.* 14, 1108–1116. doi: 10.1111/j.1461-0248.2011.01679.x

Häme, T., Stenberg, P., Andersson, K., Rauste, Y., Kennedy, P., Folving, S., et al. (2001). AVHRR-based forest proportion map of the Pan-European area. *Remote Sens. Environ.* 77, 76–91.

Härdtle, W. (1995). *Vegetation und Standort der Laubwaldgesellschaften (Querco-Fagetea) im nördlichen Schleswig-Holstein*, Vol. 48. Kiel: Mitteilungen der Arbeitsgemeinschaft Geobotanik in Schleswig-Holstein und Hamburg, 1–441.

Härdtle, W. V., Oheimb, G., and Westphal, C. (2003). The effects of light and soil conditions on the species richness of the ground vegetation of deciduous forests in northern Germany (Schleswig-Holstein). *Forest Ecol. Manag.* 182, 327–338.

Jacob, M., Viedenz, K., Polle, A., and Thomas, F. M. (2010). Leaf litter decomposition in temperate deciduous forest stands with a decreasing fraction of beech (*Fagus sylvatica*). *Oecologia* 164, 1083–1094. doi: 10.1007/s00442-010-1699-9

Jäger, E. J., and Rothmaler, W. (eds) (2017). *Rothmaler - Exkursionsflora von Deutschland. Gefäßpflanzen: Grundband*. Berlin: Springer Spektrum.

Jönsson, M. T., and Thor, G. (2012). Estimating coextinction risks from epidemic tree death: affiliate lichen communities among diseased host tree populations of *Fraxinus excelsior*. *PLoS One* 7:e45701. doi: 10.1371/journal.pone.0045701

Keesing, F., Holt, R. D., and Ostfeld, R. S. (2006). Effects of species diversity on disease risk. *Ecol. Lett.* 9, 485–498. doi: 10.1111/j.1461-0248.2006.00885.x

Kenigsvalde, K., Arhipova, N., Laiviņš, M., and Gaitnieks, T. (2010). Fungus *Chalara fraxinea* as a causal agent for ash decline in Latvia. *Mežzinātne* 21, 110–120.

Kirisitis, T., and Cech, T. L. (2009). Beobachtungen zum sexuellen stadium des eschentriebsterben-erregers *Chalara fraxinea* in österreich. *Forstschutz Aktuell.* 48, 21–25.

Kowalski, T., Bilánski, P., and Holdenrieder, O. (2015). Virulence of *Hymenoscyphus albidus* and *H. fraxineus* on *Fraxinus excelsior* and *F. pennsylvanica*. *PLoS One* 10:e0141592. doi: 10.1371/journal.pone.0141592

Kowalski, T., and Holdenrieder, O. (2008). Eine neue pilzkrankheit an esche in Europa | A new fungal disease of ash in Europe. *Swiss Forest. J.* 159, 45–50. doi: 10.3188/szf.2008.0045

Kowalski, T., Schumacher, J., and Kehr, R. (2010). "Das eschensterben in Europa - symptome, erreger und empfehlungen für die praxis: ash dieback in europe - symptoms, causes and prognosis," in *Jahrbuch der Baumpflege 2010*, ed. D. Dujesiefken (Braunschweig: Haymarket Media), 184–195.

Langenbruch, C., Helfrich, M., and Flessa, H. (2012). Effects of beech (*Fagus sylvatica*), ash (*Fraxinus excelsior*) and lime (*Tilia* spec.) on soil chemical

properties in a mixed deciduous forest. *Plant Soil* 352, 389–403. doi: 10.1007/s11104-011-1004-7

Langer, G. (2017). Collar rots in forests of Northwest Germany affected by ash dieback. *Balt. For.* 23, 4–19.

Lenz, H., and Straßer, L. (2016). *Eschentriebsterben: LWF Merkblatt 28 der Bayerischen Landesanstalt für Wald und Forstwirtschaft*. Available at: www.lwf.bayern.de (accessed April 19, 2017).

Lenz, H. D., Straßer, L., Baumann, M., and Baier, U. (2012). Boniturschlüssel zur einstufung der vitalität von alteschen. *AFZ-Der Wald* 67, 18–19.

Llur. (2012). "Die Böden Schleswig-Holsteins. Entstehung, Verbreitung, Nutzung, Eigenschaften und Gefährdung," in *Landesamt für Landwirtschaft, Umwelt und ländliche Räume des Landes Schleswig-Holstein*. 4th edn. B. Burbaum, M. Filipinski. eds Flintbek: Schriftenreihe LLUR SH - Geologie und Boden.

Londo, G. (1976). The decimal scale for releves of permanent quadrats. *Vegetatio* 33, 61–64.

Loo, J. A. (2009). Ecological impacts of non-indigenous invasive fungi as forest pathogens. *Biol. Invasions* 11, 81–96. doi: 10.1007/s10530-008-9321-3

Mack, R. N., Simberloff, D., Lonsdale, W. M., Evans, H., Clout, M., and Bazzaz, F. A. (2000). Biotic invasions: causes, epidemiology, global consequences, and control. *Ecol. App*. 10, 689–710.

Marigo, G., Peltier, J.-P., Girel, J., and Pautou, G. (2000). Success in the demographic expansion of *Fraxinus excelsior* L. *Trees* 15, 1–13. doi: 10.1007/s004680000061

Mitchell, C. E., Tilman, D., and Groth, J. V. (2002). Effects of grassland plant species diversity, abundance, and composition on foliar fungal disease. *Ecology* 83, 1713–1726.

Mitchell, R. J., Beaton, J. K., Bellamy, P. E., Broome, A., Chetcuti, J., Eaton, S., et al. (2014). Ash dieback in the UK: a review of the ecological and conservation implications and potential management options. *Biol. Conserv.* 175, 95–109. doi: 10.1016/j.biocon.2014.04.019

NW-FVA (2011). *4. Waldschutz-Info 2011: Eschentriebsterben (Info IV)*. Available at: https://www.nw-fva.de/fileadmin/user_upload/Abteilung/Waldschutz/ws-info_04-2011_21-06-2011.pdf (accessed February 14, 2019).

Oksanen, J., Blanchet, F. G., Friendly, M., Kindt, R., Legendre, P., McGlinn, D., et al. (2018). *vegan: Community Ecology Package*. Available at: https://cran.r-project.org/web/packages/vegan/index.html (accessed February 14, 2019).

Östbrant, I.-L., Vasaitis, R., Stenlid, J., Pliura, A., and Menkis, A. (2017). Natura 2000 habitats dominated by ash and elm, invaded by alien invasive fungi on the Gotland Island of Sweden: an overview. *Balt. For.* 23, 264–269.

Pautasso, M., Aas, G., Queloz, V., and Holdenrieder, O. (2013). European ash (*Fraxinus excelsior*) dieback - a conservation biology challenge. *Biol. Conserv.* 158, 37–49.

R Core Team (2017). *R: A language and Environment for Statistical Computing*. Vienna: R Core Team.

Richardson, D. M., Pyšek, P., Rejmánek, M., Barbour, M. G., Panetta, F. D., and West, C. J. (2000). Naturalization and invasion of alien plants: concepts and definitions. *Div. Distrib.* 6, 93–107.

Rutjes, H. (2017). *Die Gesellschaftliche Wahrnehmung des Eschentriebsterbens: Eine Wissenssoziologische Diskursanalyse*. Potsdam: Universitätsverlag Potsdam.

Schrautzer, J., Rinker, A., Jensen, K., Müller, F., Schwartze, P., and Dierssen, K. (2007). "Succession and restoration of drainded fens: perspectives from Northwestern Europe," in *Linking Restoration and Ecological Succesession*, eds L. Walker, J. Walker, and R. Hobbs (New York: Springer), 90–120.

Schumacher, J. (2011). The general situation regarding ash dieback in Germany and investigations concerning the invasion and distribution strategies of *Chalara fraxinea* in woody tissue. *Bull. OEPP* 41, 7–10.

Schumacher, J., Wulf, A., and Leonhard, S. (2007). Erster Nachweis von *Chalara fraxinea* T. *KOWALSKI* sp. nov. in Deutschland - ein Verursacher neuartiger Schäden an Eschen. *J. Cult. Plants* 59, 121–123.

Skovsgaard, J. P., Thomsen, I. M., Skovgaard, I. M., and Martinussen, T. (2010). Associations among symptoms of dieback in even-aged stands of ash (*Fraxinus excelsior* L.). *For. Path.* 40, 7–18.

Sugiura, N. (1978). Further analysts of the data by akaike's information criterion and the finite corrections. *Commun. Stat. A Theor.* 7, 13–26. doi: 10.1080/03610927808827599

Thomas, P. A. (2016). Biological flora of the british isles: *Fraxinus excelsior*. *J. Ecol.* 104, 1158–1209.

Timmermann, V., Nagy, N. E., Hietala, A. M., Børja, I., and Solheim, H. (2017). Progression of ash dieback in Norway related to tree age, disease history and regional aspects. *Balt. For.* 23, 150–158.

Timmermann, V., Nagy, N. E., Hietala, A. M., Kirisits, T., and Soldheim, S. (2011). Ash dieback: pathogen spread and diurnal patters of ascospore dispersal, with special emphasis on Norway. *Bull. OEPP* 41, 14–20.

Vacek, S., Vacek, Z., Bulusek, D., Putalova, T., Sarginci, M., Schwarz, O., et al. (2015). European Ash (*Fraxinus excelsior* L.) dieback: disintegrating forest in the mountain protected areas. *Czech Republic Austrian J. For. Sci.* 4, 203–223.

Wardle, P. (1959). The regeneration of *Fraxinus excelsior* in woods with a field layer of *Mercurialis perennis*. *J. Ecol.* 47, 483–497.

Wardle, P. (1961). Biological flora of the british isles. Fraxinus excelsior L. *J. Ecol.* 49, 739–751.

Zhao, Y.-J., Hosoya, T., Baral, H.-O., Hosaka, K., and Kakishima, M. (2012). *Hymenoscyphus pseudoalbidus*, the correct name for *Lambertella albida* reported from Japan. *Mycotaxon* 122, 25–41. doi: 10.5248/122.25

Zheng, H.-D., and Zhuang, W.-Y. (2014). *Hymenoscyphus albidoides* sp. nov. and *H. pseudoalbidus* from China. *Mycol. Progr.* 13, 625–638. doi: 10.1007/s11557-013-0945-z

Conflict of Interest Statement: The authors declare that the research was conducted in the absence of any commercial or financial relationships that could be construed as a potential conflict of interest.

frontiers in Plant Science

ORIGINAL RESEARCH
published: 28 October 2019
doi: 10.3389/fpls.2019.01327

Harnessing Deep Learning in Ecology: An Example Predicting Bark Beetle Outbreaks

Werner Rammer and Rupert Seidl*

Department of Forest and Soil Sciences, Institute of Silviculture, University of Natural Resources and Life Sciences (BOKU) Vienna, Vienna, Austria

Addressing current global challenges such as biodiversity loss, global change, and increasing demands for ecosystem services requires improved ecological prediction. Recent increases in data availability, process understanding, and computing power are fostering quantitative approaches in ecology. However, flexible methodological frameworks are needed to utilize these developments towards improved ecological prediction. Deep learning is a rapidly evolving branch of machine learning, yet has received only little attention in ecology to date. It refers to the training of deep neural networks (DNNs), i.e. artificial neural networks consisting of many layers and a large number of neurons. We here provide a reproducible example (including code and data) of designing, training, and applying DNNs for ecological prediction. Using bark beetle outbreaks in conifer-dominated forests as an example, we show that DNNs are well able to predict both short-term infestation risk at the local scale and long-term outbreak dynamics at the landscape level. We furthermore highlight that DNNs have better overall performance than more conventional approaches to predicting bark beetle outbreak dynamics. We conclude that DNNs have high potential to form the backbone of a comprehensive disturbance forecasting system. More broadly, we argue for an increased utilization of the predictive power of DNNs for a wide range of ecological problems.

Keywords: deep neural networks, ecological prediction, machine learning, computational ecology, forest disturbance

OPEN ACCESS

Edited by:
Christian Ammer, University of Göttingen, Germany

Reviewed by:
Alexander Zizka, German Center for Integrative Biodiversity Research, Germany
Peter Biber, Technical University of Munich, Germany

****Correspondence:***
Werner Rammer
werner.rammer@boku.ac.at

Specialty section:
This article was submitted to Functional Plant Ecology, a section of the journal Frontiers in Plant Science

Received: *31 January 2019*
Accepted: *24 September 2019*
Published: *28 October 2019*

Citation:
Rammer W and Seidl R (2019) Harnessing Deep Learning in Ecology: An Example Predicting Bark Beetle Outbreaks. Front. Plant Sci. 10:1327. doi: 10.3389/fpls.2019.01327

INTRODUCTION

Ecology is a relatively young discipline, and many of its theoretical foundations are less than a century old (Real and Brown, 1991). In recent decades, ecology has matured considerably as a scientific field, which is *inter alia* reflected by a strong increase in the application of ecological knowledge, data, and methods (e.g., Shea and Chesson, 2002), as well as a recent push towards predictive ecology (Clark et al., 2001; Evans et al., 2012; Dietze et al., 2018). Ecological prediction broadly describes the process of putting ecological knowledge, data, and methods to use for making testable, quantitative estimates about future states of an ecosystem (Luo et al., 2011). The increasing focus on prediction is motivated, amongst other things, by the growing realization that ecology is central to addressing a number of the most pressing challenges faced by humanity in the 21st century, such as to mitigate the impacts of climate change and halt biodiversity loss (Mouquet et al., 2015). Providing essential ecosystem services to society while retaining the earth within its planetary boundaries (Steffen et al., 2015) requires accurate and timely forecasts of ecosystem trajectories. Consequently, policy makers and ecosystem

managers look to scientists for providing the predictions needed to anticipate and manage global change (Clark et al., 2001).

Achieving precise and unbiased ecological predictions is more feasible today than ever before. This is the result of three simultaneous developments: First, the availability of ecological data has increased dramatically. With the advent of big data in ecology the field is in a rapid transition from an era characterized by data limitation, to one that is dominated by a wealth of data (Peters et al., 2014). Contributing to increasing data availability is the proliferation of remote sensing (Kennedy et al., 2014), large international research networks such as NEON and Fluxnet (Ershadi et al., 2014), and the use of citizen science (Jordan et al., 2015). Furthermore, the field has experienced a fundamental change in research culture in recent years, towards making ecological data accessible to the public (Whitlock, 2011). Second, recent methodological advances in the field of ecological modeling, data analysis, and statistics have drastically increased our ability to interface the growing amounts of data with our understanding of ecological systems. Given that we are facing a future characterized by no analog conditions (Williams and Jackson, 2007), such improvements in process understanding are a crucial prerequisite for successful ecological prediction (Evans, 2012). Finally, increasing computational power in general and a growing availability of high performance infrastructure for scientific computing in particular provide the technological backbone supporting both previously outlined trends. All three of these recent developments are important factors behind the recent proliferation of machine learning in ecology.

Machine learning (ML) is a family of computational algorithms that is concerned with identifying structure in complex, often nonlinear data, and generating accurate predictive models based on such data (Olden et al., 2008). Compared to classical statistical approaches such as regression, machine learning focuses on the use of computation to determine and describe complex relationships, and emphasizes predictive power over estimating parameters and confidence intervals (Breiman, 2001; Goodfellow et al., 2016). Situated at the intersection of computer sciences and statistics, and forming the core of artificial intelligence and data science, ML is a rapidly growing field (Jordan and Mitchell, 2015).

Deep learning is a relatively recent development in ML. Its main tool, the deep neural network (DNN), builds upon Artificial Neural Networks (ANNs) which were already conceived in the middle of the last century. Essentially, "deep learning" refers to a set of techniques that allow the training of larger (more neurons) and deeper (more layers) ANNs (Nielsen, 2015). These high capacity networks became possible due to the development of improved algorithms for optimizing connection weights [e.g., stochastic gradient descent (Rumelhart et al., 1986)] and a steep increase in available computing power and training data (Goodfellow et al., 2016). While these improvements may seem only gradual, current DNNs not only outperform their simpler ANN ancestors, but frequently also perform better than other ML approaches in standardized tests of prediction accuracy (e.g., Krizhevsky et al., 2012; Johnson et al., 2016; Szegedy et al., 2016).

In ecology, ML approaches were still rarely used a decade ago (Olden et al., 2008), but have seen a tremendous increase in popularity in recent years (Jordan and Mitchell, 2015). Yet, their potential is far from fully exploited, and deep learning applications in ecology remain scarce to date (see **Supplementary Material S1** for a full literature review). The overall aim of this work is to contribute to a wider recognition of deep learning in ecology (see also Reichstein et al., 2019) by demonstrating its potential for prediction based on an example application for which all necessary data and code are made available for the community. Specifically, we here chose bark beetle outbreaks in conifer-dominated forests as our example.

Bark beetles are important disturbance agents in forests around the world (Raffa et al., 2008). As a result of climate change bark beetle activity is expected to increase in the future (Seidl et al., 2017). The profound change in the structure and function of forests resulting from bark beetle outbreaks can have negative impacts on the provisioning of ecosystems services (such as clean water, timber, and climate regulation) to society (Thom and Seidl, 2016). However, given a timely knowledge of outbreak hotspots managers can contain beetle spread via removing susceptible trees and employing pheromone traps, making prediction of beetle risk a crucial task in forest management (Hlásny et al., 2019). However, these management measures are frequently applied based on ad hoc decisions of managers in the field, rather than on data-driven approaches quantifying bark beetle infestation probability.

Here we show how to predict bark beetle outbreak dynamics based on widely available information sources using deep learning. Specifically, we use a DNN (1) to estimate bark beetle outbreak probabilities based on outbreak patterns from the recent past, and (2) to predict the temporal dynamics of bark beetle outbreak waves.

MATERIALS AND METHODS

Artificial Neural Networks and Deep Learning

The basic structure of an artificial neural network (ANN) and a deep neural network (DNN) is loosely modeled after the way biological nervous systems process information (**Figure 1**). The network consists of interconnected compute units (neurons) that are organized in layers — typically an input layer (with the number of neurons corresponding to the number of input variables), hidden layer(s), and an output layer (where each dependent variable corresponds to a neuron).

The most widely used DNN type is a feedforward neural network (often also called perceptron) (Goodfellow et al., 2016). In such a feedforward network, each neuron is connected to all neurons in adjacent layers, but neurons within a layer are not connected (**Figure 1**). The connection strength between two neurons is given by an adjustable connection weight w. Every neuron calculates a single output value by computing a weighted sum of the inputs and then passing the result through a non-linear function.

An extension of a feedforward network frequently used for pattern recognition in images or time series data is the convolutional neural network (CNN). In addition to fully connected layers a CNN includes multiple stages of so-called filtering and pooling layers (LeCun et al., 2015). Filters are applied

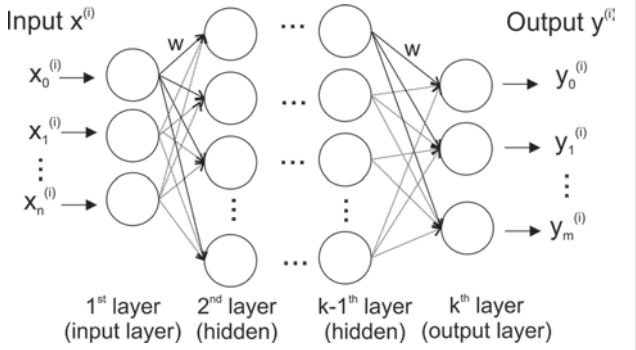

FIGURE 1 | Stylized structure of a deep feedforward neural network. Each of the *k* layers consists of a variable number of fully connected neurons (circles). Thenetwork has as many neurons in the input layer as input variables (*n*), and – for classification – as many output neurons as there are classes in the data (*m*). A neuron is connected to all neurons in the two adjacent layers via a weighted connection (*w*).

locally (e.g., to detect an edge within a subset of pixels), but use the same learned weights for all elements of the data (e.g. all the pixels in an entire image). Subsequent pooling layers merge the filter outputs into more abstract representations that are less sensitive to small shifts and distortions in the data. A series of such filtering and pooling layers is able to extract increasingly abstract patterns in data.

In the training phase of a DNN the connection weights (*w* in **Figure 1**) between neurons are iteratively updated by a training algorithm to minimize the prediction error over the training data set (see **Supplementary Material S2** for more details). In order to gauge the accuracy of predictions for new input data (i.e., data not used during training), the available data is frequently split into a training data set (used for training), and a test data set. The details of the network architecture, such as the size of the network, the selection of specific layer types, and parameters of the training process strongly determine the prediction accuracy of the network and are usually problem specific. More information on deep learning is available in e.g., Angermueller et al. (2016), LeCun et al. (2015) and Nielsen (2015). Moreover, the **Supplementary Material S2** provides a guide for designing and training of DNNs, as well as practical considerations for DNN applications.

A Deep Neural Network to Predict Bark Beetle Outbreaks

The following section presents an application of deep learning in the context of forest ecology, specifically predicting attacks by bark beetles. The example demonstrates the steps required for using DNNs, i.e. data preparation, network design and training, and finally making predictions using the trained DNN. All code and data required for reproducing the example presented here are available online https://github.com/werner-rammer/BBPredNet.

We used a 23-year time series of bark beetle (*Ips typographus* L.) infestation at the Bavarian Forest National Park (Germany), determined from annual aerial surveys at 30 m horizontal resolution over an area of 13,319 ha. The complete data set is available online (Seidl et al., 2015). More information on the dataset as well as statistical analyses of the data are provided by Seidl et al. (2016).

Our goal was to predict the risk of beetle attack for each 30 m cell and year, based on climatic information and the local outbreak pattern in the preceding two years. We used a DNN to predict the probability of bark beetle attack based on the following variables: the potential host cells in the vicinity of the target cell (i.e., grid cells in the local neighborhood (19 × 19 cells) that contain mature trees of the host tree species, Norway spruce (*Picea abies* (L.) Karst.), representing host connectivity in the vicinity of a target cell), the observed cells attacked in the last two years in the vicinity of a cell (representing local bark beetle pressure), average climatic conditions (i.e., the long-term mean annual temperature for the target cell, representing the variable climatic viability for bark beetle development at the landscape scale), and a qualitative classification of the outbreak stage at the regional scale (representing the surrounding forest area of Austria, Czech Republic, and Bavaria) in the previous two years (three classes, "background", "culmination", "gradation", determined by using the 33rd and 66th percentile of the annual timber disturbed as cutoffs), representing a broad classification of population dynamic as frequently used by forest managers). We thus used both time-invariant and temporally variable predictors in our modeling, and deliberately restricted the predictors to information that was previously published (Seidl et al., 2016) and is readily available at large spatial scales for forest managers and national park services.

The full data set comprised of 1.87 million data points for training the DNN. Each training example x_i consisted of the cells in a moving window around the focal cell (window size of 19 × 19), describing the local host tree distribution and the outbreak activity in the preceding two years, as well as the two auxiliary variables mean annual temperature and outbreak stage. Each x_i thus contained 19 x 19 = 361 + 2 = 363 input variables. The size of 19 × 19 cells represents a rectangular area with a distance from the target cell of between 270 and 382 m in each direction, which corresponds to the dispersal distance of >95% of the bark beetles (Kautz et al., 2011). The response variable y_i was the state of the focal cell (disturbed/undisturbed) in the current year.

Experiments

Experiment 1: Predicting Disturbance Probability for Individual Years

In this experiment we were interested in the capability of the DNN to predict infestation probabilities for individual years. This setup resembles an application scenario where one tries to predict future disturbance from the observed disturbance pattern of the recent past. In order to include a wide range of conditions in the test dataset, we randomly selected one year from each of the three outbreak stages (background: 1993, culmination: 1997, and gradation: 2005) as test set, while all the other years were used for training the DNN. The training set for this experiment consisted of 1.58 million data points, and the test set of 292,559 cases (15.7% of all data points).

Experiment 2: Predicting Disturbance Dynamics Over Time

The goal of the second experiment was to test the ability of the DNN to model the temporal disturbance dynamics observed for the Bavarian Forest National Park. We randomly selected 373,817 data points (20%) from the full dataset and set them aside as test set. The remaining 80% were used for training the DNN. This experiment does not reflect forward prediction, but rather aims at scrutinizing the ability of the DNN to capture the pulse dynamics of bark beetle outbreaks.

Model Design and Evaluation

Predicting bark beetle disturbance from infestation maps (see **Figure 2** for examples) can be viewed as a specific case of an image classification problem, where the network is asked to classify the focal cell of an example image either as disturbed or undisturbed. Neural Networks using convolutional layers (CNNs) are frequently applied for image classification (e.g., Krizhevsky et al., 2012; Szegedy et al., 2016), and were thus selected as the network type here. We used the dataset of Experiment 1 (setting aside individual years) for evaluating different network architectures. The hyper-parameters evaluated iteratively were network capacity (number of layers and neurons per layer), applied regularization techniques, as well as the used loss function and optimizer. The training of the individual candidate networks was stopped when the accuracy of the network on the test dataset did not increase further. The thus determined network architecture was also used for Experiment 2 (Abadi et al., 2016). All experiments and predictions were conducted using the TensorFlow framework and run on a desktop PC with an Intel QuadCore CPU (Intel i5-6600) and equipped with an NVidia GTX 1070 GPU.

We evaluated the network performance by calculating a number of different performance measures based on comparing predictions to test set data. The accuracy (defined as the ratio of correct classifications relative to the total number of examples) has only limited value as an evaluation metric here, as the class distribution is very unbalanced (only 3.48% of the data points are classified as disturbed). We therefore also calculated precision, recall, and the F1 Score, as well as Conditional Kappa and the True Skill Statistic (Allouche et al., 2006; Powers, 2011) (**Table 1**). Conditional Kappa and True Skill Statistic range from −1 to +1, where +1 indicates perfect agreement with test data, and values >0 indicate a performance than is better than random

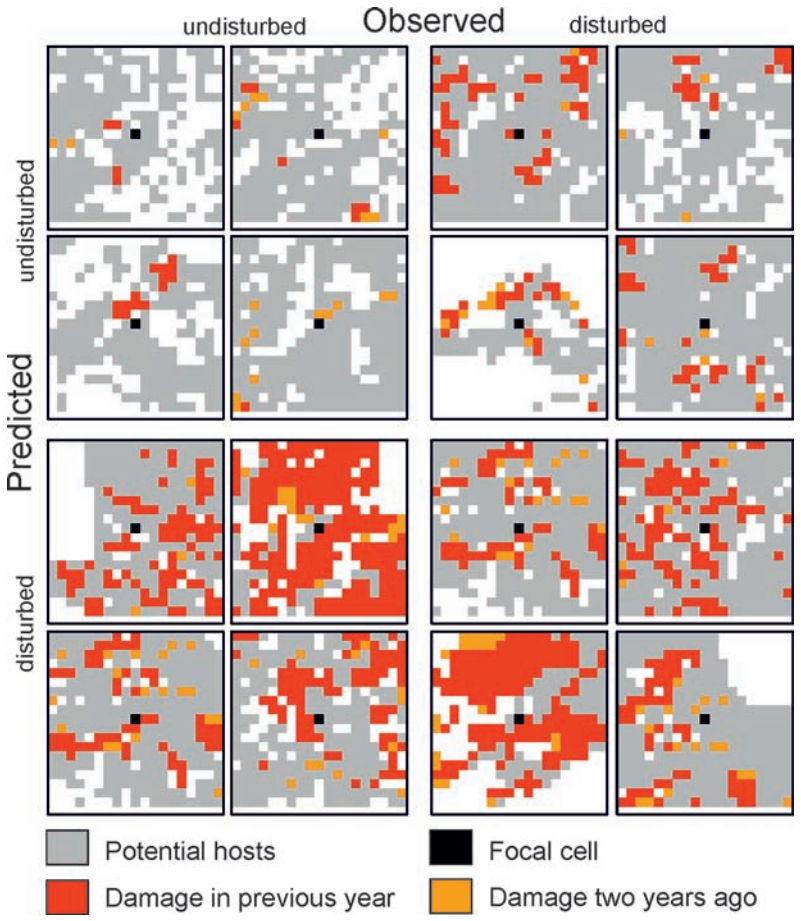

FIGURE 2 | Selected examples for 19 × 19 cell matrices (grain: 30 m) from the test dataset for which the state of the focal cell was predicted correctly (top left and bottom right quartet) and incorrectly (top right and bottom left quartet).

draws. The output of the network was a continuous disturbance probability, which was converted to a binary classification by selecting the threshold probability that yielded the highest F1 score for the training dataset. For Experiment 2 we also calculated Gleichlaeufigkeit (Buras and Wilmking, 2015), which is a measure for the similarity of two time series based on the sign of the difference between two consecutive years. Subsequently, we compared the Gleichlaeufigkeit of the DNN with the value achieved by a statistical model presented for the same system (Seidl et al., 2016).

To better contextualize the performance of the DNN, we repeated Experiments 1 and 2 using other widely used classification algorithms, i.e., distributed random forest, gradient boosting machine, and generalized linear model. We used the H2O platform (H2O.ai, 2017), which provides a set of fast and scalable learning algorithms and is integrated within the R software and environment.

RESULTS

A DNN for Predicting Bark Beetle Outbreaks

We used a convolutional neural network with five convolution layers, followed by five fully connected layers and a final softmax layer (Nielsen, 2015) for classification (for details and terminology see **Supplementary Material S2**). We used categorical cross entropy as cost function, and weight decay (Nielsen, 2015), dropout (Srivastava et al., 2014), and batch normalization (Ioffe and Szegedy, 2015) to improve generalization. **Figure S2** in the **Supplementary Material** shows the schematic structure of the DNN architecture. The presented network efficiently combines image-like pixel data with additional variables that are both numerical (climate variables) and categorical (outbreak stages). We trained the final architecture for 60 epochs, which took approximately one hour on the hardware used, and selected the epoch with the highest test set accuracy for prediction. The GitHub repository (https://github.com/werner-rammer/BBPredNet) contains the full source code for reproducing this example, and includes further details on data preprocessing and the final network architecture.

TABLE 1 | Measures for evaluating the performance of the DNN. *N* = number of examples, *tp, tn, fp; fn*, values of the confusion matrix; *tp, true positive, tn, true negative, fp, false positive, fn, false negative.*

Measure	Equation
Accuracy	$\frac{tn+tp}{N}$
Precision	$\frac{tp}{tp+fp}$
Recall	$\frac{tp}{tp+fn}$
F1 Score	$\frac{2 \cdot precision \cdot recall}{precision + recall}$
Conditional Kappa	$\frac{precision - \frac{tp+fn}{N}}{1-\frac{tp+fn}{N}}$
True Skill Statistic	$precision + \frac{tn}{tn+fn} - 1$
Gleichlaeufigkeit	$G_{ix} = \left\{ \begin{array}{c} x_{i+1} - x_i > 0 : +\frac{1}{2} \\ x_{i+1} - x_i = 0 : 0 \\ x_{i+1} - x_i > 0 : -\frac{1}{2} \end{array} \right\}$
	$G_{xy} = \frac{1}{n-1} \sum_{i=1}^{n-1} abs(G_{ix} + G_{iy})$

Predictions

Experiment 1: Predicting Disturbance Probability for Individual Years

The trained DNN was well able to predict the general disturbance level and spatial pattern observed in the years 1993, 1997, and 2005, i.e. in background, culmination, and gradation stage of the outbreak, respectively (**Figure 3**). The achieved accuracy was 0.966, with a precision of 0.652 and a recall of 0.392 (**Table 2**). The achieved conditional kappa and true skill statistic, which are less sensitive to the uneven class distribution inherent to disturbance data, were 0.637 and 0.626, respectively. **Figure 2** shows selected examples for both successful and unsuccessful classifications taken from within the landscape, illustrating the cell-level stochasticity of bark beetle activity.

Experiment 2: Predicting Disturbance Dynamics Over Time

The achieved accuracy was generally lower in Experiment 2 compared to Experiment 1 (**Table 2**). **Figure 4** shows a comparison of predicted and observed area disturbed over time. While the general pattern of two distinct outbreak waves within the 23-year study period was reproduced well by the DNN, the network had difficulties predicting the initial year of outbreak (early 1990s) and consistently underestimated the area disturbed during the gradation phase of the second outbreak wave (2003–2007). To provide additional context for the assessment of model performance, **Figure S3** in the **Supplementary Material** shows a similar time series comparison for the statistical model developed by Seidl et al. (2016). The Gleichlaeufigkeit of the DNN was with 0.750, which was slightly higher than that of the statistical model (0.727).

Comparison With Other Machine Learning Algorithms

The DNN (**Table 2**) performed better than the other tested alternative algorithms in five of the six cases; only the random forest algorithm outperformed the DNN for Experiment 2 (see **Supplementary Table S1** in the **Supplementary Material** for performance metrics). Generally, the ensemble methods (gradient boosting machine and distributed random forest) were highly proficient in extracting meaningful information from the data. Compared to the ensemble models, the generalized linear model, applying a single linear model (albeit with many predictors) had considerably lower predictive power.

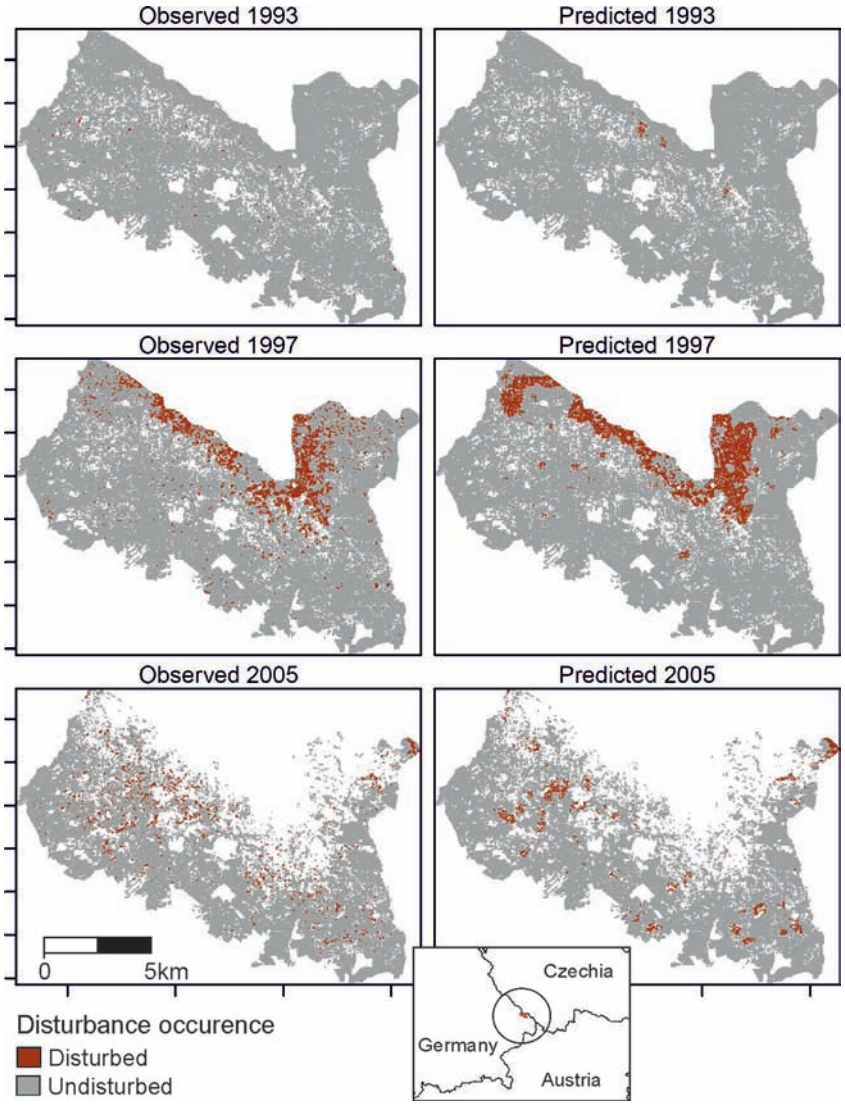

FIGURE 3 | Observed (left) and predicted (right) bark beetle disturbance in the Bavarian Forest National Park for the years 1993 (background stage), 1997 (gradation stage), and 2005 (culmination stage).

TABLE 2 | Performance measures for the two experiments. See **Table 1** for details.

Parameter	Experiment 1 (n = 292,559)	Experiment 2 (n = 373,817)
Accuracy	0.966	0.959
Precision	0.652	0.413
Recall	0.392	0.411
F1 Score	0.490	0.412
Conditional Kappa	0.637	0.392
True Skill Statistic	0.626	0.392

DISCUSSION

Deep learning is a new and powerful machine learning approach to model complex data. It is an approach under active development by a growing research community and is increasingly applied in a wide variety of fields (LeCun et al., 2015; Angermueller et al., 2016). Yet, it remains rarely used in ecology to date, as underscored by our review of the literature (see **Supplementary Material S1**). Specifically, we did not find a single study employing deep learning published in ecological flagship journals such as Ecology, Journal of Ecology, Ecology Letters, BioScience, Ecological Applications, Journal of Applied Ecology, Diversity and Distributions, or Global Ecology and Biogeography. However, deep learning has the potential to become a powerful tool for ecologists (Reichstein et al., 2019), especially as the field moves towards a more quantitative and predictive approach (Clark et al., 2001; Evans et al., 2012).

Deep learning approaches are good at generalizing beyond test data (Goodfellow et al., 2016), an ability that is of high importance in the context of prediction for applied ecological

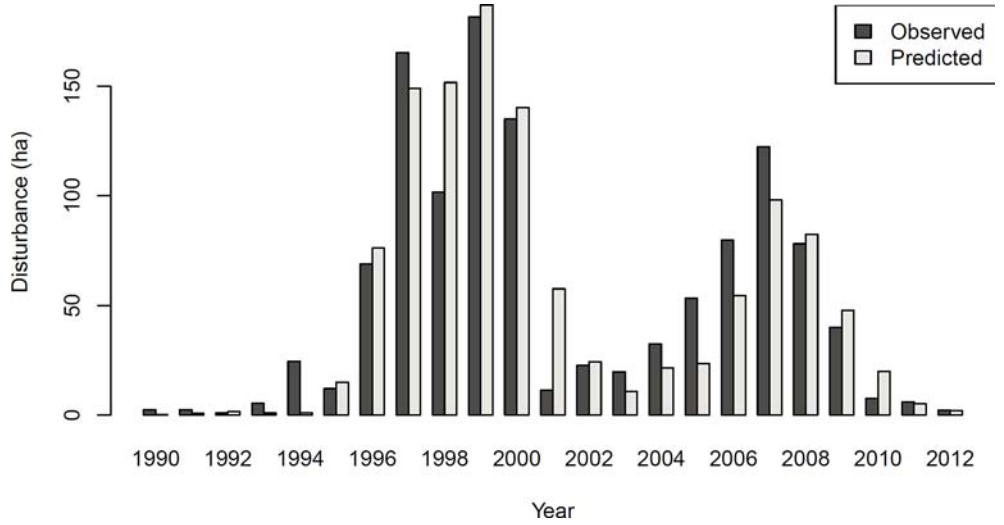

FIGURE 4 | Observed and predicted area disturbed by bark beetles in Experiment 2 (N = 373,817).

problems. A particular strength is the ability to achieve a high level of abstraction in raw data: Zhang et al. (2016), for instance, in a recent review in the context of remote sensing, concluded that DNNs are especially successful in high-level tasks such as object recognition, which are very difficult or even impossible to achieve with classic remote sensing approaches. Furthermore, deep learning may also contribute to more traditional approaches of ecological modelling for prediction, i.e. simulation modeling. For instance, DNNs could be used as powerful multi-dimensional "interpolators" to systematically analyze the growing number of simulation model ensembles (e.g., Warszawski et al., 2014), or build highly efficient meta-models of complex and computationally expensive existing simulation models (Marçais and de Dreuzy, 2017; Rammer and Seidl, 2019). Another promising approach is the hybridization of deep learning with process based models (Reichstein et al., 2019), e.g., by integrating deep learning-based sub models into a process based modeling framework, in order to advance ecological understanding.

A frequently stated reservation about applying ML in general and DNNs in particular relates to their black box character — the trained model and its weights cannot be interpreted in an intuitive way. Consequently, more traditional data models will remain an important means of inference, particularly for improving our understanding of relationships between drivers and responses in nature. It has to be noted, however, that such classical approaches make a priori assumptions on the underlying data model, which does not necessarily reflect the true relationships between driver variables and the response variable (Breiman, 2001). While conventional data models lead to more interpretable results and offer a more stringent framework for hypothesis testing, they are often characterized by a less accurate representation of reality. ML deduces relationships without making a priori assumptions about them, and is often better able to accurately describe the relationship between drivers and responses (Goodfellow et al., 2016). DNNs work particularly well with ecological data because of their ability to efficiently combine different types of data (e.g., image-like pixel data, numeric and categorical variables). In addition, their hierarchical multi-layer structure reflects the fact that ecosystems are frequently governed by a variety of processes along a nested hierarchy of scales (Raffa et al., 2008; Allen et al., 2014). We here found that DNNs outperformed all other approaches to modeling bark beetle outbreak dynamics (with the exception of another powerful ML algorithm, namely random forest).

Bark beetle outbreaks have increased considerably in many parts of the globe, and are expected to increase further under climate change (Seidl et al., 2017). Consequently, bark beetle outbreaks are a key concern for forest managers aiming to continuously supply ecosystem services to society (Hlásny et al., 2019). Precise and timely information about the probability of new bark beetle infestations would be a key asset for managing outbreaks, as it would allow a targeted application of containment measures such as sanitation logging and the deployment of pheromone traps. Here we show that DNNs have high predictive potential in the context of applied ecological issues such as bark beetle outbreaks. It has to be noted that we here deliberately excluded weather data from the vector of predictors, as such data are usually not readily available for managers. We rather focused on variables that are easily quantifiable in the field, such as infestations in the last two years, showing that already a small number of (spatially explicit) predictors can result in high predictive power when using DNNs. Future work could combine this approach with near-real time bark beetle risk mapping based on phenological models (e.g., Baier et al., 2007; Matthews et al., 2018) in order to account for weather-driven bark beetle development trajectories. Furthermore, the growing availability of remotely sensed information on past insect disturbances (Senf et al., 2017) could be integrated into future predictions of bark beetle dynamics. DNNs provide an ideal platform for such a comprehensive bark beetle forecasting system, as they are well suited to synthesize information from a wide variety of data sources (Goodfellow et al., 2016).

Deep learning is a rapidly evolving field, and DNNs have high potential beyond their application in predictive ecology. DNNs are, for instance, promising approaches for unsupervised learning (Sutskever et al., 2015), i.e. finding previously not identified patterns in data. This is particularly important in the context of the advent of big data in ecology, as the majority of big data is unlabeled. Consequently, unsupervised learning approaches in which DNNs are used to find patterns in data are expected to gain importance in the future (LeCun et al., 2015). More generally, it has been suggested that ML approaches can be applied in all stages of the scientific process, from observation to hypothesis creation and testing, to model building and prediction (Mjolsness et al., 2001). A deeper integration of ML in ecology could thus result in advances that go considerably beyond improved predictions (Peters et al., 2014). An increasing adoption of ML – and especially deep learning – can be found throughout science, technology and commerce, fueling the rapid development of methods, software, and even specialized hardware (Jordan and Mitchell, 2015). Given the substantial capacity of deep learning for ecological prediction, we maintain that adding deep learning to our arsenal of ecological methods could provide a substantial boost for quantitative ecology.

AUTHOR CONTRIBUTIONS

WR and RS jointly designed and wrote the paper. WR performed the neural network analysis.

SUPPLEMENTARY MATERIAL

The Supplementary Material for this article can be found online at: https://www.frontiersin.org/articles/10.3389/fpls.2019.01327/full#supplementary-material

REFERENCES

Abadi, M., Agarwal, A., Barham, P., Brevdo, E., Chen, Z., Citro, C., et al. (2016). TensorFlow: large-scale machine learning on heterogeneous distributed systems. 1, 19.

Allen, C. R., Angeler, D. G., Garmestani, A. S., Gunderson, L. H., and Holling, C. S. (2014). Panarchy: theory and application. *Ecosystems* 17, 578–589. doi: 10.1007/s10021-013-9744-2

Allouche, O., Tsoar, A., and Kadmon, R. (2006). Assessing the accuracy of species distribution models: prevalence, kappa and the true skill statistic (TSS). *J. Appl. Ecol.* 43, 1223–1232. doi: 10.1111/j.1365-2664.2006.01214.x

Angermueller, C., Pärnamaa, T., Parts, L., Stegle, O., and Oliver, S. (2016). Deep learning for computational biology. *Mol. Syst. Biol.* 12, 878. doi: 10.15252/msb.20156651

Baier, P., Pennerstorfer, J., and Schopf, A. (2007). PHENIPS—A comprehensive phenology model of Ips typographus (L.) (Col., Scolytinae) as a tool for hazard rating of bark beetle infestation. *For. Ecol. Manage.* 249, 171–186. doi: 10.1016/j.foreco.2007.05.020

Breiman, L. (2001). Statistical modeling: the two cultures. *Stat. Sci.* 16, 199–231. doi: 10.1214/ss/1009213726

Buras, A., and Wilmking, M. (2015). Correcting the calculation of Gleichläufigkeit. *Dendrochronologia* 34, 29–30. doi: 10.1016/j.dendro.2015.03.003

Clark, J. S., Carpenter, S. R., Barber, M., Collins, S., Dobson, A., Foley, J. A., et al. (2001). Ecological forecasts: an emerging imperative. *Science* (80-.). doi: 10.1126/science.293.5530.657

Dietze, M. C., Fox, A., Beck-Johnson, L. M., Betancourt, J. L., Hooten, M. B., Jarnevich, C. S., et al. (2018). Iterative near-term ecological forecasting: needs, opportunities, and challenges. *Proc. Natl. Acad. Sci.* 115, 1424–1432. doi: 10.1073/pnas.1710231115

Ershadi, A., McCabe, M. F., Evans, J. P., Chaney, N. W., and Wood, E. F. (2014). Multi-site evaluation of terrestrial evaporation models using FLUXNET data. *Agric. For. Meteorol.* 187, 46–61. doi: 10.1016/j.agrformet.2013.11.008

Evans, M. R. (2012). Modelling ecological systems in a changing world. *Philos. Trans. R. Soc. B Biol. Sci.* 367, 181–190. doi: 10.1098/rstb.2011.0172

Evans, M. R., Norris, K. J., and Benton, T. G. (2012). Predictive ecology: systems approaches. *Philos. Trans. R. Soc. Lond. B. Biol. Sci.* 367, 163–169. doi: 10.1098/rstb.2011.0191

Goodfellow, I., Bengio, Y., and Courville, A., (2016). *Deep Learning*. MIT Press.

H2O.ai, *H2O: Scalable Machine Learning*, 2017.

Hlásny, T., Krokene, P., Liebhold, A., Montagné-huck, C., Müller, J., Qin, H., et al. (2019). *Living with bark beetles: impacts, outlook and management options, From Science to Policy*. European Forest Institute.

Ioffe, S. and Szegedy, C. (2015). Batch Normalization: accelerating deep network training by reducing internal covariate shift. arXiv1502.03167, 1–11. doi: 10.1007/s13398-014-0173-7.2

Johnson, M., Schuster, M., Le, Q. V., Krikun, M., Wu, Y., Chen, Z., et al. (2016). Google's Multilingual Neural Machine Translation System: Enabling Zero-Shot Translation 1–16.

Jordan, M. I., and Mitchell, T. M. (2015). Machine learning: trends, perspectives, and prospects. *Science (80-.)*. doi: 10.1126/science.aaa8415

Jordan, R., Crall, A., Gray, S., Phillips, T., and Mellor, D. (2015). Citizen science as a distinct field of inquiry. *Bioscience*. doi: 10.1093/biosci/biu217

Kautz, M., Dworschak, K., Gruppe, A., and Schopf, R. (2011). Quantifying spatio-temporal dispersion of bark beetle infestations in epidemic and non-epidemic conditions. *For. Ecol. Manage.* 262, 598–608. doi: 10.1016/j.foreco.2011.04.023

Kennedy, R. E., Andréfouët, S., Cohen, W. B., Gómez, C., Griffiths, P., Hais, M., et al. (2014). Bringing an ecological view of change to Landsat-based remote sensing. *Front. Ecol. Environ.* 12, 339–346. doi: 10.1890/130066

Krizhevsky, A., Sutskever, I., and Hinton, G. E. (2012). ImageNet Classification with Deep Convolutional Neural Networks. *Adv. Neural Inf. Process. Syst.*, 1–9. doi: 10.1016/j.protcy.2014.09.007

LeCun, Y., Bengio, Y., and Hinton, G. (2015). Deep learning. *Nature* 521, 436–444. doi: 10.1038/nature14539

Luo, Y., Ogle, K., Tucker, C., Fei, S., Gao, C., LaDeau, S., et al. (2011). Ecological forecasting and data assimilation in a data-rich era. *Ecol. Appl.* 21, 1429–1442. doi: 10.1890/09-1275.1

Marçais, J., and de Dreuzy, J.-R. (2017). Prospective Interest of Deep Learning for Hydrological Inference. *Groundwater* 55, 688–692. doi: 10.1111/gwat.12557

Matthews, B., Netherer, S., Katzensteiner, K., Pennerstorfer, J., Blackwell, E., Henschke, P., et al. (2018). Transpiration deficits increase host susceptibility to bark beetle attack: experimental observations and practical outcomes for Ips typographus hazard assessment. *Agric. For. Meteorol.* 263, 69–89. doi: 10.1016/j.agrformet.2018.08.004

Mjolsness, E., DeCoste, D., Mjolsness, E., DeCoste, D., Mjolsness, E., and DeCoste, D. (2001). Machine Learning for Science : state of the art and future prospects. *Science* (80-). doi: 10.1126/science.293.5537.2051

Mouquet, N., Lagadeuc, Y., Devictor, V., Doyen, L., Duputié, A., Eveillard, D., et al. (2015). Predictive ecology in a changing world. *J. Appl. Ecol.* 52, 1293–1310. doi: 10.1111/1365-2664.12482

Nielsen, M. A. (2015). *Neural Networks and Deep Learning*. Determination Press.

Olden, J. D., Lawler, J. J., and Poff, N. L. (2008). Machine learning methods without tears: a primer for ecologists. *Q. Rev. Biol.* 83, 171–193. doi: 10.1086/587826

Peters, D. P. C., Havstad, K. M., Cushing, J., Tweedie, C., Fuentes, O., and Villanueva-Rosales, N. (2014). Harnessing the power of big data: infusing the scientific method with machine learning to transform ecology. *Ecosphere* 5, 1–15. doi: 10.1890/ES13-00359.1

Powers, D. M. W. (2011). Evaluation: from precision, recall and F-measure to ROC, informedness, markedness & correlation. *J. Mach. Learn. Technol.* 2, 37–63. doi: 10.9735/2229-3981

Raffa, K. F., Aukema, B. H., Bentz, B. J., Carroll, A. L., Hicke, J. A., Turner, M. G., et al. (2008). Cross-scale Drivers of Natural Disturbances Prone to Anthropogenic Amplification: the dynamics of bark beetle eruptions. *Bioscience* 58, 501–517. doi: 10.1641/B580607

Rammer, W., and Seidl, R. (2019). A scalable model of vegetation transitions using deep neural networks. *Methods Ecol. Evol.* 2019, 1–12. doi: 10.1111/2041-210X.13171

Real, L. E., and Brown, J. H., (1991). *Foundations of ecology: classic papers with commentaries*. Ecological Society of America, Chicago: University of Chicago Press.

Reichstein, M., Camps-Valls, G., Stevens, B., Jung, M., Denzler, J., Carvalhais, N., et al. (2019). Deep learning and process understanding for data-driven Earth system science. *Nature* 566, 195–204. doi: 10.1038/s41586-019-0912-1

Rumelhart, D. E., Hinton, G. E., and Williams, R. J. (1986). Learning representations by back-propagating errors. *Nature* 323, 533–536. doi: 10.1038/323533a0

Seidl, R., Müller, J., Hothorn, T., Bässler, C., Heurich, M., and Kautz, M. (2016). Small beetle, large-scale drivers: how regional and landscape factors affect outbreaks of the European spruce bark beetle. *J. Appl. Ecol.* 53, 530–540. doi: 10.1111/1365-2664.12540

Seidl, R., Müller, J., Hothorn, T., Bässler, C., Heurich, M., and Kautz, M. (2015). Data from: small beetle, large-scale drivers: how regional and landscape factors affect outbreaks of the European spruce bark beetle. *J. Appl. Ecol.* doi: 10.5061/dryad.c5g9s

Seidl, R., Thom, D., Kautz, M., Martin-benito, D., Peltoniemi, M., Vacchiano, G., et al. (2017). Forest disturbances under climate change. *Nat. Publ. Gr.* 7, 395–402. doi: 10.1038/nclimate3303

Senf, C., Seidl, R., and Hostert, P. (2017). Remote sensing of forest insect disturbances: current state and future directions. *Int. J. Appl. Earth Obs. Geoinf.* 60, 49–60. doi: 10.1016/j.jag.2017.04.004

Shea, K., and Chesson, P. (2002). Community ecology theory as a framework for biological invasions. *Trends Ecol. Evol.* 17, 170–176. doi: 10.1016/s0169-5347(02)02495-3

Srivastava, N., Hinton, G., Krizhevsky, A., Sutskever, I., and Salakhutdinov, R. (2014). Dropout: a simple way to prevent neural networks from overfitting. *J Mach. Learn Res.* 15, 1929–1958. doi: 10.1214/12-AOS1000

Steffen, W., Richardson, K., Rockstrom, J., Cornell, S. E., Fetzer, I., Bennett, E. M., et al. (2015). Planetary boundaries: guiding human development on a changing planet. *Science (80-)*. doi: 10.1126/science.1259855

Sutskever, I., Jozefowicz, R., Gregor, K., Rezende, D., Lillicrap, T., and Vinyals, O. (2015). Towards Principled Unsupervised Learning. *arXiv* 1–9.

Szegedy, C., Ioffe, S., Vanhoucke, V., and Alemi, A. (2016). Inception-v4, Inception-ResNet and the Impact of Residual Connections on Learning. *Arxiv* 12.

Thom, D., and Seidl, R. (2016). Natural disturbance impacts on ecosystem services and biodiversity in temperate and boreal forests. *Biol. Rev.* 91, 760–781. doi: 10.1111/brv.12193

Warszawski, L., Frieler, K., Huber, V., Piontek, F., Serdeczny, O., and Schewe, J. (2014). The Inter-Sectoral Impact Model Intercomparison Project (ISI–MIP): project framework. *Proc. Natl. Acad. Sci.* 111, 3228–3232. doi: 10.1073/pnas.1312330110

Whitlock, M. C. (2011). Data archiving in ecology and evolution: best practices. *Trends Ecol. Evol.* 26, 61–65. doi: 10.1016/j.tree.2010.11.006

Williams, J. W., and Jackson, S. T. (2007). Novel climates, no-analog communities, and ecological surprises. *Front. Ecol. Environ.* 5, 475–482. doi: 10.1890/070037

Zhang, L., Xia, G.-S., Wu, T., Lin, L., and Tai, X. C. (2016). Deep Learning for Remote Sensing Image Understanding. *J. Sensors* 2016, 1–2. doi: 10.1155/2016/7954154

Conflict of Interest: The authors declare that the research was conducted in the absence of any commercial or financial relationships that could be construed as a potential conflict of interest.

frontiers in Plant Science

ORIGINAL RESEARCH
published: 30 July 2019
doi: 10.3389/fpls.2019.00947

Functional Traits of *Pinus ponderosa* Coarse Roots in Response to Slope Conditions

R. Kasten Dumroese[1], Mattia Terzaghi[2], Donato Chiatante[2], Gabriella S. Scippa[3], Bruno Lasserre[3] and Antonio Montagnoli[2]*

[1]*Rocky Mountain Research Station, Forest Service, U.S. Department of Agriculture, Moscow, ID, United States,* [2]*Department of Biotechnology and Life Science, University of Insubria, Varese, Italy,* [3]*Department of Biosciences and Territory, University of Molise, Pesche, Italy*

We excavated the root systems of *Pinus ponderosa* trees growing on a steeply sloped, volcanic ash-influenced soil in the northern Rocky Mountains of the United States to assess their functional coarse-root traits and root system architecture. Trees, outplanted as one-year-old seedlings from a container nursery, were in their 32nd growing season on the site. We found that the trees had deployed more roots, in terms of length and volume, in the downslope and windward quadrants than in their upslope and leeward quadrants, likely a response to mechanical forces toward improving stability. Moreover, we observed the development of three types of root cages (tight, enlarged, and diffused) that likely reflect micro-site characteristics. As the cage type transitioned from tight to enlarged to diffused we measured a decrease in the overall volume of the roots associated with the cage and the taproot becoming a more prominent contributor to the overall volume of the cage. Finally, we noted the development of specialty roots, namely those with I-beam and T-beam shapes in cross section, in the downslope quadrant; these types of roots are known to better counteract compression mechanical forces. These observations improve our understanding of root plasticity and tree rooting response to environmental stimuli, which is becoming an increasingly critical topic as changes in climate increase the frequency and intensity of storms.

Keywords: functional root traits, I-beam, root cage, root system architecture, root topology, T-beam, tree anchorage

OPEN ACCESS

Edited by:
Christian Ammer, University of Göttingen, Germany

Reviewed by:
Veronica De Micco, University of Naples Federico II, Italy
Ivano Brunner, Swiss Federal Institute for Forest, Snow and Landscape Research (WSL), Switzerland

****Correspondence:***
R. Kasten Dumroese
kas.dumroese@usda.gov

Specialty section:
This article was submitted to Functional Plant Ecology, a section of the journal Frontiers in Plant Science

Received: *12 March 2019*
Accepted: *08 July 2019*
Published: *30 July 2019*

Citation:
Dumroese RK, Terzaghi M, Chiatante D, Scippa GS, Lasserre B and Montagnoli A (2019) Functional Traits of Pinus ponderosa Coarse Roots in Response to Slope Conditions. Front. Plant Sci. 10:947. doi: 10.3389/fpls.2019.00947

INTRODUCTION

The global need for forest restoration continues to increase; attempting to meet that challenge is a host of current initiatives spanning scales from local to global and addressing nearly 500 million hectares (see Haase and Davis, 2017). This focus is not surprising given that terrestrial forest ecosystems cover about one-third of the global land base and account for 70% of the carbon exchange (Waring and Schlesinger, 1985) that occurs in the biosphere. Moreover, forest ecosystems support biodiversity (Pawson et al., 2013), which is important for maintaining ecosystem resilience to changes in climate (Liang et al., 2016; Seidl et al., 2016), and sustaining social structure (Parrotta et al., 2012).

To ensure long-term results, forest restoration activities must consider current conditions as well as future, uncertain climatic conditions (e.g., Millar et al., 2007). For example, extreme weather events (i.e., drought and windstorms) that occur with greater year-to-year variation are expected to occur more frequently or with greater severity (Meehl et al., 2000; Harris et al., 2006; Allen, 2009; Allen et al., 2010). This short-term change to climate, along with longer-term changes to climatic means (i.e., temperature and precipitation) are likely important drivers of forest degradation (Stanturf et al., 2014) that will increase the need for restoration across all scales (Chen et al., 2011).

Despite a strong effort during the last few decades to better understand the contribution of the belowground portion of trees to the biosphere response to global change, advancement of our knowledge concerning roots moves slowly due to the inherent difficulty in measuring these complex structures (Nadelhoffer and Raich, 1992). Critical gaps in our knowledge of root traits remain. An exact estimation of all traits belonging to a root system is, however, necessary for correctly modeling distribution of the mechanical forces involved in tree anchorage to soil.

A complete knowledge of all the anchorage properties of trees could enable us to predict the response of trees to more severe, climate-change induced storms, as well as to inform silvicultural practices, such as thinning, toward improving the resilience of existing forest stands facing increased drought events (Fraser and Gardiner, 1967; Ruel, 1995; Danjon et al., 1999a; Puhe, 2003; Crotteau and Ritchie, 2014), especially as new models are generated (e.g., Yang et al., 2016). The effects of thinning, in particular, are important because the increased distance between trees not only affects root development (Danjon et al., 1999b) but also changes the value of the mechanical loading because both slope and wind act on tree anchorage (Quine and Gardiner, 2007; Hale et al., 2012; James et al., 2014).

Individual roots, as well as root location, promote the effective anchorage of trees. Strong anchorage near the tree base utilizes four different cross-sectional shapes of large roots: circular, oval, I-beam, and T-beam (Nicoll and Ray, 1996; Coutts et al., 1999). In particular, I- and T-beam are identified as nonsymmetrical, secondary thickening around the vertical axis through the biological center. For an I-beam, equal vertical thickening occurs above and below the biological center. The T-beam shape is characterized by an uneven lateral thickening between the upper and lower regions of the root. On sites with shallow soil and in young trees, T-beam shaped roots tend to develop close to the stem base on the leeward side. I-beam shaped roots tend to develop on the windward side approximately 2.5X farther out from the stem base than the T-beam shaped root area on the leeward side (Nicoll and Ray, 1996; Coutts et al., 1999). Both of these root shapes move the focal point of bending/hinging farther away from the stem (Nicoll and Ray, 1996; Stokes, 1999; Chiatante et al., 2003). Development of an I-beam root shape increases root stiffness nearly 300X compared to a circular-shaped root having an equal cross-sectional area (Nicoll et al., 2006b). Trees, to maintain anchorage by resisting vertical flexing, tend to develop oval or I-beam roots in response to steep slopes and wind (Nicoll and Ray, 1996; Coutts et al., 1999; Chiatante et al., 2003; Di Iorio et al., 2005). I-Beam and T-beam shaped roots were found on *Betula* spp., *Picea sitchensis*, *Pinus contorta*, *Pinus sylvestris*, and *Quercus* spp. (Anonymous, 1964; Nicoll and Ray, 1996).

The arrangement of roots into a "cage" also affects anchorage (Danjon et al., 2005). The cage is defined as a cylindrical region centered at the taproot and composed of the zone of rapid taper of horizontal surface roots as well as the numerous sinkers and deep roots that enmesh a large mass of soil. The formation of a rigid cage is common in mature *Pinus pinaster* trees (Danjon et al., 2005). As is the case with trees that develop a rigid root-soil plate through adaptive growth of their structural roots to increase the contribution of soil resistance to overturning (Coutts, 1986; Ray and Nicoll, 1998), *P. pinaster* with low cage volume are more susceptible to wind-throw than their cohorts having a larger volume of leeward roots within the cage (Danjon et al., 2005).

Pinus ponderosa is one of the most important commercial species in the United States, covering about 10.9 million ha in the west (Oliver and Ryker, 1990). While a large body of literature has been accumulated for this species, most studies have focused mainly on above-ground characteristics (e.g., Weaver, 1961; Agee, 1993; Covington and Moore, 1994; Fulé et al., 1997; Moore et al., 2004; Wright and Agee, 2004; Hessburg et al., 2005), leaving below-ground structures much less studied, especially for trees beyond the seedling stage. Notable exceptions are the works published and referenced in Curtis (1964), and a large-root biomass model based on stem diameter at breast height (DBH; ~1.3 m) (Omdal et al., 2001). At the seedling stage, the ability of *P. ponderosa* to establish better than other conifers during periods of soil moisture deficits has long been linked to the adaptability of their root systems (e.g., Larson, 1963, 1967; Larson and Schubert, 1969; Smith, 1985; Kolb and Robberecht, 1996), but, to the best of our knowledge, no empirical work has been done to understand the root system architecture of more mature trees. A better understanding of the development and deployment of root system in its rooting environment could have important implications in the effort to improve the resilience of these forests and to preserve them within a scenario of changing global climate.

We hypothesized that coarse roots would have asymmetric spatial distribution influenced by the main mechanical forces of slope and prevailing wind. A second hypothesis was that the main coarse roots of *P. ponderosa* would display an I- and/or T-beam shape in response to these forces. To test our hypothesis, length and volume of the coarse roots were analyzed as a function of their spatial distribution into soil, and main shallow roots were sectioned proximal to the taproot and their cross-sectional shapes observed. Our objective was to use an information-theoretic approach to understand how *P. ponderosa* trees modify the growth of their root systems in slope conditions on an ash-cap soil type to adjust to different rooting environment stimuli.

MATERIALS AND METHODS

Site Description and Tree Establishment

The study site is located at about 1,000 m elevation on the University of Idaho Experimental Forest in northern Idaho USA (lat 46.842240, long −116.871035). The area receives about 965 ml of annual precipitation with a seasonal drought during summer (July–September). The average, annual air temperature is 7.2°C with ~100 frost-free days (Soil Survey Staff, 2013). The prevailing wind during the growing season is west southwest (Western Regional Climate Center, 2019). Ecologically, the site is classified as a *Thuja plicata*/*Clintonia uniflora*/*Clintonia uniflora* phase habitat type (Cooper et al., 1987) that supports mixed conifer forests. It has a northeast aspect with slopes of 30–50%. The deep (~1.5 m) soil is in the Vassar series (Typic Udivitrands; Andisol), having formed in volcanic ash above material weathered from granitic (Soil Survey Staff, 2013); see **Table 1** for profile descriptions. The site was clearcut harvested and broadcast burned during 1985 with little reduction of the forest floor layer.

During March 1986, one-year-old *P. ponderosa* seedlings grown at the University of Idaho nursery in two container types (using locally collected seeds) were hand-planted on the site as part of an experiment (see Wenny et al., 1988). Twenty non-treated control seedlings of each container type were part of this outplanting in a grid having 1-m spacing between seedlings within the row (a single treatment/container combination) and 2-m spacing between rows. Each seedling was marked with a metal stake. During September 1986, every other seedling was excavated to observe first-season shoot and root growth (see Wenny et al., 1988), leaving residual trees on a 2 m × 2 m spacing. During this sample, the average bulk density, organic matter content, and pH in the rooting zone, defined as the top 25 cm of mineral soil, were determined to be 0.94 g cm^{-1}, 4.7%, and 5.9, respectively (Wenny et al., 1988). No irrigation, fertilization, weeding, or thinning was done after outplanting.

Excavation and 3-Dimensional Architecture Measurement

In early July 2017, we relocated the *P. ponderosa* trees grown in the control Styroblock 4A (313A) containers (60 ml volume, 14 cm depth, 936 cavities m^{-2}; Beaver Plastics Ltd., Acheson, AB, Canada) and randomly selected five trees for measurement (P1, P4, P5, P6, and P8). Each tree was measured for DBH (cross-slope). Using the sample tree as plot center, we measured the azimuth, distance to, and DBH of other trees (>5 cm DBH) within a 5 m radius. A single screw was driven into the bark at the root-stem interface to delineate north. After cutting the stem near the collar, we measured height. Two screws were partially drilled into the stump about 20 cm apart with their heads adjusted to horizontal level. Two more screws, perpendicular to the first two, were installed in a similar manner.

We excavated the root systems using a high-pressure air lance fitted with a 71 l s^{-1} nozzle (AirSpade 2000; AirSpade, Chicopee, MA, USA) connected to a portable air compressor (36.5 kW) that delivered air at 87 l s^{-1} at a normal effective working pressure of 0.7 MPa (XAS 185; Atlas Copco Compressors LTD, Rock Hill, SC, USA). When the resulting supersonic air stream touched a smooth object (such as a stone or root), it slipped over the surface, but when the air stream hit any tiny pore, air was compressed in the pore (it could not blow out under such a high air speed) and the pore exploded. Thus, soil was blown away while the roots and other smooth objects remain untouched (Nadezhdina and Čermák, 2003). We exposed root systems to bedrock (approximately 1–1.5 m in depth) and to distances of approximately 1.5 m from the trunk. After cutting roots that were still attached to soil, the root systems were carefully lifted from the soil and carried to the

TABLE 1 | Profile characteristics of a typical Vassar series profile (National Cooperative Soil Survey, 2019).

Horizon	Descriptions of horizon abbreviations	Depth (cm)	Texture	Bulk density (g cm^3)	Rock content > 2 mm (%)	pH	Carbon (%)	Nitrogen (%)
Oi	(O) Organic layer (i) Slightly decomposed organic matter	0–3	–	–	5	6.8	47.86	1.61
A	(A) Mineral; organic matter (humus) accumulation	3–10	Ashy silt	0.94	5	6.3	3.46	0.19
Bw1	(B) Subsurface accumulation Fe, Al, Si (w) Weak color or structure (1; suffix) horizon subdivision	10–24	Ashy silt	0.97	6	6.2	1.61	0.09
Bw2	(2; suffix) horizon subdivision	24–60	Ashy silt	0.99	4	6.3	1.20	0.07
2Bw3	(2; prefix) lithologic discontinuity (B) (w) (3; suffix) horizon subdivision	60–77	Silt	1.53	9	6.3	0.11	0.02
2BC	(2; prefix) (BC) Dominantly B characteristics but contains C horizon attributes	77–102	Loamy sand	1.56	14	6.1	0.07	0.01
2C	(2; prefix) (C) Little or no pedogenic alteration	102–136	Loamy sand	1.53	11	6.0	0.06	0.02
2Cr	(2; prefix) (C) (r) Weathered or soft bedrock	136–150	Coarse sand	–	5	6.1	0.04	0.01
Bedrock	Granite							

U.S. Department of Agriculture, Rocky Mountain Research Station, Forestry Sciences Laboratory (Moscow, ID) for analysis. At the laboratory, we positioned the root systems on four adjustable wood supports so that the exact inclination (achieved by adjusting the root so that the screw heads were at horizontal level) and north direction (positive X; see below) could be restored.

The root system was discretized by a low magnetic field digitizer (Fastrak; Polhemus, Colchester, VT, USA) and encoded in a standard format (MTG) commonly used for representing branching topological relationships using AMAPmod software at different observation scales (Godin and Caraglio, 1998). Device characteristics (Danjon et al., 1999b; Di Iorio et al., 2013) consisted of an electronic unit, a magnetic transmitter (Long Ranger; Polhemus), and a small hand-held receiver positioned at each point to be measured. The receiver measured the X, Y, and Z spatial coordinates within a sphere-wide electromagnetic field having a 4-m radius around the transmitter, which was sufficient for the root system sizes observed in this study. The transmitter was positioned approximately 1.5 m below and 2.5 m from the stump with the downslope direction in the positive X direction.

Although scientists working with the finest component of the root system define the first-order roots as those most distal (McCormack et al., 2015), in the present work the topology, (i.e., the branching hierarchic structure) was coded according to the "acropetal-development approach" (Danjon et al., 2013; Sorgonà et al., 2018) with the seed-origin radicle, the primary roots (-axis) or taproot designated order zero (pink color in **Figure 1**). Lateral roots emerging from the taproot were designated first-order roots (green color in **Figure 1**), with second-order roots then originating from these first-order laterals (blue color in **Figure 1**), and so on (Zobel and Waisel, 2010). The stump was determined subjectively as the portion of taproot with a large diameter from where most of the large horizontal surface roots originated. The taproot was the largest vertical root originating directly from the stump. We digitized starting at the root collar and followed a recursive path along the branching network as suggested by Danjon et al. (2005). Between branching points, intermediate measurements were performed in order to record changes in root direction and taper. A segment was defined as the root subdivision between two measured points. The average segment length was about 2 cm when roots were curved and approximately 15 cm when roots were straight. When a root cross-section was oblong, the largest diameter and its orientation, as well as the diameter perpendicular to the largest diameter, were recorded. All roots with a proximal diameter larger than 1 cm at the base were measured.

The output data file was analyzed using the AMAPmod software (Godin et al., 1997), which handles topological structure at several scales and also provides 3-dimensional graphical reconstruction for data checking. Extracted data were exported to other software to perform specialized processing

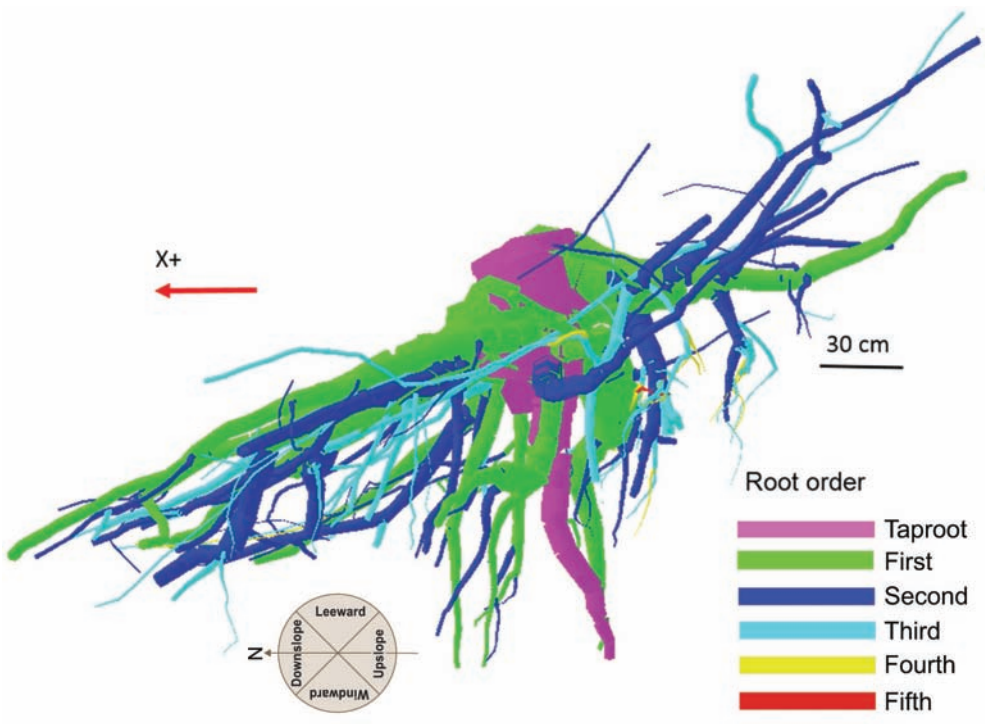

FIGURE 1 | Root hierarchy was digitized using the "acropetal-development approach" that allows each root system to be reconstructed using the AMAPmod software for 3-dimensional analysis. In this image of tree P8, the taproot appears pink, first-order lateral roots emerging from the taproot are green, and second-order roots are blue. The X + axis is oriented down slope parallel to the slope direction.

(see statistical analysis below). Root traits (i.e., length, diameter, and volume) were computed from 3-dimensional digitizing data of whole root systems. Root traits were considered as a function of up- versus down-slope direction and of west- versus east-slope direction, with the downslope direction coinciding with north and the west-east axis coinciding with the direction of the prevailing wind (**Figure 2**). Furthermore, the different root traits were assessed as a function of depth and azimuth position. After several analyses, we chose two depths for assessment: 0–30 and 30–60 cm. Within each depth, we divided the space surrounding the taproot into four quadrants: downslope (north), upslope (south), windward (west), and leeward (east).

We analyzed the root cage, defined as the cylindrical region centered at the taproot. The cage radius corresponds to the zone of rapid taper, which is calculated as the mean length of the first shallow root segments that extend from the stem base with the most rapid taper. The depth of the cage corresponds to that of the taproot (Danjon et al., 2005), and first-and second-order vertical roots were counted as sinker roots. In our study, we used an alternative definition, developed from Danjon et al. (2005) to relate the zone of rapid taper to tree size. Specifically, the zone was defined as all roots originating within a radial distance of 2.2 × DBH.

Cross-Sectional Shape of Structural Roots

On each tree in the sector with the greatest root spatial allocations, cross-sectional samples from the largest shallow roots were cut at approximately the originating branching point from the taproot. Before cutting, the top of each root was labeled. One face of each root cross section was sanded smooth to allow examination of the growth rings.

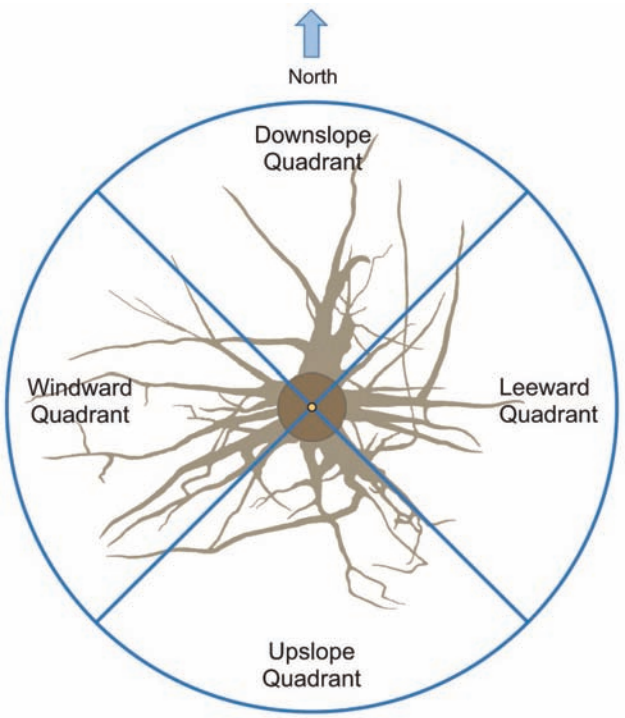

FIGURE 2 | Roots were excavated to a distance of about 1.5 m from the trunk. Traits were assessed in four quadrants: upslope, downslope, windward, and leeward.

Statistical Analysis

To evaluate the effects of abiotic factors on root apparatus architecture, we compared the length and volume of first-, second-, and third-order roots using the IBM SPSS Statistics software version 20.0 (IBM Corp.; Armonk, NY, USA). Each depth was analyzed independently. The distribution of each population was tested using the Shapiro-Wilk normality-test. Parametric comparison methods were adopted if the result was positive; otherwise, we used non-parametric comparison tests. We used tests for related (non-independent) data to analyze group means. In particular, when variables were Gaussian distributed, we employed the paired samples *t* test; otherwise, the Wilcoxon signed-rank test was performed when variables were non-Gaussian distributed. Box-plot visualizations were created using SigmaPlot (version 13.0; Systat Software, San Jose, CA, USA). Root system projections were generated using PlantGL, a Python-based geometric library for 3-dimensional plant modeling at different scales (Pradal et al., 2009). Azimuth projection and graphical reconstruction of the tree stand characteristics were produced by Excel and PowerPoint (Microsoft Office 2003 Microsoft Inc., Redmond, WA, USA) software, respectively.

RESULTS AND DISCUSSION

The variability observed among the root systems of different tree species, and within a particular species, is considered to be an adaptation response to the variability of the rooting environment (i.e., depth and nature of soil) (Henderson et al., 1983; Coutts et al., 1990). Differences between *P. ponderosa* and the species it forms mixed stands with, such as *Populus tremuloides*, *Pseudotsuga menziesii*, and *Pinus contorta*, have been noted (Berndt and Gibbons, 1958), and differences in tap root development of *P. ponderosa* occurred because of varying soil depths to bedrock (Berndt and Gibbons, 1958; Curtis, 1964).

In our study, however, the sampled area was small (132 m^2) and the trees fairly close (~2 m) (**Figure 3**). Therefore, it is reasonable to assume that the soil was uniform in terms of slope, aspect, and profile across the sampled area. Thus, any differences observed in overall root traits and architecture may represent a response of the trees to differences existing in the soil profile relative to physical and chemical properties.

Root System Traits

Overall, DBH of sampled trees ranged from 23.3 to 34.2 cm, with a median value of 24.1 cm (**Table 2**). Heights were about 16 m. Variability in root length increased with root order (topology follows the "acropetal-development approach"; Danjon et al., 2013; Sorgonà et al., 2018); that is, more variability

was observed in second-order roots compared to first-order, and more in third-order roots compared to second-order (**Table 2**). While the trend was less apparent for root volume, the third-order roots were again the most variable.

In the Vassar soil series, a lithological discontinuity occurs at about the 60 cm depth in a typical profile. At that depth, the influence of the volcanic ash dissipates, bulk density increases from about 1 to 1.5 g cm^{-3}, and percentage carbon (a reflection of overall organic matter) drops from 1.2 to 0.1% (**Table 1**). Above this discontinuity, the soil depth of 0–30 cm includes more carbon (organic matter) and nitrogen than the lower, 30–60 cm depth (**Table 1**) and this upper zone is where significant differences in root length and volume were observed (**Figures 4A,C,E,G**).

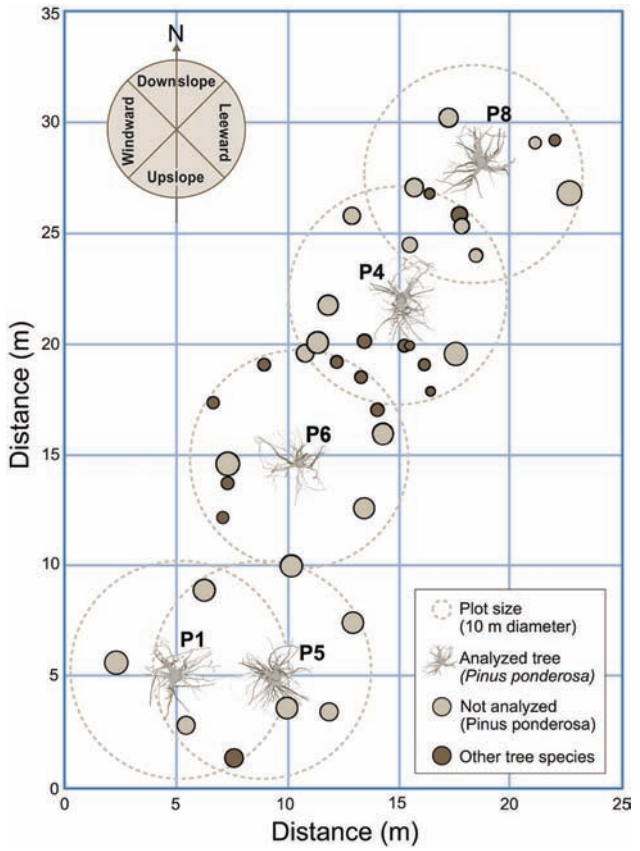

FIGURE 3 | Locations of the sampled trees and their proximity to other trees. The other tree species included *Abies grandis*, *Larix occidentalis*, and *Pseudotsuga menziesii*. Downslope was to the north and windward was to the west.

For first-order lateral roots in the 0–30 cm depth, length in the downslope quadrant was significantly different ($p = 0.0225$) than that observed in the upslope quadrant (**Figure 4A**). For volume, the downslope quadrant was significantly different than the leeward ($p = 0.0425$) and upslope ($p = 0.0490$) quadrants (**Figure 4C**). No significant differences were noted for length or volume in the 30–60 cm depth (**Figures 4B,D**).

For second-order lateral roots in the 0–30 cm depth, length in the downslope quadrant was significantly different than the leeward ($p = 0.0430$) and upslope ($p = 0.0126$) quadrants (**Figure 4E**). Volume followed the same pattern as that observed for first-order roots: the downslope quadrant was significantly different than the leeward ($p = 0.0422$) and upslope ($p = 0.0352$) quadrants (**Figure 4G**). No significant differences were noted for length or volume in the 30–60 cm depth (**Figures 4F,H**). We were unable to detect any significant differences among third-order lateral roots for length or volume in the 0–30 cm depth (all $p \geq 0.6$) (**Figures 4I–L**).

Trees grow roots in response to environmental stimuli (Rellán-Álvarez et al., 2016). On our study site, two possible displacement forces may be influencing root occurrence: prevailing wind and slope (Chiatante et al., 2003; Danjon et al., 2005; Di Iorio et al., 2005; Lombardi et al., 2017). Stokes (2002) notes that for trees undergoing mechanical stress due to the force of unidirectional wind, the roots perpendicular to the direction of possible displacement (windward-leeward direction) are held in torsion and play a marginal role in counteracting uprooting forces (Stokes, 2002). On our site with its 40% slope, it is, however, reasonable that the mechanical forces act with an upslope-downslope direction; thus more roots should grow in the upslope-downslope direction than in the windward-leeward direction. Indeed, our data indicate that two contemporaneous mechanical forces affect root spatial development: slope and prevailing wind. Lower values of first-and second-order root length and volume in the leeward and upslope

TABLE 2 | Above- and below-ground characteristics for each analyzed tree.

Tree	DBH (cm)	Height (m)	Length (cm)			Volume (cm^3)		
			Root order					
			First	Second	Third	First	Second	Third
P1	24.1	16.8	2,994	4,255	1,033	74,550	10,771	703
P4	24.1	15.2	2,859	7,482	2,492	50,640	18,192	2,099
P5	25.6	16.0	2,429	8,536	5,314	57,596	25,648	7,104
P6	23.3	17.1	3,180	4,510	1,744	30,275	22,117	1,777
P8	34.2	16.2	3,310	5,028	1953	165,406	35,263	6,826
Mean	26.3	16.3	2,954	5,962	2,507	75,693	22,398	3,702
SE	2.0	0.3	152	860	738	23,483	4,049	1,350

Total length and volume were for roots with a diameter > 1 cm.

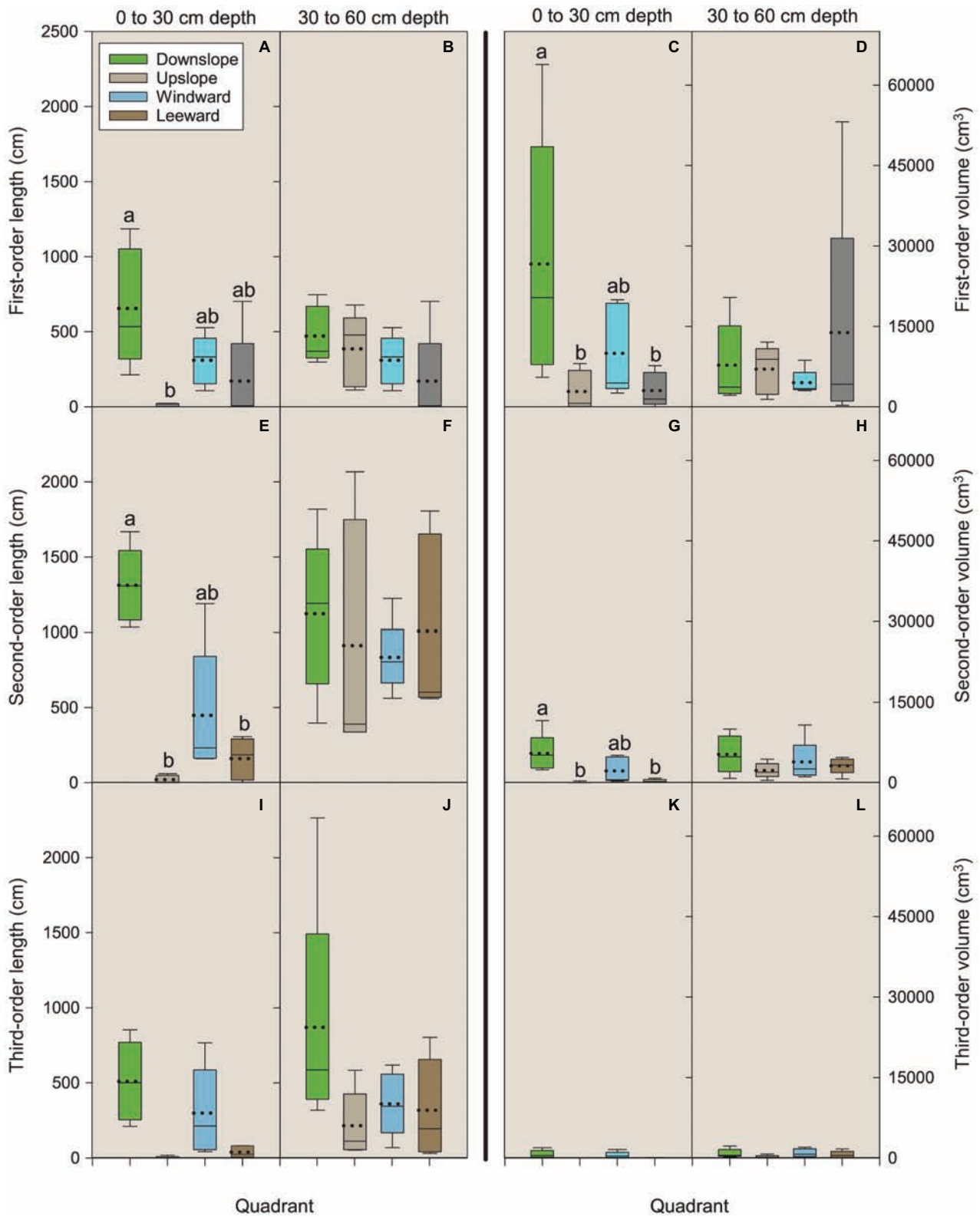

FIGURE 4 | Length and volume of first-, second-, and third-order roots by quadrant and soil depth (0–30 and 30–60 cm). Each depth was analyzed independently. Letters within each order, variable, and depth combination indicate significant differences ($p < 0.05$); absence of letters reflects that no significant difference was detected. Vertical boxes represent approximately 50% of the observations and lines extending from each box are the upper and lower 25% of the distribution. Within each box, the solid horizontal line is the median value and the dotted line is the mean.

quadrants suggest that the anchorage of *P. ponderosa* trees excavated in this study preponderantly rely on roots belonging to the downslope and windward quadrants. The latter being of lower magnitude because the windward root traits were not significantly different than the leeward side despite an observed trend. Thus, slope induces mechanical force acting on the roots with an upslope-downslope orientation (Chiatante et al., 2003; Scippa et al., 2006; Sun et al., 2008), while mechanical forces due to the wind act in the windward-leeward direction (Yang et al., 2014 and references therein). Furthermore, although the magnitude of root volume and length in the 30–60 cm soil depth is comparable to those in the 0–30 cm depth, at the deeper soil layer differences in quadrants were not detected. This finding supports our first hypothesis and indicates a probable interplay between mechanical forces, higher N concentrations, and lower bulk density that occurs in the upper part of the soil profile. These factors influence the displacement of surface roots that are important for dissipating the tree "self-loading" to the soil (Chiatante et al., 2003) because of the higher entangled soil area as well as, during the juvenile stage, for water and nutrient absorption.

Our results are opposite to those reported for an oak tree species (*Quercus pubescens*; Di Iorio et al., 2005) and a common Mediterranean shrub species (*Spartium junceum*; Lombardi et al., 2017) growing on clay soils in slope conditions; here the authors found less downslope biomass than upslope biomass. This adaptive growth behavior might be related to trees avoiding root growth into the drier portions of the soil profile. Indeed, on the downhill side on a steep slope, roots growing horizontally would grow into the drier upper soil profile and eventually emerge from the soil, but instead change direction due to decreasing soil moisture (Di Iorio et al., 2005). Thus, in this case and from a biomechanical point of view, the upslope roots' resistance to pullout and shear stress might become the main component of tree anchorage. In other species, however, preferential growth of lateral roots occurred downslope (*Arabidopsis*, Mullen et al., 2005) or even perpendicular to the slope direction when a dominant wind was present (*Picea sitchensis*, Nicoll et al., 2006a; *Robinia pseudoacacia*, Khuder et al., 2006). In our study, the higher values of root traits were found downhill in accordance with different scenarios of root displacement outlined by Ghestem et al. (2011). Indeed, from a biomechanical point of view, preferential root growth occurs either up- or down-slope, thus enhancing anchorage along the axis of static mechanical loading (Stokes et al., 2009). In our case and on one hand, the anchorage of the tree is likely attributable to the forces of the roots pushing downward rather than hanging upward. On the other hand, certainly, these roots play an important role in the exploration and exploitation of surface water and nutrients during the juvenile developmental stage, thereby shaping future root spatial displacement. Thus, from a hydrological perspective, more roots are oriented downslope than upslope (Ghestem et al., 2011). This preferential gravitropism depends on the species, on nutrients, and on the soil's physical properties.

Regarding the nature of these mechanical forces, we suggest that roots growing in the downslope and windward quadrants are subjected to compression forces, while roots in the upslope and leeward quadrants are subjected to tension forces. These forces are transferred to the soil *via* friction, so that a large root volume and length on both windward and downward side, over which the load can be distributed, is beneficial to tree anchorage (Stokes et al., 1996).

Root System Architecture

It is known that root system architecture (RSA) exhibits a great variability due to genetic and environmental factors (see Gardiner et al., 2016 for a review; Schroth, 1998; Puhe, 2003; Stokes et al., 2009; Ji et al., 2012; Yang et al., 2016). On our site, *P. ponderosa* trees growing on an ashy silt soil show a highly structured RSA with coarse roots (diameter > 1 cm). In our study, trees displayed three RSA shapes (hereafter tight, enlarged, and diffused cage) where "cage" is intended to describe the zone of the root system around the stump where the taproot and most of the sinker roots descend into the soil in a parallel pattern (Danjon et al., 2005). These RSA shapes differ considerably from the heart-shape common to other conifers (Drexhage and Gruber, 1998; Stokes, 2002). However, the anomalous RSA shapes we observed concurs, as already discussed above, with the findings of Chiatante et al. (2003) and Di Iorio et al. (2005) for root systems developing on slopes.

In our study, the differences in RSA cage shapes are mainly dependent upon the variable proportion of number of sinkers, the volume of the first-, second-, and third-order roots within the cage, and the overall behavior of the taproot (**Table 3**). We observed three cage types: tight, enlarged, and diffused. A "tight cage" is characterized by a low number of sinker roots (P1 and P8 in **Table 3**) that form proximate the taproot (P8 in **Figure 5**). Furthermore, the ratio of the taproot to the volume of the entire cage is similar (0.39 and 0.37 respectively, **Table 3**), indicating a larger contribution of the sinker roots to cage volume, thus, to tree anchorage, in respect to the taproot. An "enlarged cage" is exemplified by a similar number of sinker roots (P6 in **Table 3**) that form proximate as well as distant from the taproot (P6 in **Figure 5**). Here the ratio of the taproot volume to the total cage volume is 50% showing an equal contribution by the taproot and the rest of the roots composing the cage to tree anchorage than that found in a tight cage. The highest number of sinkers (P4 and P5 in **Table 3**), located more distant from the taproot than other cage types, characterizes a "diffused cage" (P5 in **Figure 5**). For both P4 and P5 trees, the taproot volume is about 40% greater than the cumulative volume of the first-, second-, and third-order roots (**Table 3**; ratio of 0.59); here the taproot provides the greatest contribution to the cage and the overall anchorage of the tree compared to the other cage types.

Within a root system, the zone of rapid taper is a compartment including the portion of all the shallow roots that branch off from the taproot and undergo the most rapid decrease of diameter (Danjon et al., 2005). The zone of rapid taper along with the sinker roots plays a dominant role in tree anchorage with the taproot being the first mechanical contributor to tree anchorage strength (Yang et al., 2014, 2016). Nevertheless, we observed that, transitioning from the tight cage to the

TABLE 3 | Characteristics of root system architecture for analyzed *Pinus ponderosa* trees: the number of first- and second-order sinker roots; the length and volume of the first-, second-, and third-order roots (>1 cm diameter) within a radius of 2.2 × DBH (diameter breast height); the length and volume of the taproot; the total cage volume (sum of first-, second-, and third-order roots and taproot); and the ratio of taproot volume to total cage.

Tree	Sinker roots (number)		First-, second-, and third-order roots		Taproot		Total	Taproot/total
	Order							
	First	Second	Length (cm)	Volume (cm³)	Length (cm)	Volume (cm³)	Volume (cm³)	Volume (cm³)
P1	6	13	2,254	63,786	116	41,169	104,955	0.39
P4	4	20	2,617	36,619	157	52,686	89,305	0.59
P5	2	22	3,406	49,913	272	72,258	122,171	0.59
P6	3	9	2,541	37,077	124	37,496	74,573	0.50
P8	6	11	3,762	144,529	165	86,195	230,724	0.37

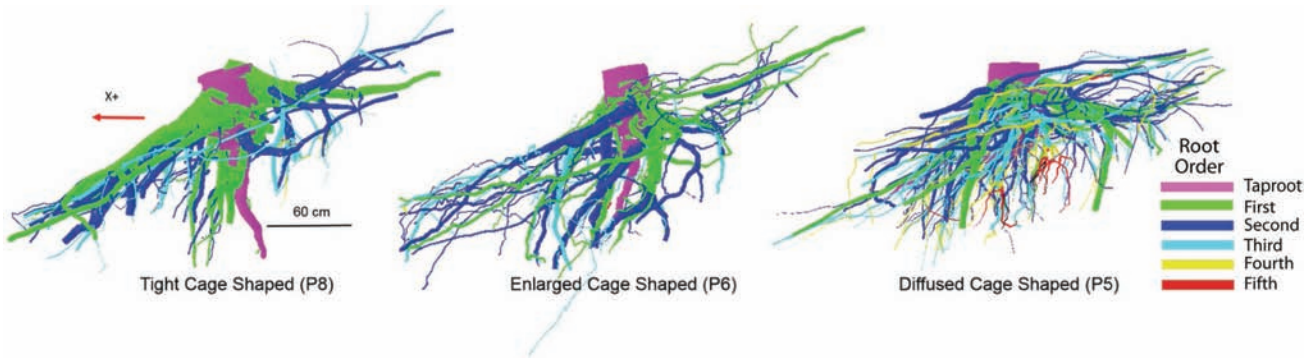

FIGURE 5 | An example of the three different root system architectures (tight, enlarged, and diffused cages) related to differences in the zone around the stump where the taproot and most of the sinker roots descend into the soil in a parallel pattern. Different colors indicate differences in branching order.

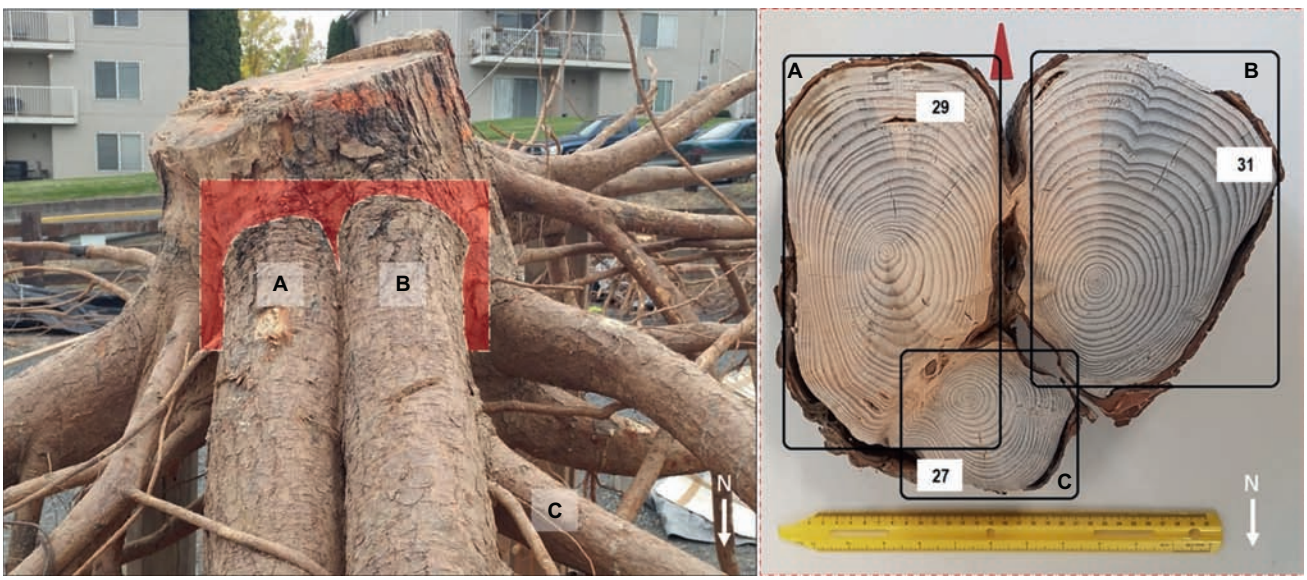

FIGURE 6 | Tree P8 (left panel) with two first-order lateral roots **(A,B)** north-oriented (downslope) and a second-order root **(C)** bending eastward (leeward). These same three roots in cross section (right panel); both first-order roots are subjected to mechanical induction and show asymmetry in the rings with different shapes: I-beam **(A)** T-beam **(B)**. White arrows indicate the north direction and the red arrow in the right panel points toward the soil surface. The number of growth rings in each root is reported in the white boxes.

diffuse cage, total cage volume decreases while the contribution of the taproot to the root cage increases. This suggests that in *P. ponderosa*, the taproot and the rest of the cage roots contribute differently to tree anchorage depending on the high plasticity of the root at the individual plant level.

At an individual root level, we observed that shallow roots in the 0–30 cm soil depth in the downslope quadrant could develop both I- and T-beam shaped roots at their branching point from the taproot. This finding supports our second hypothesis. Compared to I-beam development, most roots (83%) in the down-slope quadrant displayed T-beam development. This adaptive growth strategy strengthens the anchorage because the T-beam is particularly well designed to resist compressive forces (Nicoll and Ray, 1996), which on our sites was likely caused by the force of gravity occurring downslope.

These cross sectional root shapes have been observed in conifer and broadleaved trees with shallow structural roots (Nicoll and Ray, 1996; Coutts et al., 1999; Nicoll et al., 2006a; Danjon et al., 2013) particularly in response to wind movement (Coutts et al., 1999). These shapes maximize resistance to bending or flexing and increase rigidity of the root-soil plate with minimum wood production (Coutts et al., 1999 and references therein). Therefore, in our case, this particular root shape could represent the response of trees to the need to increase their mechanical contribution to anchorage due to mechanical stimuli as a result of slope. We noted that roots with I- and T-beam shape were present in the downslope quadrant (**Figure 6**) along with the observation that root length and volume were also greatest in this quadrant. Thus, our findings concur with those of Stokes et al. (1996) that related the increase in buttress surface area of these roots obtained with either an I- or T-beam shape with a better counteracting of the compression mechanical forces by transferring those forces to the soil.

CONCLUSIONS

Limited literature has discussed the root system architecture of *P. ponderosa*, with a paucity of information about this topic for trees growing on sloping ash-cap soils. On this site after 32 growing seasons, *P. ponderosa* trees appear to have deployed roots in response to mechanical forces due to both slope and prevailing wind by devoting more root resources downslope and windward toward improving stability. We noted growth of roots with I- and T-beam shapes in the downslope quadrant that better counteract the compression mechanical forces. Although this architectural pattern was common to all trees analyzed, we observed that the contribution of the taproot to the root cage, and thus to the tree anchorage, may vary depending on the plasticity of the root system in relation to the micro-soil conditions. Finally, these results unveil a powerful mechanism that involves modulation of root spatial displacement and morphology to increase tree stability. Thus, such an understanding of RSA provides useful information in terms of tree adaptation in the scenario of increasing frequency and intensity of storms.

DATA AVAILABILITY

The datasets generated for this study are available on request to the corresponding author.

AUTHOR CONTRIBUTIONS

KD and DC conceived the research project. KD provided primary funding. AM, KD, and DC developed the study plan. AM was responsible for field excavations and data collection and analysis. AM and MT equally contributed to the field activities. AM performed the digitalization and provided the 3D visualization. BL performed the three-dimensional data arrangement and analysis. GS provided important insights into the study plan and research process. KD, DC, and AM prepared the manuscript.

FUNDING

This study was supported by the University of Insubria, the University of Molise, the U.S. Department of Agriculture, Forest Service (USFS) Rocky Mountain Research Station, and the USFS National Center for Reforestation, Nurseries, and Genetic Resources.

ACKNOWLEDGMENTS

For their assistance with data collection, we thank Dr. Robert Keefe and his crew at the University of Idaho Experimental Forest, as well as Evan Lunning, Brian Mora, Kyle Peterson, and Melissa Topping at the U.S. Department of Agriculture, Forest Service. Authors are in debt to Dr. Frédéric Danjon of the French National Institute of Agronomic Research (INRA) at Bordeaux for help with digitalization and data processing, and Dr. Barbara Giussani at the University of Insubria for assistance with the nonparametric statistics and interpretation. We thank Mario Oriani, University of Insubria, for informatics support and Jim Marin for some of the visualizations used in this paper.

REFERENCES

Agee, J. K. (1993). *Fire ecology of Pacific Northwest forests*. Washington, DC: Island Press.

Allen, C. D. (2009). Climate-induced forest dieback: an escalating global phenomenon. *Unasylva* 60, 43–49.

Allen, C. D., Macalady, A. K., Chenchouni, H., Bachelet, D., McDowell, N., Vennetier, M., et al. (2010). A global overview of drought and heat-induced tree mortality reveals emerging climate change risks for forests. *For. Ecol. Manag.* 259, 660–684. doi: 10.1016/j.foreco.2009.09.001

Anonymous (1964). Liability of trees on peat to windthrow. *Scott. For.* 18, 38–43.

Berndt, H. W., and Gibbons, R. D. (1958). Root distribution of some native trees and understory plants growing on three sites within ponderosa pine watersheds in Colorado. Fort Collins, CO: U.S. Department of Agriculture, Forest Service, Rocky Mountain Forest and Range Experiment Station, Station Paper 37. 14 p.

Chen, I.-C., Hill, J. K., Ohlemüller, R., Roy, D. B., and Thomas, C. D. (2011). Rapid range shifts of species associated with high levels of climate warming. *Science* 333, 1024–1026. doi: 10.1126/science.1206432

Chiatante, D., Scippa, G. S., Di Iorio, A., and Sarnataro, M. (2003). The influence of steep slopes on root system development. *J. Plant Growth Regul.* 21, 247–260. doi: 10.1007/s00344-003-0012-0

Cooper, S. T., Neiman, K. E., Steele, R., and Roberts, D. W. (1987). Forest habitat types of northern Idaho: a second approximation. Ogden, UT: U.S. Department of Agriculture, Forest Service, Intermountain Research Station. General Technical Report INT–236. 135 p.

Coutts, M. P. (1986). Components of tree stability in Sitka spruce on peaty gley soil. *Forestry* 59, 173–197. doi: 10.1093/forestry/59.2.173

Coutts, M. P., Nielsen, C. C. N., and Nicoll, B. C. (1999). The development of symmetry, rigidity and anchorage in the structural root system of conifers. *Plant Soil* 217, 1–5. doi: 10.1023/A:1004578032481

Coutts, M. P., Walker, C., and Burnand, A. C. (1990). Effects of establishment method on root form of lodgepole pine and Sitka spruce on the production of adventitious roots. *Forestry* 63, 143–159. doi: 10.1093/forestry/63.2.143

Covington, W. W., and Moore, M. M. (1994). Southwestern ponderosa forest structure: change since Euro-American settlement. *J. For.* 92, 39–47. doi: 10.1093/jof/92.1.39

Crotteau, J. S., and Ritchie, M. W. (2014). Long-term stand growth of interior ponderosa pine stands in response to structural modifications and burning treatments in northeastern California. *J. For.* 112, 412–423. doi: 10.5849/jof.13-090

Curtis, J. D. (1964). Roots of a ponderosa pine. Ogden, UT: U.S. Department of Agriculture, Forest Service, Intermountain Forest and Range Experiment Station. Research Paper INT–9. 10 p.

Danjon, F., Bert, D., Godin, C., and Trichet, P. (1999a). Structural root architecture of 5-year-old *Pinus pinaster* measured by 3D digitising and analysed with AMAPmod. *Plant Soil* 217, 49–63. doi: 10.1023/A:1004686119796

Danjon, F., Fourcaud, T., and Bert, D. (2005). Root architecture and wind-firmness of mature *Pinus pinaster*. *New Phytol.* 168, 387–400. doi: 10.1111/j.1469-8137.2005.01497.x

Danjon, F., Khuder, H., and Stokes, A. (2013). Deep phenotyping of coarse root architecture in *R. pseudoacacia* reveals that tree root system plasticity is confined within its architectural model. *PLoS One* 8:e83548. doi: 10.1371/journal.pone.0083548

Danjon, F., Sinoquet, H., Godin, C., Colin, F., and Drexhage, M. (1999b). Characterization of structural tree root architecture using 3D digitizing and AMAPmod software. *Plant Soil* 211, 241–258. doi: 10.1023/A:1004680824612

Di Iorio, A., Lasserre, B., Scippa, G. S., and Chiatante, D. (2005). Root system of *Quercus pubescens* trees growing on different sloping conditions. *Ann. Bot.* 95, 351–361. doi: 10.1093/aob/mci033

Di Iorio, A., Montagnoli, A., Terzaghi, M., Scippa, G. S., and Chiatante, D. (2013). Effect of tree density on root distribution in *Fagus sylvatica* stands: a semi-automatic digitising device approach to trench wall method. *Trees* 27, 1503–1513. doi: 10.1007/s00468-013-0897-6

Drexhage, M., and Gruber, F. (1998). Architecture of the skeletal root system of 40-year-old *Picea abies* on strongly acidified soils in the Harz Mountains (Germany). *Can. J. For. Res.* 28, 13–22. doi: 10.1139/x97-181

Fraser, A. I., and Gardiner, J. B. H. (1967). *Rooting and stability in Sitka spruce. Issue 40 of Forestry commission bulletin*. London: Forestry Commission, HMSO, 28.

Fulé, P. Z., Covington, W. W., and Moore, M. M. (1997). Determining reference conditions for ecosystem management of southwestern ponderosa pine forests. *Ecol. Appl.* 7, 895–908. doi: 10.1890/1051-0761(1997)007[0895:DRCFEM]2.0.CO;2

Gardiner, B., Berry, P., and Moulia, B. (2016). Review: wind impacts on plant growth, mechanics and damage. *Plant Sci.* 245, 94–118. doi: 10.1016/j.plantsci.2016.01.006

Ghestem, M., Sidle, R. C., and Stokes, A. (2011). The influence of plant root systems on subsurface flow: implications for slope stability. *Bioscience* 61, 869–879. doi: 10.1525/bio.2011.61.11.6

Godin, C., and Caraglio, Y. (1998). A multiscale model of plant topological structures. *J. Theor. Biol.* 191, 1–46. doi: 10.1006/jtbi.1997.0561

Godin, C., Costes, E., and Caraglio, Y. (1997). Exploring plant topological structure with the AMAPmod software: an outline. *Silva Fenn.* 31, 357–368.

Haase, D. L., and Davis, A. S. (2017). Developing and supporting quality nursery facilities and staff are necessary to meet global forest and landscape restoration needs. *Reforesta* 4, 69–93. doi: 10.21750/REFOR.4.06.45

Hale, S. E., Gardiner, B. A., Wellpott, A., Nicoll, B. C., and Achim, A. (2012). Wind loading of trees: influence of tree size and competition. *Eur. J. For. Res.* 131, 203–217. doi: 10.1007/s10342-010-0448-2

Harris, J. A., Hobbs, R. J., Higgs, E., and Aronson, J. (2006). Ecological restoration and global climate change. *Restor. Ecol.* 14, 170–176. doi: 10.1111/j.1526-100X.2006.00136.x

Henderson, R., Ford, E. D., Renshaw, E., and Deans, J. D. (1983). Morphology of the structural root system of Sitka spruce 1. Analysis and quantitative description. *Forestry* 56, 121–135. doi: 10.1093/forestry/56.2.121

Hessburg, P. F., Agee, J. K., and Franklin, J. F. (2005). Dry forests and wildland fires of the Inland Northwest USA: contrasting the landscape ecology of the pre-settlement and modern eras. *For. Ecol. Manag.* 211, 117–139. doi: 10.1016/j.foreco.2005.02.016

James, K. R., Dahle, G. A., Grabosky, J., Kane, B., and Detter, A. (2014). Tree biomechanics literature review: dynamics. *Arboric. Urban For.* 40, 1–15.

Ji, J., Kokutse, N., Genet, M., Fourcaud, T., and Zhang, Z. (2012). Effect of spatial variation of tree root characteristics on slope stability. A case study on black locust (*Robinia pseudoacacia*) and arborvitae (*Platycladus orientalis*) stands on the Loess Plateau, China. *Catena* 92, 139–154. doi: 10.1016/j.catena.2011.12.008

Khuder, H., Danjon, F., Stokes, A., and Fourcaud, T. (2006). "Growth response and root architecture of black locust seedlings growing on slopes and subjected to mechanical perturbation" in *Proceedings of the 5th plant biomechanics conference*. ed. L. Salmen (Stockholm: STFI-Packforsk AB), 299–304.

Kolb, P. F., and Robberecht, R. (1996). *Pinus ponderosa* seedling establishment and the influence of competition with the bunchgrass *Agropyron spicatum*. *Int. J. Plant Sci.* 157, 509–515. doi: 10.1086/297369

Larson, M. M. (1963). Initial root development of ponderosa pine seedlings as related to germination date and size of seed. *For. Sci.* 9, 456–460. doi: 10.1093/forestscience/9.4.456

Larson, M. M. (1967). Effect of temperature on initial development of ponderosa pine seedlings from three sources. *For. Sci.* 13, 286–294. doi: 10.1093/forestscience/13.3.286

Larson, M. M., and Schubert, G. H. (1969). Effect of osmotic water stress on germination and initial development of ponderosa pine seedlings. *For. Sci.* 15, 30–36. doi: 10.1093/forestscience/15.1.30

Liang, J., Crowther, T. W., Picard, N., Wiser, S., Zhou, M., and Alberti, G. (2016). Positive biodiversity-productivity relationship predominant in global forests. *Science* 354:aaf8957. doi: 10.1126/science.aaf8957

Lombardi, F., Scippa, G. S., Lasserre, B., Montagnoli, A., Tognetti, R., Marchetti, M., et al. (2017). The influence of slope on *Spartium junceum* root system: morphological, anatomical and biomechanical adaptation. *J. Plant Res.* 130, 515–525. doi: 10.1007/s10265-017-0919-3

McCormack, M. L., Dickie, I. A., Eissenstat, D. M., Fahey, T. J., Fernandez, C. W., Guo, D., et al. (2015). Redefining fine roots improves understanding of belowground contributions to terrestrial biosphere processes. *New Phytol.* 207, 505–518. doi: 10.1111/nph.13363

Meehl, G. A., Zwiers, F., Evans, J., Knutson, T., Mearns, L., and Whetton, P. (2000). Trends in extreme weather and climate events: issues related to modeling extremes in projections of future climate change. *Bull. Am. Meteorol. Soc.* 81, 427–436. doi: 10.1175/1520-0477(2000)081<0427:TIEWAC>2.3.CO;2

Millar, C. I., Stephenson, N. L., and Stephens, S. L. (2007). Climate change and forests of the future: managing in the face of uncertainty. *Ecol. Appl.* 17, 2145–2151. doi: 10.1890/06-1715.1

Moore, M. M., Huffman, D. W., Fulé, P. Z., Covington, W. W., and Crouse, J. E. (2004). Comparison of historical and contemporary forest structure and composition on permanent plots in southwestern ponderosa pine forests. *For. Sci.* 50, 162–176. doi: 10.1093/forestscience/50.2.162

Mullen, J. L., Wolverton, C., and Hangarter, R. P. (2005). Apical control, gravitropic signaling, and the growth of lateral roots in *Arabidopsis*. *Adv. Space Res.* 36, 1211–1217. doi: 10.1016/j.asr.2005.03.103

Nadelhoffer, K. J., and Raich, J. W. (1992). Fine root production estimates and belowground carbon allocation in forest ecosystems. *Ecology* 73, 1139–1147. doi: 10.2307/1940664

Nadezhdina, N., and Čermák, J. (2003). Instrumental methods for studies of structure and function of root systems of large trees. *J. Exp. Bot.* 54, 1511–1521. doi: 10.1093/jxb/erg154

National Cooperative Soil Survey (2019). National cooperative soil survey characterization database. Available at: https://ncsslabdatamart.sc.egov.usda.gov/ (Accessed January 24, 2019).

Nicoll, B. C., Berthier, S., Achim, A., Gouskou, K., Danjon, F., and van Beek, L. P. H. (2006a). The architecture of *Picea sitchensis* structural root systems on horizontal and sloping terrain. *Trees* 20, 701–712. doi: 10.1007/s00468-006-0085-z

Nicoll, B. C., Gardiner, B. A., Rayner, B., and Peace, A. J. (2006b). Anchorage of coniferous trees in relation to species, soil type, and rooting depth. *Can. J. For. Res.* 36, 1871–1883. doi: 10.1139/x06-072

Nicoll, B. C., and Ray, D. (1996). Adaptive growth of tree root systems in response to wind action and site conditions. *Tree Physiol.* 16, 891–898. doi: 10.1093/treephys/16.11-12.891

Oliver, W. W., and Ryker, R. A. (1990). "*Pinus ponderosa* Dougl. ex Laws., Ponderosa pine" in *Silvics of North America, volume 1, conifers. Agriculture Handbook*. eds. R. M. Burns and B. H. Honkala (Washington, DC: U.S. Department of Agriculture, Forest Service), 654, 413–424.

Omdal, D. W., Jacobi, W. R., and Shaw, C. G. III (2001). Estimating large-root biomass from breast-height diameters for ponderosa pine in northern New Mexico. *West. J. Appl. For.* 16, 18–21. doi: 10.1093/wjaf/16.1.18

Parrotta, J. A., Wildburger, C., and Mansourian, S. (eds.) (2012). *Understanding relationships between biodiversity, carbon, forests and people: The key to achieving REDD + objectives. World series.* Vol. 31, (Vienna: International Union of Forest Research Organizations).

Pawson, S. M., Brin, A., Brockerhoff, E. G., Lamb, D., Payn, T. W., Paquette, A., et al. (2013). Plantation forests, climate change and biodiversity. *Biodivers. Conserv.* 22, 1203–1227. doi: 10.1007/s10531-013-0458-8

Pradal, C., Boudon, F., Nouguier, C., Chopard, J., and Godin, C. (2009). PlantGL: a python-based geometric library for 3D plant modelling at different scales. *Graph. Model.* 71, 1–21. doi: 10.1016/j.gmod.2008.10.001

Puhe, J. (2003). Growth and development of the root system of Norway spruce (*Picea abies*) in forest stands—a review. *For. Ecol. Manag.* 175, 253–273. doi: 10.1016/S0378-1127(02)00134-2

Quine, C. P., and Gardiner, B. A. (2007). "Understanding how the interaction of wind and trees results in windthrow, stem breakage and canopy gap formation" in *Plant disturbance ecology: The process and the response*. eds. E. Johnson and K. Miyanishi (Amsterdam: Elsevier Academic Press), 103–156.

Ray, D., and Nicoll, B. C. (1998). The effect of soil water-table depth on root-plate development and stability of Sitka spruce. *Forestry* 71, 169–182. doi: 10.1093/forestry/71.2.169

Rellán-Álvarez, R., Lobet, G., and Dinneny, J. R. (2016). Environmental control of root system biology. *Annu. Rev. Plant Biol.* 67, 1–26. doi: 10.1146/annurev-arplant-043015-111848

Ruel, J. C. (1995). Understanding windthrow: silvicultural implications. *For. Chron.* 71, 434–445. doi: 10.5558/tfc71434-4

Schroth, G. (1998). A review of belowground interactions in agroforestry, focusing on mechanisms and management options. *Agrofor. Syst.* 43, 5–34. doi: 10.1023/A:1026443018920

Scippa, G. S., Di Michele, M., Di Iorio, A., Costa, A., Lasserre, B., and Chiatante, D. (2006). The response of *Spartium junceum* roots to slope: anchorage and gene factors. *Ann. Bot.* 97, 857–866. doi: 10.1093/aob/mcj603

Seidl, R., Spies, T. A., Peterson, D. L., Stephens, S. L., and Hicke, J. A. (2016). Searching for resilience: addressing the impacts of changing disturbance regimes on forest ecosystem services. *J. Appl. Ecol.* 53, 120–129. doi: 10.1111/1365-2664.12511

Smith, W. K. (1985). "Montane forests" in *Physiological ecology of North American plant communities*. eds. B. F. Chabot and H. A. Mooney (New York: Chapman & Hall), 95–126.

Soil Survey Staff (2013). Available at: https://soilseries.sc.egov.usda.gov/OSD_Docs/V/VASSAR.html (Accessed January 24, 2019).

Sorgonà, A., Proto, A. R., Abenavoli, L. M., and Di Iorio, A. (2018). Spatial distribution of coarse root biomass and carbon in a high-density olive orchard: effects of mechanical harvesting methods. *Trees* 32, 919–931. doi: 10.1007/s00468-018-1686-z

Stanturf, J. A., Palik, B. J., Williams, M. I., Dumroese, R. K., and Madsen, P. (2014). Forest restoration paradigms. *J. Sustainable For.* 33, S161–S194. doi: 10.1080/10549811.2014.884004

Stokes, A. (1999). Strain distribution during anchorage failure of *Pinus pinaster* at different ages and tree growth response to wind-induced root movement. *Plant Soil* 217, 17–27. doi: 10.1023/A:1004613126353

Stokes, A. (2002). "Biomechanics of tree root anchorage" in *Plant roots: The hidden half.* 3rd Edn. eds. Y. Weisel, A. Eshel and U. Kafkafi (New York: Marcel Dekker), 175–186.

Stokes, A., Atger, C., Bengough, A. G., Fourcaud, T., and Sidle, R. C. (2009). Desirable plant root traits for protecting natural and engineered slopes against landslides. *Plant Soil* 324, 1–30. doi: 10.1007/s11104-009-0159-y

Stokes, A., Ball, J., Fitter, A. H., Brain, P., and Coutts, M. P. (1996). An experimental investigation of the resistance of model root systems to uprooting. *Ann. Bot.* 78, 415–421. doi: 10.1006/anbo.1996.0137

Sun, H.-L., Lia, S.-C., Xiong, W.-L., Yang, Z.-R., Cui, B.-S., and Yang, T. (2008). Influence of slope on root system anchorage of *Pinus yunnanensis*. *Ecol. Eng.* 32, 60–67. doi: 10.1016/j.ecoleng.2007.09.002

Waring, R. H., and Schlesinger, W. H. (1985). *Forest ecosystems: Concepts and management*. San Diego, CA: Academic Press, Inc. 340.

Weaver, H. (1961). Ecological changes in the ponderosa pine forest of cedar valley in southern Washington. *Ecology* 42, 416–420. doi: 10.2307/1932097

Wenny, D. L., Liu, Y., Dumroese, R. K., and Osborne, H. L. (1988). First year field growth of chemically root pruned containerized seedlings. *New For.* 2, 111–118. doi: 10.1007/BF00027762

Western Regional Climate Center (2019). Prevailing wind direction. Available at: https://wrcc.dri.edu/Climate/comp_table_show.php?stype=wind_dir_avg (Accessed February 15, 2019).

Wright, C. S., and Agee, J. K. (2004). Fire and vegetation history in the eastern Cascade Mountains, Washington. *Ecol. Appl.* 14, 443–459. doi: 10.1890/02-5349

Yang, M., Défossez, P., Danjon, F., Dupont, S., and Fourcaud, T. (2016). Which root architectural elements contribute the best to anchorage of *Pinus* species? Insights from *in silico* experiments. *Plant Soil* 411, 275–291. doi: 10.1007/s11104-016-2992-0

Yang, M., Défossez, P., Danjon, F., and Fourcaud, T. (2014). Tree stability under wind: simulating uprooting with root breakage using a finite element method. *Ann. Bot.* 114, 695–709. doi: 10.1093/aob/mcu122

Zobel, R. W., and Waisel, Y. (2010). A plant root system architectural taxonomy: a framework for root nomenclature. *Plant Biosyst.* 144, 507–512. doi: 10.1080/11263501003764483

Conflict of Interest Statement: The authors declare that the research was conducted in the absence of any commercial or financial relationships that could be construed as a potential conflict of interest.

frontiers in Plant Science

ORIGINAL RESEARCH
published: 09 May 2019
doi: 10.3389/fpls.2019.00537

Frost Survival Mechanism of Vegetative Buds in Temperate Trees: Deep Supercooling and Extraorgan Freezing vs. Ice Tolerance

Gilbert Neuner, Kristina Monitzer, Dominik Kaplenig and Julia Ingruber*

Unit Functional Plant Biology, Department of Botany, University of Innsbruck, Innsbruck, Austria

In temperate climates, overwintering buds of trees are often less cold hardy than adjoining stem tissues or evergreen leaves. However, data are scarce regarding the freezing resistance (FR) of buds and the underlying functional frost survival mechanism that in case of supercooling can restrict the geographic distribution. Twigs of 37 temperate woody species were sampled in midwinter 2016 in the Austrian Inn valley. After assessment of FR, infrared-video-thermography and cryo-microscopy were used to study the freezing pattern in and around overwintering vegetative buds. Only in four species, after controlled ice nucleation in the stem (−1.6 ± 0.9°C) ice was observed to immediately invade the bud. These buds tolerated extracellular ice and were the most freezing resistant (−61.8°C mean LT_{50}). In all other species (33), the buds remained supercooled and free of ice, despite a frozen stem. A structural ice barrier prevents ice penetration. Extraorgan ice masses grew in the stem and scales but in 50% of the species between premature supercooled leaves. Two types of supercooled buds were observed: in temporary supercooling buds (14 species) ice spontaneously nucleated at −20.5 ± 4,6°C. This freezing process appeared to be intracellular as it matched the bud killing temperature (−22.8°C mean LT_{50}). This response rendered temporarily supercooled buds as least cold hardy. In 19 species, the buds remained persistently supercooled down to below the killing temperature without indication for the cause of damage. Although having a moderate midwinter FR of −31.6°C (LT_{50}), some species within this group attained a FR similar to ice tolerant buds. The present study represents the first comprehensive overview of frost survival mechanisms of vegetative buds of temperate trees. Except for four species that were ice tolerant, the majority of buds survive in a supercooled state, remaining free of ice. In 50% of species, extraorgan ice masses harmlessly grew between premature supercooled leaves. Despite exposure to the same environmental demand, midwinter FR of buds varied intra-specifically between −17.0 and −90.0°C. Particularly, species, whose buds are killed after temporary supercooling, have a lower maximum FR, which limits their geographic distribution.

Keywords: freeze dehydration, freezing pattern, freezing resistance, ice nucleation, stem cells, supercooling, translocated ice, vegetative buds

OPEN ACCESS

Edited by:
Guenter Hoch,
Universität Basel, Switzerland

Reviewed by:
Seizo Fujikawa,
Hokkaido University, Japan
YeonKyeong Lee,
Norwegian University of Life Sciences, Norway

****Correspondence:***
Gilbert Neuner
gilbert.neuner@uibk.ac.at

Specialty section:
This article was submitted to Functional Plant Ecology, a section of the journal Frontiers in Plant Science

Received: *05 February 2019*
Accepted: *08 April 2019*
Published: *09 May 2019*

Citation:
Neuner G, Monitzer K, Kaplenig D and Ingruber J (2019) Frost Survival Mechanism of Vegetative Buds in Temperate Trees: Deep Supercooling and Extraorgan Freezing vs. Ice Tolerance. Front. Plant Sci. 10:537. doi: 10.3389/fpls.2019.00537

INTRODUCTION

In temperate woody plants, vegetative buds are often less cold hardy than adjoining stem tissues and evergreen leaves (Bannister and Neuner, 2001). Additionally, buds have been reported to survive freezing by various frost survival mechanisms (Sakai and Larcher, 1987). Buds of temperate conifers have been shown to survive by deep supercooling and extraorgan freezing (Ishikawa and Sakai, 1982; Sakai, 1982), except for *Pinus* species. Buds of pines were shown to exhibit extracellular freezing (Sakai and Eiga, 1985; Quamme, 1995; Ide et al., 1998). While reproductive buds of many angiosperms exhibit deep supercooling (Quamme, 1995), their vegetative buds, based upon previous studies, have been suggested to survive freezing temperatures 10 to 15°C lower than reproductive buds, by undergoing extracellular freezing (Sakai and Larcher, 1987). Exceptions, however, have been reported (*Pyrus syriaca*: Rajashekar and Burke, 1978) and more recently added (*Acer japonicum*: Ishikawa et al., 1997; *Malus domestica*: Pramsohler and Neuner, 2013; *Alnus alnobetula*: Neuner et al., 2019).

Ice formation and concomitant extracellular freezing do not occur in the buds that exhibit extraorgan freezing. Rather intra- and extracellular water in the buds remains supercooled down to a critical freezing temperature, at which the buds are injured. While the bud tissues are supercooling, water migrates from the cells to locations that lie outside of the bud, such as the subtending stem or the bud scales. In *A. alnobetula*, ice masses can even form inside the bud between the premature leaves (Neuner et al., 2019). This process of external formation of ice masses and subsequent freeze dehydration of the bud tissues has been termed extraorgan freezing (Ishikawa and Sakai, 1982; Sakai, 1982). Three types of extraorgan freezing have been differentiated by Sakai and Larcher (1987), based on the extent of freeze dehydration and the maximum frost hardiness of the bud. *Type I* buds are very dehydration-tolerant and, under proper conditions, can dehydrate until no freezable water remains. Such buds can survive liquid nitrogen temperatures. Lateral buds of *A. japonicum* have been shown, using NMR micro imaging, to belong to *Type I* (Ishikawa et al., 1997). *Type II* buds are not fully freeze dehydration-tolerant and become frost damaged between −35 and −50°C. Apple buds could be assigned to *Type II* based on studies using infrared differential thermal analysis (IDTA) (Pramsohler and Neuner, 2013). *Type III* buds remain only partially dehydrated. Instead, freezable water remains inside the bud cells, the cells are killed when temperatures fall below the supercooling ability of the buds (−25 to −30°C), and intracellular ice formation occurs. *Type III* extraorgan freezing has been experimentally proven in the buds of several conifers and in the reproductive buds of many temperate woody angiosperms (Sakai and Larcher, 1987; Quamme, 1995). In contrast, until now only a few vegetative buds of woody angiosperm species have been classified as *Type III* (*P. syriaca*: Rajashekar and Burke, 1978; terminal buds of *A. japonicum*: Ishikawa et al., 1997). In general, experimental evidence on the frost survival mechanism of overwintering vegetative buds of woody angiosperms is scarce.

The freezing processes in and around buds can be determined using differential thermal analysis (DTA). Upon freezing of extracellular water in the stem, a high-temperature exotherm (HTE) representing the release of heat as water changes from a liquid to a solid phase (Burke et al., 1976) is recorded in buds. In supercooling buds, additionally, freezing of supercooled intracellular water is evidenced by a low-temperature exotherm (LTE). This freezing event is associated with the death of the bud cells, which was first demonstrated by Graham and Mullin (1976) in the reproductive buds of *Rhododendron*. Using DTA, the reproductive buds of several woody angiosperms were subsequently shown to survive freezing temperatures by supercooling (*Type III*, Sakai and Larcher, 1987). LTEs could not be detected, however, in the small reproductive buds in other species, hence their frost survival mechanism remained ambiguous (Sakai and Larcher, 1987). Bud size may have also limited the ability to detect LTEs in the DTA of vegetative buds of many other angiosperms listed by Sakai and Larcher (1987). These limitations can be overcome using more sensitive technologies, such as ^{1}H-nuclear magnetic resonance (NMR) microscopy (Ishikawa et al., 1997; Price et al., 1997; Ide et al., 1998) or IDTA (Neuner and Kuprian, 2014; Wisniewski et al., 2015). IDTA has recently been used to study the overall freezing response, i.e., ice nucleation, propagation, and supercooling, within and around overwintering buds of *P. abies* (Kuprian et al., 2017, 2018). In contrast to NMR microscopy (Ishikawa et al., 1997), which can observe freezing phenomena at a high level of resolution, IDTA demonstrated that the buds of *P. abies* remain free of ice despite the presence of ice in the subtending stem. Ice entrance into the bud was impeded by a bowl-like ice barrier tissue that prevents ice propagation into the supercooled bud. Cryo-microscopic inspection revealed the growth of large extraorgan ice masses in the adjoining stem below (Kuprian et al., 2017). A breakdown of supercooling was observed to occur at −18°C, triggered by an intrinsic ice nucleation event inside the bud while the ice barrier remained intact. Freezing of the bud cells proceeded within seconds and matched the frost killing-temperature, and as a result, the ice formation was suggested to be intracellular.

Based on the findings regarding the frost survival mechanism of buds of *P. abies,* the objective of the present study was, after assessment of FR, to utilize IDTA and cryo-microscopy to study the freezing response in overwintering buds of other temperate woody plants, particularly vegetative buds of angiosperms, which have not been extensively examined.

We wanted to obtain a more comprehensive understanding of the functional frost survival mechanisms of overwintering buds of temperate trees by studying the freezing pattern in and around vegetative buds. While functional frost survival mechanisms of vegetative buds are quite well understood in conifers, they are not in angiosperms. Based on individual findings (Rajashekar and Burke, 1978; Ishikawa et al., 1997; Neuner et al., 2019), we hypothesized that the majority of vegetative angiosperm buds may not be ice tolerant. In case of supercooled buds, we aimed to determine whether, and how lethal, freezing is initiated in the supercooled bud tissue and where translocated ice masses preferentially form. Further, we hypothesized that midwinter bud

FR should be related to the functional frost survival strategy of overwintering buds that may define maximum bud FR. Additionally, we expected little intra-specific variation between bud FR from trees exposed to the same environmental demand.

MATERIALS AND METHODS

Plant Material

Buds of 37 woody plant species were investigated (**Supplementary Table 1**). Twigs ∼40 cm in length were collected in the Inn Valley close to the city of Innsbruck, Austria. Stems were typically obtained from at least three individual plants, except in the case of ornamental species, where samples were taken from a single individual. The twigs were immediately transported to the Institute of Botany in Innsbruck. Samples collected in midwinter, from 7 Jan to 23 Feb 2016, were immediately subjected to measurements and observations or stored in a cold room at 4°C for no more than 3 days. Twigs collected between 24 Feb and 2 Mar 2016 were wrapped in wet paper towels placed inside sealed plastic bags and stored in a laboratory freezer at −5°C until they were used in the experiments. Terminal buds were used in all of the experiments. Air temperature in winter 2015/16 is shown in **Supplementary Figure 1**.

Differential Thermal Analysis

Differential thermal analysis (DTA) was conducted according to Burke et al. (1976) using an improved measurement procedure detailed in Kuprian et al. (2017). Computer-controlled freezing treatments were conducted in a laboratory freezer (Profiline Taurus 0986, National Lab, Mölln, Germany). Temperature control in the freezer compartment, which was set at a constant low temperature, was regulated using internal heaters controlled by temperature measurement and control software (programmed in Lab View by O. Buchner). Continuous ventilation by a ventilator (Sunon, Sunonwealth Electronic Machine Industry Co., Kaohsiung, Taiwan) inside the freezing compartment provided uniform temperature conditions. DTA measurements of living and dead (oven-dried at 80°C for 3 d) bud samples were conducted using thermocouples (Type-T) connected to a data logger (CR10, Campbell Scientific Inc., Utah, USA). Temperatures were recorded every 10 s and stored on an external storage device (SM4M Storage Modul, Campbell Scientific Inc., Utah, USA).

Twig segments (3 cm) bearing a terminal bud were excised from collected twigs. Typically, 17 samples per species were prepared for DTA. All lateral buds were removed. The solder junction of a thermocouple was fixed to the surface of the outermost bud scales of the investigated bud with a thermally conducting, self-adhesive pad (Laird Technologies, Earth City, Missouri, USA). Additionally, a 1 cm incision was made with a razor blade on the side of the stem opposite of the bud. A length of wetted sisal yarn was inserted into this incision and fixed with a knot. The bud and surrounding pad were then wrapped in aluminum foil and inserted into wells (6 to 10 mm in diameter) that had been drilled into aluminum cylinders (diameter 10 cm, height 10 cm). Dead bud samples of the same size as the living samples were similarly prepared to use as a reference. The free ends of the sisal yarns were then bundled and placed into a small beaker filled with water containing ice nucleation active (INA) bacteria (*Pseudomonas syringae* van Hall 1902) that was itself immersed in a plastic tray filled with an ice slurry. Altogether, the aluminum cylinders with the inserted samples, the bundled sisal yarn, and the plastic tray containing the ice slurry and INA solution were then transferred into the freezing compartment of the freezer. All parts were thoroughly covered with wetted paper towels and enveloped in plastic film (food wrap). This prevented drying of the sisal yarn inside the ventilated freezing compartment. After initially precooling the samples at 5°C for 45 min, a controlled temperature program was initiated with a cooling rate of −5 K/h. Ultimate target low temperatures depended on the frost killing temperature of the investigated buds, which was between −45 and −80°C.

The recorded temperature data were transferred to a computer and the temperature differential between the living and dead buds was determined by subtraction of the temperature of the dead reference sample bud from the temperature of living buds (Microsoft Office Excel, Microsoft Corporation, Redmond, USA). The differential temperature was then plotted against the temperature of the dead sample. Freezing events in the live buds could then be observed as peaks rising from a flat base line. A high-temperature exotherm (HTE), originating from the freezing of extracellular water in the stem and bud scales (triggered by INA bacteria), and a low-temperature exotherm (LTE) that originates from lethal freezing of supercooled, intracellular water inside the bud cells, could be determined in the DTA plots.

Infrared Differential Thermal Analysis (IDTA)

The temperature-controlled freezer employed in the DTA measurements was also used to conduct IDTA of the samples. Sample temperatures were also recorded with six thermocouples. Bud infrared images were recorded using FLIR S60 or FLIR T650sc (FLIR Systems, Oregon, USA) infrared cameras during successive lowering of the temperature by −4 K/h down to below the frost killing temperature of the investigated bud. Depending on the number of samples or the size of the investigated buds, either no close-up lens or a 25 μm or 50 μm close-up lens (FLIR Systems, Oregon, USA) was used. Infrared cameras were either used from outside the freezer where the sample could be viewed through an infrared permeable inspection window (10 x 10 x 0.5 cm glass made of zinc oxide, ZnS clear grade; Vitron, Jena-Maua, Germany) or the whole camera was put inside a thermally insulated plastic box and used inside the freezer (Neuner and Kuprian, 2014). Fifteen images per second were recorded and subsequently stored as image sequences on a PC.

One to five ca. 3 cm-long twig pieces bearing a terminal bud were cut off from random branch samples collected from the different species. These twig pieces were then sectioned longitudinally with a razor blade to obtain better visibility of the overall freezing pattern. Preliminary tests using intact and longitudinally dissected twig pieces indicated that no major changes in the freezing response occurred as a result of the

sectioning (data not shown). The bark side of the sectioned twig was then fixed to a thermally conducting, self-adhesive pad (Laird Technologies, Earth City, Missouri, USA) that had been mounted on a lifting plate in order to horizontally orient the cut surface of the twig piece. Six thermocouples were mounted all around but not attached to the twig sample at a 1 mm distance from each other in order to determine the sample temperature. A small ventilator (20 × 20 mm) was positioned on the side of the sample to ensure a homogenous temperature distribution on the surface of the investigated sample. The HTE was triggered by use of INA bacteria via sisal yarn (as in DTA) that was fixed to an incision in the stem opposite of the bud. The mounted bud samples were placed into a temperature-controlled freezer, and the infrared camera was focused onto the cut surface of a single twig piece when a close-up lens was employed or on the cut surface of all 15 twig pieces at once when the close-up lens was not employed.

Infrared images and video sequences were further processed using FLIR ResearchIR Max software (FLIR Systems, Oregon, USA). The thermal data of whole video sequences could be subtracted from immediately before the onset of a freezing process using this software to obtain IDTA images (Hacker and Neuner, 2007). This greatly enhanced the ability to detect where ice nucleation occurred and how it propagated. It also provided the ability to determine which, if any, tissues remained supercooled and free of ice. Relevant images were then extracted to illustrate the freezing pattern in and around buds in image plates (PowerPoint, Microsoft Corporation, Redmond, USA).

Cryo-Microscopy

For cryo-microscopic investigation, twigs were exposed in the cooling compartment of the same temperature-controlled freezer as described above. The freezing treatment started at +5°C and was followed by a cooling rate of −3 K/h down to −10°C. The samples remained at −10°C for ∼20 h before the frozen buds still inside the cooling compartment of the freezer were longitudinally dissected with a pre-cooled razor blade. For cryo-microscopic inspection, a light microscope (SZX12, Olympus Austria GmbH., Vienna, Austria) was mounted inside the same freezing compartment. By this, the dissected buds could be immediately placed on the microscope stage that had an equal temperature (−10°C) as the sample. The dissected buds could then be inspected for places where extraorgan ice masses had grown around and inside the bud and where tissues remained free of ice.

Freezing Resistance of Buds

Freezing resistance (FR) of buds was investigated by exposing whole twigs to a set of different freezing temperatures, thus simulating low temperature stresses of various degrees. Twigs were cut to ∼10 cm in length. Twigs bearing at least 10 buds were then put into sealable plastic bags (16.5 × 25 cm) that contained a layer of wet paper towels. Controlled freezing treatments were conducted inside the freezing compartment of computer-controlled laboratory freezers (Profiline Taurus 0986, National Lab, Mölln, Germany and GT 2102, Liebherr, Lienz, Austria) as described above. One control sample was maintained at 4°C throughout the experiment. After an initial settling time of 45 min at 5°C, samples were cooled at a rate of −5 K/h down to five different target temperatures (−10, −20, −30, −40, and −50°C) and held for 5 h. Subsequent warming also occurred at a rate of +5 K/h. All samples then remained under moderate illumination (40 μmol photons $m^{-2}s^{-1}$) at room temperature for 1 week. Twigs were then removed from the plastic bags and the buds were longitudinally dissected for visual inspection of frost injury. The degree of frost damage to the bud was ranked in three different classes: no damage, partial damage (50%), and total loss (100%). The percent of frost damage was then plotted against the target temperature and a logistic function (Boltzmann function) was fitted to the data using OriginPro 7G SR4 (OriginLab Corporation, Northhampton, MA, USA) software. The logistic function was used to assess LT_{50}, i.e., the temperature resulting in 50% lethality of the tissue.

Statistical Analysis

Mean values and standard error of HTE, LTE and LT_{50} of the investigated buds were calculated using IBM SPSS Statistics for Windows (Version 21.0. IBM Corp., Armonk, NY, USA). Differences between mean values of different species and bud types were tested with a one-way analysis of variance (ANOVA) and a subsequent Duncan *post hoc* test, homoscedasticity provided. In the case of a negative Levene test, the Mann–Whitney *U*-test was used as a non-parametric *post hoc* test. All analyses were conducted at a significance level of $p \leq 0.05$.

RESULTS

IDTA analysis provided the ability to directly observe the freezing pattern in and around buds, and to determine whether or not ice forms in the bud tissue. Three significantly different freezing patterns were observed. The first pattern, where ice immediately propagated from the surrounding tissue during the HTE into the bud, was observed in only four of the 37 examined species. This freezing pattern was exhibited in *Pinus cembra* buds and is shown in **Figure 1A** (**Supplementary Video 1**). This freezing pattern was also seen in *Pinus sylvestris* and two angiosperm species, *Sambucus nigra*, and *Elaeagnus rhamnoides*. In the majority (33 out of 37, or 89.2%) of the tested species, the bud tissue remained free of ice during the occurrence of the HTE (**Table 1**). The initial ice wave stopped below the bud, and the bud cells remained ice-free in a supercooled state. Propagation of ice from the stem into the bud was inhibited by an ice barrier in the tissue between the stem and the bud. Two types of supercooling buds were observed. In one group, a second freezing event occurred at a much lower freezing temperature than the HTE and, in addition to the infrared observations, was recorded in the DTA as a low-temperature exotherm (LTE). IDTA indicated that the LTE was localized and originated from within the bud itself. This pattern of freezing is exemplified in *Acer platanoides* (**Figure 1B**, **Supplementary Video 2**). The LTE was triggered by an ice nucleation event inside the bud in all buds that exhibited temporary supercooling. A breakdown of the ice barrier, i.e., propagation of ice from the frozen stem below a critical threshold freezing temperature, was never observed. Once ice formation was initiated in a single spot

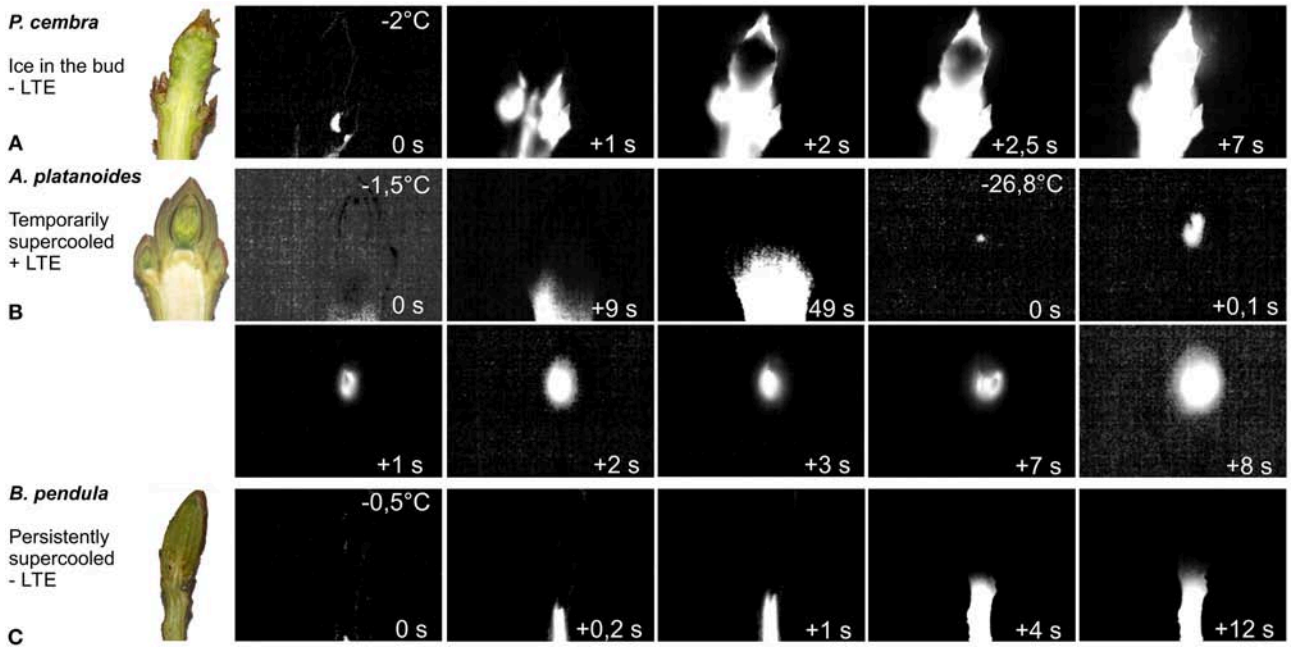

FIGURE 1 | Digital color image (left) of longitudinally sectioned shoots bearing vegetative buds prior to freezing (enlarged images: **Supplementary Figure 2**) and IDTA images of the buds during controlled freezing at 4 K/h. Images were obtained at temperatures indicated in the upper right corner. **(A)** *P. cembra,* an example of buds that exhibit extracellular freezing (**Supplementary Video 1**). **(B)** *A. platanoides*: buds that exhibit supercooling. Initial ice formation occurs at −1.5°C below the bud in the adjoining stem but does not enter the bud (**Supplementary Video 2**). More than 6 h later, below a certain critical threshold temperature (−26.8°C), an ice nucleation event inside the bud triggers intracellular lethal freezing of all of the bud cells within 8 s (**Supplementary Video 3**). **(C)** *B. pendula*: buds supercool after the initial freezing of the surrounding tissue at −0.5°C, which stops below the bud (**Supplementary Video 4**). No further freezing process is detected, even at temperatures below the frost killing temperature. Freezing exotherm temperatures are indicated in the top right corner of each image. The time span during each freezing exotherm (in seconds) is indicated in the bottom right corner.

(tentatively a single cell), ice spread rapidly throughout the whole bud within seconds (**Supplementary Video 3**). In the second group of supercooled buds, no distinct LTE could be detected despite cooling the buds below the temperature at which the buds are killed. This freezing pattern of persistently supercooled buds, without the occurrence of a distinct LTE, is exemplified by the freezing response of *Betula pendula* (**Figure 1C**, **Supplementary Video 4**).

Although DTA does not allow one to determine the location where ice forms in tissues, it is very sensitive and can detect small freezing events. When properly configured, it also allows one to measure a considerable number of buds as replicates at the same time. HTEs in buds of the 37 species were detected at a mean freezing temperature of −1.6 ± 0.9°C (SD). The temperature of the HTE varied slightly among the tested species (**Table 1**). Collectively, HTEs occurred between −0.5°C in *Fagus sylvatica* and −3.2°C in *Celtis occidentalis*. In the majority of the species (73%), however, water in stem tissues froze extracellularly between −1.0 and −2.1°C. Buds that exhibited an absence of any supercooling exhibited a mean HTE that occurred at a slightly but significantly higher freezing temperature (−1.2°C) than in the other bud types. Buds that exhibited supercooling, but no LTE, had a mean HTE of −1.5°C; meanwhile, while buds that exhibited temporary supercooling and a LTE had a mean HTE of −1.7°C. A distinct LTE could be detected by DTA analysis during controlled freezing in 14 (38%) of the examined species (**Figure 2**). These results corresponded with the results obtained by IDTA fully (**Table 1**). More specifically, intracellular freezing of the bud tissue could be visualized by IDTA at a temperature similar to the LTE detected during DTA. Mean values of the recorded LTEs ranged between −14.2°C (*Aesculus hippocastanum*) and −29.8°C (*Ilex aquifolium*) with an overall mean of −20.5 ± 4.6 SD°C. Mean ± SD of FR (LT_{50}) was −22.8 ± 4.4°C, and LTE temperatures correlated well with the FR (LT_{50}) of buds (**Figure 3**).

Representative DTA-plots that depict the three different freezing pattern types are shown in **Figure 4**. Buds of *S. nigra* freeze extracellularly during the occurrence of the HTE. The HTE in buds that did not supercool was typically a distinct, long-lasting exotherm in the DTA-plot. Buds of *A. hippocastanum* and *F. sylvatica* supercool but exhibit an LTE when the temperature falls below their ability to supercool. The HTE in supercooled buds that exhibit an LTE is distinct and can be similar (*A. hippocastanum*) or much shorter (*F. sylvatica*) than the HTE in buds that freeze extracellularly and do not supercool. LTEs in these buds were often short and pinnacle (*F. sylvatica*) freezing exotherms in the DTA but could also appear as a small hillock (*A. hippocastanum*), the latter indicating a slower freezing process. Lastly, buds that supercool but do not exhibit a distinct LTE are exemplified by *B. pendula*. The DTA-plot in these types of

TABLE 1 | The freezing pattern around and in buds of the 37 investigated woody species could be assigned to three different types by infrared differential thermal analysis (IDTA): *Type A* Extracellular ice formation during HTE in the bud (no ice barrier), *Type B* Temporarily supercooled and ice-free during HTE, but killed by spontaneous ice nucleation in the bud (with LTE) and *Type C* persistently supercooled and ice-free during HTE, but no ice formation down to below the frost killing temperature (no LTE).

Bud frost survival type	Plant species	HTE ± SE (°C)	LTE ± SE (°C)	FR (±SE,°C)	Bud FR (°C) after others	Extraorgan ice masses
Type A	*E. rhamnoides*	−1.4 ± 0.1	No	−41.3 ± 1.3		-
	P. cembra	−1.3 ± 0.1	No	−75.2 ± 4.9	−70,3[l]/−90[a]	-
	P. sylvestris	−1.2 ± 0.1	No	-	−70[b]/−90[a]	-
	S. nigra	−0.8 ± 0.1	No	-		-
Type B	*A. platanoides*	−1.1 ± 0.1	−23.6 ± 0.4	−32.5 ± 1.5	−40[b]	S/Sc
	A. pseudoplatanus	−1.2 ± 0.1	−22.4 ± 0.4	−23.8 ± 0.8	−25[b]	S/Sc*
	A. hippocastanum	−1.5 ± 0.1	−14.2 ± 0.6	−18.1 ± 0.2	−25[b]/−40[c]	Sc/L
	C. bignoniodes	−1.9 ± 0.2	−24.8 ± 0.2	-		L
	C. occidentalis	−3.2 ± 0.3	−21.6 ± 0.7	−25.0 ± 0.0		-
	C. mas	−1.5 ± 0.1	−22.3 ± 0.6	−24.0 ± 1.0	−30[b]	L
	C. monogyna	−0.7 ± 0.1	−17.7 ± 0.5	−17.0 ± 0.0		S/L
	F. sylvatica	−0.5 ± 0.1	−15.1 ± 0.4	−22.2 ± 2.3	−27[b]/−29.6[d]/−40[h]	Sc
	I. aquifolium	−1.3 ± 0.2	−29.8 ± 0.4	−28.0 ± 0.6	−18[b]	S/Sc/L
	J. regia	−2.1 ± 0.1	−15.9 ± 0.3	−17.7 ± 0.9	−18.5[e]	S
	L. tulipifera	−3.1 ± 0.2	−20.1 ± 0.1	−23.0 ± 0.6	−25[b]/−30[b]	S/Sc
	P. abies	−1.7 ± 0.2	−24.8 ± 0.2	−25.5 ± 1.1	−24,2[i]/−40[b]/−50[k]	S
	P. x hispanica	−2.7 ± 0.2	−17.5 ± 0.2	−21.5 ± 0.6	−30[b]	L
	R. ferrugineum	−1.4 ± 0.1	−15.3 ± 0.4	−17.7 ± 0.9	−25[c]	L
Type C	*A. incana*	−1.5 ± 0.1	No	−28.8 ± 1.3		L
	A. alnobetula	−1.2 ± 0.1	No	−42.5 ± 7.6	−50[g]/−45[i]	L
	B. pendula	−1.4 ± 0.2	No	−90.0 ± 3.3	−70[b]/−86.7[n]/−93.3[n]	L
	C. betulus	−1.0 ± 0.1	No	−25.7 ± 0.8	<-74[m]	L
	C. sativa	−3.0 ± 0.2	No	−22.0 ± 0.8	−27[f]	nd
	C. avellana	−1.0 ± 0.1	No	−23.7 ± 1.2	−31.9[m]	Sc
	E. europaeus	−1.4 ± 0.2	No	−19.0 ± 1.0		L
	L. anagyroides	−2.4 ± 0.3	No	−47.0 ± 0.4		nd
	M. nigra	−1.5 ± 0.2	No	−35.0 ± 0.0	−28.0[m]	L
	O. carpinifolia	−2.6 ± 0.2	No	−29.6 ± 3.0	−40[f]	L
	P. tremula	−1.1 ± 0.1	No	−32.0 ± 2.5	−42.4[m]	Sc/L
	P. avium	−1.6 ± 0.2	No	−20.0 ± 0.0	−30[o]	L
	Q. rubra	−1.3 ± 0.1	No	−20.8 ± 0.2	−30[b]	nd
	S. caprea	−0.7 ± 0.1	No	-	<-74[m]	nd
	S. helvetica	−1.0 ± 0.1	No	−48.1 ± 3.8	−59.9[m]	L**
	S. aucuparia	−2.8 ± 0.1	No	−32.2 ± 3.9	−40.4[m]	Sc
	T. cordata	−1.0 ± 0.1	No	−42.1 ± 1.7	<-70[b]	L
	U. glabra	−1.2 ± 0.1	No	−25.8 ± 0.8	<-70[b]	-
	V. lantana	−1.2 ± 0.1	No	−39.4 ± 0.7		S/L

Species are grouped accordingly. The table lists the species examined, the mean temperature (°C) of the high temperature exotherm (HTE) and the low temperature exotherm (LTE) as determined by differential thermal analysis (DTA) and mean midwinter FR (LT_{50}) of winter 2015/16, and the midwinter FR reported by other authors. For supercooling buds, locations of formation of extraorgan ice masses are additionally shown: S, subtending stem; Sc, inside bud scales; L, between premature leaves; nd, not detectable; –, not examined.
*[a]Bannister and Neuner (2001); [b]Sakai (1982); [c]Sakai and Larcher (1987); [d]Hofmann et al. (2015); [e]Charrier et al. (2013); [f]Filippi (1986), [g]Benowicz et al. (2000); [h]Lenz et al. (2016); [i]Neuner et al. (2019); [j]Kuprian et al. (2017); [k]Beuker et al. (1998); [l]Buchner and Neuner (2011); [m]Schiffmann (2017); [n]Riikonen et al. (2013); [o]Vitra et al. (2017); *Dereuddre (1979); **between innermost scale and leaves.*

buds is characterized by a short but distinct HTE and the absence of any LTE.

Under the winter conditions of 2015/16, buds did not frost harden to the midwinter maximum reported in the literature, but differences in FR of functional groups was similar (**Figure 5**). The most frost hardy, with a mean midwinter LT_{50} of −61.8°C, were buds that exhibited ice tolerance. Temporarily supercooled buds that exhibited an LTE, with some exceptions, were the least frost hardy, exhibiting a mean LT_{50} of −22.8°C. Buds that supercooled but that did not exhibit an LTE exhibited an intermediate level of FR (LT_{50} −31.6°C). Some species within this group, however, were very frost susceptible, such as *Euonymus europaeus* with an LT_{50} of −19.0°C, while others, such as *B. pendula,* exhibited a level of FR similar to buds that froze extracellularly and did not supercool or exhibit an LTE.

In supercooling buds, formation of extraorgan ice masses was monitored by cryo-microscopy (**Table 1**). At −10°C in the

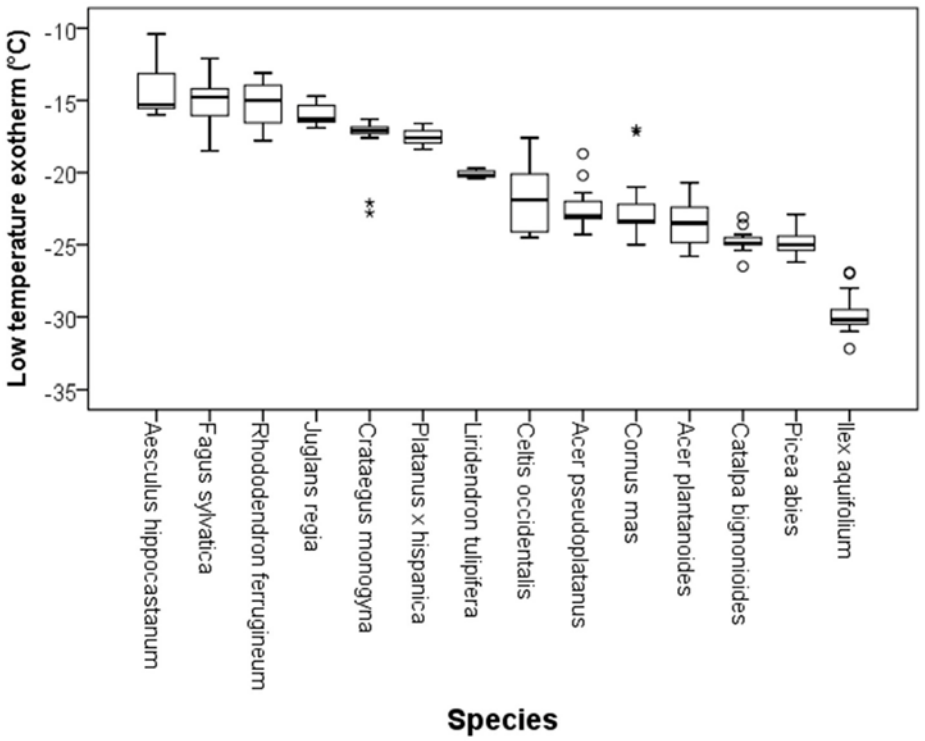

FIGURE 2 | Variability in the temperatures at which low temperature exotherms (LTEs, °C) were detected by DTA in temporary supercooled buds of excised twigs of different species ($N = 17$). Ice nucleation during LTE was always initiated inside the bud. The box plots indicate the median (= second quartile; line inside the box) and extend from the first to the third quartile. The whiskers indicate at maximum the 1.5-fold interquartile range. Outliers are shown as dots, extreme outliers as stars.

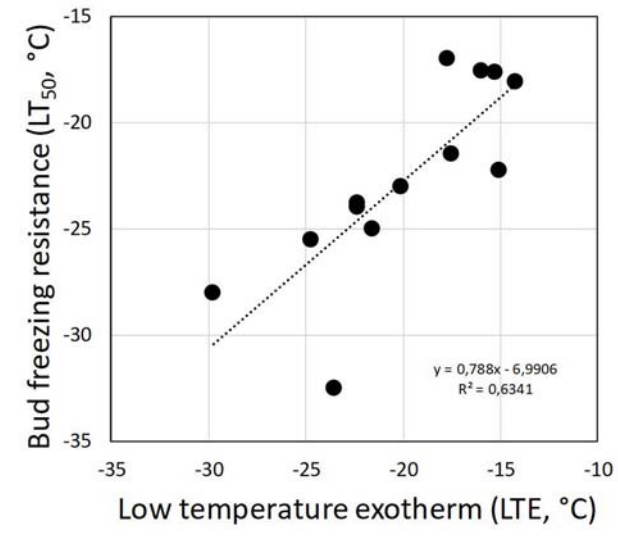

FIGURE 3 | Correlation between the detected low-temperature exotherms (LTEs, °C) in temporary supercooled buds and measured FR (LT_{50}, °C).

majority of the investigated species, extraorgan ice masses could be detected either in the adjoining stem (**Figure 6A**), in the bud scales (**Figure 6B**) or inside the bud around the premature leaves (**Figures 6C,D**). The exceptions were four species with persistently supercooling buds (*Castanea sativa, L. anagryoides, Quercus rubra, Salix caprea*), where no large ice masses could be found inside or in close vicinity to the bud (**Figure 6E**). In 50% of all tested species, translocated ice masses formed exclusively around the premature leaves inside the bud. While in DTA, no freezing exotherms were detectable during formation of translocated ice between the premature leaves, in some species in IDTA occasionally exiguous freezing processes were recorded (e.g., *A. alnobetula*: Neuner et al., 2019). In temporarily supercooled buds, no preferential location of ice masses could be found (**Figure 7**). In persistently supercooled buds, except for the species lacking ice masses, ice crystals mostly could be found close to premature leaves, but in *Populus tremula* and *Corylus avellana* they could additionally be found in the scales and in *Viburnum lantana* additionally in the stem—and only in *Sorbus aucuparia* was ice exclusively seen in the bud scales.

DISCUSSION

Frost Survival Mechanisms of Vegetative Buds

Extracellular Freezing of Buds (Type A)

Vegetative buds that freeze extracellularly, i.e., Type A buds, have not been experimentally proven until now in angiosperms (Sakai and Larcher, 1987) but have been found in *S. nigra* and *E. rhamnoides*. Interestingly, reproductive buds in *Sambucus*

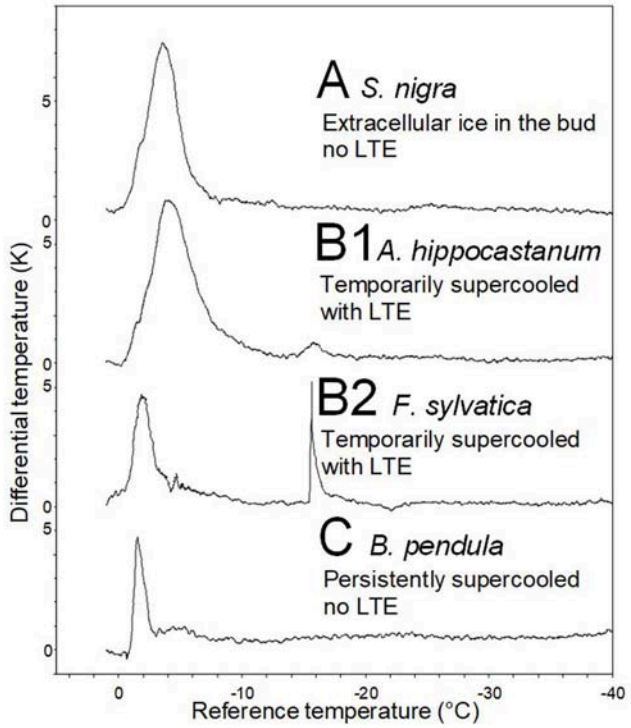

FIGURE 4 | Representative differential thermal analysis plots (DTA-plots) obtained from buds during controlled freezing treatments (cooling rate: 5 K/h). Three freezing patterns could be distinguished by the DTA-plots: **(A)** *S. nigra,* whose buds freeze extracellularly during HTE, **(B1)** *A. hippocastanum* and **(B2)** *F. sylvatica,* whose buds supercool temporary but freeze intracellularly at some critical threshold temperature as indicated by the low temperature exotherm (LTE), and **(C)** *B. pendula,* where buds also supercool but do not freeze intracellularly (No LTE).

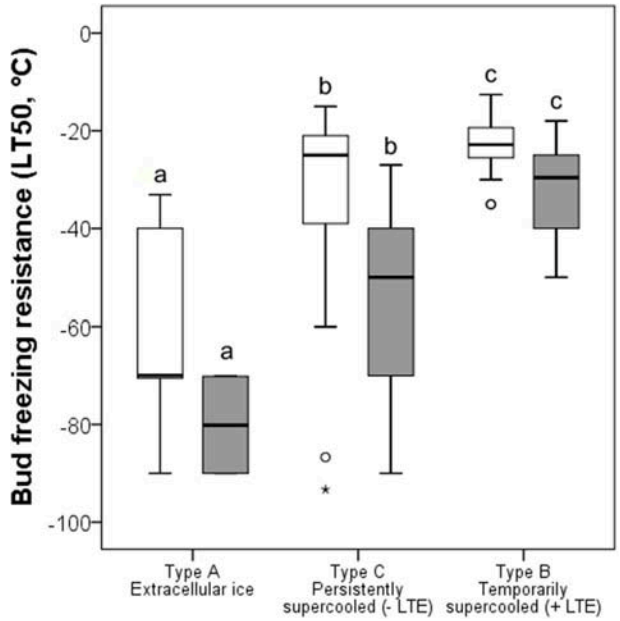

FIGURE 5 | Comparison of bud FR (LT_{50}, °C) determined (white bars) in the current study and (gray bars) by other authors (see **Table 1**) grouped by contrasting frost survival mechanisms: *Type A* extracellular freezing (ice tolerant), *Type B* temporarily supercooled with the occurrence of intracellular freezing as evidenced by an LTE, and *Type C* persistently supercooled without lethal intracellular freezing (no LTE). The box plots indicate the median (= second quartile; line inside the box) and extend from the first to the third quartile. The whiskers indicate, at maximum, the 1.5-fold interquartile range. Outliers are shown as dots, extreme outliers as stars. The significance of difference between bud FR of different bud types is indicated by different letters ($P < 0.05$).

racemosa, in contrast to the many reproductive buds of angiosperm woody species (Ashworth, 1982, 1990; Quamme, 1995), also did not exhibit an LTE (Ishikawa and Sakai, 1982); this suggests that another FR mechanism exists other than deep supercooling. With respect to conifers, the results obtained in *P. cembra* and *P. sylvestris* corroborate earlier findings that buds of pines survive by extracellular freezing (Sakai and Eiga, 1985; Price et al., 1997; Ide et al., 1998). Buds that only exhibit extracellular freezing with an absence of any supercooling were the most frost hardy, corroborating earlier reports on the FR of *P. cembra* and *P. sylvestris* that exhibited a maximum FR at midwinter of −90°C (Sakai and Okada, 1971). Opposed to other conifers that have buds that supercool (Quamme, 1995), in pines, ice forms in the buds at the same time when ice forms in subtending stem tissues, and no supercooling occurs (Ide et al., 1998). In contrast to other *Pinaceae*, such as *Abies* (Sakai, 1978; Ide et al., 1998) and *Picea* (Sakai, 1979; Kuprian et al., 2017, 2018), pines also do not have crown tissue at the base of the bud, which serves as an ice barrier that keeps the bud free of ice. Similar to pines, the two angiosperms examined in the present study, *S. nigra* and *E. rhamnoides,* also do not have structural barriers that impede ice propagation from the stem into the bud. Additionally, a barrier against extrinsic ice nucleation from the bud surface does not appear to exist in buds that exhibit extracellular freezing. *S. nigra* buds for instance differ from other buds as they lack a compact, tight coverage of buds by layers of bud scales. In supercooling buds, an impermeable ice barrier can be brought about by a sophisticated bud scale architecture (*P. abies,* Kuprian et al., 2017) or, as only recently reported, by surface impregnation with lipophilic substances (Neuner et al., 2019).

Ice nucleation was triggered in the stem by the use of ice-nucleation-active (INA) bacteria. It is important to artificially nucleate the twig samples, as otherwise ice nucleation would occur at much lower freezing temperatures than those found in natural settings (data not shown). This has been recently demonstrated in *P. abies,* where ice nucleation in detached twigs does not occur at temperatures warmer than −8.4°C in the absence of INA bacteria. However, when INA bacteria are used, ice nucleation is triggered around −2.9°C (Kuprian et al., 2017). The temperature range (−0.5 to −3.2°C), wherein HTEs occurred in the detached twigs of the 37 species examined in the present study, was similar to the range of temperatures within which ice nucleation has been reported to occur in intact woody plants in nature, i.e., > −3.4°C (Beck et al., 1982;

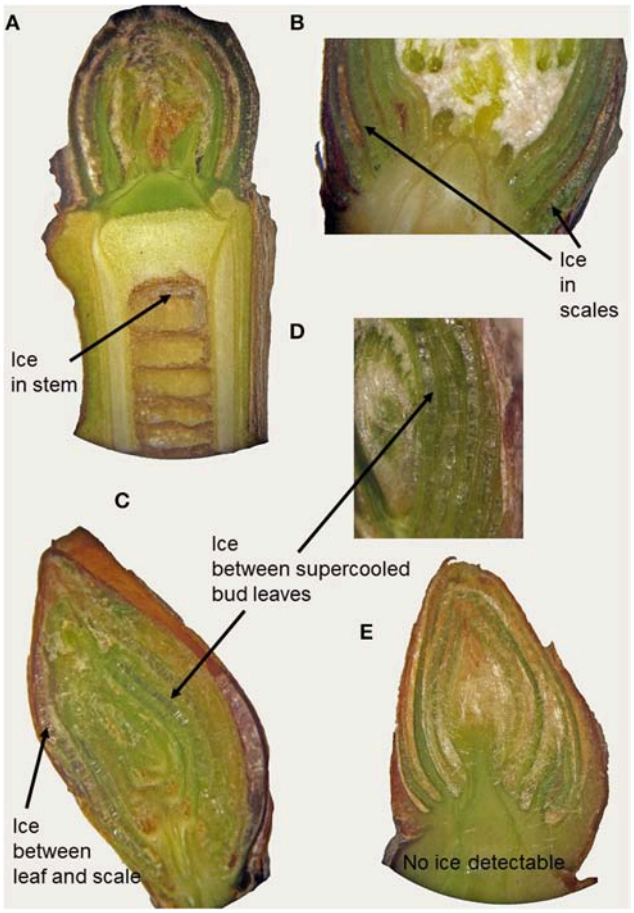

FIGURE 6 | By cryo-microscopy extra organ ice masses could be detected in different locations in buds sectioned longitudinally in the frozen state (−10°C). Ice was found either in **(A)** the subtending stem (*J. regia*), in **(B)** the bud scales (*A. hippocastanum*) or inside the bud around the premature leaves as in **(C)** *B. pendula* and in **(D)** *O. carpinifolia* or **(E)** no ice could be found inside the bud or in tissues in close vicinity to the bud.

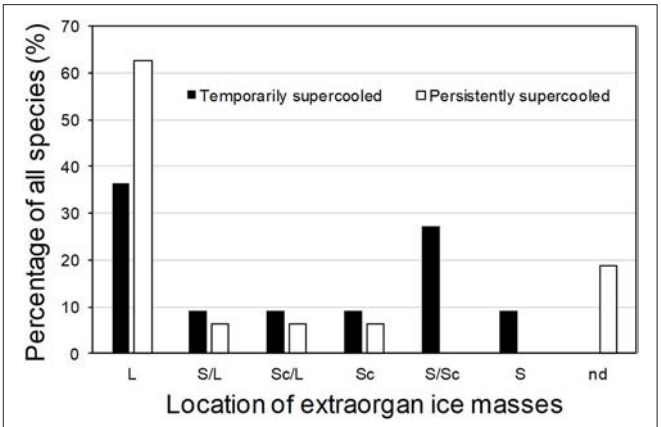

FIGURE 7 | In supercooled buds, translocated ice masses can be found either in (S) the adjoining stem, in (Sc) the bud scales or inside (L) the bud around the premature leaves. In some buds, (nd) no large ice masses could be found inside or in close vicinity to the bud. Percentage of all species using the respective locations for translocated ice masses are given for (■) temporarily supercooled and (□) persistently supercooled buds.

Ashworth and Davis, 1986; Mayr et al., 2006; Buchner and Neuner, 2011; Pramsohler et al., 2012). In nature, ice nucleation in stem tissues at relatively warm sub-zero temperatures appears to be advantageous. The water potential gradient from the liquid cellular water to the surrounding extracellular ice is temperature-dependent and increases significantly with decreasing temperature. Artificial supercooling could expose cells to a steep water potential gradient when ice forms that could potentially result in injury that otherwise would not be seen.

Buds Surviving Free of Ice

In the majority (89.2%) of the investigated species, buds remained free of ice during and after the HTE. Deviating from earlier expectations (Sakai and Larcher, 1987), most vegetative buds of angiosperms survive freezing temperatures free of ice, and this appears to be the general rule rather than the exception. Only a few reports have suggested this type of freezing response in vegetative buds of angiosperms, including *P. syriaca* (Rajashekar and Burke, 1978), *A. japonicum* (Ishikawa et al., 1997), and *M. domestica* (Pramsohler and Neuner, 2013). In contrast, this type of freezing response is generally accepted to be the major mechanism in most vegetative buds of conifers, with the exception of pines (Zwiazek et al., 2001).

Maintenance of an ice-free bud during and after the HTE requires the presence of external and internal ice barriers. Once ice has formed anywhere in the plant (in nature > -3.4°C) and comes into contact with xylem-conducting elements, it usually spreads rapidly (at high rates of up to 27 cm.s^{-1}) into all plant parts that are colder than 0°C. Furthermore, the ice is able to spread into areas that are not protected by an ice barrier (Wisniewski et al., 1997; Hacker and Neuner, 2007, 2008; Hacker et al., 2008). Therefore, an internal ice barrier that prevents the spread of ice into a bud is necessary. By IDTA, for all supercooling buds it could be shown that ice propagation from the frozen subtending stem into the bud is prevented by an internal ice barrier. Nevertheless, the bud also needs to be protected from extrinsic nucleation events that occur on the bud surface. These structural requirements may be met by a unique water/ice proof bud architecture where the scales and cuticle play an important role as an impermeable barrier (Kuprian et al., 2017) or by surface impregnation with lipophilic substances (triterpenoids and flavonoid aglycones: Neuner et al., 2019). Similarly, in some species, premature leaves are spaced by a dense trichome felt that we suggest might have a comparable function.

In addition to the presence of ice barriers, maintenance of the supercooled state requires regulatory mechanisms that are involved in the freezing response, including potential biochemical components that have supercooling stabilizing activity, ice nucleation activity and/or antifreeze activity (Ishikawa et al., 2009). The biochemical mechanisms involved in

freeze regulation that likely determine freezing response remain unclear (Ishikawa et al., 2009, 2015; Wisniewski et al., 2009, 2014; Kishimoto et al., 2014).

Freeze dehydration of the supercooled bud could also play a role in maintaining the supercooled state (Ide et al., 1998); however, desiccation alone did not increase the supercooling capacity of buds in *P. abies* (Kuprian et al., 2018). Still, the freezing of apoplastic water in the stem and subtending bud scales, while buds remain ice-free, produces a steep water potential gradient that must be managed. Typically, water migrates from the bud across the barrier tissue to the site of the ice, which has been labeled as extraorgan freezing (Sakai, 1982). Different degrees of freeze dehydration are also the basis of the postulated bud survival typology described by Sakai and Larcher (1987). Recently, temperature-dependent freeze dehydration of supercooled buds was demonstrated in *P. abies* (*Type III*) (Kuprian et al., 2017). Strikingly, the extent of freeze dehydration, as indicated by measuring the water potential of buds, was not much different than that reported for buds of *M. domestica* (Pramsohler and Neuner, 2013), which are *Type II* buds. These results suggest that differences in the extent of freeze dehydration may not explain the differences that exist between the low-temperature survival of *Type II* and *III* buds. Our typology does not use the amount of freeze dehydration for classification.

Extraorgan freezing depends on the presence of ice sinks in the subtending stem, at the base of the bud scales or, as has been recently shown, between the premature leaves inside the bud (Neuner et al., 2019). In *P. abies* (Kuprian et al., 2017), translocated water freezes and forms large ice masses in voids in the pith tissue of the subtending stem. By stereo-light microscopy and cryo-SEM it could be shown that in *Larix kaempferi* large extraorgan ice masses form in the subtending stem in the space below the crown tissue and within basal areas of scales (Endoh et al., 2009), which is a typical pattern of extraorgan freezing in conifers (Sakai, 1979, 1982). Freezing exotherms that are provoked by formation of translocated ice are usually not detectable by DTA, as the freezing process may be too slow. In some species, such as *A. alnobetula*, exiguous freezing signals from ice formation between the leaves could be seen in IDTA (Neuner et al., 2019). However, as in *P. abies*, no freezing exotherm may be recorded by IDTA (Kuprian et al., 2017). Supercooled buds of angiosperms have also been shown to accumulate large ice masses within the basal parts of bud scales and the upper part of the immature pith of the subtending stem, as has been reported for *A. japonicum,* (Ishikawa et al., 1997) and *Acer pseudoplatanus* (Dereuddre, 1979). The ice masses create cavities that can be seen as such when the stem and bud tissues thaw. Interestingly, our results suggest that in more than 50% of the investigated species, and in most of the persistently supercooling buds, translocated ice masses harmlessly form between the premature leaves, such as what was recently reported for *A. alnobetula* (Neuner et al., 2019). While in stems and bud scales the growing ice masses disrupt the tissue, this is not the case in the latter, which may be advantageous.

Temporarily vs. Persistently Supercooled Buds

Two different frost survival mechanisms could be distinguished in buds that remain free of ice during and after the HTE. In the first mechanism, buds continued to supercool but were killed by an intracellular freezing event initiated within the bud when the temperature fell below the ability of the buds to maintain supercooling. This freezing event was detectable by an LTE and such buds were termed Type B buds, which corresponds to the *Type III* buds of Sakai and Larcher (1987). As supercooling in Type B buds can suddenly break down, we term it ***temporarily supercooled***. In the second mechanism, the buds remain supercooled; however, no further freezing occurs. This type of response represents *Type I* or *II* buds (Sakai and Larcher, 1987), where *Type I* buds are thought to be fully dehydration-tolerant with unlimited FR and *Type II* buds can be intensively dehydrated, although they are not dehydration-tolerant with limited FR (−35 to −50°C). Freeze dehydration was not examined in the current study, and the level of FR measured in winter 2015/16 may not be the species-specific maximum. Therefore, a clear assignment of the buds examined in this current study as *Type I* or *II* buds is not possible. Additionally, freeze dehydration of many buds that remain supercooled without a detectable LTE is generally difficult to assess. Therefore, we suggestively term this group of buds Type C, or ***persistently supercooled***.

Temporarily Supercooled Buds (Type B)

In 14 of the examined species, the ice-free, supercooled bud cells were observed to freeze intracellularly in a sudden event, detectable as an LTE. This occurred at a temperature below a certain threshold freezing temperature that corresponded to the frost killing temperature. Similar to the observations on Norway spruce buds (Kuprian et al., 2017), ice never penetrated the ice barrier between the adjoining stem and the bud, but lethal freezing was in all temporarily supercooling species initiated by an independent, separate ice nucleation event inside the bud tissue. Once ice had nucleated, the bud tissue froze within seconds. The FR of these temporarily supercooled buds was much less, relative to the other bud types. The LT_{50} in these species ranged from −17.0°C in *Crataegus monogyna* to −32.5°C in *A. platanoides* (mean −22.8°C). Other species with Type B buds have been reported to attain similar moderate levels of midwinter FR, such as *A. pseudoplatanus,* with a mean FR of −21°C (Larcher, 1985) and *Juglans regia,* with a mean FR of −18.5°C (Charrier et al., 2013). The maximum observed FR of −32.5°C corresponds to the FR limit (−25 to −30°C) indicated by Sakai and Larcher (1987) for this type of buds. Other reports on maximum midwinter FR obtained for temporarily supercooling vegetative buds of angiosperms, however, suggest that in extreme survival of freezing temperatures for the majority of down to −40°C is possible, exceptionally even as low as −50°C (*P. abies*: Beuker et al., 1998). For example, maximum midwinter FR of *F. sylvatica* buds was reported to reach −40°C (Lenz et al., 2013, 2016; Kreyling et al., 2014), which is similar to the level (−40°C) reported for *A. hippocastanum* (Sakai and Larcher, 1987). Nevertheless, the limited maximum FR of temporarily supercooling buds likely limits the northern distribution of

species that employ this functional frost survival strategy. A similar conclusion was drawn by Quamme (1995) on the basis of knowledge at that time for deep supercooling buds of conifers and reproductive buds of angiosperms.

Persistently Supercooled Buds (Type C)

In 51.4% of the investigated species, vegetative buds remained ice-free during and after the HTE and did not exhibit any further freezing event (LTE) that was associated with frost injury. Such freezing behavior is also known for flower buds of angiosperms that do not exhibit an LTE (e.g., apple: Quamme, 1991). FR of Type C buds was intermediate. Some species were rather frost susceptible, while others were among the most frost hardy. For example, overwintering buds of *B. pendula* have been reported to survive liquid hydrogen temperatures (−253°C) if properly acclimated (Sakai and Larcher, 1987). It was suggested that Type C buds become freeze-dehydrated to such an extent that no freezable water remains that could be involved in producing an LTE. This could suggest that another injurious process, other than intracellular freezing, occurs in Type C buds (Sakai and Larcher, 1987). However, as when the intracellular freezing process is insignificantly below the resolution limit of DTA and IDTA, intracellular freezing as a cause of frost damage to Type C buds cannot be completely excluded. Previous DTA studies showed that experimental settings such as slow cooling rates (Endoh et al., 2009) or prolonged exposure to freezing conditions that promote dehydration (Sakai, 1979) can lead to failure of detection of an LTE in buds. Similarly, xylem ray parenchyma cells of boreal trees showed deep supercooling in a cryo-SEM study, while DTA did not provide an LTE (Kuroda et al., 2003). Further studies are needed to clarify how these persistently supercooled buds are killed.

Variability of Midwinter Bud FR

In winter 2015/16—compared to earlier reports—the tested species were less frost hardy, which can be addressed to milder site conditions and the relatively moderate winter temperatures. Midwinter bud FR is attained after a long frost hardening period that is initiated in autumn by decreasing photoperiod and colder temperatures (Horvath et al., 2003). In the dormant state, actual bud FR can largely fluctuate in response to abrupt temperature variations (Hänninen, 2016; Lenz et al., 2016; Vitra et al., 2017). For instance, in Norway spruce inter-annual differences in winter temperatures caused different midwinter bud FR between years and sudden low temperature exposure enforced immediate additional frost hardening in the buds (Beuker et al., 1998).

Despite exposure to similar environmental conditions, midwinter bud FR differed intra-specifically between −17.0 and −90.0°C. The extreme differences between species can only partly be explained by different frost survival mechanisms. The results clearly point out that the temporarily supercooled buds have a limited midwinter bud FR for most species down to −40°C, or at the extreme −50°C. Extracellularly freezing buds generally belong to the frost hardiest group (−90°C). Strikingly, within the species that have persistently supercooled buds, a similar heterogeneity with respect to FR was observed (−19.0 to −90.0°C) as between all species. This may be indicative for currently unknown mechanistic differences within this frost survival type. The extreme intra-specific differences in midwinter FR developed under similar environmental conditions point out that besides winter temperature, there is also a strong functional and genetic component effectively leaving species with dramatically different safety margins from frost damage.

AUTHOR CONTRIBUTIONS

GN designed the research, wrote the manuscript and interpreted the results. DK, JI, and KM were responsible for the performance of the research, data analysis, collection and interpretation.

FUNDING

The experiments were conducted in the frame of research project P23681-B16 granted by the Austrian Science Fund (FWF) to GN.

ACKNOWLEDGMENTS

The authors would like to thank Konrad Pagitz and Caecilia Lechner-Pagitz for helping to collect sample twigs and checking scientific names. We are grateful to the staff of the Botanical Garden of the University of Innsbruck and of the Alpine Zoo Innsbruck for permission to collect samples from cultivated woody species.

SUPPLEMENTARY MATERIAL

The Supplementary Material for this article can be found online at: https://www.frontiersin.org/articles/10.3389/fpls.2019.00537/full#supplementary-material

REFERENCES

Ashworth, E. N. (1982). Properties of peach flower buds which facilitate supercooling. *Plant Physiol.* 70, 1475–1479. doi: 10.1104/pp.70.5.1475

Ashworth, E. N. (1990). The formation and distribution of ice within Forsythia flower buds. *Plant Physiol.* 92, 718–725. doi: 10.1104/pp.92.3.718

Ashworth, E. N., and Davis, G. A. (1986). Ice formation in woody plants under field conditions. Hort. *Sci.* 21, 1233–1234.

Bannister, P., and Neuner, G. (2001). "Frost resistance and the distribution of conifers," in *Conifer Cold Hardiness*, eds F. J. Bigras and S. J. Colombo (Dordrecht: Kluwer Academiv Publisher), 3–22. doi: 10.1007/978-94-015-9650-3_1

Beck, E., Senser, M., Scheibe, R., Steiger, H.-M., and Pongratz, P. (1982). Frost avoidance and freezing tolerance in Afroalpine "giant rosette" plant. *Plant Cell Environ.* 5, 215–222.

Benowicz, A., El-Kassaby, Y. A., Guy, R. D., and Ying, C. C. (2000). Sitka alder (Alnus sinuata RYDB.) genetic diversity in germination, frost hardiness and growth attributes. *Silv. Genet.* 49, 206–212.

Beuker, E., Valtonen, E., and Repo, T. (1998). Seasonal variation in the frost hardiness of Scots pine and Norway spruce in old provenance experiments

in Finland. *For. Ecol. Manag.* 107, 87–98. doi: 10.1016/S0378-1127(97)00344-7

Buchner, O., and Neuner, G. (2011). Winter frost resistance of Pinus cembra measured *in situ* at the alpine timberline as affected by temperature conditions. *Tree Physiol.* 31, 1217–1227. doi: 10.1093/treephys/tpr103

Burke, M. J., Gusta, L. V., Quamme, H. A., Weiser, C. J., and Li, P. H. (1976). Freezing and injury in plants. *Ann. Rev. Plant Physiol.* 27, 507–528. doi: 10.1146/annurev.pp.27.060176.002451

Charrier, G., Poirier, M., Bonhomme, M., Lacointe, A., and Améglio, T. (2013). Frost hardiness in walnut trees (*Juglans regia L.*): how to link physiology and modelling? *Tree Physiol.* 33, 1229–1241. doi: 10.1093/treephys/tpt090

Dereuddre, J. (1979). Etude comparative du comportement des bourgeons d'arbres en vie ralentie, pendant un refroidissenment graduel des rameaux. *Bull. Soc. Botan. France Lett. Bot.* 126, 399–411.

Endoh, K., Kasuga, J., Arakawa, K., Ito, T., and Fujikawa, S. (2009). Cryo-scanning electron mircoscopic study on freezing behaviors of tissue cells indormant buds of larch (Larix kaempferi). *Cryobiology* 59, 214–222. doi: 10.1016/j.cryobiol.2009.07.010

Filippi (1986). *Gefrierverhalten submediterraner Holzpflanzen.* Diploma thesis, University of Innsbruck, Innsbruck.

Graham, P. R., and Mullin, R. (1976). The determination of lethal freezing temperatures in buds and stems of deciduous azalea by a freezing curve method. *J. Amer. Soc. Hort. Sci.* 101, 3–7.

Hacker, J., and Neuner, G. (2007). Ice propagation in plants visualized at the tissue level by IDTA (infrared differential thermal analysis). *Tree Physiol.* 27, 1661–1670. doi: 10.1093/treephys/27.12.1661

Hacker, J., and Neuner, G. (2008). Ice propagation in dehardened alpine plant species studied by infrared differential thermal analysis (IDTA). *Arc. Antarc. Alp. Res.* 40, 660–670. doi: 10.1657/1523-0430(07-077)[HACKER]2.0.CO;2

Hacker, J., Spindelböck, J. P., and Neuner, G. (2008). Mesophyll freezing and effects of freeze dehydration visualized by simultaneous measurement of IDTA and differential imaging chlorophyll fluorescence. *Plant Cell Environ.* 31, 1725–1733. doi: 10.1111/j.1365-3040.2008.01881.x

Hänninen, H. (2016). *Boreal and Temperate Trees in a Changing Climate.* Dordrecht: Springer. doi: 10.1007/978-94-017-7549-6

Hofmann, M., Durka, W., Liesebach, M., and Bruelheide, H. (2015). Intraspecific variability in frost hardiness of *Fagus sylvatica L. Europ. J. For. Res.* 134, 433–441. doi: 10.1007/s10342-015-0862-6

Horvath, D. P., Anderson, J. V., Chao, W. S., and Foley, M. E. (2003). Knowing when to grow: signals regulating bud dormancy. *Trends Plant Sci.* 8, 534–540. doi: 10.1016/j.tplants.2003.09.013

Ide, H., Price, W. S., Arata, Y., and Ishikawa, M. (1998). Freezing behaviors in leaf buds of cold-hardy conifers visualized by NMR microscopy. *Tree Physiol.* 18, 451–458. doi: 10.1093/treephys/18.7.451

Ishikawa, M., Ide, H., Price, W. S., Arata, Y., Nakamura, T., and Kishimoto, T. (2009). "Freezing behaviours in plant tissues: Visualization using NMR micro-imaging and biochemical regulatory factors involved," in *Plant Cold Hardiness: From the Laboratory to the Field*, eds. L. V. Gusta, M. E. Wisniewski, and K. K. Tanino (Cambridge: CAB International), 19–28.

Ishikawa, M., Ishikawa, M., Toyomasu, T., Aoki, T., and Price, W. S. (2015). Ice nucleation activity in various tissues of Rhododendron flower buds: their relevance to extraorgan freezing. *Front. Plant Sci.* 6:149. doi: 10.3389/fpls.2015.00149

Ishikawa, M., Price, W. S., Ide, H., and Arata, Y. (1997). Visualization of freezing behaviors in leaf and flower buds of full-moon maple by nuclear magnetic resonance microscopy. *Plant Physiol.* 115, 1515–1524. doi: 10.1104/pp.115.4.1515

Ishikawa, M., and Sakai, A. (1982). "Characterization of freezing avoidance in comparison with freezing tolerance. A demonstration of extraorgan freezing," in *Plant Cold Hardiness and Freezing Stress: Mechanisms and Crop Implications,* Vol. 2, eds P. H. Li and A. Sakai (New York, NY: Academic Press), 325–340.

Kishimoto, T., Yamazaki, H., Saruwatari, A., Murakawa, H., Sekozawa, Y., Kuchitsu, K., et al. (2014). High ice nucleation activity located in blueberry stem bark is linked to primary freeze initiation and adaptive freezing behaviour of the bark. *AoB Plants* 6, 1–17. doi: 10.1093/aobpla/plu044

Kreyling, J., Buhk, C., Backhaus, S., Hallinger, M., Huber, G., Huber, L., et al. (2014). Local adaptations to frost in marginal and central populations of the dominant forest tree *Fagus sylvatica L.* as affected by temperature and extreme drought in common garden experiments. *Ecol. Evol.* 4, 594–605. doi: 10.1002/ece3.971

Kuprian, E., Munkler, C., Resnyak, A., and Neuner, G. (2018). Does winter dehydration account for seasonal increase in supercooling ability of Norway spruce bud primordia. *Tree Physiol.* 38, 591–601. doi: 10.1093/treephys/tpx142

Kuprian, E., Munkler, C., Resnyak, A., Zimmermann, S., Tuong, T. D., Gierlinger, N., et al. (2017). Complex bud architecture and cell-specific chemical patterns enable supercooling of Picea abies bud primordia. *Plant Cell Environ.* 40, 3101–3112. doi: 10.1111/pce.13078

Kuroda, K., Kasuga, J., Arakawa, K., and Fujikawa, S. (2003). Xylem ray parenchyma cells in boreal hardwood species respond to subfreezing temperatures by deep supercooling that is accompanied by incomplete desiccation. *Plant Physiol.* 131, 736–744. doi: 10.1104/pp.011601

Larcher, W. (1985). "Kälte und Frost," in *Handbuch der Pflanzenkrankheiten*, *found,* ed P. Sorauer (Berlin: Parey), 107–320.

Lenz, A., Hoch, G., and Vitasse, Y. (2016). Fast acclimation of freezing resistance suggests no influence of winter minimum temperature on the range limit of European beech. *Tree Physiol.* 36, 490–501. doi: 10.1093/treephys/tpv147

Lenz, A., Hoch, G., Vitasse, Y., and Körner, C. (2013). European deciduous trees exhibit similar safety margins against damage by spring freeze events along elevational gradients. *New Phytol.* 200, 1166–1175. doi: 10.1111/nph.12452

Mayr, S., Wieser, G., and Bauer, H. (2006). Xylem temperatures during winter in conifers at the alpine timberline. *Agri. For. Meteorol.* 137, 81–88. doi: 10.1016/j.agrformet.2006.02.013

Neuner, G., Kreische, B., Kaplenig, D., Monitzer, K., and Miller, R. (2019). Deep supercooling enabled by surface impregnation with lipophilic substances explains the survival of overwintering buds at extreme freezing. *Plant Cell Environ.* doi: 10.1111/pce.13545. [Epub ahead of print].

Neuner, G., and Kuprian, E. (2014). "Infrared thermal analysis of plant freezing processes," in *Methods in Molecular Biology: Plant Cold Acclimation*, eds. D. Hincha and E. Zuther (New York, NY: Springer), 91–98.

Pramsohler, M., Hacker, J., and Neuner, G. (2012). Freezing pattern and frost killing temperature of apple (Malus domestica) wood under controlled conditions and in nature. *Tree Physiol.* 32, 819–828. doi: 10.1093/treephys/tps046

Pramsohler, M., and Neuner, G. (2013). Dehydration and osmotic adjustment in apple stem tissue during winter as it relates to the frost resistance of buds. *Tree Physiol.* 33, 807–816. doi: 10.1093/treephys/tpt057

Price, W. S., Ide, H., Arata, Y., and Ishikawa, M. (1997). Visualisation of freezing behaviours in flower bud tissues of cold-hardy Rhododendron japonicum by nuclear magnetic resonance micro-imaging. *Austr. J. Plant Physiol.* 24, 599–605. doi: 10.1071/PP97049

Quamme, H.A. (1991). Application of thermal analysis to breeding fruit crops for increased cold hardiness. *Hortscience* 26, 513–517. doi: 10.21273/HORTSCI.26.5.513

Quamme, H.A. (1995). "Deep supercooling in buds of woody plants," in *Biological Ice Nucleation and Its Application*, eds R. E. Lee, G. J. Warren, and L. V. Gusta (St. Paul: APS Press), 183–200.

Rajashekar, C., and Burke, M.J. (1978). "The occurrence of deep supercooling in the genera Pyrus, Prunus and Rosa. A preliminary report," *in Plant Cold Hardiness and Freezing Stress*, Vol. 1, eds P. H. Li and A. Sakai (New York, NY: Academic Press), 213–225.

Riikonen, J., Kontunen-Soppela, S., Vapaavuori, E., Tervahauta, A., Tuomainen, M., and Oksanen, E. (2013). Carbohydrate concentrations and freezing stress resistance of silver birch buds grown under elevated temperature and ozone. *Tree Physiol.* 33, 311–319. doi: 10.1093/treephys/tpt001

Sakai, A. (1978). Low temperature exotherms of winter buds of hardy conifers. *Plant Cell Physiol.* 19, 1439–1446.

Sakai, A. (1979). Freezing avoidance mechanism of primordial shoots of conifer buds. *Plant Cell Physiol.* 20, 1381–1390. doi: 10.1093/oxfordjournals.pcp.a075937

Sakai, A. (1982). "Extraorgan freezing of primordial shoots of winter buds of conifer," in *Plant Cold Hardiness and Freezing Stress. Mechanisms and Crop Implications*, Vol. 2, eds. P. H. Li and A. Sakai (New York, NY: Academic Press), 199–209.

Sakai, A., and Eiga, S. (1985). "Physiological and ecological aspects of cold adaptation of boreal conifers," in *Plant Production in the North,* eds Å. Kaurin, O. Juntilla, and J. Nilsen (Tromsø: Norwegian University Press), 157–170.

Sakai, A., and Larcher, W. (1987). *Frost Survival of Plants: Responses and Adaptation to Freezing Stress*, Vol. 62. Ecological Studies. Berlin: Springer.

Sakai, A., and Okada, S. (1971). Freezing resistance of conifers. *Silv. Gen*. 20, 91–97.

Schiffmann, F. (2017). *Gefrierdehydrierung von Typ I und Typ II Knospenprimordien und die direkte Anwendung für den Unterricht.* Diploma thesis, University of Innsbruck, Innsbruck.

Vitra, A., Lenz, A., and Vitasse, Y. (2017). Frost hardening and dehardening potenrial in temperate trees from wintert o budburst. *New Phytol.* 216, 113–123. doi: 10.1111/nph.14698

Wisniewski, M., Gusta, L., and Neuner, G. (2014). Adaptive mechanisms of freeze avoidance in plants: a brief update. *Env. Exp. Bot*. 99, 133–140. doi: 10.1016/j.envexpbot.2013.11.011

Wisniewski, M., Gusta, L.V., Fuller, M.P., and Karlson, D. (2009). "Ice nucleation. Propagation and deep supercooling: the lost tribes of freezing studies," in *Plant Cold Hardiness: From the Laboratory to the Field*, eds L. V. Gusta, K. Tannino, and M. Wisniewski (Cambridge: CABI), 19–28.

Wisniewski, M., Lindow, S. E., and Ashworth, E. N. (1997). Observations of ice nucleation and propagation in plants using infrared video thermography. *Plant Physiol*. 113, 327–334. doi: 10.1104/pp.113.2.327

Wisniewski, M., Neuner, G., and Gusta, L. (2015). The use of High-Resolution Infrared Thermography (HRIT) for the study of ice nucleation and ice propagation in plants. *JoVE* 99:52703. doi: 10.3791/52703

Zwiazek, J. J., Renault, S., Croser, C., Hansen, J., and Beck, E. (2001). "Biochemical and biophysical changes in relation to cold hardiness," in *Conifer Cold Hardiness*, eds F. J. Bigras and S. J. Colombo (Dordrecht: Kluwer Academic Publisher), 165–186.

Conflict of Interest Statement: The authors declare that the research was conducted in the absence of any commercial or financial relationships that could be construed as a potential conflict of interest.

frontiers in Plant Science

ORIGINAL RESEARCH
published: 18 September 2019
doi: 10.3389/fpls.2019.01100

Complex Above- and Below-Ground Growth Responses of Two Urban Tree Species Following Root, Stem, and Foliage Damage—An Experimental Approach

Valentina Vitali[1], Jorge A. Ramirez[1,2], Guillaume Perrette[1], Sylvain Delagrange[3], Alain Paquette[1] and Christian Messier[1,3]*

[1] Faculté des sciences, Département des sciences biologiques, Centre d'Étude de la Forêt (CEF), Université du Québec à Montréal, Montréal, Canada, [2] Facultad de Ciencias Agrarias, Universidad del Cauca, Popayán, Colombia, [3] Institut des Sciences de la Foret Tempérée, Université du Québec en Outaouais, Ripon, Canada

OPEN ACCESS

Edited by:
Henrik Hartmann, Max-Planck-Institut für Biogeochemie, Germany

Reviewed by:
Chiara Cirillo, University of Naples Federico II, Italy
Miguel Montoro Girona, Swedish University of Agricultural Sciences, Sweden

***Correspondence:**
Valentina Vitali
valentina.vitali@wsl.ch

Specialty section:
This article was submitted to Functional Plant Ecology, a section of the journal Frontiers in Plant Science

Received: *05 April 2019*
Accepted: *09 August 2019*
Published: *18 September 2019*

Citation:
Vitali V, Ramirez JA, Perrette G, Delagrange S, Paquette A and Messier C (2019) Complex Above- and Below-Ground Growth Responses of Two Urban Tree Species Following Root, Stem, and Foliage Damage—An Experimental Approach. Front. Plant Sci. 10:1100. doi: 10.3389/fpls.2019.01100

Urban trees are subjected to numerous biotic and mechanical damages, which can affect their growth rates and health. However, for most species, a systematic analysis of tree above- and below-ground growth reactions to a variety of damages is still lacking. Under a fully factorial experimental setup, using two common urban trees (*Celtis occidentalis*, *Fraxinus pennsylvanica*), we tested the effects of various degrees of frequently occurring damage as defoliation, root reduction, and stem injuries for a total of 18 treatments. We hypothesized that (i) an increasing amount of damage would proportionally negatively affect both root and stem growth; (ii) there would be a lag or lasting effect on growth; and (iii) both species would react similarly to the treatments. Contrary to our expectation, increasing levels of single or combined damage did not have an incremental effect on either stem or root growth. Although *Celtis* was significantly less vigorous than *Fraxinus*, it did not react strongly to damage treatments compared to the control. Interestingly, *Celtis* that experienced stem damage alone or in combination with other damages showed higher growth rates than the control. For *Celtis*, root injury was the treatment having the most impact, decreasing both root and stem growth consistently throughout the 5 years following treatments, whereas defoliation decreased growth only in the first 2 years. All damage treatments negatively affected stem and root growth of *Fraxinus* trees. Stem growth was affected the most by defoliation in the first year following the treatment, while root injury became the driving factor in subsequent years. For both species, stem injury showed the least influence on growth rates. The control and low-level damage treatments often affected growth rates in a similar way, suggesting that low-intensity stress triggers compensatory reactions stimulating photosynthetic rates and nutrient utilization. The slower-growing tree species, *Celtis*, showed a less negative reaction to all damage treatments compared to *Fraxinus*. This study illustrates that various types of above- and below-ground injuries do not have a

simple additive effect on tree growth and that trees are capable of compensating for the loss of foliage, roots, or phloem to meet their metabolic demand.

Keywords: *Celtis occidentalis*, damage and stress, *Fraxinus pennsylvanica*, tree growth, urban environment

INTRODUCTION

Trees growing in urban landscapes are an invaluable asset as they provide numerous environmental, social, cultural, and economic benefits (Konijnendijk et al., 2005; Tanner et al., 2014). Yet, urban environments are often characterized by low water availability, higher temperatures induced by the urban heat island phenomenon, and limited space (Sieghardt et al., 2005; Moser-Reischl et al., 2018). All too frequently, urban trees are also damaged by bystanders or during construction or maintenance work on urban infrastructure. Consequently, these trees have to withstand a wide variety of damages and accidental injuries, such as root trenching for road work or sidewalk placement or reparation; trunk scarification damage caused by construction and infrastructure maintenance; and crown reduction or defoliation through pruning, drought stress or insect infestation (Clair-Maczulajtys et al., 1999; Millet and Bouchard, 2003; Smiley, 2008; Jacquet et al., 2012). Such levels of damage and stress, alone or in combination, can dramatically affect tree growth and vitality and lead to mortality, thereby increasing costs for removal and replacement.

Such deviation from the typical growth environment of trees affects several physiological mechanisms, which can lead to drastic changes in growth rates in different parts of the tree (Boege, 2005; Jacquet et al., 2014; Freschet et al., 2018). Thus, tree growth is maximal when both above- and below-ground environmental conditions and resources are optimal and declines when these values are suboptimal (Niinemets and Valladares, 2008; Niinemets, 2010b). Overall, tree species that have the capacity to tolerate the most extreme environmental conditions have low plasticity and low growth rates (Niinemets, 2010b), possibly due to the associated carbon cost of maintaining a positive carbon balance during acclimation (Ramirez, 2017)

Trees growing in urbanized conditions face several stressors that can act alone or in combination (Jutras et al., 2010; Calfapietra et al., 2015) and can generate a unique set of responses due to a mitigation effect (Mittler, 2006; Niinemets, 2010a). Their growth response may be more severe due to negative interactions between stressors or less severe due to mitigation effects (Mittler, 2006; Niinemets, 2010a). Although there is a strong interest in ensuring vigorous and healthy trees in urban settings, our understanding of urban tree reactions to injury, and in particular to a combination of injuries, is still poor (Niinemets, 2010a; Ferrini et al., 2014). In this study, we focus on single and combined effects of three types of injuries, which typically affect urban trees: defoliation, root reduction, and stem damage.

Defoliation can cause a decrease in tree photosynthetic capacity, reducing available carbon for growth, and build-up of reserves (Eyles et al., 2009; Pinkard et al., 2011). This damage can also activate short- and long-term physiological mechanisms including the reduction of biomass allocation to coarse roots (Eyles et al., 2009) and the mobilization of carbohydrate reserves from branches, stems, and roots to increase the metabolism of remaining leaves to compensate for the decreased supply of carbohydrates (Quentin et al., 2010). Root reduction affects the hydraulic system and water uptake, reducing the amount of water available for transpiration and further affecting photosynthesis, while actively removing storage organs (Vysotskaya et al., 2004). Stem damage impacts both water and sugar translocation between above- and below-ground organs affecting reserves build-up and photosynthetic rates (Fajstavr et al., 2017) and, in extreme cases, can induce wilting when the damage reaches deep into the xylem and water transportation is drastically reduced (Moore, 2013), or even tree death by starvation when translocation of sugars is strongly decreased (Adams et al., 2013; Oberhuber et al., 2017). After a stress episode, different tree species will show different capacities to recover from the damage and maintain or increase growth rates. This capability is based on life history traits of the species and its resource allocation to growth and defense (Grime and Hunt, 1975). It is expected that functionally different species will exhibit variation in carbon allocation and therefore in recovery after damage (Poorter and Kitajima, 2007).

All injuries affect physiological mechanisms, which can be evaluated through changes in growth rates in different parts of the tree. It is expected that these injuries lead to shifts in the carbon allocation priorities to maintain their metabolic activities and to start compensatory growth. In this study, we will use tree-ring data to assess the effect on growth and resilience to multiple kinds of mechanical damage, single and combined, in two commonly used urban species in Eastern North America: North American hackberry (*Celtis occidentalis L.*) and green ash (*Fraxinus pennsylvanica* Marsh.). Furthermore, these species show distinctly different resource utilization strategies; where the North American hackberry shows a lower growth speed and a conservative use of resources (i.e., photosynthetic products), ash is growing faster and uses resources more intensively (Ramirez, 2017). We will compare the growth response in stem and roots of both species to determine whether biomass allocation above- and below ground was altered by various types and levels of damage treatments, and if there was a lag or lasting effect on growth rates in the years after the damage, treatments were applied to address the following hypotheses:

(1) An increase in damage intensity results in a simple additive negative growth response:
   (i) Main stem and large roots show greater declines in growth when treated with multiple types and high damage intensities.
   (ii) The combination of both root reduction and defoliation causes lower decline of overall tree growth at independently of the treatment intensity.

(2) Species strategies to compensate for damages change with species-specific physiology. A resource-conservative species (*Celtis*) will be less affected by mechanical damages than a resource-intensive species (*Fraxinus*).
(3) Above- and below-ground growths of the two species return to pretreatment levels in the years after the treatment.

METHODS

Study Site

This study was conducted in the municipal nursery of the City of Montreal, province of Quebec, Canada. The site lies at 45°49′59″ N, 73°24′44″ W, at about 35 m of elevation. The mean annual precipitation is 978 mm (215 mm snow and 763 mm rain), and the mean annual temperature is 6.2°C (mean growing season temperature is 14.4°C). The mean daily maximum and minimum temperatures are 10.5°C and 0°C. Annually, there is an average of 1,958 h of sunshine, 2.8 degree-days below 10°C, and 1,099 degree-days above 10°C. Temperatures below 0°C occur between October and April (period 1971–2000; Environment Canada, climate.weather.gc.ca) and the winter season commonly extends from mid-November to the end of March (Boyer et al., 1985). Soil structure is mainly composed of a loamy clay.

Study Species

We studied two tree species commonly planted in the city of Montreal: *C. occidentalis* L. (common hackberry) and *F. pennsylvanica* Marsh. (Red ash), hereafter referred to as *Celtis* and *Fraxinus,* respectively. Both species show a large variability across their geographical range, but they are generally characterized as medium-sized (*Celtis* reaching 15 m and *Fraxinus* 25 m in height), with a medium lifespan (100 years for *Fraxinus* and 150 years for *Celtis*), and are in generally considered fast growing, although they show distinctively different growth rates (Farrar, 1995). *Celtis* is a more resource conservative species since it has a higher foliar carbon/nitrogen ratio, lower photosynthetic capacity, and higher wood density than *Fraxinus* (Ramirez, 2017). Moreover, *Celtis* is capable of growing in very inhospitable conditions (Gucker, 2011), while *Fraxinus*, although showing a broad climate adaptability, prefers growing in mesic to humid sites (Gucker, 2005). The exemplars for this experiment were donated by the City of Montréal. At the seedling stage, there were no apparent differences in vigor between the species. However, after e-planting, *Celtis* showed signs of growth decline independent from the application of treatments. Trees at the beginning of the study (2012) were between 1.6 and 4.5 m tall for *Celtis*, and 2.6 to 6.1 m tall for *Fraxinus*. Therefore, the results presented hereafter compare both two different species and two states of vigor (**Figure 1**). A total of 202 trees were planted in 2009 and 2010, 116 *Celtis* from field-grown seedlings propagated in 2004, and 86 *Fraxinus* seedlings propagated in 2003.

Experimental Design: Damage Treatments

A fully factorial experiment was set up; where in addition to the control with no damage treatment, all other trees were randomly assigned to the following damage treatments: two intensities of defoliation (37%, 75%), two intensities of root reduction (37%, 75%), and one intensity of stem damage (50%) (**Table 1**, **Figure 2**). All possible combinations among these three treatments were reproduced, resulting in 18 types and levels of damage treatment. The number of replicates per treatment was 6 in *Celtis* and 4 in

FIGURE 1 | Examples of control trees of **(A)** *Celtis* and **(B)** *Fraxinus* taken at the end of the experiment period in 2017. Ruler for scale is 1m in length.

TABLE 1 | Description of the damage treatments performed in 2012 and 2013 [more details about stress treatments in Ramirez (2017)]. For *Fraxinus*, we used six trees per treatment on average, with the exception of nine for the maximum damage treatment group, while *Celtis* on average had four trees per treatment and eight for the maximum damage treatment group.

Treatment		Method	Intensity
DEFOLIATION	(DF)	Manual removal of leaves at the base of the petiole for all branches	High = 75% Low = 37% Control = no treatment
ROOT REDUCTION	(RR)	Tree spade machine cutting at 30-cm radius from stem base	High = 75% Low = 37% Control = no treatment
STEM DAMAGE	(SD)	40-mm-wide strip removal, 30 cm above root base. Only cambium and phloem connection were removed	Damage 50% Control = no treatment

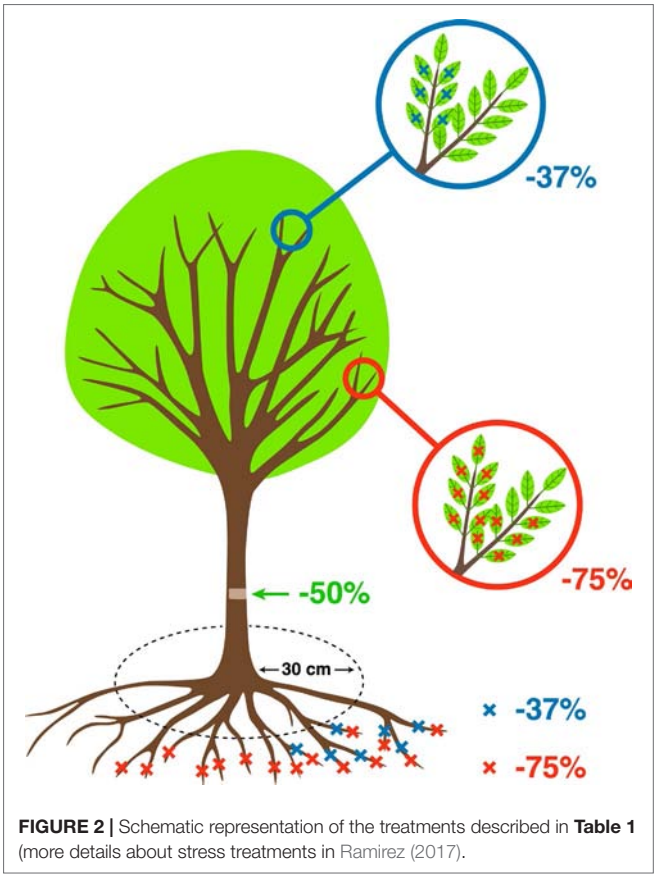

FIGURE 2 | Schematic representation of the treatments described in **Table 1** (more details about stress treatments in Ramirez (2017).

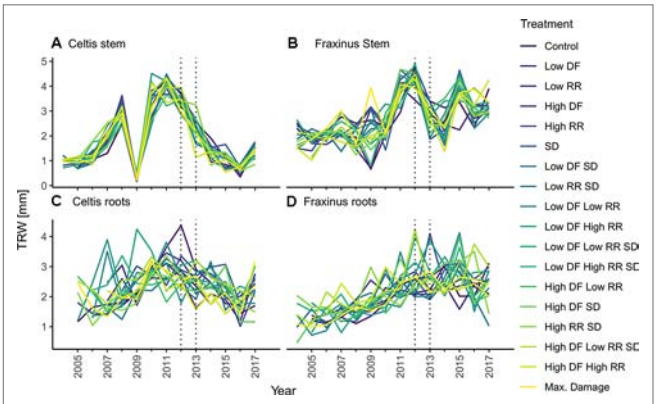

FIGURE 3 | Tree-ring chronologies of **(A)** *Celtis* stem growth, **(C)** *Celtis* average root growth, and **(B)** *Fraxinus* stem growth, and **(D)** *Fraxinus* average root growth for each combination of damage treatments. Low growth in 2009 for *Celtis* and 2009 and 2010 for *Fraxinus* is related to replanting operations. Damage treatments were applied in 2012–2013 as indicated by the two vertical dotted lines. Damage treatment levels are described as follows: DF, defoliation; RR, root reduction and SD, stem damage indicated as low = 37% damage and high = 75% damage.

Fraxinus due to the availability of trees, and this varied slightly between treatments to ensure sufficient trees in case of mortality. Treatments were applied in July, which corresponded to the month of maximum leaf area in both 2012 and 2013. At the beginning of the dormant season in autumn 2015, a reduction pruning of the main stem was performed on all trees with the removal of the lower half of the living crown. This treatment was applied to all trees, but its effect will not be investigated in this instance as analyses specific to crown recovery and architecture have been carried out in a separate study.

Sample Collection and Dendrochronological Measurements

For each tree, the stem discs were collected at 1.3-m height, and three large roots were cut at 5 cm from the stem base in winter 2017. These cross sections were left to air dry and subsequently sanded down to 400 grit sandpaper (Schweingruber, 1988). Tree ring widths were measured with WINDENDRO™ (Regents Instruments, Quebec). Data quality of single tree chronologies was controlled through visual and statistical cross dating (i.e., gleichläufigkeit). Cross-dating analyses were performed with the dplr package (Bunn, 2010), and mean tree chronologies were created from the average of the three radiuses per cross section from stem and roots (**Figure 3**). All computations were performed using R version 3.4.3 (R Core Team, 2017). Considering the short time span analyzed and the even age status of the trees, we decided to perform our calculations on both raw tree ring widths and on converted basal area increment (BAI) data, obtained with the function bai.out function in the dplr package (Bunn, 2010). This decision was to ensure the preservation of small year-to-year variability that could be potentially concealed through standardization of the chronology (Fritts, 1976).

It is to be noted that *Celtis* showed a replanting shock reaction in 2009, while *Fraxinus* showed a smaller growth decline due to replanting, which occurred in 2009 and 2010. Overall, it should be observed that controls for *Celtis* showed a declining growth rate, while *Fraxinus* showed a vigorous growth trend. Therefore, the effect of the treatments should be related to the actual growth trends of the two species, and the results presented are relative to these growth trends.

Data Analyses

Mixed Models: Overall Treatment Effects

To evaluate the effects of each treatment, alone and in combination with other damage treatments, on the growth response of stems and roots for each species, we created a mixed model that considered growth data from the years 2012–2015.

$$G_{ij} = \beta_{0i} + S_{0ij} + \beta_{1i} X1_{ij} + e_{ij} \quad \text{(Eq.1)}$$

where G_{ij} is the response variable (tree ring width of stem and root samples for each tree in each year), β_0 is the intercept, β_1 is the parameter estimate, S_{0ij} is the random effect (for consecutive years measurement and tree identity), X1 is the fixed effect representing the treatment level, which ranges from the control (damage = 0) to the maximum damage (where damage SD = 50%, DF = 75%, RR = 75%), and e_i is the error. All computations were performed with the lme4 package (Bates et al., 2015).

GBM Model: Year-by-Year Treatment Effects

Boosted regression tree (GBM) models were used to evaluate the effect and relative importance of every single damage treatment on the annual growth of *Celtis* and *Fraxinus*. Boosted regression trees (GBM models) have important advantages for tree-based statistical methods. They can handle different types of predictor variables, cope with small sample sizes, and automatically handle interaction effects between predictors (Cutler et al., 2007; Elith et al., 2008; Olden et al., 2008).

The learning algorithm for additive GBM is based on the sequential building of "weak" trees, built atop some randomly chosen variables, which are fitted simultaneously, improving the model with every iteration. Each GBM analysis was based on the mean squared loss function; analysis of variance (ANOVA) model with three-way interactions; 1,000 trees; 5-fold cross validation (Friedman, 2002). Next, the best of these models was chosen, based on the residual sum of squares criterion (Friedman, 2001; Natekin and Knoll, 2013). The calculations were performed with the gbm.step (gbm package) function, and the learning rate and bag fraction were kept constant between the models (Ridgeway et al., 2019).

To visualize the results of the GBM model, we created two types of plots: relative variable influence plots and partial dependence plots. The former shows how important each treatment is to growth, but it does not provide any explanation about how the variable affects the response. The relative influences were further standardized to add up to 100% so that each of the treatments could explain a percentage of the growth rates. The partial dependence plots subdivide the contribution of each level of treatment to the estimated growth. The partial dependence plots display the average change in predicted growth as we vary the effect of each treatment while holding all other variables constant. Summing up the estimate for any combination of DF, RR, and SD levels will determine the estimated growth for that treatment.

Above- and Below-Ground Biomass and Root Architecture in 2017

The entire root system from all trees was excavated mechanically in autumn 2017 allowing for a complete assessment and measurement of fine and larger structural roots. All roots with diameter greater than 3 mm were measured and inventoried for the calculation of roots total diameter increment. The presence of the finer roots was recorded as percent cover within the inner 20-cm radius of the stump center. To assess differences between the intensities and combinations of damage treatments and the control, ANOVA and *post hoc* Tukey tests were used. A simple linear model was used to evaluate the above- and below-ground diametric growth:

$$Y_i = \beta_0 + \beta_1 Z1_i + e_i \quad \text{(Eq. 2)}$$

where Y_i is the sum of all measured root diameters for each tree i, β_0 is the intercept, and β_1 is the parameter estimates of Z1, which is the diameter at breast height (DBH) value in 2017. All computations were performed using R version 3.4.3 (R Core Team, 2017).

To compensate for the root measurement threshold of 3 mm, fine root abundance was estimated for the 20-cm radius area surrounding the stump. In this zone, the area covered by fine roots was visually estimated, where 5% indicates an almost absence of fine roots, and 90% to 100% a dense reticulum of fine roots.

RESULTS

Mixed Models to Evaluate Overall Effects for All Years

Overall, both stem and root growth of *Celtis* were less affected by the various levels and combinations of damage treatments than *Fraxinus*, showing few significant growth differences when compared to the control; in some cases, the stem damage treatment stimulated growth (**Table S.1** and **Figures 4A**, **C**). On the contrary,

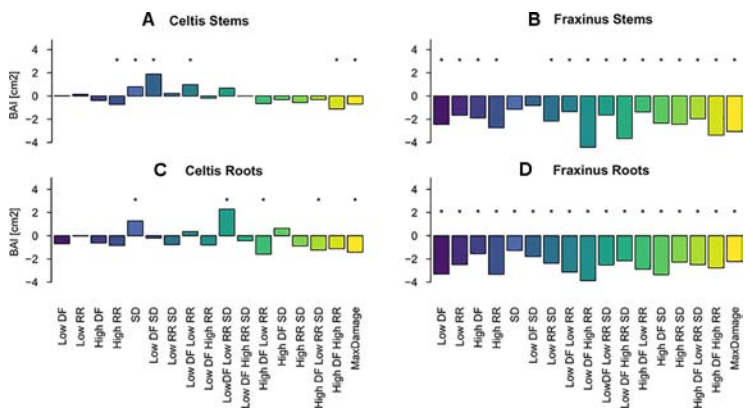

FIGURE 4 | Estimated coefficients of the linear model effect sizes for basal area increment (BAI) growth of *Celtis* (**A** for stem and **C** for roots) and *Fraxinus* (**B** stem and **D** for roots) in the period 2012–2015 (years following last damage treatment), and in relation to the damage treatment level (1–18 treatments are color-coded; DF, defoliation; RR, root reduction; and SD = stem damage, indicated as low = 37% damage and high = 75% damage). r^2 ~0.1 for all models. For simplicity, asterisks in the figure indicate a significant effect of the variable for $P < 0.05$, discrimination between significance levels can be found in **Table S.1**. The standard deviations for the random effects for the year and the tree id were *Celtis* stems: 0.9 and 1.09, *Fraxinus* stems: 1.53 and 1.8, *Celtis* roots: 0.3 and 1.9, *Fraxinus* roots: 0.76 and 1.75.

stem and root growth of *Fraxinus* were, in general, significantly negatively affected by most damage treatments, both alone and in combination, especially the combinations of defoliation and root damage (at both high and low intensities) where it had the lowest stem growth (**Table S1** and **Figures 4B**, **D**). *Fraxinus* root growth was consistently reduced by all damage treatments. Only following SD and low DF-SD treatments, *Fraxinus* did show a nonsignificant decrease in growth compared to the control.

Results GBM Model: Year-by-Year Treatment Effect

The results calculated by the GBM models indicating the effect of the three damage treatments in the years after they were applied are shown in **Figure 5**. Defoliation had the strongest impact on both *Celtis* and *Fraxinus* stem growth in the 2 years after the damage treatments. However, in the subsequent years, root reduction had the strongest impact. Stem damage had only a minor effect on stem growth (**Figures 5A**, **B**), but it had a stronger impact on root growth for both *Celtis* and *Fraxinus* throughout the years (**Figures 5C**, **D**). *Celtis* root growth was more strongly impacted by defoliation than by root reduction in the 2 years after the damage treatments and vice versa in the later years, while the impact of defoliation and root reduction on *Fraxinus* root growth was similar in all years.

The marginal effects of each treatment level on the decomposition of stems (**Figure 6D**) and root growth (**Figures 6E–H**) for both species in the first year (2012) and last year (2015) are shown in **Figure 6**. The variable with the highest relative influence is also the one accounting for the greatest differences in growth; when a variable is more influential, the fitted growth shows a positive or negative trend depending on the effect of the damage treatment (i.e., from 0 = control, low = 37% damage, and high = 75% damage, see **Table 1**). The mean annual growth for each treatment can be calculated by summing the GBM fitted results in **Figure 6** for the respective treatment level.

High defoliation in *Celtis* showed the lowest contribution to growth rates in 2012, while low defoliation and no defoliation damage treatments had similar contribution rates (**Figure 6A**). On the contrary, in 2015, root reduction played the biggest part in differentiating growth rates, which was indirectly proportional to its intensity (**Figure 6B**). Similar patterns can be observed for *Celtis* root growth; however, in 2015, the differences between the damage treatment levels are more evident (**Figures 6E**, **F**). Interestingly, in this case, low defoliation shows higher growth than the null and high damage treatments, while root reduction contribution is still decreasing with increasing intensity of damage treatments (**Figure 6F**).

The decomposition of *Fraxinus* growth shows a more even distribution among the damage treatments. Interestingly, the low intensity DF and RR damage treatments show a more similar effect than their control counterparts for stem growth (**Figures 6C**, **D**, **H**). The trend of the DF contribution to growth drastically changes in 2015, showing a higher contribution to growth from high DF than the null and low intensity damage treatments (**Figures 6D**, **H**), while high intensity RR shows the lowest contribution to the growth of roots (**Figure 6E**). For both species, in most cases, the SD treatment has either an equal or a higher contribution than the no stem damage.

Stem Size, Larger Root Area, and Root Architecture in 2017

In 2017, the final DBH and the total root area cover showed a nonsignificant difference between the damaged trees and the controls in most cases (**Figures 7A**, **B**). DBH in *Fraxinus* trees was significantly lower than control in low DF/high RR, low DF/high RR/SD, and high DF/high RR treatments. *Celtis* showed no significant differences in DBH but showed a higher growth of roots in the trees with low DF/low RR, low DF/high RR, high DF/low RR, and high DF/high RR/SD than in the control. There was an increase in production of finer roots with increasing

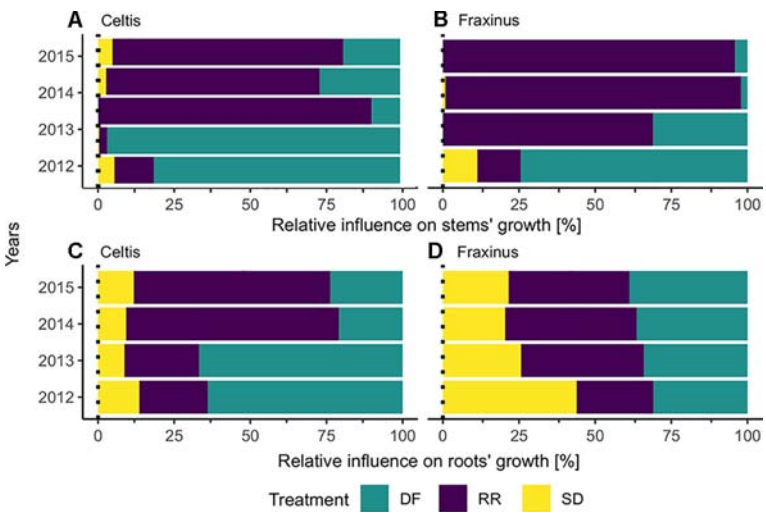

FIGURE 5 | Results from the boosted regression trees: relative influence of each treatment on **(A)** *Celtis* and **(B)** *Fraxinus* stems, **(C)** *Celtis*, and **(D)** *Fraxinus* roots, in the years following damage treatment. DF, defoliation; RR, root reduction and SD, stem damage.

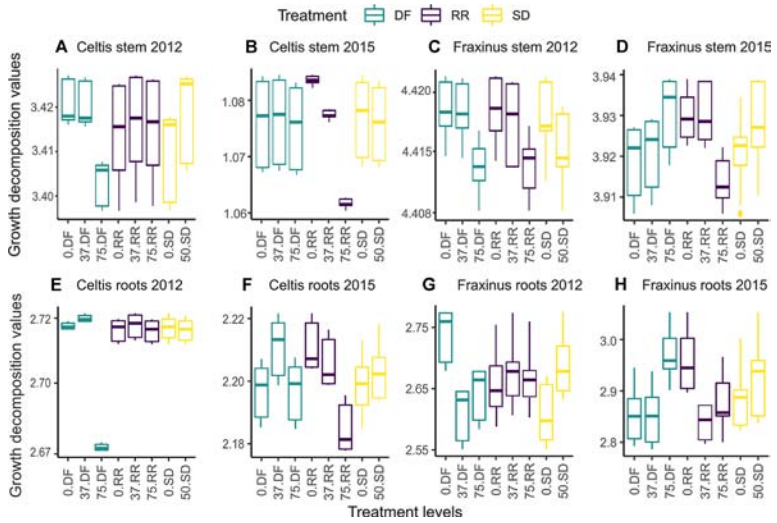

FIGURE 6 | Partial dependence plots showing tree ring growth decomposition between the different levels of damage treatments obtained by the GBM model for the first year (2012) and last year (2015) following damage treatment. DF, defoliation; RR, root reduction; and SD = stem damage, 0 = null treatment, 37 = low intensity treatment, 75 = high intensity treatment. Panels **(A** and **B)** for the stem growth of *Celtis*, **(C** and **D)** for the stem growth of *Fraxinus*, **(E** and **F)** for the root growth of *Celtis*, and **(G** and **H)** for the root growth of *Fraxinus*. Scales are different in each panel to maximize the visibility of the differences between the treatment levels. The vertical lines represent the "whiskers" for the 5th and 95th percentiles of the data distribution.

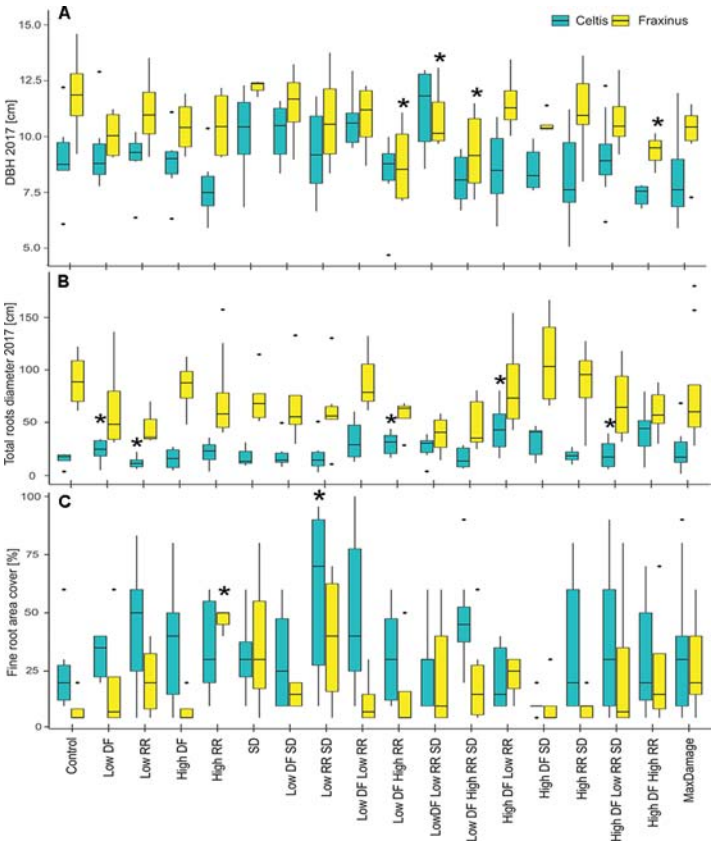

FIGURE 7 | (A) DBH measurements in 2017, **(B)** total larger roots area, measured at 20 cm from the stem center, and **(C)** percent area covered by fine roots for the two tree species and all damage treatments, alone and in combination. All damage treatments are compared to the control group for the respective species. Significant difference performance is indicated by an asterisk (ANOVA $P > 0.05$). The difference between the two species growth is also significant in all three cases.

intensity of the damage treatments, particularly for the low RR/SD treatment in *Celtis*, and high RR in *Fraxinus* (**Figure 7C**).

The correlations between DBH and total larger root diameter in 2017 were strong for both species (r^2 = 0.7 for *Celtis* and r^2 = 0.5 for *Fraxinus* for both treatments). Damage treatments did not have a significant ($P > 0.5$) effect on *Fraxinus* correlations, while the damage treatment combination of low DF/high RR significantly and positively affected *Celtis* abundance of roots (**Figure 8**).

DISCUSSION

Multiple Damage Effects Are Not Simply Cumulative

Multiple damages did not have a simple cumulative effect on growth contrary to our first hypothesis. In most cases, they led to a less negative effect on tree growth than expected. In fact, the maximum damage treatment (DF 75%, RR 75%, and SD) did not have the most negative effect on stem and root growth for either species. Above- and below-ground woody production was decreased by all damage treatments for *Fraxinus* trees, but this decrease was relatively independent of treatment intensity and similar in all 18 damage treatments. In contrast, *Celtis*, which was experiencing a growth decline when damage treatments were applied, showed only a slight both positive and negative growth responses to treatments.

Interestingly, the effect of increasing intensity or number of damage treatments applied did not show a linear cumulative pattern. The effects of low or high intensity damage to only roots or the foliage did not affect the overall tree growth differently compared to the combined root and foliage damage treatments. Similar results can be found in urban oak where compensatory pruning was administrated following root loss to reduce water demand and crown dieback (Watson, 1998). Paired treatments did not decrease growth further; rather, it was similar to the reduction caused by a single treatment of defoliation or root reduction (Watson, 1998). This may indicate a synergistic effect of the damage treatments, inducing physiological responses that protect the trees from the second type of damage (Rennenberg et al., 2006; Bansal et al., 2013). It may also indicate that, in response to any significant stress, trees rapidly stop their growth to reallocate resources (i.e., mainly C from their photosynthesis or reserve pools) to cope with maintenance respiration, tissue reconstruction, or new tissue production (Körner, 2003; Muller et al., 2011; Körner, 2015).

Celtis and *Fraxinus* Did Not Respond Similarly to the Damage Treatments

The different types, intensities, and combinations of damage treatments affected *Celtis* less than *Fraxinus*, 2 years after the last application, contrary to our second hypothesis. Moreover, trees treated with stem damage showed a greater stem growth compared to the control (**Figures 4** and **7**). This increased growth could be explained by a reaction to the injury and consequent compensatory growth to maintain tree viability, especially in trees already showing a decline in growth. Also, following stem damage like girdling, carbohydrates tend to accumulate in the upper parts of the tree (Winkler and Oberhuber, 2017), allowing above-ground compartments to be insensitive to or even to benefit from such treatment. Similarly, the low defoliation treatment in combination with stem damage had a boosting effect on both stem and root growth (**Figures 4** and **7**). In fact, the inclusion of stem damage with other damage treatments tended to reduce the negative effects of these other treatments, presumably due to the triggering of compensatory growth as has been shown in earlier studies (Mcnaughton, 1983; Gill, 1992; Watson, 1998). However, the small growth response of *Celtis* to any combination of treatments should take into account the low growth trend shown by this species following replanting (**Figure 1A**), and the additional stresses did not worsen the already observed decline.

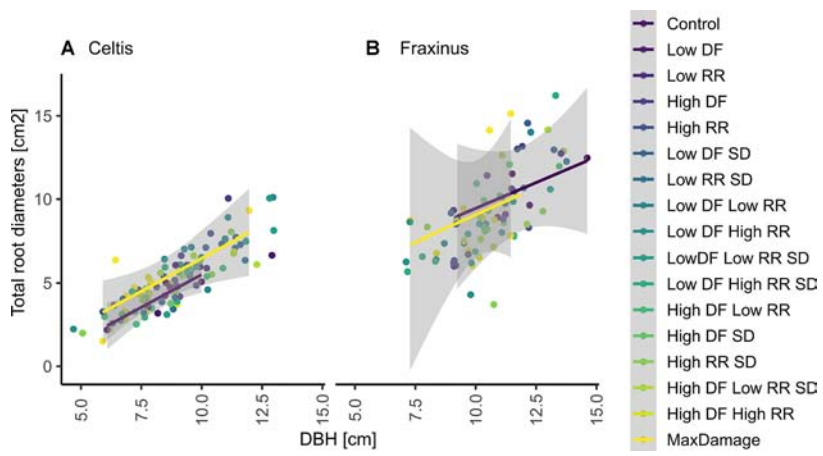

FIGURE 8 | Correlation between DBH and the sum of all larger root diameters at 20 cm from the stump center in 2017 on **(A)** *Celtis* and **(B)** *Fraxinus*. The fitted linear model shows a positive linear correlation with the control group (blue line) and with the maximum combination of damage treatment (yellow line) where r^2 = 0.7 for *Celtis* and r^2 = 0.5 for *Fraxinus*, respectively, for both treatments. None of the groups were significantly different for *Fraxinus* ($P > 0.5$); similarly, all groups for *Celtis* were not significantly different, but the "low DF low RR," which showed a significant reduction in root growth.

This would reinforce the hypothesis that under stress or with tissue damage, this species expresses a particularly high control of resource allocation to its C sinks to maintain its carbon balance (Hoch, 2015). Indeed, under stress, *Celtis* seems to be able to minimize growth and avoid mortality, sustaining "minimum growth levels" for several years. Such strategy may allow for the preservation of scarce resources and provide the capability of dealing with stress and associated secondary metabolism (Muller et al., 2011; Hartmann and Trumbore, 2016).

Fraxinus, which recovered well from replanting (**Figure 1B**), reacted more negatively to all treatments but for a shorter period of time compared to *Celtis* (**Figures 1** and **4**). The trees reacting to treatments, which combined similar levels of defoliation and root reduction, did not fare better than those following a single damage treatment. Growth showed a similar reduction when affected by single damage treatments compared to multiple damage treatments. Only trees undergoing stem damage, or stem damage paired with low defoliation, were not significantly different from the control. Roots showed a significant growth reduction with all damage treatments regardless of the type, intensity, or combination of damage, except in the trees that experienced only stem damage. This result refutes the hypothesis that damage to both above- and below-ground parts can minimize the negative impact on growth by balancing relative activity occurring both above- and below-ground. One should rather acknowledge that trees need to deal with each stress independently perhaps even simultaneously (see next section below). Hence, there is no benefit, nor apparent disadvantage, in trying to compensate for above- or below-ground damage by a similar reduction above- or below-ground.

Damage Treatments Are Time Dependent

In answer to our third question, the three main damage treatments influence on growth shifted in importance and intensity in the years following their application. For stem growth, defoliation had a strong effect right after the damage treatment, while root reduction showed the highest negative effect in the long term (**Figures 5** and **6**). Stem damage was the factor with the lowest influence on stem growth, while it had a relatively strong effect on root growth. On the contrary, all damage treatments had equal weight in the contribution to root growth, and their effects remained constant in the years following the treatments. *Fraxinus* roots were the most affected by stem damage in the first year after treatment and equally affected by all three treatments thereafter. *Celtis* roots were affected most by defoliation in the first 2 years after damage treatment, while root reduction drove the differences in growth afterward.

In some cases, defoliation may reduce tree growth, or, on the contrary, photosynthetic up-regulation reactions may compensate for the loss of foliage resulting in a smaller impact on growth (Pinkard and Beadle, 1998; Vanderklein and Reich, 1999; Eyles et al., 2009; Li et al., 2016). In our study, *Celtis* stem growth rate had little response to defoliation, since growth of this species was actually already affected by other unknown factors. Nevertheless, there are numerous examples showing the lack of effect of low intensity defoliation on tree growth. For example, trees can compensate for a 25% or more defoliation treatment, showing no changes in concentration of nonstructural carbohydrates (Körner, 2003; Boege, 2005; Würth et al., 2005). A crown removal of 50% in Eucalyptus species showed no significant reduction in height and diameter increments over a 2-year period (Alcorn et al., 2008; Alcorn et al., 2013), indicating the great capability of trees to maintain above-ground growth rate from their reserve pools despite loss of foliage. On the contrary, *Fraxinus* stem growth responded to defoliation, by showing reduced growth rate initially, but recovering in the second year after the treatment, and remaining consistent in the following years (**Figure S1**). This compensation response after defoliation has already been reported and associated with the enhancement of photosynthetic efficiency after leaf loss and movement of resources to storage (Pinkard and Beadle, 1998; Quentin et al., 2012; Liu et al., 2019). The null and low root reduction and defoliation treatments showed a similar contribution to *Fraxinus* stem growth, while 75% of treatments showed the lowest contribution in the first 2 years after the treatment (**Figure 6**, **Figure S1**). Interestingly, in 2014 and 2015, high defoliation had a higher contribution to growth than the treatments of lower intensities.

In all cases, null and low root removal treatments showed similar growth contribution. Therefore, to maintain growth, low root removal might have a positive effect on remaining root activities, due to compensatory mechanisms enhancing water and nitrogen utilization efficiency (Blake, 1983; Ferree et al., 1999). However, this enhancement seemed to be insufficient or absent under higher root removal. Similarly, studies of root removal treatments on *Cunninghamia lanceolata* have also indicated multiple compensatory responses associated with root pruning, although above-ground biomass production was significantly negatively associated with increasing root removal (Dong et al., 2016). Trees treated with root removal exhibited higher water use efficiency, both right after the treatment and in the long term, along with an increase in fine root production. Root pruning at the 25% level seemed to be the most effective treatment to enhance photosynthetic nitrogen-use efficiency and stem dry mass accumulation (Dong et al., 2016).

Damage Treatments Do Not Affect Above- and Below-Ground Growth Relationships in the Long Term

Surprisingly, the negative effects of the damage treatments were less pronounced than expected, showing no dramatic reduction when compared to the control, both above- and below-ground. Fine root production found near the stump increased in some of the damaged *Celtis* trees, especially those with the low root damage treatment. However, *Fraxinus* did not show any significant increase in fine root production in relation to the various damage treatments. The correlations between DBH and root production also show only minor differences among the damage treatments, and only the low DF/high RR showed a significant reduction for *Celtis*, probably due to a shift in resource allocation to a higher production of small roots and structural roots. The lack of significant differences between DBH and the larger root area produced in 2017 suggests that although these two species have different strategies when reacting to damage treatments and different growth rates and vitality, they both show that the impacts of damage treatments are not cumulative on tree growth.

Nonetheless, these results should be considered in light of the very different growth patterns of *Celtis* and *Fraxinus* in the growing

conditions of this experiment, regardless of the treatments applied. Where *Celtis* showed low annual increments, *Fraxinus* showed high annual increments and a larger root system (Gucker, 2005; Gucker, 2011). Whereas *Celtis* control trees had reached an average of 8 cm DBH in 2017, *Fraxinus* reached a DBH of 11 cm, showing a 37.5% larger stem (**Figure 7**). Greater differences were found at the root level where *Fraxinus* grew 167% more roots than *Celtis*, although *Celtis* had a higher production of fine roots (on average 5% vs. 30%–40% of area covered by fine roots). In the event of a damage treatment, *Fraxinus* tended to keep the entire crown alive while sacrificing stem growth for a short period of time, whereas *Celtis* tended to sacrifice crown development and overall growth in order to maintain minimal stem and root increment (**Figure 3**). It is also interesting to notice how the correlation between roots produced and diameter growth did not drastically differ between the species and the treated groups (**Figure 8**), suggesting the capacity of both species to reach an equilibrium in above- and below-ground production, only 3 to 4 years after application of damage treatments. The only group showing a significantly higher root production was *Celtis* low DF/low RR. As discussed above, this is also evidence of a root-oriented compensatory mechanisms in *Celtis*, which stimulates root growth when low root removal is applied (Fare, 2014; Dong et al., 2016).

Furthermore, these species-specific differences need to be accounted for to understand any reaction to stress treatments. Overall, *Celtis* showed a system that focuses on the survival of the individual, possibly through a laborious and high-C demanding compartmentation and repair. One consequence is a long-term reduction or cessation of growth, to reduce structural growth sink and save C to cope with this stress response. The considerably low growth rates, probably associated with the shock of replanting, are consistent with trees that are capable of naturally growing in ravines and very rocky, unfavorable soils (Gucker, 2011). *Celtis* has been rated as the most damage-resistant species following hurricane damage (Xi and Peet, 2008), and a successful species in the rehabilitation of mining sites (Ashby et al., 1984). On the contrary, *Fraxinus* shows a high capacity for resource acquisition, compartmentalization after wounds, and growth recovery. This possibly explains its wide distribution across North America, ranging from southeastern Alberta, through central Montana to southeastern Texas, Florida, and up the east coast to Halifax (Kindscher and Holah, 1998). Although this species shows good climate adaptability, it is most often described in association with riparian areas, floodplains, and swamps, but is also found in areas that experience drought.

Finally, increasing stress does not imply a greater reduction in woody mass production. Although differences in their tolerance to damage were evident, neither species showed mortality with increasing stress. This indicates their suitability as urban trees. However, although this experiment shows the high capacity for adaptability of both *Celtis* and *Fraxinus*, it should be noted that physical damage still increases the occurrence of fungal and pathogenic infections, and vulnerability to insects, and therefore, injury should be avoided whenever possible (Clair-Maczulajtys et al., 1999). These conclusions do not take into account the emerald ash borer, which is posing a serious threat to *Fraxinus* health and vitality, and call into question the recommendation of planting *Fraxinus* in the urban setting (Klooster et al., 2018).

CONCLUSION AND STUDY LIMITATIONS

Both in vigorous or declining trees, multiple damage treatments do not have a cumulative effect on growth. Furthermore, for the vigorous *Fraxinus*, low intensity damage treatments stimulated growth after one or two growing seasons, which allowed a compensatory growth and at times an enhanced growth compared to control trees. This highlights the fact that damage can have a negative effect only above a certain threshold. Moreover, when surveying tree health, monitoring of damage impact should thus be done not only in the short term, but also years after damage occurs.

This experiment attempted to disentangle the effect of three types of damage commonly occurring in urban environments, at different levels of intensity both alone and in combination. However, there are three main limitations to the extrapolation of these results to urban trees. First, our sample trees were young, and it is difficult to extrapolate our results to a more advanced growth stage when growth and reserve storage change considerably. However, although direct comparisons between young and old trees' reactions to damage were not carried out, it has been seen that growth of mature trees is significantly negatively affected by defoliation, which, for example, affected 80-year-old aspen for 2 to 3 years after the loss of foliage (Perrette et al., 2014), or major root removal (Dujesiefken and Stobbe, 2002). Mature spruce and beech trees showed a 3- or 4-year time lag before recovering from root trenching (Pretzsch et al., 2016). Second, 3 years of observations is a short period for evaluating the full effects of damage on trees. However, long-term experiments of this type are rare or nonexistent, so this study is a first step toward gaining a better understanding of the complexity of these damage treatments on tree growth. Third, our trees were growing in a rich and open agricultural field; it is not representative of a typical urban growing environment: the trees had plenty of water and space to grow and did not suffer from any pollution or high temperatures (Birkmann et al., 2010; Moser-Reischl et al., 2018). Although these growing conditions did not include common stresses that species can encounter in highly urbanized conditions, the differences in the growth trend of the control trees did highlight fundamental differences in vigor, showing a slow-growing *Celtis* and a fast-growing *Fraxinus*. Therefore, *Celtis* results reflect a "nonvigorous" population of trees, which may have been different if this species had not been experiencing a growth decline. Although no direct factor could be identified to justify *Celtis* low growth rate, it might be related to the shock of replanting in 2009, and roots system show a less clear pattern in reduction due to their larger variability.

This study did not intend to be an exhaustive compendium of species' reactions to mechanical stress, but rather an unprecedented experiment aimed at assessing the effects of a large number of treatments and providing a unique insight into common reactions of urban tree species to mechanical stresses. Further experiments are needed to evaluate the threshold of stress treatments that shift the balance between positive reaction, a sustained negative impact, and growth collapse. This threshold is species-specific. In this study, *Fraxinus* growth was equally affected by all treatments regardless of intensity, whereas *Celtis*, while already declining at the time of planting, showed no enhanced negative impact on growth after the application of treatments and even marginally benefited from

some specific low levels of damage. However, in this experiment, we could not provide further clarification about tree mortality; therefore, future research and long-term monitoring in urban environments are needed. Finally, both species, especially at a young stage, although through different strategies, seem to be particularly resistant and resilient to various levels and combinations of above- and below-ground damages often found in urban settings. Such high resistance and resilience to single or multiple damages do not seem to occur at the detriment of decreasing levels of reserve found in the trees (Ramirez et al., 2018). Further studies done on more tree species under more stressful conditions such as found in urban areas are necessary to generalize our results.

DATA AVAILABILITY

The datasets for this manuscript are not publicly available because data still in use for further publications. Requests to access the datasets should be directed to valentina.vitali89@gmail.com.

AUTHOR CONTRIBUTIONS

VV produced and processed the roots data, performed the analyses on the roots and stem data, and wrote the paper; JR and GP supervised and carried out the experimental procedures and helped with the evaluation and discussion of the results; CM and JR conceived the study idea, developed the study design, and cowrote the paper; and AP and SD also cowrote the paper.

FUNDING

This research was supported by the NSERC/Hydro-Quebec research chair on tree growth control and by a scholarship from the Quebec research funds for nature and technology.

ACKNOWLEDGMENTS

The authors thank David Andres Herrera, Sergio Martinez, Mathieu Messier, Bastien Lecigne, Éric Larose, and Maria Isabel Carol-Aristizabal for their support in the field activities and Kim Bannon for field logistics. We also thank Martin Gaudet, Michel Desilets, and all the employees of the Montreal nursery for their technical, professional, and overall support and openness throughout this project. This research was supported by the NSERC/Hydro-Quebec research chair on tree growth control and by a scholarship from the Quebec research funds for nature and technology. We thank Justine Fontaine-Topaloff and Maria Isabel Carol-Aristizabal who cleaned, measured, and sampled the roots for the experiment and helped with the processing and measurement of tree-ring samples.

SUPPLEMENTARY MATERIAL

The Supplementary Material for this article can be found online at: https://www.frontiersin.org/articles/10.3389/fpls.2019.01100/full#supplementary-material

REFERENCES

Adams, H. D., Germino, M. J., Breshears, D. D., Barron-Gafford, G. A., Guardiola-Claramonte, M., Zou, C. B., et al. (2013). Nonstructural leaf carbohydrate dynamics of *Pinus edulis* during drought-induced tree mortality reveal role for carbon metabolism in mortality mechanism. *New Phytol.* 197, 1142–1151. doi: 10.1111/nph.12102

Alcorn, P., Forrester, D., Thomas, D., James, R., Smith, R., Nicotra, A., et al. (2013). Changes in whole-tree water use following live-crown pruning in young plantation-grown *Eucalyptus pilularis* and *Eucalyptus cloeziana*. *Forests* 4, 106–121. doi: 10.3390/f4010106

Alcorn, P. J., Bauhus, J., Thomas, D. S., James, R. N., Smith, R. G. B., and Nicotra, A. B. (2008). Photosynthetic response to green crown pruning in young plantation-grown *Eucalyptus pilularis* and *E. cloeziana*. *For. Ecol. Manage.* 255, 3827–3838. doi: 10.1016/j.foreco.2008.03.030

Ashby, W. C., Vogel, W. G., Kolar, C. A., and Philo, G. R. (1984). Productivity of stony soils on strip mines 1. *Erosion and Productivity Soils Containing rock Fragments*, 13, 31–44.

Bansal, S., Hallsby, G., Löfvenius, M. O., and Nilsson, M.-C. (2013). Synergistic, additive and antagonistic impacts of drought and herbivory on *Pinus sylvestris*: leaf, tissue and whole-plant responses and recovery. *Tree Physiol.* 33, 451–463. doi: 10.1093/treephys/tpt019

Bates, D., Mächler, M., Bolker, B., and Walker, S. (2015). Fitting linear mixed-effects models using lme4. *J. Stat. Soft.* 67 (1): 1–48. doi: 10.18637/jss.v067.i01

Birkmann, J., Garschagen, M., Kraas, F., and Quang, N. (2010). Adaptive urban governance: new challenges for the second generation of urban adaptation strategies to climate change. *Sustain Sci.* 5, 185–206. doi: 10.1007/s11625-010-0111-3

Blake, T. J. (1983). Transplanting shock in white spruce; effect of cold-storage and root pruning on water relations and stomatal conditioning. *Physiol. Plant* 57, 210–216. doi: 10.1111/j.1399-3054.1983.tb00901.x

Boege, K. (2005). Influence of plant ontogeny on compensation to leaf damage. *Am. J. Bot.* 92, 1632–1640. doi: 10.3732/ajb.92.10.1632

Boyer, L., Bensoussan, A., Durand, M., Grice, R. H., and Berard, J. (1985). Geology of Montreal, Province of Quebec, Canada. 22:333–394. *Bull. Assoc. Eng. Geo.* 22, 333–394. doi: 10.2113/gseegeosci.xxii.4.329

Bunn, A. G. (2010). Statistical and visual crossdating in R using the dplR library. *Dendrochronologia* 28, 251–258. doi: 10.1016/j.dendro.2009.12.001

Calfapietra, C., Peñuelas, J., and Niinemets, Ü. (2015). Urban plant physiology: adaptation-mitigation strategies under permanent stress. *Trends Plant Sci.* 20, 72–75. doi: 10.1016/j.tplants.2014.11.001

Clair-Maczulajtys, D., Le Disquet, I., and Bory, G. (1999). Pruning stress: changes in tree physiology and their effects on tree health. *Acta Hortic.*, 496 (39), 317–324. doi: 10.17660/ActaHortic.1999.496.39

Cutler, D. R., Edwards, T. C., Beard, K. H., Cutler, A., Hess, K. T., Gibson, J., et al. (2007). Random forests for classification in ecology. *Ecology* 88, 2783–2792. doi: 10.1890/07-0539.1

Dong, T., Duan, B., Zhang, S., Korpelainen, H., Niinemets, Ü., and Li, C. (2016). Growth, biomass allocation and photosynthetic responses are related to intensity of root severance and soil moisture conditions in the plantation tree *Cunninghamia lanceolata*. *Tree Physiol.* 36, 807–817. doi: 10.1093/treephys/tpw025

Dujesiefken, D., and Stobbe, H. (2002). The Hamburg Tree Pruning System—a framework for pruning of individual trees. *Urban For. Urban Gree* 1, 75–82. doi: 10.1078/1618-8667-00008

Elith, J., Leathwick, J. R., and Hastie, T. (2008). A working guide to boosted regression trees. *J. Anim. Ecol.* 77, 802–813. doi: 10.1111/j.1365-2656.2008.01390.x

Eyles, A., Pinkard, E. A., and Mohammed, C. (2009). Shifts in biomass and resource allocation patterns following defoliation in *Eucalyptus globulus* growing with varying water and nutrient supplies. *Tree Physiol.* 29, 753–764. doi: 10.1093/treephys/tpp014

Fajstavr, M., Giagli, K., Vavrčík, H., Gryc, V., and Urban, J. (2017). The effect of stem girdling on xylem and phloem formation in Scots pine. *Silva Fenn.* 51 (4), artID1760. doi: 10.14214/sf.1760

Fare, D. (2014). Effects of root pruning on container-grown maple and oak. *J. Environ. Hortic.* 32, 208–214. doi: 10.1371/journal.

Farrar, J. L. (1995). *Trees in Canada*. (Ottawa, ON: Fitzhenry and Whiteside, Markham, ON, and Canadian Forest Service). 502.

Ferree, D. C., Scurlock, D. M., and Schmid, J. C. (1999). Root pruning reduces photosynthesis, transpiration, growth, and fruiting of container-grown French-American hybrid grapevines. *HortScience* 34, 1064–1067. doi: 10.21273/HORTSCI.34.6.1064

Ferrini, F., Bussotti, F., Tattini, M., and Fini, A. (2014). Trees in the urban environment: response mechanisms and benefits for the ecosystem should guide plant selection for future plantings. *Agrochimica* 58, 234–246.

Freschet, G. T., Violle, C., Bourget, M. Y., Scherer-Lorenzen, M., and Fort, F. (2018). Allocation, morphology, physiology, architecture: the multiple facets of plant above- and below-ground responses to resource stress. *New Phytol.* 219, 1338–1352. doi: 10.1111/nph.15225

Friedman, J. H. (2001). Greedy function approximation: a gradient boosting machine. *Ann. Stat.* 29, 1189–1232. doi: 10.1214/aos/1013203451

Friedman, J. H. (2002). Stochastic gradient boosting. *Comput. Stat. Data Anal.* 38, 367–378. doi: 10.1016/S0167-9473(01)00065-2

Fritts, H. C. (1976). *Tree rings and climate*. London: Academic Press.

Gill, R. M. A. (1992). A review of damage by mammals in north temperate forests: 3. Impact on trees and forests. *Forestry* 65, 363–388. doi: 10.1093/forestry/65.4.363-a

Grime, J. P., and Hunt, R. (1975). Relative growth-rate: its range and adaptive significance in a local flora. *J. Ecol.* 63, 393. doi: 10.2307/2258728

Gucker, C. L. (2005). "*Fraxinus pennsylvanica*.," in *Fire effects information system*. *[online]* U.S. Department of Agriculture, Forest Service, Rocky Mountain Research Station, Fire Sciences Laboratory. Available at https://www.fs.fed.us/database/feis/plants/tree/frapen/all.html.

Gucker, C. L. (2011). "*Celtis occidentalis*.," in *Fire effects information system*. *[online]*. U.S. Department of Agriculture, Forest Service, Rocky Mountain Research Station, Fire Sciences Laboratory. Available at www.fs.fed.us/database/feis/plants/tree/celocc/all.html.

Hartmann, H., and Trumbore, S. (2016). Understanding the roles of nonstructural carbohydrates in forest trees—from what we can measure to what we want to know. *New Phytol.* 211, 386–403. doi: 10.1111/nph.13955

Hoch, G. (2015). "Carbon reserves as indicators for carbon limitation in trees," in *Progress in botany*, vol. 76. Eds. U. Lüttge and W. Beyschlag (Cham: Springer International Publishing) p. 321–346. doi: 10.1007/978-3-319-08807-5_13

Jacquet, J.-S., Bosc, A., O'Grady, A., and Jactel, H. (2014). Combined effects of defoliation and water stress on pine growth and non-structural carbohydrates. *Tree Physiol.* 34, 367–376. doi: 10.1093/treephys/tpu018

Jacquet, J.-S., Orazio, C., and Jactel, H. (2012). Defoliation by processionary moth significantly reduces tree growth: a quantitative review. *Ann. For. Sci.* 69, 857–866. doi: 10.1007/s13595-012-0209-0

Jutras, P., Prasher, S., and Mehuys, G. R. (2010). Appraisal of key abiotic parameters affecting street tree growth. *Arboric Urban For.* 36, 1–10.

Kindscher, K., and Holah, J. (1998). *An old-growth definition for western hardwood gallery forests*. Asheville, NC: U.S. Department of Agriculture, Forest Service, Southern Research Station. doi: 10.2737/SRS-GTR-22

Klooster, W., Gandhi, K., Long, L., Perry, K., Rice, K., and Herms, D. (2018). Ecological impacts of emerald ash borer in forests at the epicenter of the invasion in North America. *Forests* 9, 250. doi: 10.3390/f9050250

Konijnendijk, C., Nilsson, K., Randrup, T., Schipperijn J., editors. (2005). *Urban forests and trees*. Berlin, Heidelberg: Springer Berlin Heidelberg. doi: 10.1007/3-540-27684-X

Körner, C. (2003). Carbon limitation in trees. *J. Ecol.* 91, 4–17. doi: 10.1046/j.1365-2745.2003.00742.x

Körner, C. (2015). Paradigm shift in plant growth control. *Curr. Opin. Plant Biol.* 25, 107–114. doi: 10.1016/j.pbi.2015.05.003

Li, N., He, N., Yu, G., Wang, Q., and Sun, J. (2016). Leaf non-structural carbohydrates regulated by plant functional groups and climate: evidences from a tropical to cold-temperate forest transect. *Ecol. Indic.* 62, 22–31. doi: 10.1016/j.ecolind.2015.11.017

Liu, M., Gong, J., Li, Y., Li, X., Yang, B., Zhang, Z., et al. (2019). Growth-defense trade-off regulated by hormones in grass plants growing under different grazing intensities. *Physiol. Plant* 166, 553–539. doi: 10.1111/ppl.12802

Mcnaughton, S. J. Compensatory plant growth as a response to herbivory. Proceedings of a Symposium, 1981 September 14-18, Kevo, Finland. Wiley on behalf of Nordic Society Oikos (1983). 40:3, 329-336. doi: 10.2307/3544305

Millet, J., and Bouchard, A. (2003). Architecture of silver maple and its response to pruning near the power distribution network. *Can. J. For. Res.* 33, 726–739. doi: 10.1139/x02-206

Mittler, R. (2006). Abiotic stress, the field environment and stress combination. *Trends Plant Sci.* 11, 15–19. doi: 10.1016/j.tplants.2005.11.002

Moore, G. M. (2013). *Ring-barking and girdling: how much vascular connection do you need between roots and crown?*. Richmond. Burnley College: University of Melbourne.

Moser-Reischl, A., Uhl, E., Rötzer, T., Biber, P., van Con, T., Tan, N. T., et al. (2018). Effects of the urban heat island and climate change on the growth of Khaya senegalensis in Hanoi, Vietnam. *For. Ecosyst.* 5, 295. doi: 10.1186/s40663-018-0155-x

Muller, B., Pantin, F., Génard, M., Turc, O., Freixes, S., Piques, M., et al. (2011). Water deficits uncouple growth from photosynthesis, increase C content, and modify the relationships between C and growth in sink organs. *J. Exp. Bot.* 62, 1715–1729. doi: 10.1093/jxb/erq438

Natekin, A., and Knoll, A. (2013). Gradient boosting machines, a tutorial. *Front. Neurorobot.* 7, 21. doi: 10.3389/fnbot.2013.00021

Niinemets, Ü. (2010a). Mild versus severe stress and BVOCs: thresholds, priming and consequences. *Trends Plant Sci.* 15, 145–153. doi: 10.1016/j.tplants.2009.11.008

Niinemets, Ü. (2010b). Responses of forest trees to single and multiple environmental stresses from seedlings to mature plants: past stress history, stress interactions, tolerance and acclimation. *For. Ecol. Manage.* 260, 1623–1639. doi: 10.1016/j.foreco.2010.07.054

Niinemets, Ü., and Valladares, F. (2008). "Environmental tolerance," in *Encyclopedia of ecology*. Ed. B. Fath (Amsterdam: Elsevier), 1370–1376. doi: 10.1016/B978-008045405-4.00826-0

Oberhuber, W., Gruber, A., Lethaus, G., Winkler, A., and Wieser, G. (2017). Stem girdling indicates prioritized carbon allocation to the root system at the expense of radial stem growth in Norway spruce under drought conditions. *Environ. Exp. Bot.* 138, 109–118. doi: 10.1016/j.envexpbot.2017.03.004

Olden, J. D., Lawler, J. J., and Poff, N. L. (2008). Machine learning methods without tears: a primer for ecologists. *Q. Rev. Biol.* 83, 171–193. doi: 10.1086/587826

Perrette, G., Lorenzetti, F., Moulinier, J., and Bergeron, Y. (2014). Site factors contribute to aspen decline and stand vulnerability following a forest tent caterpillar outbreak in the Canadian Clay Belt. *For. Ecol. Manage.* 323, 126–137. doi: 10.1016/j.foreco.2014.03.013

Pinkard, E. A., Battaglia, M., Roxburgh, S., and O'Grady, A. P. (2011). Estimating forest net primary production under changing climate: adding pests into the equation. *Tree Physiol.* 31, 686–699. doi: 10.1093/treephys/tpr054

Pinkard, E. A., and Beadle, C. L. (1998). Regulation of photosynthesis in *Eucalyptus nitens* (Deane and Maiden) Maiden following green pruning. *Trees* 12, 366–376. doi: 10.1007/PL00009722

Poorter, L., and Kitajima, K. (2007). Carbohydrate storage and light requirements of tropical moist and dry forest tree species. *Ecology* 88, 1000–1011. doi: 10.1890/06-0984

Pretzsch, H., Bauerle, T., Häberle, K. H., Matyssek, R., Schütze, G., and Rötzer, T. (2016). Tree diameter growth after root trenching in a mature mixed stand of Norway spruce (*Picea abies* [L.] Karst) and European beech (*Fagus sylvatica* [L.]). *Trees* 30, 1761–1773. doi: 10.1007/s00468-016-1406-5

Quentin, A. G., O'Grady, A. P., Beadle, C. L., Mohammed, C., and Pinkard, E. A. (2012). Interactive effects of water supply and defoliation on photosynthesis, plant water status and growth of *Eucalyptus globulus* Labill. *Tree Physiol.* 32, 958–967. doi: 10.1093/treephys/tps066

Quentin, A. G., Pinkard, E. A., Beadle, C. L., Wardlaw, T. J., O'Grady, A. P., Paterson, S., et al. (2010). Do artificial and natural defoliation have similar effects on physiology of *Eucalyptus globulus* Labill. seedlings? *Ann. For. Sci.* 67, 203. doi: 10.1051/forest/2009096

R Core Team (2017). *R: a language and environment for statistical computing*. Austria: Vienna.

Ramirez, J. A. (2017). *The functional role of carbohydrate reserves in the growth and survival of trees. PhD thesis.* Montréal, Canada: PhD Université du Québec à Montréal (UQAM).

Ramirez, J. A., Handa, I. T., Posada, J. M., Delagrange, S., and Messier, C. (2018). Carbohydrate dynamics in roots, stems, and branches after maintenance pruning in two common urban tree species of North America. *Urban For. Urban Gree* 30, 24–31. doi: 10.1016/j.ufug.2018.01.013

Rennenberg, H., Loreto, F., Polle, A., Brilli, F., Fares, S., Beniwal, R. S., et al. (2006). Physiological responses of forest trees to heat and drought. *Plant Biol. (Stuttg)* 8, 556–571. doi: 10.1055/s-2006-924084

Ridgeway, G., Boehmke, B., and Cunningham, J. (2019). gbm, 2.1.5: generalized boosted regression models. *R package version* 1. 1–39.

Schweingruber, F. H. (1988). *Tree rings: basics and applications of dendrochronology*. Dordrecht: Springer Netherlands. doi: 10.1007/978-94-009-1273-1

Sieghardt, M., Mursch-Radlgruber, E., Paoletti, E., Couenberg, E., Dimitrakopoulus, A., Rego, F., et al. (2005). "The abiotic urban environment: impact of urban growing conditions on urban vegetation," in *Urban forests and trees: A reference book/Cecil C. Konijnendijk*. Ed. C. C. Konijnendijk et al. (Berlin, Great Britain: Springer), 281–323. doi: 10.1007/3-540-27684-X_12

Smiley, E. (2008). Root pruning and stability of young willow oak. *Arboric Urban For.* 34 (2), 123–128.

Tanner, C. J., Adler, F. R., Grimm, N. B., Groffman, P. M., Levin, S. A., Munshi-South, J., et al. (2014). Urban ecology: advancing science and society. *Front. Ecol. Environ.* 12, 574–581. doi: 10.1890/140019

Vanderklein, D. W., and Reich, P. B. (1999). The effect of defoliation intensity and history on photosynthesis, growth and carbon reserves of two conifers with contrasting leaf lifespans and growth habits. *New Phytol.* 144, 121–132. doi: 10.1046/j.1469-8137.1999.00496.x

Vysotskaya, L. B., Arkhipova, T. N., Timergalina, L. N., Dedov, A. V., Veselov, S. Y., and Kudoyarova, G. R. (2004). Effect of partial root excision on transpiration, root hydraulic conductance and leaf growth in wheat seedlings. *Plant Physiol. Biochem.* 42, 251–255. doi: 10.1016/j.plaphy.2004.01.004

Watson, G. W. (1998). Tree growth after trenching and compensatory crown pruning. *J. Arboric* 24, 47–53.

Winkler, A., and Oberhuber, W. (2017). Cambial response of Norway spruce to modified carbon availability by phloem girdling. *Tree Physiol.* 37, 1527–1535. doi: 10.1093/treephys/tpx077

Würth, M. K. R., Peláez-Riedl, S., Wright, S. J., and Körner, C. (2005). Non-structural carbohydrate pools in a tropical forest. *Oecologia* 143, 11–24. doi: 10.1007/s00442-004-1773-2

Xi, W., and Peet, R. K. (2008). Hurricane effects on the piedmont forests: patterns and implications. *Ecol. Restor.* 26, 295–298. doi: 10.3368/er.26.4.295

Conflict of Interest Statement: The authors declare that the research was conducted in the absence of any commercial or financial relationships that could be construed as a potential conflict of interest.

Advantages of publishing in Frontiers

OPEN ACCESS
Articles are free to read for greatest visibility and readership

FAST PUBLICATION
Around 90 days from submission to decision

HIGH QUALITY PEER-REVIEW
Rigorous, collaborative, and constructive peer-review

TRANSPARENT PEER-REVIEW
Editors and reviewers acknowledged by name on published articles

Frontiers
Avenue du Tribunal-Fédéral 34
1005 Lausanne | Switzerland

Visit us: www.frontiersin.org
Contact us: info@frontiersin.org | +41 21 510 17 00

REPRODUCIBILITY OF RESEARCH
Support open data and methods to enhance research reproducibility

DIGITAL PUBLISHING
Articles designed for optimal readership across devices

FOLLOW US
@frontiersin

IMPACT METRICS
Advanced article metrics track visibility across digital media

EXTENSIVE PROMOTION
Marketing and promotion of impactful research

LOOP RESEARCH NETWORK
Our network increases your article's readership